DIFFERENCES IN DROUGHT SENSITIVITY AMONG PRAIRIE COMMUNITIES AND AMONG MANAGEMENT HISTORIES: A REMOTE SENSING ANALYSIS OF 221 PRAIRIES IN THE NORTHERN GREAT PLAINS

By

Jarrod J. Morrice

A THESIS

Submitted to
Michigan State University
in partial fulfillment of the requirements
for the degree of

MASTER OF SCIENCE

Plant Biology

2011

ABSTRACT

DIFFERENCES IN DROUGHT SENSITIVITY AMONG PRAIRIE COMMUNITIES AND AMONG MANAGEMENT HISTORIES: A REMOTE SENSING ANALYSIS OF 221 PRAIRIES IN THE NORTHERN GREAT PLAINS

By

Jarrod J. Morrice

The relationship between primary production and precipitation in grasslands has long been an issue of great interest both to ecologists and managers who graze livestock and/or maintain conservation properties. Data from remote sensors are now obtained at higher spatial resolutions on a near daily basis providing new methods to explore broad scale relationships between grassland production and moisture availability. To promote remote sensing-based analysis of grasslands in North America, I developed the Prairie Spatial Database (PSD) for the northern Great Plains. To develop the PSD, I obtained geospatial coordinates and ecological data from conservation managers for 261 prairies. Sites were filtered for suitability for remote sensing studies, and 221 were selected for further analysis; representing a mix of shortgrass, mixedgrass, and tallgrass prairie types and different C_3/C_4 dominances. Using time series weather data (PRISM), I next derived Palmer's Drought Severity Index (PDSI) values and produced a time series of normalized difference vegetation index (NDVI) values for each site for 2000 – 2008 from the Moderate Resolution Imaging Spectroradiometer (MODIS). Mixed modeling techniques allowed me next to compare the influence of soil moisture on growing season time integrated NDVI (TINDVI) and maximum NDVI across prairie types. Selection of best-fit models highlighted the contingency of biomass production on soil moisture availability and a hidden relationship between TINDVI and soil moisture within tallgrass prairies.

I dedicate this thesis to my loving wife Lina, who has supported and encouraged me through the completion of this thesis.

ACKNOWLEDGEMENTS

I would like to acknowledge my thesis advisor, Dr. Carolyn Malmstrom, for the hard work and many hours she has provided in guiding the research and the writing behind this thesis. I would also like to thank the current and former members of my graduate committee, Dr. David Lusch, Dr. Lars Brudvig, and Dr. Kay Gross for their assistance with these projects. This work could not have been done without the pleasant help and hardwork of the many natural areas land managers who provided data during the development of the Prairie Spatial Database. The list of names is too long to mention within this section, but I have dedicated Appendix A to acknowledging these people and organizations. My lab mates helped in reading and revising various portions of this document. I thank all of you for all of your support.

TABLE OF CONTENTS

LIST OF TABLES

LIST OF FIGURES

Chapter 1. Prairie Vegetation Responses to Weather Perturbations as Assessed By Satellite Remote Sensing: A Review

I. Overview

Prairie ecosystems composed of grasses and forbs once dominated the Great Plains region of central North America, but now are considered to be threatened and endangered over much of this area. The high fertility of their soils made many prairies attractive for agricultural development over the past two centuries, and the substantial conversion of prairies to agriculture has raised concerns about the possible loss of prairie species and ecosystem services and led to efforts to restore prairie habitat.

Projected changes in climate change pose a challenge for conservation and restoration managers who are constructing habitats now to conserve species for the future. Within the Great Plains, temperature is expected to increase by as much as 4^{o}C by 2080 (Christensen *et al.* 2007, Meehl *et al.* 2007) and precipitation is expected to decrease slightly, with a concomitant increase in the intensity of precipitation events (Tebaldi *et al.* 2006). Because prairie ecosystems are strongly shaped by moisture conditions (Smoliak 1986, Sala *et al.* 1988, Briggs & Knapp 1995), these projected changes in climate may substantially alter prairie structure and function and may make it more difficult for prairie managers to meet biodiversity objectives within managed prairies. The aim of my research is to investigate climate sensitivity of Great Plains prairies to develop a deeper understanding of how these ecosystems respond to extreme weather events and to assist managers in decision-making.

Remote sensing techniques can provide invaluable information about change in vegetation dynamics across regions overtime, thus serving as excellent tools for investigations of biotic changes to climatic change. Vegetation indexes used with remote sensing can be

employed to monitor net primary production (NPP) and other ecosystem functions over large areas through quantification of patterns of vegetation greenness. Satellite sensors such as the Moderate Resolution Imaging Spectroradiometer (MODIS) onboard the United States National Aeronautic Space Administration (NASA) Terra satellite provide frequent temporal monitoring of vegetation across wide regions. The ability to compare the function of prairies across a large spatial area may help elucidate the impacts of regional changes, such as climate change, on prairies.

Within this chapter, I present an overview of the literature pertaining to prairie conservation and monitoring prairies using remote sensing. In section II, I discuss prairies in general and some conservation concerns associated with them. Section III compares field and remote sensing methods for observing structural and functional attributes of prairies. In this section, I also highlight the need for additional functional assessments of ecosystems. Section IV discusses specific techniques used with remote sensing that can be used to attain functional attributes, particularly biomass changes, of prairies. Section V provides an introduction to the influence of several weather attributes on prairies, a topic which I expand in subsequent analysis in which I compare the biomass response to drought among prairies within northern Great Plains.

II. Central North American Prairies

What is a prairie?

Grasslands are ecosystems dominated by grasses and forbs (Beard 1978, Axelrod 1985). Depending on the continent, grasslands may be referred to as steppe (Asia), veldt (Africa), pampas (South America) or prairie (North America). Collectively, grassland regions comprise approximately 20% of the terrestrial environment (Scurlock & Hall 1998, Lemmens *et al.* 2006).

Prairies were once a large component of the central United States (U. S.), also known as the Great Plains. Their pre-European extent has been estimated as 149 - 370 million ha (Samson & Knopf 1994, Sims & Risser 2000) and their historical range extended in central North America from the southern United States into southern Canada (Transeau 1935, Weaver & Albertson 1956, Olson *et al.* 2001) (See Figures 1.1 and 1.2). In this region, precipitation increases from west to east and temperatures increase from north to south (Figure 1.3). These precipitation and temperature gradients significantly affect the composition of vegetation communities within the landscape. Three broad categories of vegetation can be defined based on the precipitation gradient: shortgrass prairie in the west, mixedgrass prairie in the central region, and tallgrass prairie to the east (Table 1.1). The north-to-south temperature gradient predominately influences the photosynthetic pathway that dominates a particular prairie. Vegetation that uses the C_3 pathway thrives in cooler climates, while the C_4 pathway dominates in southern latitudes.

Figure 1.1. The historic range of prairie in central North America. Based on data obtained from the World Wildlife Fund (Olson, Dinerstein *et al.* 2001). For interpretation of the references to color in this and all other figures, the reader is referred to the electronic version of this thesis.

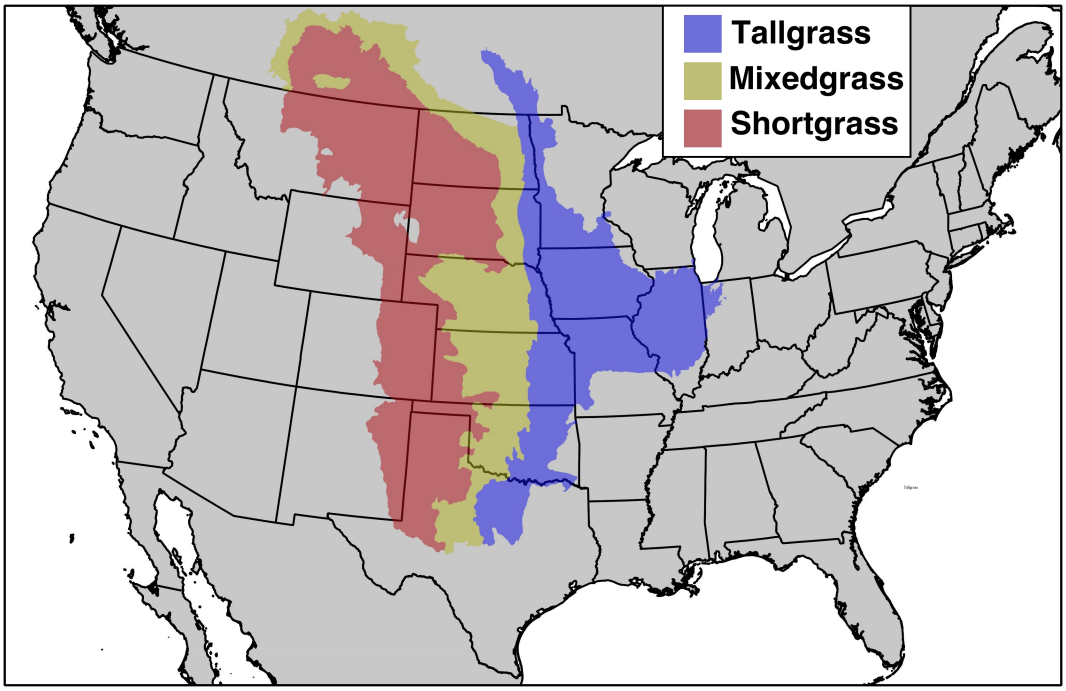

Figure 1.2. Transeau's depiction of the Prairie Peninsula based on observation personal observation and communication with other experts (Transeau 1935). Black areas represent historic prairie regions.

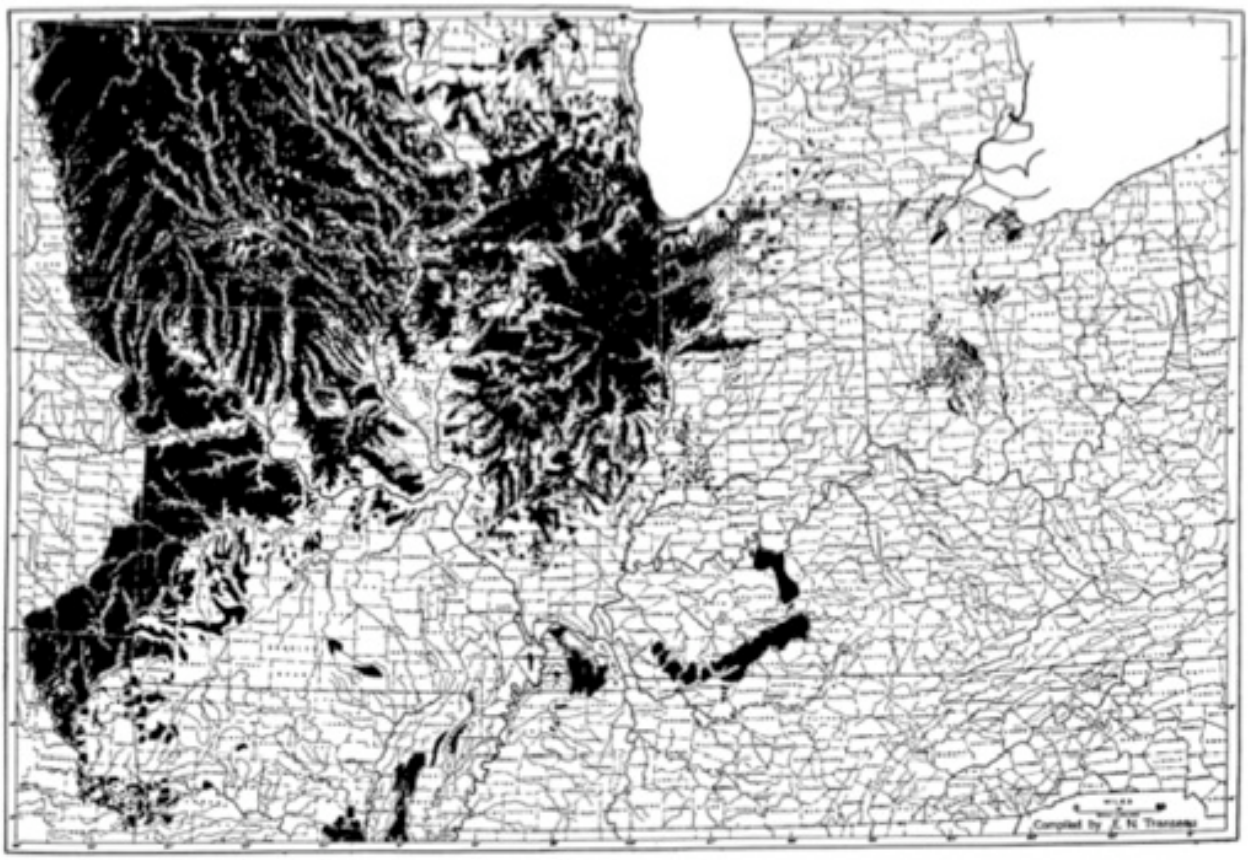

Figure 1.3. (A) Pattern of precipitation (cm) and (B) maximum temperature (^{o}C) within the U.S. Gradients are yearly averages from 1971-2000 and were obtained from the PRISM dataset (Daly 2009).

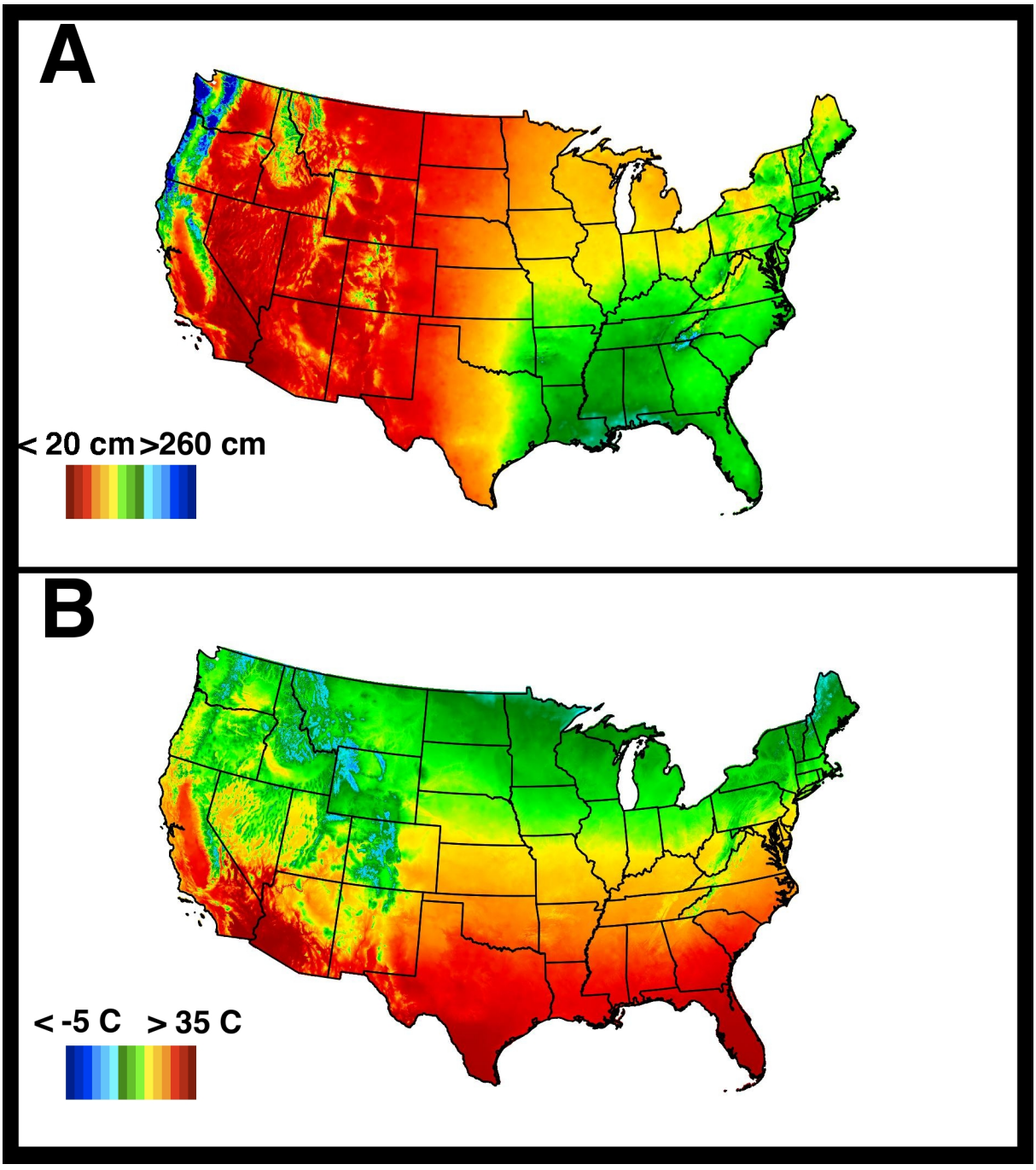

Table 1.1. Comparison of the three main prairie types located in central North America.

Prairie Type	Short-grass	Mixed-grass	Tall-grass
Mean precipitation *	30 cm yr^{-1}	50 cm yr^{-1}	100 cm yr^{-1}
Historic extent **	18 million ha	62 million ha	68 million ha
Present extent **	4 million ha	21 million ha	2 million ha
Dominant species *	*Buchloë dactyloides*	*Pseudoroegneria spp.*	*Andropogon gerardii*
	Pascopyrum smithii	*Schyzachrium spp.*	*Panicum virgatum*
	Bouteloua gracilis	*Stipa spp.*	*Sorghastrum nutans*
		Elymus spp.	
		Pascopyrum spp.	
		Calamovilfa spp.	
		Bouteloua spp.	
		Sporobolus spp.	

* From Sims and Risser (2000)

** From Samson and Knopf (1994)

Distribution and dominance of C_3 and C_4 species

Several studies have examined the modern day boundary between C_3 and C_4 dominance within the central U. S. (Table 1.2). For example, based on species richness data for C_3 and C_4 groups at 32 sites in the Great Plains, higher richness for C_4 species was found southward from 40^{o}N (Teeri & Stowe 1976). In another approach, using model simulations based on temperature and light, Ehleringer (1978) estimated the boundary between C_3 and C_4 dominance to lie at 45^{o}N. Epstein *et al*. (1997b) found similar results in a study in which they quantified biomass productivity by C_3 and C_4 grasses using data collected from Natural Resources Conservation Service (NRCS) range site descriptions. They found that the dominance of these two functional

Table 1.2. This table compares studies that have defined the transition latitude for C_3 and C_4 species in the central United States. Transition lines represent the approximate latitude at which C_3 species dominate to the north and C_4 species dominate to the south.

Reference	Transition Latitude	Method
Teeri and Stowe 1976	40° N	Sampling sites for species richness
Ehleringer 1978	45° N	Modeling from temperature and light intensity
Epstein, Lauenroth et al. 1997	43° N	Biomass data and modeling
vonFischer, Tieszen et al. 2008	45° N	Isotopic analysis of soil organic matter

groups could be characterized using a precipitation and temperature curve, which indicated a C_3/C_4 grass boundary at 43°N. Similarly, isotopic data from soil organic matter show C_3 dominance northward of 45°N (vonFischer *et al.* 2008). Additional studies have shown a similar transition line between 40° - 45°N (Woodward & Lomas 2004, Woodward *et al.* 2004).

Conservation of North American prairies

Conservation efforts for prairies in North America developed during the Dust Bowl Era of the 1930s (Kindscher & Tieszen 1998, Allison 2002). At that time, it became apparent that great tracts of prairie had been lost to agriculture (Kindscher & Tieszen 1998). Currently, an estimated 80% of the former prairie extent has been lost in North America (Samson & Knopf 1994). Much of this loss can be attributed to land conversion for agriculture (Sims & Risser 2000) and to the alteration of ecosystem processes such as changes in fire frequencies after European settlement. Tallgrass prairies have been most affected by land conversion (Table 1.1) and are now considered an endangered ecosystem in the U. S. (Noss *et al.* 1995, Noss & Peters 1995). It has been estimated that 99% of all tallgrass prairies have been eliminated east of the Missouri river and 85% west of the Missouri river (Noss *et al.* 1995). Depending on region, the

proportion of shortgrass prairie lost has been estimated at 20-85% and the loss of mixedgrass prairie ranges at 30–99% (Samson & Knopf 1994).

Decline in prairie habitat has significantly influenced the conservation status of many animal and plan species. Approximately 330 (75%) of the bird species that breed within the U. S. do so within the Great Plains (Samson & Knopf 1994). Declines in these bird species have ranged from 17–91% depending on region (Samson & Knopf 1994). Populations of prairie dogs, a keystone species (Kotliar *et al.* 1999, Kotliar 2000), have sharply declined since European settlement (Samson & Knopf 1994, Magle & Crooks 2009). Another species affected by this loss is the black-footed ferret, a predator of prairie dogs, which is now endangered (Grenier *et al.* 2009). Plant species have been affected by the loss of prairie area as well. The United States Fisheries and Wildlife Service (USFWS) maintains a list of threatened or endangered species, which includes *Platanthera leucophaea* (Eastern prairie fringed orchid), *Platanthera praeclara* (Western prairie fringed orchid), *Boltonia decurrens* (Decurrent false aster), *Delea foliosa* (Leafy prairie clover), *Asclepias meadii* (Mead's milkweed), and *Lespedeza leptostachya* (Prairie bush clover)(USFWS 2009). The decline in the number of individuals of such species has motivated agencies such as The Nature Conservancy, Prairie Plains Resource Institute, and state and federal agencies to invest in prairie restoration.

III. Assessing ecosystem structure and function in North American prairies

Biodiversity and Function Can be Assessed by Both Field and Remote Sensing Methods

Ecosystem assessment is important for conservation and restoration activities (Clark 1997, Whisenant 1999). It provides a means of evaluating how previous management activities have helped achieve restoration goals and direction for future work. When managing and assessing ecosystems, there are two components that must be considered: structure and function (Bradshaw 1997). The structure of a system is defined by the physical organization of the biotic and abiotic parts of the ecosystem, such as the diversity of organisms and their occurrence within an ecosystem. The function of an ecosystem is comprised of the various processes that occur within the system which include, but are not limited to, the cycling of nutrients, energy, and water. Some extend the definition of function to also include ecosystem services (Hooper *et al.* 2005). Preservation efforts should aim to maintain ecosystem structure and function in each conservation plan (Clark 1997, Camill *et al.* 2004, Martin *et al.* 2005).

Ecosystem assessments have been traditionally performed through fieldwork (i.e. visiting a site and acquiring direct measurements of the ecosystem). However, high costs in terms of time and financial resources associated with this method may be responsible for the relative lack of assessments conducted in natural systems. A nationwide database of stream restorations showed that only 10% of the projects were conducting assessment activities (Bernhardt *et al.* 2005). Additionally, a meta-analysis of restoration studies showed that even these assessments may not be satisfactory, revealing a tendency within restoration projects to conduct structural assessments, such as species surveys, rather than functional assessments (Ruiz-Jaen & Aide 2005). Remote sensing offers an alternative method for assessing ecosystem characteristics (Kerr & Ostrovsky 2003, Zhang *et al.* 2003, Malmstrom *et al.* 2008, Zheng & Moskal 2009) that

may reduce the direct cost of assessment for conservation agencies. The term 'remote sensing' can be applied to any technology that acquires environmental information from a distance, but typically refers to the acquisition of spectral reflectance data. Although the types of data that are acquired through remote sensing are usually coarser than field data, they can be collected over a much larger area, and more frequently, than may typically be achieved by fieldwork alone.

Several indicators are used for assessing ecosystem structure and function in prairies through fieldwork or by remote sensing. Some measures of ecosystem structure include vegetation height, vegetation cover, and species composition. Simple measurements in the field may be acquired to estimate ecosystem structure, but remote sensing methods can capture many of these same characteristics. For example, Light Detecting and Ranging (LIDAR) is a special type of airborne remote sensor that can measure the height of vegetation in grasslands by emitting laser pulses and timing their return (Bork & Su 2007). Additionally, special algorithms have been developed to analyze spectral reflectance data that can estimate leaf area (Alfieri *et al.* 2009). Remote sensing is also capable of identifying certain species (Martin *et al.* 1998). However, identification can only be done for larger species (Turner *et al.* 2003) with high spatial or spectral resolutions, and an assessment of species composition for an ecosystem cannot be accomplished using this method.

There are many techniques used to assess the function of ecosystems in the field. Some specific examples include examining soil samples to monitor nutrient sequestration (Christian & Wilson 1999), biomass harvesting to understand energy and nutrient cycling (Tilman & Downing 1994), and measurement of soil CO_2 flux (McCarron *et al.* 2003). In terms of remote sensing, an eddy flux system is a stationary unit that is also capable of conducting nutrient cycling measurements at fine scales by measuring the concentration and direction of movement

of molecules (such as CO_2) in the atmosphere (Goulden *et al.* 1996). Additionally, changes in canopy greenness have been monitored using spectral reflectance sensors (Sellers 1987, Reed *et al.* 1994, Yang *et al.* 1998, Xiao & Moody 2004, Pettorelli *et al.* 2005). Tracking changes in vegetation greenness can provide insight into other important ecosystem functions such as nutrient, energy, and water cycling. Energy efficiency can also be monitored using surface brightness temperature measurements; however, few ecologists have used this measurement (Kerr & Ostrovsky 2003).

Most previous assessments of ecological status of prairies have examined species richness and diversity

Species richness has been a common measure used to assess the ecological status of prairie restorations (Kindscher & Tieszen 1998, Allison 2002, Camill *et al.* 2004, Ruiz-Jaen & Aide 2005, Kucharik *et al.* 2006). Greater species richness or diversity is often assumed to enhance ecosystem function. For example, Tilman and Downing (1994) showed that species diversity influences the resilience of grassland systems in response to drought. In their experiment, they used random assemblages of species and evaluated the biomass differences before and after a drought and found that greater diversity leads to more resilience (Tilman & Downing 1994). Since then, other studies have revealed that ecosystem function may depend upon the specific makeup of species in the community (Symstad *et al.* 1998), likely resulting from the diversity of functional groups represented (Grime 1997, Symstad *et al.* 1998, Díaz & Cabido 2001, Hooper *et al.* 2005). However, the relationship between diversity and ecosystem function is complex and not well understood in many ecosystems (Mertz *et al.* 2007). Until this relationship is characterized, biodiversity assessments will continue to provide valuable

information on structural characteristics of ecosystems, but other measurements should be used for investigating function.

Assessment of ecosystem function is also important for management

Kerr and Ostrovsky (2003) argue that understanding ecosystem function should be one of the main focuses within ecological science. Ecosystem functions influence which species are able to persist in a given system as well as which ecological services are provided for humans including water filtration, carbon sequestration, flower pollination, soil augmentation, and many others (Christensen *et al.* 1996). The value of these ecosystem services have been estimated at \$16-54 trillion yr^{-1} (US) globally, which highlights the economic incentive for conserving ecosystem function (Costanza *et al.* 1998).

Multiple factors influence ecosystem function within prairies, including vegetative composition (Christian & Wilson 1999, Smith & Knapp 2003), weather patterns (Yang *et al.* 1998, Xiao & Moody 2004, Fay *et al.* 2008), management practices (Engle & Bidwell 2001, Fuhlendorf *et al.* 2008), and herbivory (Fuhlendorf *et al.* 2008, Derner *et al.* 2009). However, because of the complexity of these interacting factors, there is still much that is unknown about ecosystem function (Christensen *et al.* 1996) and how it varies geographically.

Understanding prairie function therefore has been an important objective within prairie restoration (Camill *et al.* 2004, Martin *et al.* 2005, Kucharik *et al.* 2006). Achieving sustainable restoration of an ecosystem requires consideration of the ecosystem's function. To this end, several studies have focused on analyzing the relationship between restoration and function. For example, Baer *et al*. (2002) examined several functional traits in a restored prairie chronosequence. Their study was conducted on restorations completed through the Conservation

Reserve Program (CRP), a U.S. government program that promotes conversion of agricultural land to more natural landscapes in order to promote ecosystem functions. They found that restored prairie sites were able to produce soil carbon (C) at rates similar to native prairies after 12 years. Soil nitrogen (N) also increased through time, but at a lesser rate (Baer *et al.* 2002). In Wisconsin, Kucharik *et al*. (2006) analyzed some of the functional differences between a native prairie and the Curtis prairie, the oldest recorded prairie restoration. They discovered that soil C and N were significantly higher at the remnant site at all soil layers (Kucharik *et al.* 2006). They also measured aboveground net primary productivity (NPP) and found that for two years the sites were similar despite different fire regimes (Kucharik *et al.* 2006). Studies such as these are good examples of functional assessments of restoration. Yet, the number of assessments is relatively low in comparison to the number of restorations that currently exist.

IV. Using MODIS time series to assess ecosystem function in prairies

Using phenology to assess changes in NPP and other ecosystem function

Phenology can be defined as 'the study [and description] of the timing of recurring biological events, the causes of their timing with regard to biotic and abiotic forces, and the interrelation among phases of the same or different species' (Leith 1974). In the past, phenology studies of vegetation were largely field-oriented and focused on flowering times (Gentry 1974, Rathcke & Lacey 1985), but introduction of the Advanced Very High Resolution Radiometer (AVHRR) on-board the NOAA polar-orbiting satellites in 1979 allowed frequent measurements of ecosystem vegetation on a global scale and generated interest in using remote sensing for phenology applications. The phenology techniques that developed from this remote sensing approach primarily related to the growth and senescence of green vegetation (Figure 1.4; Reed *et al.* 1994, Zhang *et al.* 2003, White *et al.* 2009). Under the assumptions that spectral reflectance

measures are corrected for atmospheric distortion and that it captures information from all canopy layers, these remote sensing methods can be used to estimate net primary productivity (NPP) (Paruelo *et al.* 1997) and photosynthetic activity (Sellers 1987, Myneni *et al.* 1995). Additionally, since vegetative growth is associated with the flux of nutrients and energy within an ecosystem (Baldocchi *et al.* 2001), phenology can be used as a general indicator for changes in ecosystem function. Following the introduction of AVHRR, technologically advanced sensors such as the Moderate Resolution Imaging Spectroradiometer (MODIS) on-board the polar-orbiting Terra and Aqua satellites (launched in December 1999 and May 2002, respectively) have enhanced the ability of

Figure 1.4. Phenology variables obtained using common remote sensing methods. The curves represent one year of NDVI data obtained for a single point. The black line is the raw data and the gray line is the smoothed data. MaxV = the maximum NDVI value; RateUP = the rate of greenup; RateDOWN = the rate of senescence; TINDVI = the time integrated NDVI for the growing season, which is represented by the shaded area; SOS = the start of the growing season; EOS = the end of the growing season, and MaxD = the date the maximum NDVI value occurs. Note that growing season can be determined by subtracting SOS from EOS.

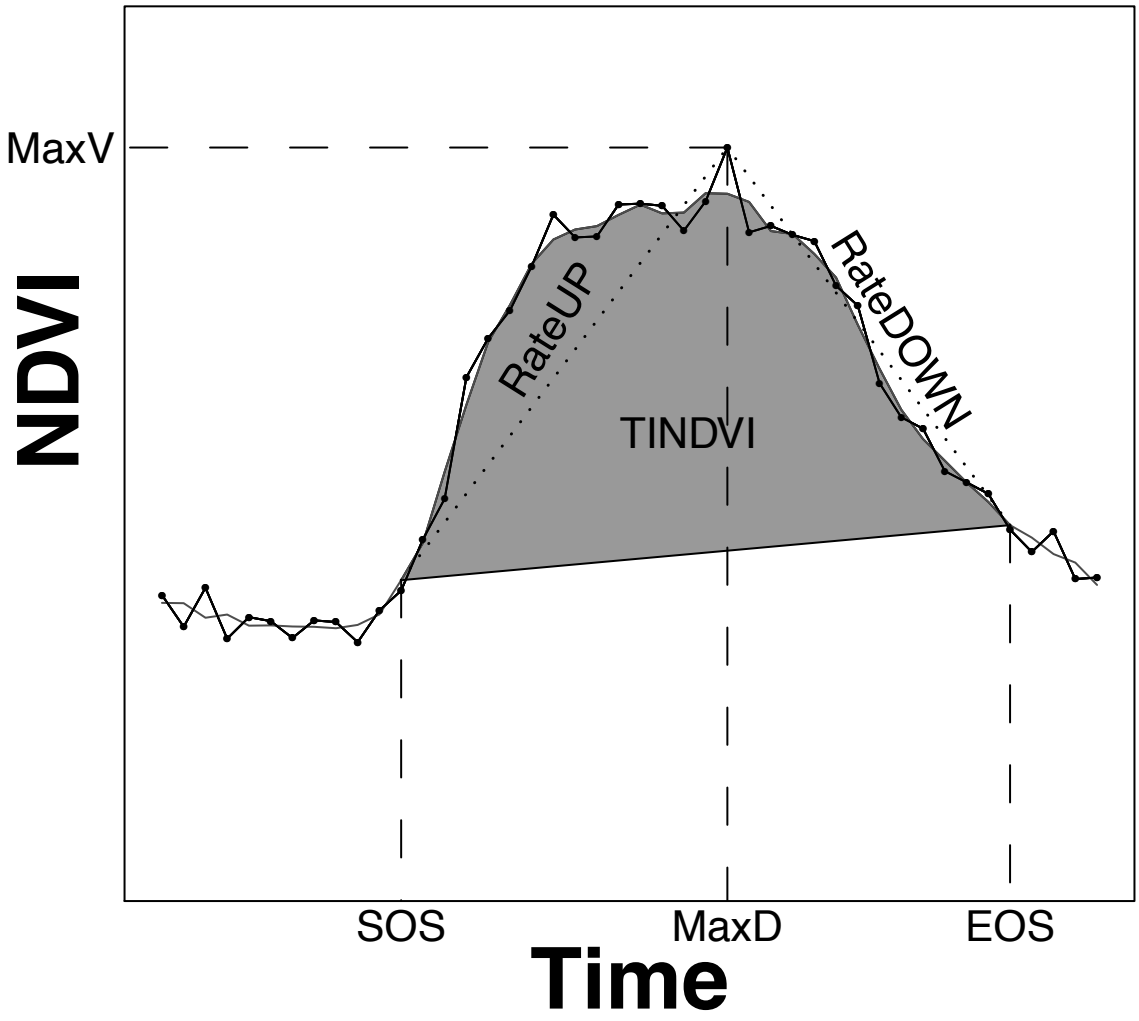

scientists to quantify phenological phenomenon at a landscape to global-scale (see Table 1.3 for comparison of satellite sensors).

MODIS imagery represents a significant improvement over that from AVHRR. MODIS is equipped with 36 spectral bands that range in spectral resolution from 0.62 – 14.385 μm. Its imagery for vegetation analyses can be acquired at a finer spatial scale than that of AVHRR (250m as opposed to 1.1 km) and is available at least twice as frequently (every 1-2 d as compared to every 4-5 d; Lillesand *et al.* 2004). MODIS is also better than Landsat imagery for phenological studies because of its finer temporal scale. Although Landsat TM and ETM+ have much finer *spatial* resolution (30 m), they acquire imagery on a more prolonged 15-d cycle (when comparing individual satellites). Moreover, current Landsat acquisitions are limited by technical problems: Landsat 7 (with ETM+ onboard) is no longer functioning properly (due to problems with its scan line corrector); Landsat 5 (with TM on-board) has substantially exceeded its duty-cycle; and replacement satellites will not be launched until 2013.

MODIS data processing and data types

MODIS data are split into five levels that represent different degrees of processing (Figure 1.5). Level 0 data are obtained directly from the sensor and contain the raw binary data collected from the sensor (Masuoka *et al.* 1998, Xiong *et al.* 2006). These data are then transformed into a hierarchical data file (HDF) format with data values in the form of digital numbers that make up the Level 1A data type (Xiong *et al.* 2006). Geolocation values and calibration tables are combined with Level 1A data to form Level 1B data (Xiong *et al.* 2006). Level 2 data are produced from the Level 1B

Table 1.3. This table describes technical aspects of three popularly used satellite remote sensors. Based on information from Lillesand, Kiefer *et al.* (2004) and Masuoka, Fleig *et al.* (1998). "---" represent data that is not applicable to that sensor.

	AVHRR	**TM/ETM+**	**MODIS**
Satellite(s)	NOAA-6 to NOAA-17	Landsat 4 to Landsat 7	Terra & Aqua
First Launch	6/27/79	7/16/82	12/18/99
Swath Width	2400 km	185 km	2330 km
IFOV at nadir	1.1 km	30 m	250 m[1]
Temporal Resolution	4-5 days[2]	16 days	1-2 days
Bands			
Blue	---	0.45-0.52 μm	0.46-0.48 μm
Red	0.58-0.68 μm	0.63-0.69 μm	0.62-0.67 μm
NIR	0.72-1.10 μm	0.76-0.90 μm	0.84-0.88 μm

[1] Only the red and NIR bands for MODIS have 250 m resolution.

[2] Applies to the daytime sensors equipped on NOAA-6, NOAA-8, NOAA-10, NOAA-12, NOAA-15, and NOAA-17 satellites.

data and maintain the same observation and location information. Three separate 'recipe' codes are used on the Level 2 data depending on the output: snow, ice, and fire products receive R1, surface reflectance data uses R3, and land surface temperatures receive R4. Level 2G and Level 3 data are the outputs of Level 2 data after they have been placed into an 'earth referenced grid' (Masuoka *et al.* 1998, Wolfe & Saleous 2006). Finally, Level 4 data are associated with products that use models for final production (Wolfe & Saleous 2006).

The Land Processes Distributed Active Archive Center (LPDAAC) houses the variety of MODIS Land images used for examining the terrestrial landscape (https://lpdaac.usgs.gov/). These data can be obtained on daily, eight-day, or monthly

Figure 1.5. Flowchart depicting the workflow of MODIS data products. Parallelograms represent input data and squares represent procedures performed upon the data (Masuoka et al. 1998, Xiong et al. 2006, Wolfe & Saleous 2006).

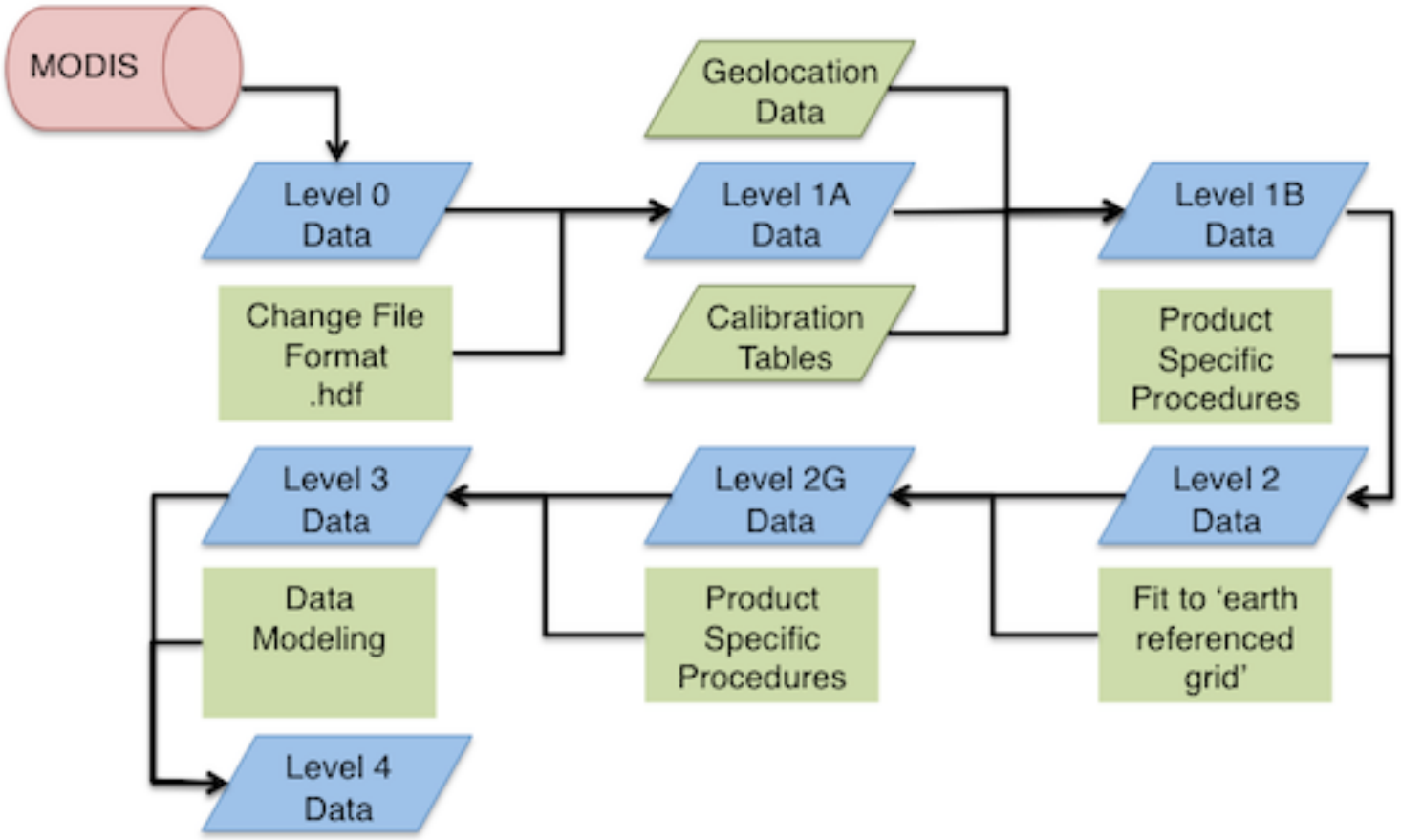

frequencies (Salomonson *et al.* 2006).

The MODIS team, creates eight-day and monthly composite images using maximum value compositing to reduce the influence of clouds and other spectral contaminants (Masuoka *et al.* 1998). Indices commonly employed for monitoring temporal changes in vegetation, the Normalized Difference Vegetation Index (NDVI) (Reed *et al.* 1994, Jönsson & Eklundh 2004, Beck *et al.* 2006, Hermance *et al.* 2007) and the Enhanced Vegetation Index (EVI) (Zhang *et al.* 2003, Zhang *et al.* 2009), are available from MODIS as standard products and can be used to evaluate vegetation dynamics in prairies. When greater temporal resolutions are desired these same indices can be generated directly by users from spectral reflectance data that have been corrected for Rayleigh scattering, aerosols, gaseous absorption, and adjacency effects (Vermote & Vermeulen 1999). For instance, the NDVI dataset available through LPDAAC is derived from 16 - day to monthly composites, but NDVI can be easily calculated directly by users from 8 - day composites of surface reflectance data.

NDVI vs. EVI for monitoring grassland phenology

Determining the most appropriate MODIS-based vegetation index to use (NDVI vs. EVI) for monitoring grassland phenology depends on several factors, which include spatial resolution and spectral sensitivity for prairie ecosystems. The fragmented nature of prairie ecosystems means that there will be smaller tracts of prairie within the landscape. To detect these sites, higher spatial resolutions will be required. Grassland canopy cover ranges from dry litter cover to high levels of green vegetation cover. The index must be sensitive within this range of vegetation cover, especially during the growing season.

The most commonly used vegetation index is NDVI (Tucker *et al.* 1985, Sellers *et al.* 1994, Goetz 1997, Huete *et al.* 2002, Wang *et al.* 2003, Xiao & Moody 2004, Beck *et al.* 2006). NDVI can be correlated with the fraction of photosynthetically active radiation (fPAR) absorbed by a canopy (Sellers 1987, Law & Waring 1994), as well as with related properties such as leaf area index (LAI) (Sellers 1987, Law & Waring 1994), and green biomass (Tucker *et al.* 1985, Butterfield & Malmstrom 2009).

NDVI is calculated as

$$NDVI = \frac{\rho_{NIR} - \rho_{red}}{\rho_{NIR} + \rho_{red}},$$

where ρ_{NIR} and ρ_{red} represent near-infrared and red reflectance (Rouse *et al.* 1973, Tucker 1979, Tucker *et al.* 1985). MODIS captures both ρ_{NIR} and ρ_{red} at a 250 m resolution, which allows NDVI to be calculated at this same resolution. NDVI ranges from -1 to 1 with higher values representing greater canopy greenness. Low NDVI values typically represent bare ground, snow, water, cloud cover, or senesced plants. Pettorelli *et al*. (2005) suggest that NDVI is most useful as a quantitative tool in areas where the leaf area index (LAI) ranges from 3 to 6. Below this range, too much noise may be generated from the soil background and above this range the red spectrum oversaturates and limits the capability of distinguishing various levels of vegetation (Huete *et al.* 2002).

In comparison to NDVI, EVI is a newer index developed for implementation with MODIS data. EVI was designed to give more precise measurements of vegetation than NDVI by accounting for aerosol scattering using the blue spectrum and adjusting for canopy background (Huete *et al.* 2002). EVI is calculated as

$$EVI = 2.5 \times \frac{(\rho_{NIR} - \rho_{red})}{(\rho_{NIR} + C_1 \times \rho_{red} - C_2 \times \ _{blue} + L},$$

where ρ_{NIR} is near infrared reflectance, ρ_{red} is the red reflectance, ρ_{blue} is the blue reflectance, C_1 and C_2 are correction coefficients for aerosols, and L is and adjustment accounting for canopy background (Huete *et al.* 1997, Huete *et al.* 1999). The coefficients C_1, C_2, and L vary depending on atmospheric corrections that the reflectance data have undergone (Huete *et al.* 1997), and on MODIS these coefficients were determined as 6.0, 7.5, and 1.0, respectively (Huete *et al.* 1999). EVI exhibits less sensitivity to changes in the red spectrum, which permits detection of differences in high biomass areas (Huete *et al.* 2002). Unfortunately, with MODIS, ρ_{blue} is captured with a 500 m resolution, which limits the spatial resolution of EVI.

Both EVI (Zhang *et al.* 2009) and NDVI (Reed *et al.* 1994, Yang *et al.* 1998, Xiao & Moody 2004) have been used to monitor grassland phenology. Grassland vegetation cover for the Great Plains region has generally been characterized as exhibiting an LAI ranging between two and six, which is well within the range of both vegetation indices (Shaw *et al.* 1997, Scurlock *et al.* 2001, Suyker & Verma 2001, Kucharik *et al.* 2006). Yet, NDVI does exhibit more sensitivity to vegetation within this range, making it the better index on MODIS for examining prairie phenology. Additionally, the finer spatial resolution of the MODIS NDVI product lends itself to detecting smaller areas of vegetation, which is necessary for fragmented prairies.

Methods for calculating phenology

From a time series of imagery, specific algorithms can be used to determine phenology by detecting the start and end of growing seasons. There are three broad types of models used: threshold, derivative, and moving average. Within these categories, different techniques can be employed to account for specific biases within the data.

Preprocessing of Satellite Data

Current phenological algorithms estimate phenological parameters based solely on a time series of remote sensing imagery, assuming it reflects vegetation growth on the ground. However, there are many factors that can influence the reflectance of a pixel that may force an algorithm to delineate the onset or end of the growing season prematurely. To prevent these occurrences, smoothing algorithms are typically employed to eliminate sudden changes in the vegetation index while maintaining short- and long-term trends in the data (Reed *et al.* 2003). Early phenology studies implemented simple smoothing algorithms such as running medians (Reed *et al.* 1994) or best index slope extraction (BISE) (Viovy *et al.* 1992) techniques. These techniques are advantageous in that they are simple to implement and preserve the original values of the NDVI time-series. Modern smoothing techniques such as piecewise logistic functions (Zhang *et al.* 2003), asymmetric gaussian (Jönsson & Eklundh 2004), double logistic functions (Beck *et al.* 2006), and high order splines (Hermance *et al.* 2007) are more complex and typically require site-specific coefficients for calculation. These complex techniques have also shown sensitivity to high noise levels in time-series data causing erroneous phenological predictions if the contaminated data points are not first removed (Jönsson & Eklundh 2004, Pettorelli *et al.* 2005). Special processing of data in areas where prolonged snow cover occurs is required and typically results in the replacement of snow cover data points with alternative values that represent previous vegetation conditions or soil reflectance (Zhang *et al.* 2003, Beck *et al.* 2006, Hird & McDermid 2009). Hird and McDermid (2009) conducted a comparison of select smoothing algorithms, which revealed that the double logistic and asymmetric Gaussian techniques gave superior results in terms of noise reduction.

Threshold method

The first phenological detection method to be used was the threshold method developed by Lloyd (1990). In this method, the user determines a particular NDVI or EVI value to represent baseline vegetation conditions (Figure 1.6 a). When the time-series data first exceeds the threshold value in a year, this point is declared to be the start of the growing season, and when values first fall below it, the end of the growing season is considered to have occurred. This method is easy to implement, but setting a biologically meaningful threshold is problematic. Growth dynamics can differ markedly among ecosystems or regions; therefore, the same threshold cannot be used across large regions. In response to this, White *et al*. (1997) modified the threshold method by defining the threshold as the average of the maximum and minimum NDVI points in the overall time series. In their study, they determined that the averaged NDVI value correlated with the date at which the fastest increase in greenness occurred. They argued that this rapid increase in NDVI has more biological relevance than declaring an arbitrarily set threshold (White *et al.* 1997). Other studies have created modified versions of this method. Instead of using the midpoint NDVI for the entire series, Jönsson and Eklundh (2004) developed a separate threshold for each growing season (Figure 1.6 b). They declared the start and end of the growing season to be the points when NDVI reached a determined percentage (typically 20%) of the difference between that growing season's maximum and minimum NDVI values (Jönsson & Eklundh 2004).

Derivative method

The derivative method for phenology detection is based on detecting the greatest rate of increase in vegetative growth (Studer *et al.* 2007). Sparse vegetative cover typically produces low NDVI values because of the strong soil contribution; therefore, increases in vegetation cover should produce notable increases in NDVI. In this method, the date of greatest NDVI increase is declared to be the growing season start, while the date with the greatest decrease in NDVI is declared to be the season's end (Figure 1.6 c). This method has been combined with a piecewise logistic smoothing algorithm to identify the date of vegetation maturity and start of senescence in addition to the start and end of the growing season (Zhang *et al.* 2003).

Moving average method

Developed by Reed *et al*. (1994), the moving average method detects points at which NDVI values deviate from a normal vegetation trend (Figure 1.6 d). In their study, Reed *et al.* created a moving average from an AVHRR time series, by averaging in a 9 image window to obtain the "normal trend" in the vegetation. Next, they produced a three point running median from the same raw data. The point at which the median becomes greater than the moving average marks the start of the growing season. The end of the growing season is determined by using the same technique on the reverse ordered data.

Figure 1.6. A comparison of four remote sensing phenology methods for determining the start and end of the growing season. (A) Threshold method declares a pre-defined value ("Thresh") set by the user to indicate SOS and EOS (Lloyd 1990). (B) TIMESAT method first detects the maximum NDVI point (MaxV). Then the minimum point on both sides of the curve is found (MinV1 and MinV2). The difference between the maximum value and minimum values are then multiplied by a user specified percentage to obtain the SOS and EOS. SOS was calculated for this example as: MinV1 + (MaxV – MinV1) * 0.2 (Jönsson and Eklundh 2004). (C) Derivative method is performed by calculating the slope between each set of points (graphed as dashed line). The maximum slope detects SOS while the minimum slope detects EOS (Studer *et al.* 2007). (D) Moving average method is obtained by creating a secondary curve that is formed by taking an *n*-size moving average (shown as dashed line). SOS is obtained when the moving average is calculated in the forward direction and EOS is obtained by reversing the direction of the moving average. When raw data exceeds the moving average is where SOS or EOS is detected. Two growing seasons are shown in this plot to demonstrate the time lapse between the moving average and the raw data (Reed *et al.* 1994).

Figure 1.6 (cont'd)

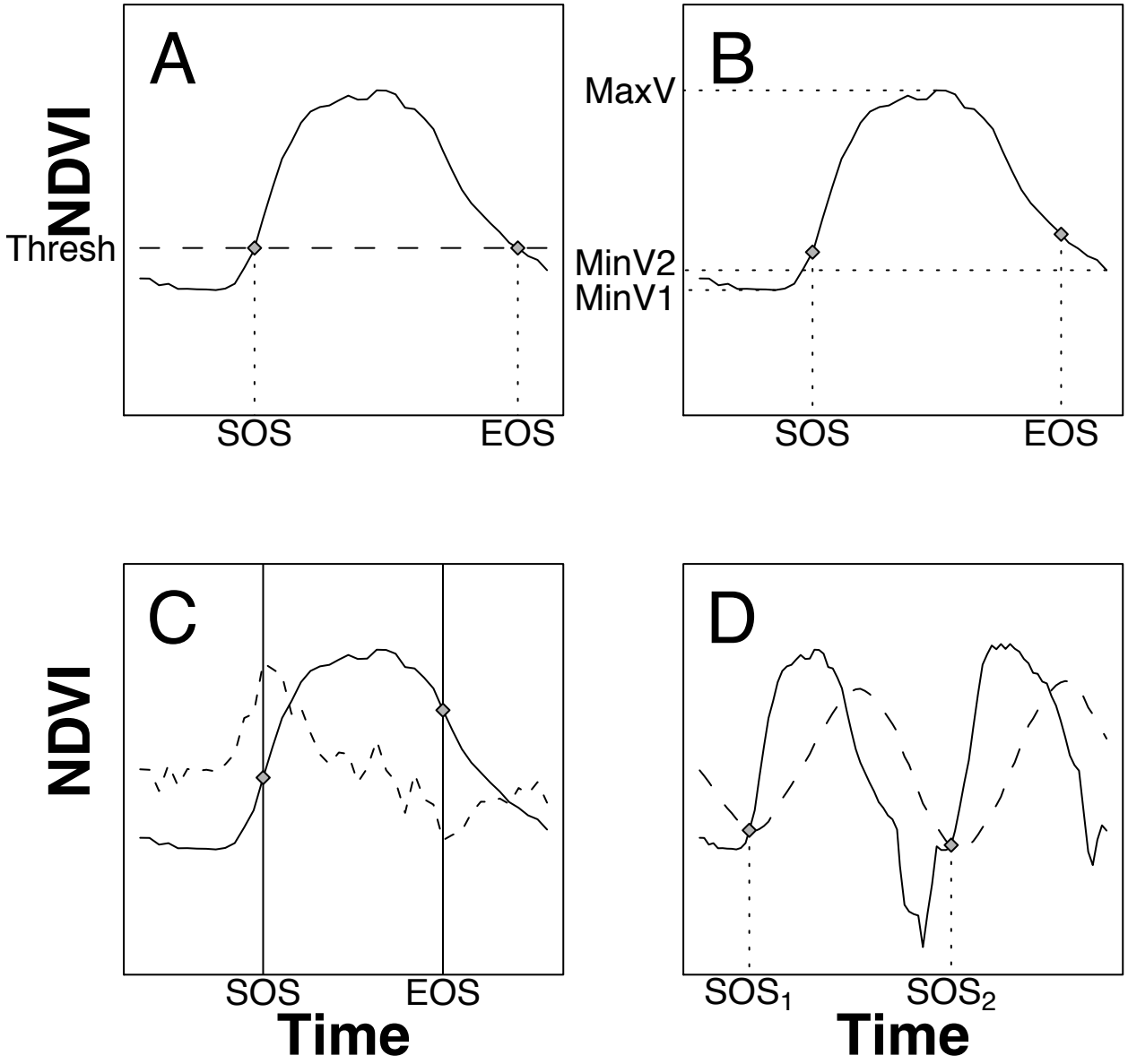

Algorithm Selection

Determining a universal detection method requires the adoption of a technique that compares well to field observations. However, few studies have been conducted to compare phenology detection techniques with simultaneous ground data. In such studies, it is clear that each detection method provides slightly different results while none has proven superior for all applications (Schwartz *et al.* 2002, Studer *et al.* 2007, White *et al.* 2009). Schwartz *et al.* (2002) compared the ability of the moving average method and the midpoint threshold method (White *et al.* 1997) to detect the onset of the growing season in deciduous forests by comparing them to a calculated spring index based from field observations. They concluded that both methods adequately detected the start of the growing season, but that the moving average technique was more accurate in southern latitudes (Schwartz *et al.* 2002). The results of the moving average method also depend strongly upon the length of the period for which moving average is calculated. The original moving average period length was set in a subjective manner that would be difficult to repeat for data from sensors other than AVHRR, for which the original method was developed. In a comparison between the midpoint threshold and derivative methods, Studer *et al*. (2007) found the midpoint threshold method to be less sensitive to snowmelt. This finding is further supported in a recent comparison of several detection and smoothing algorithms, where the midpoint threshold method was found to more closely resemble observational data and spring indicators (White *et al.* 2009). Given these results and the occurrence of snow within the northern Great Plains, it is most likely that the midpoint threshold method would most accurately detect significant changes in phenological dates in this region.

V. Weather perturbations in the central North-American prairie

Weather and climate of the Great Plains

Climate (the long-term trends in meteorological events) has been a point of interest in many recent ecological studies. Alterations in the phenology of birds, insects, and vegetation are predicted to result from increases in global mean temperatures, and some such changes have been already observed (Penuelas & Filella 2001). The current climate for the northern Great Plains is described by mean annual temperatures that range from 1°C to 15°C and mean annual precipitation that varies between 25 cm and 160 cm (Daly 2009), where snowfall typically accounts for 20% of the annual precipitation (Barker & Whitman 1988). The temperature and precipitation in this region are expected to increase by 2–3°C (Plummer *et al.* 2006) and 20–40% (Cook *et al.* 2008) within the next century, respectively. Although precipitation is expected to increase, precipitation events are predicted to become both more infrequent and more intense, which may lead to an increase in the frequency and intensity of droughts in this region (Christensen *et al.* 2007, Meehl *et al.* 2007).

Studying the response of vegetation to climate trends requires an extensive historical record for vegetation, a record that has not yet been attained by MODIS. However, weather patterns occur at timescales from days to months, which can be easily observed using MODIS. Additionally, observing the response of vegetation to short-term weather responses may provide an indicator of how vegetation may respond under alternate climatic regimes. In the following sections, I review several meteorological weather variables and the response that prairie vegetation exhibits to them.

Precipitation

Correlations between precipitation and vegetative growth in grassland systems have been well documented (Sims *et al.* 1978, Webb *et al.* 1978, Prins 1988, Sala *et al.* 1988, Lauenroth & Sala 1992, Briggs & Knapp 1995, Xiao & Moody 2004, Fay *et al.* 2008). For example, Xiao and Moody (2004) found that in more arid environments, such as prairies, growth depends more strongly on precipitation than on temperature values. Reed *et al*. (1994) characterized the vegetation dynamics of several biomes in the U.S. and found that arid grasslands tended to have more stochastic growth periods than other biomes, which they attributed to the timing of precipitation events. In a shortgrass prairie, precipitation explained 39–45% of the forage production variance (Lauenroth & Sala 1992). Additionally, Webb *et al*. (1978) found that shortgrass prairie production was correlated with the previous year's precipitation. They hypothesized that the precipitation helped to establish more seeds within the soil, as well as to increase carbohydrate reserves that may aid bud formation. Several other studies have indicated that spring precipitation is closely related to growing season primary production for the year (Rogler & Haas 1947, Smoliak 1956). Other responses to precipitation in grasslands include altering soil respiration (Fay *et al.* 2008) and flowering phenology (Cleland *et al.* 2006).

Snow

Only a few studies have examined the effects of snow on vegetative growth of prairies, particularly within the northern Great Plains, which may receive between 50 – 100 cm of snow each year (Barker & Whitman 1988). Blumenthal *et al*. (2008) found, for example, that increased spring snow cover can facilitate the establishment of invading species while having little impact on already-established vegetation. The authors attributed this relationship to the

increase in available soil moisture (Blumenthal *et al.* 2008). With snow cover, the repeated freezing and thawing of soil has been also shown to increase growing season production (Kreyling *et al.* 2007). Kreyling *et al.* hypothesize that the increase in production may be from the prevention of damage caused by deep soil freezing. Early spring thawing of soil followed by snow cover may insulate the soil and prevent further deep-freezing.

Temperature

Temperature has been shown to influence the growing dynamics of prairie vegetation, but to a lesser extent than precipitation in prairies. Sims *et al*. (1978) found that belowground biomass was best estimated using temperature related measures rather than precipitation. Regarding the aboveground biomass of grasslands, temperature has accounted for up to 40% of the variability in NPP for grasslands receiving less than 80 cm precipitation, but for only 7% of the NPP variability in grasslands receiving more (Epstein *et al.* 1997a). Several studies have also indicated that temperature may play a larger role in grassland growth dynamics during the beginning and end of the growing season (Wang *et al.* 2003, Jolly *et al.* 2005). Temperature may contribute to other ecosystem dynamics such as water use efficiency (Lemmens *et al.* 2006), photosynthetic rates (Lemmens *et al.* 2006), flowering phenology (Cleland *et al.* 2006), and carbon cycling (Davidson & Janssens 2006). However, the effects of temperature may depend upon the species being considered. A study conducted by Nippert *et al*. (2009) showed that *Andropogon gerardii* may be more influenced by temperature conditions, while *Sorghastrum nutans* is regulated primarily through precipitation.

Drought

The effects of drought on prairies can be seen in reductions in ecosystem primary production (Sala *et al.* 1982, Sala *et al.* 1988, Heitschmidt & Vermeire 2006). Such loss of productivity may be due to the ecophysiological effects that drought has on individual prairie species, such as decreases in osmotic potential (Knapp 1984), which lead to decreases in photosynthetic activity. A time lag may occur between the period when a drought occurs and when the effects are observed in the vegetation. Ji and Peters (2003) suggest that this time lag is a period of 3 months. However, loss of production in grasslands may also occur in the years following a drought (Oesterheld *et al.* 2001) and may influence long term vegetation dynamics (Haddad *et al.* 2002).

Drought can be defined in several ways, depending upon the environmental focus: meteorological drought focuses on the occurrence of abnormally low amounts of precipitation, hydrological drought uses stream flow as an indicator, and agricultural drought occurs when crop production is hindered (Dracup *et al.* 1980). Indices have been developed in order to facilitate comparisons of drought, when it occurs, and how long it lasts. The most frequently used indices include the Palmer's Drought Severity Index (PDSI; Palmer 1965) and the Standardized Precipitation Index (SPI; McKee *et al.* 1993).

PDSI uses a budgetary analysis of soil moisture on a monthly basis to determine when a drought or wet spell has occurred. This budget is developed through a series of equations that estimate the natural hydrology of the study area. A key element is the equation that describes the amount of precipitation ($P_{i,j}$) that is "climatically appropriate for existing conditions", or CAFEC precipitation:

$$P_{i,j} = \alpha_j PE_{i,j} + \beta_j PR_{i,j} + \gamma_j PRO_{i,j} - \delta_j PL_{i,j},$$

where α is the potential evapotranspiration coefficient, PE is the potential evapotranspiration, β is the potential soil moisture recharge coefficient, PR is the potential soil moisture recharge, γ is the potential run-off coefficient, PRO is the potential run-off, δ is the potential soil moisture loss coefficient, PL is the potential soil moisture loss for each year (*i*) and month (*j*). The coefficients for each hydrological variable are based upon the long-term averages of each hydrological variable. Within this equation, Palmer accounts for two major factors that influence soil moisture: temperature (through PE) and the soil's ability to hold water (PR). Once CAFEC precipitation for *i*, *j* is calculated, it is then subtracted from the actual precipitation to determine whether a deficit or surplus of water exists for month *j*. Next, Palmer normalized the differences in precipitation and placed them on a scale from -4 to 4 with negative values representing increasing severities of drought and positive values representing more extreme moisture conditions. When Palmer tested his original index, he noted differences in the drought extremes for different regions. To account for these differences Palmer geographically normalized PDSI using observed data that he gathered in the central U.S.

McKee *et al.* (1993) developed another index based on the idea that most definitions of drought relate to a deficiency in moisture or precipitation. The standardized precipitation index (SPI) is based solely on a time series of precipitation and does not account for other factors that may influence moisture availability (such as temperature and potential evapotranspiration). SPI requires at least 30 years of monthly precipitation values and is calculated based on the precipitation average for the previous set of months (2 – 48 months). A probability is then associated with each precipitation value and used with its normal inverse value to determine the difference in precipitation, which is then used as the SPI value. The SPI value ranges from -2 to 0 with lower values representing more severe drought.

Currently, there is no drought index that has proven superior to all other drought indices (Heim 2002). Carefully weighing the strengths and weaknesses of the index with the objectives of the study is the only way to select the most appropriate index. The advantage of PDSI is that it relies on estimating specific factors such as evapotranspiration and the soil's available water content (AWC), factors that are likely to influence the amount of moisture available to vegetation. However, the multiple factors used to calculate PDSI may not always be readily available or may be difficult to estimate. Alternatively, SPI is based on relative probability of precipitation, a relatively common dataset. Yet, the lack of factors within SPI may provide an overly simplistic model of drought and may fail to accurately portray drought patterns, particularly if temperatures change.

Weather Summary

Previous work indicates that precipitation seems to be an important factor controlling vegetation growth for many prairies. If the reason for this correlation is moisture in general, then it is reasonable to assume that snow and drought would also be important factors to consider. Studies that establish the effects of snow and drought on prairie vegetation growth are needed. Predictions from global climate models that indicate an increase in the frequency and severity of droughts for the Great Plains region highlight the importance of such studies.

VI. Conclusion

Conserving and restoring prairies during a period of climate change will require a thorough ecological understanding of prairies at a regional scale. Advances in spatial technology offer methods that may help characterize spatial patterns of ecosystem function across a terrestrial landscape. Remote sensing is a cost effective method for obtaining spectral information that can be correlated with vegetative characteristics. MODIS, in particular, is valuable for studying prairies because of its high temporal frequency, which permits detection of short-duration changes in vegetation growth, and its moderate pixel size, which permits analysis of fragmented land covers.

This thesis examines the regional responses of prairie vegetation to weather perturbations. Since conditions in the Great Plains are expected to become drier, I focus on responses to drought and moisture conditions. In Chapter 2, I describe the development of a spatial prairie database and existing associated resources that can be used with the database. In Chapter 3, I examine the response of different prairies types to drought (calculated as PDSI) over the period 2000–2008. For the analysis, prairies are grouped by community type, dominant photosynthetic pathway, and restoration history.

REFERENCES

VII. References

Alfieri JG, Xiao X, Nyhogi D, Sr. RAP, Chen F, LeMone M (2009) Satellite-based modeling of transpiration from the grasslands in the Southern Great Plains, USA. *Global and Planetary Change,* **67**, 78-86.

Allison SK (2002) When is a restoration successful? Results from a 45-year-old tallgrass prairie restoration. *Ecological Restoration,* **20**, 10-17.

Axelrod DI (1985) Rise of the grassland biome, central North America. *The Botanical Review,* **51**, 164-201.

Baer SG, Kitchen DJ, Blair JM, Rice CW (2002) Changes in ecosystem structure and function along a chronosequence of restored grasslands. *Ecological Applications,* **12**, 1688-1701.

Baldocchi D, Falge E, Gu L*, et al.* (2001) FLUXNET: A New Tool to Study the Temporal and Spatial Variability of Ecosystem-Scale Carbon Dioxide, Water Vapor, and Energy Flux Densities. *Bulletin of the American Meteorological Society,* **28**, 2415-2434.

Barker WT, Whitman WC (1988) Vegetation of the Northern Great Plains. *Rangelands,* **10**, 266-272.

Beard JS (1978) The Physiognomic Approach. In: *Classification of Plant Communities* Vol. 2 (ed Whittaker RH), pp. 408. Dr. W. Junk b.v. Publishers, Boston.

Beck PSA, Atzberger C, Høgda KA, Johansen B, Skidmore AK (2006) Improved monitoring of vegetation dynamics at very high latitudes: A new method using MODIS NDVI. *Remote Sensing of Environment,* **100**, 321-334.

Bernhardt ES, Palmer MA, Allan JD*, et al.* (2005) Synthesizing U.S. River Restoration Efforts. *Science,* **308**, 636-637.

Blumenthal D, Chimner RA, Welker JM, Morgan JA (2008) Increased snow facilitates plant invasion in mixedgrass prairie. *New Phytologist,* **179**, 440-448.

Bork EW, Su JG (2007) Integrating LIDAR data and multispectral imagery for enhanced classification of rangeland vegetation: A meta analysis. *Remote Sensing of Environment,* **111**, 11-24.

Bradshaw AD (1997) What do we mean by restoration? In: *Restoration Ecology and Sustainable Development* (eds Urbanska KM, Webb NR, Edwards PJ), pp. 4-14. Cambridge University Press, Cambridge.

Briggs JM, Knapp AK (1995) Interannual variability in primary production in tallgrass prairie: climate, soil moisture, topographic position, and fire as detminants of aboveground biomass. *American Journal of Botany,* **82**, 1024-1030.

Butterfield HS, Malmstrom CM (2009) The effects of phenology on indirect measures of aboveground biomass in annual grasses. *International Journal of Remote Sensing,* **30**, 3133-3146.

Camill P, McKone MJ, Sturges ST*, et al.* (2004) Community- and ecosystem-level changes in a species-rich tallgrass prairie restoration. *Ecological Applications,* **14**, 1680-1694.

Christensen JH, Hewitson B, Busuioc A*, et al.* (2007) Regional Climate Projections. In: *Climate Change 2007: The Physical Science Basis. Contribution of Working Group I to the Fourth Assessment Report of the Intergovernmental Panel on Climate Change* (eds Solomon S, Qin D, Manning M*, et al.*). Cambridge University Press, Cambridge, United Kingdom and New York, NY, USA.

Christensen NL, Bartuska AM, Brown JH*, et al.* (1996) The report of the Ecological Society of America Committee on the Scientific Basis for Ecosystem Management. *Ecological Applications,* **6**, 665-691.

Christian JM, Wilson SD (1999) Long-term ecosystem impacts of an introduced grass in the northern great plains. *Ecology,* **80**, 2397-2407.

Clark MJ (1997) Ecological restoration - the magnitude of the challenge: an outsider's view. In: *Restoration Ecology and Sustainable Development* (eds Urbanska KM, Webb NR, Edwards PJ), pp. 353-377. The Syndicate Press of the University of Cambridge, Cambridge.

Cleland EE, Chiariello NR, Loarie SR, Mooney HA, Field CB (2006) Diverse responses of phenology to global changes in a grassland ecosystem. *Proceedings of the National Academy of Sciences,* **103**, 13740-11374.

Cook KH, Vizy EK, Launer ZS, Patricola CM (2008) Springtime intensification of the Great Plains low-level jet and midwest precipitation in GCM simulations of the twenty-first century. *Journal of Climate,* **21**, 6321-6340.

Costanza R, d'Arge R, Groot Rd*, et al.* (1998) The value of the world's ecosystem services and natural capital. *Ecological Economics,* **25**, 3-15.

Daly C (2009) *PRISM Climate Group,* Oregon State University, Accessed on May, 2009 at www.prism.oregonstate.edu.

Davidson EA, Janssens IA (2006) Temperature sensitivity of soil carbon decomposition and feedbacks to climate change. *Nature,* **440**, 165-173.

Derner JD, Lauenroth WK, Stapp P, Augustine DJ (2009) Livestock as ecosystem engineers for grassland bird habitat in the Western Great Plains of North America. *Rangeland Ecology and Management,* **62**, 111-118.

Díaz S, Cabido M (2001) Vive la différence: plant functional diversity matters to ecosystem processes. *Trends in Ecology & Evolution,* **16**, 646-655.

Dracup JA, Lee KS, Jr. EGP (1980) On the definition of droughts. *Water Resources Research,* **16**, 297-302.

Ehleringer JR (1978) Implications of quantum yield differences on the distributions of C_3 and C_4 grasses. *Oecologia,* **31**, 255-267.

Engle DM, Bidwell TG (2001) Viewpoint: The response of central North American prairies to seasonal fire. *Journal of Range Management,* **54**, 2-10.

Epstein HE, Lauenroth WK, Burke IC (1997a) Effects of temperature and soil texture on ANPP in the U.S. Great Plains. *Ecology,* **78**, 2628-2631.

Epstein HE, Lauenroth WK, Burke IC, Coffin DP (1997b) Productivity patterns of C_3 and C_4 functional types in the U.S. Great Plains. *Ecology,* **78**, 722-731.

Fay PA, Kaufman DM, Nippert JB, Carlisle JD, Harper CW (2008) Changes in grassland ecosystem function due to extreme rainfall events: implications for responses to climate change. *Global Change Biology,* **14**, 1600-1608.

Fuhlendorf SD, Engle DM, Kerby J, Hamilton R (2008) Pyric herbivory: Rewilding landscapes through the recoupling of fire and grazing. *Conservation Biology,* **23**, 588-598.

Gentry AH (1974) Phenology and diversity in tropical Bignoniaceae. *Biotropica,* **6**, 64-68.

Goetz SJ (1997) Multi-sensor analysis of NDVI, surface temperature and biophysical variables at a mixed grassland site. *International Journal of Remote Sensing,* **18**, 71-94.

Goulden ML, Munger JW, Fan S-M, Daube BC, Wofsy SC (1996) Measurements of carbon sequestration by long-term eddy covariance: methods and a critical evaluation of accuracy. *Global Change Biology,* **2**, 169-182.

Grenier MB, Buskirk SW, Anderson-Sprecher R (2009) Population indices versus correlated density estimates of black-footed ferret abundance. *Journal of Wildlife Management,* **73**, 669-676.

Grime JP (1997) Biodiversity and Ecosystem Function: The Debate Deepens. *Science,* **277**, 1260-1261.

Haddad NM, Tilman D, Knops JMH (2002) Long-term oscillations in grassland productivity induced by drought. *Ecology Letters,* **5**, 110-120.

Heim RR (2002) A review of twentieth-century drought indices used in the United States. *Bulletin of the American Meteorological Society,* **83**, 1149-1165.

Heitschmidt RK, Vermeire LT (2006) Can abundant summer precipitation counter losses in herbage production caused by spring drought? *Rangeland Ecology and Management,* **59**, 392-399.

Hermance JF, Jacob RW, Bradley BA, Mustard JF (2007) Extracting phenological signals from multiyear AVHRR NDVI time series: framework for applying high-order annual splines with roughness damping. *IEEE Transactions on Geoscience and Remote Sensing,* **45**, 3264-3276.

Hird JN, McDermid GJ (2009) Noise reduction of NDVI time series: An empirical comparison of selected techniques. *Remote Sensing of Environment,* **113**, 248-258.

Hooper DU, Chapin FS, III, Ewel JJ*, et al.* (2005) Effects of Biodiversity on ecosystem functioning: A consensus of current knowledge. *Ecological Monographs,* **75**, 3-35.

Huete A, Didan K, Miura T, Rodriguez EP, Gao X, Fereira LG (2002) Overview of the radiometric and biophysical performance of the MODIS vegetation indices. *Remote Sensing of Environment,* **83**, 195-213.

Huete A, Justice C, Leeuwen Wv (1999) *MODIS Vegetation Index (MOD13), EOS MODIS Algorithm-Theoretical Basis Document.* National Aeronautics and Space Administration, Greenbelt, Maryland

Huete AR, Liu HQ, Batchily K, Leeuwen Wv (1997) A comparison of vegetation indices over a global set of TM images for EOS-MODIS. *Remote Sensing of Environment,* **59**, 440-451.

Ji L, Peters AJ (2003) Assessing vegetation response to drought in the northern Great Plains using vegetation and drought indices. *Remote Sensing of Environment,* **87**, 85-98.

Jolly WM, Nemani R, Running SW (2005) A generalized, bioclimatic index to predict foliar phenology in response to climate. *Global Change Biology,* **11**, 619-632.

Jönsson P, Eklundh L (2004) TIMESAT - a program for analyzing time-series of satellite sensor data. *Computers & Geosciences,* **30**, 833-845.

Kerr JT, Ostrovsky M (2003) From space to species: ecological applications for remote sensing. *Trends in Ecology & Evolution,* **18**, 299-305.

Kindscher K, Tieszen LL (1998) Floristic and soil organic matter changes after five and thirty-five years of native tallgrass prairie restoration. *Restoration Ecology,* **6**, 181-196.

Knapp AK (1984) Water relations and growth of three grasses during wet and drought years in a tallgrass prairie. *Oecologia,* **65**, 35-43.

Kotliar NB (2000) Application of the New Keystone-Species Concept to Prairie Dogs: How Well Does It Work? *Conservation Biology,* **14**, 1715-1721.

Kotliar NB, Baker BD, Whicker AD (1999) A Critical Review of Assumptions About the Prairie Dog as a Keyston Species. *Environmental Management,* **24**, 177-192.

Kreyling J, Beierkuhnlein C, Pritsch K, Schloter M, Jentsch A (2007) Recurrent soil freeze-thaw cycles enhance grassland productivity. *New Phytologist,* **177**, 938-945.

Kucharik CJ, Fayram NJ, Cahill KN (2006) A paired study of prairie carbon stocks, fluxes, and phenology: comparing the world's oldest prairie restoration with an adjacent remnant. *Global Change Biology,* **12**, 122-139.

Lauenroth WK, Sala OE (1992) Long-term forage production of North American short-grass steppe. *Ecological Applications,* **2**, 397-403.

Law BE, Waring RH (1994) Remote sensing of leaf area index and radiation intercepted by understory vegetation. *Ecological Applications,* **4**, 272-279.

Lemmens CMHM, DeBoeck HJ, Gielen B*, et al.* (2006) End-of-season effects of elevated temperature on ecophysiological processes in grassland species at different species richness levels. *Environmental and Experimental Botany,* **56**, 245-254.

Lillesand TM, Kiefer RW, Chipman JW (2004) *Remote Sensing and Image Interpretation.* John Wiley & Sons, New Aster.

Lloyd D (1990) A phenological classification of terrestrial vegetation cover using shortwave vegetation index imagery. *International Journal of Remote Sensing,* **11**, 2269-2279.

Magle SB, Crooks KR (2009) Investigating the distribution of prairie dogs in an urban landscape. *Animal Conservation,* **12**, 192-203.

Malmstrom CM, Butterfield HS, Barber C*, et al.* (2008) Using remote sensing to evaluate the influence of grassland restoration activities on ecosystem forage provisioning services. *Restoration Ecology,* **16**, 1-13.

Martin LM, Moloney KA, Wilsey BJ (2005) An assessment of grassland restoration success using species diversity components. *Journal of Applied Ecology,* **42**, 327-336.

Martin ME, Newman SD, Aber JD, Congalton RG (1998) Determining Forest Species Composition Using High Spectral Resolution Remote Sensing Data. *Remote Sensing of Environment,* **65**, 249-254.

Masuoka E, Fleig A, Wolfe RE, Patt F (1998) Key characteristics of MODIS data products. *IEEE Transactions on Geoscience and Remote Sensing,* **36**, 1313-1323.

McCarron JK, Knapp AK, Blair JM (2003) Soil C and N responses to woody plant expansion in a mesic grassland. *Plant and Soil,* **257**, 183-192.

McKee TB, Doesken NJ, Kleist J (1993) The relationship of drought frequency and duration to time scales. In: *Eighth Conference on Applied Climatology*. American Meteorological Society, Anaheim, California.

Meehl GA, Stocker TF, Collins WD*, et al.* (2007) Global Climate Projections. In: *Climate Change 2007: The Physical Science Basis. Contribution of Working Group I to the Fourth Assessment Report of the Intergovernmental Panel on Climate Change* (eds Solomon S, Qin D, Manning M*, et al.*). Cambridge University Press, Cambridge, United Kingdom and New York, NY, USA.

Mertz O, Ravnborg HM, Lovei GL, Nielsen I, Konijnendijk CC (2007) Ecosystem services and biodiversity in developing countries. *Biodiversity and Conservation,* **16**, 2729-2737.

Myneni RB, Hall FG, Sellers PJ, Marshak AL (1995) The Interpretation of Spectral Vegetation Indexes. *IEEE Transactions on Geoscience and Remote Sensing,* **33**, 481-486.

Nippert JB, Fay PA, Carlisle JD, Knapp AK, Smith MD (2009) Ecophysiological responses of two dominant grasses to altered temperature and precipitation regimes. *Acta Oecologica,* **35**, 400-408.

Noss RF, III ETL, Scott JM (1995) *Endangered Ecosystems of the United States: A preliminary assessment of loss and degredation.* United States Geological Survey, Washington D.C.

Noss RF, Peters RL (1995) *Endangered Ecosystems: A Status Report on America's Vanishing Habitat and Wildlife.* Defenders of Wildlife, Washington, DC.

Oesterheld M, Loreti J, Semmartin M, Sala OE (2001) Inter-annual variation in primary-production of semi-arid grassland related to previous year production *Journal of Vegetation Science,* **12**, 137-142.

Olson DM, Dinerstein E, Wikramanayake ED*, et al.* (2001) Terrestrial ecoregions of the world: A new map of life on Earth. *BioScience,* **51**, 933-938.

Palmer WC (1965) *Meteorological Drought. Research Paper No. 45.* United States Department of Commerce, Washington D. C. .

Paruelo JM, Epstein HE, Lauenroth WK, Burke IC (1997) ANPP estimates from NDVI for the central grassland region of the United States. *Ecology,* **78**, 953-958.

Penuelas J, Filella I (2001) Responses to a Warming World. *Science,* **294**, 793-795.

Pettorelli N, Vik JO, Mysterud A, Gaillard J-M, Tucker CJ, Stenseth NC (2005) Using the satellite-derived NDVI to assess ecological responses to environmental change. *Trends in Ecology & Evolution,* **20**, 503-510.

Plummer DA, Caya D, Frigon A*, et al.* (2006) Climate and climate change over North America as simulated by the Canadian RCM. *Journal of Climate,* **19**, 3112-3132.

Prins HHT (1988) Plant phenology patterns in Lake Manyara National Park, Tanzania. *Journal of Biogeography,* **15**, 465-480.

Rathcke B, Lacey EP (1985) Phenological patterns of terrestrial plants. *Annual Review of Ecological Systems,* **16**, 179-214.

Reed BC, Brown JF, VanderZee D, Loveland TR, Merchant JW, Ohlen DO (1994) Measuring phenological variability from satellite imagery *Journal of Vegetation Science,* **5**, 703-714.

Reed BC, White M, Brown JF (2003) Remote Sensing Phenology. In: *Phenology: an integrative environmental science* (ed Schwartz MD), pp. 365-382. Kluwer Academic Publishers, Dordrecht.

Rogler GA, Haas HJ (1947) Range production as related to soil moisture and precipitation on the northern great plains. *Journal of Agronomy,* **39**, 378-389.

Rouse JW, Haas RH, Deering DW, Schell JA (1973) *Monitoring the vernal advancement and retrogradation (green wave effect) of natural vegetation.* National Aeronautics and Space Administration, Greenbelt, Maryland.

Ruiz-Jaen MC, Aide TM (2005) Restoration Success: How Is It Being Measured? *Restoration Ecology,* **13**, 569-577.

Sala OE, Lauenroth WK, Parton WJ (1982) Plant recovery following prolonged drought in a shortgrass steppe. *Agricultural Meteorology,* **27**, 49-58.

Sala OE, Parton WJ, Joyce LA, Lauenroth WK (1988) Primary production of the central grassland region of the United States. *Ecology,* **69**, 40-45.

Salomonson VV, Barnes W, Masuoka EJ (2006) Introduction to MODIS and an Overview of Associated Activities. In: *Earth Science Satellite Remote Sensing* Vol. Vol 1: Science and Instruments (eds Qu JJ, Gao W, Kafatos M, Murphy RE, Salomonson VV). Tsinghua University Press & Springer-Verlag GmbH, Beijing & Berlin Heidelberg.

Samson F, Knopf F (1994) Prairie Conservation in North America. *BioScience,* **44**, 418-421.

Schwartz MD, Reed BC, White MA (2002) Assessing satellite-derived start-of-season measures in the conterminous USA. *International Journal of Climatology,* **22**, 1793-1805.

Scurlock JMO, Asner GP, Gower ST (2001) *Worldwide Historical Estimates of Leaf Area Index, 1932-2000*. Oak Ridge National Laboratory, Oak Ridge.

Scurlock JMO, Hall DO (1998) The global carbon sink: a grassland perspective. *Global Change Biology,* **4**, 229-233.

Sellers PJ (1987) Canopy reflectance, photosynthesis, and transpiration. II. The role of biophysics in the linearity of their interdependence. *Remote Sensing of Environment,* **21**, 143-183.

Sellers PJ, Tucker CJ, Collatz GJ, Los SO, Justice CO, Dazlich DA, Randall DA (1994) A global 1° by 1° NDVI data set for climate studies. Part 2: The generation of global fields of terrestrial biophysical parameters from the NDVI. *International Journal of Remote Sensing,* **15**, 3519-3545.

Shaw BL, Pielke RA, Ziegler CL (1997) A three-dimensional numerical simulation of a Great Plains Dryline. *Monthly Weather Review,* **125**, 1489-1506.

Sims PL, Risser PG (2000) Grasslands. In: *North American Terrestrial Vegetation* (eds Barbour MG, Billings WD), pp. 323-356. Cambridge University Press, Cambridge.

Sims PL, Singh JS, Lauenroth WK (1978) The structure and function of ten western North American grasslands: I. Abiotic and vegetational characteristics. *Journal of Ecology,* **66**, 251-285.

Smith MD, Knapp AK (2003) Dominant species maintain ecosystem function with non-random species loss. *Ecology Letters,* **6**, 509-517.

Smoliak S (1956) Influence of climatic conditions on forage production of shortgrass rangeland. *Journal of Range Management,* **9**, 89-91.

Smoliak S (1986) Influence of Climatic Conditions on Production of *Stipa-Bouteloua* Prairie over a 50-Year Period. *Journal of Range Management,* **39**, 100-103.

Studer S, Stöckli R, Appenzeller C, Vidale PL (2007) A comparitive study of satellite and ground-based phenology. *International Journal of Biometeorology,* **51**, 405-414.

Suyker AE, Verma SB (2001) Year-round observations of the net ecosystem exchange of carbon dioxide in a native tallgrass prairie. *Global Change Biology,* **7**, 279-289.

Symstad AJ, Tilman D, Willson J, Knops JMH (1998) Species loss and ecosystem functioning: effects of species identity and community composition. *Oikos,* **81**, 389-397.

Tebaldi C, Hayhoe K, Arblaster JM, Meehl GA (2006) Going to the extremes: An intercomparison of model-simulated historical and future changes in extreme events. *Climatic Change,* **79**, 185-211.

Teeri JA, Stowe LG (1976) Climatic Patterns and the Distribution of C_4 Grasses in North America. *Oecologia,* **23**, 1-12.

Tilman D, Downing JA (1994) Biodiversity and stability in grasslands. *Nature,* **367**, 363-365.

Transeau EN (1935) The Prairie Peninsula. *Ecology,* **16**, 423-437.

Tucker CJ (1979) Red and photographic infrared linear combinations for monitoring vegetation. *Remote Sensing of Environment,* **8**, 127-150.

Tucker CJ, Townshend JRG, Goff TE (1985) African land-cover classification using satellite data. *Science,* **227**, 369-375.

Turner W, Spector S, Gardiner N, Fladeland M, Sterling E, Steininger M (2003) Remote sensing for biodiversity science and conservation. *Trends in Ecology & Evolution,* **18**, 306-314.

USFWS (2009) *Endangered Species Program,* United States Fisheries and Wildlife, Accessed on June, 2009 at www.fws.gov/endangered/.

Vermote EF, Vermeulen A (1999) *Atmospheric Correction Algorithm: Spectral Reflectances (MOD09).* National Aeronautics and Space Administration, Greenbelt, Maryland

Viovy N, Arino O, Belward AS (1992) The best index slop extraction: A method for reducing noise in NDVI time series. *International Journal of Remote Sensing,* **13**, 1585-1590.

vonFischer JC, Tieszen LL, Schimel DS (2008) Climate controls on C_3 vs. C_4 productivity in North American grasslands from carbon isotope composition of soil organic matter. *Global Change Biology,* **14**, 1141-1155.

Wang J, Rich PM, Price KP (2003) Temporal responses of NDVI to precipitation and temperature in the central Great Plains, USA *International Journal of Remote Sensing,* **24**, 2345-2364.

Weaver JE, Albertson FW (1956) *Grasslands of the Great Plains: their nature and use.* Johnsen Publishing, Lincoln.

Webb W, Szarek S, Lauenroth W, Kinerson R, Smith M (1978) Primary productivity and water use in native forest, grassland, and desert ecosystems. *Ecology,* **59**, 1239-1247.

Whisenant SG (1999) *Repairing Damaged Wildlands.* Press Syndicate of the University of Cambridge, Cambridge.

White MA, Beurs KMd, Didan K*, et al.* (2009) Intercomparison, interpretation, and assessment of spring phenology in North America estimated from remote sensing for 1982-2006. *Global Change Biology,* **15**, 2335-2359.

White MA, Thrornton PE, Running SW (1997) A continental phenology model for monitoring vegetation responses to interannual climatic variability. *Globel Biogeochemical Cycles,* **11**, 217-234.

Wolfe RE, Saleous N (2006) MODIS Land Products and Data Processing. In: *Earth Science Satellite Remote Sensing* Vol. Volume 1: Science and Instruments (eds Qu JJ, Gao W, Kafatos M, Murphy RE, Salomonson VV), pp. 111-122. Tsinghua University Press & Springer-Verlag GmbH, Beijing & Berlin Heidelberg

Woodward FI, Lomas MR (2004) Vegetation dynamics - simulating responses to climatic change. *Biological Reviews,* **79**, 643-670.

Woodward FI, Lomas MR, Kelly CK (2004) Global climate and the distribution of plant biomes. *Philosophical Transactions of the Royal Society of London,* **239**, 1465-1476.

Xiao J, Moody A (2004) Photosynthetic activity of US biomes: responses to the spatial variability of seasonality of precipitation and temperature. *Global Change Biology,* **10**, 437-451.

Xiong X, Isaacman A, Barnes W (2006) MODIS Level-1B Products. In: *Earth Science Satellite Remote Sensing* Vol. 1 (eds Qu JJ, Gao W, Kafatos M, Murphy RE, Salomonson VV), pp. 33-49. Tsinghua University Press & Springer-Verlag GmbH, Beijing & Berlin Heidelberg

Yang L, Wylie BK, Tieszen LL, Reed BC (1998) An analysis of relationships among climate forcing and time-integrated NDVI of grasslands over the U.S. northern and central Great Plains. *Remote Sensing of Environment,* **65**, 25-37.

Zhang X, Friedl MA, Schaa CB*, et al.* (2003) Monitoring vegetation phenology using MODIS. *Remote Sensing of Environment,* **84**, 471-475.

Zhang X, Friedl MA, Schaaf CB (2009) Sensitivity of vegetation phenology detection to the temporal resolution of satellite data. *International Journal of Remote Sensing,* **30**, 2061-2074.

Zheng G, Moskal LM (2009) Retrieving Leaf Area Index (LAI) using remote sensing: theories, methods, and sensors. *Sensors,* **9**, 2719-2745.

Chapter 2: Development of a Spatially Explicit Prairie Database for Regional Studies

I. Introduction

Concerns about projected climate changes (Plummer *et al.* 2006, Christensen *et al.* 2007, Meehl *et al.* 2007) have highlighted the need for understanding fundamental ecological processes at regional and global scales. In conservation biology, the response of species to climate change is particularly important because species may need to adapt or migrate within fragmented landscapes. Endangered ecosystems (Noss *et al.* 1995, Noss & Peters 1995) are of further conservation concern because they support species that are likely to also be endangered. Additionally, ecosystem services from these endangered sites may be particularly vulnerable to climate change due to the lower frequency of these systems in the landscape. Development of more comprehensive data resources to enhance our understanding of regional biotic and abiotic interactions is critical in conservation planning for mitigation of predicted global changes.

Field studies of regional processes have typically been difficult to conduct due to the large number of resources required to sample a region. This limitation of field studies has led to alternative approaches, including spectral remote sensing, which has become a reliable method for evaluating regional biotic environments (Yang *et al.* 1998, Ricotta & Avena 2000, Pettorelli *et al.* 2005). Indices used in remote sensing, such as the Normalized Difference Vegetation Index (NDVI; Tucker 1979), have been correlated with vegetative properties including the fraction of photosynthetically active radiation absorbed by canopies (fPAR; Sellers 1987), leaf area (Sellers 1987, Law & Waring 1994), and green biomass (Sellers 1987, Butterfield & Malmstrom 2009), which has helped promote the use of remote sensing in many biological studies (Reed *et al.* 1994, Ji & Peters 2003, Xiao & Moody 2004). Landscape attributes, including geo-location of specific ecosystems, can be combined with remote sensing data within

Geographic Information Systems (GIS) to evaluate the functional dynamics of specific ecosystems over time (Reed *et al.* 1994, Ji & Peters 2003, Xiao & Moody 2004).

One common method for defining ecosystem boundaries for remote sensing analyses has been to develop land cover maps (Reed *et al.* 1994, Ji & Peters 2003, Xiao & Moody 2004). Land cover maps are synthesized by integrating multiple forms of digitized spatial data (such as remote sensing imagery) to predict or describe the location of ecosystems or land types within a region (Loveland *et al.* 1991). Though land cover maps are useful for providing initial assessments of ecosystem boundaries, they typically have low spatial accuracies. Assessments of land cover maps have revealed that typical spatial accuracies do not exceed 80% (Xian *et al.* 2009, Ran *et al.* 2010). Therefore, studies that rely on land cover maps to delineate ecosystem boundaries inherit a substantial amount of error that may potentially alter the outcome of statistical analyses. A better system for determining ecosystem boundaries is needed for remote sensing applications.

The Global Positioning System (GPS) allows users to accurately trilaterate their position on the Earth's surface using a network of satellites (Getting 1993). Obtaining locations of natural systems using GPS often requires extensive fieldwork to delineate even small land areas. However, since the initial implementation of GPS into non-military applications in the mid-1980s, GPS has been harnessed by conservation agencies for monitoring and managing ecosystems at local scales (Getting 1993). The composite of these local scale efforts presents an alternative method for producing regional scale maps of ecosystems, which could be used for analyzing regional ecosystem processes.

To provide a more accurate regional perspective of prairie locations in the northern Great Plains, we have created a new prairie geodatabase, called the Prairie Spatial Database (PSD).

The database focuses on prairie ecosystems because of their conservation status (Samson & Knopf 1994, Noss *et al.* 1995, Noss & Peters 1995). This database was created by synthesizing geospatial vector files and management information from land managers in 43 organizations that manage natural areas in the northern Great Plains. To prepare the database for use with remote sensing applications, we also determined which prairies were suitable for analysis with imaging from the Moderate Resolution Imaging Spectroradiometer (MODIS). The objectives of this chapter are to document the development of the PSD and to introduce existing spatial datasets that complement the PSD. With the development of a prairie geodatabase, we hope to increase understanding of regional processes and spatial differences among prairies to promote their conservation.

II. Prairie Database Development

Locating Northern Great Plains Prairies

The historical extent of prairie ecosystems in the North American Great Plains (Figure 2.1) has been documented from south-central Canada to south-central United States (U.S.) and ranges longitudinally from Colorado to Illinois with pockets occurring as far east as Michigan and Ohio (Transeau 1935, Weaver & Albertson 1956, Olson *et al.* 2001). In creating a prairie database, we aimed to include a large amount of the inherent diversity within the historical prairie extent. The northern Great Plains encompasses several vegetation communities including shortgrass, mixedgrass, and tallgrass prairies as well as the transition between C_3 and C_4 dominant prairie communities (Ehleringer 1978, Epstein *et al.* 1997, Tieszen *et al.* 1997). A large range of climatic variability is also included in this region, providing a suitable area of focus for the development of an initial prairie database.

Geospatial information about prairie locations within the northern Great Plains was obtained through collaboration with governmental and conservation agencies within ten states (see Appendix A). Prairies were defined as 'areas dominated by grasses' (Beard 1978, Faber-Langendoen 2001). Landowner privacy requirements prevented some agencies from sharing all prairie sites, while other agencies were able to share coordinates of privately owned land with the understanding that such data would not be made publicly available. To ensure an exact understanding of the spatial location of prairies, all data received from agencies were conveyed in the form of coordinate vector files. In some cases, prairie sites were located using online geographic databases. We located the prairie sites from vector files by conducting keyword searches of the site attributes with "prairie", "grassland", and "savannah." We ensured that all data were collected using GPS or through digitizing orthorectified aerial imagery.

Creating a Prairie Database

We constructed a hybrid database using ArcGIS (ESRI Inc.; Redlands, CA) to store spatial data and Microsoft Access 2003 (Microsoft Corporation; Redmond, WA) to organize and store ancillary data associated with each prairie. To integrate with later work (Chapter 3), we prepared the database for use with MODIS spectral data by determining in advance which MODIS pixels represent reflectances from vegetation at our prairie sites. Additionally, we obtained information about the physical attributes of the prairies that might influence the results of remote sensing studies, including percent grass cover and historical management, to increase database utility. Below we outline further steps we took to prepare the database for use with MODIS imagery, and how we obtained the information about the additional physical attributes.

Figure 2.1. Extent of North American grasslands, based on Olson *et al.* (2001).

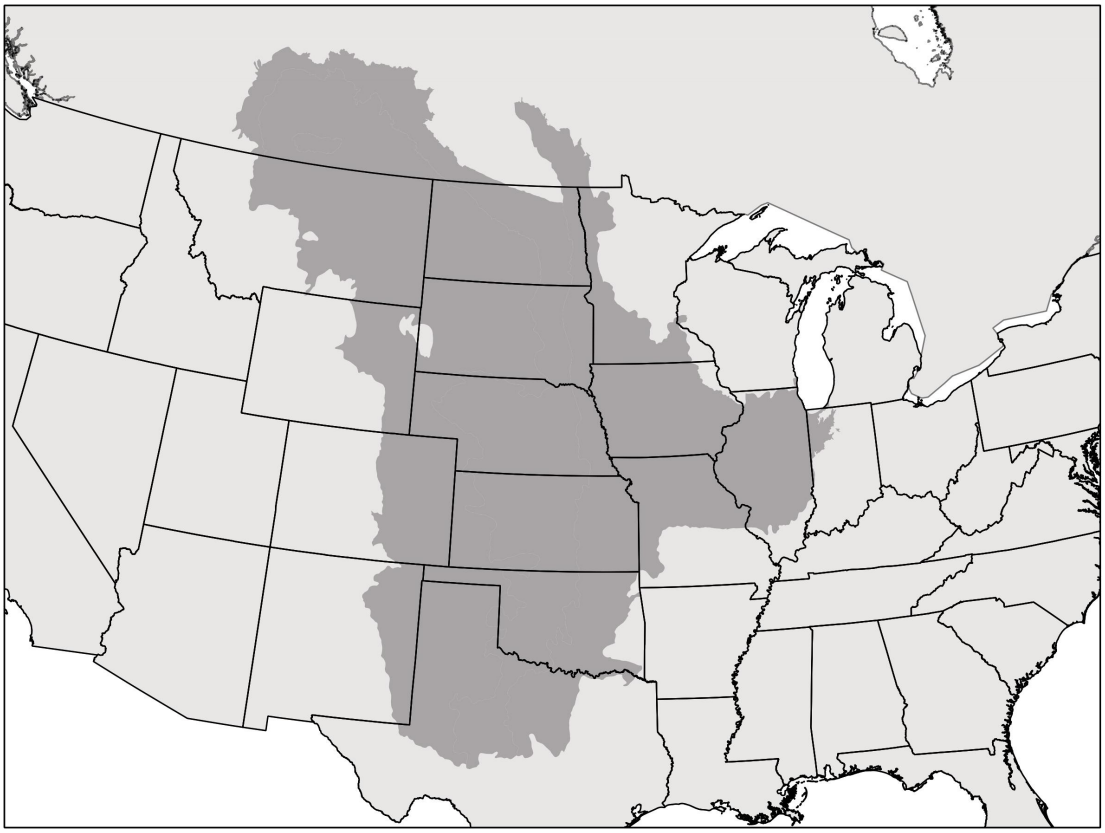

Decision to Use MODIS Data

To facilitate use of this database in analyses of MODIS imagery, we identified a set of prairies that would be compatible with MODIS Terra data for analysis (See section IV of this chapter for a detailed description of MODIS). We chose MODIS over other satellite sensors because we desired imagery that was widely available, regularly collected, and appropriate for evaluating relatively small patches in fragmented systems. MODIS is among the few satellite sensors with freely available, no-cost imagery that allows scientists and land managers to conduct affordable time-series analysis of prairie vegetation (for descriptive comparison of satellite sensors, see Chapter 1).

Determining Which MODIS Pixels Represent a Prairie's Spectral Reflectance

We evaluated the suitability of each prairie for MODIS-based analyses. The first concern was to ensure that prairie size was compatible with MODIS pixel size. Various land cover types exhibit different spectral reflectances (Reed *et al.* 1994) making it difficult to interpret remotely sensed data when multiple land cover types occupy a single pixel. To avoid error introduced by non-target land cover types, analysis should consider only pixels that are completely bounded by the prairie's border. Evaluating pixel suitability requires determining the placement of pixels relative to the prairie boundary, and consideration of the geolocation error associated with the imagery. Geolocation error represents a sensor's limits of consistently capturing data for a location with the same pixel with each pass. The geolocation error for MODIS is 50 m at nadir (Wolfe 2006) and 113 m off-nadir (Knight *et al.* 2006).

To determine which MODIS pixels would best represent each prairie in our geospatial database, we first accounted for the 113 m off-nadir geolocation error in MODIS data by

drawing a new boundary for each prairie 125 m within the original prairie boundary as delineated by its vector file (Figure 2.2A). MODIS pixels that fit entirely within this new boundary were selected and their outlines were vectorized (Figure 2.2B) for further work, including the determination of herbaceous material within the prairie.

Herbaceous Composition

In our second filtering process, we evaluated whether each site met our definition of herbaceous dominance for prairies (Transeau 1935, Sims *et al.* 1978, Axelrod 1985, Sims & Risser 2000). To do this, we quantified the area of each site that was dominated by herbaceous species by using a maximum likelihood supervised classification of aerial imagery in ENVI (ITT 2009) to separate images into two categories, "herbaceous" and "other" (Figures 2.2C and 2.2D). All aerial photos were obtained from the U. S. Geological Survey through MapCard (www.mapcard.com) and were taken between 2000 and 2006 at a 2 m spatial resolution. The areal extent of vegetation evaluated was a region that included the vectorized pixels (see previous section) and a 125 m buffer outside the pixel boundary to account for geolocational error (Figure 2.2D). Percent herbaceous cover was calculated using the external pixel boundary. Any prairies with less than 50% herbaceous cover were not considered to fit the definition of prairie and were not included in the database.

Management History

Third, we sought information about prairie management history and characteristics to allow categorization of prairies as remnant or restored. Management practices impact diversity (Allison 2002, Polley *et al.* 2005, Fuhlendorf *et al.* 2008), nutrient cycles

Figure 2.2. The process for selecting MODIS pixels to represent prairies and then determining the percent cover of herbaceous vegetation. A) The original vector file obtained from conservation agencies (red) overlaid on a MODIS Terra image. A 125 m interior buffer (blue) was then created from the original file to account for geolocation error. B) The pixels that are fully contained by the interior buffer are then selected (purple). C) Aerial imagery was then obtained and D) classified into herbaceous (red regions) and other (green regions). A 125 m boundary is formed around the pixels selected in B and the outer boundary is used to determine the percent herbaceous cover.

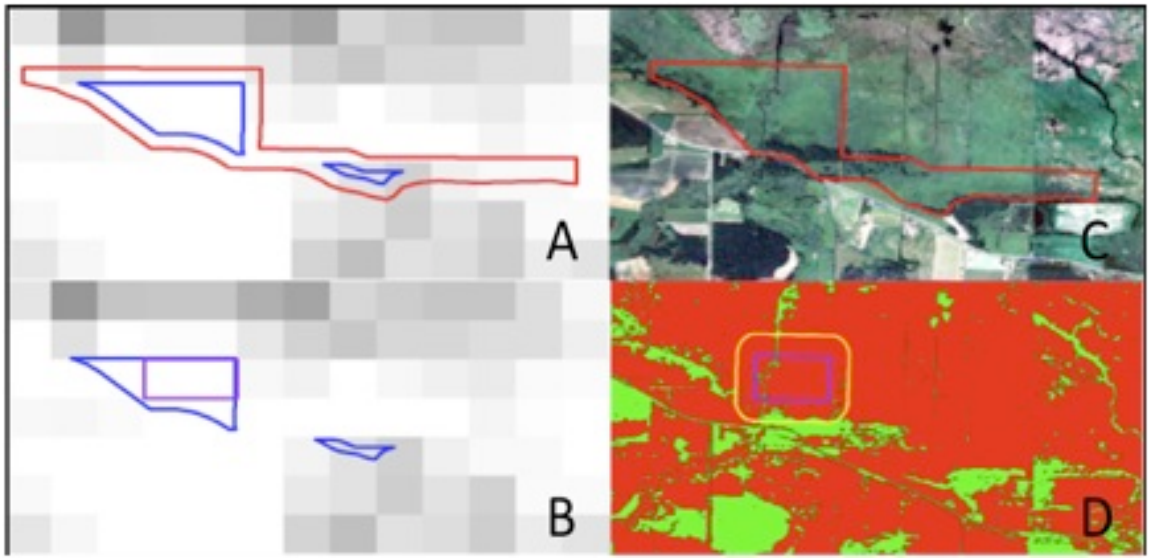

(Baer *et al.* 2002, Anderson *et al.* 2006, Han *et al.* 2008), species evenness (Polley *et al.* 2005), and species composition (Towne *et al.* 2005) of prairies. When possible, based upon information provided by land managers, we reported information regarding the fire, mowing, or grazing conducted at each site. Data included the time of year when management was conducted and how long and frequently such management was implemented at the site. Additionally, we determined whether the site had ever been converted to another land type, such as crop agriculture, and what specifically that land type was.

Prairie Spatial Database Description

From our filtering process, we produced a Prairie Spatial Database that contains 261 prairies spread across seven states (Figure 2.3). These prairies have ≥ 50% herbaceous cover and are suitable for evaluation with MODIS imagery (see section III). Of these prairies, 220 contain ≥ 80% herbaceous cover and 187 prairies have ≥ 90% herbaceous cover. The mean size of prairies in the database is 3.5 km^2 with the smallest prairie measured at 0.46 km^2 and the largest prairie measured at 35 km^2. Nebraska was the primary source of prairies within the database, accounting for 165 prairies. Conversely, only four prairies that met our criteria were found in each of two states: Wisconsin and North Dakota.

Management history was obtained for 25 prairies. Six of these prairies were at some point used in agriculture and then converted back to prairie. Thirteen sites had historical records indicating that they were remnant prairie carried over from the pre-settlement era. The remaining six sites contained areas of both; some areas of agriculture that had been converted back to prairie and some areas that have always been prairie.

Figure 2.3. Modeled transition line separating the dominance of C_3 and C_4 vegetation. The light gray area to the north represents C_3 dominance and the dark gray area to the south represents C_4 dominance. Points on this graph represent the positions of prairies within the Prairie Spatial Database that have been prepared for use with MODIS imagery. Transition line was modeled based from data in Epstein et al. (1997).

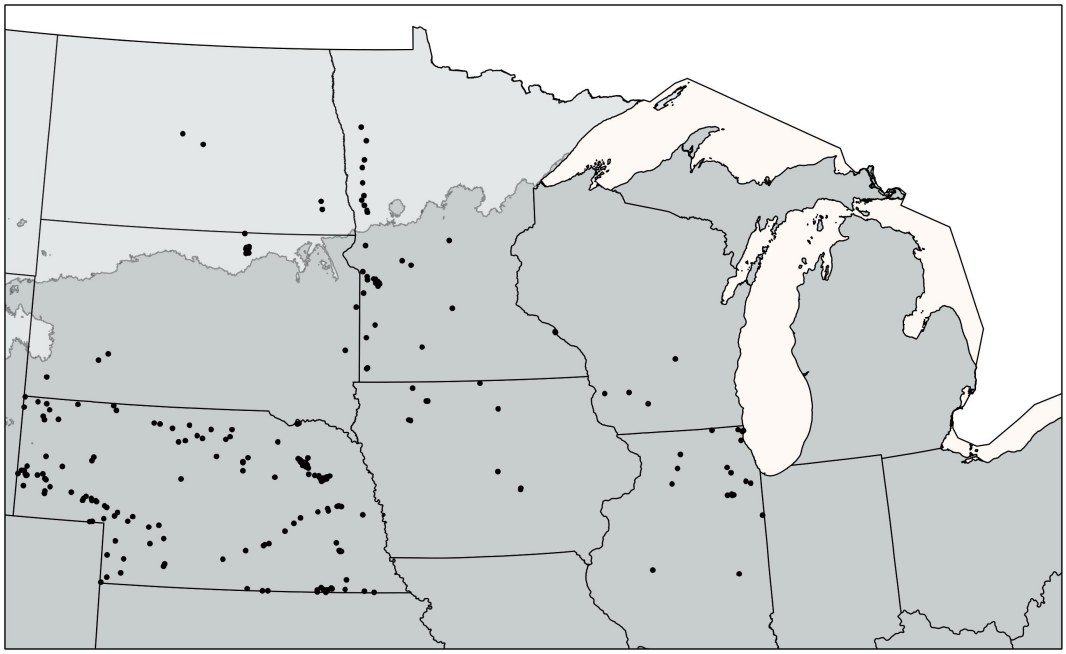

Of the management techniques analyzed, prescribed burning was the most commonly used. The frequency of mowing, grazing, or prescribed burning events usually occurred every 4 years or more, though there were some sites that used these techniques on an annual basis.

III. Existing Data for Use With the Regional Prairie Database

The main purpose of developing the Prairie Spatial Database was to provide an accurate tool for locating prairies in the northern Great Plains that could be used in regional ecological studies, particularly with remote sensing. In the following section, I summarize characteristics of MODIS imagery and other types of data that may be used in conjunction with this database, including weather, ecological, and soils resources.

MODIS Imagery

The Moderate Resolution Imaging Spectroradiometer (MODIS) is a spectral sensor onboard the Terra and Aqua satellites (Salomonson *et al.* 2006). MODIS collects 36 spectral bands at three spatial resolutions (250 m, 500 m, and 1,000 m) covering a 2330 km swath width (Salomonson *et al.* 2006). After the data are collected, they are prepared for public distribution, which, for some products, includes correcting the spectral values to account for Rayleigh scattering, aerosols, gaseous absorption, and adjacency effects (Vermote & Vermeulen 1999).

MODIS and similar sensors have been used with vegetation indexes in numerous studies to quantify the growth dynamics of vegetation at regional scales (Zhang *et al.* 2003, Guo *et al.* 2004). MODIS, in particular, offers near-daily repeat frequency at 250 m spatial resolutions (Salomonson *et al.* 2006) and provides a useful dataset for studying temporal trends in spatially fragmented prairie systems.

MODIS imagery is regularly submitted to multiple production programs (Masuoka *et al.* 1998) to yield multiple data products that can be downloaded from the Land Processes Distributed Active Archive Center (LPDAAC) website. Two indexes easily used for monitoring vegetation result from this process: the Normalized Difference Vegetation Index (NDVI) and the Enhanced Vegetation Index (EVI). A comparison of the use of NDVI and EVI within prairie ecosystems is presented in Chapter 1.

Weather Datasets

Weather variables such as precipitation and temperature influence the net primary productivity of prairie vegetation (Rogler & Haas 1947, Smoliak 1956, Schimel *et al.* 1991, Lauenroth & Sala 1992, Briggs & Knapp 1995, Yang *et al.* 1998, Henebry 2003, Wang *et al.* 2003, Knapp *et al.* 2006, Fay *et al.* 2008, Nippert *et al.* 2009, Zavalloni *et al.* 2009). There are at least three sources of weather information that could be used to characterize weather fluctuations in the central U.S. In the following sections, the strengths and weaknesses of the National Climatic Data Center (NCDC) weather station database, the North American Regional Reanalysis (NARR) database, and the PRISM database are presented (see Table 2.1).

NCDC Weather Stations

The National Climatic Data Center (NCDC) associated with the National Oceanic and Atmospheric Association (NOAA) collects and archives weather information for the

Table 2.1. Comparison of three weather databases; National Climatic Data Center (NCDC), North American Regional Reanalysis (NARR), and Parameter-Elevation on Independent Slopes Model (PRISM).

Dataset	NCDC	NARR	PRISM
Spatial Extent	Worldwide	North America	Contiguous U.S.
Spatial Type	Point	Raster	Raster
Spatial Resolution	-	32 km	4 km
Historic Length	1825*	1979	1895
Temporal Interval	Daily	3-hourly	Monthly
Variables			
Precipitation	✓	✓	✓
Max. Temperature	✓	✓	✓
Min. Temperature	✓	✓	✓
Wind	✓	✓	-
Pressure	✓	✓	-
Snow	✓	-	-
Other variables	✓	-	-

* Start of weather collection for Pittsburgh, Pennsylvania. Not all stations are this old.
\- Does not apply to this dataset

entire world (Center 1995). NCDC offers multiple sources of data relating to weather, including remote sensing systems, aircraft, and National Weather Service (NWS) cooperative observers (Center 2008). This overview provides information about surface data measurements obtained from a network of weather stations.

NCDC's daily surface weather data can be downloaded from their website (http://www.ncdc.noaa.gov/oa/ncdc.html) where over 1.2 petabytes of digital information is stored (Center, 2008). Within the U.S., there are nearly 8,000 NCDC weather stations spread across the landscape in a non-uniform pattern (Figure 2.4). Most commonly these stations record precipitation, temperature, evaporative demand, wind, and snow; however, the weather variables collected vary from station to station and depend on available equipment. The time frame within which data are collected also varies by station. Some stations have collected data for more than a century and continue to collect data; other stations may have only recently started collecting

data; and yet other stations may have started and stopped collecting data midway in the timescale. Malfunctions in equipment further complicate the availability of any single weather variable from a particular station, leaving gaps within the data that may span several months.

NARR

The North American Regional Reanalysis (NARR) dataset was developed by the National Centers for Environmental Prediction (NCEP), which is a part of the United States National Oceanic and Atmospheric Administration (NOAA). The NARR raster dataset focuses on the North American continent and was created to improve upon the spatial and informational accuracy of the Global Reanalysis dataset (Black 1994), a dataset providing spatially coarse weather measurements of the entire earth. NARR uses the Eta model to predict weather variables, which allows for both horizontal and vertical estimates (Black 1994). Data from NARR are reported from 1979 to present at a 32 km spatial resolution for 45 atmospheric layers, in 3 hour time increments (Mesinger *et al.* 2006). The spatial interpolations computed within the NARR Eta model are performed for precipitation, temperature, pressure, and wind, which are estimated from rawinsonde, dropsonde, pibal, aircraft, surface, and geostationary satellite data sets (Kalnay *et al.* 1996, Mesinger *et al.* 2006).

PRISM

The Parameter-Elevation Regressions on Independent Slopes Model (PRISM) is used to generate precipitation and temperature data at monthly time intervals for the

Figure 2.4. Locations of the weather stations associated with the National Climatic Data Center within the U.S. Each dot represents one weather station.

conterminous U.S. (Daly *et al.* 1994, Daly *et al.* 2004, Daly *et al.* 2008). This model has been used to develop a series of raster layers at a 4 km spatial resolution at monthly time intervals extending as far back as 1895. The raster dataset was originally designed to provide better estimations of weather variables in areas with substantial changes in topography, but it is also suitable for use on smooth topographies (Daly *et al.* 2008). To enhance data accuracy, the model incorporates weather data from multiple sources including the National Weather Service Cooperative Observer Program (COOP), the Weather Bureau Army Navy (WBAN), the USDA NRCS Snow Telemetry (SNOTEL) network, the USDA Forest Service and Bureau of Land Management Remote Automatic Weather Stations (RAWS), as well as from several other sources, older raster layers are more limited in the number of data stations used (Daly *et al.* 2008).

Selecting a Weather Dataset

Determining the best dataset to use with the prairie database ultimately depends upon the goals of the study being conducted. Data derived from the NCDC point dataset may be the most accurate, but its usability is most limited. To harness the accuracy of the NCDC, prairies must be in close proximity to the weather station. Analysis may be further limited if key data variables are not recorded at stations of interest during the study period. Although the accuracy of the interpolated raster datasets (NARR and PRISM) cannot match the accuracy of the NCDC dataset at the locations of the weather stations, they are likely to have better accuracy at locations not situated near weather stations.

There are several key factors that influence the choice of whether to use NARR or PRISM data for prairie response analysis. NARR is superior to PRISM in both its temporal

resolution and in the weather factors it incorporates. Researchers examining within-day or daily responses of prairies would find NARR more suitable. Additionally, NARR would be a good option for studies that incorporate wind or atmospheric pressure. Alternatively, PRISM has a longer historical record (as early as 1895 as opposed to 1979), as well as a finer spatial resolution (4 km vs 32 km) in comparison to NARR. Therefore, PRISM would be a better choice for studies with more extensive timeframes or for studies that require more spatial precision.

Vegetation Communities

Composition of vegetation within a prairie influences many ecosystem processes such as carbon sequestration and net primary productivity (Christian & Wilson 1999, Smith & Knapp 2003). However, it has not been logistically feasible to include field descriptions of vegetation communities within PSD at this point. Therefore, determining the similarity in community structure between prairies must rely on the delineation of major vegetation communities established in land cover maps.

Numerous landcover maps have been generated to characterize the vegetation of North America and many of them can be found at the Land Cover Institute (LCI - http://landcover.usgs.gov/index.php), which is associated with the U.S. Geologic Survey (USGS). One of the land cover maps that portrays the prairie extent according to historical descriptions (Transeau 1935, Weaver 1954, Weaver & Albertson 1956, Sims & Risser 2000) is the eco-region map of Olson et al. (2001). This global map of the earth's eco-regions was developed using current biotic distributions of animals and plants, as well as published regional data and personal consultation with experts (Olson *et al.* 2001). Though this delineation of

prairie types does not address species associated with each grouping, it provides a general grouping of similar species.

Dominant Photosynthetic Pathways

Vegetation with different photosynthetic pathways (C_3 vs C_4) has been shown to exhibit differences in seasonality (Foody & Dash 2007), as well as in response to environmental perturbations (Ward *et al.* 1999). C_3 species are better adapted to cooler temperatures while C_4 species thrive in warmer temperatures (Tieszen *et al.* 1997, Foody & Dash 2007). The relative dominance of either of these photosynthetic types would be an important consideration for analysis of temporal differences in vegetation growth (Tieszen *et al.* 1997).

Within the central U.S., the transition in dominant photosynthetic pathways has been related to a function of mean annual precipitation (MAP) and mean annual temperatures (MAT) (Epstein *et al.* 1997). In their study, Epstein et al. (1997) produced a transition boundary between areas where C_3 and C_4 vegetation dominate that follows the 43° N latitude line and closely follows other estimates of this transition (Teeri & Stowe 1976, Ehleringer 1978, Woodward & Lomas 2004, Woodward *et al.* 2004, vonFischer *et al.* 2008). The algorithm from Epstein et al. (1997)can be summarized as:

$$MAT_{thresh} = -1/3 \times MAP + 21,$$

where MAT_{thresh} represents the threshold for mean annual temperature. If the MAT for a prairie is below MAT_{thresh}, then the prairies is considered to be C_3 dominated. We applied this algorithm to the PRISM dataset (Daly 2009), averaged for 1971-2000, for temperature (average of maximum and minimum) and precipitation. This algorithm generated a similar boundary located between 43° and 45°N for the central portion of the U.S (Figure 2.3).

SSURGO Soils

Soil is an important part of ecosystem structure and helps quantify environmental moisture conditions in indices like Palmer's Drought Severity Index (PDSI). Accounting for moisture conditions is especially important in prairies because of the strong correlation in these systems between moisture and vegetation growth (Rogler & Haas 1947, Smoliak 1956, Schimel *et al.* 1991, Lauenroth & Sala 1992, Briggs & Knapp 1995, Yang *et al.* 1998, Wang *et al.* 2003, Knapp *et al.* 2006, Fay *et al.* 2008, Nippert *et al.* 2009). The Soil Survey Geographic (SSURGO) database is a polygon-based geospatial representation of soils within the U.S. and describes, among many other parameters, the available water content (AWC) of soils across the U.S., which is a measurement of the soil's ability to hold water (Staff 2009). The information within the SSURGO database was derived from detailed soil survey maps (Staff 2009). The soil Map Units (the spatial representation of the data) are composed of multiple soil types each with several horizons. Spatial placement of the soil Map Units were determined through auger sampling in the field, statistical analysis of soil transect data, and air-photo interpretation, so the size and shape of soil Map Units varies (Staff 2009).

The SSURGO database structure is split into three levels of information. Map Units are the coarsest level of information within SSURGO and describe the spatial distributions of multiple soil types. The second level within the database describes the individual soil series that are attributed to each Map Unit. The final level of the database provides data about each individual horizon in each soil series. The physical properties of the soil, such as AWC, are contained in the horizon level of the database. Therefore, developing regional estimates of soil properties requires aggregating across all three levels.

IV. Summary

PSD is a geographically explicit database that integrates geospatial and management information from a diverse pool of conservation agencies. PSD is spatially defined in an unprojected geographic coordinate system (WGS84 datum using decimal degrees) and contains 261 prairies ready to use with MODIS imagery. Additionally, there are numerous sources of geographic data that complement PSD and can be used for examining prairie regional processes occurring across the northern Great Plains. The compilation of PSD represents an important first step in the development of a larger more comprehensive prairie database.

PSD currently focuses on the northern Great Plains, which is an important transition point in terms of community type (shortgrass, mixedgrass, and tallgrass) and dominant photosynthetic pathway (C_3 and C_4). However, a more comprehensive database should be sought and future expansions of this database should extend coverage throughout the entire historical extent of prairies (Transeau 1935, Weaver & Albertson 1956, Olson *et al.* 2001). Additionally, there are more sources of information that could be explored within the current extent of PSD. For instance, though North Dakota and South Dakota are located in the central Great Plains, very few prairies were located within these two states. Although this may truly reflect the current status of GIS resources for prairies in those states, the technology is continually being updated; providing new sources of information that should be continually examined and updated.

PSD is readily usable with MODIS imagery, aiding the study of vegetation for the 2000-present time period. However, testing compatibility with other sensors would open up new opportunities for studying additional prairies, as well as extending the period of time considered. In comparison to MODIS, Landsat has a much smaller pixel size (30 m vs 250 m), a longer

acquisition history, and its imagery has recently become freely available. Screening prairies against imagery from this sensor would likely allow the inclusion of a larger sampling of prairies, which could be studied for a longer historical period. However, studies of recent prairie vegetation may be difficult to conduct with Landsat ETM+ due to a breakdown in its scan line corrector in 2003. The Landsat 5 Thematic Mapper (TM) continues to provide imagery, however this sensor has encountered several technical difficulties within the past years, which have disrupted the continuity of data transmission. AVHRR is another sensor from which data could be made compatible with PSD. AVHRR can provide a longer historical view of prairies with usable imagery currently being collected. Yet the larger pixel size of AVHRR (1.1 km) would diminish the number of prairies that could be used with this dataset.

A majority of North American prairies have been lost from the natural landscape and those that remain may be threatened by future global changes. PSD is an important step to developing a larger more comprehensive database while providing conservationists with an important tool for studying prairie ecosystems.

REFERENCES

V. References

Allison SK (2002) When is a restoration successful? Results from a 45-year-old tallgrass prairie restoration. *Ecological Restoration,* **20**, 10-17.

Anderson RH, Fuhlendorf SD, Engle DM (2006) Soil nitrogen availability in tallgrass prairie under the fire-grazing interaction. *Rangeland Ecology and Management,* **59**, 625-631.

Axelrod DI (1985) Rise of the grassland biome, central North America. *The Botanical Review,* **51**, 164-201.

Baer SG, Kitchen DJ, Blair JM, Rice CW (2002) Changes in ecosystem structure and function along a chronosequence of restored grasslands. *Ecological Applications,* **12**, 1688-1701.

Beard JS (1978) The Physiognomic Approach. In: *Classification of Plant Communities* Vol. 2 (ed Whittaker RH), pp. 408. Dr. W. Junk b.v. Publishers, Boston.

Black TL (1994) The new NMC Mesoscale Eta Model: Description and Forecast Examples. *Weather and Forecasting,* **9**, 265-278.

Briggs JM, Knapp AK (1995) Interannual variability in primary production in tallgrass prairie: climate, soil moisture, topographic position, and fire as detminants of aboveground biomass. *American Journal of Botany,* **82**, 1024-1030.

Butterfield HS, Malmstrom CM (2009) The effects of phenology on indirect measures of aboveground biomass in annual grasses. *International Journal of Remote Sensing,* **30**, 3133-3146.

Center NCD (1995) *Monthly Climatic Data for the World.* Asheville, North Carolina.

Center NCD (September 30, 2008) *What is NCDC?,* National Climatic Data Center, Accessed on May 28, 2010 at http://www.ncdc.noaa.gov/oa/about/whatisncdc.html.

Christensen JH, Hewitson B, Busuioc A*, et al.* (2007) Regional Climate Projections. In: *Climate Change 2007: The Physical Science Basis. Contribution of Working Group I to the Fourth Assessment Report of the Intergovernmental Panel on Climate Change* (eds Solomon S, Qin D, Manning M*, et al.*). Cambridge University Press, Cambridge, United Kingdom and New York, NY, USA.

Christian JM, Wilson SD (1999) Long-term ecosystem impacts of an introduced grass in the northern great plains. *Ecology,* **80**, 2397-2407.

Daly C *PRISM Climate Group, Oregon State University,* Oregon State University, Accessed on 2009 at www.prism.oregonstate.edu.

Daly C, Gibson W, Doggett M, Smith J, Taylor G (2004) Up-to-date monthly climate maps for the conterminous United States. In: *14th American Meteorological Society Conference on Applied Climatology.* American Meteorological Society, Seattle, WA.

Daly C, Halbleib M, Smith JI*, et al.* (2008) Physiographically sensitive mapping of climatological temperature and precipitation across the conterminous United States. *International Journal of Climatology,* **28**, 2031-2064.

Daly C, Neilson RP, Phillips DL (1994) A statistical-topographic model for mapping climatological precipitation over mountainous terrain. *Journal of Applied Meteorology,* **33**, 140-158.

Ehleringer JR (1978) Implications of quantum yield differences on the distributions of C_3 and C_4 grasses. *Oecologia,* **31**, 255-267.

Epstein HE, Lauenroth WK, Burke IC, Coffin DP (1997) Productivity patterns of C3 and C4 functional types in the U.S. Great Plains. *Ecology,* **78**, 722-731.

Faber-Langendoen D (Ed.) (2001) *Plant communities of the Midwest: Classification in an ecological context,* Association for Biodiversity Information, Arlington, VA.

Fay PA, Kaufman DM, Nippert JB, Carlisle JD, Harper CW (2008) Changes in grassland ecosystem function due to extreme rainfall events: implications for responses to climate change. *Global Change Biology,* **14**, 1600-1608.

Foody GM, Dash J (2007) Discriminating and mapping the C3 and C4 composition of grasslands in the northern Great Plains, USA. *Ecological Informatics,* **2**, 89-93.

Fuhlendorf SD, Engle DM, Kerby J, Hamilton R (2008) Pyric herbivory: Rewilding landscapes through the recoupling of fire and grazing. *Conservation Biology,* **23**, 588-598.

Getting IA (1993) The Global Positioning System. *IEEE Spectrum*, 36-47.

Guo X, Gao W, Richard P, Lu Y, Zheng Y, Pietroniro E (2004) Canadian prairie drought assessment through MODIS vegetation indices. *Remote Sensing and Modeling of Ecosystems for Sustainability,* **5544**, 149-158.

Han G, Hao X, Zhao M, Wang M, Ellert BH, Willms W, Wang M (2008) Effect of grazing intensity on carbon and nitrogen in soil and vegetation in a meadow steppe in Inner Mongolia. *Agriculture, Ecosystems and Environment,* **125**, 21-32.

Henebry GM (2003) Grasslands of the North American Great Plains. In: *Phenology: an integrative environmental science* (ed Schwartz MD), pp. 157-174. Kluwer Academic Publishers, Dordrecht.

ITT (2009). ITT Visual Imaging Solutions, www.ittvis.com, Boulder, CO.

Ji L, Peters AJ (2003) Assessing vegetation response to drought in the northern Great Plains using vegetation and drought indices. *Remote Sensing of Environment,* **87**, 85-98.

Kalnay E, Kanamitsu M, Kistler R*, et al.* (1996) The NCEP/NCAR 40-year Reanalysis Project. *Bulletin of the American Meteorological Society,* **77**, 437-471.

Knapp AK, Burns CE, Fynn RWS, Kirkman KP, Morris CD, Smith MD (2006) Convergence and contingency in production-precipitation relationships in North American and South African C4 grasslands. *Oecologia,* **149**, 456-464.

Knight JF, Lunetta RS, Ediriwickrema J, Khorram S (2006) Regional scale land cover characterization using MODIS NDVI 250m multi-temporal imagery: A phenology-based approach. *GIScience and Remote Sensing,* **43**, 1-23.

Lauenroth WK, Sala OE (1992) Long-term forage production of North American short-grass steppe. *Ecological Applications,* **2**, 397-403.

Law BE, Waring RH (1994) Remote sensing of leaf area index and radiation intercepted by understory vegetation. *Ecological Applications,* **4**, 272-279.

Loveland TR, Merchant JW, Ohlen DO, Brown JF (1991) Development of a land-cover charactersitics database fore the conterminous U.S. *Photogrammetric Engineering & Remote Sensing,* **57**, 1453-1463.

Masuoka E, Fleig A, Wolfe RE, Patt F (1998) Key characteristics of MODIS data products. *IEEE Transactions on Geoscience and Remote Sensing,* **36**, 1313-1323.

Meehl GA, Stocker TF, Collins WD*, et al.* (2007) Global Climate Projections. In: *Climate Change 2007: The Physical Science Basis. Contribution of Working Group I to the Fourth Assessment Report of the Intergovernmental Panel on Climate Change* (eds Solomon S, Qin D, Manning M*, et al.*). Cabridge University Press, Cambridge, United Kingdom and New York, NY, USA.

Mesinger F, DiMego G, Kalnay E*, et al.* (2006) North American Regional Reanalysis. *Bulletin of the American Meteorological Society,* **87**, 343-360.

Nippert JB, Fay PA, Carlisle JD, Knapp AK, Smith MD (2009) Ecophysiological responses of two dominant grasses to altered temperature and precipitation regimes. *Acta Oecologica,* **35**, 400-408.

Noss RF, III ETL, Scott JM (1995) *Endangered Ecosystems of the United States: A preliminary assessment of loss and degredation.* Goverment Printing Office, Washington D.C.

Noss RF, Peters RL (1995) *Endangered Ecosystems: A Status Report on America's Vanishing Habitat and Wildlife.* Defenders of Wildlife, Washington, DC.

Olson DM, Dinerstein E, Wikramanayake ED*, et al.* (2001) Terrestrial ecoregions of the world: A new map of life on Earth. *BioScience,* **51**, 933-938.

Paruelo JM, Epstein HE, Lauenroth WK, Burke IC (1997) ANPP estimates from NDVI for the central grassland region of the United States. *Ecology,* **78**, 953-958.

Pettorelli N, Vik JO, Mysterud A, Gaillard J-M, Tucker CJ, Stenseth NC (2005) Using the satellite-derived NDVI to assess ecological responses to environmental change. *Trends in Ecology & Evolution,* **20**, 503-510.

Plummer DA, Caya D, Frigon A*, et al.* (2006) Climate and climate change over North America as simulated by the Canadian RCM. *Journal of Climate,* **19**, 3112-3132.

Polley HW, Derner JD, Wilsey BJ (2005) Patterns of plant species diversity in remnant and restored tallgrass prairies. *Restoration Ecology,* **13**, 480-487.

Ran Y, Li X, Lu L (2010) Evaluation of four remote sensing based land cover products over China. *International Journal of Remote Sensing,* **31**, 391-401.

Reed BC, Brown JF, VanderZee D, Loveland TR, Merchant JW, Ohlen DO (1994) Measuring phenological variability from satellite imagery *Journal of Vegetation Science,* **5**, 703-714.

Ricotta C, Avena GC (2000) The remote sensing approach in broad-scale phenological studies. *Applied Vegetation Science,* **3**, 117-122.

Rogler GA, Haas HJ (1947) Range production as related to soil moisture and precipitation on the northern great plains. *Journal of Agronomy,* **39**, 378-389.

Salomonson VV, Barnes W, Masuoka EJ (2006) Introduction to MODIS and an Overview of Associated Activities. In: *Earth Science Satellite Remote Sensing* Vol. Vol 1: Science and Instruments (eds Qu JJ, Gao W, Kafatos M, Murphy RE, Salomonson VV). Tsinghua University Press & Springer-Verlag GmbH, Beijing & Berlin Heidelberg.

Samson F, Knopf F (1994) Prairie Conservation in North America. *BioScience,* **44**, 418-421.

Schimel DS, Kittel TGF, Knapp AK, Seastedt TR, Parton WJ, Brown VB (1991) Physiological Interactions Along Resource Gradients in a Tallgrass Prairie. *Ecology,* **72**, 672-684.

Sellers PJ (1987) Canopy reflectance, photosynthesis, and transpiration. II. The role of biophysics in the linearity of their interdependence. *Remote Sensing of Environment,* **21**, 143-183.

Sims PL, Risser PG (2000) Grasslands. In: *North American Terrestrial Vegetation* (eds Barbour MG, Billings WD), pp. 323-356. Cambridge University Press, Cambridge.

Sims PL, Singh JS, Lauenroth WK (1978) The structure and function of ten western North American grasslands: I. Abiotic and vegetational characteristics. *Journal of Ecology,* **66**, 251-285.

Smith MD, Knapp AK (2003) Dominant species maintain ecosystem function with non-random species loss. *Ecology Letters,* **6**, 509-517.

Smoliak S (1956) Influence of climatic conditions on forage production of shortgrass rangeland. *Journal of Range Management,* **9**, 89-91.

Staff SS (2009) Soil Survey Geographic (SSURGO) Database for the United States. United States Department of Agriculture, Natural Resources Conservation Service. Available online at http://soildatamart.nrcs.usda.gov.

Teeri JA, Stowe LG (1976) Climatic Patterns and the Distribution of C4 Grasses in North America. *Oecologia,* **23**, 1-12.

Tieszen LL, Reed BC, Bliss NB, Wylie BK, DeJong DD (1997) NDVI, C3 and C4 production, and distributions in Great Plains grassland land cover classes. *Ecological Applications,* **7**, 59-78.

Towne EG, Hartnett DC, Cochran RC (2005) Vegetation trends in tallgrass prairie from bison and cattle grazing. *Ecology,* **15**, 1550-1559.

Transeau EN (1935) The Prairie Peninsula. *Ecology,* **16**, 423-437.

Tucker CJ (1979) Red and photographic infrared linear combinations for monitoring vegetation. *Remote Sensing of Environment,* **8**, 127-150.

Vermote EF, Vermeulen A (1999) *Atmospheric Correction Algorithm: Spectral Reflectances (MOD09).* Goddard Space Flight Center, Greenbelt Maryland 20771, USA.

vonFischer JC, Tieszen LL, Schimel DS (2008) Climate controls on C_3 vs. C_4 productivity in North American grasslands from carbon isotope composition of soil organic matter. *Global Change Biology,* **14**, 1141-1155.

Wang J, Rich PM, Price KP (2003) Temporal responses of NDVI to precipitation and temperature in the central great plains, USA *International Journal of Remote Sensing,* **24**, 2345-2364.

Ward JK, Tissue DT, Thomas RB, Strain BR (1999) Comparative responses of model C3 and C4 plants to drought in low and elevated CO_2 *Global Change Biology,* **5**, 857-867.

Weaver JE (1954) *North American Prairie.* Johnsen Publishing Company, Lincoln, NE.

Weaver JE, Albertson FW (1956) *Grasslands of the Great Plains: their nature and use.* Johnsen Publishing, Lincoln.

Wolfe RE (2006) MODIS Geolocation. In: *Earth Science Satellite Remote Sensing* Vol. Vol 1: Science and Instruments (eds Qu JJ, Gao W, Kafatos M, Murphy RE, Salomonson VV), pp. 50-73. Tsinghua University Press & Springer-Verlag GmbH, Beijing & Berlin Heidelberg

Woodward FI, Lomas MR (2004) Vegetation dynamics - simulating responses to climatic change. *Biological Reviews,* **79**, 643-670.

Woodward FI, Lomas MR, Kelly CK (2004) Global climate and the distribution of plant biomes. *Philosophical Transactions of the Royal Society of London,* **239**, 1465-1476.

Xian G, Homer C, Fry J (2009) Updating the 2001 National Land Cover Database land cover classifacation to 2006 by using Landsat imagery change detection methods. *Remote Sensing of Environment,* **113**, 1133-1147.

Xiao J, Moody A (2004) Photosynthetic activity of US biomes: responses to the spatial variability of seasonality of precipitation and temperature. *Global Change Biology,* **10**, 437-451.

Yang L, Wylie BK, Tieszen LL, Reed BC (1998) An analysis of relationships among climate forcing and time-integrated NDVI of grasslands over the U.S. northern and central Great Plains. *Remote Sensing of Environment,* **65**, 25-37.

Zavalloni C, Gielen B, Boeck HJD, Lemmens CMHM, Ceulemans R, Nijs I (2009) Greater impact of extreme drought on photosynthesis of grasslands exposed to a warmer climate in spite of acclimation. *Physiologia Plantarum,* **136**, 57-72.

Zhang X, Friedl MA, Schaa CB*, et al.* (2003) Monitoring vegetation phenology using MODIS. *Remote Sensing of Environment,* **84**, 471-475.

Chapter 3: Drought Sensitivity of North American Prairie Types: Assessment of MODIS NDVI Time Series for 221 Sites in the Northern Great Plains

I. Introduction

The relationship between primary production and precipitation in grasslands has long been an issue of great interest both to ecologists and to managers who graze livestock and/or maintain conservation properties (Smoliak 1956, Knapp 1984b, Smoliak 1986, Sala *et al.* 1988a, Sala *et al.* 1992, Briggs & Knapp 1995, Knapp *et al.* 2006). Over the last several decades, field studies of grassland production dynamics have sought to identify general relationships between production and moisture availability within North American grasslands and elsewhere (Smoliak 1986, Briggs & Knapp 1995, Oesterheld *et al.* 2001, Knapp *et al.* 2006, Smart *et al.* 2007). These studies have generated invaluable insight, but also require extensive resources to conduct, which has limited their frequency and extent.

New developments in remote sensing science, specifically the recent accumulation of highly detailed time series of low cost imagery (e.g. Salomonson *et al.* 2006), now allow these relationships to be reexamined in much more detail and over broader scales than has ever before been possible. Here we use a time series of 8-day composite imagery from the Moderate Resolution Imaging Spectroradiometer (MODIS) instrument onboard the Terra satellite to examine the influence of interannual soil moisture on productivity in 221 prairie communities within the North American Great Plains region for the period 2000-2008. We use multi-level modeling (Pinheiro & Bates 2000, Merlo 2003, Gelman & Hill 2009) to analyze relationships between values of the Palmer Drought Severity Index (PDSI) (Palmer 1965, Weber & Nkemdirim 1998) experienced by prairie communities over time and their growth response as captured by the Normalized Difference Vegetation Index (NDVI) (Rouse *et al.* 1973, Tucker

1979). We evaluate relationships between PDSI and two NDVI-based metrics for each growing season: (i) maximum NDVI values, as a measure of maximum relative photosynthetic activity (Sellers 1987), and (ii) the integration of NDVI over the growing season, as a proxy for aboveground productivity (Goward *et al.* 1985, Paruelo *et al.* 1997).

The North American prairie region represents an excellent study system for this analysis because it encompasses several different prairie community types, whose distribution (Figure 3.1a) is strongly shaped by precipitation and temperature gradients (Sala *et al.* 1988b, Epstein *et al.* 1996, 1997, Xiao & Moody 2004, Bradford *et al.* 2006, Grosso *et al.* 2008). Mean annual precipitation increases from west to east in this region (Figure 3.1c) and strongly influences the stature, distribution, and mean productivity of prairie types, which are generally categorized--in order of increasing mean annual precipitation and plant stature--as shortgrass, mixedgrass, and tallgrass communities (Weaver 1954, Sims & Risser 2000). Mean annual temperature, on the other hand, generally decreases with increasing latitude (Figure 3.1d) and influences which photosynthetic pathway (C_3 or C_4) predominates within communities (Epstein *et al.* 1997). Over the last 200 yrs, these prairie communities were reduced to less than 20% of their original extent (Samson & Knopf 1994), largely because of conversion to agriculture. As a result, restoration of these prairies is a conservation priority, and the most limited prairie type (tallgrass prairie, ca. 99% converted) is now considered an endangered ecosystem (Noss *et al.* 1995, Noss & Peters 1995). It is therefore also useful to consider differences among restored and remnant prairie sites.

Previous field studies indicate that prairie productivity is influenced by yearly weather patterns, and that responses to weather variability may differ among prairie community types. For example, production in shortgrass prairie has been found to be more sensitive to moisture

Figure 3.1. (A) Locations of prairies within the central United States (Olson et al. 2001). Shortgrass prairie denoted in red, mixedgrass prairies denoted in yellow, and tallgrass prairie denoted in blue. (B) Distribution of prairies for this study (black dots). Light colors represent areas dominated by C3 species and darker colors represent areas dominated by C4 species. Red colors represent shortgrass prairies, yellow represent mixedgrass prairies, blue represents tallgrass prairies, and gray represents an area not denoted as a prairie dominated region. A precipitation map (C) and temperature map (D) were created using a 30 year mean for yearly data between 1971 – 2000 for the region (Daly 2009).

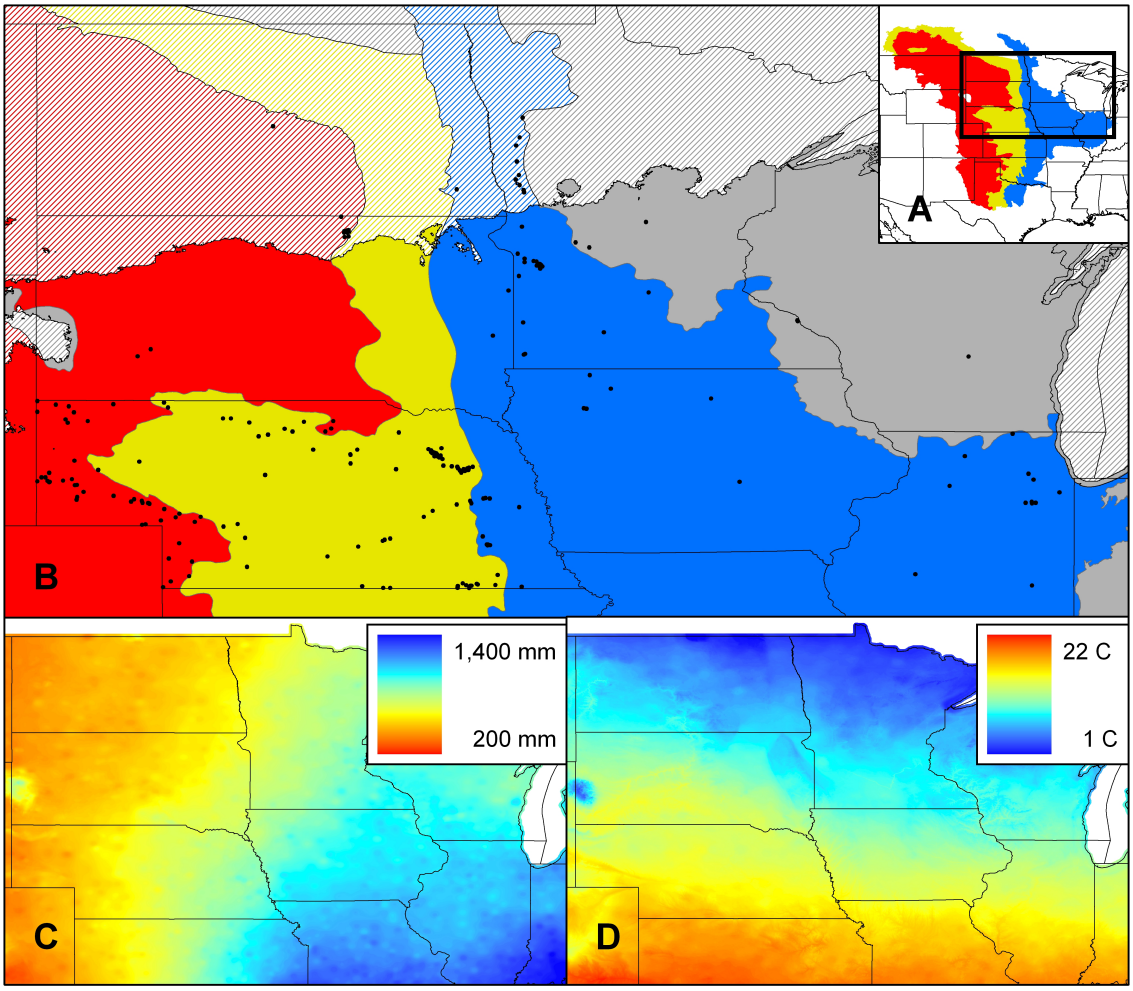

availability than that in the tallgrass prairie, in which precipitation totals are greater (Lauenroth & Sala 1992, Briggs & Knapp 1995). Field data also suggest that multi-year relationships may be important. For example, long-term studies indicate that in shortgrass and mixedgrass prairies production is influenced by precipitation values in the previous growing season (Smoliak 1986, Smart *et al.* 2007). Likewise, in a 50-year analysis, Oesterheld *et al.* (2001) found that biomass production in shortgrass and mixedgrass prairie was slightly greater in dry years if the previous growing season had been wet, but very reduced if the previous year had been dry; in tallgrass prairie, reduced data availability limited analysis. In a related manner, (Yahdjian & Sala 2006) likewise found that more of the variance in production data in the Patagonian Steppe could be explained when production in the previous year was added as an explanatory variable, suggesting the importance of multi-year feedbacks.

Remote sensing studies offer powerful means to expand investigation of the relationships between primary productivity and moisture availability. The earliest uses of remote sensing vegetation indices include innovative monitoring of drought effects in the African Sahel with the Normalized Difference Vegetation Index (NDVI), which is a measure of vegetation greenness (Tucker *et al.* 1986). In the North American Great Plains, grassland dynamics have been evaluated with several remote sensing approaches, with the most extensive previous studies examining NDVI time series derived from1-km AVHRR imagery (e.g. Goward *et al.* 1985, Paruelo *et al.* 1997, Tieszen *et al.* 1997, Yang *et al.* 1998, Ji & Peters 2003). In this region, time-integrated NDVI has been found to serve as a reasonable surrogate for ANPP (Goward *et al.* 1985, Paruelo *et al.* 1997). Quantitative relationships between NDVI and weather variables were documented by Yang et al. (Yang *et al.* 1998) for many grassland communities within the Great

Plains. Ji and Peters (2003) further demonstrated the seasonal dependence of NDVI – moisture relationships and found that correlations were strongest for June and July.

The development of 250-m MODIS imagery now permits more rigorous evaluation of relationships between NDVI and moisture dynamics at finer spatial scales than were previously possible with the coarser 1-km AVHRR data. The improvement in scale offered by MODIS data promises new insight into the dynamics of the tallgrass prairie community in particular, because this prairie type has been most fragmented by human activities. The majority of remnant and restored tallgrass prairies are smaller in size than can be well evaluated at a 1-km scale and thus have had to be overlooked in most previous remote sensing analyses.

The objective of this study is to evaluate the relationship between growing season soil moisture conditions and primary production in grasslands in the northern Great Plains prairie region for the 2000-2008 period of MODIS data availability, with improved spatial precision and increased focus on tallgrass prairies. To facilitate this analysis, we make use of a new geospatial database we created that delineates locations of extant prairies. We develop multilevel models to describe the response of NDVI metrics to inter-annual weather patterns, as a function of prairie community type (shortgrass, mixedgrass, or tallgrass), dominant photosynthetic pathway (C_3 or C_4), and restoration history (restored or remnant); we focus primarily on community types in our analysis because it was our most robust comparison. In general, we expected that primary production in grasslands would be most reduced when drought periods extended for more than one year. Based on previous findings and plant ecophysiology, we further predicted that prairie dynamics would differ among prairie types, as follows: i) shortgrass prairies would be most sensitive to growing season moisture availability and tallgrass prairies least sensitive; ii) C_3-dominated prairies would respond more strongly to interannual variability in soil moisture than

C_4-dominated prairies, due to their lower water use efficiencies; and iii) restored prairies would be more sensitive to inter-annual moisture patterns because of their lower biodiversity.

II. Methods

Identifying Prairie Locations and Categorizing Prairies

To evaluate relationships between soil moisture availability and prairie growth responses, we examined a group of 221 prairies within the northern Great Plains, which represent a suite of community types (Figure 3.1c; Sims & Risser 2000) and dominant photosynthetic pathways (Epstein *et al.* 1997). To identify specific prairie locations, we obtained GIS polygon files from local conservation organizations (Figure 3.1b). We next categorized these 221 prairies by community type (shortgrass, mixedgrass, or tallgrass), dominance of C_3 or C_4 species, and restoration status (restored, remnant or mixed). Classification of shortgrass, mixedgrass and tallgrass prairies was determined according to the World Wildlife Fund's eco-region map (Olson *et al.* 2001). The eco-region map was constructed by using biogeographic realms, biome systems, floristic and zoogeographic provinces, and expert consultation (Olson *et al.* 2001). The prairie types outlined within the eco-region map follow the same general pattern described from previous reports of prairie ecosystems (Transeau 1935, Weaver & Albertson 1956). A major strength of our analysis is that tallgrass prairies are located with precision and represent 61 of the 221 prairies evaluated.

To delineate the regional dominance of C_3 and C_4 pathways, we used methods developed by Epstein *et al*. (1997) who characterized the separation of the dominance of these two pathways using mean annual temperature (MAT) and mean annual precipitation (MAP). Using 800 m resolution PRISM climate data averaged over 1971-2000 (Daly 2009), we generated a

map delineating the dominance of photosynthetic pathways in this region. To derive MAT, we averaged the minimum and maximum temperatures generated by PRISM. We applied the following algorithm to the precipitation map based on absolute production algorithms in Epstein *et al.* (1997):

$$TEMP_{thresh} = -1/3 \times PRECIP + 21,$$

where PRECIP represents the precipitation (cm) and $TEMP_{thresh}$ represents the threshold temperature in degrees C. When the temperature at a given location exceeded $TEMP_{thresh}$ then that location was considered to be C_4-dominated, otherwise it was considered C_3-dominated. This approach delineated a boundary separating C_3- and C_4-dominated prairies, where locations south of the 45° N latitude line were classified as C_4-dominated. The map generally agrees with previous studies of C_3-C_4 delineation in this area (Teeri & Stowe 1976, Ehleringer 1978, Woodward & Lomas 2004, Woodward *et al.* 2004, vonFischer *et al.* 2008).

For restoration status, we were able to categorize a subset of the prairie sites (25/221) as remnant, restored, or mixed, based upon information provided by land managers. An original goal of this study was to determine restoration status for all prairies considered, but management information proved more difficult to obtain than we initially thought. We defined restored prairies as sites that had been converted to another land cover, such as crop agriculture, and then converted back to prairie. We defined remnant sites as areas that were historically prairie and had remained so until the present. Since some of the prairies were extremely large, it was also necessary to consider some prairies as mixed, which means that the prairie has areas of both restored and remnant prairie within its boundary.

Several constraints influenced the choice of prairies evaluated. Most importantly, although we were able to consider much smaller prairies than possible in an AVHRR-based

analysis, we still were required to impose a minimum prairie size for our analysis; we did not include prairies in our study when they were too small to be fairly compared with 250-m MODIS pixels. This means that our sample may underestimate the impact of edge effects and other phenomena most evident in even smaller prairies, but our study nonetheless represents a notable improvement over coarser analyses. In addition, our sample is weighted more heavily towards C_4-dominated systems (n = 196) than to C_3 prairies (n=25), which were less common and largely restricted to the northern states of Minnesota, South Dakota, and North Dakota (Figure 3.1b). In addition, relying on conservation managers to provide information about prairie locations may have increased the chance that the prairie sites we studied are under some form of management, which might have influenced community compositions or response dynamics. Finally, categorizing prairies using dominant photosynthetic pathways and community types has potential to confound these factors with the environmental gradients (e.g, temperature, precipitation) used to delineate the location of these prairie types.

Examining Prairie Vegetation with MODIS

The MODIS Sensor

To evaluate prairie response to changes in soil moisture availability at a scale finer than 1-km, we assessed vegetation using remotely sensed imagery obtained from MODIS onboard the National Aeronautic and Space Adminstration (NASA) polar orbiting Terra satellite. MODIS is a multispectral sensor with a near-daily temporal repeat frequency and spatial resolution ranging from 250-1000 m. We chose to use MODIS because of its reliable image acquisition, its short return frequency, and the ease of acquiring its data sets, and because its moderate spatial resolution permits analysis of many smaller prairie sites. Landsat Thematic Mapper or Enhanced

Thematic Mapper imagery would offer similar comparisons at an even finer resolution (30 m), but data gaps and much longer repeat cycles limit the value of Landsat time series for the study conducted here.

For the MODIS analysis, we obtained 250 m spatial resolution surface reflectance (MOD09Q1) imagery from the U.S. Land Processes Distributed Active Archive Center (LPDAAC - lpdaac.usgs.gov) for the paths and row of v4 h10 and v4 h11 during the period February 2000 – September 2008. The near-daily imagery was processed by the MODIS team to correct for rayleigh scattering, aerosols, gaseous absorption, and adjacency effects (Vermote & Vermeulen 1999). Additionally, the MOD09Q1 product is an 8-day, maximum-value composite, which reduces the inclusion of low values generated by clouds.

Normalized Difference Vegetation Index

To assess vegetation dynamics, we next calculated the Normalized Difference Vegetation Index (NDVI) from the MOD09Q1 imagery. We chose NDVI because we were able to calculate the index at a moderate spatial resolution (250 m) and because NDVI is correlated with the fraction of photosynthetically active radiation (Sellers 1987, Sellers *et al*. 1992) and has been used as an indicator of vegetation growth and primary production (Tucker 1979, Goward *et al*. 1985, Paruelo *et al*. 1997, Xiao & Moody 2004). NDVI is calculated as:

$$NDVI = \frac{(\rho_{NIR} - \rho_{red})}{(\rho_{NIR} + \rho_{red})},$$

where ρ_{red} is the spectral reflectance in the red spectrum (MODIS Band 1) and ρ_{NIR} is the reflectance obtained in the near infrared (MODIS Band 2) (Rouse et al. 1973, Tucker 1979). The Enhanced Vegetation Index (EVI) is an alternative MODIS product with less tendency to

saturate when vegetation is dense (Huete *et al.* 1994, Salomonson *et al.* 2006), but its pixel size (500 m) was too coarse for analyses (see below).

Identification of Pixels Representing Prairie

Spectral reflectance patterns captured by satellite imagery differ with land cover (Reed et al. 1994), so we took several steps to reduce inadvertent inclusion of multiple land cover types within our study polygons. One potential cause of inclusion of multiple land cover types is geolocational error associated with the remote sensor. Geolocational error occurs when there are differences among the geographic placements of images that nominally represent the same location. For example, a prairie might be represented by a single MODIS pixel during one satellite overpass but in the next overpass that same pixel may be geographically shifted and now encompass both prairie and another land cover adjacent to it. The current geolocational error associated with MODIS has been estimated to be 50 m at nadir (Wolfe 2006) and 113 m off-nadir (Knight et al. 2006). A second cause of inclusion of multiple land covers is simply that another land cover may occur within the boundary of a prairie as delineated by geographic polygons used for management, as is even more likely to be problematic with 1-km AVHRR images used in previous studies.

We accounted for each of these possibilities by evaluating data only from (i) MODIS pixels that fell within an interior region of each prairie polygon and (ii) prairies that contained at least 80% herbaceous vegetation. First, we modified each prairie polygon to account for potential MODIS geolocational error by creating a new internal boundary for each prairie polygon 125 m within the original polygon, and then analyzed data only from those MODIS pixels that fell entirely within this internal boundary. Next, to evaluate vegetation composition within the study

polygons, we analyzed USDA National Agriculture Imagery Program true color high-resolution aerial imagery (2m pixels) obtained from MapCard (Billings, MT) taken during the summers of 2002-2006. To account for the MODIS geolocational error in this analysis, we developed a polygon 125 m outside the group of pixels representing the prairie. With the image processing software ENVI (ITT 2009), we conducted a supervised classification of the aerial imagery using maximum likelihood methods to separate herbaceous cover from all other land cover (roads, water, forest, etc.). We used only sites that contained a minimum of 80% herbaceous vegetation for further analysis.

Measures of Prairie Response

We developed a time series of vegetation greenness for each prairie, with an 8-day time step from 2000 to 2008, using MODIS-derived NDVI values that were averaged over all pixels in each prairie polygon for each time step (Figure 3.2; Appendix B). Time-series curves were smoothed using a 3-frame moving average. We attempted to use several automated algorithms to detect the start and the end of the growing season for each prairie (Reed *et al.* 1994, Studer *et al.* 2007), but these algorithms performed poorly with bi-modal data, which was prevalent within the western prairies. Therefore, we manually determined the onset and end of the growing season to avoid extraneous variability due to fluctuations in snow cover, which depresses NDVI values (Dye & Tucker 2003, Hird & McDermid 2009). We inspected all NDVI time series curve to determine the earliest seasonal date in all time series at which NDVI exceeded 0 and the latest date at which NDVI in all time series not drop below 0. Based on this analysis, we defined the growing season as the period between Julian day 89 (March 29/30) and Julian day 273 (September 29-30) to minimize the effect of snow cover on the NDVI time series. Additionally,

Figure 3.2. NDVI time series obtained from MODIS 8 day composite images. (A) A single year time series for one prairie represented by 45 temporally linked images. Time integrated NDVI (TINDVI), represented by the shaded area, was calculated by summing the values under the NDVI curve throughout the growing season, where growing season was defined as julian days 89 - 273. The dashed line represents the point obtained for the MaxNDVI. (B) Typical NDVI curves (solid line) generated from 382 temporally linked MODIS images for tallgrass, mixedgrass, and shortgrass prairies are presented along with a time series of 108 monthly PDSI values (dotted line). White regions represent growing season used to estimate TINDVI and MaxNDVI values while shaded areas were not examined in this study.

Figure 3.2. (cont'd)

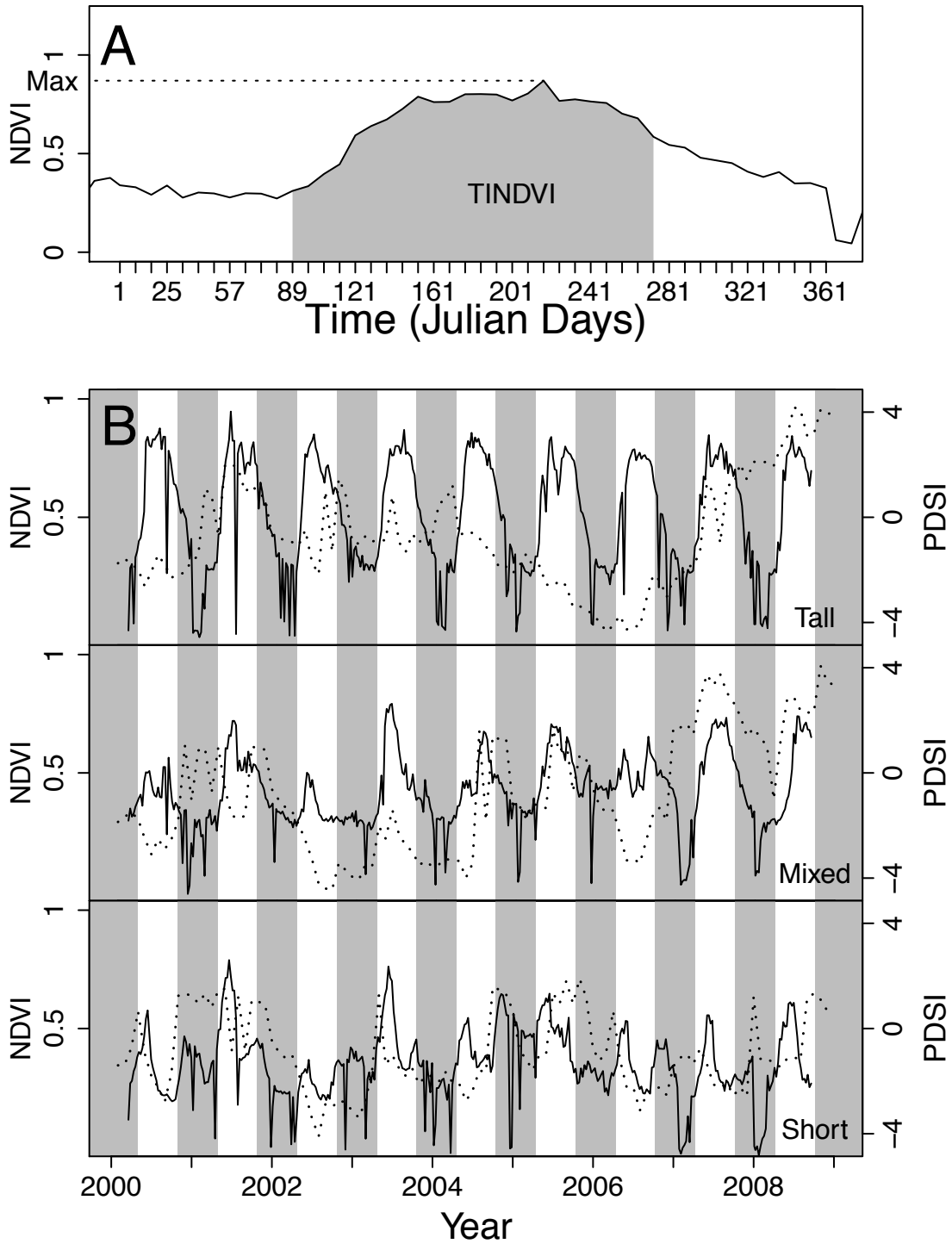

we also reduced the effects of dates including snow by altering any point below an NDVI value of 0.1 within the defined growing season to equal 0.1 (Beck *et al.* 2006, Hird & McDermid 2009). Data were missing for Julian day 217 in 2000 and Julian day 169 in 2001 due to sensor malfunctions, so we estimated these data points by using the NDVI value from the previous image in the time series.

To assess the effects of soil moisture availability on prairie dynamics, we examined two variables derived from the NDVI time-series data for each growing season period: (i) Time-Integrated NDVI (TINDVI; Figure 3.2a) and (ii) Maximum NDVI (MaxNDVI). TINDVI calculated for the growing season period is a measure of total greenness that has been correlated with yearly net primary productivity (Goward *et al.* 1985). MaxNDVI is a metric of peak greenness and was quantified as a measure of maximum relative photosynthetic activity (Sellers 1987, Sellers *et al.* 1992).

Drought Assessment

The Palmer Drought Severity Index (PDSI) is a monthly drought index calculated by estimating and comparing monthly anomalies to long term (>30 years) moisture patterns (Palmer 1965, Weber & Nkemdirim 1998). We chose PDSI for this study over other drought indices because it considers multiple hydrologic parameters that are likely to influence plant growth, such as evapo-transpiration and soil available water capacity (AWC), in addition to precipitation. The index contains defined wetness categories for values ranging from -4 to 4 (Table 3.1) with lower values representing more severe drought, higher values representing increasingly wet conditions, and values near zero representing normal moisture conditions. This index is appropriate for our study area

Table 3.1. Interpretation of Palmer's Drought Severity Index (Palmer 1965).

PDSI Range	Interpretation
≥ 4.0	Extremely Wet
3.0 to 3.9	Severely Wet
2.0 to 2.9	Moderately Wet
1.0 to 1.9	Mildly Wet
-0.9 to 0.9	Normal Moisture Conditions
-1.9 to -1.0	Mildly Dry
-2.9 to -2.0	Moderately Dry
-3.0 to -3.0	Severely Dry
≤ -4.0	Extremely Dry

since it incorporates a spatial normalization process that was developed and tested within this region (Palmer 1965). Additionally, PDSI has a temporal continuity component that accounts for values of recent months and adjusts the index accordingly. For example, if the previous month were excessively dry, then the current month requires more moisture in order to attain a "normal" status for the index. This index is particularly useful because it considers not only precipitation, but also temperature and soil moisture-holding capacity, and thereby produces more realistic assessments of the extent to which drought is experienced by vegetation.

To calculate PDSI, we used monthly precipitation and minimum and maximum temperature values from PRISM raster grids that cover the entire U.S. with a 4 km spatial resolution (Daly 2009). PRISM weather estimates have been produced for the period 1895--present by spatial interpolation from an extensive network of weather stations using an algorithm that accounts for weather differences due to elevation (Daly *et al.* 1994, Daly *et al.* 2004). PDSI requires at least 30 years of data for its calculation, so we used PRISM estimates from 1970-2008. Weather values were estimated from the pixel located in the center of each prairie

polygon; the temperature estimates used for the PDSI calculations were derived by averaging maximum and minimum temperature values.

The available water-holding capacity (AWC) of the soil was estimated for PDSI calculations by using the United States Department of Agriculture Soil Survey Geographic (SSURGO) Database (USDA 2009). SSURGO is a geospatial database that describes the extent, depth, and other characteristics of soils for the entire U.S. AWC values for prairie soils were not directly linked to the geospatial layer of the SSURGO database. To derive AWC values it was necessary to use a weighted average to combine the AWC estimates of locally similar soils as well as the estimates for each soil horizon. We converted the AWC values from the soil database to a volumetric measure by multiplying the depth of the soil (150 cm) by the percentage value listed in the database. We selected 1.5 m as the soil depth for this study because it was the most common maximum depth reported in the SSURGO database and it is close to the mean rooting depth typically found in grassland systems (Canadell *et al.* 1996). To understand the consequences of this choice for our analysis, we also evaluated the sensitivity of PDSI calculations to the choice of soil depth, for the different prairie categories.

To assess drought severity for each year for the period 2000-2008, we used several metrics based on PDSI in a single year: (i) average growing season PDSI (AvgPDSI); (ii) minimum growing season PDSI (MinPDSI); and (iii) average PDSI in June and July (JnJlPDSI). We considered the latter factor because NDVI is sometimes correlated with other measures of drought in June and July (Ji & Peters 2003). In addition, we considered the extent of growing season drought in previous years by also evaluating $PDSI_{(n-1)}$, $PDSI_{(n-2)}$, and $PDSI_{(n-3)}$, where n is the current year.

Statistical Models

Model Type

The data we analyzed included repeated measurements of a set of subjects (prairies); therefore, we chose to use a mixed level model for our comparisons (Gelman & Hill 2009). The mixed level model works differently from normal regression in that it models each subject separately, producing more accurate estimations for layered (observation level and subject level) datasets. All analyses were conducted in R (Team 2009) using the *lme* function within the *nlme* library (Pinheiro & Bates 2000). In addition, to account for the influence of temporal correlation, we used a time-based, autoregressive correlation structure (accounting for year). The combinations of fixed effects used in our models are listed in Table 3.2.

NDVI Dynamics

To assess differences in overall NDVI patterns among prairie types (community type, photosynthetic dominance, and restoration history), we conducted multiple mixed-level ANOVAs with an autoregressive correlation structure for time. TINDVI, MaxNDVI, and the date of MaxNDVI for all sites and years were modeled using prairie type as the sole explanatory variable. To estimate the relative variation in NDVI patterns within each prairie type across years, we calculated the coefficient of variation (CV) across all prairies for all years.

Table 3.2. List of model structures considered in this study in their general form. Group represents one of the different prairie grouping methods (community type, C_3 or C_4 dominance, or restoration history). PDSI represents one of the three PDSI variables considered (AvgPDSI, JnJlPDSI, MinPDSI). Lag1, Lag2, and Lag3 represent drought from one, two, and three years previous to the current year. The labels from these models will be used in subsequent tables and the text. To simplify reading models, the interaction term with 'Group' was not included in any of the models.

Label	ModelStructure
A	Group+PDSI
B	Group+PDSI+Lag1+PDSI:Lag1
C	Group+PDSI+Lag2+PDSI:Lag2
D	Group+PDSI+Lag3+PDSI:Lag3
E	Group+PDSI+PDSI^2
F	Group+PDSI+PDSI^2+Lag1+PDSI:Lag1+PDSI^2:Lag1
G	Group+PDSI+PDSI^2+Lag2+PDSI:Lag2+PDSI^2:Lag2
H	Group+PDSI+PDSI^2+Lag3+PDSI:Lag3+PDSI^2:Lag3
I	Group+Lag1
J	Group+Lag1+Lag1^2
K	Group+Lag2
L	Group+Lag2+Lag2^2
M	Group+Lag3
N	Group+Lag3+Lag3^2

Prairie Response to Drought

To determine differences in drought response, we conducted mixed-level, two-way, repeated measures ANCOVA using the prairie category and PDSI factors to explain NDVI. Incomplete blocks within the data (Figure 3.3) did not allow developing a model that simultaneously compared all categories together for this analysis. Therefore, we developed independent models using three categorical variables describing prairie types (community type, photosynthetic dominance, and restoration status), two response variables (TINDVI and MaxNDVI), and three covariates describing drought (AvgPDSI, MinPDSI, and AvgJnJlPDSI).

Since moisture does not generally have a strict linear relationship with vegetative growth, we tested quadratic models in addition to linear models for drought. To avoid correlation between the linear and quadratic terms, orthogonal polynomials were used. Interpretation of quadratic coefficients depends on both sign and absolute value. Negative quadratic coefficients indicate a reduction in the response variable at both low and high water availability, whereas positive coefficients indicate increases at both moisture levels. A higher absolute value of the quadratic coefficient indicates more curvature within the response curve, indicating a more rapid response. We used an arcsine transformation for MaxNDVI to attain normality within the MaxNDVI dataset (Ahrens et al. 1990).

Model Selection and Variation

We compared models using the Bayesian Information Criterion (BIC) (Lewis et al. 2010). We compared models for each combination of response variable (TINDVI or MaxNDVI) and prairie category (all prairies, community type, photosynthetic dominance, and restoration status) (Table 3.2). Once a best-fit model was determined for each combination, we then quantified the amount of variation explained by the fixed effects of the model using R^2.

Sensitivity of Analysis to Operator-Defined Parameters

Within our study there are two types of parameters that were defined by the operator: the depth of soil used for defining AWC in the PDSI calculations and the growing season length. To test the sensitivity of our results to these parameters, we re- analyzed the data while slightly altering these parameters. To examine the influence of soil depth on PDSI values, we

Figure 3.3. Distribution of prairies within each category. Vertical lines between bars separate the groupings used within (A) community type, (B) dominant photosynthetic pathway, and (C) restoration history. Numbers in parentheses next to each heading represents the sum for that group. Note that the "No Type" group represents prairies that fall outside the grassland region described in Olson *et al.* (2001).

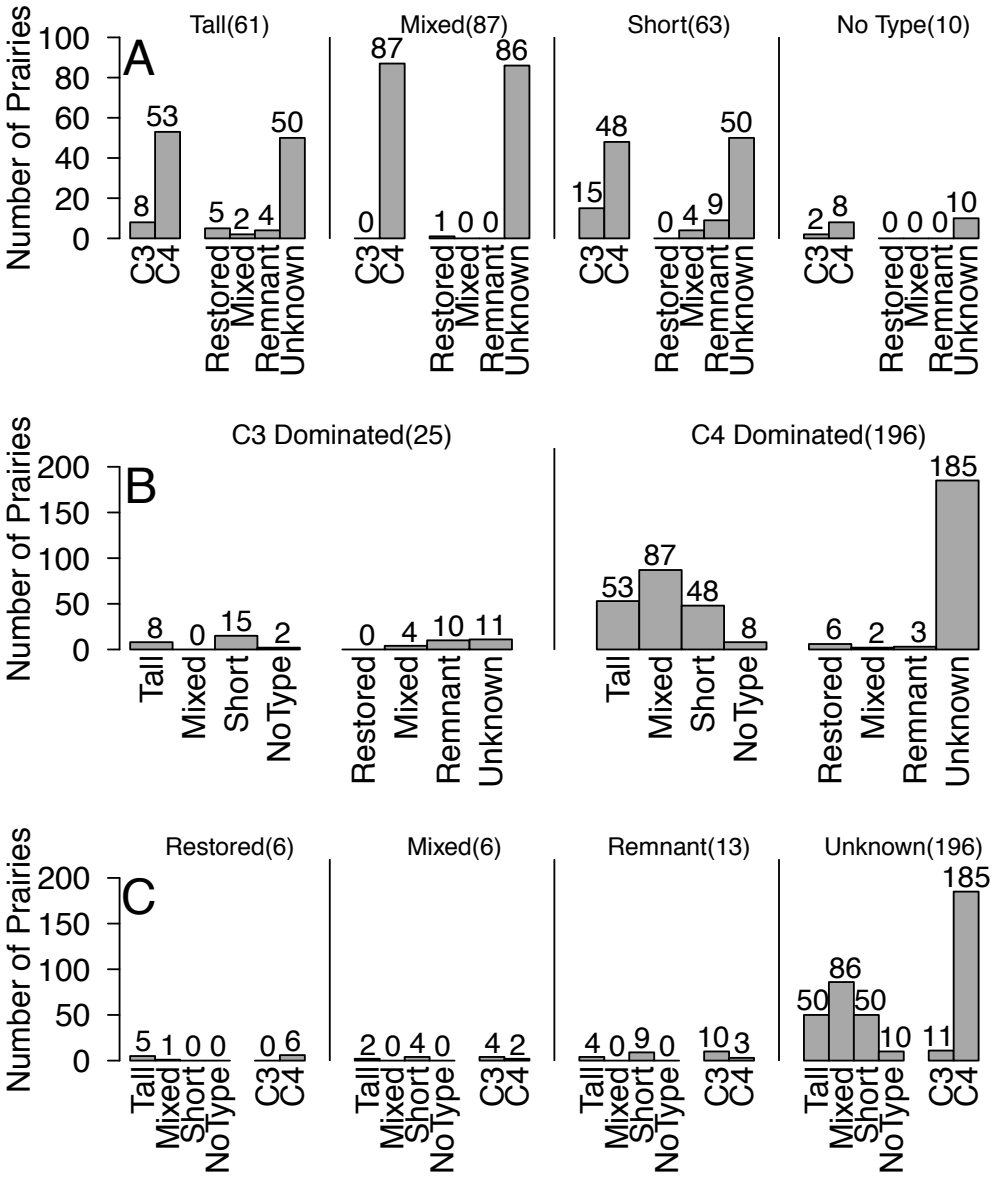

recalculated AWC using soil depths of 0.5 m, 1.0 m, 2.0 m, and 2.5 m, to compare to our initial setting of 1.5 m. In regards to the influence of the choice of growing season length, the calendar-based thresholds that we defined (Julian Days 89 & 273) were more likely to truncate the growing season than to include too much of the winter season. Therefore, we tested the sensitivity of PDSI and TINDVI calculations to growing season length by independently extending the beginning (start one month earlier) and end (end 3 months later) of the growing season.

III. Results

Differences in Overall NDVI dynamics

Community Types

MODIS time series captured expected differences in mean growing season NDVI among prairie communities (shortgrass, mixedgrass, and tallgrass). Averaged across all sites for the period 2000-2008, mean TINDVI (a measure of ANPP) in tallgrass prairie was about 30% greater than in shortgrass prairie, and about 12% greater than in mixed grass communities (ANCOVA: $p < 0.0001$, $df = 207$, $f = 90.39$, Figure 3.4a). MaxNDVI, quantifying maximum photosynthetic rates, was greatest in tallgrass prairies (0.83), about 24% greater than shortgrass prairie (0.63), and 11% greater than mixedgrass (0.74), and (ANCOVA: $p < 0.0001$, $df = 207$, $f = 88.63$, data not shown).

In inter-annual analysis, NDVI time series from tallgrass prairie locations exhibited less variability in both TINDVI and MaxNDVI values across years (TINDVI CV = 0.11 & MaxNDVI CV = 0.06) than did mixedgrass (TINDVI CV = 0.15 & MaxNDVI CV = 0.12) or shortgrass prairies (TINDVI CV = 0.23 & MaxNDVI CV = 0.21; Figure 3.2b), which

experienced the most. On average, shortgrass sites exhibited their MaxNDVI earlier in the year (Julian date 184) in comparison to mixedgrass (Julian date 198) and tallgrass (Julian date 191) communities (ANCOVA: $p < 0.0001$, $df = 207$, $f = 18.38$).

C_3- and C_4-Dominated Prairies

C_3- and C_4-dominated prairies exhibited similar mean TINDVI values (averaged for 2000-2008, $p = 0.30$, Figure 3.4b), but growing season peak values were 9% greater on average in C_3 prairies than in C_4 prairies (MaxNDVI = 0.80 vs 0.73; ANCOVA $p = 0.0032$, data not shown). The inter-annual variability of TINDVI and MaxNDVI was 33% and 50% lower in C_3 prairies in comparison to C_4-dominated prairies (TINDVI CV: 0.14 vs. 0.21 & MaxNDVI CV: 0.09 vs. 0.18). No differences were observed between C_3 and C_4 prairies in the timing of MaxNDVI (ANOVA $p = 0.45$).

Remnant and Restored Prairies

Limited availability of information about restoration histories constrained this comparison to only a small subsample of sites (25/221), primarily located in South Dakota and Illinois (Figure 3.2). However, the comparison provides useful preliminary information because regional comparisons of function between restored and remnant prairies over time have been so few. In this comparison, mean TINDVI of restored prairies was about 11% greater than in remnant prairies (Figure 3.4c, $p = 0.028$), and mean MaxNDVI was about 7% greater (0.86 vs 0.80 values, $p = 0.041$, data not show).

Figure 3.4. Average growing season NDVI by (A) community type, (B) photosynthetic pathway dominance, and (C) restoration history. Different letters above bars represent significant differences (Average precipitation received during drought (PDSI < -1), normal (PDSI between -1 and 1), and wet (PDSI > 1) conditions for (D) community type, (E) photosynthetic pathway dominance, and (F) restoration history. Data is based from estimates between 2000 and 2008.

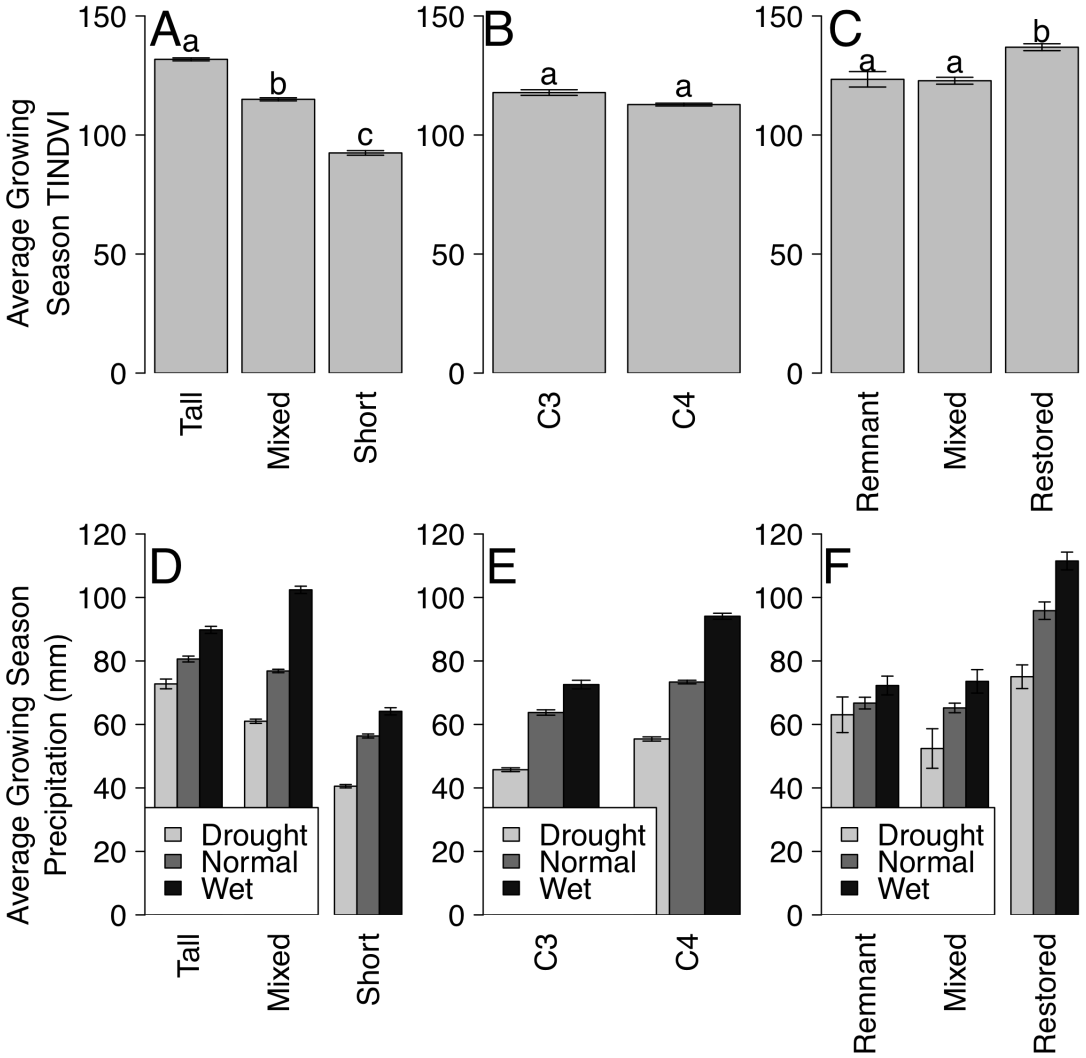

Because shortgrass prairie was not represented among the restored prairies (0/6 restorations vs 9/13 for remnants, Figure 3.3c), we also evaluated differences between restored and remnant sites within tallgrass prairies alone (N=11). Within this small subset, TINDVI and MaxNDVI were both slightly greater in restored prairies (TINDVI = 144.84 vs. 140.73; MaxNDVI = 0.88 vs. 0.86), but not significantly so ($p = 0.5414$ and 0.1412 respectively). Inter-annual variability was slightly higher for restored prairies for
TINDVI (CV 0.13 vs 0.12), but was 30% lower for MaxNDVI (CV 0.06 vs 0.09). No differences were observed between restored and remnant prairies in the timing of their MaxNDVI (ANOVA $p = 0.25$).

Prairie Response to Drought

Nature of Droughts 2000-2008

Inspection of PDSI times series within the northern Great Plains revealed three major droughts in the region. In 2000 and again in 2002, extreme growing season droughts (PDSI < -4) occurred in the western and southern portions of the study area (Nebraska). Another extreme drought occurred in 2006 within the eastern portion of the study area (Illinois and Wisconsin). In general, the western prairies encountered drier conditions during the study period, with PDSI values frequently below -2. Eastern prairies also frequently encountered drought during the growing season, but its magnitude was not as great as in the western prairies.

Table 3.3. The BIC values for models of TINDVI. Model structure is taken from Table 3.2. Groups are represented by the larger clusters in this table (Community type, Dominant Photosynthetic Pathway, and Restoration History). PDSI and the corresponding Lag factors are represented by the smaller clusters within this table (Avg = AvgPDSI,JnJl = JnJlPDSI, Min = MinPDSI). Lower values indicate a better fitting model. B = The best fitting model using BIC for a prairie group. * = Models within 10 units of the lowest BIC scores for a particular group.

	AllPrairies			Community Type			Photosynthetic Pathway			Restoration History		
Model	Avg	JnJl	Min	Avg	JnJl	Min	Avg	JnJl	Min	Avg	JnJl	Min
A	12730	12733	12794	11944	11916	11962	12735	12728	12783	1344	1347	1350
B	12490	12592	12591	11613 *	11748	11713	12471	12586	12572	1356	1366	1370
C	12667	12637	12723	11870	11847	11884	12689	12662	12734	1312B	1318 *	1316 *
D	12617	12691	12672	11819	11883	11856	12630	12699	12673	1369	1373	1370
E	12611	12584	12586	11863	11815	11804	12628	12604	12605	1348	1343	1353
F	12383B	12460	12391 *	11607B	11705	11661	12390B	12471	12421	1373	1347	1384
G	12597	12545	12583	11857	11797	11807	12623	12579	12614	1328	1338	1333
H	12507	12562	12508	11758	11808	11762	12533	12599	12545	1387	1384	1388
I	12785	12788	12836	11999	12024	12055	12758	12758	12808	1368	1367	1366
J	12720	12743	12673	11932	11983	11897	12719	12729	12685	1376	1375	1376
K	13192	13185	13201	12482	12484	12435	13194	13192	13196	1330	1342	1332
L	13160	13147	13164	12467	12467	12409	13175	13164	13174	1345	1357	1342
M	13018	13015	12978	12317	12316	12264	13024	13024	12982	1365	1362	1360
N	13023	13011	12971	12311	12318	12252	13032	13026	12987	1376	1369	1375

Table 3.4. The BIC values for models of MaxNDVI. Model structure is taken from Table 3.2. Groups are represented by the larger clusters in this table (Community type, Dominant Photosynthetic Pathway, and Restoration History). PDSI and the corresponding Lag factors are represented by the smaller clusters within this table (Avg = AvgPDSI, JnJl = JnJlPDSI,Min = MinPDSI). Lower values indicate a better fitting model. B = The best fitting model using BIC for a prairie group. * = Models within 10 units of the lowest BIC scores for a particular group.

	AllPrairies			Community Type			Photosynthetic Pathway			Restoration History		
Model	Avg	JnJl	Min	Avg	JnJl	Min	Avg	JnJl	Min	Avg	JnJl	Min
A	-3361	-3464	-3370	-3311	-3411	-3329	-3353	-3455	-3369	-359	-370	-353
B	-3389	-3477	-3392	-3415	-3478 *	-3421	-3370	-3460	-3382	-345	-353	-341
C	-3384	-3488	-3396	-3302	-3397	-3325	-3383	-3471	-3398	-350	-350	-344
D	-3378	-3483	-3387	-3351	-3427	-3380	-3370	-3488	-3381	-360	-380B	-353
E	-3391	-3522	-3451	-3307	-3428	-3370	-3388	-3514	-3439	-354	-359	-346
F	-3412	-3524	-3473	-3389	-3481B	-3415	-3391	-3512	-3455	-317	-328	-318
G	-3404	-3511	-3452	-3280	-3380	-3320	-3389	-3486	-3431	-326	-327	-326
H	-3400	-3537B	-3469	-3322	-3419	-3384	-3386	-3584B	-3448	-338	-360	-337
I	-3283	-3283	-3271	-3205	-3228	-3191	-3283	-3282	-3270	-351	-353	-350
J	-3305	-3327	-3331	-3254	-3280	-3296	-3303	-3330	-3323	-343	-347	-335
K	-3248	-3248	-3254	-3152	-3156	-3159	-3251	-3244	-3262	-356	-353	-354
L	-3263	-3268	-3273	-3147	-3151	-3165	-3251	-3257	-3264	-349	-345	-342
M	-3266	-3275	-3270	-3178	-3180	-3197	-3270	-3289	-3269	-366	-377 *	-365
N	-3259	-3268	-3263	-3163	-3164	-3185	-3264	-3286	-3257	-354	-366	-359

Table 3.5. The models that were used for analysis for each of the response by prairie group combinations. The variables in Response, Group, and Drought are the terms used within the selected model from Table 3.2.

Number	Response	Group	Drought	Model
1	TINDVI	Community	AvgPDSI	F
2	TINDVI	Photosynthesis	AvgPDSI	F
3	TINDVI	Restoration	AvgPDSI	C
4	MaxNDVI	Community	JnJlPDSI	F
5	MaxNDVI	Photosynthesis	JnJlPDSI	H
6	MaxNDVI	Restoration	JnJlPDSI	D

Model Selection

For all comparisons of prairies and response variables, the selected best-fit models (Tables 3.3, 3.4, and 3.5) included some factor accounting for soil moisture availability in previous years. However, the inclusion of previous moisture conditions did not increase the amount of explained variability (measured by R^2) within the fixed effects. AvgPDSI best described TINDVI relationships with drought whereas JnJlPDSI best described MaxNDVI dynamics. Soil moisture effects were most evident in analyses across prairie community types (TINDVI $R^2 = 0.47$ and MaxNDVI $R^2 = 0.45$) followed by analyses across restoration history (TINDVI $R^2 = 0.24$ and MaxNDVI $R^2 = 0.36$). Moisture effects were least evident in comparisons of C_3 and C_4 prairies (TINDVI $R^2 = 0.09$ and MaxNDVI $R^2 = 0.15$).

Community Type

Overall, ANCOVA results indicated that TINDVI-drought relationships differed among communities (ANCOVA $p = 0.0001$, $df = 207$, $f = 90.45$). Shortgrass prairies were most different in their responses from tallgrass and mixedgrass prairies (Table 3.6), and their TINDVI showed the greatest drought response, fluctuating nearly 40 TINDVI

Table 3.6. Summary statistics for the best fit models describing TINDVI and MaxNDVI. The column 'Num.' refers to the selected model number in Table 3.5. R^2 refers to the R^2 of the fixed effects. Different letters next to each coefficient indicate significantly different groups ($p < 0.05$).

Num.	Model R^2	Subject	Intersect	PDSI	$PDSI^2$	$PDSI_{(n-1)}$	$PDSI:PDSI_{(n-1)}$	$PDSI^2:PDSI_{(n-1)}$	Sub-model R^2
1	0.47	Tall	130.659 a	94.529 a	-25.788 a	-0.129 a	25.516 ab	-9.595 a	0
		Mixed	116.085 b	119.265 a	-26.444 a	-1.467 b	45.575 a	-10.426 a	0.09
		Short	93.346 c	232.171 b	-88.597 b	-2.079 c	18.171 b	-13.816 a	0.16
2	0.09	C3	111.574 a	554.495 a	-224.138 a	1.443 a	-79.88 a	1.447 a	0.18
		C4	113.086 a	154.745 b	-71.562 b	-1.37 b	37.235 b	-11.988 a	0.08
3	0.24	Restored	137.27 a	2.487 a	NA	-2.353 a	0.477 a	NA	0
		Mixed	124.104 a	3.437 a	NA	-2.488 a	-0.326 a	NA	0.4
		Remnant	124.427 a	2.084 a	NA	-1.865 a	-0.085 a	NA	0.1
4	0.45	Tall	0.98 a	0.635 a	-0.256 a	0.006 a	-0.063 a	-0.054 a	0.02
		Mixed	0.841 b	0.798 a	-0.559 a	-0.005 b	-0.002 a	-0.155 a	0.04
		Short	0.692 c	1.624 b	-0.406 a	-0.016 c	0.117 a	0.248 b	0.18
5	0.15	C3	0.956 a	1.458 a	-0.278 a	-0.021 a	-0.03 a	0.073 a	0.24
		C4	0.834 b	1.248 a	-0.738 a	-0.004 b	0.01 a	-0.191 a	0.11
6	0.36	Restored	1.048 a	0.014 a	NA	0.007 a	-0.002 a	NA	0.29
		Mixed	0.988 ab	0.005 a	NA	-0.023 b	0.005 a	NA	0.33
		Remnant	0.954 b	0.018 a	NA	-0.019 b	-0.001 a	NA	0.20

Figure 3.5. Modeled TINDVI response for different restoration histories using the best-fit model. Model has 'F' structure (Table 3.2) and uses average growing season PDSI (AvgPDSI) values as the current and previous drought (PDSI(n-1); previous year) prediction variables ($R^2 = 0.47$). Predictions and R^2 values are based on fixed effects of model.

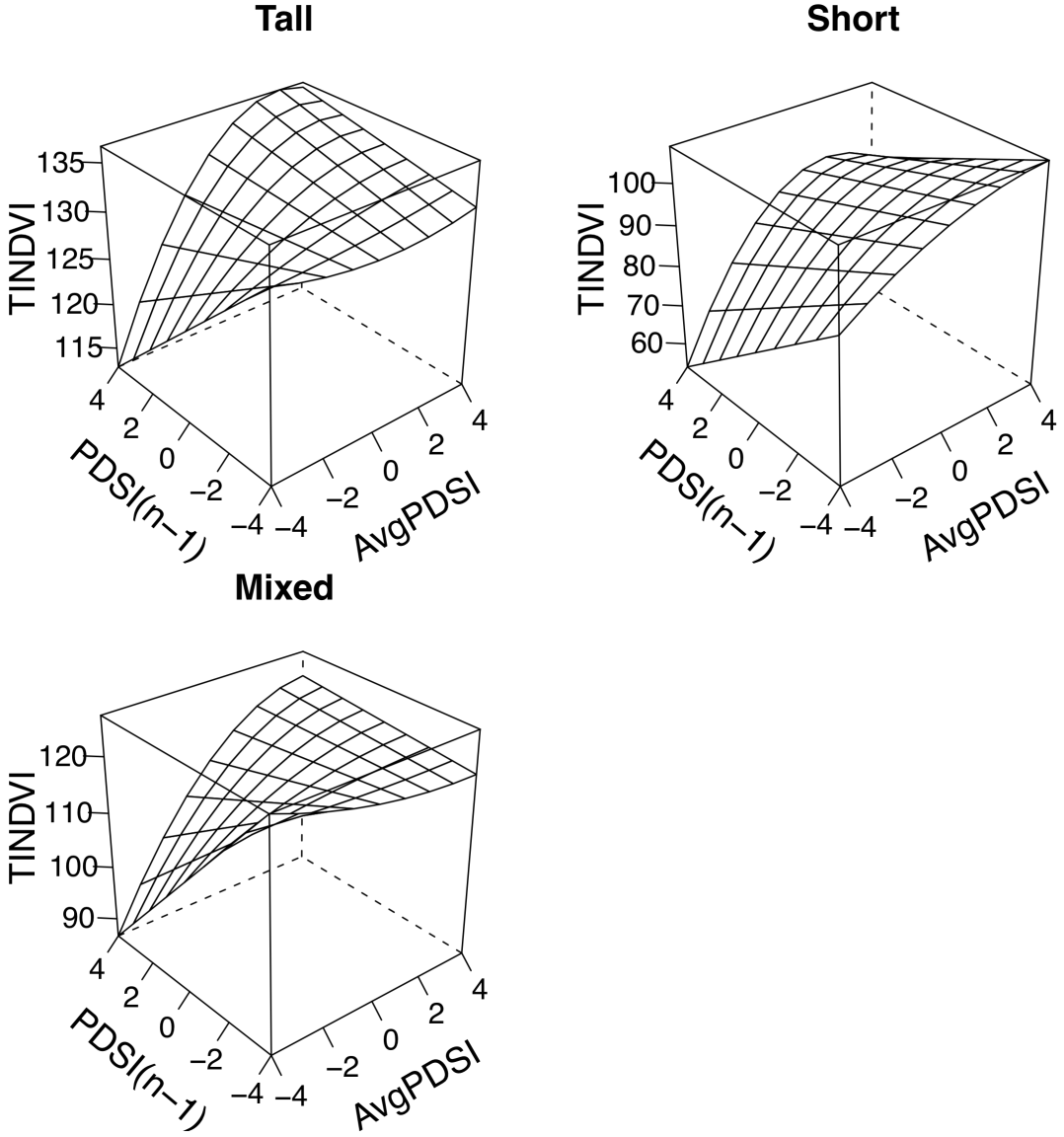

units from peak to depression (cf. tallgrass ~10 TINDVI units and mixedgrass ~ 30 TINDVI units).

For all community types, best-fit models indicated that TINDVI was lowest in a dry year that was preceded by a wet year (dry←wet) (Figure 3.5). TINDVI values for all other two-year patterns (including dry←dry, wet←dry, wet←wet) were notably greater. In tall and mixedgrass prairies, TINDVI values for the dry←dry, wet←dry, and wet←wet patterns were similar, whereas in shortgrass prairies TINDVI was greatest when a wet year followed a dry year (wet←dry, Figure 3.5).

The best-fit model of MaxNDVI likewise exhibited both dependency on previous year moisture conditions and differences among community types (ANCOVA $p = 0.0001$, $df = 207$, $f = 92.38$). The responses of shortgrass and tallgrass prairies differed most notably. When the previous year was wet, tallgrass prairies exhibited a curvilinear response to current year drought while shortgrass prairies displayed a linear response to current year drought (Figure 3.6). Of the three communities, shortgrass prairies showed the largest differences in MaxNDVI with a range ~ 0.25 MaxNDVI units (Figure 3.6)

C_3- and C_4-Dominated Prairies

Multi-year models of drought and TINDVI showed differential responses between dominant photosynthetic pathways (ANCOVA, $p = 0.1$, $df = 218$, $f = 2.73$). C_3- and C_4-dominated prairies shared similar responses for most multi-year combinations, but TINDVI for C_3-dominated prairies was significantly reduced when conditions were consistently dry (Figure 3.7). In comparison, TINDVI values for C_4-dominated prairies were reduced most when a dry year followed a wet year (dry←wet), as in the community type comparison (Figure 3.5).

Additionally, C_3-dominated prairies showed greater sensitivity to fluctuations in drought patterns, varying by as much as 80 TINDVI units (C_4-dominated prairies ~ 35 TINDVI units).

Although there was general similarity, some differences were observed between dominant photosynthetic pathways for the multi-year model of MaxNDVI (ANCOVA, $p = 0.001$, $df = 218$, $f = 11.22$). C_3 prairies exhibited a more linear relationship whereas the function describing C_4 dominated prairies were more curvilinear when previous moisture conditions were wet (Figure 3.8). For both community types, MaxNDVI was best predicted by drought conditions from the growing season three years previous.

Remnant and Restored Prairies

Best-fit models of responses of TINDVI and MaxNDVI in remnant and restored prairies described similar relationships to those seen in the analysis of community types. Restored prairies, which are mostly tallgrass prairies, resembled tallgrass prairie drought dynamics while remnant prairies, which are predominantly shortgrass prairies, resembled shortgrass prairie trends. For MaxNDVI, the pronounced curvature within community type models is due to the inclusion of the quadratic form of PDSI within the model, which is lacking in the management history models. Despite this difference between community types and management histories, the overall response surfaces share general similarities. Differences among management histories for MaxNDVI were limited to the influence of the previous year's drought, whereas none of the differences among restoration histories for TINDVI was statistically significant (Table 3.6). Additionally, the best-fit models for the comparison between remnant and restored prairies (Figures 3.9

Figure 3.6. Modeled MaxNDVI (arcsine transformed) response for different community types using the best-fit model. Model has 'F' structure (Table 3.2) and uses average June and July PDSI (JnJlPDSI) values as the current and previous drought (PDSI(n-1); previous year) prediction variables ($R^2 = 0.45$). Predictions and R^2 values are based on fixed effects of model.

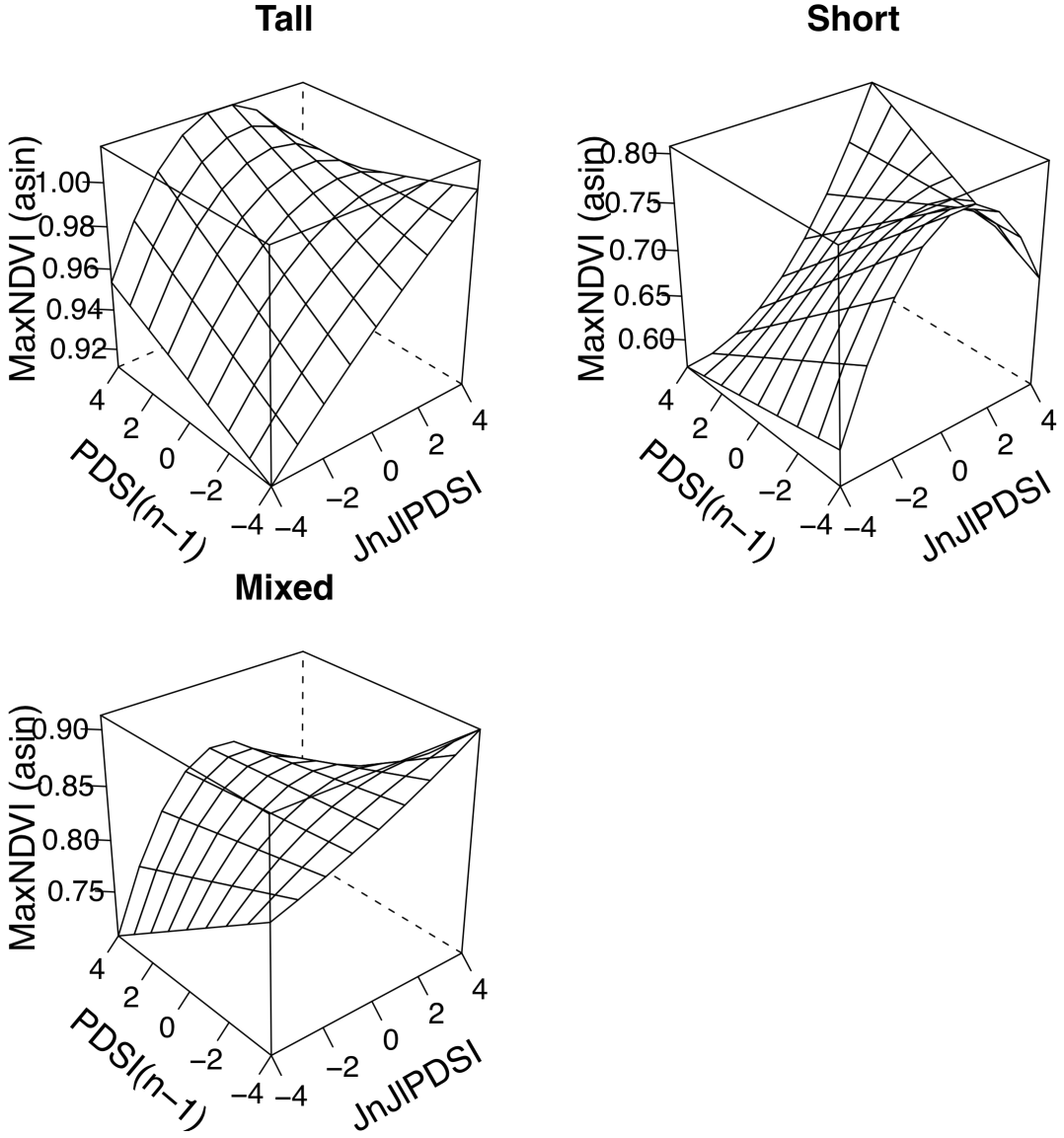

Figure 3.7. Modeled TINDVI response for different dominant photosynthetic pathways using the best-fit model. Model has 'F' structure (Table 3.2) and uses average growing season PDSI (AvgPDSI) values as the current and previous drought (PDSI(n-1); previous year) prediction variables ($R^2 = 0.09$). Predictions and R^2 values are based on fixed effects of model.

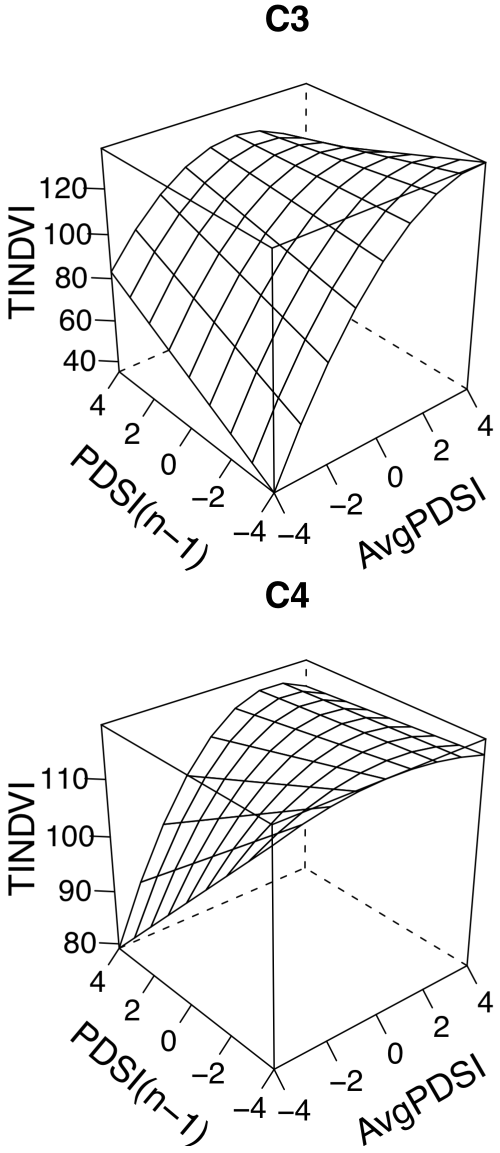

Figure 3.8. Modeled MaxNDVI (arcsine transformed) response for different dominant photosynthetic pathways using the best-fit model. Model has 'H' structure (Table 3.2) and uses average June and July PDSI (JnJlPDSI) values as the current and previous drought (PDSI(n-3); 3 years previous) prediction variables ($R^2 = 0.15$). Predictions and R^2 values are based on fixed effects of model.

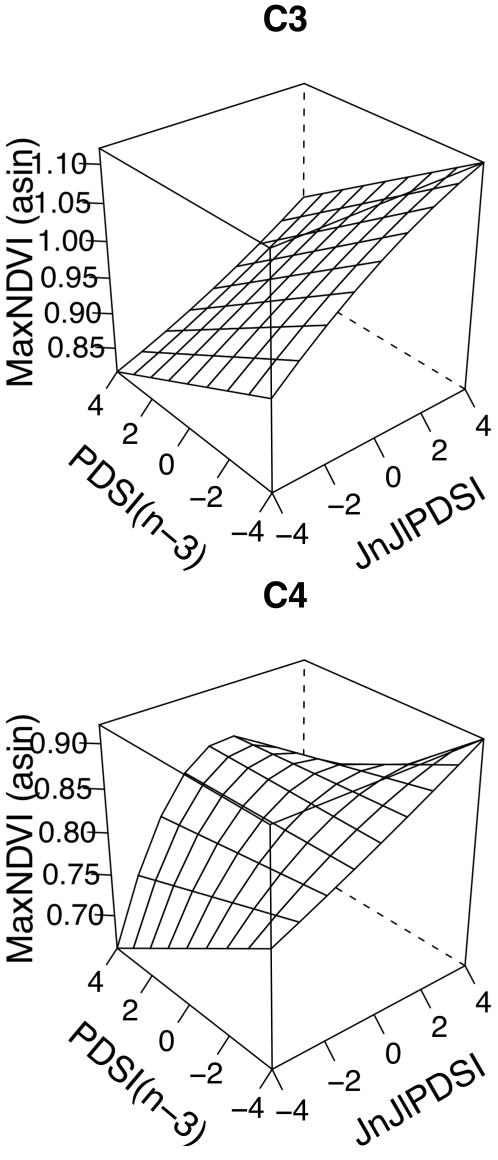

and 3.10) used drought conditions from two (TINDVI) and three (MaxNDVI) years previous.

Sensitivity of Analysis to Operator-Defined Parameters

The choice of soil depth used to calculate PDSI did not strongly influence predictions of relationships between TINDVI and soil moisture conditions. In our sensitivity tests, the TINDVI from each prairie group (except C_3-dominated prairies) continued to be the most reduced in a dry year that followed a wet year (dry←wet). Additionally, shortgrass and C_3-dominated prairies continued to be those most sensitive to soil moisture conditions.

However, the TINDVI analysis was sensitive to the choice of growing season length, particularly to the choice of the date for the growing season start (Figure 3.11); the choice of date for the end of the growing season was less consequential (Figure 3.12). If the growing season start is moved earlier in the year (e.g., from JD 89 to JD 49), three relationships are altered: (i) TINDVI in tallgrass and mixedgrass prairies is now substantially reduced when a wet year follows a dry year (wet←dry). (ii) Tallgrass prairies no longer exhibit a strong reduction in TINDVI when a dry year follows a wet year (dry←wet), although this pattern remains evident in mixedgrass communities. (iii) The TINDVI response of C_3–dominated prairies becomes more similar to that of C_4 prairies, with the greatest reduction in TINDVI evident in dry years following wet years (dry←wet).

Figure 3.9. Modeled TINDVI response for different restoration histories using the best-fit model. Model has 'C' structure (Table 3.2) and uses average growing season PDSI (AvgPDSI) values as the current and previous drought (PDSI(n-2); 2 years previous) prediction variables ($R^2 = 0.24$). Predictions and R^2 values are based on fixed effects of model.

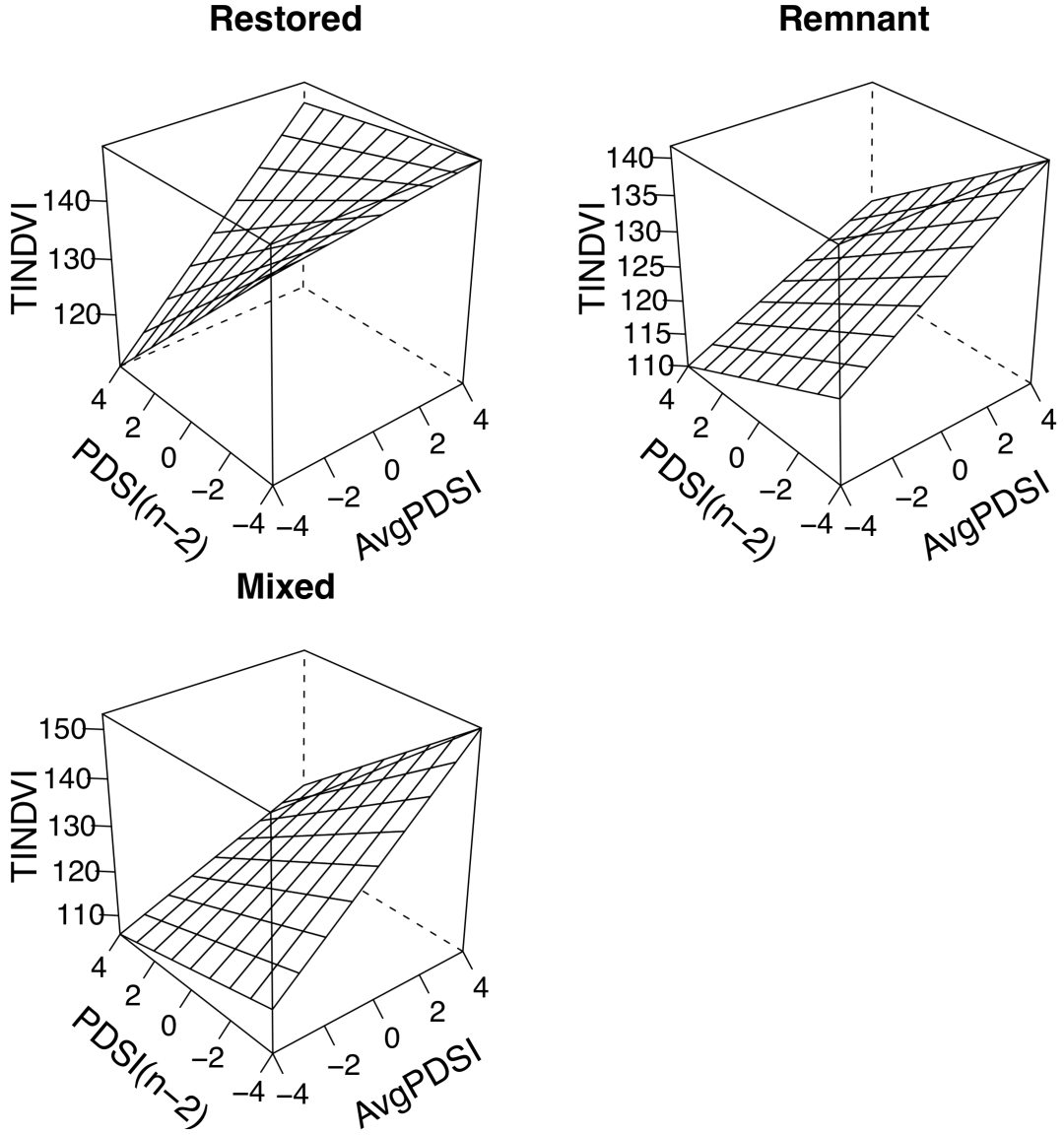

Figure 3.10. Modeled MaxNDVI (arcsine transformed) response for different restoration histories using the best-fit model. Model has 'D' structure (Table 3.2) and uses average June and July PDSI (JnJlPDSI) values as the current and previous drought (PDSI(n-3); 3 years previous) prediction variables ($R^2 = 0.36$). Predictions and R^2 values are based on fixed effects of model.

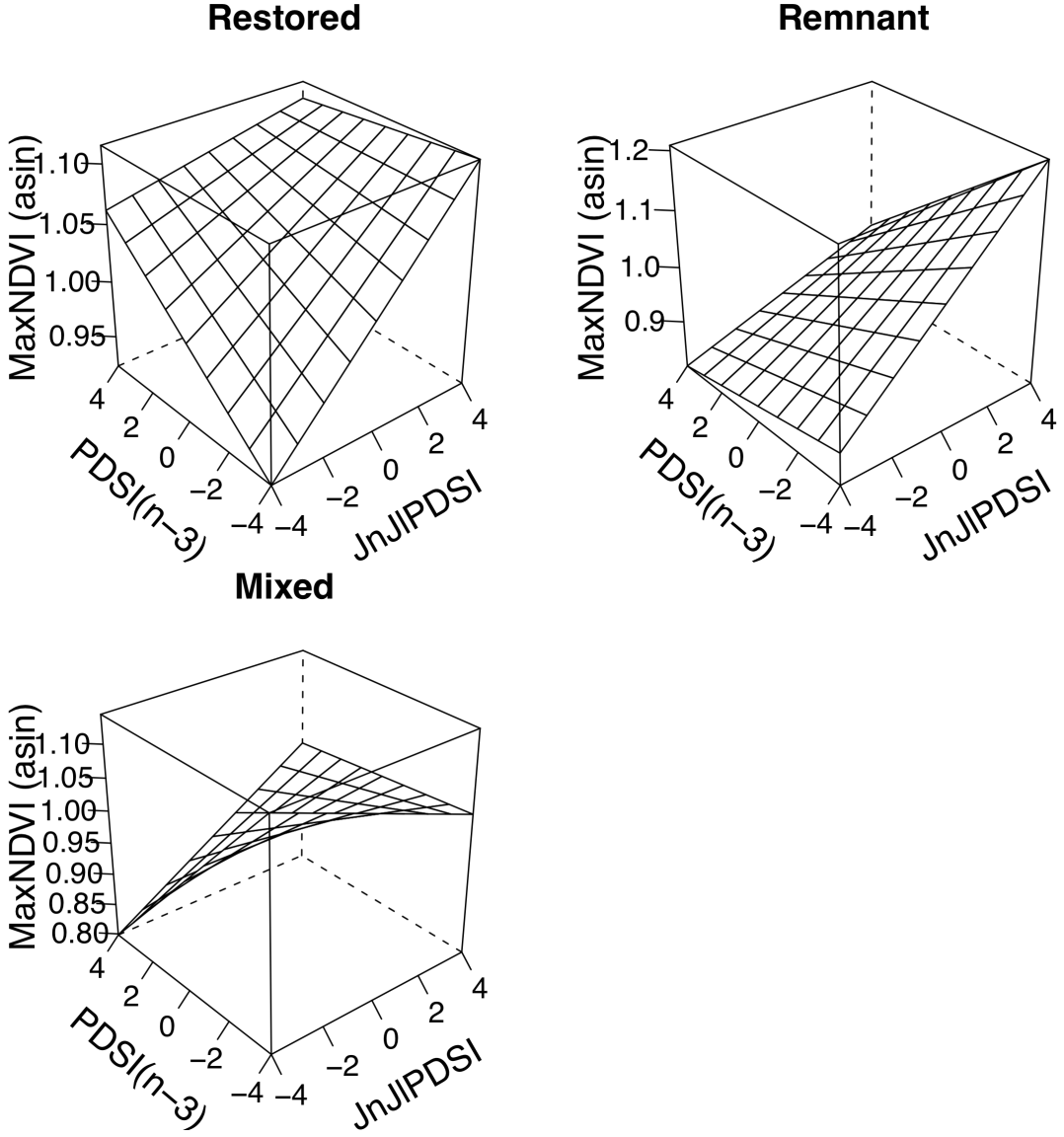

Figure 3.11. Sensitivity analysis of the effects of extending the start of the growing season. Growing season for this analysis encompasses Julian dates 49-273. Top row of graphs depict the three community types, the middle row of graphs depict the dominant photosynthetic pathway, and the bottom row of graphs depict the management histories.

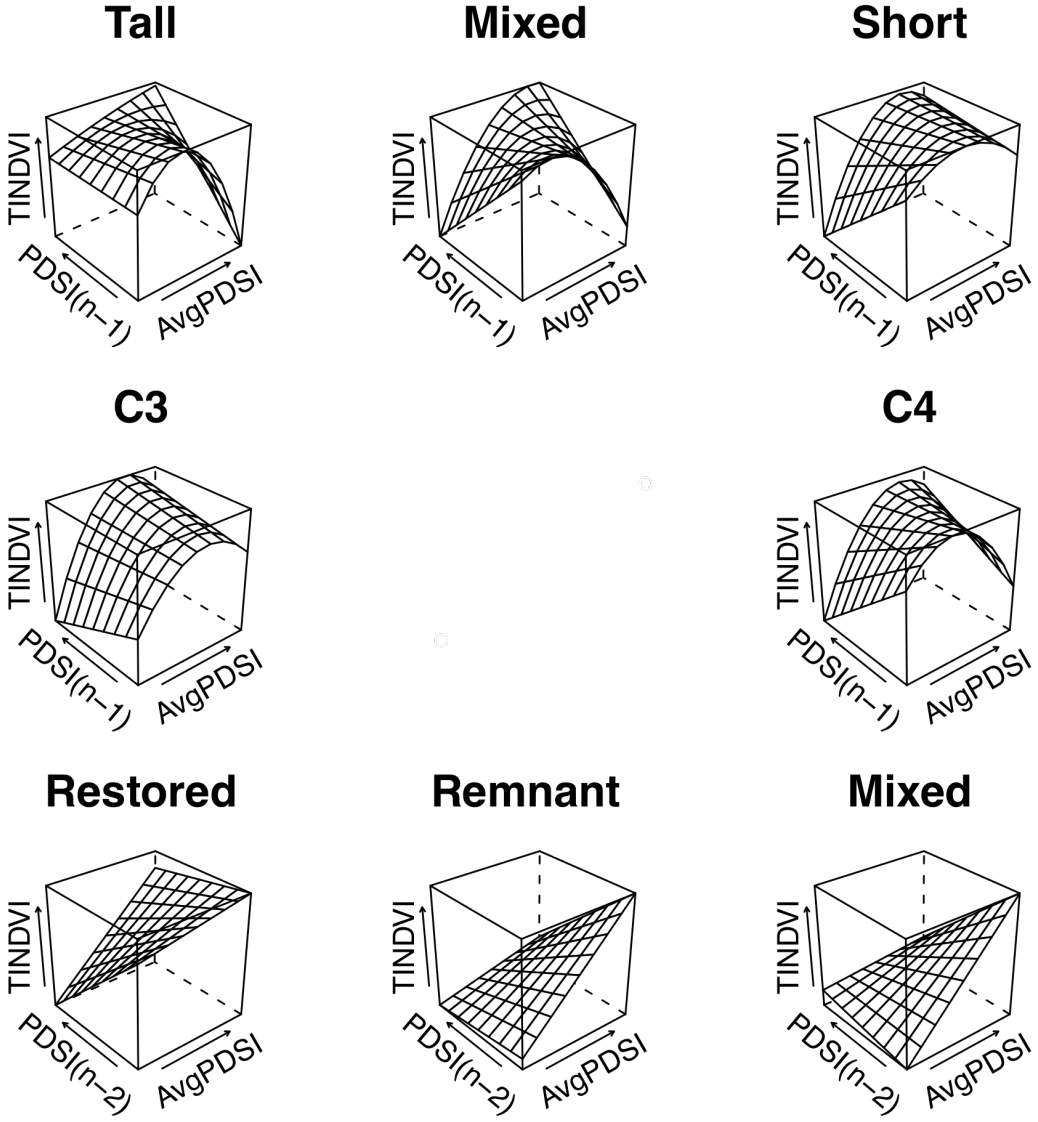

Figure 3.12. Sensitivity analysis of the effects of extending the end of the growing season. Growing season for this analysis encompasses Julian dates 89-365. Top row of graphs depict the three community types, the middle row of graphs depict the dominant photosynthetic pathway, and the bottom row of graphs depict the management histories.

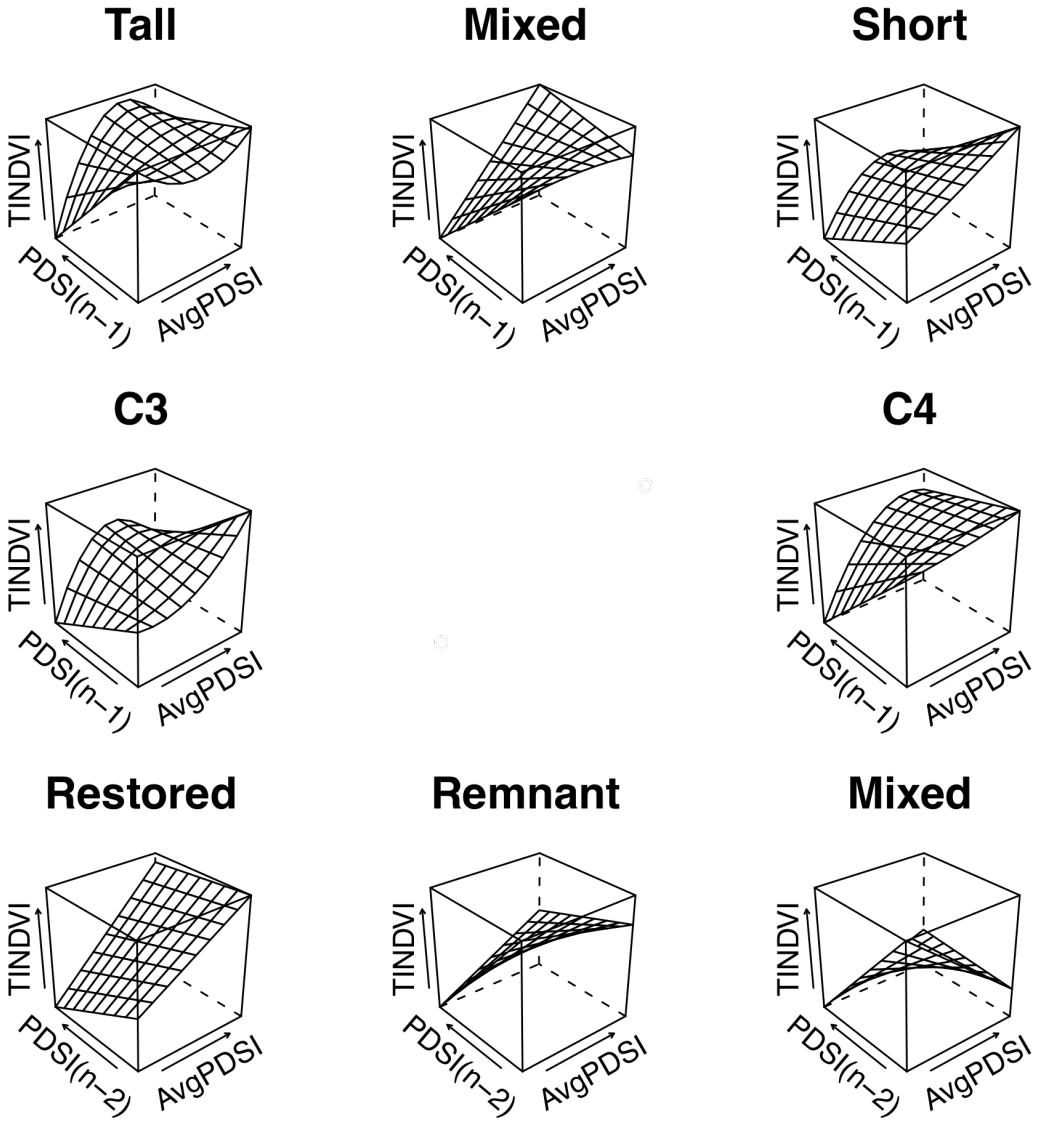

IV. Discussion

Our MODIS-based analysis of soil moisture sensitivity of northern Great Plains prairies found notable differences in drought responses among prairie communities and offers new insight into the dynamics of tallgrass prairies in particular. Consistent with previous field studies (Sala *et al.* 1992, Briggs & Knapp 1995, Edwards *et al.* 2010), we found the drought sensitivity of TINDVI (a surrogate for ANPP) to be greatest in shortgrass and C_3-dominated prairies. Best-fit models indicated that for all prairie types considered TINDVI and MaxNDVI were influenced by moisture conditions in preceding years, as has also been suggested by field studies (Smoliak 1986, Oesterheld *et al.* 2001, Yahdjian & Sala 2006, Smart *et al.* 2007). For most prairie categories, our analysis of TINDVI for JD 89-273 indicated that TINDVI was lowest in drought years that followed very wet years (dry←wet). This relationship was reversed (TINDVI lowest in wet←dry years) in tallgrass prairies when the growing season start was advanced from JD 89 (March 29/30) to JD 49 (February 18), but this reversal is likely to reflect artifactual depression of TINDVI values by spring snow cover. The finding that TINDVI is reduced in dry years following wet years (dry←wet) is most striking in tallgrass prairies, which typically are less moisture-limited and thus show less direct responsiveness to inter-annual variation in soil moisture. The phenomenon observed here thus may represent feedbacks to productivity mediated through secondary factors such as detritus and/or pathogens that accumulate in preceding wet years and exert effects that cannot be entirely overcome when the following year is dry. Our findings differ from field studies in more westerly shortgrass prairies in which increased production in a previous year increases production in the current year irrespective of current year moisture dynamics (Oesterheld *et al.* 2001). The capabilities of recent remote sensing systems, such as that used in this study, provide new ways of quantifying spatio-temporal dynamics of

ecosystems and may detect relationships not previously evident in field studies or coarser resolution remote sensing analyses.

Prairie Group Response Comparison

C_4-Dominated Prairies Are More Drought Tolerant Than C_3-Dominated Prairies

Differences in drought sensitivity between C_3- and C_4-dominated prairies agreed with expectations. C_4 plants perform better than C_3 plants under higher temperatures when there is more evaporative demand because they concentrate CO_2 within bundle sheath cells which allows rubisco to bind more efficiently (Chaves *et al.* 2003, Edwards *et al.* 2010). As a result better water use efficiency is typically found within C_4 plants. Spatial studies of C_3 and C_4 species distribution also indicate that C_4 vegetation tends to outcompete C_3 plants in southern areas of the U.S., where there is a potentially higher moisture demand during the growing season (Teeri & Stowe 1976, Ehleringer 1978, Epstein *et al.* 1997). Within our study, we observed more variability in the TINDVI of C_3-dominated prairies, indicating a higher sensitivity to drought and correspond with the studies mentioned above.

Dry Prairies Are More Responsive to Drought Conditions

Our analysis confirms the relative sensitivities of prairie communities to drought that have been observed in previous studies. Of the three prairie types (shortgrass, mixedgrass, and tallgrass), shortgrass prairie biomass has been observed to be the most sensitive to availability of precipitation (Lauenroth & Sala 1992, Smart *et al.* 2007). However, temporal variance in tallgrass prairie ANPP has not previously been associated strongly with precipitation fluctuations except in cases in which management practices or topographical position allow precipitation to

be the limiting factor in this system (Briggs & Knapp 1995). Although our data suggest that tallgrass prairie TINDVI is sensitive to drought, the tallgrass prairies showed less sensitivity than shortgrass prairies.

Although shortgrass prairies were the most sensitive to changes in soil moisture, this does not necessarily mean that these prairies will be reduced in their extent if soil moisture becomes drier in the future. Reducing ANPP during times of insufficient water availability may be an adaptive trait of shortgrass vegetation rather than an indication that this community is unable to cope with dry environmental conditions.

Potential Differences in TINDVI Between Prairies with Different Management Histories

Our comparison of restored and remnant prairies, which was limited by sample size, did not detect significant differences in mean levels of TINDVI or drought responses. Both prairie types exhibited a large decrease in TINDVI when a drought year followed a wet year (as seen in the community types) and the fluctuation of TINDVI values was relatively similar between both management groups. Larger management datasets are needed to permit more definitive comparisons.

Multi-year Studies Uncover Relationships Between ANPP and Available Moisture

Single Year Relationships Between Grassland and Precipitation

Previous studies have demonstrated that current year precipitation can be an important determining factor for ANPP for some grassland community types. Shortgrass prairie ANPP has been correlated with growing season and annual precipitation (Lauenroth & Sala 1992) whereas the ANPP of tallgrass prairies is often not significantly correlated with precipitation unless the

site is upland with a continued history of burning (Briggs & Knapp 1995, Knapp *et al.* 2006). Grassland communities in regions beyond the North American Great Plains also seem to exhibit variability in their relationship with precipitation. For example, the Patagonian steppe is similar to the shortgrass prairie both in its climate and in its ANPP response to annual precipitation (Lauenroth & Sala 1992, Yahdjian & Sala 2006), whereas production in South African grasslands was more closely linked to precipitation than that in tallgrass prairies despite the systems' similar climates (Knapp *et al.* 2006).

Drought Response Depends on Drought Conditions of Previous Year

Our best fit models indicated that the relationship between TINDVI and drought within the current year depends on the moisture conditions from a previous year. The most consistent pattern among the modeled TINDVI of prairies in our study was the prediction that the lowest TINDVI values occurring during dry years that follow wet years (dry ← wet). This pattern was observed in all prairie groups except for C_3-dominated prairies, which showed diminished TINDVI values during two consecutive dry years. Extension of the growing season start slightly altered these patterns. For example, C_3-dominated prairies then manifested the pattern of dry ← wet TINDVI depression and tallgrass prairies exhibited an alternate response (TINDVI most reduced when wet ← dry). Despite these group-specific responses, the general pattern that TINDVI is most reduced in dry years following wet years (dry ← wet) was most prevalent throughout our analyses.

Reduction of TINDVI in dry years following wet years (dry ← wet) differs from the pattern that Oesterheld *et al.* (2001) identified in an analysis of field measurements in western shortgrass prairie. In this system, production was slightly greater in years following wet years

(wet/dry ← wet), and somewhat reduced following a dry year (wet/dry ← dry). This difference in results may reflect either a difference in the systems studied or a methodological difference in vegetation sampling. Biomass estimates from Oesterheld *et al.*'s study included both standing live and dead biomass, which may artificially inflate the biomass production for the current year by also including that from the previous year. In contrast, standing litter in our study was more likely to reduce NDVI values by obscuring green growth.

In tallgrass prairies, our analysis indicates that TINDVI is relatively unchanged unless a dry year follows a wet year (dry ← wet), in which case TINDVI drops significantly. This finding agrees in many respects with previous studies that have found little direct connection between productivity and precipitation fluctuations in tallgrass prairie under most conditions. For example, single-year studies within tallgrass prairies in Kansas demonstrate only weak correlations between biomass and precipitation unless the site is upland and annually burned (Briggs & Knapp 1995, Knapp *et al.* 2006). Likewise, when Oesterheld *et al.* (2001) re-examined a time series of data from the same tallgrass prairie site, they found no significant relationships between production and precipitation. The much expanded spatial extent of our dataset (61 tallgrass prairies considered) allows our analysis to uncover an otherwise hidden relationship within tallgrass prairies that is evident only for the specific case of the dry ← wet pattern; further extension of the MODIS time series would permit more robust tests of this relationship.

The reduction of TINDVI in dry years following wet (dry ← wet) may be explained by indirect negative feedbacks resulting from moisture-sensitive processes such as accumulation of detritus or pathogens. During wet years, for example, a thicker layer of detritus may accumulate which can potentially reduce vegetation growth the following year by i) blocking

photosynthetically active radiation (Knapp 1984a), ii) reducing photosynthesis rates (Knapp & Gilliam 1985), and iii) reducing the amount of inorganic nitrogen supplied by precipitation (Seastedt 1985, Knapp & Seastedt 1986). Alternatively, wet years may promote disease, such as root infections. Widespread pathogen pressure in a previous year would then further strain vegetation during a year of severe drought and could contribute to the drop in TINDVI observed across prairie types.

Our study monitors changes in soil moisture availability as opposed to changes in precipitation alone. Soil moisture availability is a better indicator of water stress within plants than precipitation, as documented in studies that have manipulated precipitation timing while maintaining overall precipitation amounts. Results indicate that precipitation timing has considerable influence on the amount of soil moisture available to plants throughout the growing season (Heisler-White *et al.* 2009) and demonstrates the need to consider soil moisture availability measurements. However, most studies of grassland response to moisture have considered only precipitation values and none have explicitly analyzed the link between soil moisture and ANPP. For instance, Flanagan and Johnson (2005) graphically showed the similarities in pattern between biomass and soil moisture patterns but did not statistically link these two variables.

Additionally, our study also showed that our multiyear patterns for TINDVI within tallgrass prairies depends upon how the growing season is defined. In order to determine which of these growing season scenarios (start JD = 49 versus start JD = 89) is more likely, it is necessary to compare slices of the current year trends within the three dimensional models in our study to the single year studies that currently dominate the literature. When the previous year is wet, the extended growing season start (JD = 49) exhibits no relationship between TINDVI and

PDSI whereas the growing season start for the main analysis (JD = 89) produces a positive relationship (Figures 3.5 & 3.11). Alternatively, when the previous year is dry, the extended growing season start (JD = 49) exhibits a negative relationship, whereas the growing season start used in the main analysis (JD = 89) exhibits no relationship. The relationship between tallgrass vegetation production and precipitation observed in other studies shows a positive relationship with these variables (Briggs & Knapp 1995), which supports using the results from the main analysis (JD = 89) as opposed to the extended growing season (JD = 49). The difference between the two growing season analyses may be response from including more snow contaminated NDVI when extending the growing season start.

Qualifications

The TINDVI results of this analysis were determined to be sensitive to the date of the start of the growing season was declared. The differences observed among individual prairie groups in their response to changing the start of the growing season suggest that an algorithm is needed to determine growing season for each individual prairie for each year. However, when we initially attempted to use several of the currently used algorithms (Reed *et al.* 1994, Studer *et al.* 2007) to do this, much of the growing season was cut off for prairies that had a bi-modal NDVI curve. The method we used, detecting the portion of the NDVI curve that was uninfluenced by large drops in NDVI, obtains the main vegetation response during the growing season while minimizing the effects of snow cover. This procedure is likely the ideal method to use until an algorithm is determined to consistently detect the major vegetation changes within these grassland systems.

Next Steps

Our broad-area MODIS- based analysis has uncovered evidence of a multi-year dependency between soil moisture and NPP within tallgrass prairies that has not been previously detected in field studies or coarse-grain remote sensing analysis. Previous field studies that have considered multiyear relationships of moisture and ANPP have focused on few locations and the vegetation sampling done within those studies were conducted in relatively small plots, whereas previous remote sensing studies were conducted at spatial resolutions that are too coarse to permit consideration of the tallgrass prairie fragments we identified. We recommend further study of the multi-year dependencies identified, perhaps in field studies that consider multiple tallgrass prairie sites and monitor both precipitation and soil moisture.

REFERENCES

V. References

Ahrens WH, Cox DJ, Budhwar G (1990) Use of the arcsine and square root transformations for subjectively determined percentage data. *Weed Science,* **38**, 452-458.

Beck PSA, Atzberger C, Høgda KA, Johansen B, Skidmore AK (2006) Improved monitoring of vegetation dynamics at very high latitudes: A new method using MODIS NDVI. *Remote Sensing of Environment,* **100**, 321-334.

Bradford JB, Lauenroth WK, Burke IC, Paruelo JM (2006) The Influence of climate, soils, weather, and land use on primary production and biomass seasonality in the U.S. Great Plains. *Ecosystems,* **9**, 934-950.

Briggs JM, Knapp AK (1995) Interannual variability in primary production in tallgrass prairie: climate, soil moisture, topographic position, and fire as detminants of aboveground biomass. *American Journal of Botany,* **82**, 1024-1030.

Canadell J, Jackson RB, Ehleringer JR, Mooney HA, O.E.Sala, Schulze ED (1996) Maximum rooting depth of vegetation types at the global scale. *Oecologia,* **108**, 583-595.

Chaves MM, Maroco JP, Pereira JS (2003) Understanding plant responses to drought- from genes to the whole plant. *Functional Plant Biology,* **30**, 239-264.

Daly C (2009) *PRISM Climate Group,* Oregon State University, Accessed on May, 2009 at www.prism.oregonstate.edu.

Daly C, Gibson W, Doggett M, Smith J, Taylor G (2004) Up-to-date monthly climate maps for the conterminous United States. In: *14th American Meteorological Society Conference on Applied Climatology.* American Meteorological Society, Seattle, WA.

Daly C, Neilson RP, Phillips DL (1994) A statistical-topographic model for mapping climatological precipitation over mountainous terrain. *Journal of Applied Meteorology,* **33**, 140-158.

Dye DG, Tucker CJ (2003) Seasonality and trends of snow-cover, vegetation index, and temperature in northern Eurasia. *Geophysical Research Letters,* **30**, 58-51:58-53.

Edwards EJ, Osborne CP, Strömberg CAE, Smith SA, Consortium CG (2010) The origins of C_4 grasslands: Integrating evolutionary and ecosystem science. *Science,* **328**, 587-591.

Ehleringer JR (1978) Implications of quantum yield differences on the distributions of C_3 and C_4 grasses. *Oecologia,* **31**, 255-267.

Epstein HE, Lauenroth WK, Burke IC, Coffin DP (1996) Ecological responses of dominant grasses along two climatic gradients in the Great Plains of the United States. *Journal of Vegetation Science,* **7**, 777-788.

Epstein HE, Lauenroth WK, Burke IC, Coffin DP (1997) Productivity patterns of C_3 and C_4 functional types in the U.S. Great Plains. *Ecology,* **78**, 722-731.

Flanagan LB, Johnson BG (2005) Interacting effects of temperature, soil moisture and plant biomass production on ecosystem respiration in a northern temperate grassland. *Agricultural and Forest Meteorology,* **130**, 237-253.

Gelman A, Hill J (2009) *Data analysis using regression and multilevel/hierarchical models.* Cambridge University Press, New York.

Goward SN, Tucker CJ, Dye DG (1985) North American vegetation patterns observed with the NOAA-7 Advanced Very High Resolution Radiometer. *Vegetatio,* **64**, 3-14.

Grosso SD, Parton W, Stohlgren T*, et al.* (2008) Global potential net primary production predicted from vegetation class, precipitation, and temperature. *Ecology,* **89**, 2117-2126.

Heisler-White JL, Blair JM, Kelly EF, Harmoney K, Knapp AK (2009) Contingent productivity responses to more extreme rainfall regimes across a grassland biome. *Global Change Biology,* **15**, 2894-2904.

Hird JN, McDermid GJ (2009) Noise reduction of NDVI time series: An empirical comparison of selected techniques. *Remote Sensing of Environment,* **113**, 248-258.

Huete A, Justice C, Liu H (1994) Development of vegetation and soil indices for MODIS-EOS. *Remote Sensing of Environment,* **49**, 224-234.

ITT (2009). ITT Visual Imaging Solutions, www.ittvis.com, Boulder, CO.

Ji L, Peters AJ (2003) Assessing vegetation response to drought in the northern Great Plains using vegetation and drought indices. *Remote Sensing of Environment,* **87**, 85-98.

Knapp AK (1984a) Post-burn differences in solar radiation, leaf temperature and water stress influencing production in lowland tallgrass prairie. *American Journal of Botany,* **71**, 220-227.

Knapp AK (1984b) Water relations and growth of three grasses during wet and drought years in a tallgrass prairie. *Oecologia,* **65**, 35-43.

Knapp AK, Burns CE, Fynn RWS, Kirkman KP, Morris CD, Smith MD (2006) Convergence and contingency in production-precipitation relationships in North American and South African C_4 grasslands. *Oecologia,* **149**, 456-464.

Knapp AK, Gilliam FS (1985) Response of Andropogon gerardii (Poaceae) to fire-induced high vs low irradiance environments in tallgrass prairie: Leaf structure and photosynthetic pigments. *American Journal of Botany,* **72**, 1668-1671.

Knapp AK, Seastedt TR (1986) Detritus accumulation limits productivity of tallgrass prairie. *BioScience,* **36**, 662-668.

Knight JF, Lunetta RS, Ediriwickrema J, Khorram S (2006) Regional scale land cover characterization using MODIS NDVI 250m multi-temporal imagery: A phenology-based approach. *GIScience and Remote Sensing,* **43**, 1-23.

Lauenroth WK, Sala OE (1992) Long-term forage production of North American short-grass steppe. *Ecological Applications,* **2**, 397-403.

Lewis F, Butler A, Gilbert L (2010) A unified approach to model selection using the likelihood ratio test. *Methods in Ecology & Evolution,*

Merlo J (2003) Multilevel analytical approaches in social epidemiology: Measures of health variation compared with traditional measures of association. *Journal of Epidemiology and Community Health,* **57**, 550-552.

Noss RF, III ETL, Scott JM (1995) *Endangered ecosystems of the United States: A preliminary assessment of loss and degredation.* United States Geological Survey, Washington D.C.

Noss RF, Peters RL (1995) *Endangered ecosystems: A status report on America's vanishing habitat and wildlife.* Defenders of Wildlife, Washington, DC.

Oesterheld M, Loreti J, Semmartin M, Sala OE (2001) Inter-annual variation in primary-production of semi-arid grassland related to previous year production *Journal of Vegetation Science,* **12**, 137-142.

Olson DM, Dinerstein E, Wikramanayake ED*, et al.* (2001) Terrestrial ecoregions of the world: A new map of life on Earth. *BioScience,* **51**, 933-938.

Palmer WC (1965) *Meteorological drought. Research paper No. 45.* United States Department of Commerce, Washington D. C. .

Paruelo JM, Epstein HE, Lauenroth WK, Burke IC (1997) ANPP estimates from NDVI for the central grassland region of the United States. *Ecology,* **78**, 953-958.

Pinheiro JC, Bates DM (2000) *Mixed-effects models in S and S-PLUS.* Springer-Verlag, New York.

Reed BC, Brown JF, VanderZee D, Loveland TR, Merchant JW, Ohlen DO (1994) Measuring phenological variability from satellite imagery *Journal of Vegetation Science,* **5**, 703-714.

Rouse JW, Haas RH, Deering DW, Schell JA (1973) *Monitoring the vernal advancement and retrogradation (green wave effect) of natural vegetation.* National Aeronautics and Space Administration, Greenbelt, Maryland.

Sala OE, Lauenroth WK, Parton WJ (1992) Long-term soil water dynamics in the shortgrass steppe. *Ecology,* **73**, 1175-1181.

Sala OE, Parton WJ, Joyce LA, Lauenroth WK (1988a) Primary production of the central grassland region of the United States. *Ecology,* **69**, 40-45.

Sala OE, Parton WJ, Joyce LA, Lauenroth WK (1988b) Primary production of the central grassland region of the United States *Ecology,* **69**, 40-45.

Salomonson VV, Barnes W, Masuoka EJ (2006) Introduction to MODIS and an overview of associated activities. In: *Earth Science Satellite Remote Sensing* Vol. Vol 1: Science and Instruments (eds Qu JJ, Gao W, Kafatos M, Murphy RE, Salomonson VV). Tsinghua University Press & Springer-Verlag GmbH, Beijing & Berlin Heidelberg.

Samson F, Knopf F (1994) Prairie conservation in North America. *BioScience,* **44**, 418-421.

Seastedt TR (1985) Canopy interception of nitrogen in bulk precipitation by annually burned and unburned tallgrass prairie. *Oecologia,* **66**, 88-92.

Sellers PJ (1987) Canopy reflectance, photosynthesis, and transpiration. II. The role of biophysics in the linearity of their interdependence. *Remote Sensing of Environment,* **21**, 143-183.

Sellers PJ, Berry JA, Collatz GJ, Field CB, Hall FG (1992) Canopy reflectance, photosynthesis and transpiration. III. A re-analysis using improved leaf models and a new canopy integration scheme. *Remote Sensing of Environment,* **42**, 187-216.

Sims PL, Risser PG (2000) Grasslands. In: *North American Terrestrial Vegetation* (eds Barbour MG, Billings WD), pp. 323-356. Cambridge University Press, Cambridge.

Smart AJ, Dunn BH, Johnson PS, Xu L, Gates RN (2007) Using weather data to explain herbage yield on three Great Plains plant communities. *Rangeland Ecology and Management,* **60**, 146-153.

Smoliak S (1956) Influence of climatic conditions on forage production of shortgrass rangeland. *Journal of Range Management,* **9**, 89-91.

Smoliak S (1986) Influence of climatic conditions on production of *Stipa-Bouteloua* prairie over a 50-year period. *Journal of Range Management,* **39**, 100-103.

Studer S, Stöckli R, Appenzeller C, Vidale PL (2007) A comparative study of satellite and ground-based phenology. *International Journal of Biometeorology,* **51**, 405-414.

Team RDC (2009). R Foundation for Statistical Computing, Vienna, Austria.

Teeri JA, Stowe LG (1976) Climatic patterns and the distribution of C_4 grasses in North America. *Oecologia,* **23**, 1-12.

Tieszen LL, Reed BC, Bliss NB, Wylie BK, DeJong DD (1997) NDVI, C_3 and C_4 production, and distributions in Great Plains grassland land cover classes. *Ecological Applications,* **7**, 59-78.

Transeau EN (1935) The prairie peninsula. *Ecology,* **16**, 423-437.

Tucker C, Justice C, Prince S (1986) Monitoring the grasslands of the Sahel: 1984-1985. *International Journal of Remote Sensing,* **7**, 1571-1582.

Tucker CJ (1979) Red and photographic infrared linear combinations for monitoring vegetation. *Remote Sensing of Environment,* **8**, 127-150.

USDA SSS (2009) Soil Survey Geographic (SSURGO) Database for the United States. United States Department of Agriculture, Natural Resources Conservation Service. Available online at http://soildatamart.nrcs.usda.gov.

Vermote EF, Vermeulen A (1999) *Atmospheric correction algorithm: Spectral reflectances (MOD09).* National Aeronautics and Space Administration, Greenbelt, Maryland

vonFischer JC, Tieszen LL, Schimel DS (2008) Climate controls on C_3 vs. C_4 productivity in North American grasslands from carbon isotope composition of soil organic matter. *Global Change Biology,* **14**, 1141-1155.

Weaver JE (1954) *North American prairie.* Johnsen Publishing Company, Lincoln, NE.

Weaver JE, Albertson FW (1956) *Grasslands of the Great Plains: Their nature and use.* Johnsen Publishing, Lincoln.

Weber L, Nkemdirim L (1998) Palmer's drought indices revisited. *Geografiska Annaler. Series A, Physical Geography,* **80**, 153-172.

Wolfe RE (2006) MODIS geolocation. In: *Earth Science Satellite Remote Sensing* Vol. Vol 1: Science and Instruments (eds Qu JJ, Gao W, Kafatos M, Murphy RE, Salomonson VV), pp. 50-73. Tsinghua University Press & Springer-Verlag GmbH, Beijing & Berlin Heidelberg

Woodward FI, Lomas MR (2004) Vegetation dynamics - simulating responses to climatic change. *Biological Reviews,* **79**, 643-670.

Woodward FI, Lomas MR, Kelly CK (2004) Global climate and the distribution of plant biomes. *Philosophical Transactions of the Royal Society of London,* **239**, 1465-1476.

Xiao J, Moody A (2004) Photosynthetic activity of US biomes: responses to the spatial variability of seasonality of precipitation and temperature. *Global Change Biology,* **10**, 437-451.

Yahdjian L, Sala OE (2006) Vegetation structure constrains primary production response to water availability in the patagonian steppe. *Ecology,* **87**, 952-962.

Yang L, Wylie BK, Tieszen LL, Reed BC (1998) An analysis of relationships among climate forcing and time-integrated NDVI of grasslands over the U.S. northern and central Great Plains. *Remote Sensing of Environment,* **65**, 25-37.

APPENDIX

APPENDIX A

Appendix A acknowledges all the people, offices, and organizations that helped in producing the data to create the Prairie Spatial Database described in Chapter 2. The data in this appendix is presented as a series of tables.

Table A.1. Organizations contacted in the development of the Prairie Spatial Database.

Agencies
Ann Arbor City Parks
Army Corps of Engineers
Audubon
Augustana College
Ducks Unlimited
Fisheries and Wildlife Service
Illinois Department of Natural Resources
Indiana Department of Natural Resources
Indiana University
Institute of Natural Resource Sustainability
Iowa Department of Natural Resources
Iowa Natural Heritage Foundation
Iowa Prairie Network
Iowa State University
Michigan Department of Natural Resources
Michigan Department of Technology Management and Budget
Michigan Natural Features Inventory
Michigan State University
Minnesota Department of Natural Resources
National Park Service
Natural Resources Trust
Nebraska Department of Natural Resources
Nebraska Game and Park Commission
Nebraska Wildlife Federation
North Dakota Game and Fish Department
North Dakota State Government
Ohio Department of Natural Resources
Ohio Office of Information Technology
Ohio Metroparks
Pheasants Forever
Prairie Plains Resource Institute
South Dakota Department of Environment and Natural Resources
South Dakota State University
Southern Illinois University
The Nature Conservancy

Table A.1 (cont'd)

The Prairie Enthusiasts
United States Department of Agriculture (USDA)
United States Geological Service (USGS)
University of Michigan
University of North Dakota
University of Wisconsin
Wisconsin Department of Natural Resources
Wisconsin State Cartographer's Office

Table A.2. Table of agencies and offices that were contacted during the development of the Prairie Spatial Database. NWR stands for National Wildlife Refuge.

State	Agency	Office
IL	Army Corps of Engineers	Rock Island
IL	Augustana College	Dziadyk Lab
IL	Department of Natural Resources	Main Office
IL	Department of Natural Resources	Natural History Survey
IL	Department of Natural Resources	Office of Reality and Environment
IL	Fisheries and Wildlife Service	Upper Mississippi River NWR
IL	Fisheries and Wildlife Service	Savanna District
IL	Fisheries and Wildlife Service	Lost Mound
IL	Fisheries and Wildlife Service	Crab Orchard NWR
IL	Institute of Natural Resource Sustainability	Illinois Natural History Survey
IL	National Park Service	Lincoln Home National Historic Site
IL	Pheasants Forever	Main Office
IL	Southern Illinois University	Baer Lab
IL	The Nature Conservancy	Chicago Office
IL	The Nature Conservancy	Nachusa Grasslands
IL	United States Department of Agriculture (USDA)	Natural Resource Conservation Service
IL	United States Geological Service (USGS)	Main Office
IN	Department of Natural Resources	Parks and Reservoirs - Indianapolis Central Office
IN	Fisheries and Wildlife Service	Main Office
IN	Indiana University	Letsinger Lab
IN	Pheasants Forever	Main Office
IN	The Nature Conservancy	Indiana Field Office
IN	United States Geological Service (USGS)	Main Office
IA	Department of Natural Resources	Iowa Department of Natural Resources
IA	Fisheries and Wildlife Service	Rock Island Field Office - Ecological Services
IA	Fisheries and Wildlife Service	Neal Smith National Wildlife Refuge
IA	Fisheries and Wildlife Service	McGregor Office
IA	Iowa Natural Heritage Foundation	Iowa Natural Heritage Foundation

Table A.2 (cont'd)

IA	Iowa Prairie Network	Iowa Prairie Network
IA	Iowa State University	GIS Support and Research Facility
IA	Iowa State University	Otis Lab
IA	Iowa State University	Debinski Lab
IA	National Park Service	Effigy Mounds National Monument
IA	National Park Service	Herbert Hoover National Historic Site
IA	Pheasants Forever	Main Office
IA	The Nature Conservancy	Iowa Office
IA	United States Geological Service (USGS)	Iowa Geological Survey
MI	Ann Arbor City Parks	Parks and Recreation
MI	Fisheries and Wildlife Service	Shiawassee Office
MI	Fisheries and Wildlife Service	Kirtland Warbler Refuge
MI	Fisheries and Wildlife Service	Michigan Islands NWR
MI	Fisheries and Wildlife Service	Harbor Island NWR
MI	Fisheries and Wildlife Service	Whitefish Point NWR
MI	Fisheries and Wildlife Service	Seney NWR
MI	Fisheries and Wildlife Service	Huron NWR
MI	Fisheries and Wildlife Service	Detroit River IWR
MI	Michigan Department of Technology Management and Budget	Center for Geographic Information
MI	Michigan Natural Features Inventory	Michigan Natural Features Inventory
MI	Michigan State University	Remote Sensing and Geographic Information Science Research and Outreach Services
MI	National Park Service	Sleeping Bear Dunes National Lakeshore
MI	The Nature Conservancy	West Michigan Field Office
MI	The Nature Conservancy	East Michigan Field Office
MI	The Nature Conservancy	Shiawassee River Program Office
MI	University of Michigan	Spatial and Numeric Data (SAND) Services
MN	Army Corps of Engineers	Environmental and Economic Resources Branch
MN	Department of Natural Resources	Minnesota DNR

Table A.2 (cont'd)

MN	Department of Natural Resources	Minnesota DNR Data Deli
MN	Fisheries and Wildlife Service	Upper Mississippi National Wildlife and Fish Refuge Headquarters
MN	Fisheries and Wildlife Service	Habitat and Population Evaluation Team
MN	Fisheries and Wildlife Service	Northern Tallgrass Prairie NWR
MN	Fisheries and Wildlife Service	Realty Division
MN	National Park Service	Pipestone National Monument
MN	Pheasants Forever	Main Office
MN	The Nature Conservancy	Minnesota Office
MN	The Nature Conservancy	Northern Tallgrass Prairie Ecoregion Office
MN	The Nature Conservancy	Tallgrass Aspen Parkland Office
NE	Audubon	Wachiska
NE	Department of Natural Resources	Nebraska DNR GIS Processing
NE	Fisheries and Wildlife Service	Nebraska Ecological Services Field Office
NE	Fisheries and Wildlife Service	Nebraska Fisheries and Wildlife Office
NE	Game and Park Commission	Nebraska Game and Park Commission
NE	National Park Service	Scotts Bluff National Monument
NE	National Park Service	Niobrara National Scenic River
NE	National Park Service	Scotts Bluff National Monument
NE	National Park Service	Agate Fossil Beds National Monument
NE	National Park Service	Homestead National Monument
NE	National Park Service	Niobrara National Scenic River
NE	Nebraska Wildlife Federation	Nebraska Wildlife Federation
NE	Pheasants Forever	Main Office
NE	Prairie Plains Resource Institute	Prairie Plains Resource Institute
NE	The Nature Conservancy	Nebraska Field Office
ND	Fisheries and Wildlife Service	Arrowwood Wildlife Refuge
ND	Fisheries and Wildlife Service	Audubon NWR
ND	Fisheries and Wildlife Service	Chase Lake Prarie Project
ND	Fisheries and Wildlife Service	Dakota Prairie Grasslands
ND	Fisheries and Wildlife Service	J. Clark Salyer NWR
ND	Fisheries and Wildlife Service	Long Lake NWR
ND	Fisheries and Wildlife Service	Lostwood NWR
ND	Fisheries and Wildlife Service	Tewaukon NWR
ND	Fisheries and Wildlife Service	Upper Souris NWR

Table A.2 (cont'd)

ND	Fisheries and Wildlife Service	Chase Lake Prairie Project Wetland
ND	Fisheries and Wildlife Service	Kulm Wetland Management District
ND	Fisheries and Wildlife Service	Crosby Wetland Management District
ND	Fisheries and Wildlife Service	Habitat and Population Evaluation Team
ND	Fisheries and Wildlife Service	Devils Lake Wetland Management District
ND	Fisheries and Wildlife Service	Private Lands
ND	Fisheries and Wildlife Service	Regional Office
ND	Game and Fish Department	Game and Fish Main Office
ND	National Park Service	Devils Lake State Park
ND	National Park Service	Ft. Abraham Lincoln State Park
ND	National Park Service	Fort Union Trading Post NHS
ND	National Park Service	Knife River Indian Villages NHS
ND	National Park Service	Theodore Roosevelt National Park - North
ND	National Park Service	Theodore Roosevelt National Park - South
ND	National Park Service	Inventory and Monitoring Program
ND	Natural Resources Trust	North Dakota Natural Resources Trust
ND	North Dakota State Government	North Dakota GIS
ND	Pheasants Forever	Main Office
ND	The Nature Conservancy	North Dakota Office
ND	United States Geological Service	Northern Prairie Wildlife Research Center
ND	University of North Dakota	Beeri Lab
OH	Department of Natural Resources	Geographic Information Management Systems
OH	Department of Natural Resources	Ohio DNR Division of Wildlife
OH	Department of Natural Resources	Division of Natural Areas and Preserves
OH	Department of Natural Resources	Ohio Natural Heritage Program
OH	National Park Service	Cuyahoga Valley National Park
OH	National Park Service	Hopewell Culture National Historical Park
OH	Office of Information Technology	GIS Support Center
OH	Ohio Metroparks	Columbus Metroparks
OH	Ohio Metroparks	Toledo Metroparks
OH	Pheasants Forever	Main Office
OH	The Nature Conservancy	Ohio Chapter
OH	The Nature Conservancy	Oak Openings Region
SD	Department of Environment and Natural Resources	Main Office

Table A.2 (cont'd)

SD	Ducks Unlimited	Goebel Ranch
SD	Fisheries and Wildlife Service	Wildlife Division
SD	Fisheries and Wildlife Service	Parks and Recreation
SD	Fisheries and Wildlife Service	Custer State Park
SD	Fisheries and Wildlife Service	Newton Hills State Park
SD	National Park Service	Badlands National Park
SD	National Park Service	Wind Cave National Park
SD	National Park Service	Spirit Mound Historic Prairie
SD	Pheasants Forever	Main Office
SD	South Dakota State University	O'Neill Lab
SD	South Dakota State University	Gritzner Lab
SD	South Dakota State University	Larson Lab
SD	South Dakota State University	Toelstrup Lab
SD	The Nature Conservancy	Samuel H. Ordway Prairie
SD	The Nature Conservancy	Prairie Coteau Office
SD	The Nature Conservancy	South Dakota Nature Conservancy
SD	The Nature Conservancy	Western Dakotas Program
SD	United States Geological Service (USGS)	Earth Resource Observation & Science (EROS) center
WI	Department of Natural Resources	Wisconsin DNR
WI	Department of Natural Resources	GIS Services
WI	Fisheries and Wildlife Service	Gravel Island NWR
WI	Fisheries and Wildlife Service	Horicon NWR
WI	Fisheries and Wildlife Service	Necedah NWR
WI	Fisheries and Wildlife Service	Trempealeau NWR
WI	Fisheries and Wildlife Service	Fox River NWR
WI	Fisheries and Wildlife Service	St. Croix NWR
WI	Fisheries and Wildlife Service	Whittlesey Creek NWR
WI	Fisheries and Wildlife Service	La Crosse
WI	Fisheries and Wildlife Service	Madison
WI	Pheasants Forever	Main Office
WI	State Cartographer's Office	Wisconsin Land Information Clearinghouse
WI	The Nature Conservancy	Madison Field Office
WI	The Prairie Enthusiasts	The Prairie Enthusiasts

Table A.2 (cont'd)

WI	United States Geological Service (USGS)	Upper Midwest Environmental Sciences Center
WI	University of Wisconsin	GIS and Geospatial Data
WI	University of Wisconsin	Herbarium

Table A.3. Table of contacts who provided assistance during the development of the Prairie Spatial Database.

State	Agency	Name
IL	Army Corps of Engineers	Chuck Gerdes
IL	Augustana College	Bohdan Dziadyk
IL	Department of Natural Resources	John Buhnerkempe
IL	Department of Natural Resources	William Handel
IL	Department of Natural Resources	Mary Honer
IL	Department of Natural Resources	Tara Kieninger
IL	Department of Natural Resources	Dan Sallee
IL	Department of Natural Resources	Diane Szafoni
IL	Department of Natural Resources	Renee Thakali
IL	Department of Natural Resources	John Wilker
IL	Department of Natural Resources	Sheryl Oliver
IL	Fisheries and Wildlife Service	Alan Anderson
IL	Fisheries and Wildlife Service	Ed Britton
IL	Fisheries and Wildlife Service	Deb Green
IL	Fisheries and Wildlife Service	Thomas Palmer
IL	National Park Service	Randy Heidorn
IL	National Park Service	Bill McClain
IL	National Park Service	Tim Townsend
IL	National Park Service	Karen Witter
IL	Pheasants Forever	Matt Bradshaw
IL	Southern Illinois University	Sara Baer
IL	The Nature Conservancy	Bill Kleiman
IL	The Nature Conservancy	Karen Tharp
IL	The Nature Conservancy	Josh Thompson
IL	The Nature Conservancy	Jeff Walk
IL	United States Department of Agriculture (USDA)	Terry Conway
IL	University Illinois Urbana Champain	Diane Szafoni
IL	Unknown	Don Gardner
IN	Department of Natural Resources	Ron Hellmich
IN	Indiana University	Sally Letsinger
IN	Pheasants Forever	Brian Grossman
IN	The Nature Conservancy	Chip O'leary
IN	The Nature Conservancy	Helen Rowe
IN	The Nature Conservancy	Chip Sutton

Table A.3 (cont'd)

IA	Department of Natural Resources	Kathryne Clark
IA	Department of Natural Resources	Casey Kohrt
IA	Department of Natural Resources	John Pearson
IA	Fisheries and Wildlife Service	Pauline Drobney
IA	Fisheries and Wildlife Service	Mary Mitchell
IA	Fisheries and Wildlife Service	Karen Viste-Sparkman
IA	Fisheries and Wildlife Service	Tim Yager
IA	Iowa Natural Heritage Foundation	Kathryne Clark
IA	Iowa Prairie Network	Judy Felder
IA	Iowa Prairie Network	MJ Hatfield
IA	Iowa Prairie Network	Cindy Hildebrand
IA	Iowa Prairie Network	Jean Wiedenheft
IA	Iowa State University	Diane Debinski
IA	Iowa State University	Rolf Koford
IA	Iowa State University	Dave Otis
IA	National Park Service	Ken Block
IA	National Park Service	Sherry Middlemis-Brown
IA	National Park Service	Rodney Rovang
IA	Pheasants Forever	Tom Fuller
IA	Pheasants Forever	John Linquist
IA	Pheasants Forever	Dave Van Waus
IA	The Nature Conservancy	Jennifer Filipiak
MI	Ann Arbor City Parks	Dave Borneman
MI	Fisheries and Wildlife Service	Greg Corace
MI	Fisheries and Wildlife Service	Jim Dastyck
MI	Fisheries and Wildlife Service	Steve Dushane
MI	Fisheries and Wildlife Service	Steve Kahl
MI	Fisheries and Wildlife Service	Dave Olson
MI	Michigan Department of Technology Management and Budget	Everrett Root
MI	Michigan Natural Features Inventory	Ed Schools
MI	National Park Service	Ken Hyde
MI	The Nature Conservancy	Rebecca Hagerman
MI	The Nature Conservancy	Mike Parker
MI	The Nature Conservancy	Lara Rainbolt
MI	University of Michigan	Jen Green

Table A.3 (cont'd)

MN	Army Corps of Engineers	Dan Wilcox
MN	Department of Natural Resources	Jason Eckstein
MN	Department of Natural Resources	Jaime Edwards
MN	Department of Natural Resources	Jason Garmes
MN	Department of Natural Resources	Lisa Joyal
MN	Department of Natural Resources	Matt Mecklinberg
MN	Fisheries and Wildlife Service	Alice Hanley
MN	Fisheries and Wildlife Service	Rex Johnson
MN	Fisheries and Wildlife Service	Sean Killen
MN	Fisheries and Wildlife Service	Eric Nelson
MN	Fisheries and Wildlife Service	Lisa Pember
MN	Fisheries and Wildlife Service	Mary Stefanski
MN	Fisheries and Wildlife Service	Tom Worthington
MN	Pheasants Forever	Aaron Kuehl
MN	Pheasants Forever	Eran Sandquist
MN	The Nature Conservancy	Erik Anthonisen
MN	The Nature Conservancy	Meredith Cornett
MN	The Nature Conservancy	Sandi Edmunds
MN	The Nature Conservancy	Rich Johnson
NE	Audubon	Tim Knott
NE	Audubon	Arnold Mendenhall
NE	Audubon	Arlys Reitan
NE	Audubon	Ernie Rousek
NE	Department of Natural Resources	Tim Hermansen
NE	Department of Natural Resources	Gerry Steinauer
NE	Department of Natural Resources	Mahendra Bansal
NE	Department of Natural Resources	Kim Menke
NE	Fisheries and Wildlife Service	Andy Bishop
NE	Fisheries and Wildlife Service	Jarren Kuipers
NE	Game and Park Commission	Emily Munter
NE	Game and Park Commission	Rick Schneider
NE	Game and Park Commission	Rachel Simpson
NE	Game and Park Commission	Gerry Steinauer
NE	Game and Park Commission	Scott Taylor
NE	National Park Service	Jesse Bolli
NE	National Park Service	Robert Manasek

Table A.3 (cont'd)

NE	National Park Service	Lil Mansfield
NE	National Park Service	David Peitz
NE	National Park Service	Pam Sprenkle
NE	National Park Service	Stephen Wilson
NE	Nebraska Wildlife Federation	Penny Perkins
NE	Pheasants Forever	Keith Brus
NE	Pheasants Forever	Drew Larsen
NE	Prairie Plains Resource Institute	Mike Bullerman
NE	Prairie Plains Resource Institute	Bill Whitney
NE	The Nature Conservancy	Chris Helzer
NE	The Nature Conservancy	Mardell Jasnowski
ND	Fisheries and Wildlife Service	Dave Azure
ND	Fisheries and Wildlife Service	Cami Dixon
ND	Fisheries and Wildlife Service	Mike Estey
ND	Fisheries and Wildlife Service	Todd Grant
ND	Fisheries and Wildlife Service	Tim Kessler
ND	Fisheries and Wildlife Service	Wayne King
ND	Fisheries and Wildlife Service	Chuck Loesch
ND	Fisheries and Wildlife Service	Connie Mueller
ND	Fisheries and Wildlife Service	Scott Ralston
ND	Fisheries and Wildlife Service	Ron Reynolds
ND	Fisheries and Wildlife Service	Phil Sjursen
ND	Fisheries and Wildlife Service	Kevin Willis
ND	Game and Fish Department	Scott Peterson
ND	National Park Service	Marsha
ND	National Park Service	Andy Banta
ND	National Park Service	Sean Dekeyser
ND	National Park Service	Taryn Flesjer
ND	National Park Service	Bob Gibson
ND	National Park Service	Scott Ralston
ND	National Park Service	Chad Sexton
ND	National Park Service	Rod Skullsky
ND	Natural Resources Trust	Terry Albee
ND	Natural Resources Trust	Karen Kreil
ND	North Dakota State Government	Bob Nutsch
ND	North Dakota State Government	Rebecca Phillips

Table A.3 (cont'd)

ND	Pheasants Forever	Dan Hare
ND	The Nature Conservancy	Rich Johnson
ND	The Nature Conservancy	Eric Rosenquist
ND	United States Geological Service	Larry Igl
ND	United States Geological Service	David Mushet
ND	United States Geological Service	Larry Strong
ND	University of North Dakota	Ofer Beeri
Ohio	Department of Natural Resources	Jennifer
Ohio	Department of Natural Resources	Tom Arbour
Ohio	Department of Natural Resources	David Crecelius
Ohio	Department of Natural Resources	Rick Gardner
Ohio	Department of Natural Resources	Jennifer Windus
Ohio	National Park Service	Anthony Gareau
Ohio	National Park Service	Darlene Kelback
Ohio	National Park Service	Carrie Morrow
Ohio	National Park Service	Tim Schetter
Ohio	Pheasants Forever	Jim Inglis
SD	Ducks Unlimited	Bruce Toay
SD	Fisheries and Wildlife Service	Gary Brundige
SD	Fisheries and Wildlife Service	Dave Ode
SD	Fisheries and Wildlife Service	Eric Stouwe
SD	National Park Service	Eddie Childers
SD	National Park Service	Marie Curtin
SD	National Park Service	Brian Kenner
SD	National Park Service	Eric VanderStouwe
SD	Pheasants Forever	Ben Bigalke
SD	South Dakota State Government	Erik Nelson
SD	South Dakota State University	Janet Gritzner
SD	South Dakota State University	Gary Larson
SD	South Dakota State University	Mary O'Neill
SD	South Dakota State University	Nels Troelstrup
SD	The Nature Conservancy	Pete Bauman
SD	The Nature Conservancy	Joe Blastick
SD	The Nature Conservancy	Rich Johnson
SD	The Nature Conservancy	Mary Miller
SD	The Nature Conservancy	Bob Paulson

Table A.3 (cont'd)

SD	United States Geological Service	Jennifer Rover
SD	United States Geological Service	Bruce Wylie
WI	Department of Natural Resources	Armund Bartz
WI	Department of Natural Resources	Julie Bleser
WI	Department of Natural Resources	Catherine Eleser
WI	Department of Natural Resources	Harvey Halvorsen
WI	Department of Natural Resources	Dawn Hinebaugh
WI	Department of Natural Resources	Randolph Hoffman
WI	Department of Natural Resources	Deborah Konkel
WI	Department of Natural Resources	Mark Martin
WI	Department of Natural Resources	Thomas Meyer
WI	Department of Natural Resources	Rori Paloski
WI	Department of Natural Resources	Kenneth Parsons
WI	Department of Natural Resources	Emily Rusch
WI	Department of Natural Resources	Jerry Sullivan
WI	Department of Natural Resources	Craig Thompson
WI	Fisheries and Wildlife Service	Katie Goodwin
WI	Fisheries and Wildlife Service	Vickie Hirschboeck
WI	Fisheries and Wildlife Service	Rich King
WI	Fisheries and Wildlife Service	David McConnell
WI	Fisheries and Wildlife Service	Darienne McNamara
WI	Fisheries and Wildlife Service	Jim Nissen
WI	Fisheries and Wildlife Service	Sadie O'dell
WI	Fisheries and Wildlife Service	Shawn Papon
WI	Fisheries and Wildlife Service	Wendy Woyczik
WI	Pheasants Forever	Jeff Gaska
WI	State Cartographer's Office	Jim Lacy
WI	The Nature Conservancy	Steve Richter
WI	The Prairie Enthusiasts	Rich Henderson
WI	United States Geological Service	James Rogala
WI	University of Wisconsin	Tim Cochrane
WI	University of Wisconsin	John A. Harrington

APPENDIX B

Graphs describing the time-series of NDVI, drought, precipitation, maximum temperature, and minimum temperature for each prairie considered within the analysis for Chapter 3. The title from each graph includes the unique alpha-numeric code that identifies each prairie in the PSD. NDVI is estimated at an 8 – day timescale and was obtained from Moderate Resolution Imaging Spectroradiometer (MODIS). Weather variables were estimated at a monthly temporal frequency and were based on data from the PRISM Group (Daly 2009). The drought index is represented by the calculation of the Palmer's Drought Severity Index (PDSI; Palmer 1968). The dashed lines in these graphs mark 1 and -1, the index values that indicate the onset of higher moisture conditions or below normal moisture conditions respectively (Palmer, 1968).

Figure B.1. Time series curves for iam.
The community type for this prairie is Tall.
The dominant photosynthetic pathway for this prairie is C4.
The restoration status for this prairie is Remnant.

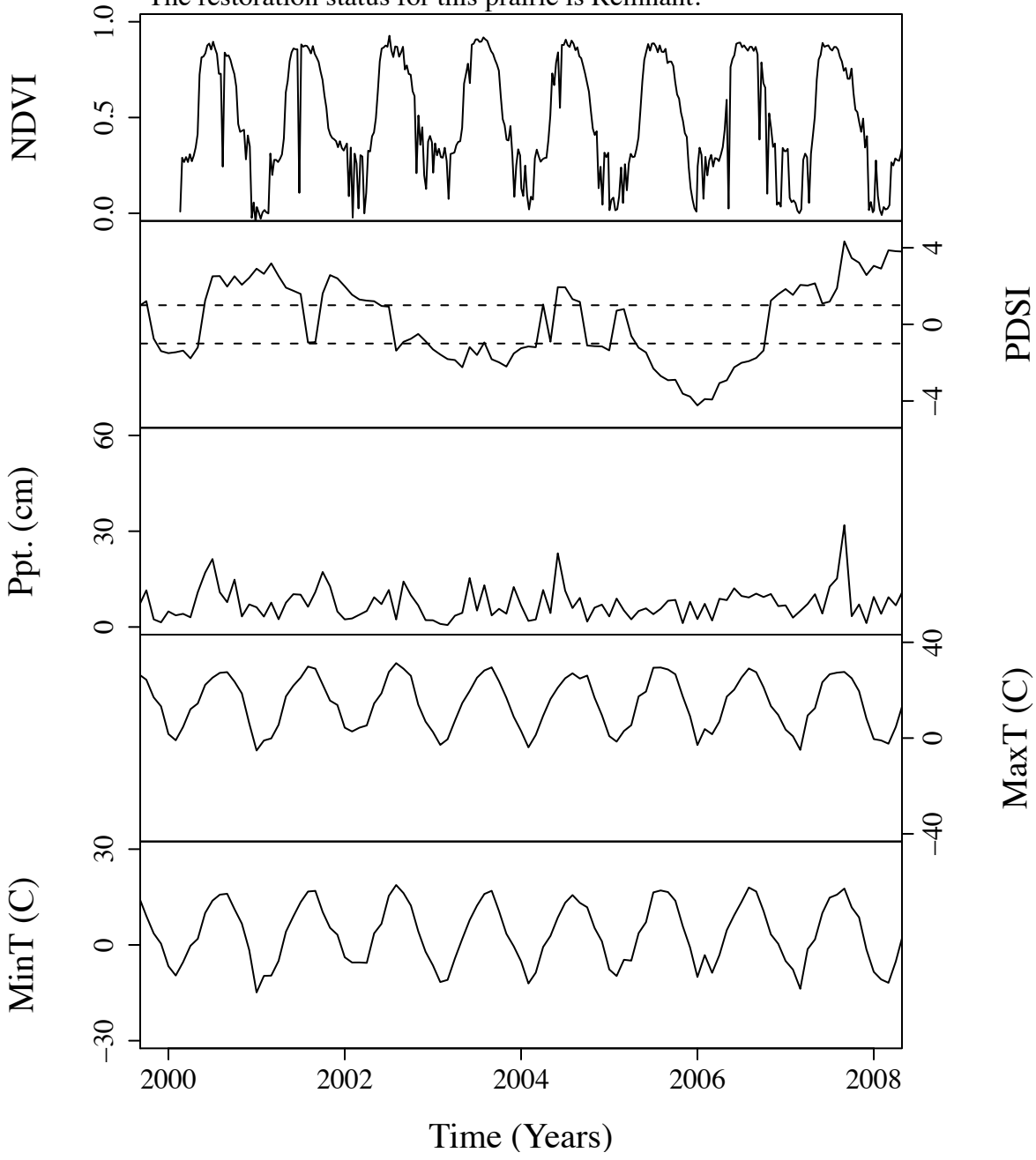

Figure B.2. Time series curves for iba369.
The community type for this prairie is Tall.
The dominant photosynthetic pathway for this prairie is C4.
The restoration status for this prairie is Restored.

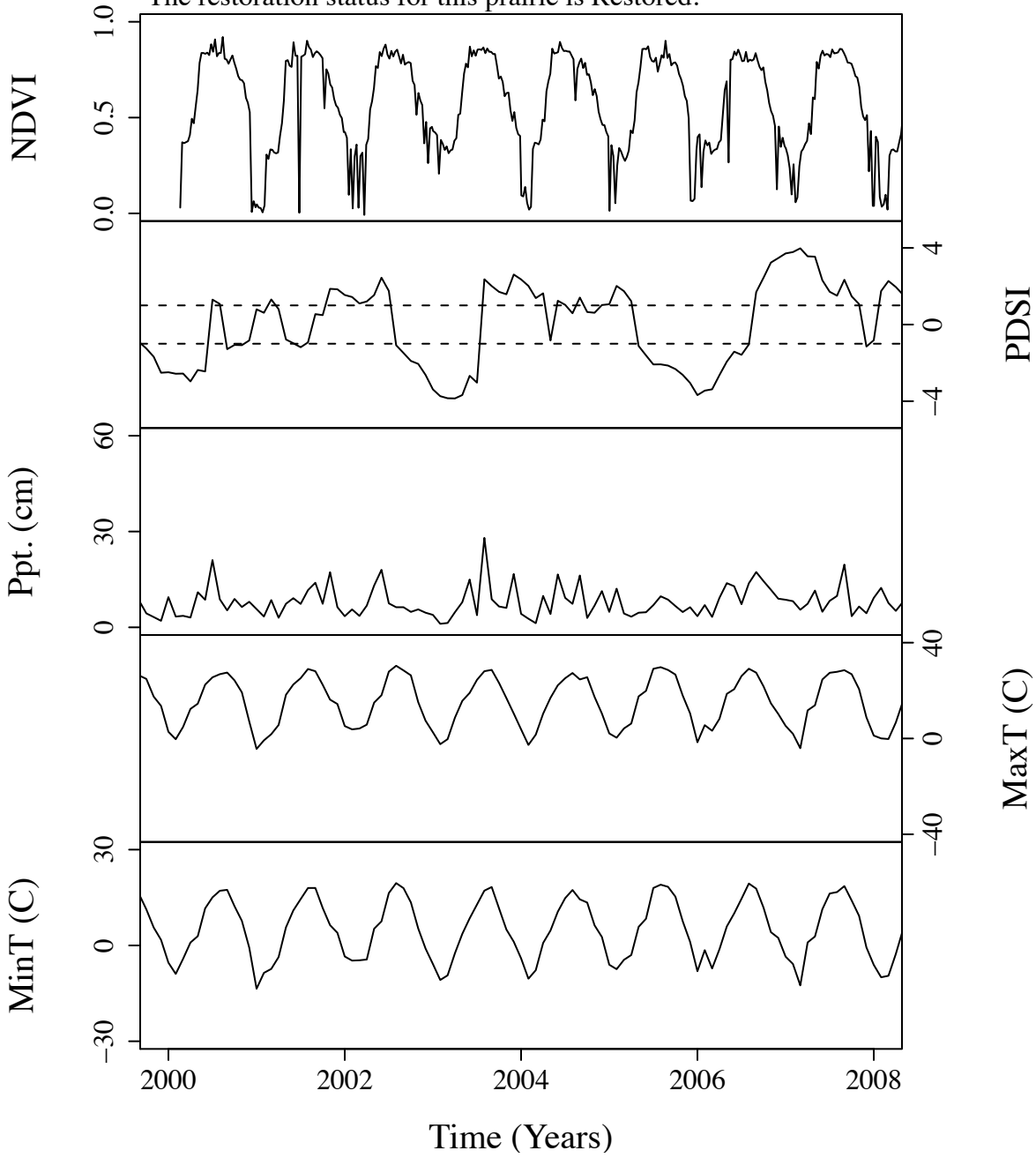

Figure B.3. Time series curves for ibh.
The community type for this prairie is Tall.
The dominant photosynthetic pathway for this prairie is C4.
The restoration status for this prairie is Restored.

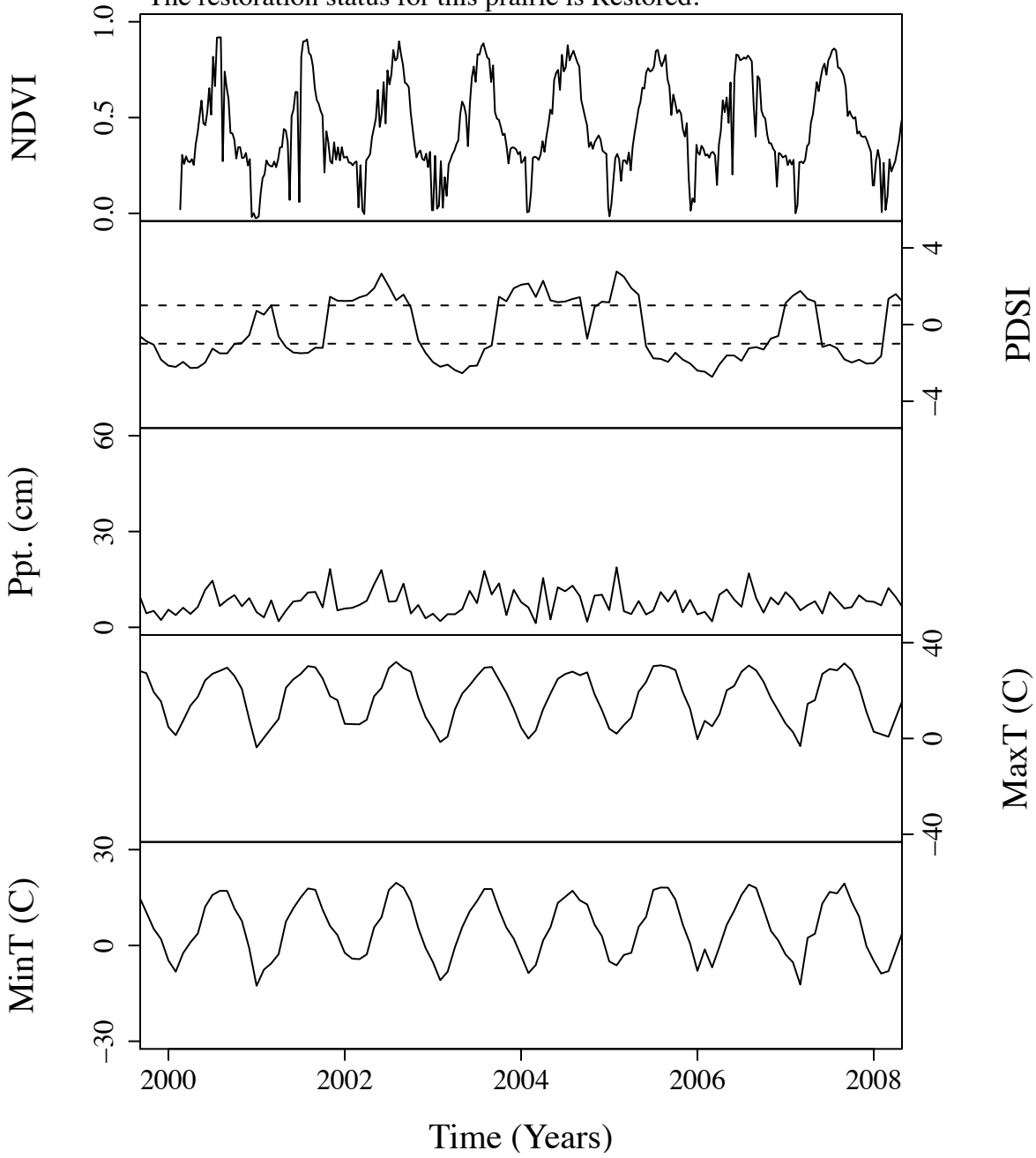

Figure B.4. Time series curves for ibr.
The community type for this prairie is Tall.
The dominant photosynthetic pathway for this prairie is C4.
The restoration status for this prairie is Remnant.

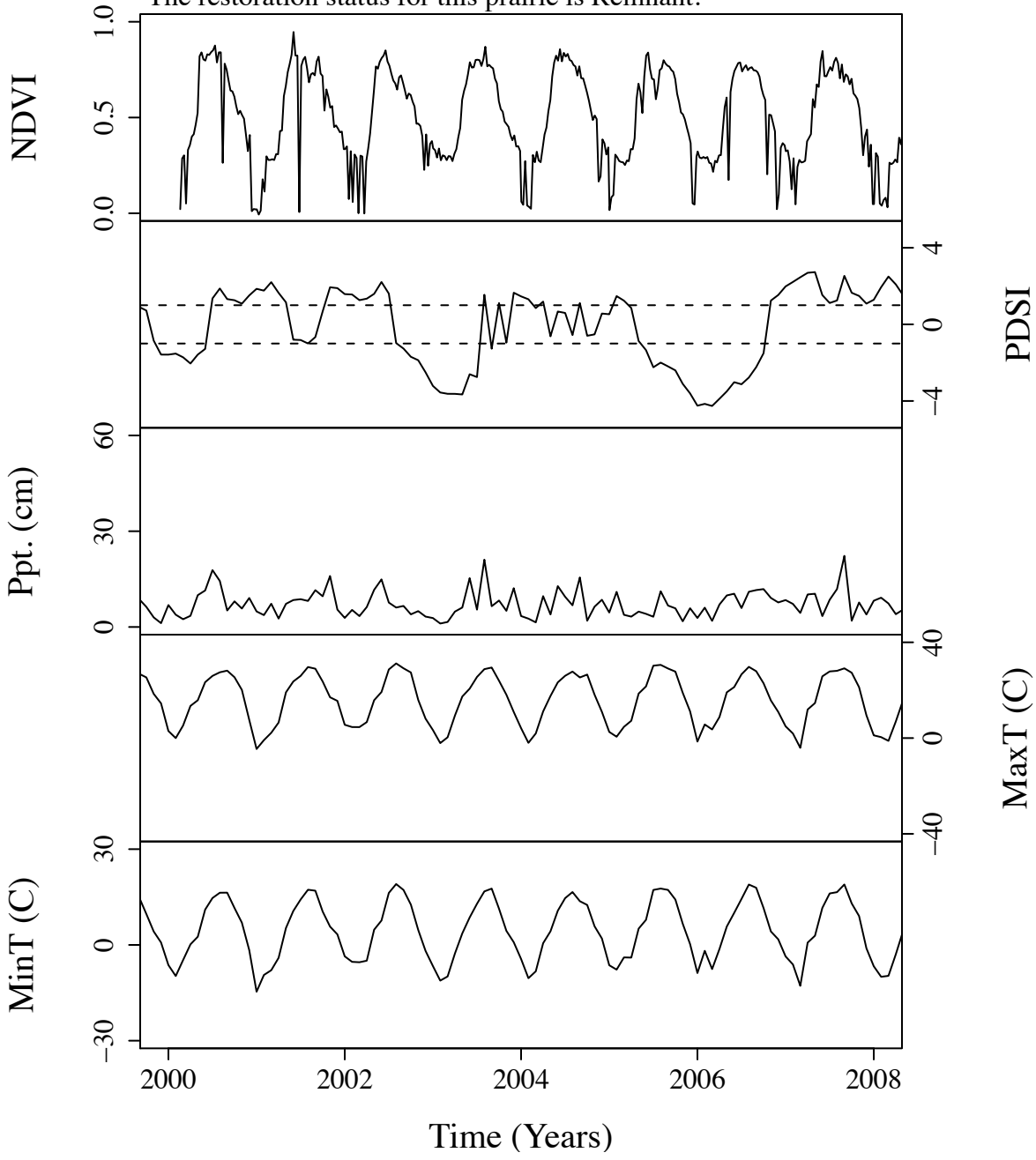

Figure B.5. Time series curves for ica1174.
The community type for this prairie is Tall.
The dominant photosynthetic pathway for this prairie is C4.
The restoration status for this prairie is Unknown.

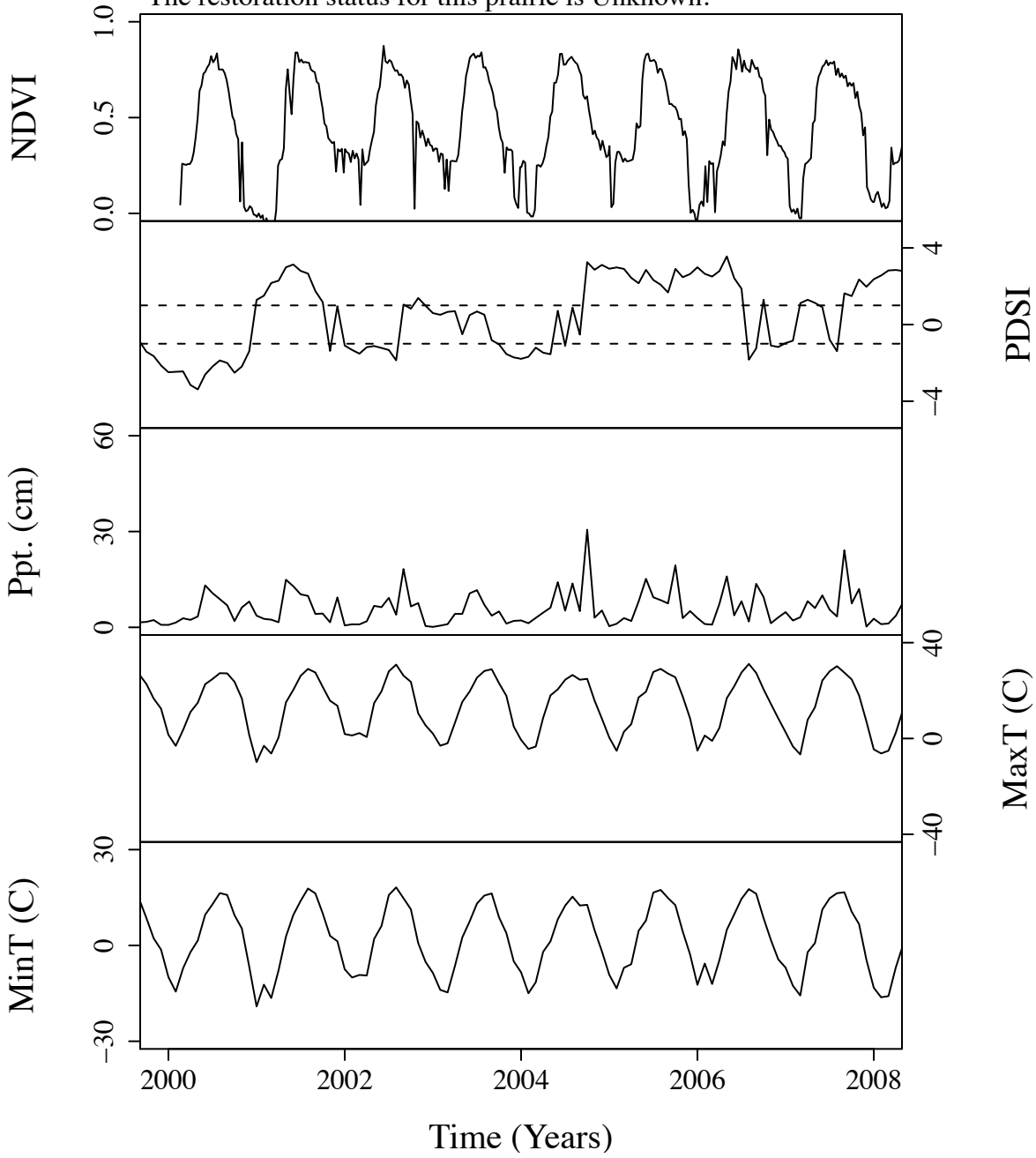

Figure B.6. Time series curves for idp.
The community type for this prairie is Tall.
The dominant photosynthetic pathway for this prairie is C4.
The restoration status for this prairie is Remnant.

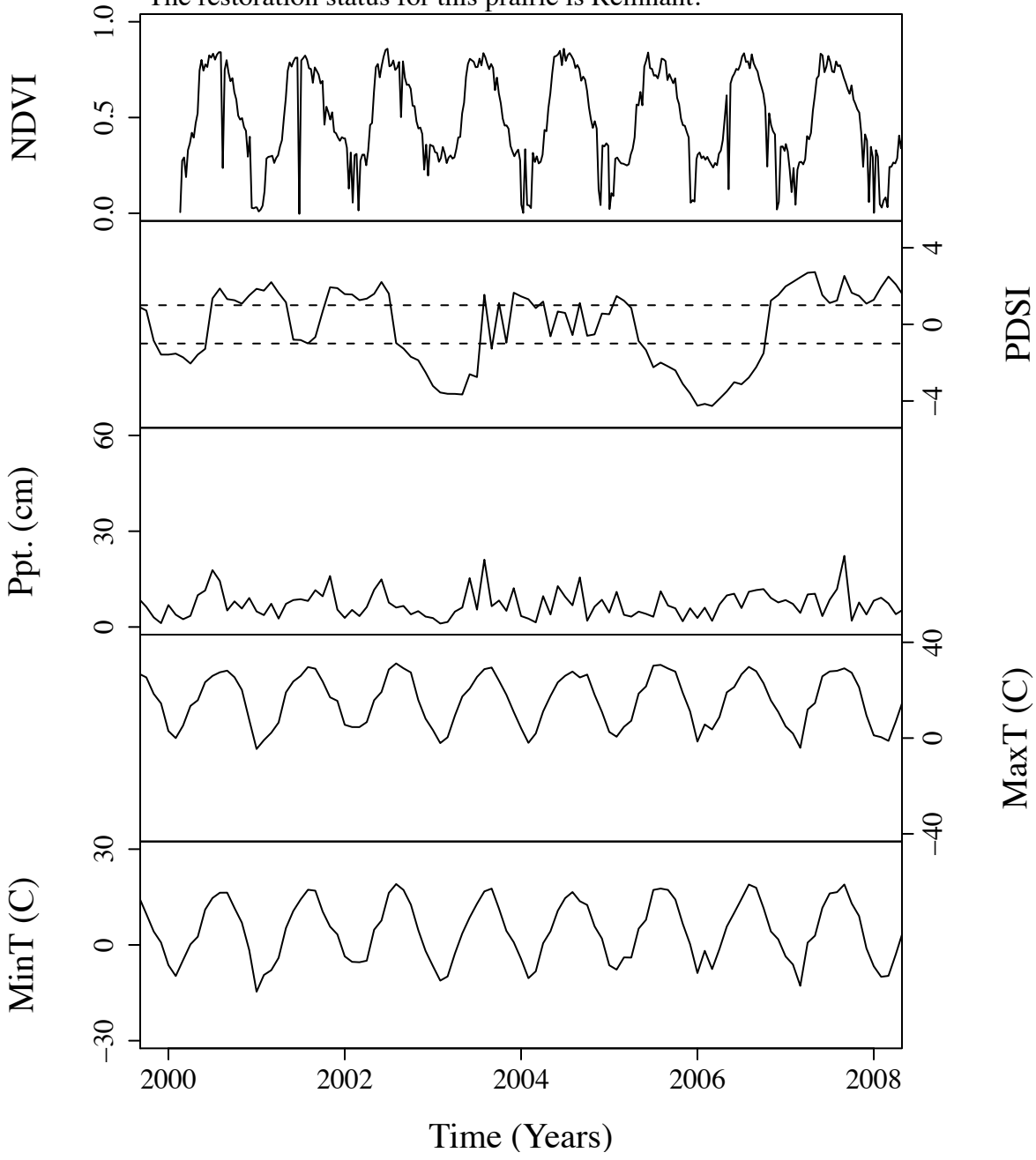

Figure B.7. Time series curves for ife.
The community type for this prairie is Tall.
The dominant photosynthetic pathway for this prairie is C4.
The restoration status for this prairie is Unknown.

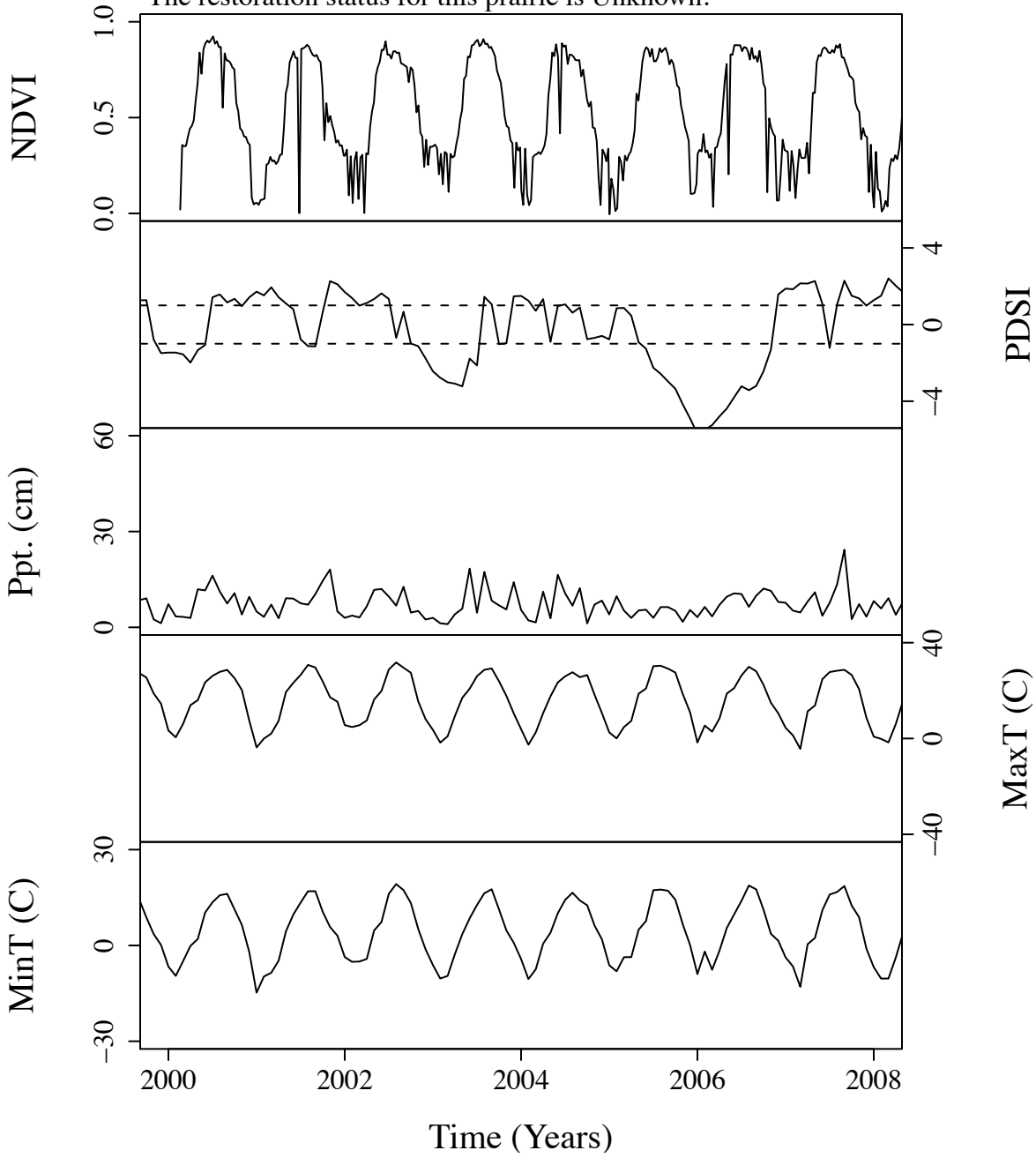

Figure B.8. Time series curves for igr.
The community type for this prairie is Tall.
The dominant photosynthetic pathway for this prairie is C4.
The restoration status for this prairie is Unknown.

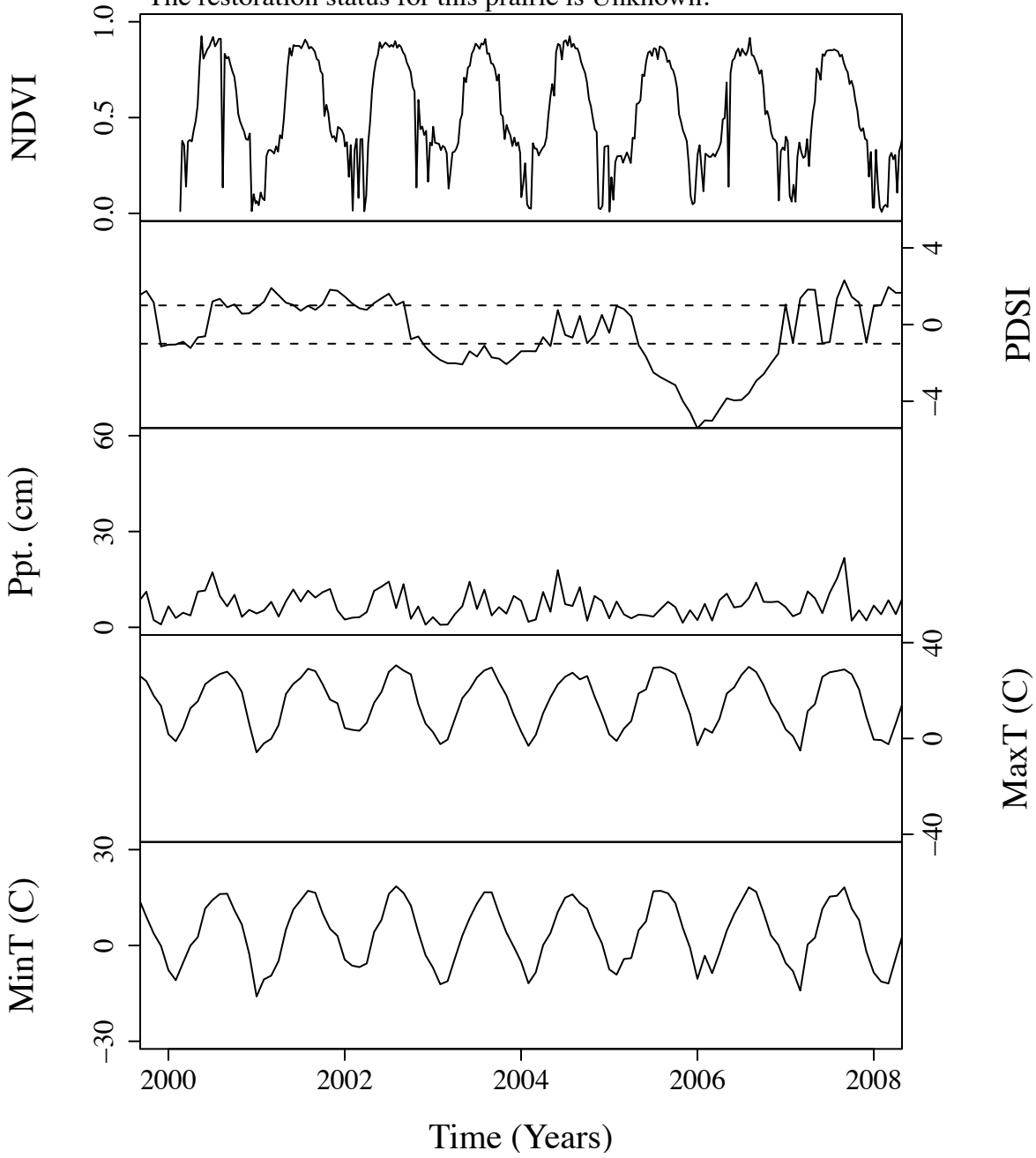

Figure B.9. Time series curves for igs.
The community type for this prairie is Tall.
The dominant photosynthetic pathway for this prairie is C4.
The restoration status for this prairie is Restored.

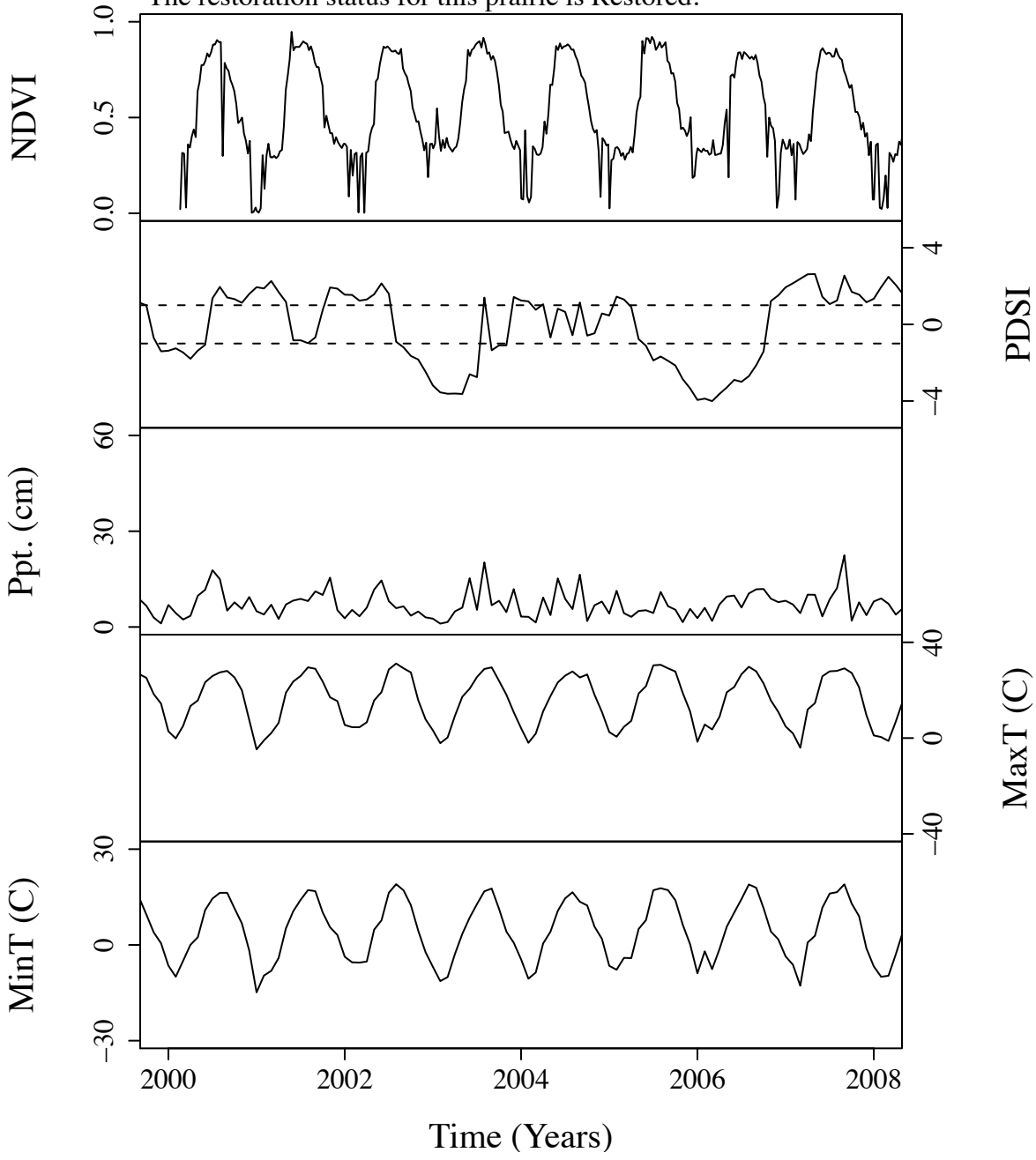

Figure B.10. Time series curves for ijo16.
The community type for this prairie is Tall.
The dominant photosynthetic pathway for this prairie is C4.
The restoration status for this prairie is Unknown.

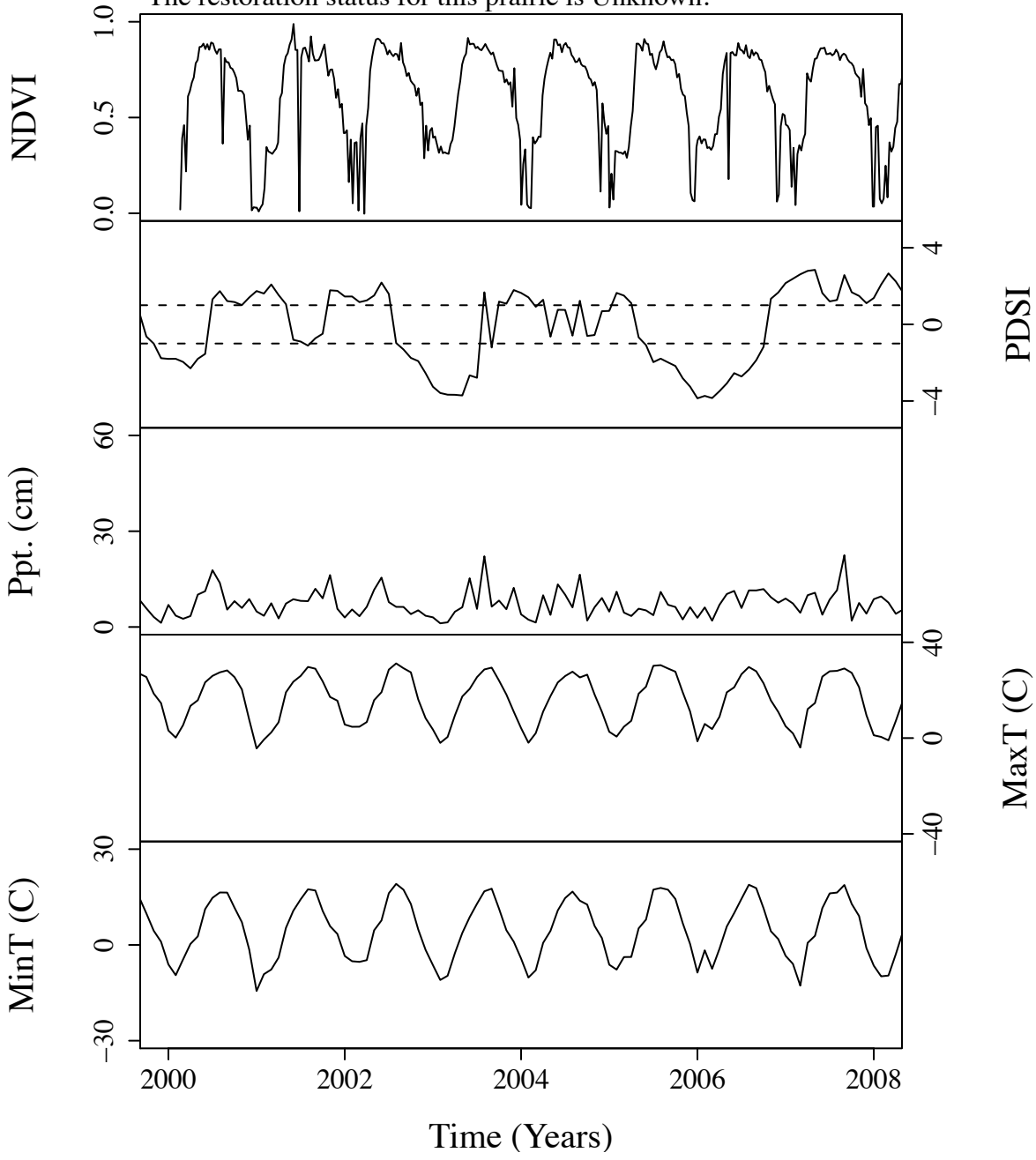

Figure B.11. Time series curves for ijr.
The community type for this prairie is Tall.
The dominant photosynthetic pathway for this prairie is C4.
The restoration status for this prairie is Restored.

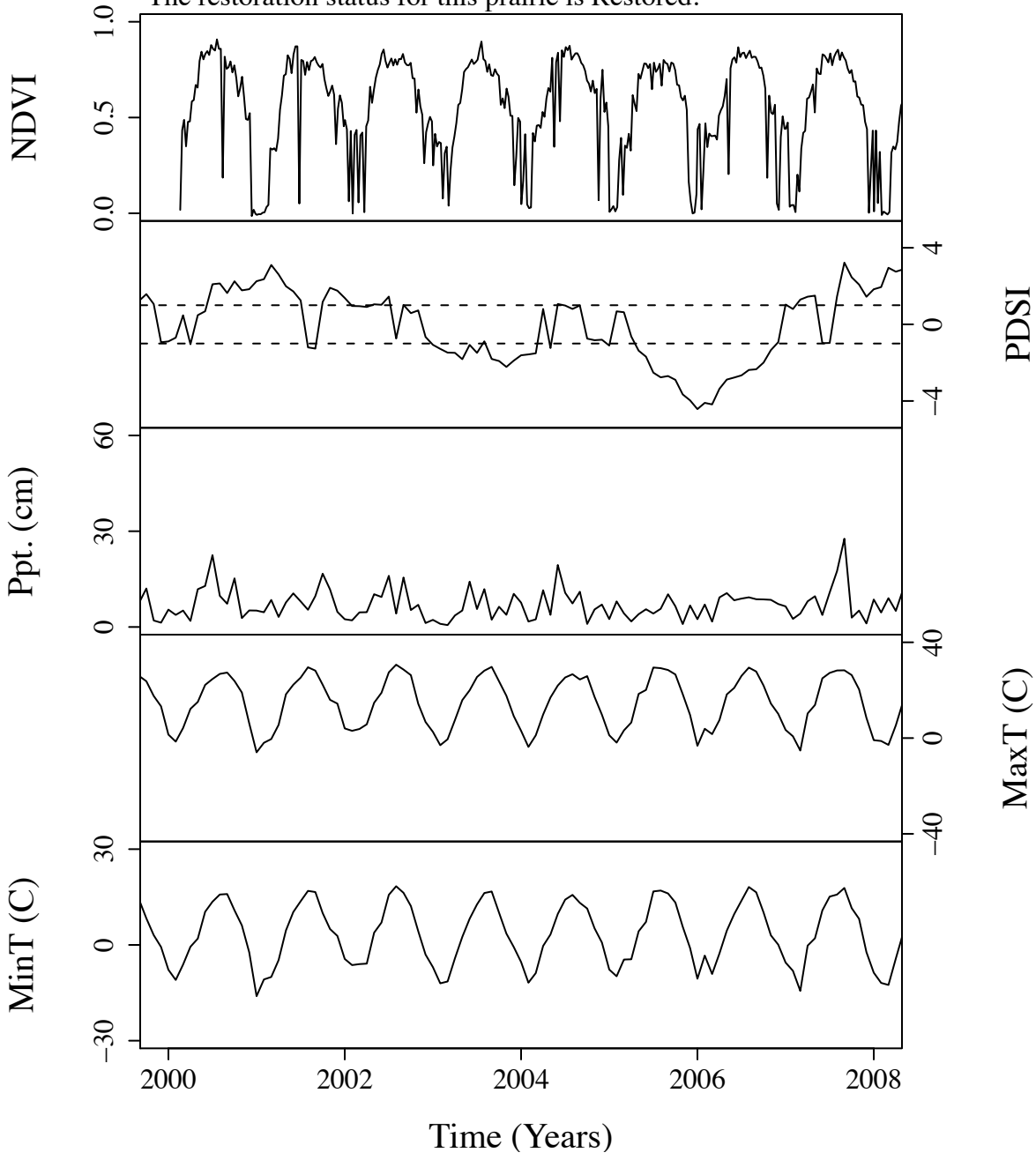

Figure B.12. Time series curves for ilb.
The community type for this prairie is Tall.
The dominant photosynthetic pathway for this prairie is C4.
The restoration status for this prairie is Unknown.

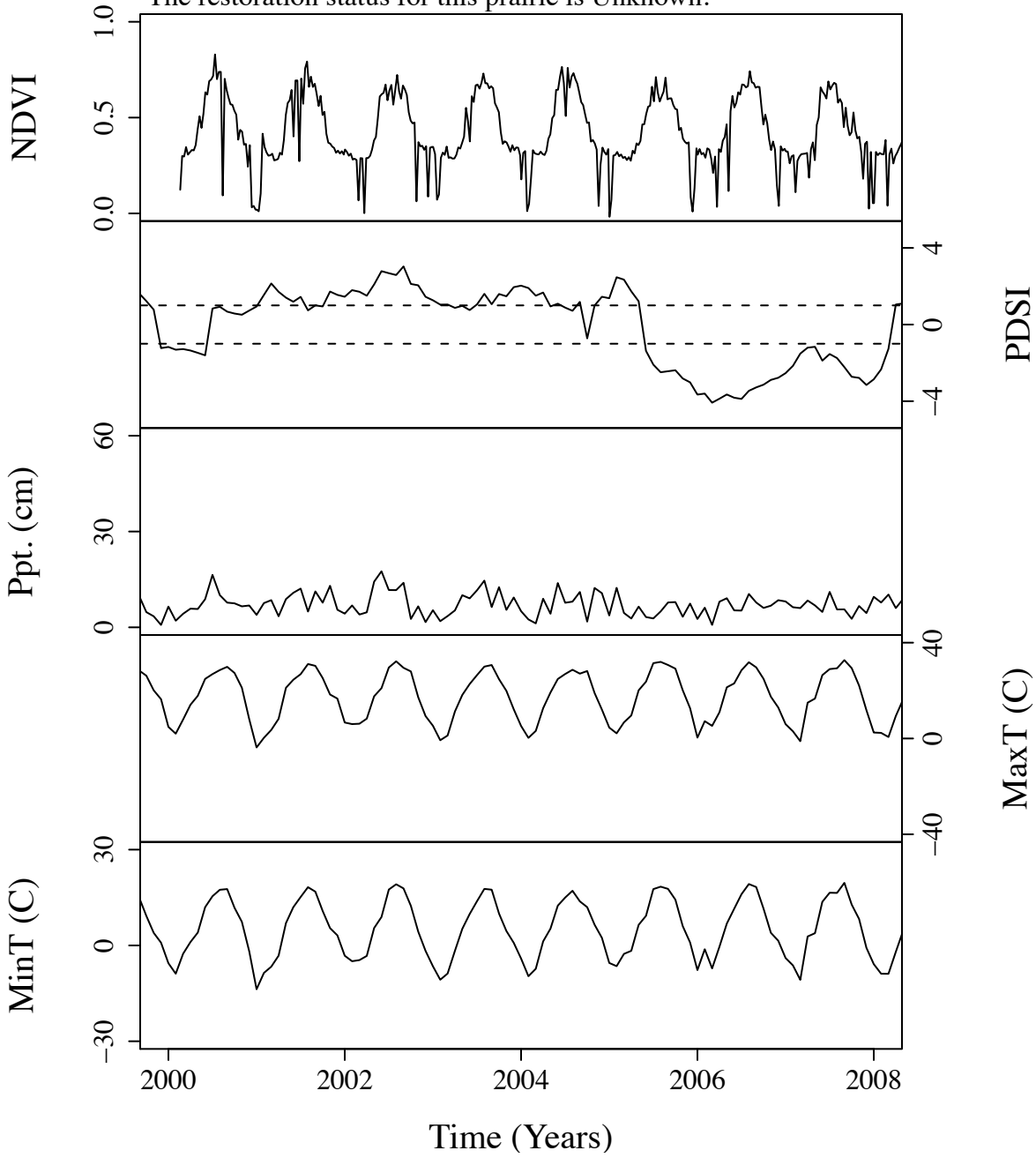

Figure B.13. Time series curves for ilo1330.
The community type for this prairie is Tall.
The dominant photosynthetic pathway for this prairie is C4.
The restoration status for this prairie is Unknown.

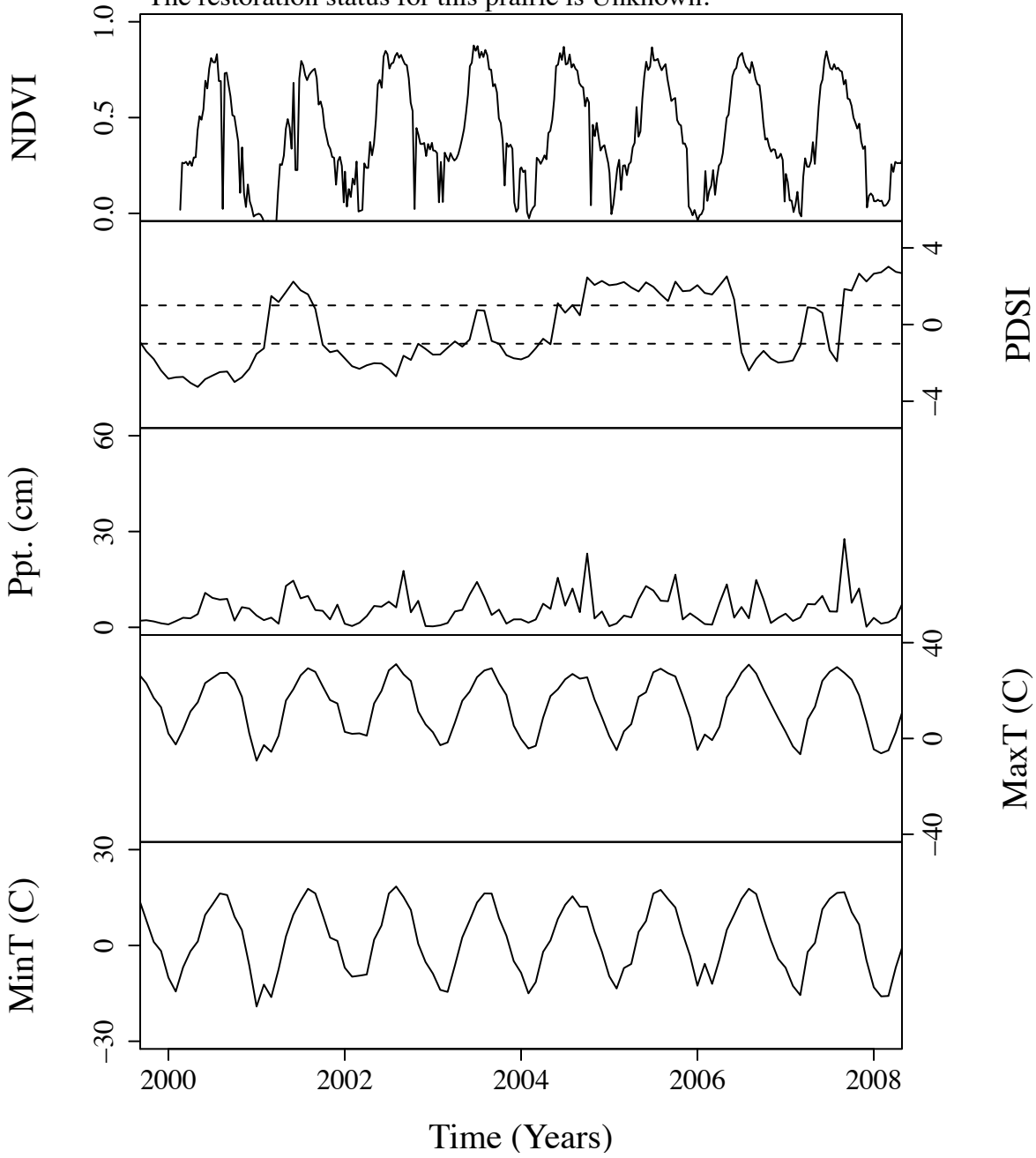

Figure B.14. Time series curves for ipr3452.
The community type for this prairie is Tall.
The dominant photosynthetic pathway for this prairie is C4.
The restoration status for this prairie is Unknown.

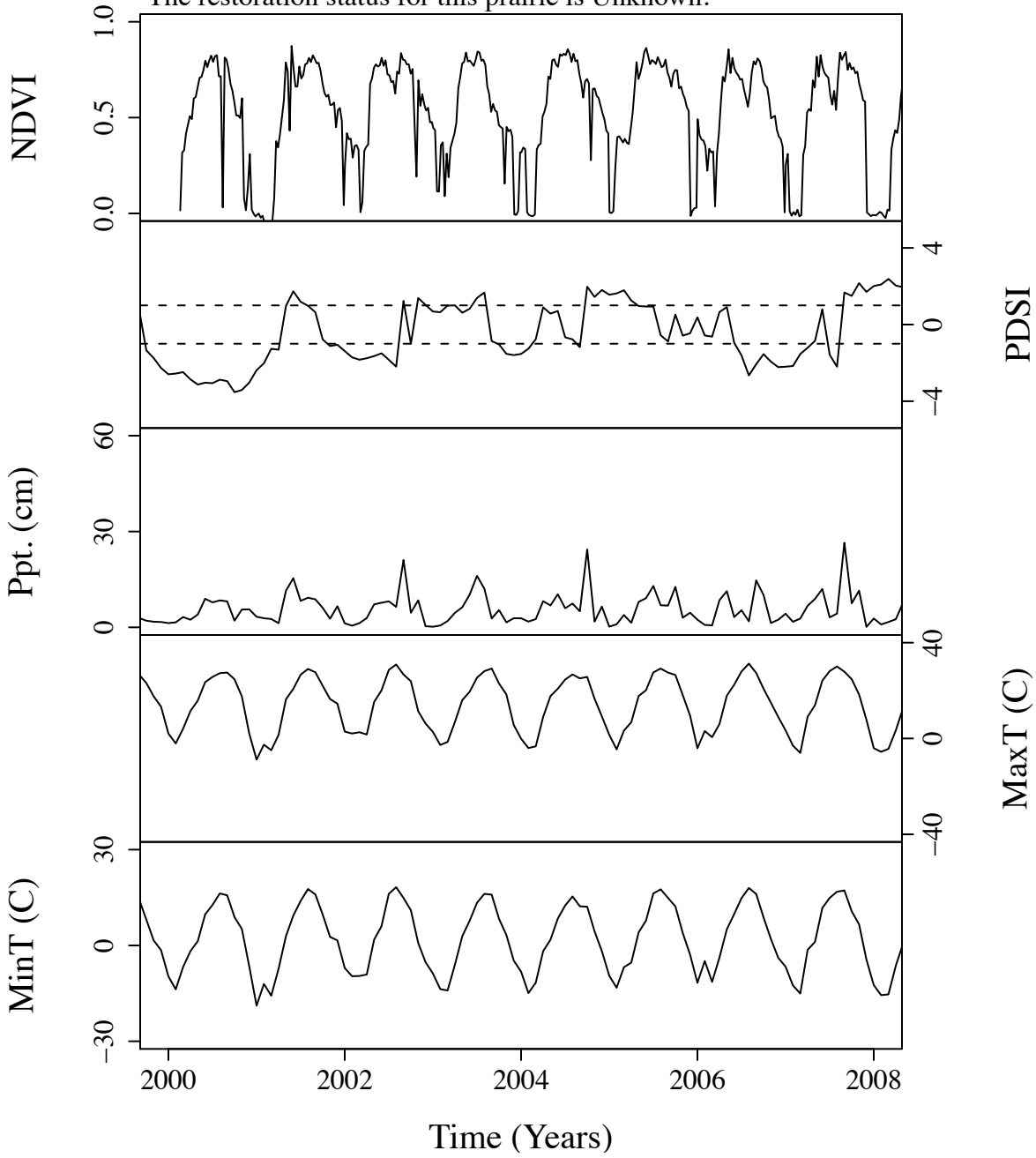

Figure B.15. Time series curves for ipr654.
The community type for this prairie is Tall.
The dominant photosynthetic pathway for this prairie is C4.
The restoration status for this prairie is Unknown.

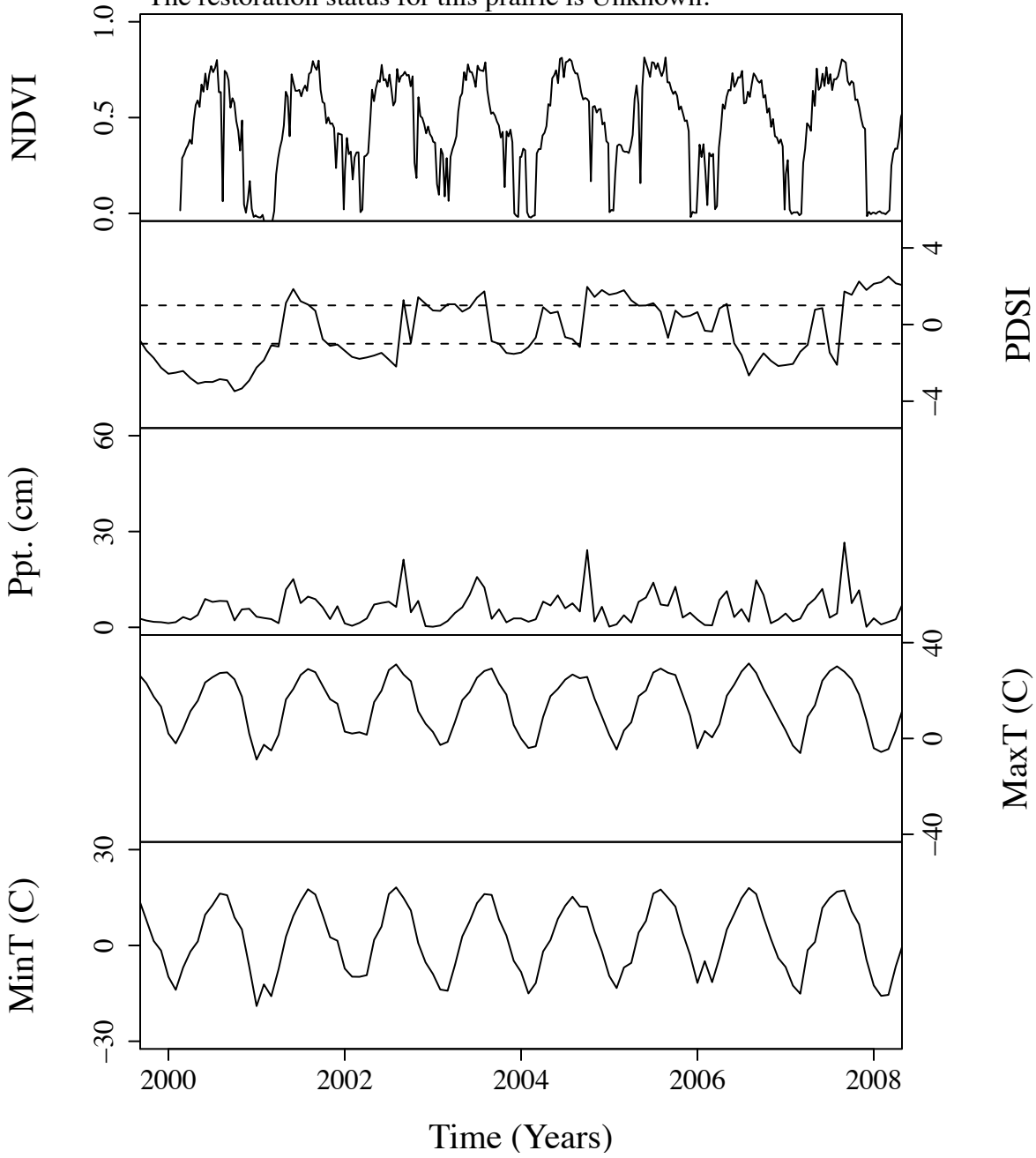

Figure B.16. Time series curves for ire3461.
The community type for this prairie is Tall.
The dominant photosynthetic pathway for this prairie is C4.
The restoration status for this prairie is Unknown.

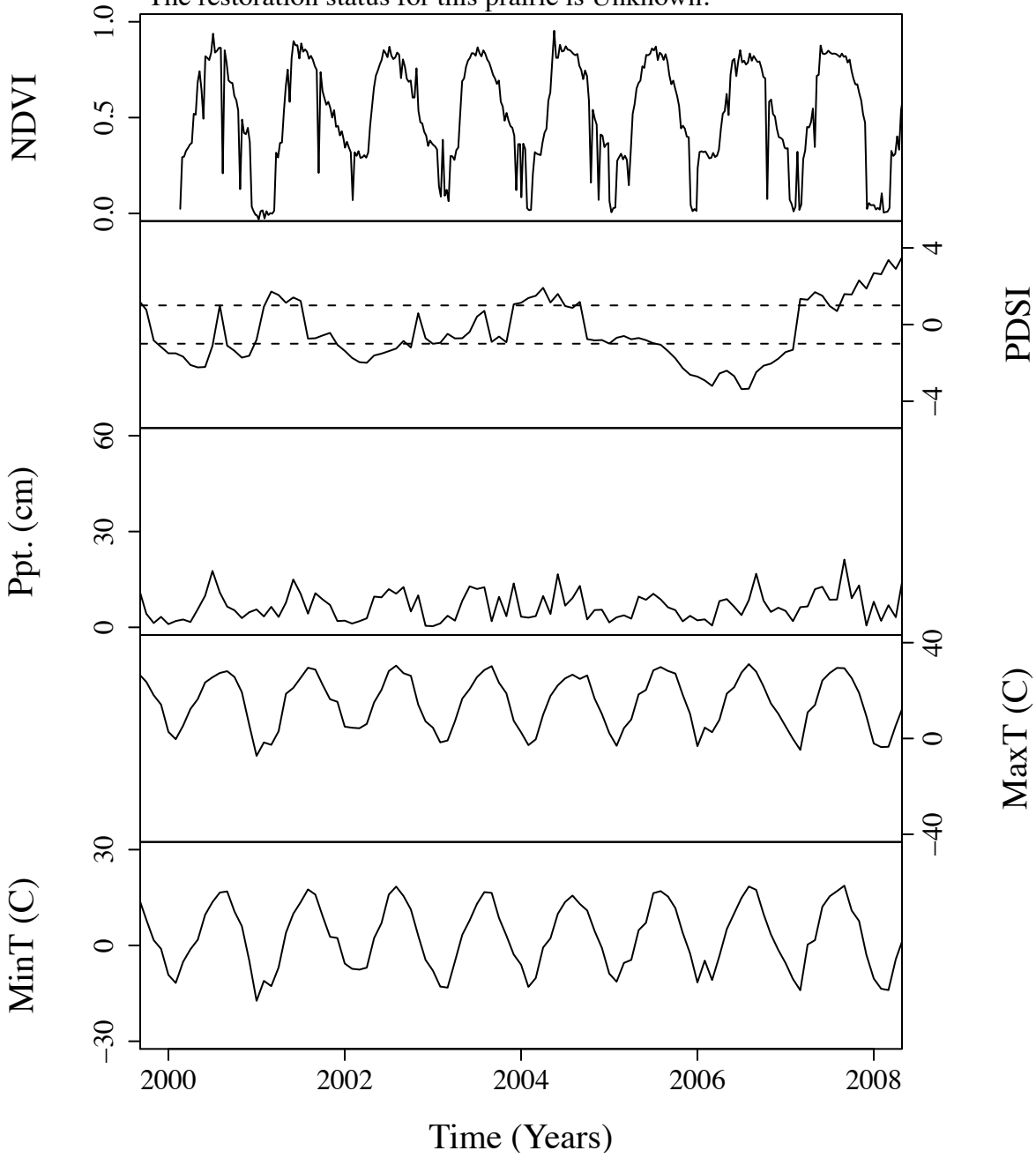

Figure B.17. Time series curves for isp.
The community type for this prairie is Tall.
The dominant photosynthetic pathway for this prairie is C4.
The restoration status for this prairie is Unknown.

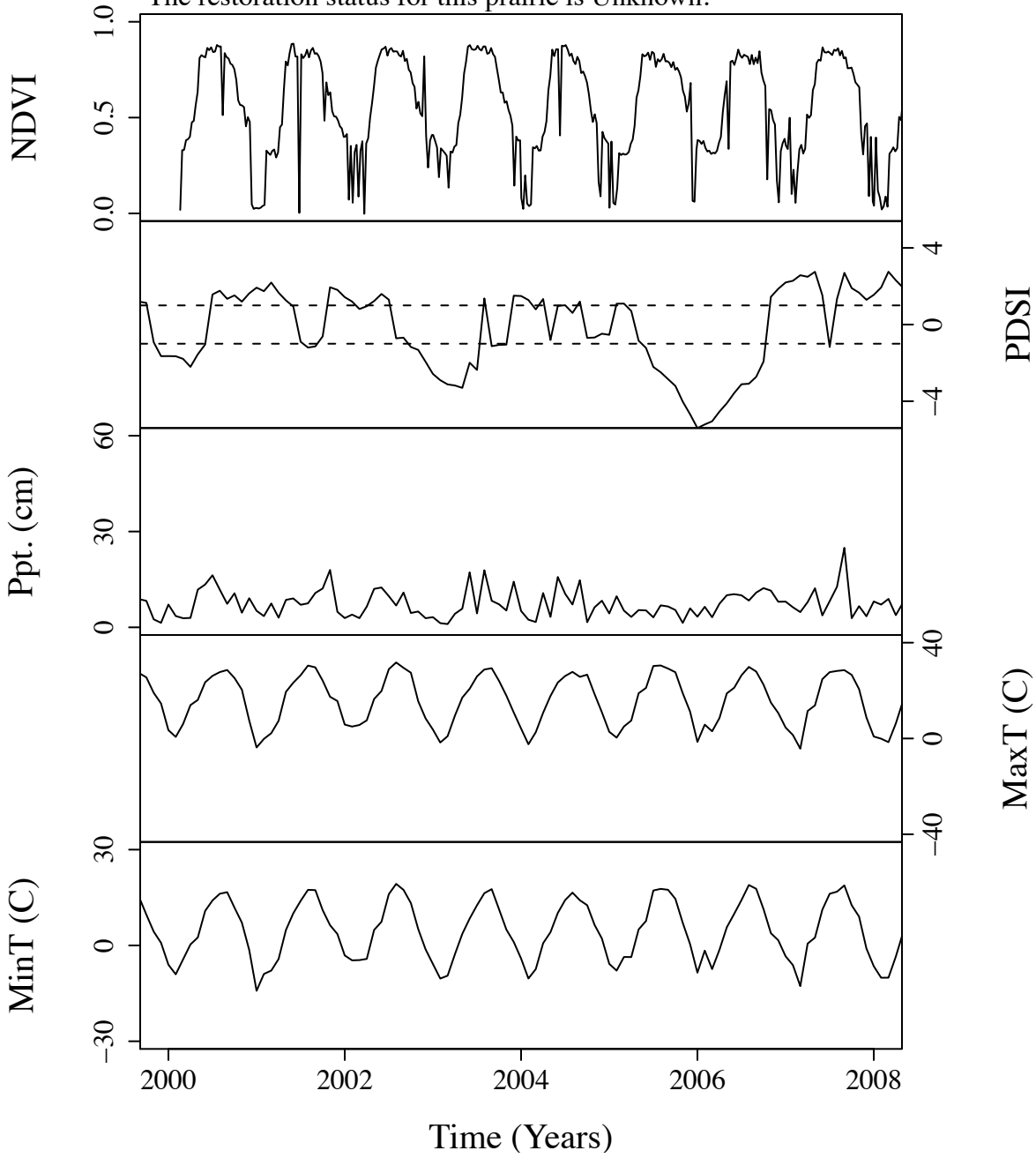

Figure B.18. Time series curves for iwa605.
The community type for this prairie is Tall.
The dominant photosynthetic pathway for this prairie is C4.
The restoration status for this prairie is Restored.

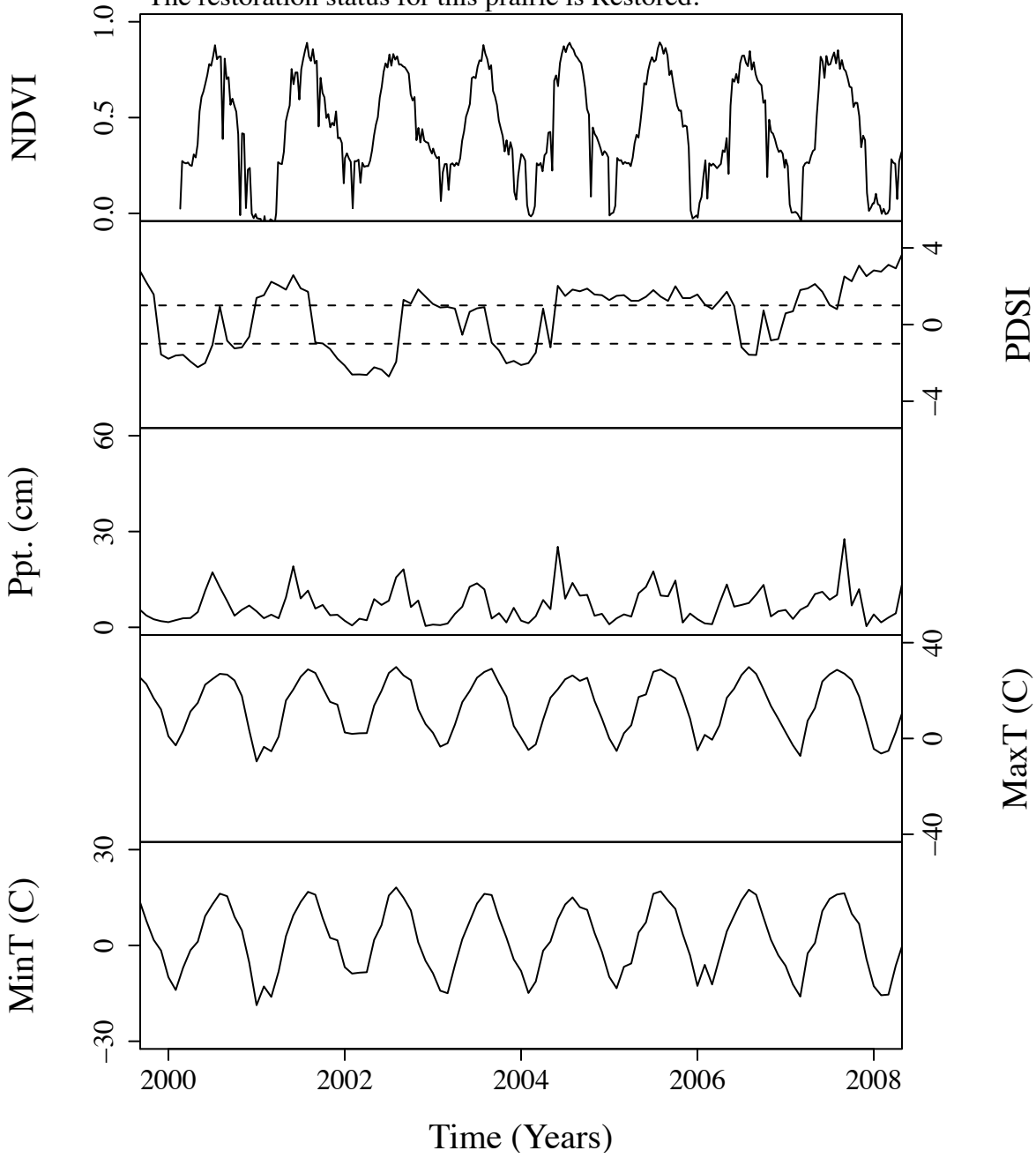

Figure B.19. Time series curves for mag0.
The community type for this prairie is NoType.
The dominant photosynthetic pathway for this prairie is C3.
The restoration status for this prairie is Unknown.

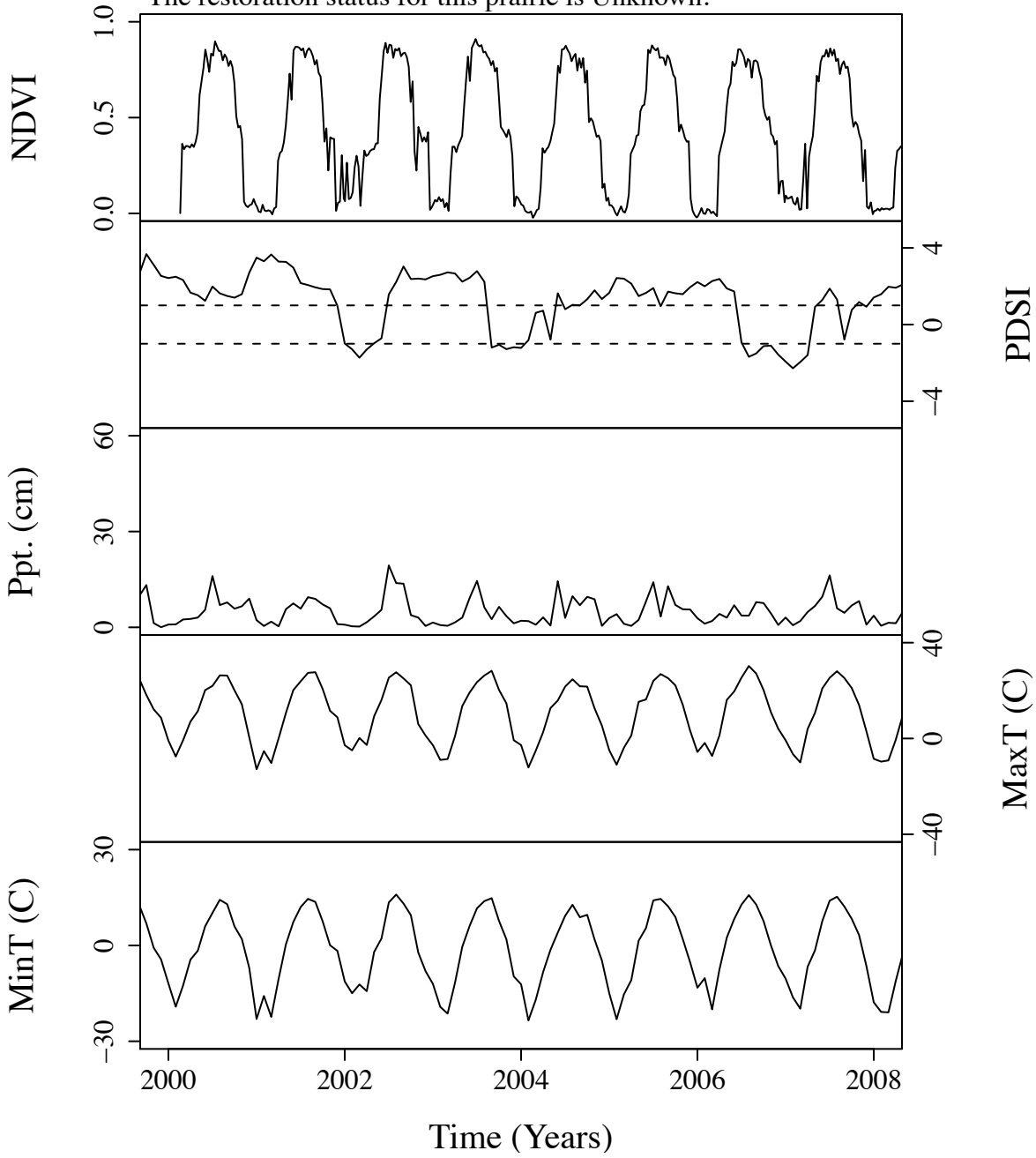

Figure B.20. Time series curves for man1.
The community type for this prairie is Tall.
The dominant photosynthetic pathway for this prairie is C4.
The restoration status for this prairie is Unknown.

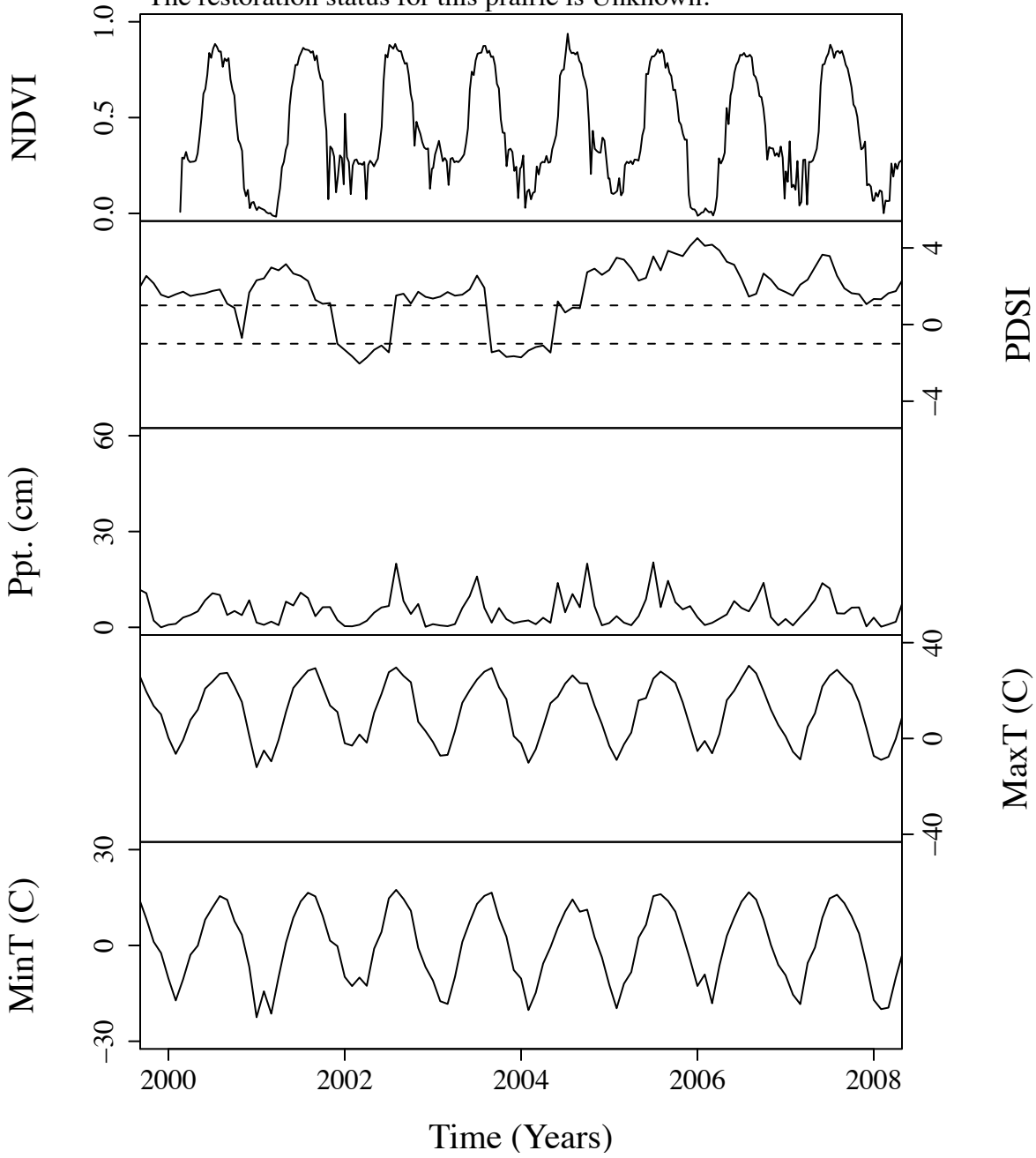

Figure B.21. Time series curves for mbl2.
The community type for this prairie is Tall.
The dominant photosynthetic pathway for this prairie is C3.
The restoration status for this prairie is Unknown.

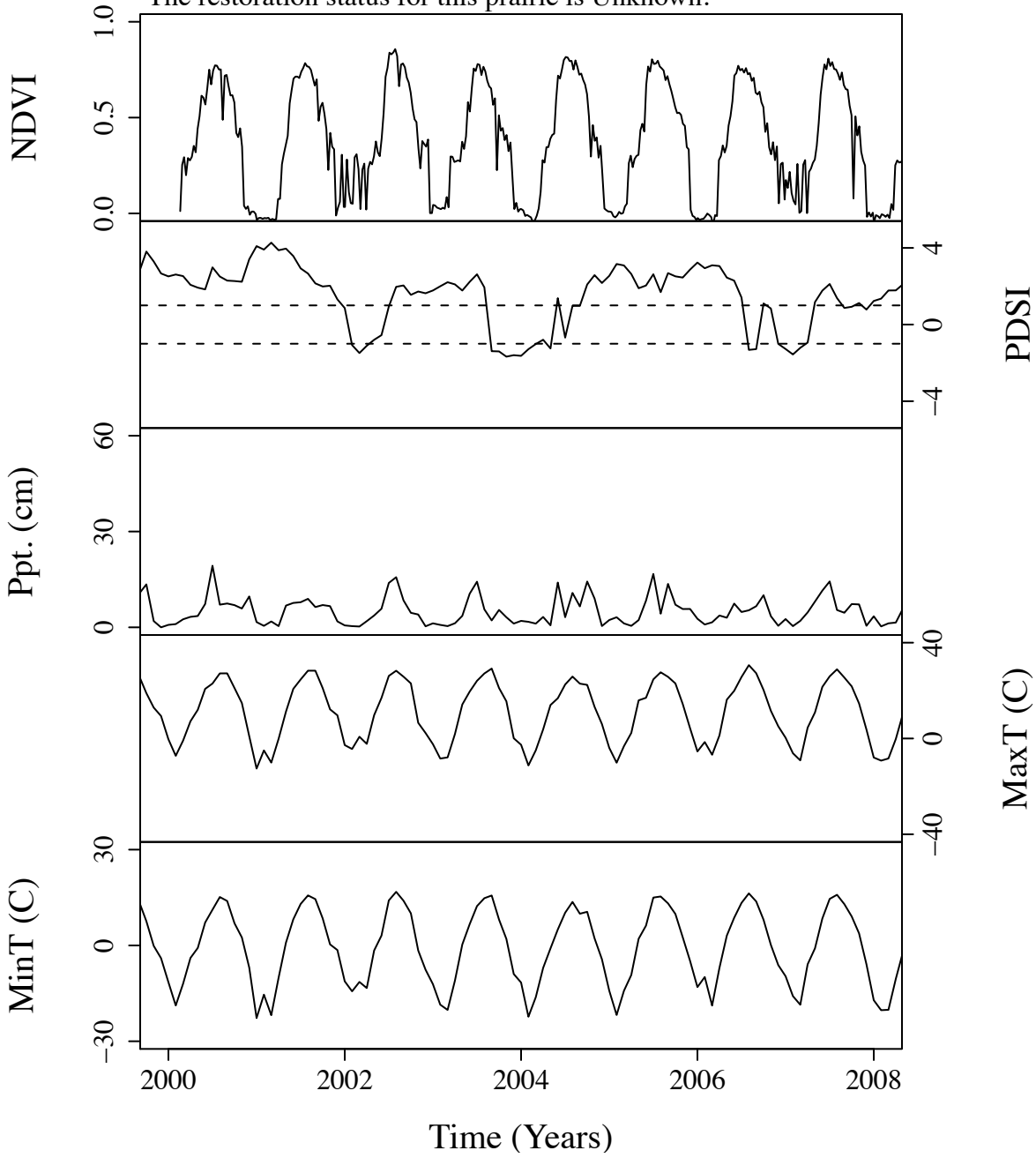

Figure B.22. Time series curves for mfo4.
The community type for this prairie is Tall.
The dominant photosynthetic pathway for this prairie is C3.
The restoration status for this prairie is Unknown.

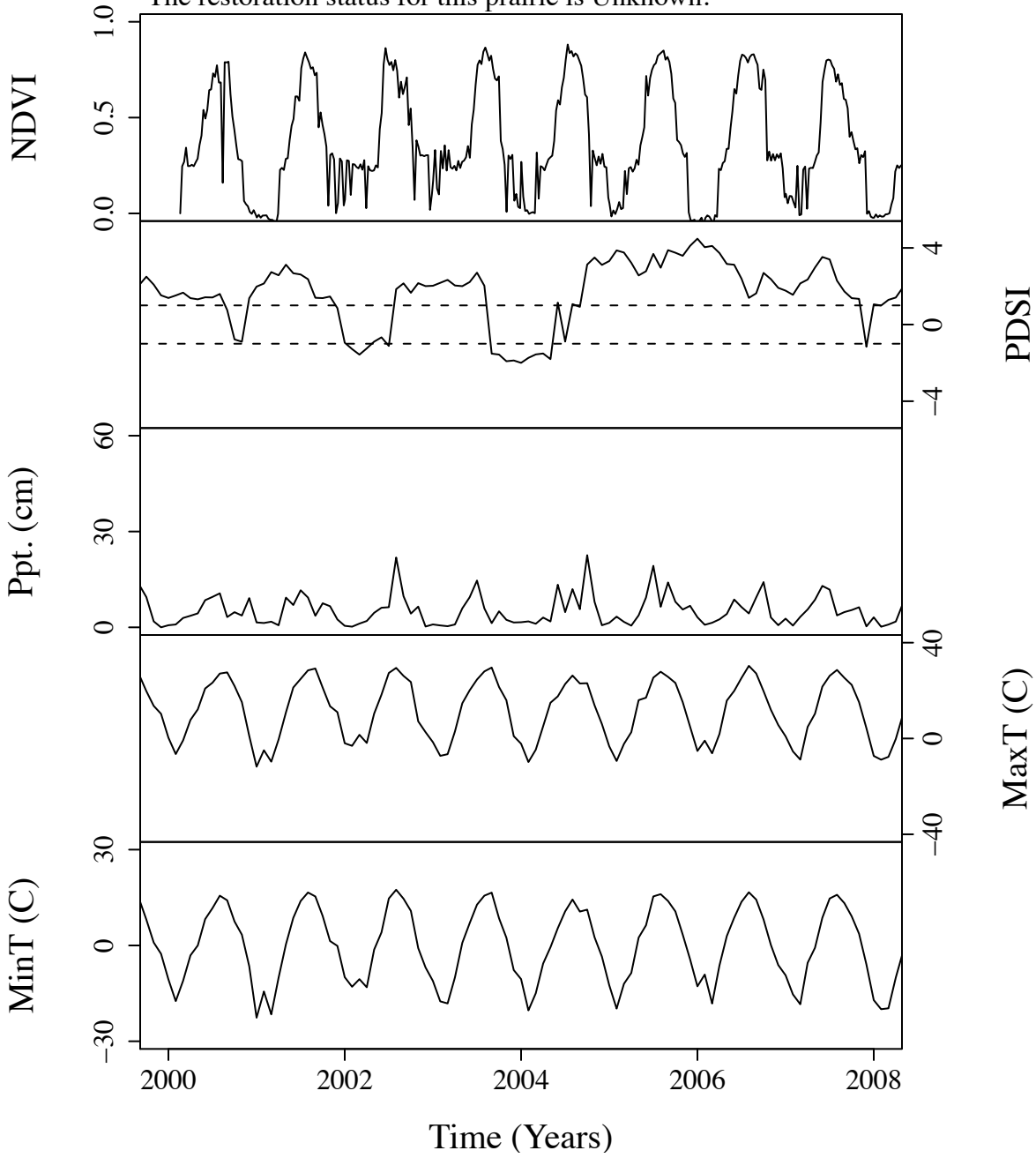

Figure B.23. Time series curves for mho14.
The community type for this prairie is Tall.
The dominant photosynthetic pathway for this prairie is C4.
The restoration status for this prairie is Unknown.

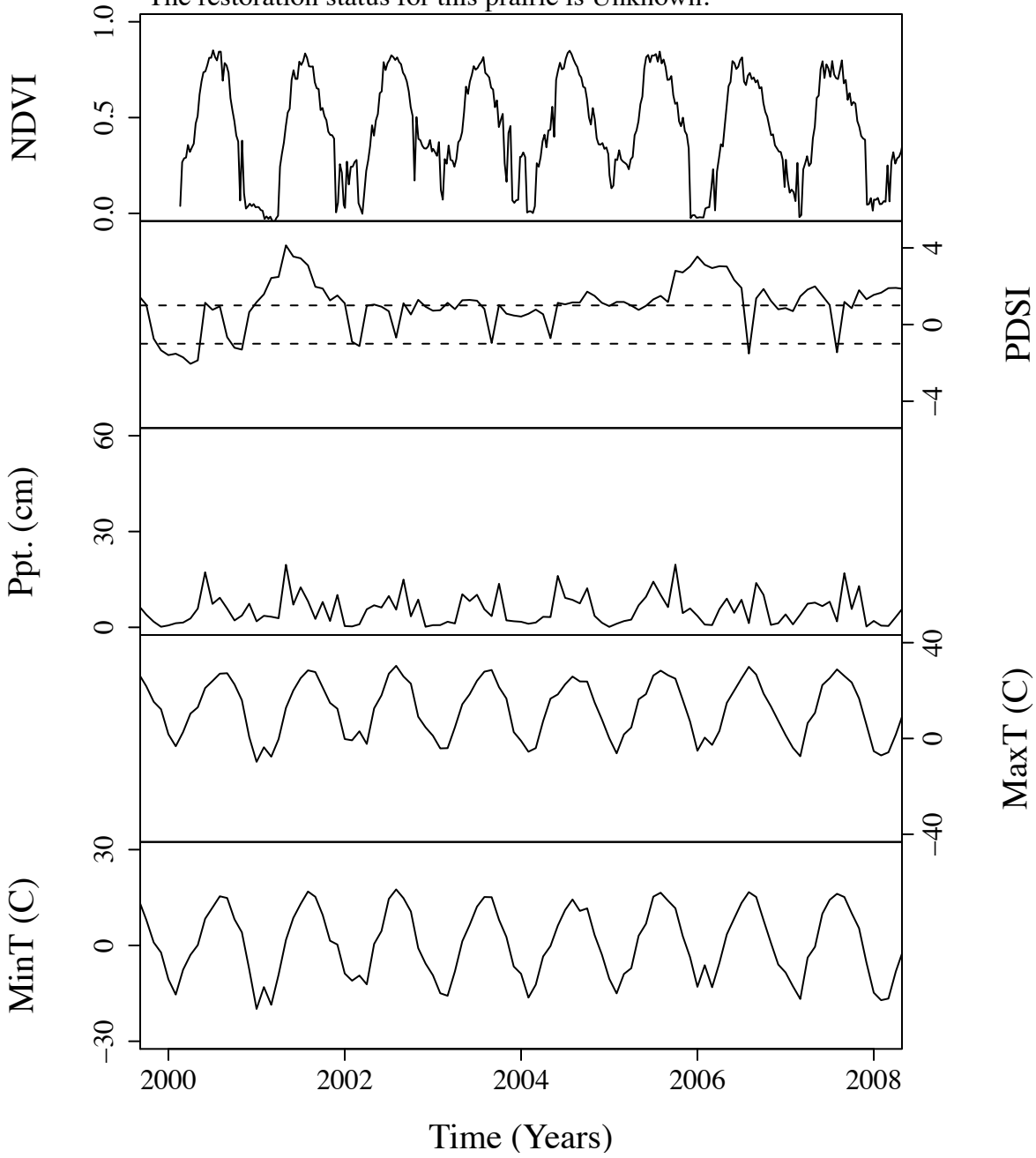

Figure B.24. Time series curves for mke6.
The community type for this prairie is Tall.
The dominant photosynthetic pathway for this prairie is C3.
The restoration status for this prairie is Unknown.

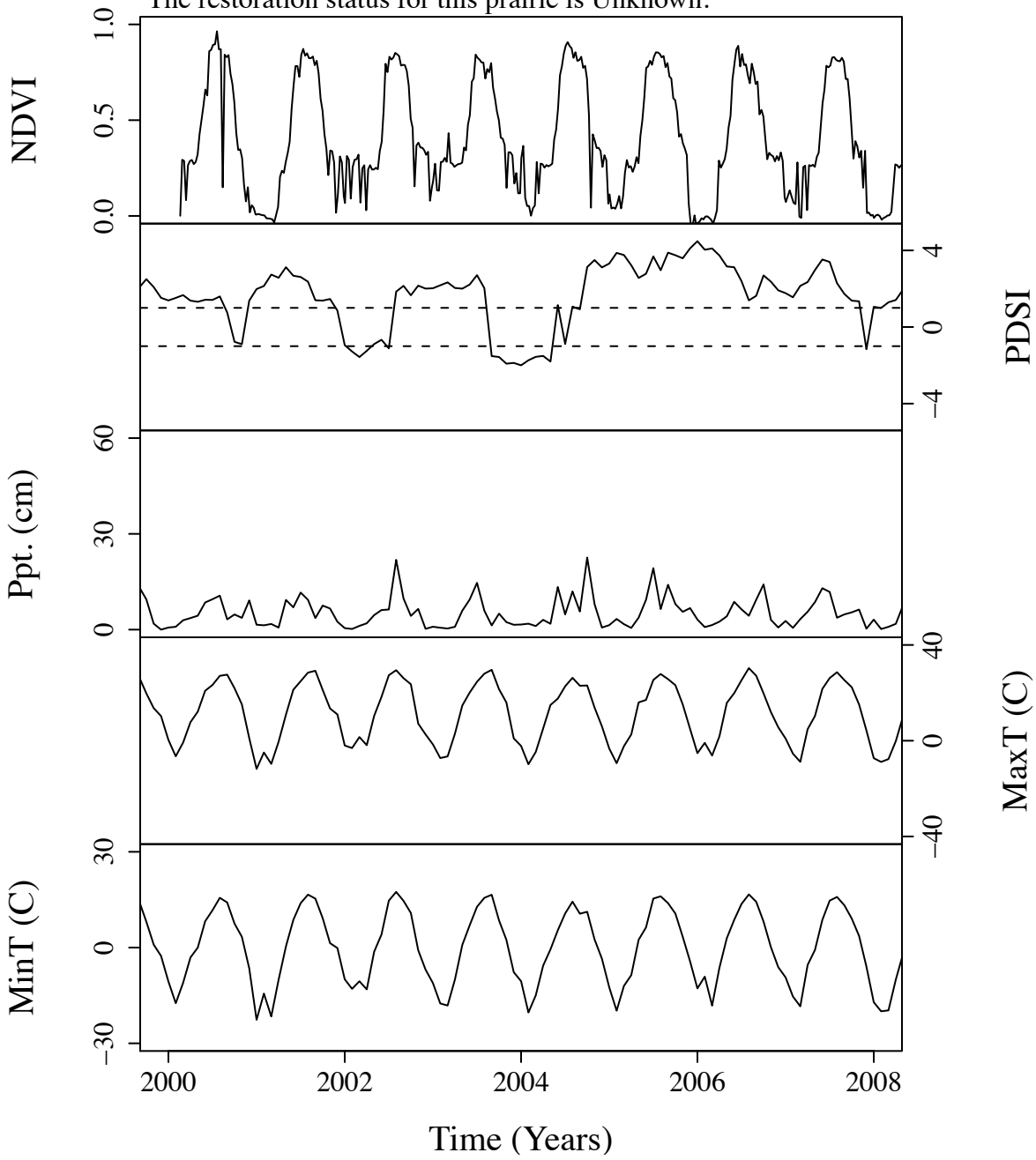

Figure B.25. Time series curves for mma20.
The community type for this prairie is NoType.
The dominant photosynthetic pathway for this prairie is C4.
The restoration status for this prairie is Unknown.

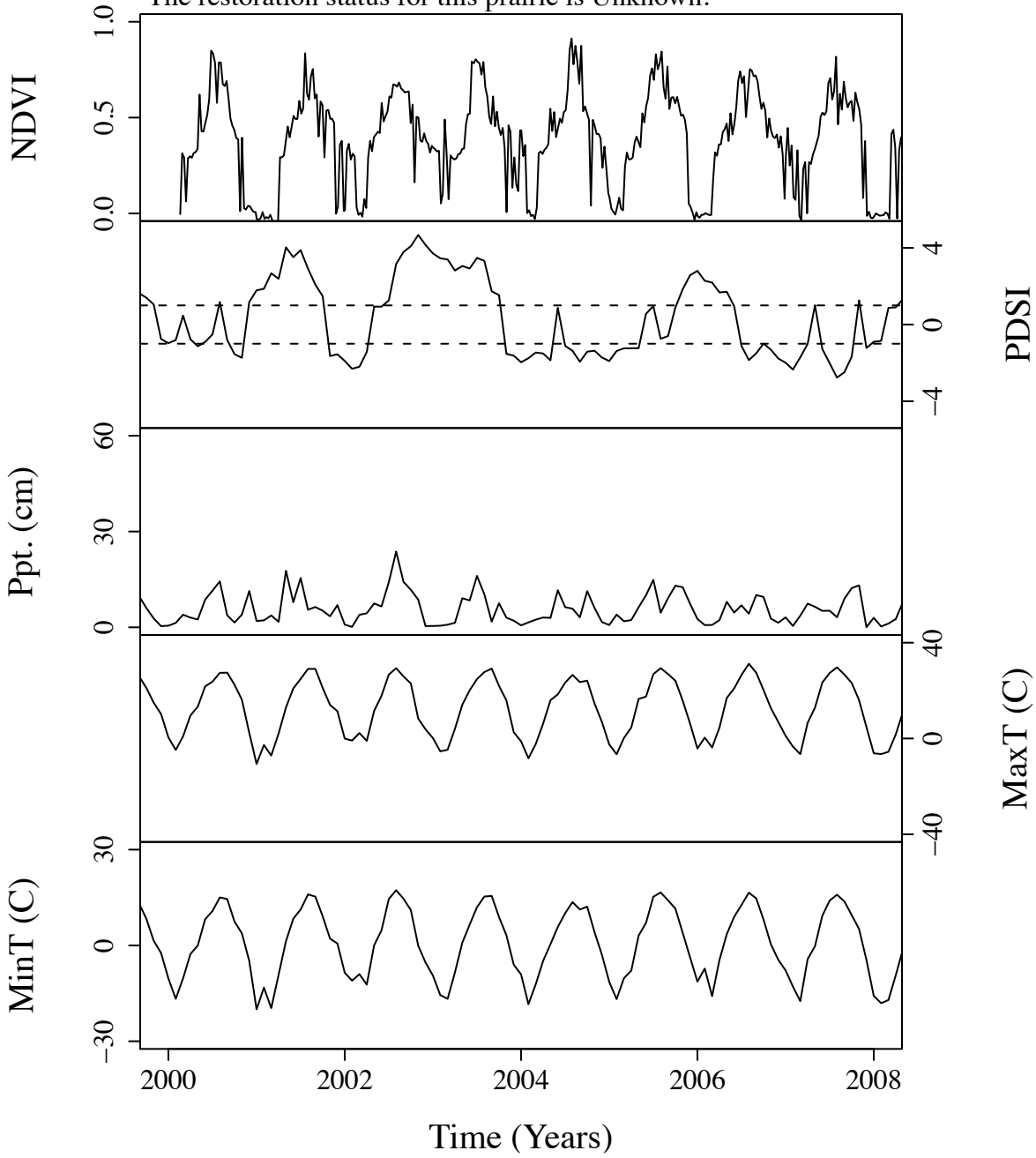

Figure B.26. Time series curves for mma8.
The community type for this prairie is Tall.
The dominant photosynthetic pathway for this prairie is C3.
The restoration status for this prairie is Unknown.

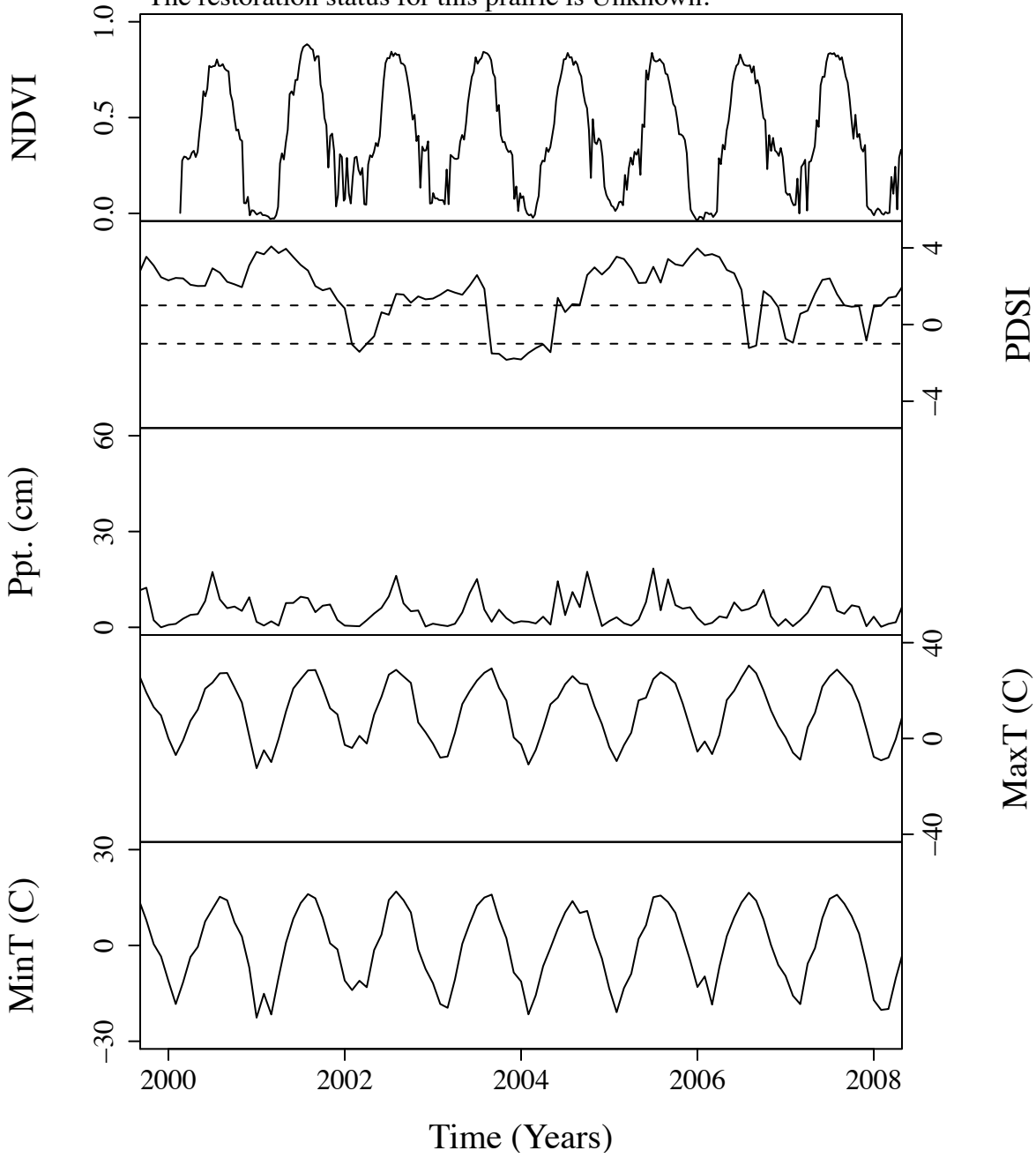

Figure B.27. Time series curves for mmi9.
The community type for this prairie is Tall.
The dominant photosynthetic pathway for this prairie is C4.
The restoration status for this prairie is Unknown.

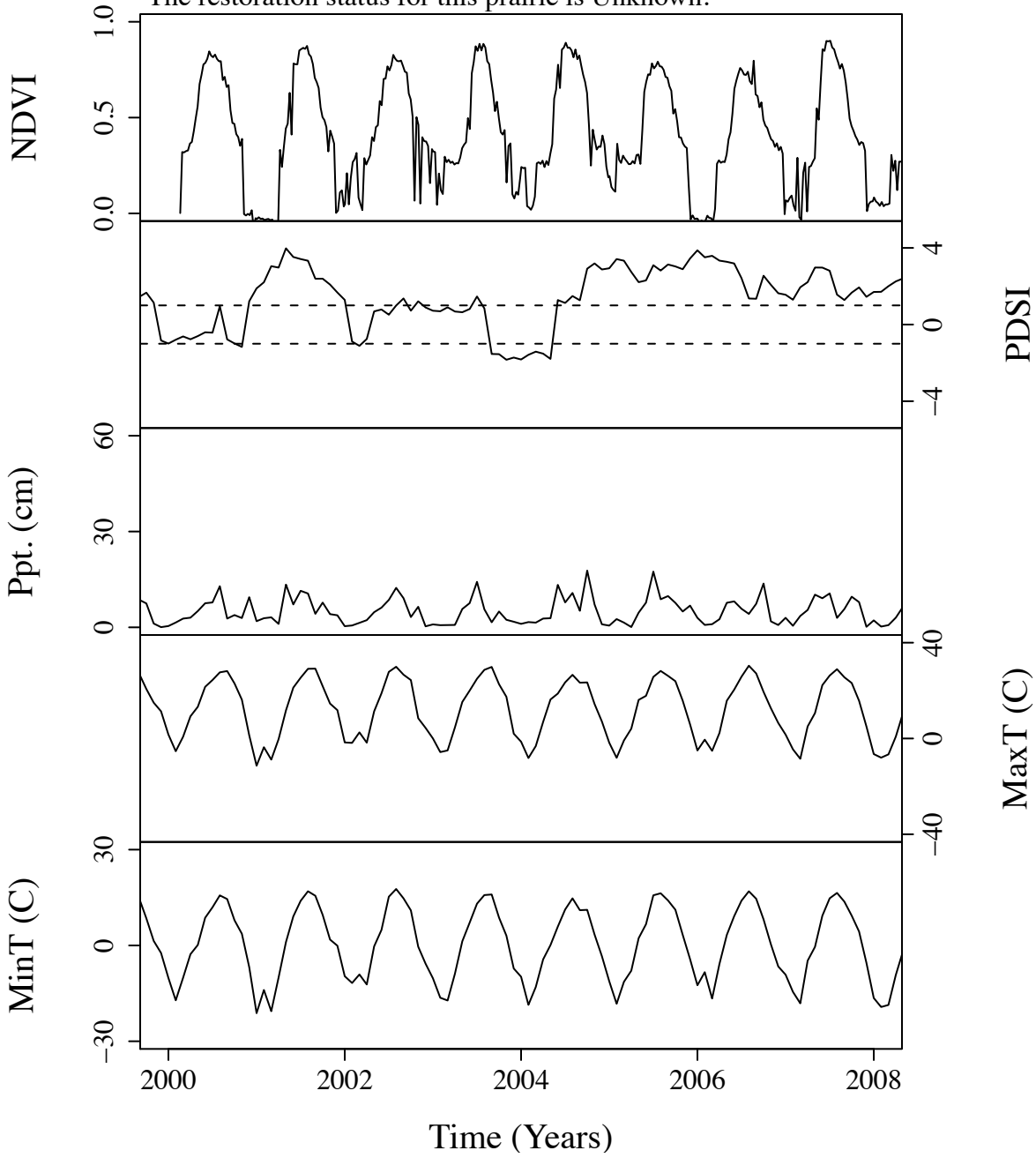

Figure B.28. Time series curves for mno33.
The community type for this prairie is Tall.
The dominant photosynthetic pathway for this prairie is C4.
The restoration status for this prairie is Mixed.

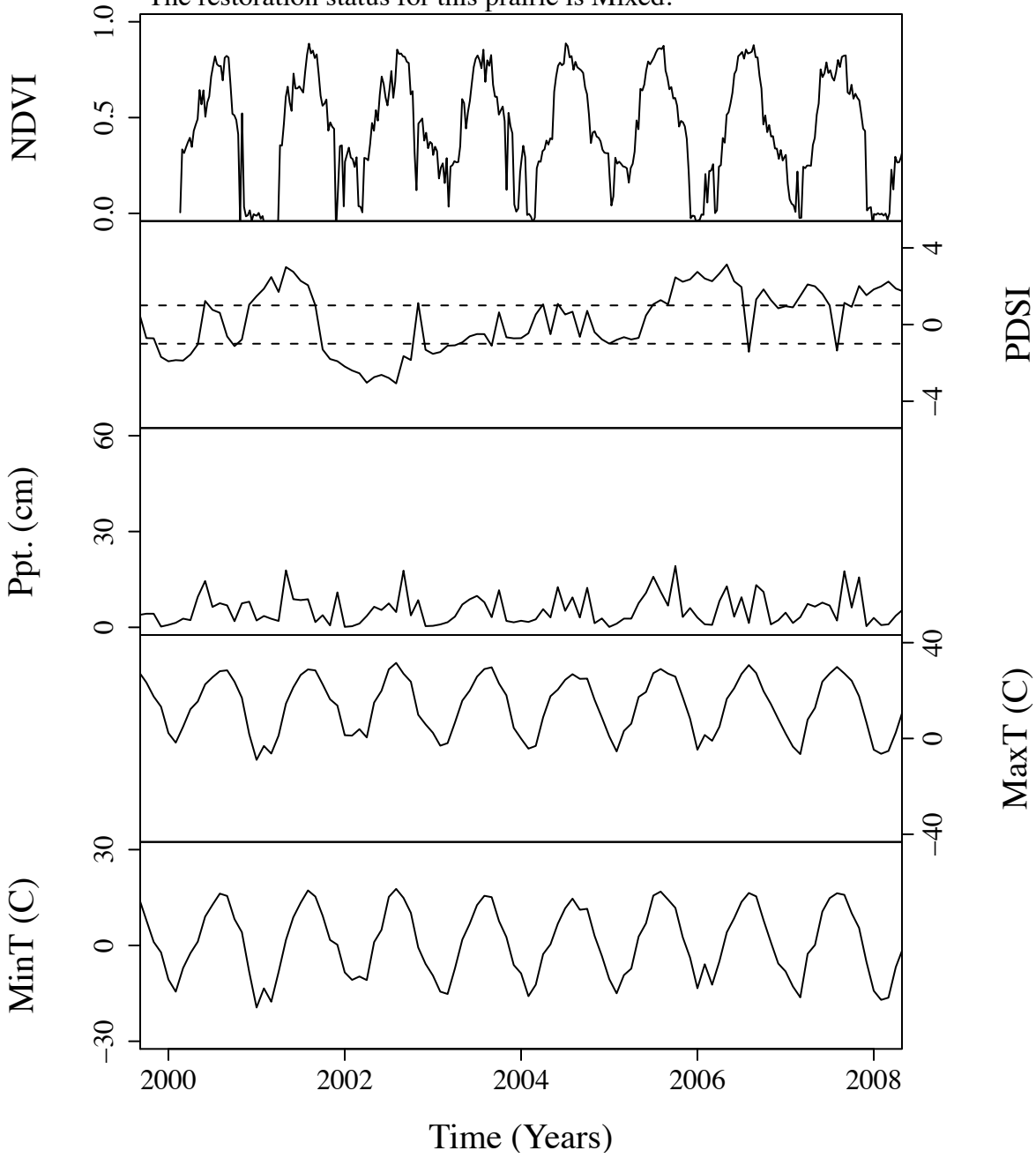

Figure B.29. Time series curves for mno36.
The community type for this prairie is Tall.
The dominant photosynthetic pathway for this prairie is C4.
The restoration status for this prairie is Mixed.

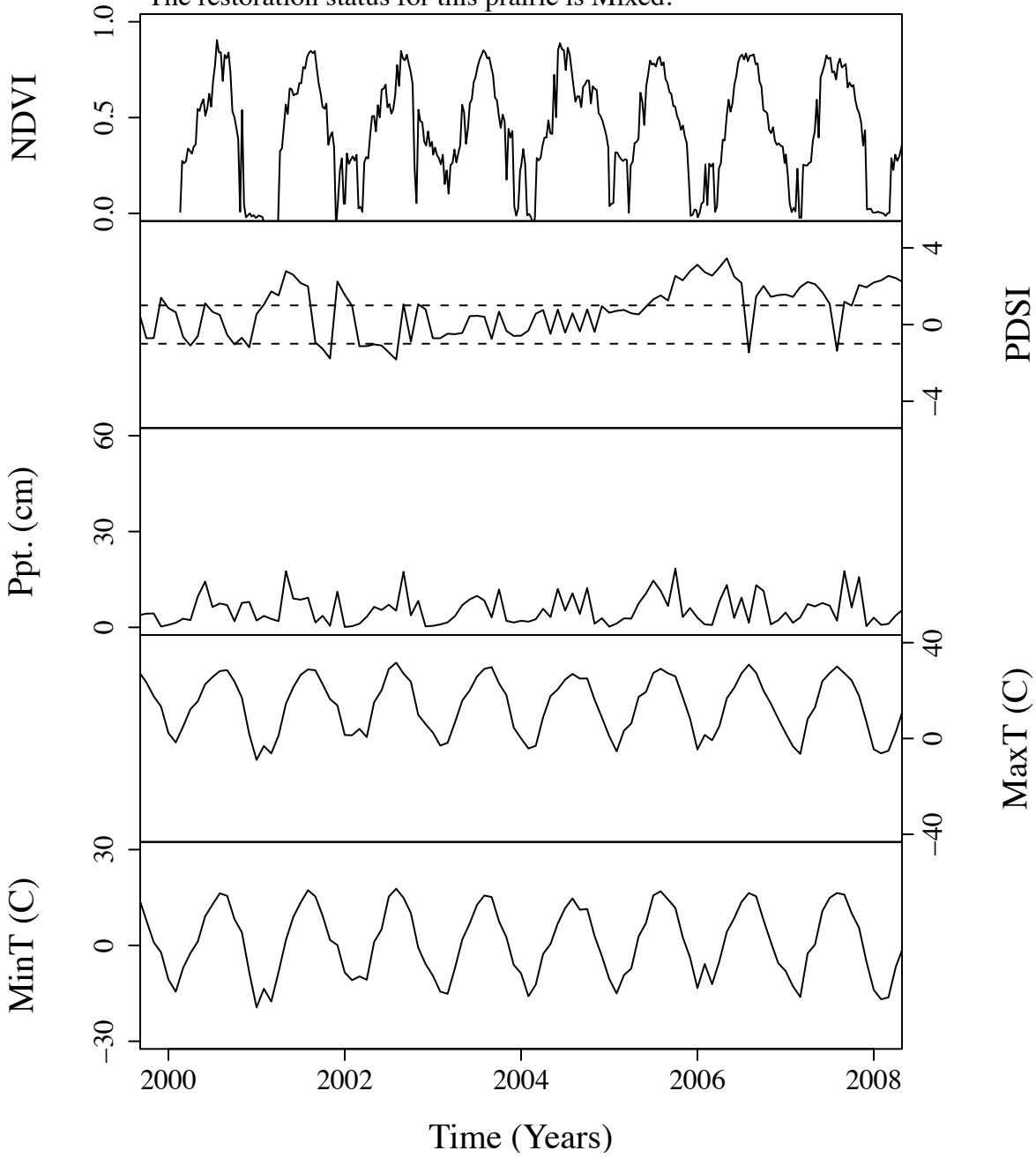

Figure B.30. Time series curves for mr.12.
The community type for this prairie is Tall.
The dominant photosynthetic pathway for this prairie is C3.
The restoration status for this prairie is Unknown.

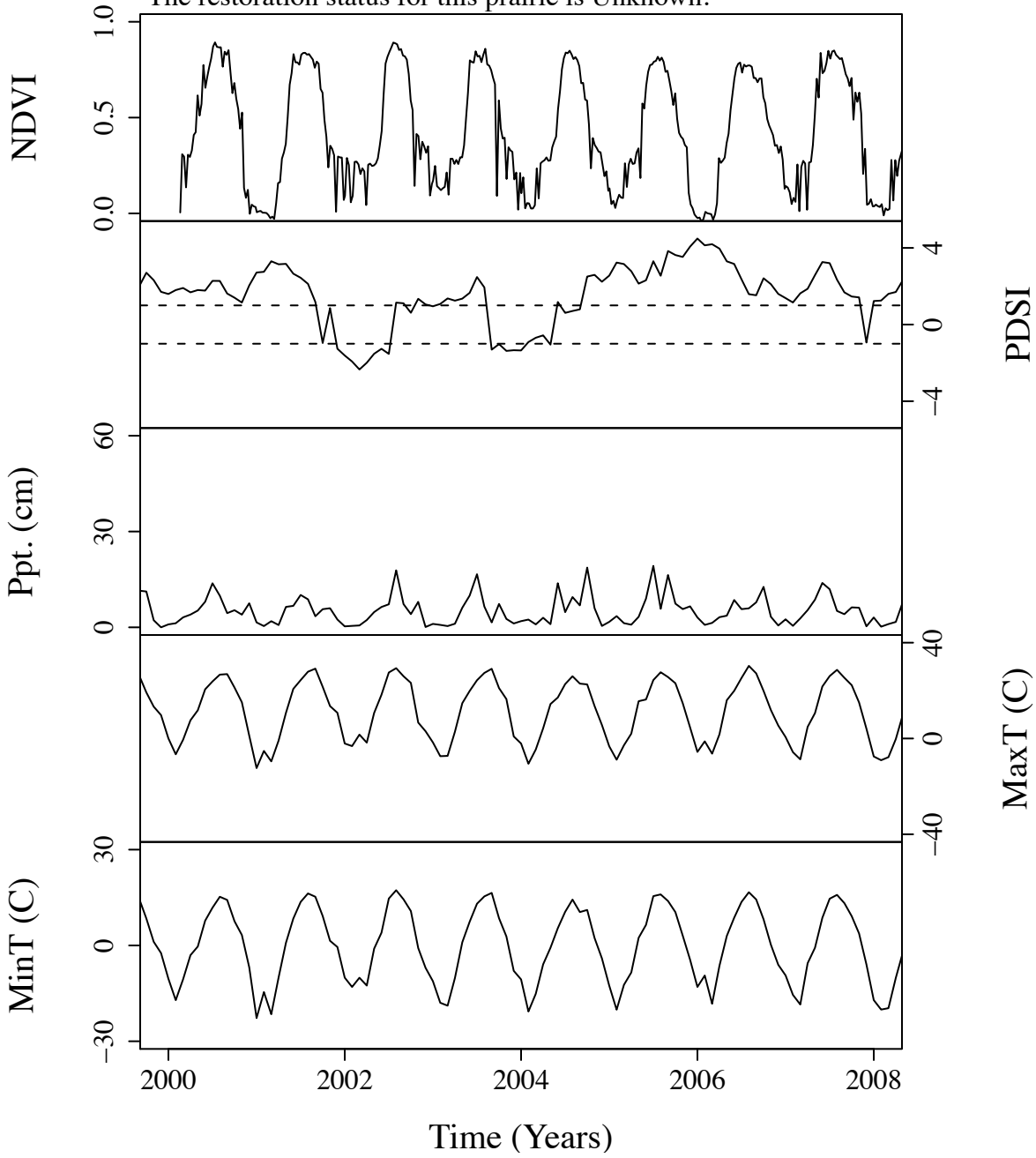

Figure B.31. Time series curves for mre37.
The community type for this prairie is Tall.
The dominant photosynthetic pathway for this prairie is C4.
The restoration status for this prairie is Unknown.

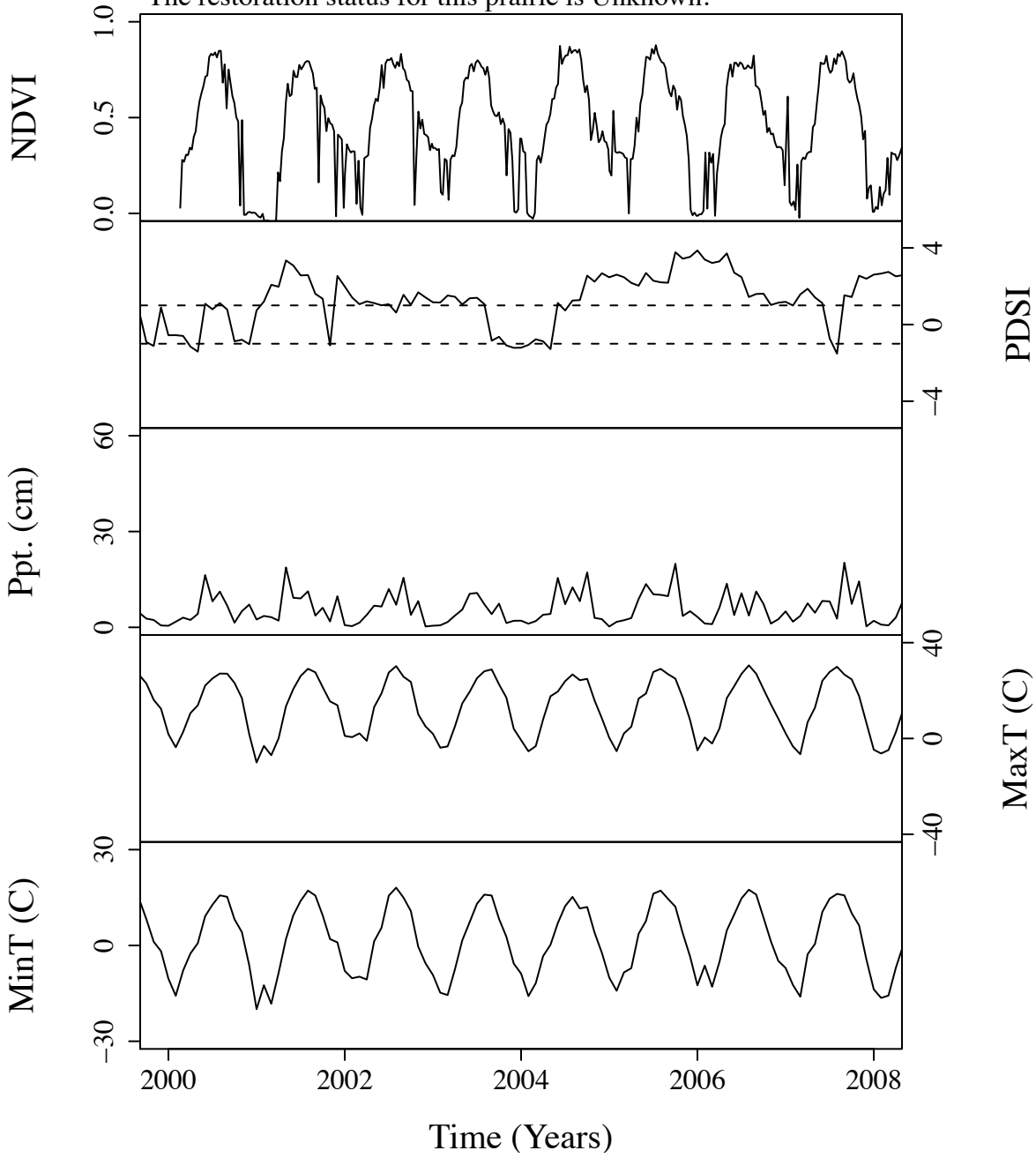

Figure B.32. Time series curves for msc42.
The community type for this prairie is Tall.
The dominant photosynthetic pathway for this prairie is C4.
The restoration status for this prairie is Unknown.

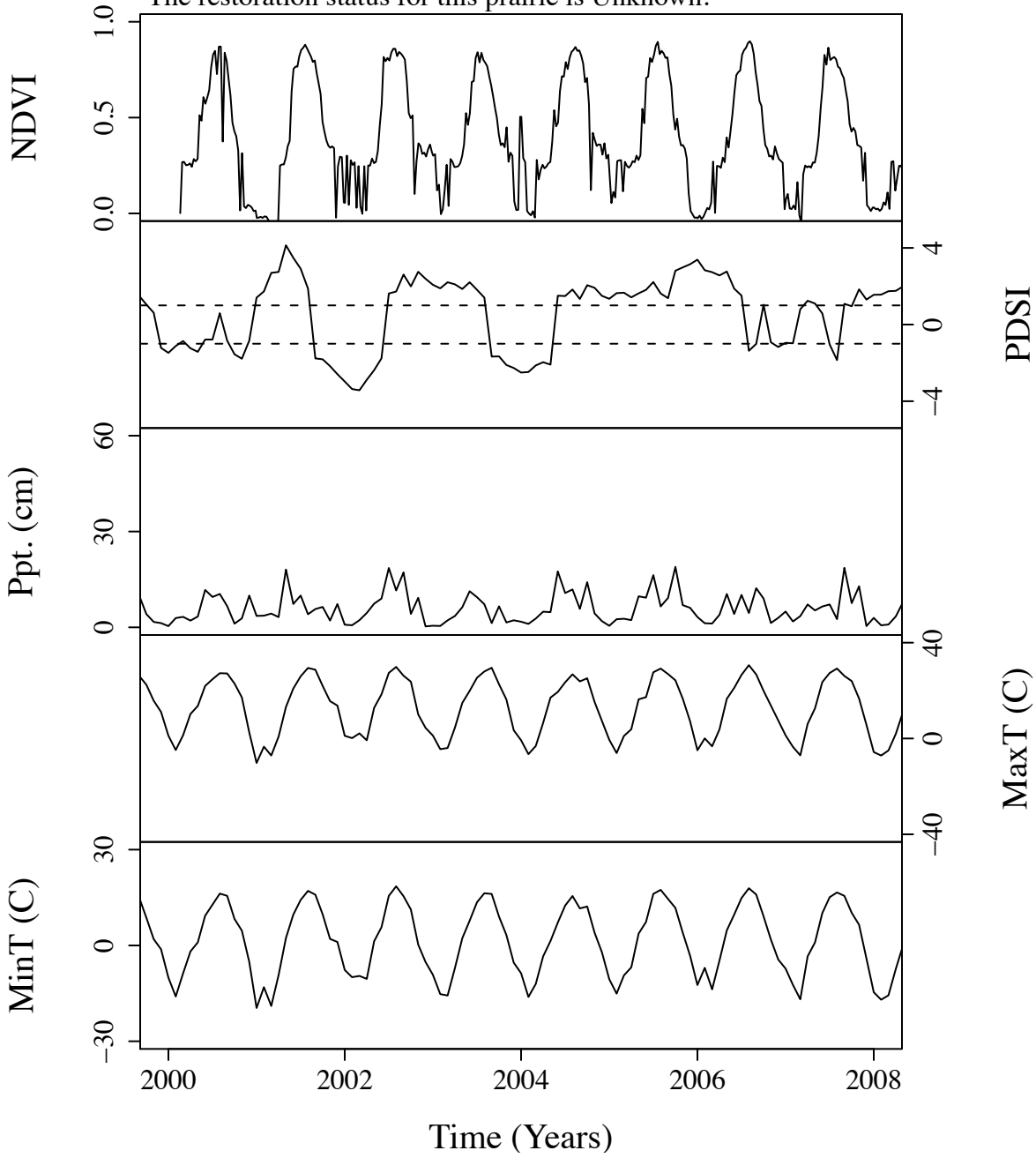

Figure B.33. Time series curves for mtw17.
The community type for this prairie is Tall.
The dominant photosynthetic pathway for this prairie is C3.
The restoration status for this prairie is Unknown.

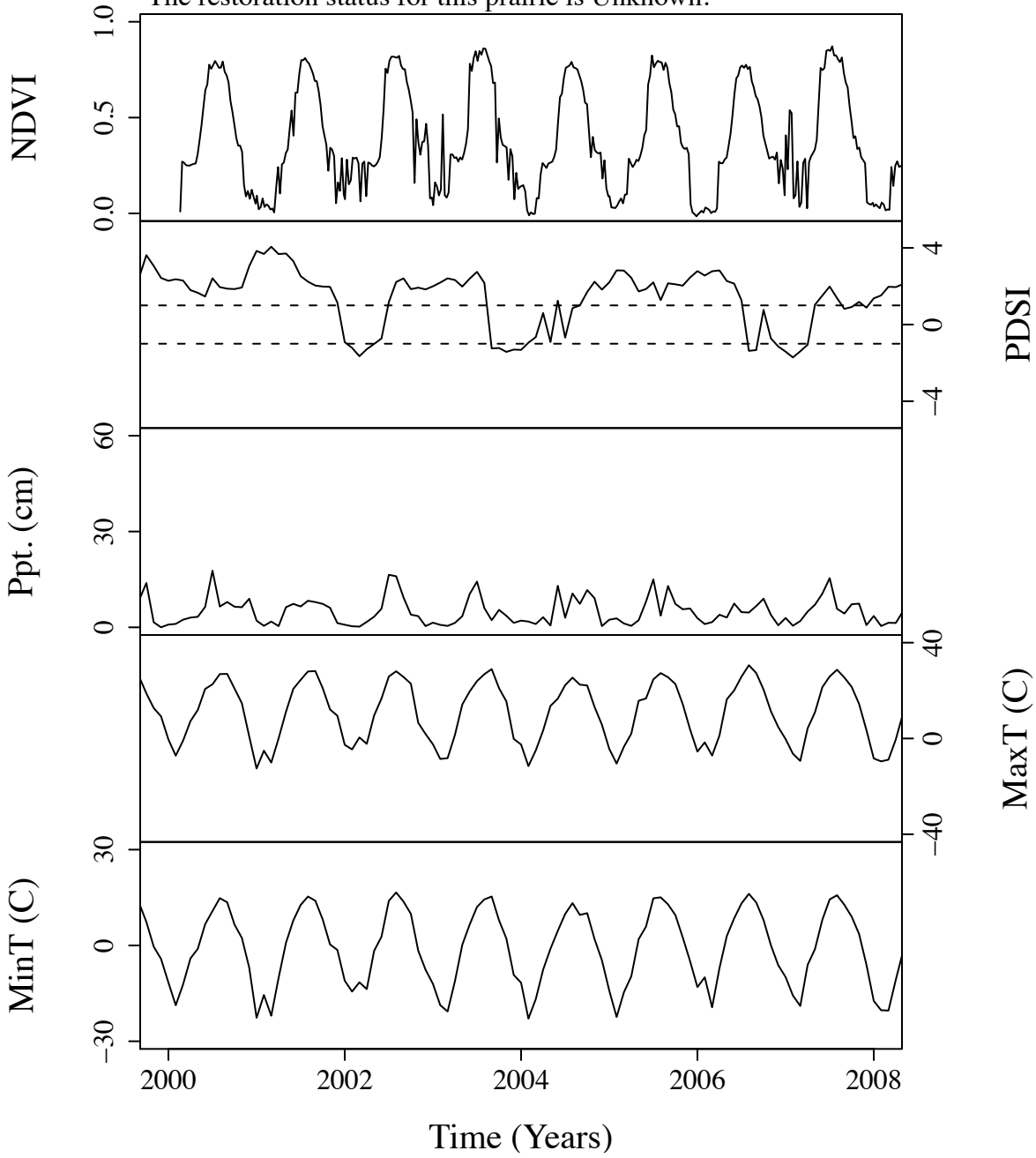

Figure B.34. Time series curves for mup1097.
The community type for this prairie is Tall.
The dominant photosynthetic pathway for this prairie is C4.
The restoration status for this prairie is Unknown.

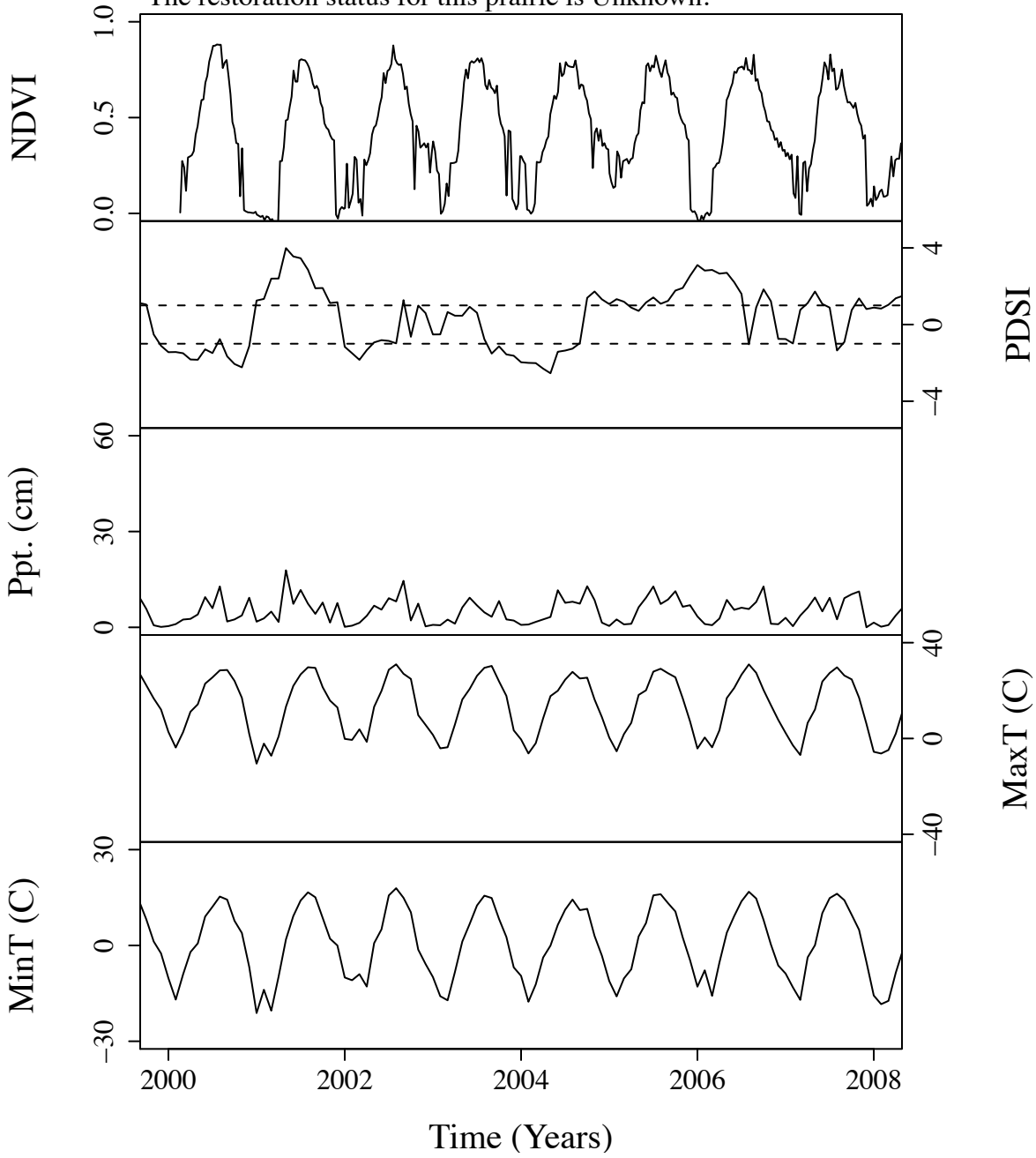

Figure B.35. Time series curves for mup1163.
The community type for this prairie is Tall.
The dominant photosynthetic pathway for this prairie is C4.
The restoration status for this prairie is Unknown.

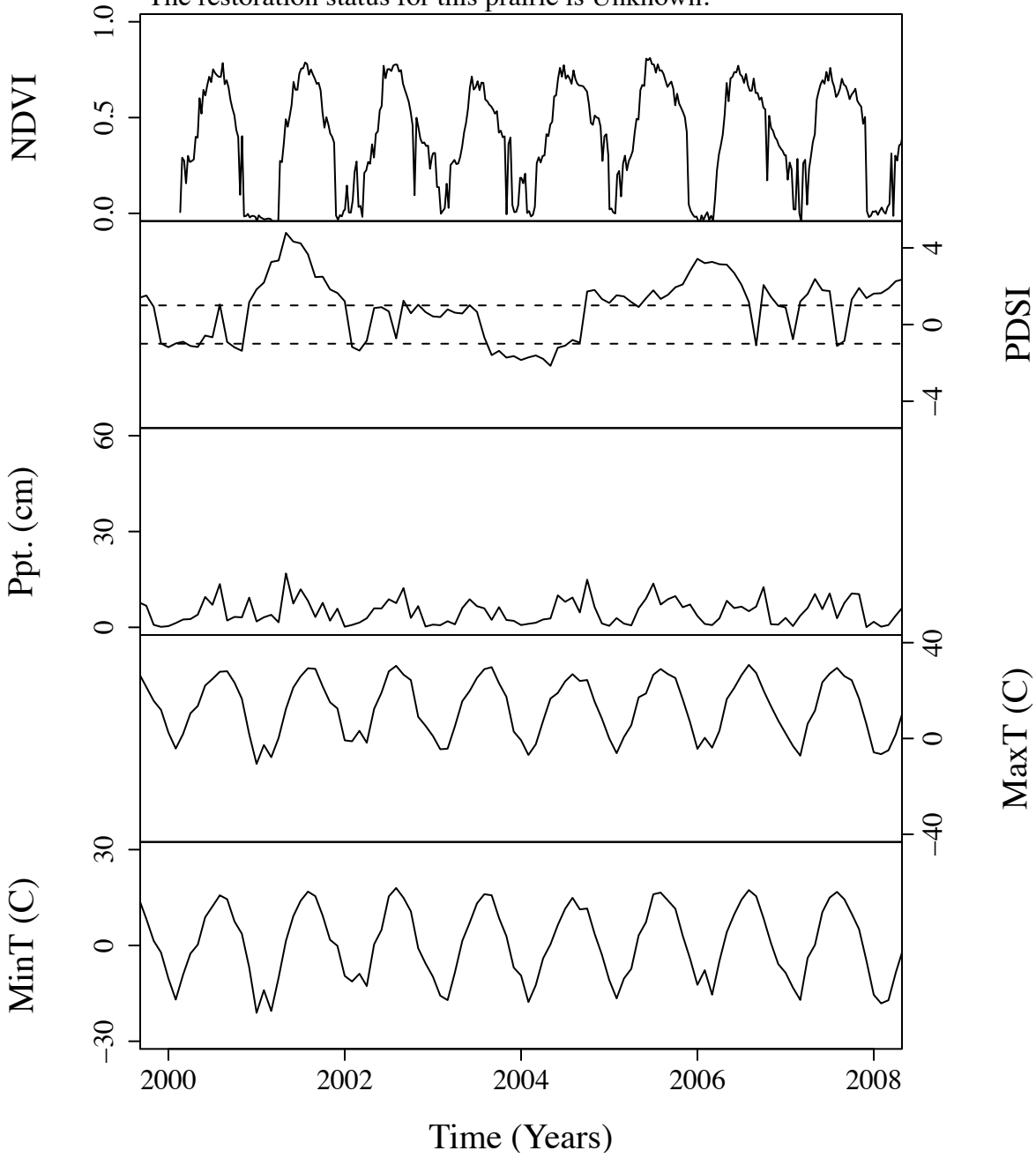

Figure B.36. Time series curves for mup1262.
The community type for this prairie is Tall.
The dominant photosynthetic pathway for this prairie is C4.
The restoration status for this prairie is Unknown.

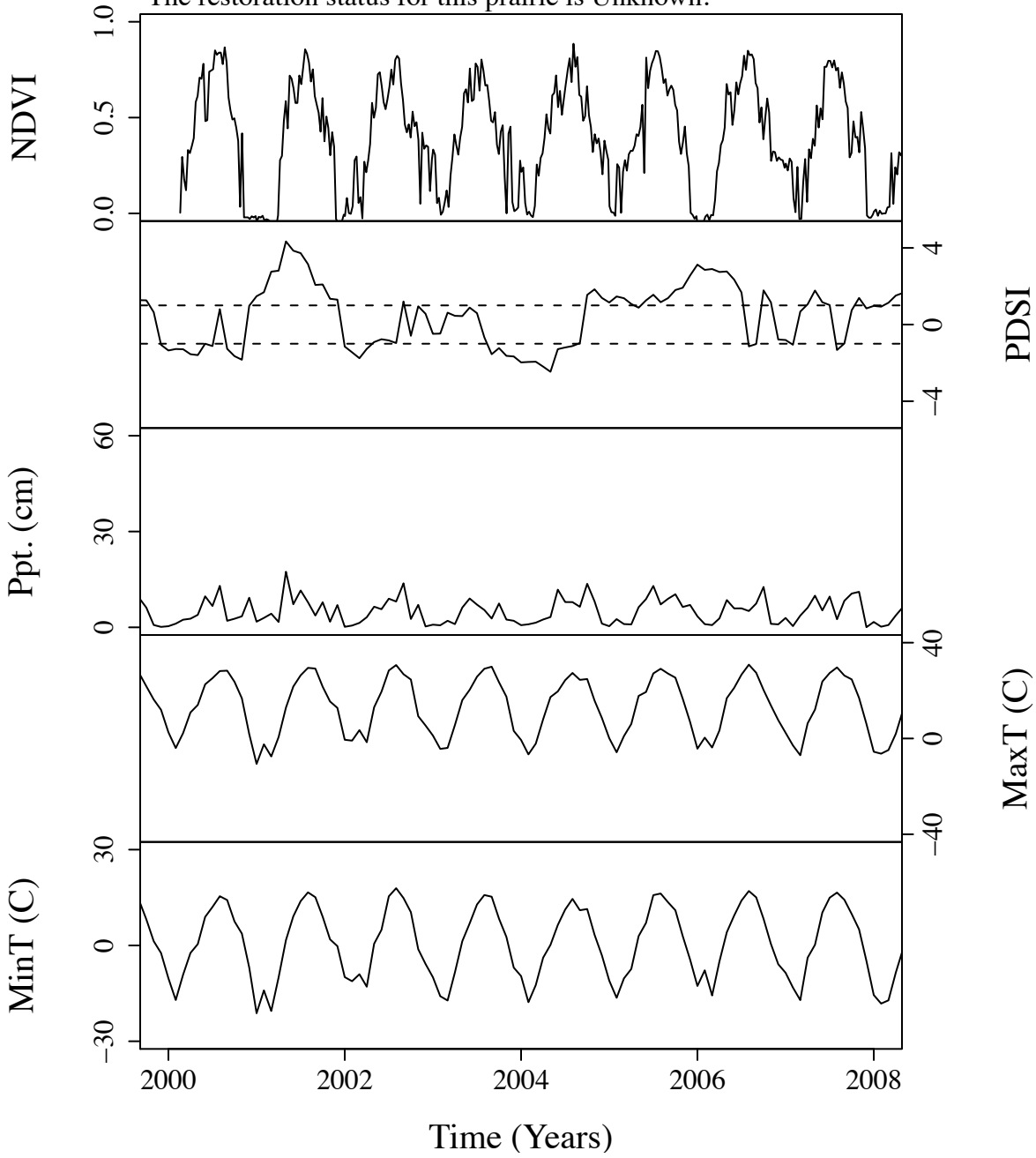

Figure B.37. Time series curves for mup1281.
The community type for this prairie is Tall.
The dominant photosynthetic pathway for this prairie is C4.
The restoration status for this prairie is Unknown.

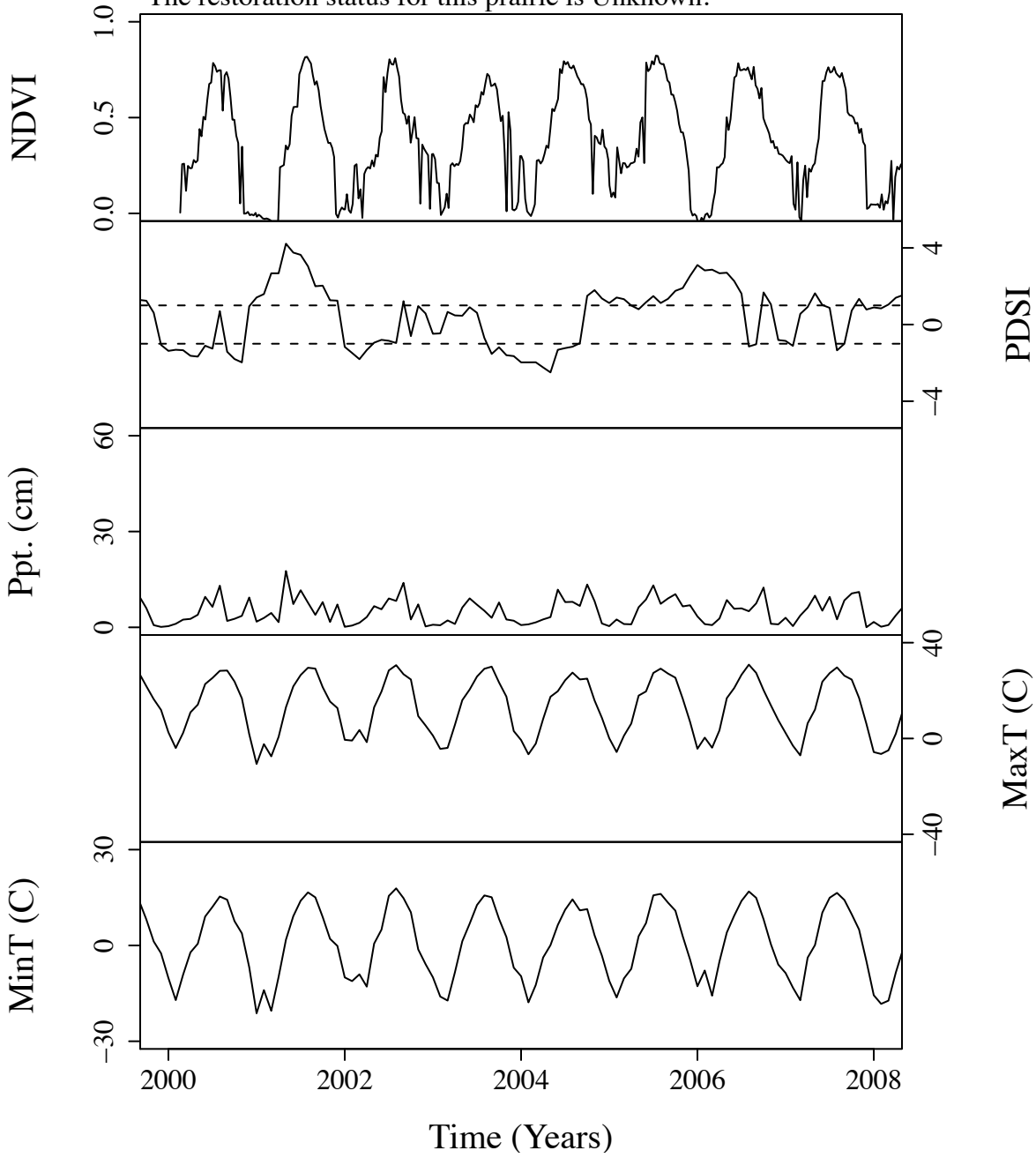

Figure B.38. Time series curves for mup1289.
The community type for this prairie is Tall.
The dominant photosynthetic pathway for this prairie is C4.
The restoration status for this prairie is Unknown.

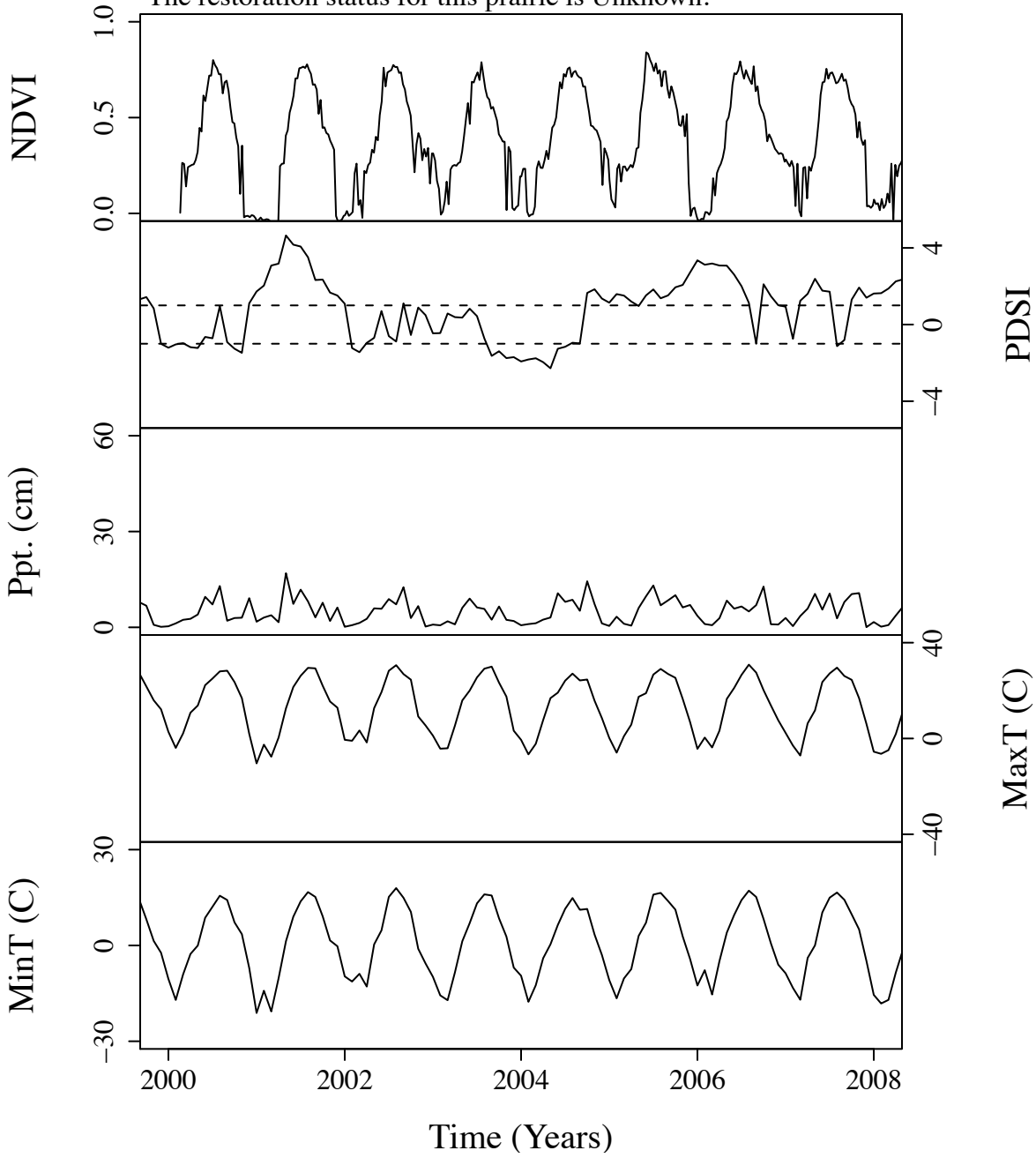

Figure B.39. Time series curves for mup1348.
The community type for this prairie is Tall.
The dominant photosynthetic pathway for this prairie is C4.
The restoration status for this prairie is Unknown.

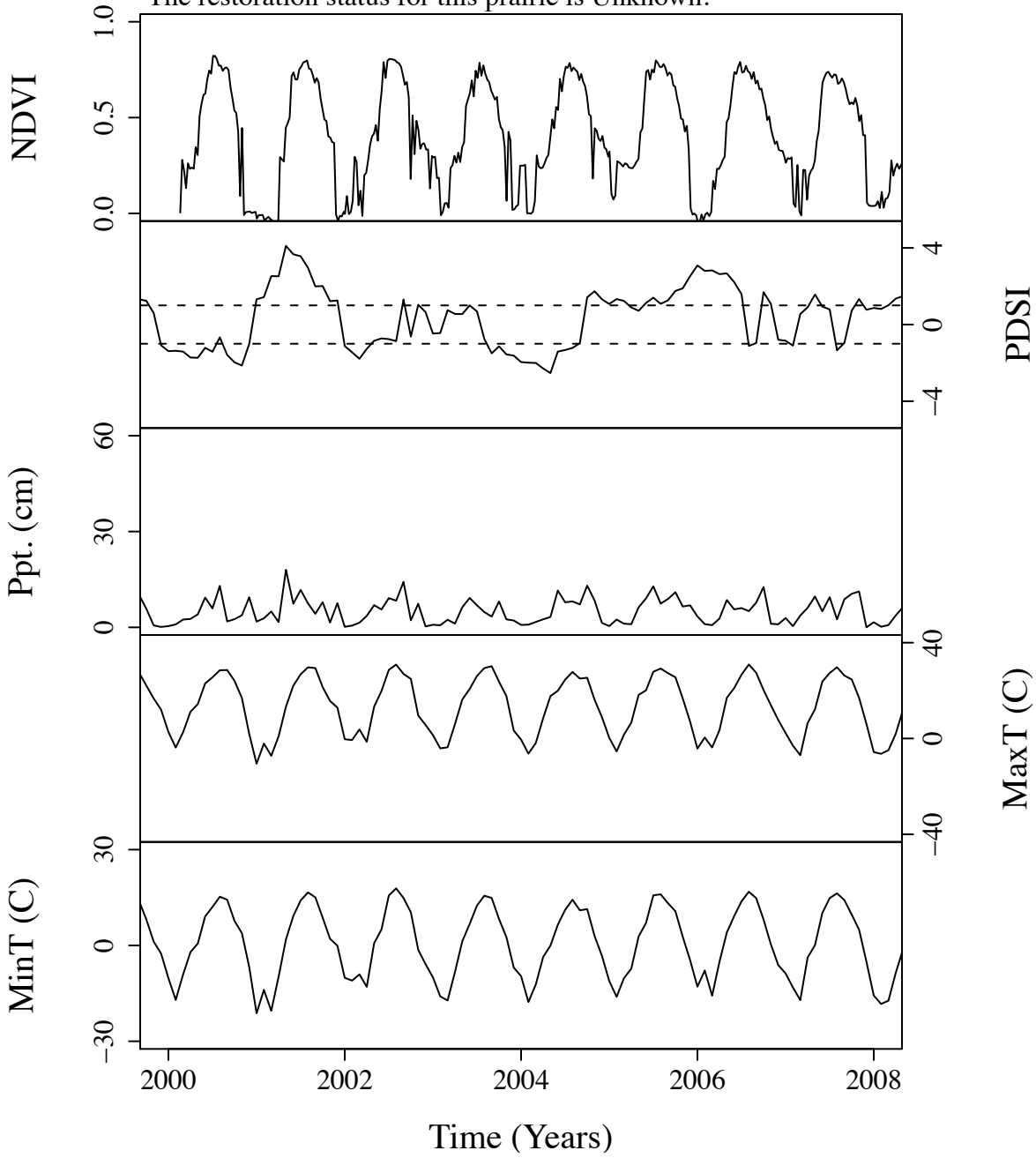

Figure B.40. Time series curves for mup1355.
The community type for this prairie is Tall.
The dominant photosynthetic pathway for this prairie is C4.
The restoration status for this prairie is Unknown.

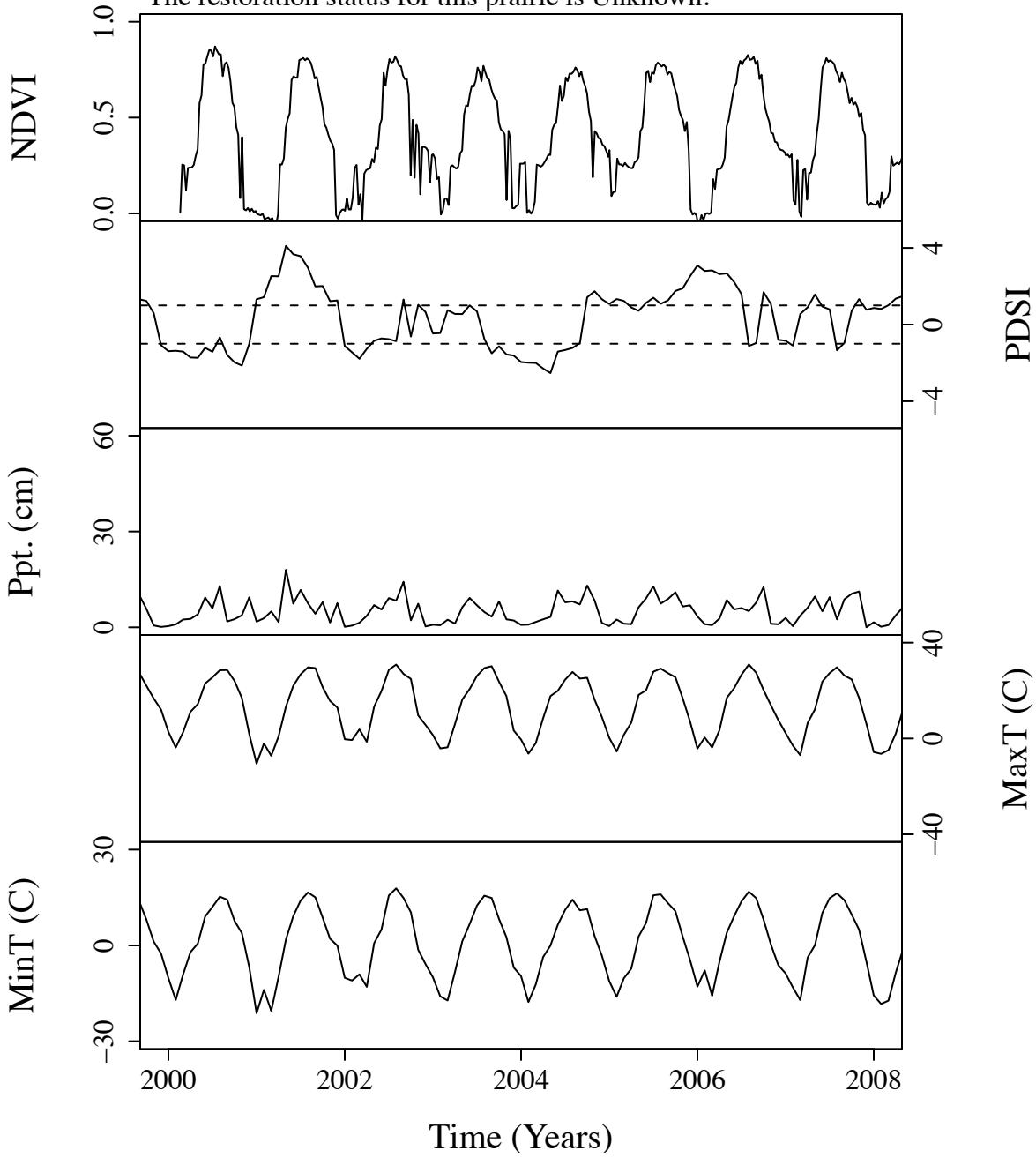

Figure B.41. Time series curves for mup1363.
The community type for this prairie is Tall.
The dominant photosynthetic pathway for this prairie is C4.
The restoration status for this prairie is Unknown.

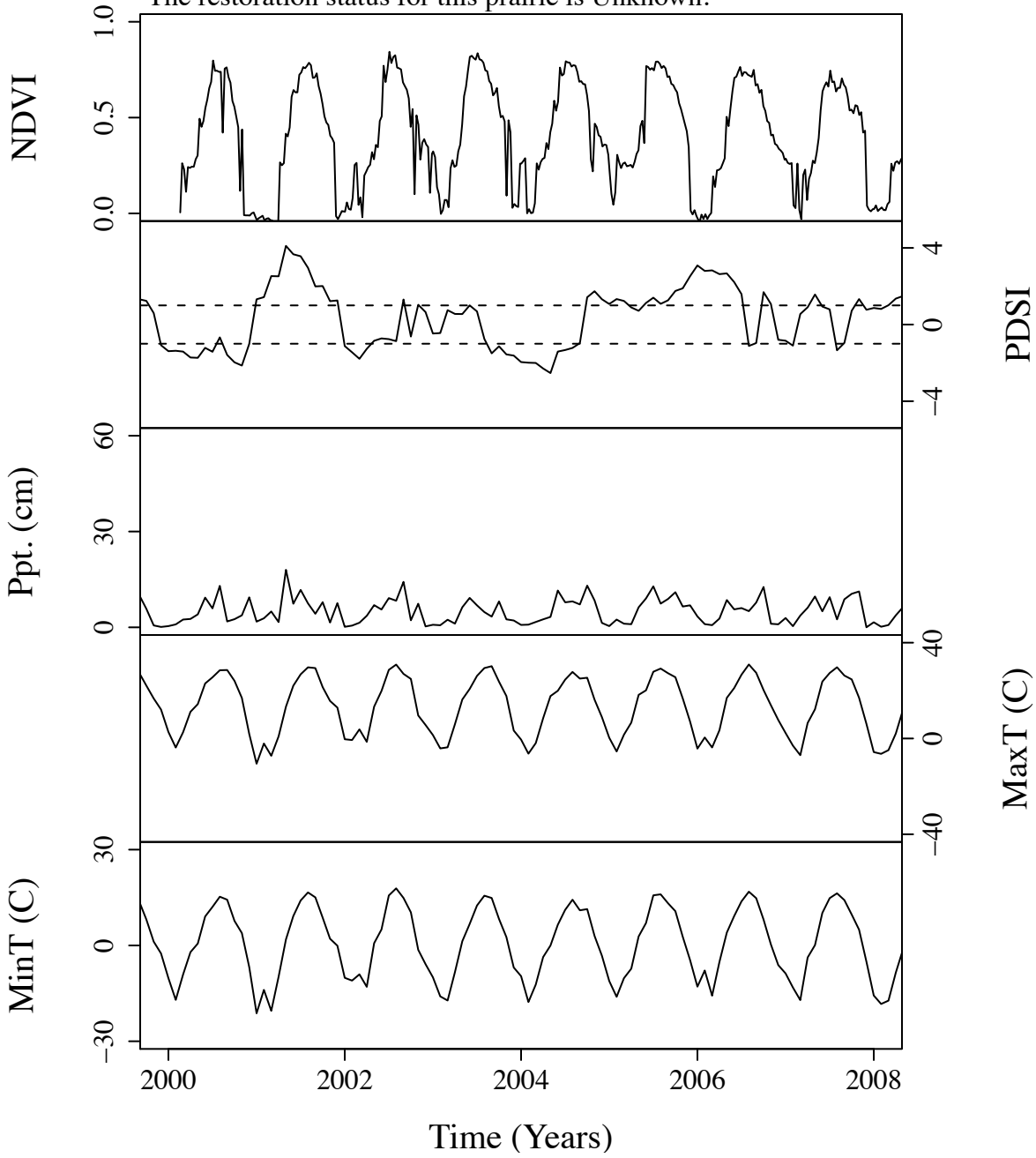

Figure B.42. Time series curves for mup1376.
The community type for this prairie is Tall.
The dominant photosynthetic pathway for this prairie is C4.
The restoration status for this prairie is Unknown.

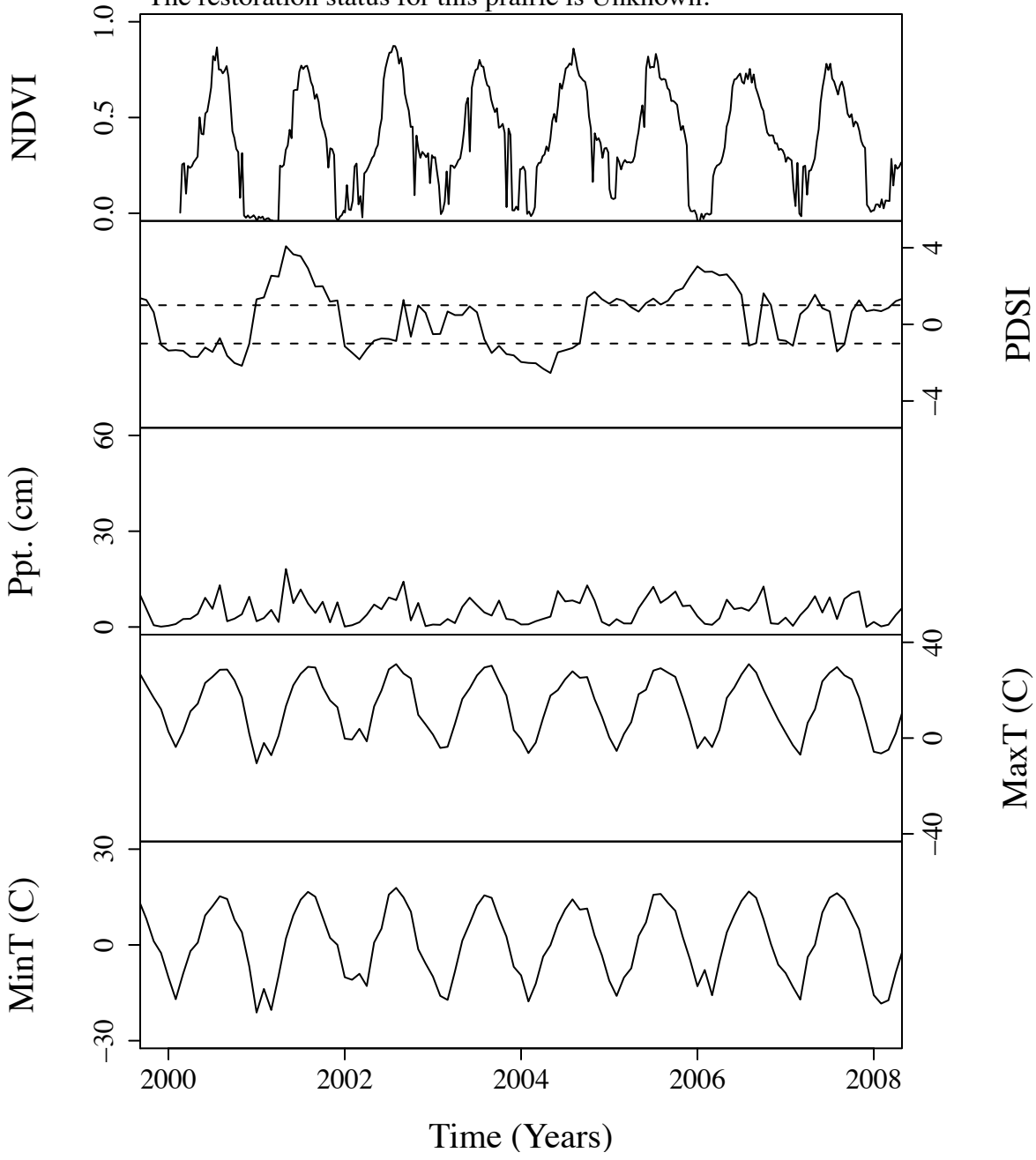

Figure B.43. Time series curves for mup1397.
The community type for this prairie is Tall.
The dominant photosynthetic pathway for this prairie is C4.
The restoration status for this prairie is Unknown.

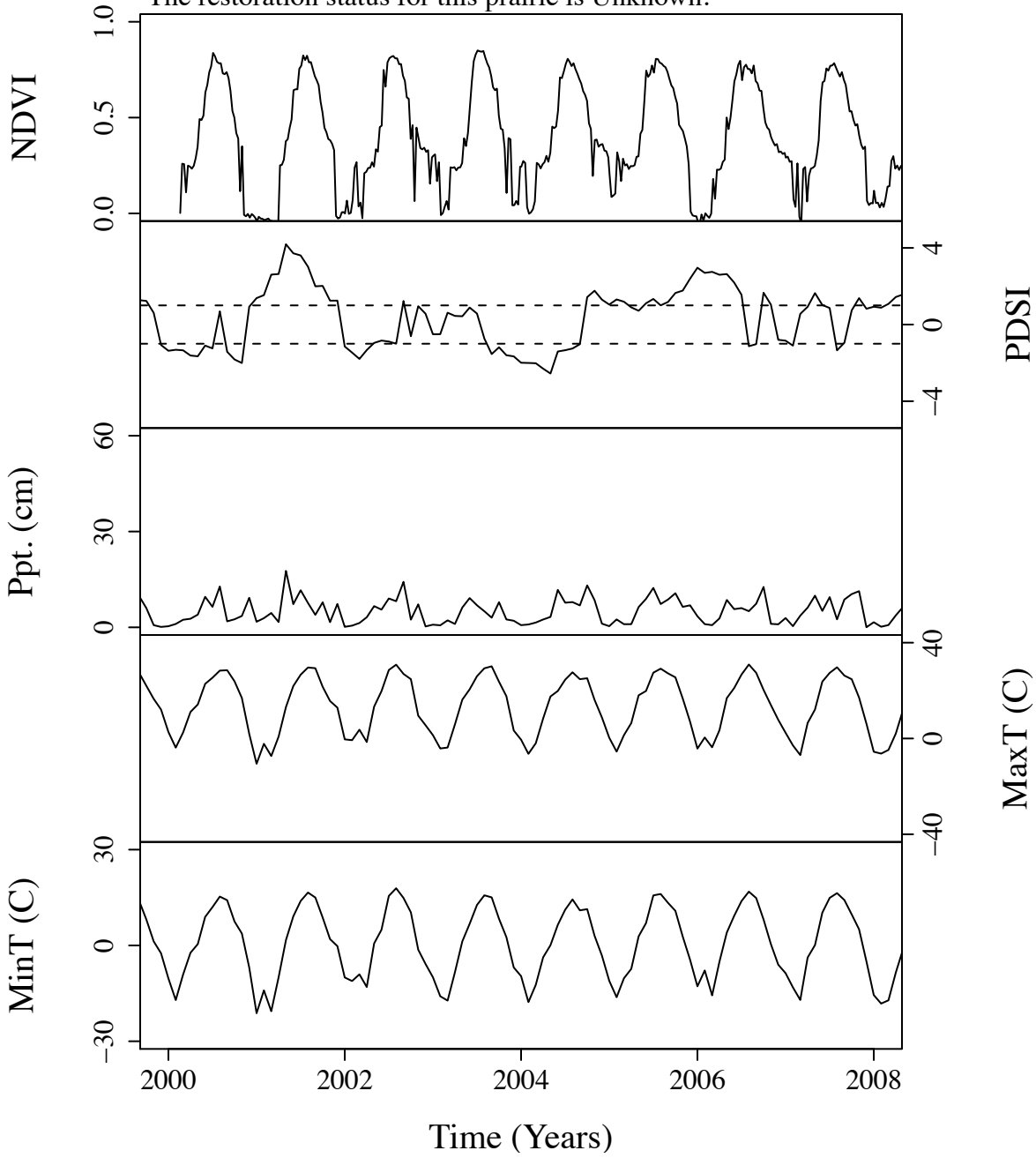

Figure B.44. Time series curves for mup1399.
The community type for this prairie is Tall.
The dominant photosynthetic pathway for this prairie is C4.
The restoration status for this prairie is Unknown.

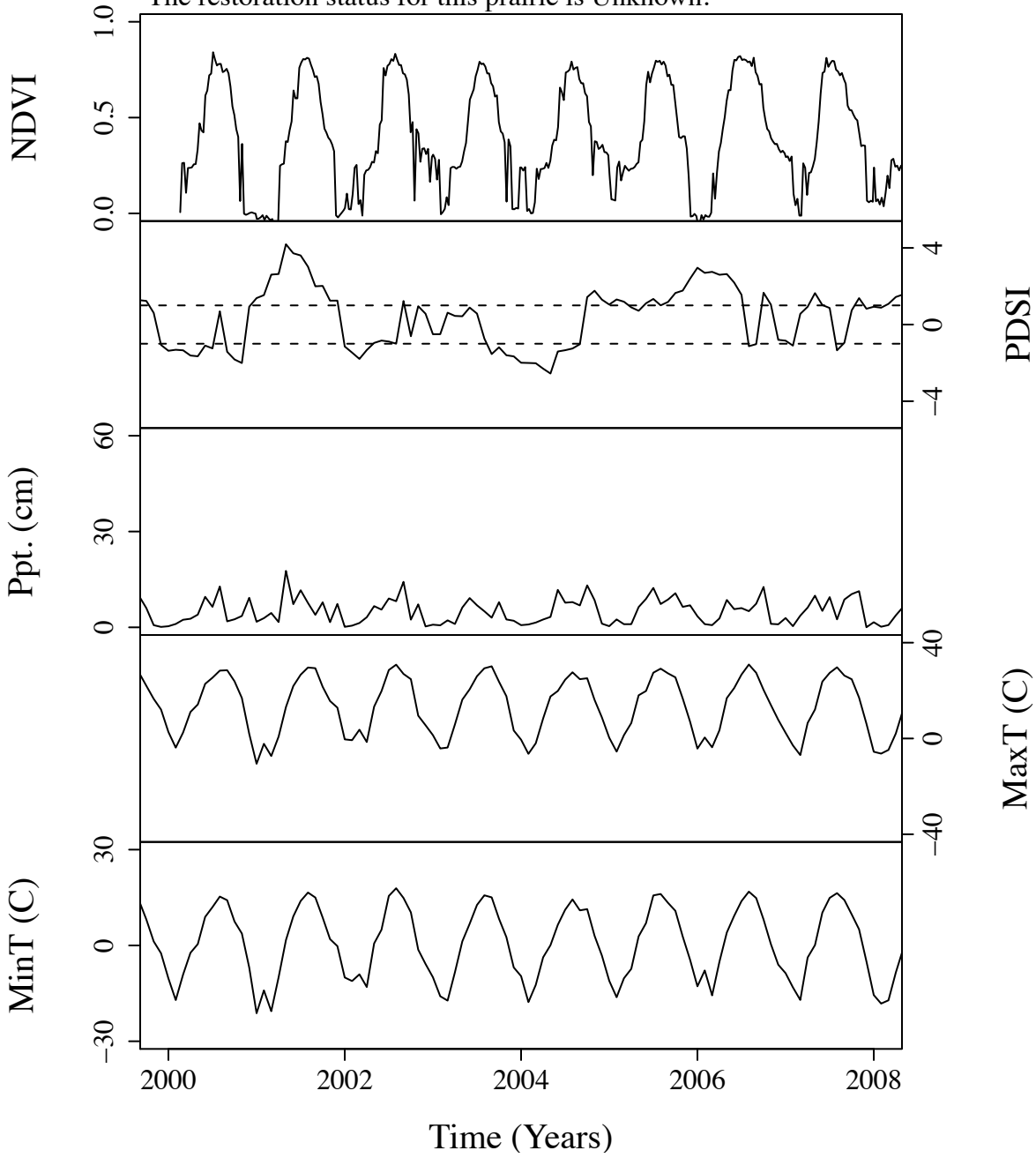

Figure B.45. Time series curves for mup1426.
The community type for this prairie is Tall.
The dominant photosynthetic pathway for this prairie is C4.
The restoration status for this prairie is Unknown.

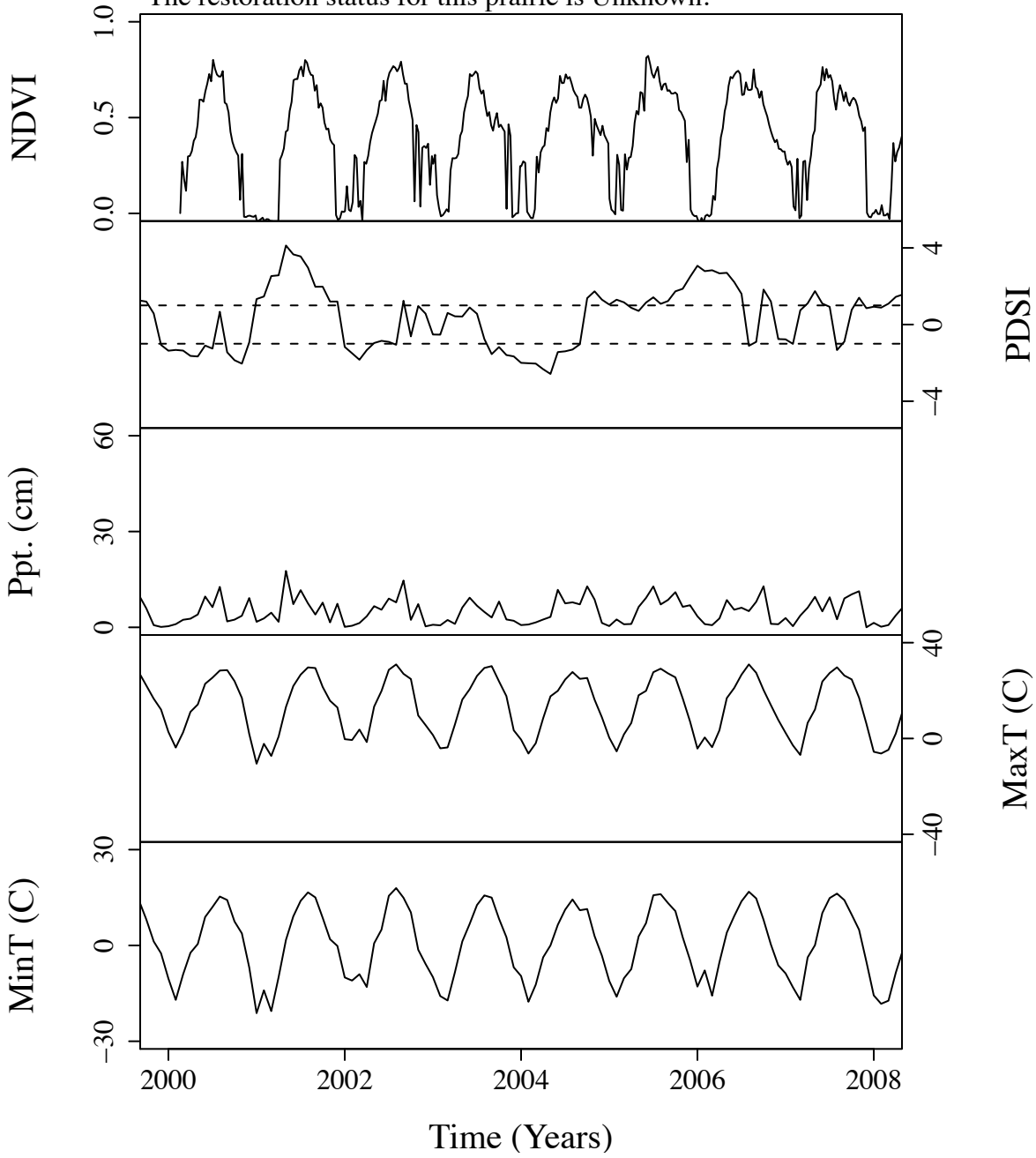

Figure B.46. Time series curves for mup1442.
The community type for this prairie is Tall.
The dominant photosynthetic pathway for this prairie is C4.
The restoration status for this prairie is Unknown.

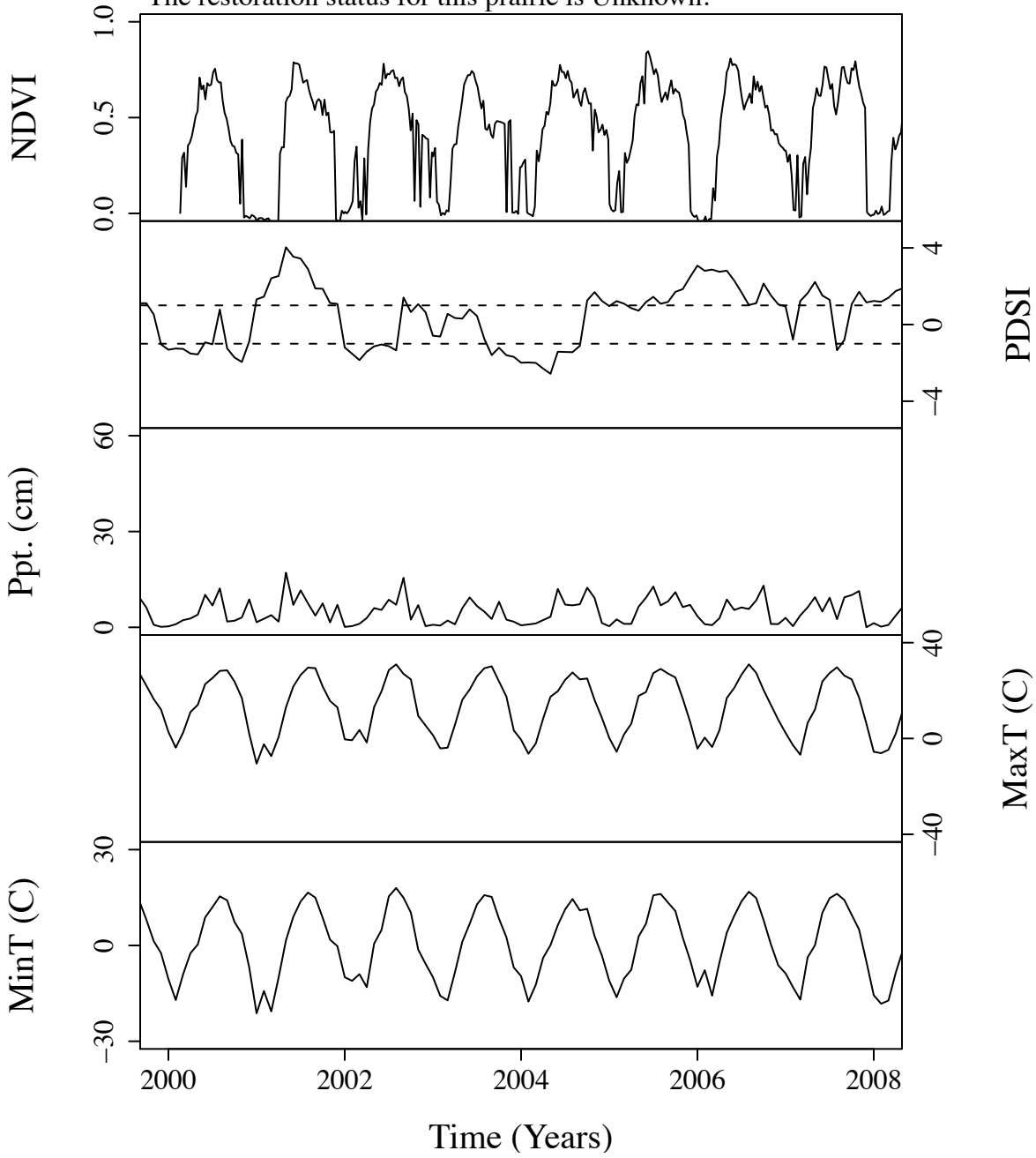

Figure B.47. Time series curves for mup2255.
The community type for this prairie is NoType.
The dominant photosynthetic pathway for this prairie is C4.
The restoration status for this prairie is Unknown.

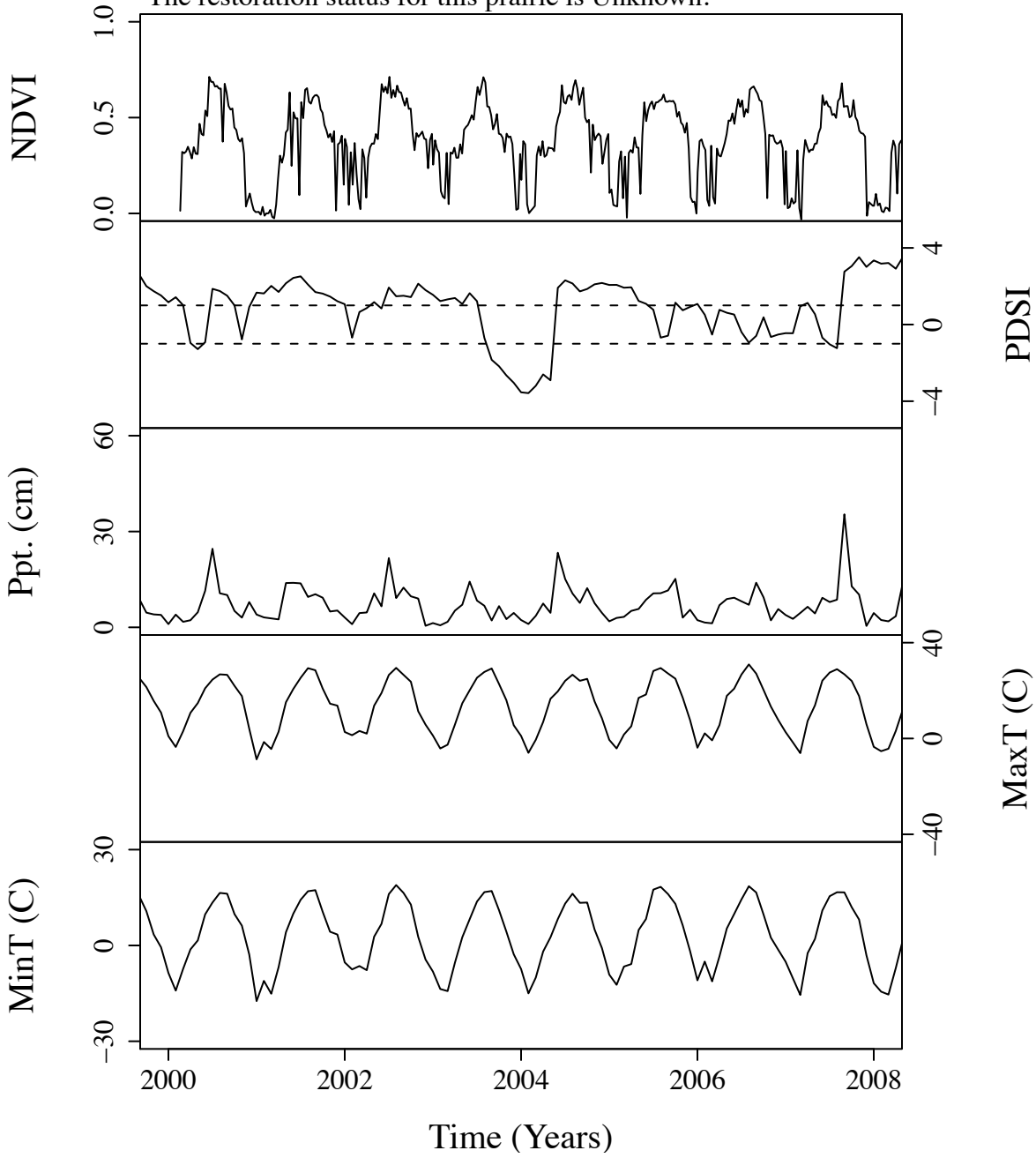

Figure B.48. Time series curves for mup2263.
The community type for this prairie is NoType.
The dominant photosynthetic pathway for this prairie is C4.
The restoration status for this prairie is Unknown.

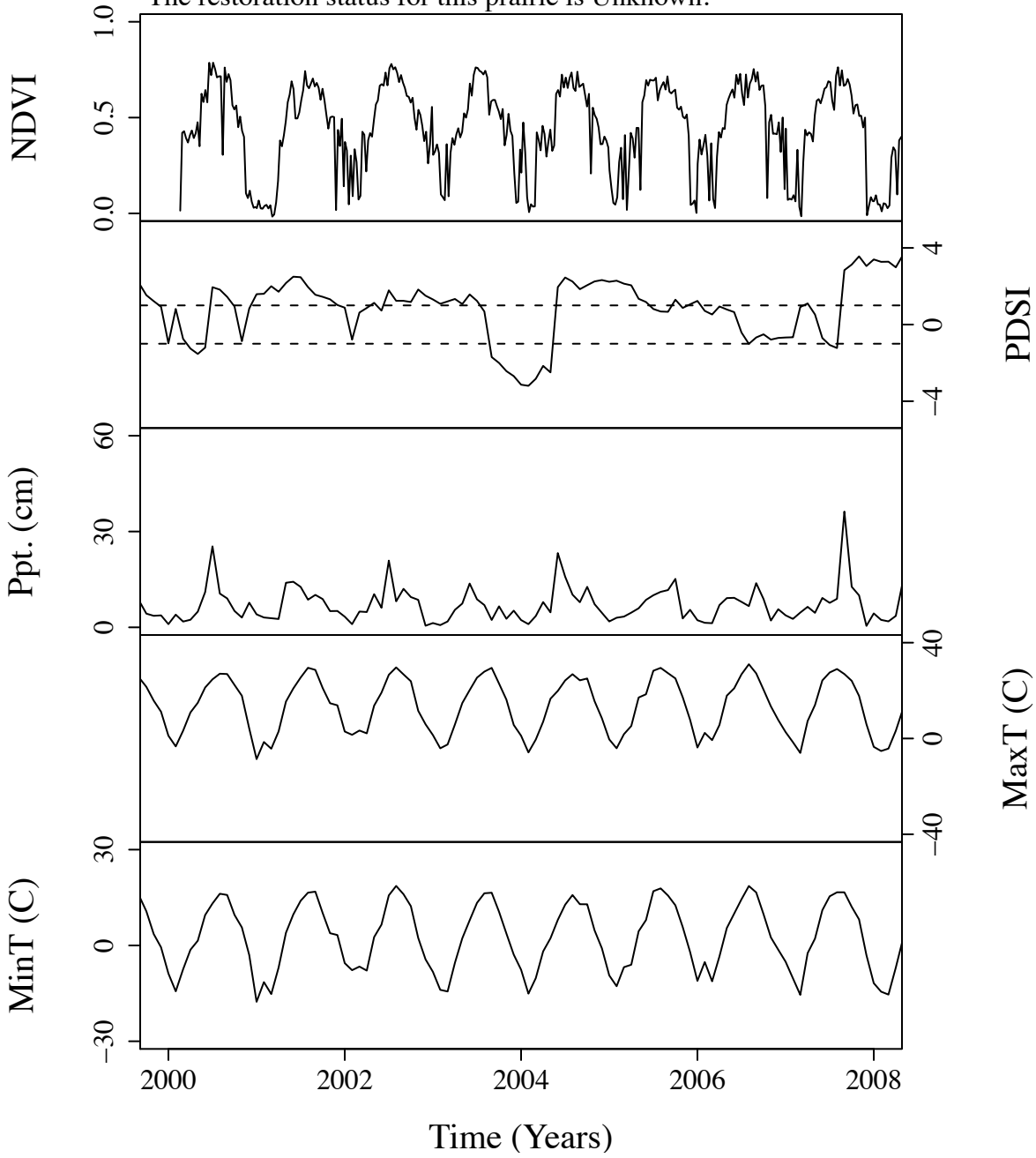

Figure B.49. Time series curves for mup412.
The community type for this prairie is NoType.
The dominant photosynthetic pathway for this prairie is C4.
The restoration status for this prairie is Unknown.

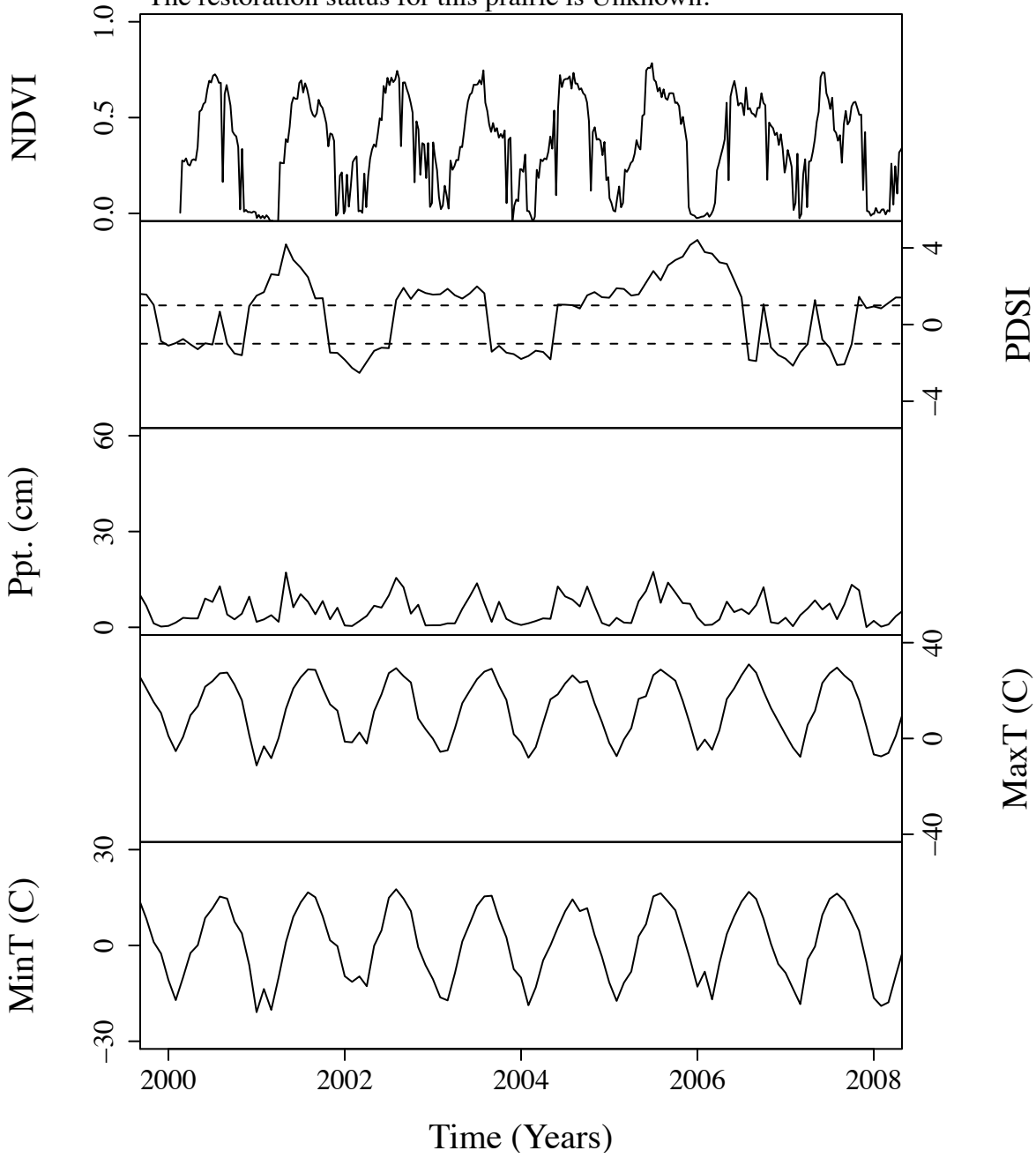

Figure B.50. Time series curves for mup704.
The community type for this prairie is NoType.
The dominant photosynthetic pathway for this prairie is C4.
The restoration status for this prairie is Unknown.

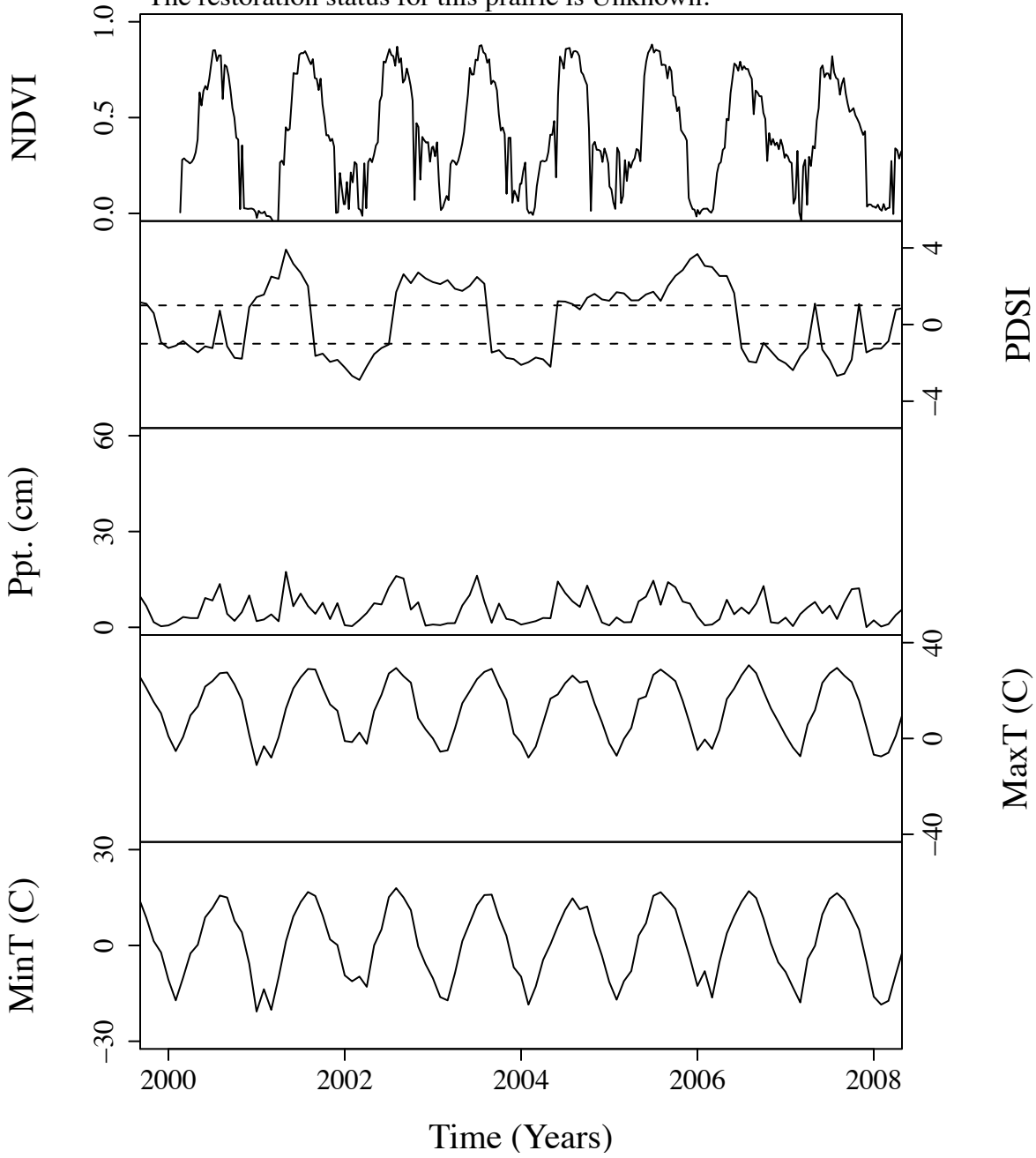

Figure B.51. Time series curves for mup979.
The community type for this prairie is Tall.
The dominant photosynthetic pathway for this prairie is C4.
The restoration status for this prairie is Unknown.

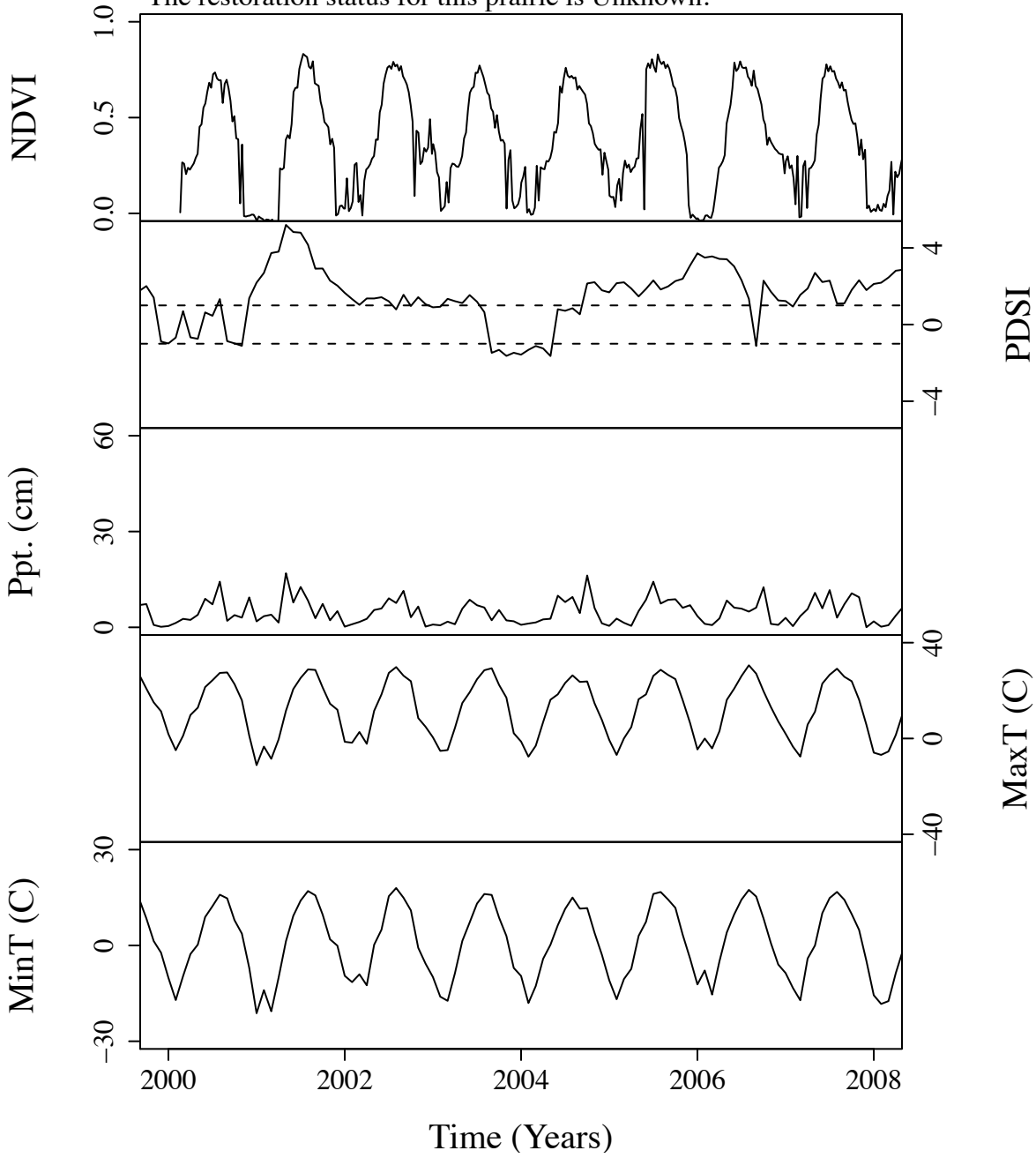

Figure B.52. Time series curves for mwe18.
The community type for this prairie is Tall.
The dominant photosynthetic pathway for this prairie is C3.
The restoration status for this prairie is Unknown.

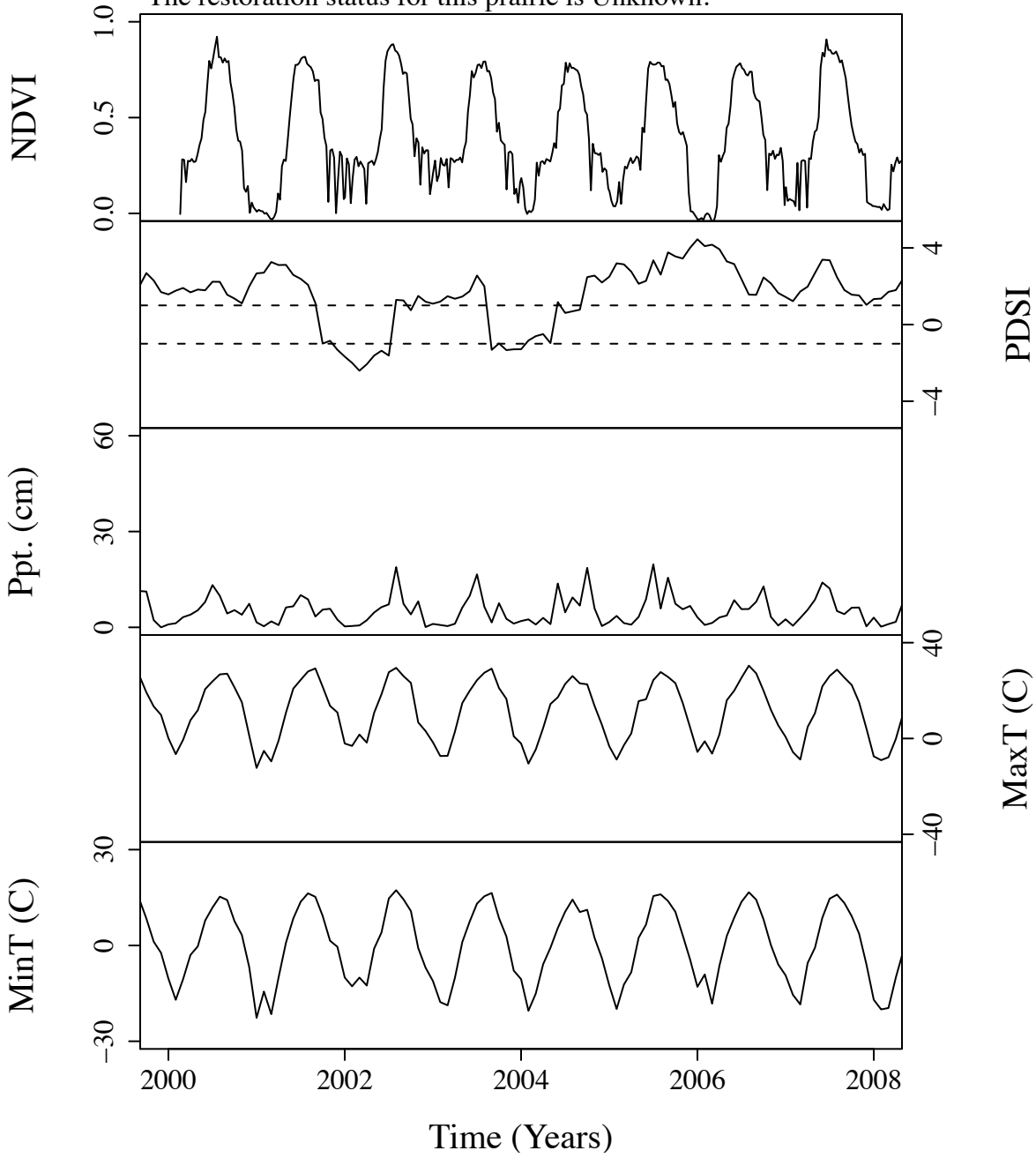

Figure B.53. Time series curves for mwp1533.
The community type for this prairie is Tall.
The dominant photosynthetic pathway for this prairie is C4.
The restoration status for this prairie is Unknown.

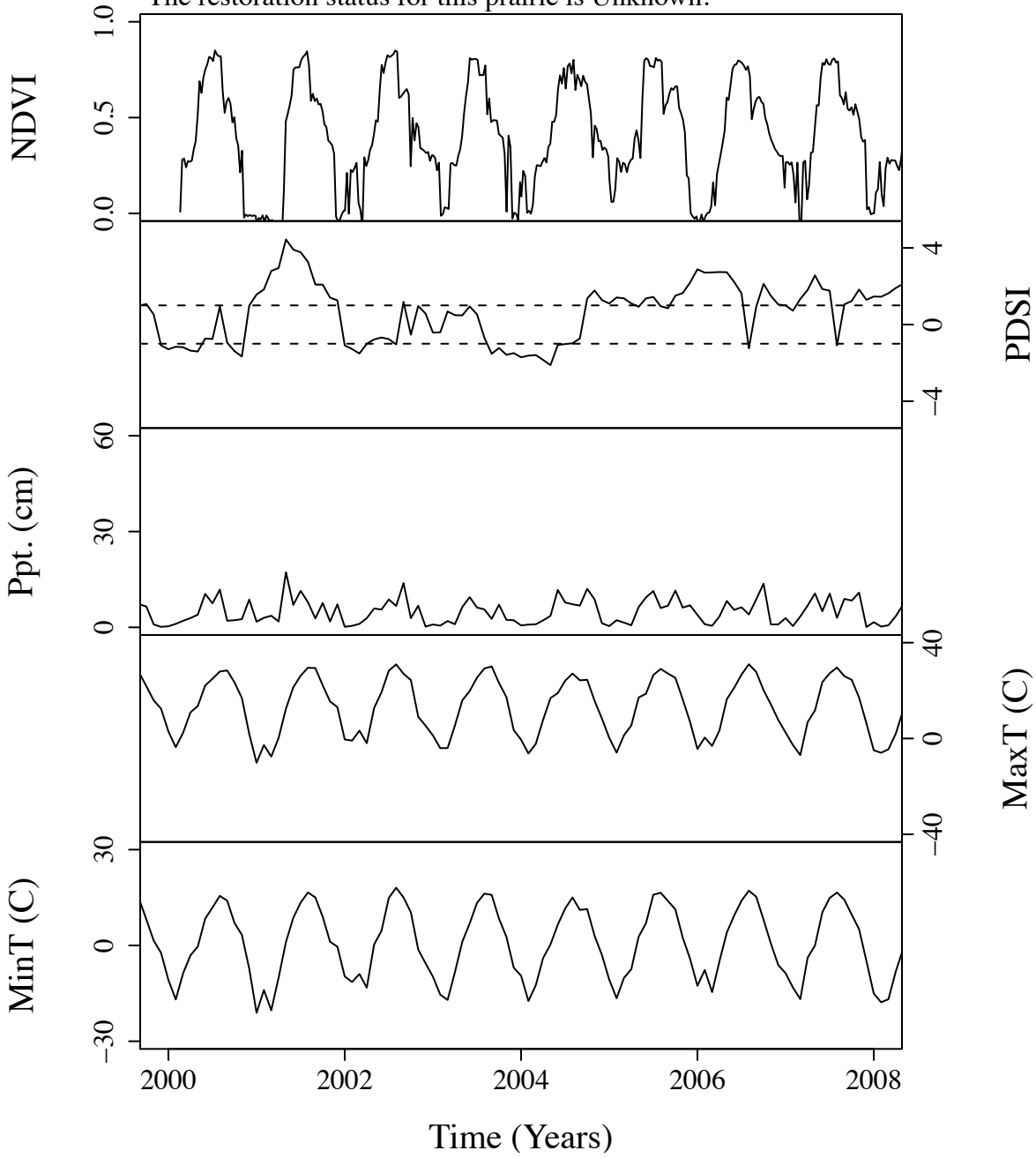

Figure B.54. Time series curves for nbr0.
The community type for this prairie is Tall.
The dominant photosynthetic pathway for this prairie is C3.
The restoration status for this prairie is Remnant.

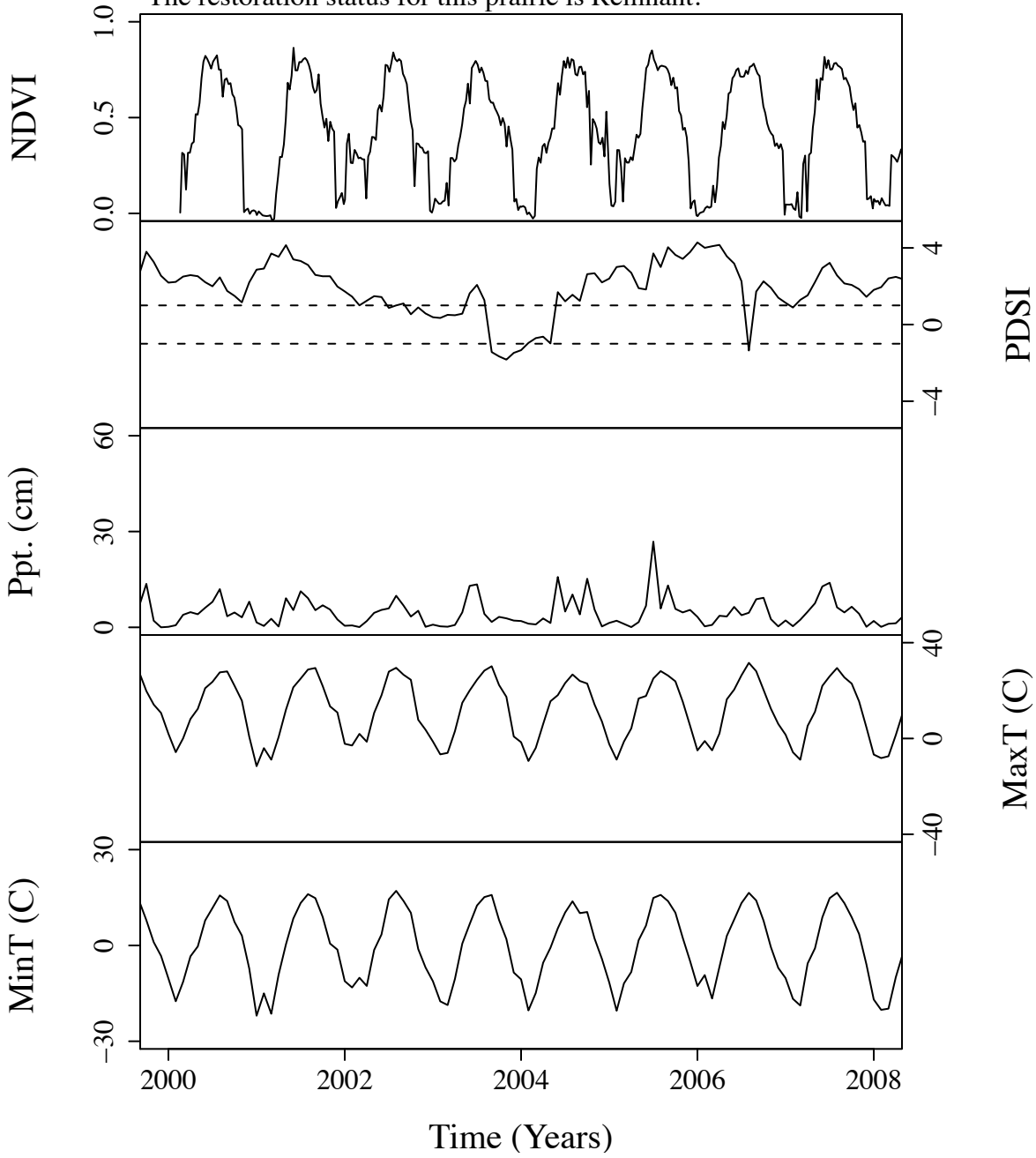

Figure B.55. Time series curves for nda2.
The community type for this prairie is Short.
The dominant photosynthetic pathway for this prairie is C3.
The restoration status for this prairie is Remnant.

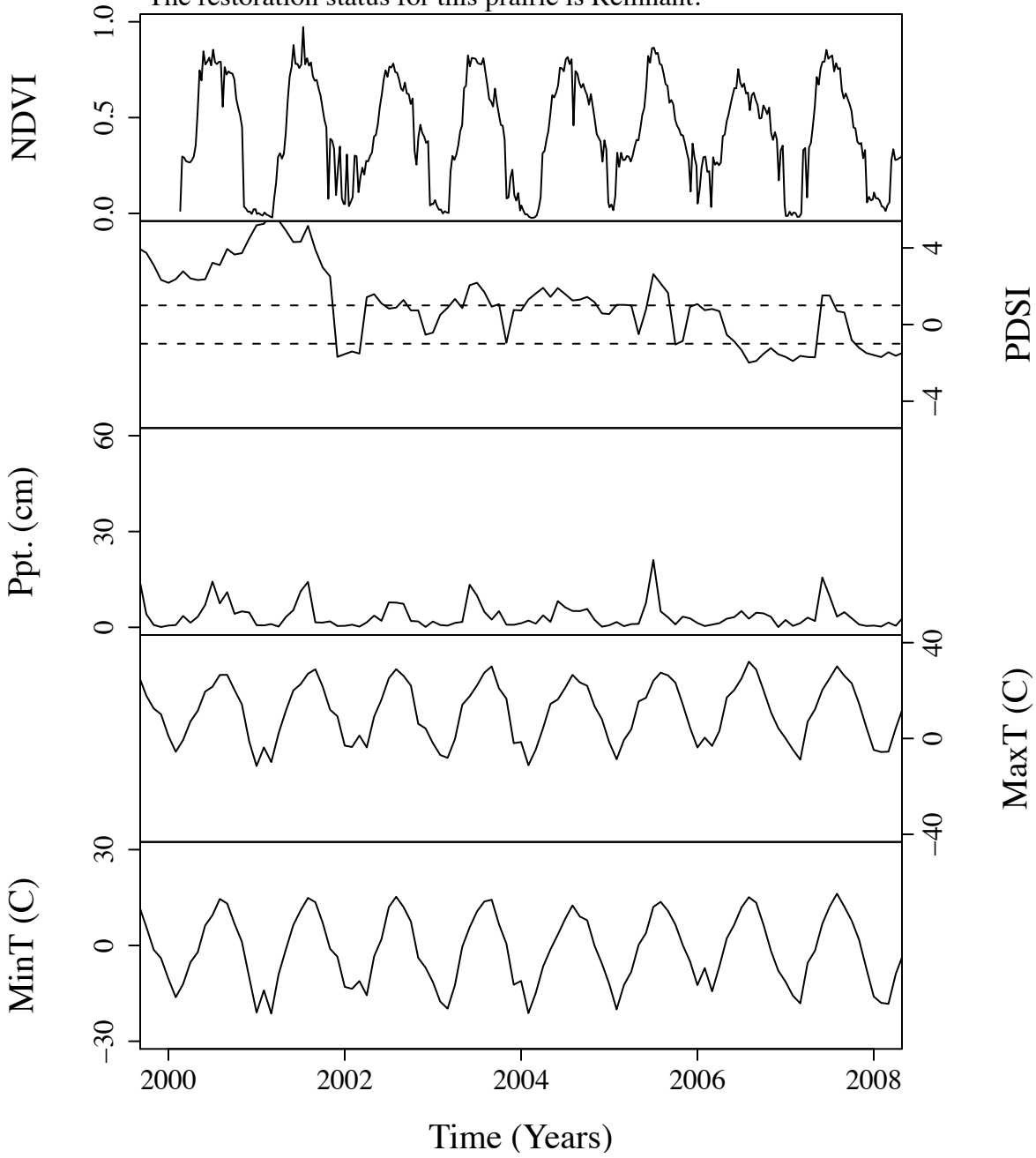

Figure B.56. Time series curves for nea131.
The community type for this prairie is Mixed.
The dominant photosynthetic pathway for this prairie is C4.
The restoration status for this prairie is Unknown.

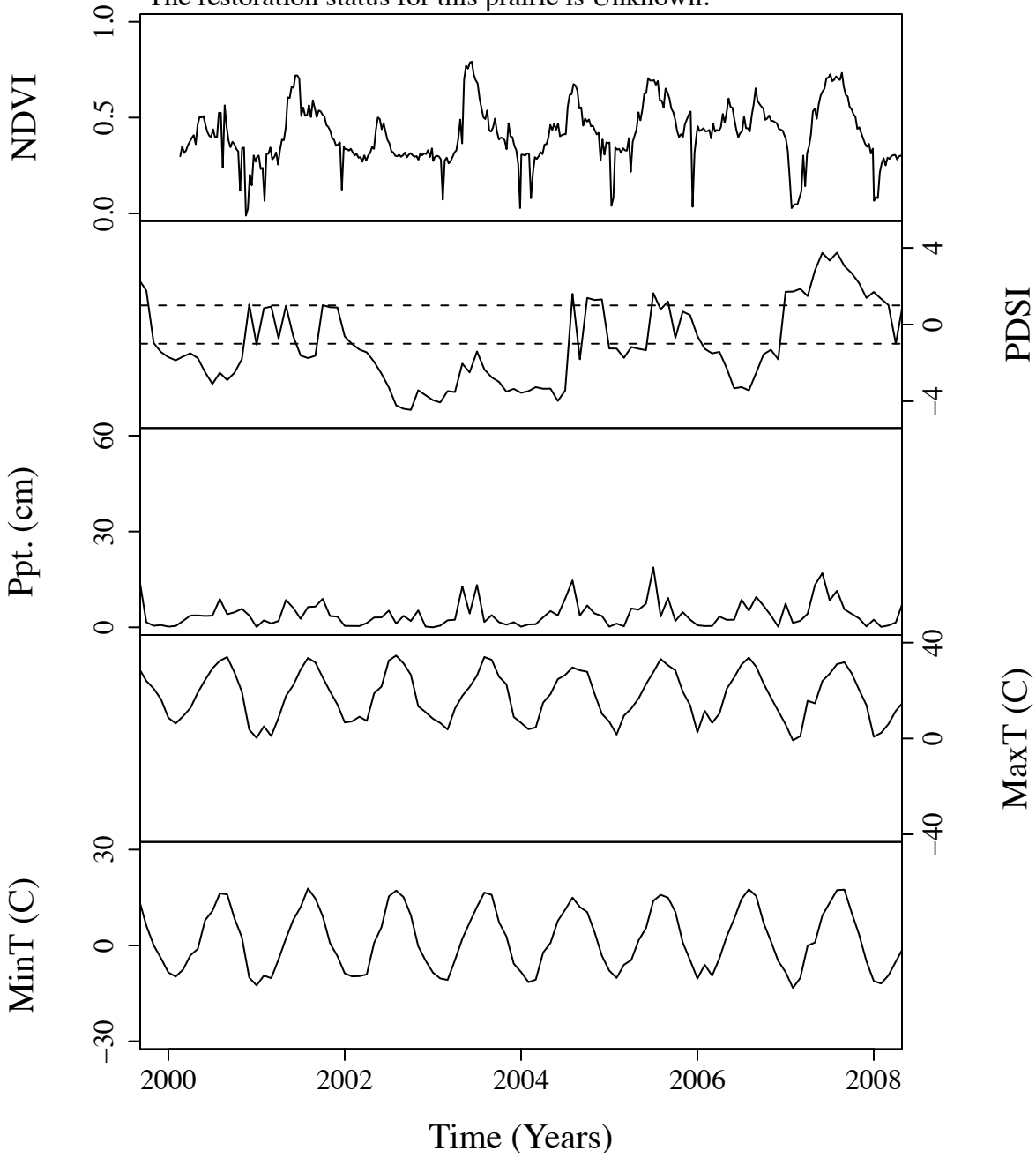

Figure B.57. Time series curves for nea146.
The community type for this prairie is Mixed.
The dominant photosynthetic pathway for this prairie is C4.
The restoration status for this prairie is Unknown.

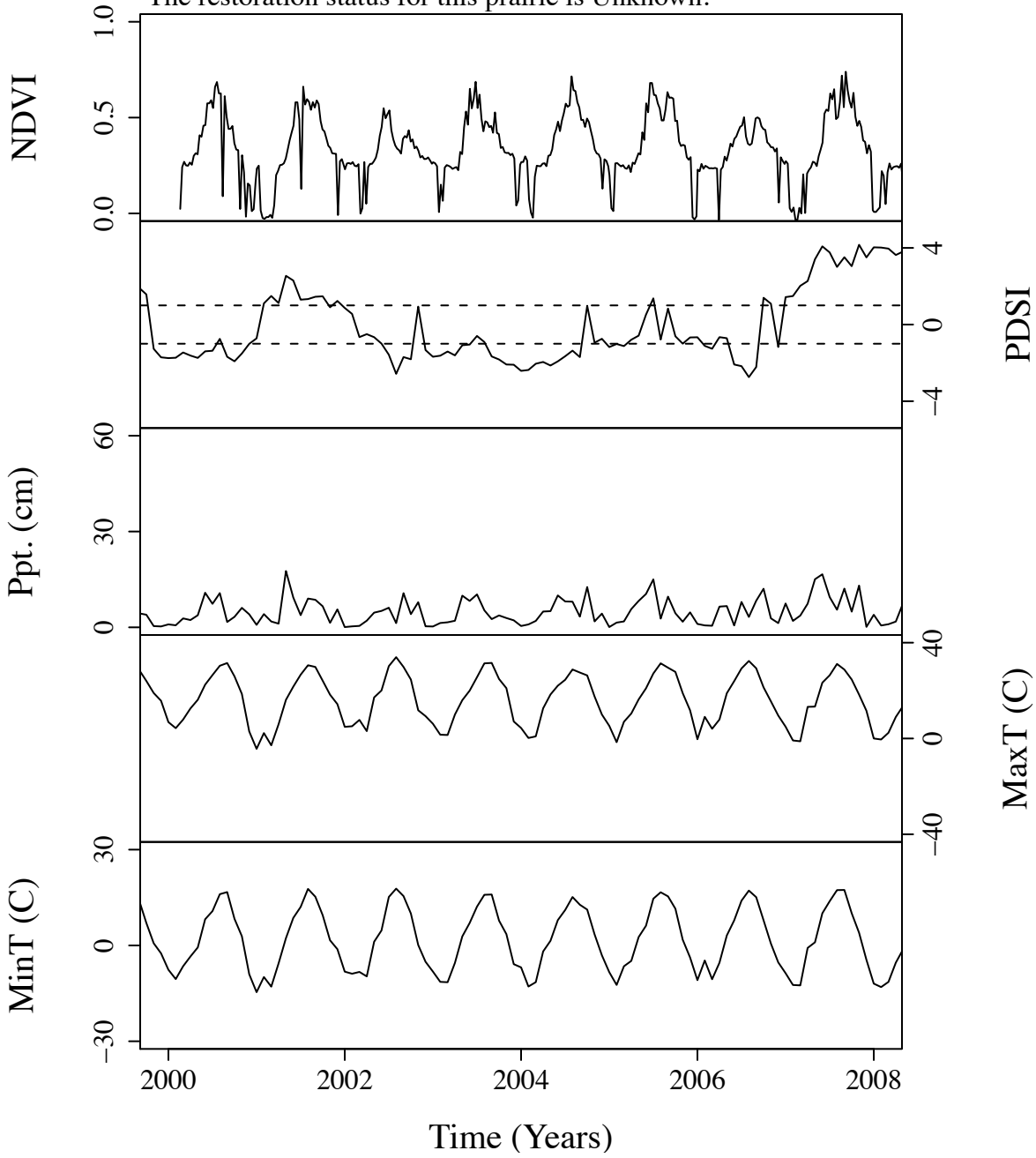

Figure B.58. Time series curves for nea419.
The community type for this prairie is Mixed.
The dominant photosynthetic pathway for this prairie is C4.
The restoration status for this prairie is Unknown.

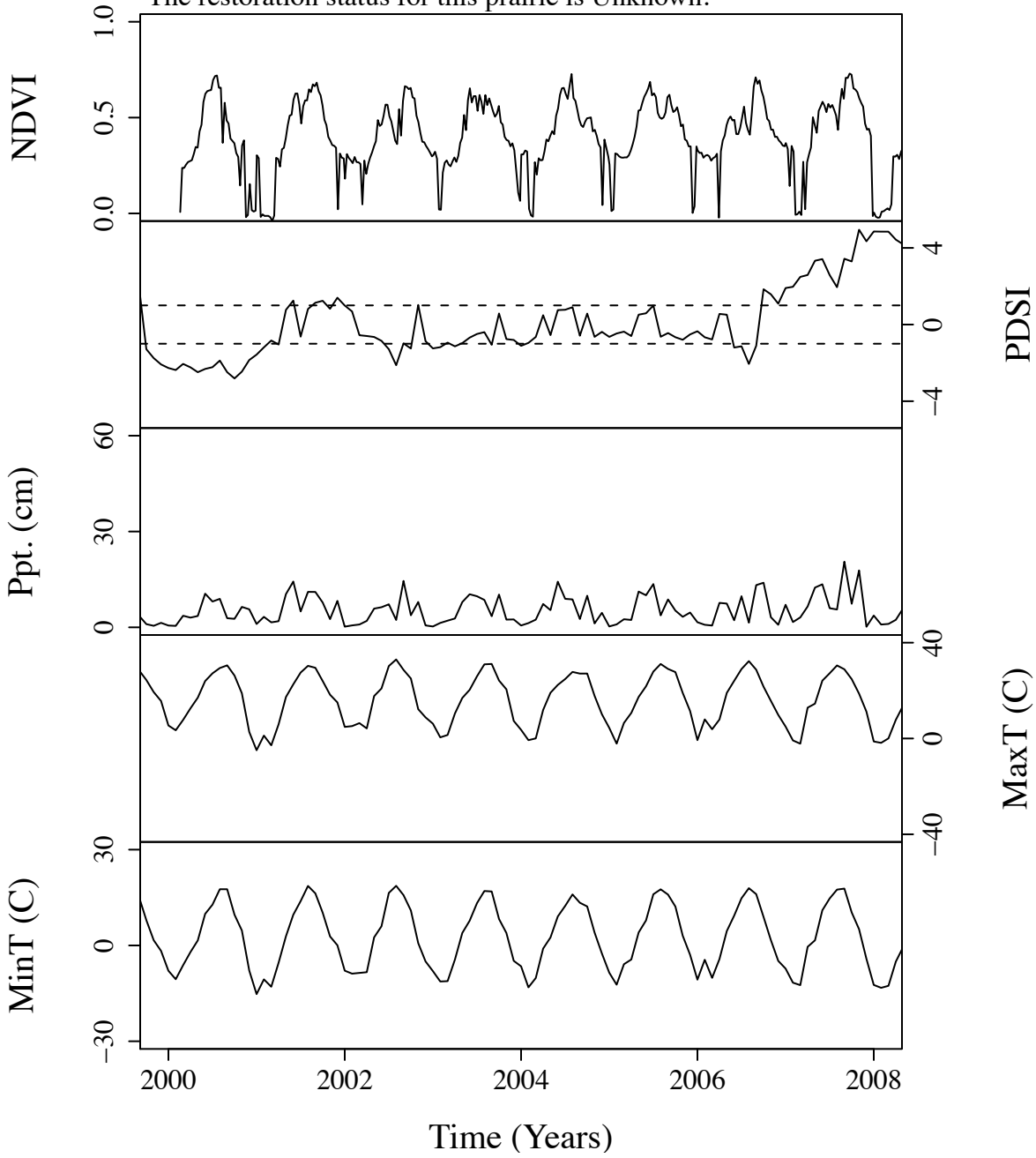

Figure B.59. Time series curves for nea420.
The community type for this prairie is Mixed.
The dominant photosynthetic pathway for this prairie is C4.
The restoration status for this prairie is Unknown.

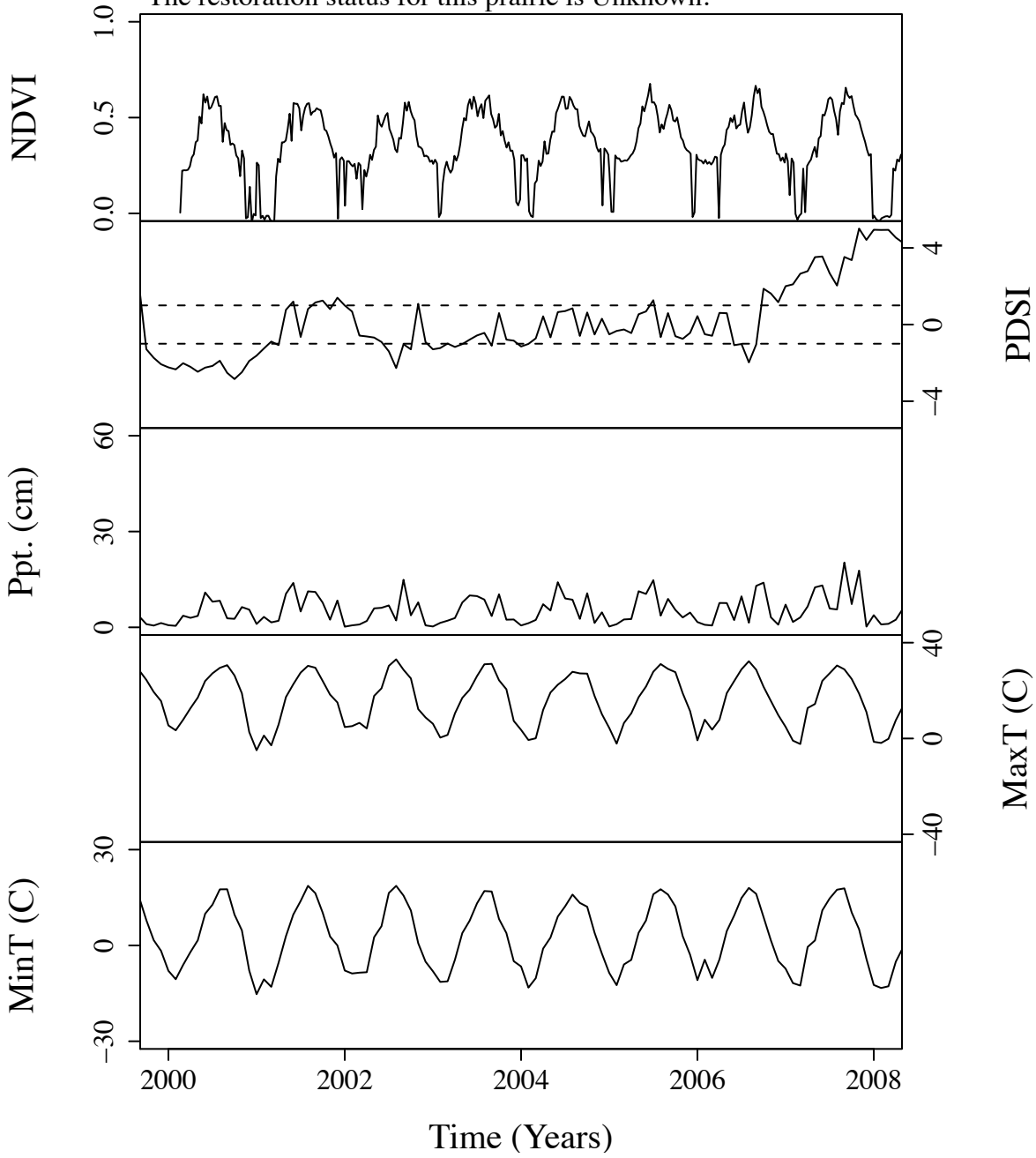

Figure B.60. Time series curves for nea424.
The community type for this prairie is Mixed.
The dominant photosynthetic pathway for this prairie is C4.
The restoration status for this prairie is Unknown.

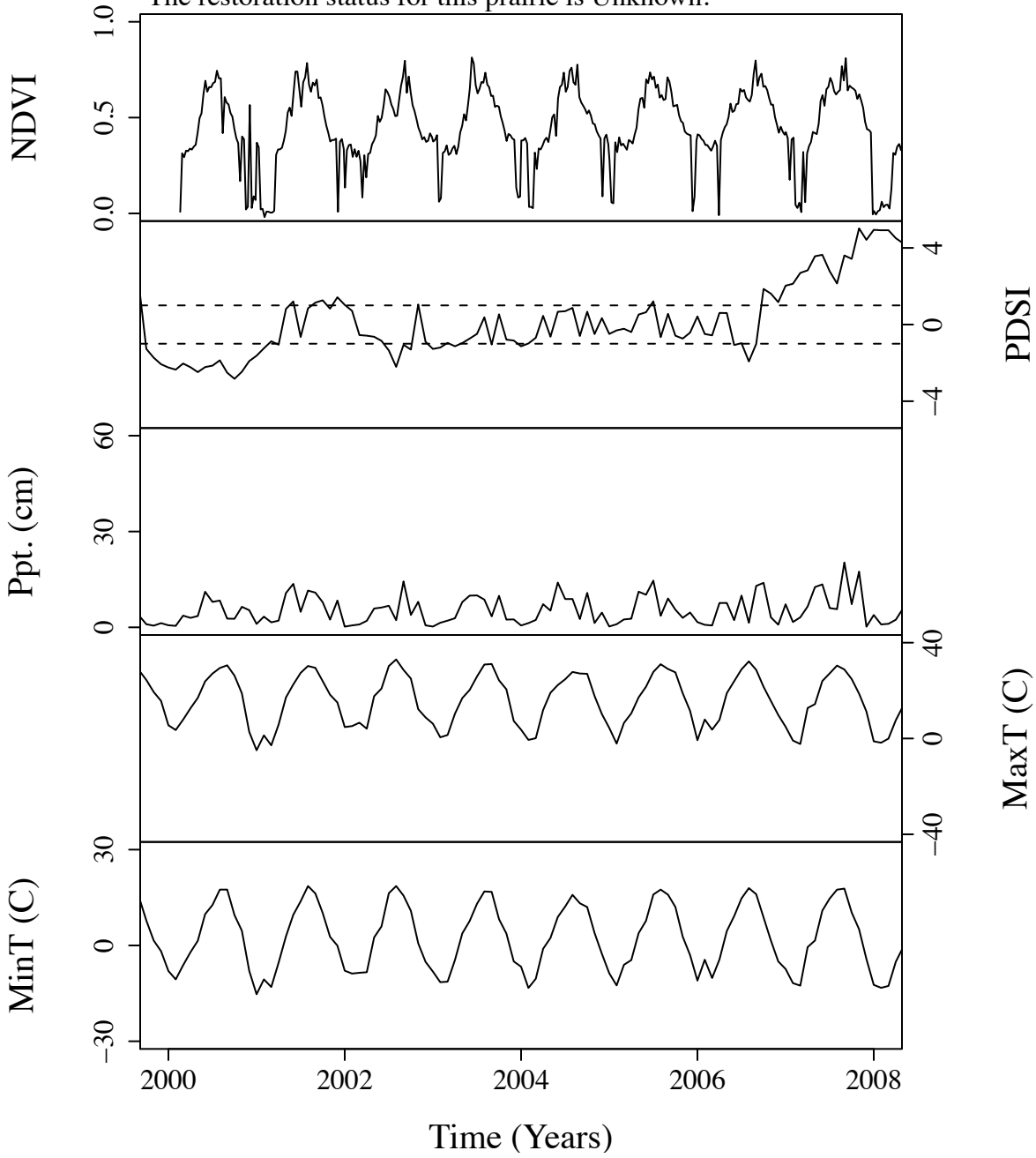

Figure B.61. Time series curves for nea425.
The community type for this prairie is Mixed.
The dominant photosynthetic pathway for this prairie is C4.
The restoration status for this prairie is Unknown.

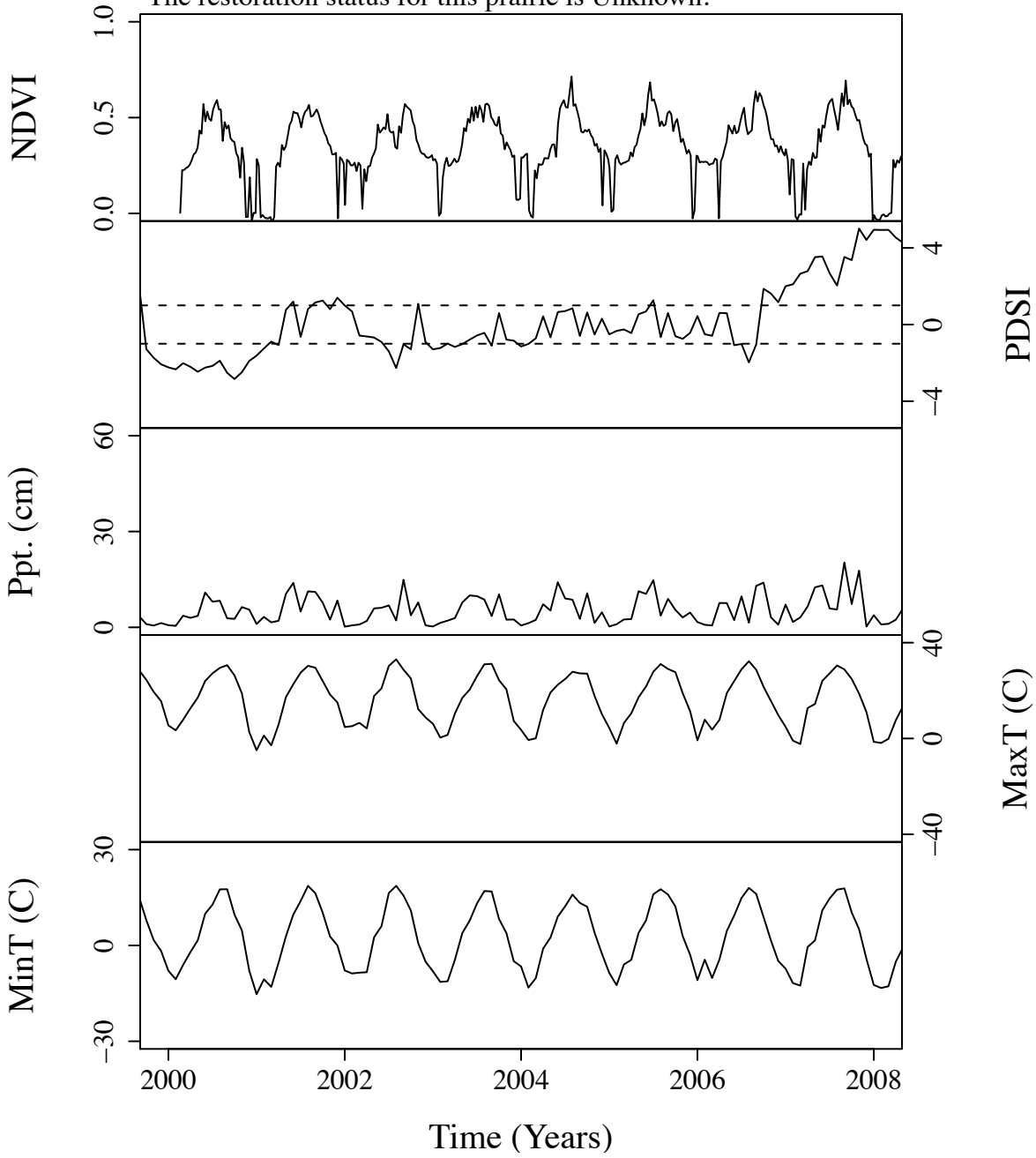

Figure B.62. Time series curves for nea426.
The community type for this prairie is Mixed.
The dominant photosynthetic pathway for this prairie is C4.
The restoration status for this prairie is Unknown.

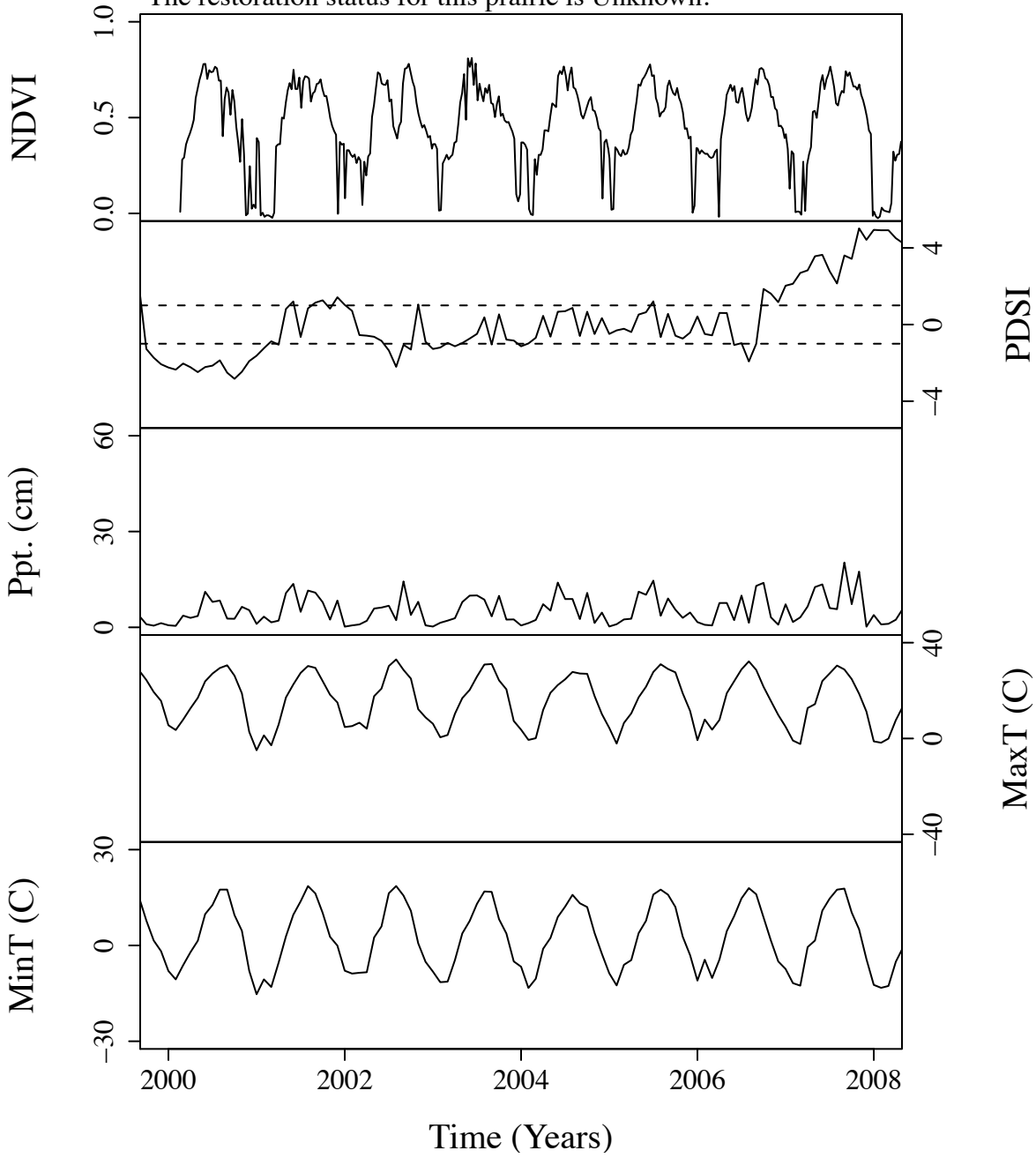

Figure B.63. Time series curves for nea427.
The community type for this prairie is Mixed.
The dominant photosynthetic pathway for this prairie is C4.
The restoration status for this prairie is Unknown.

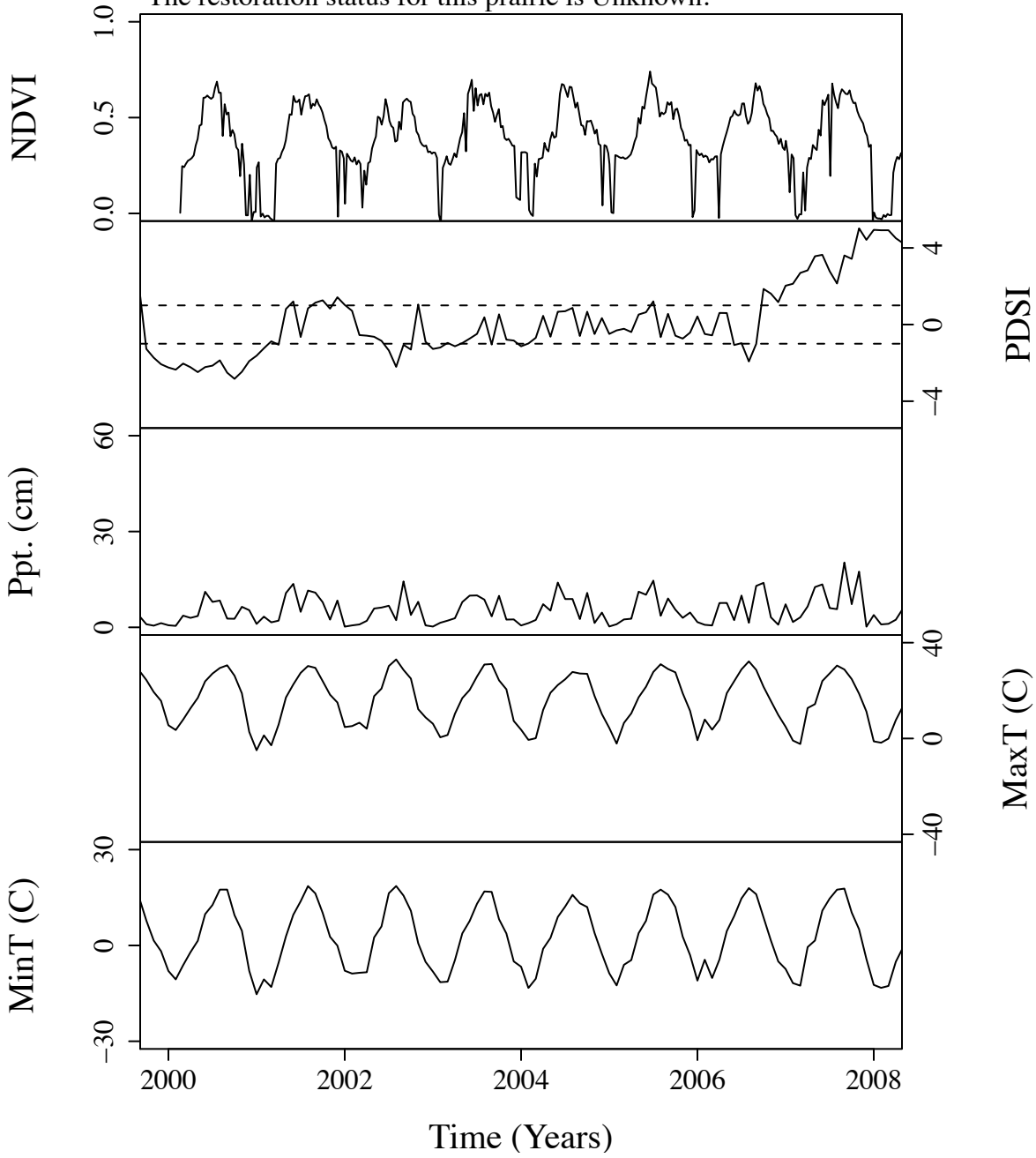

Figure B.64. Time series curves for nea431.
The community type for this prairie is Mixed.
The dominant photosynthetic pathway for this prairie is C4.
The restoration status for this prairie is Unknown.

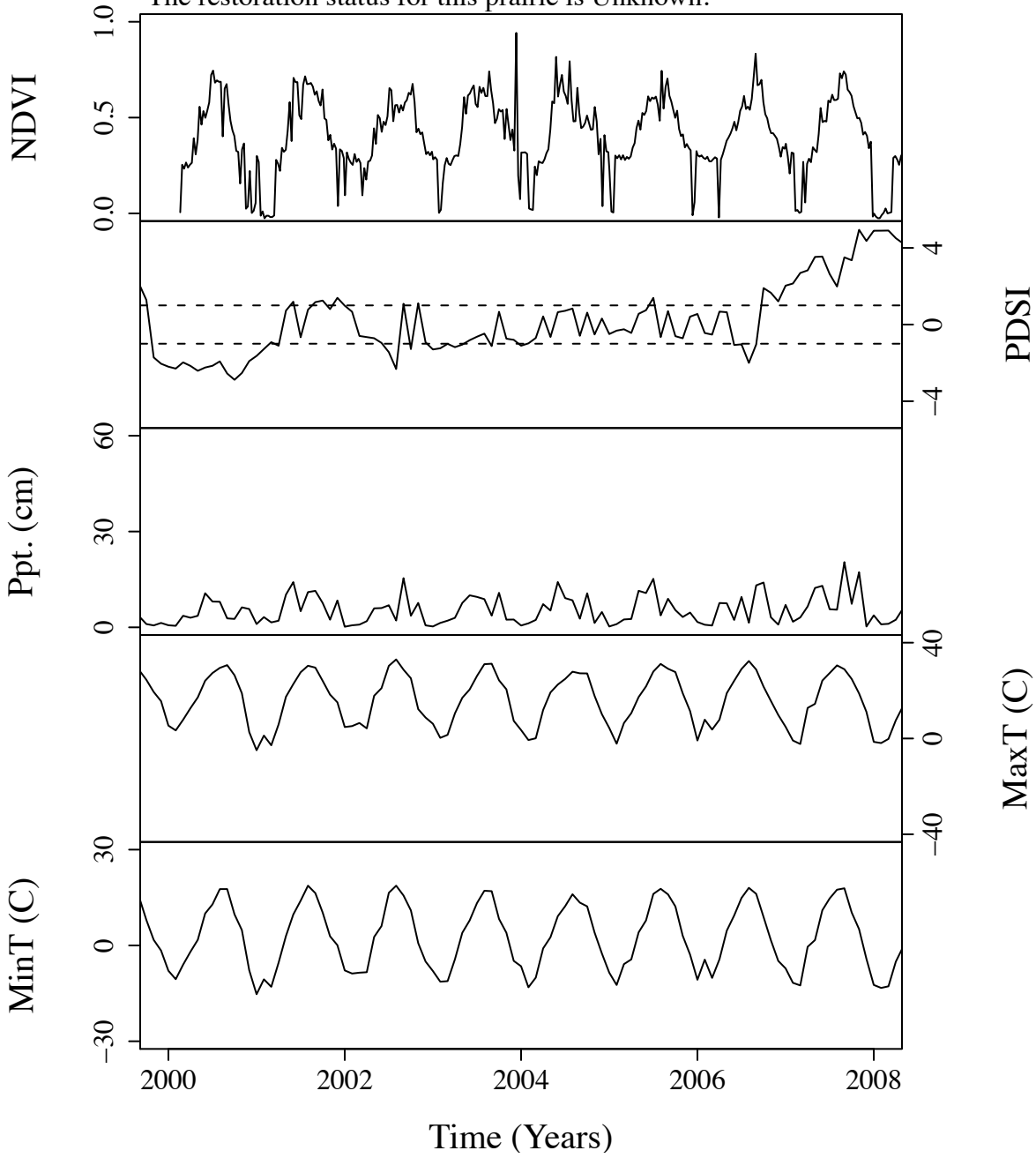

Figure B.65. Time series curves for nea433.
The community type for this prairie is Mixed.
The dominant photosynthetic pathway for this prairie is C4.
The restoration status for this prairie is Unknown.

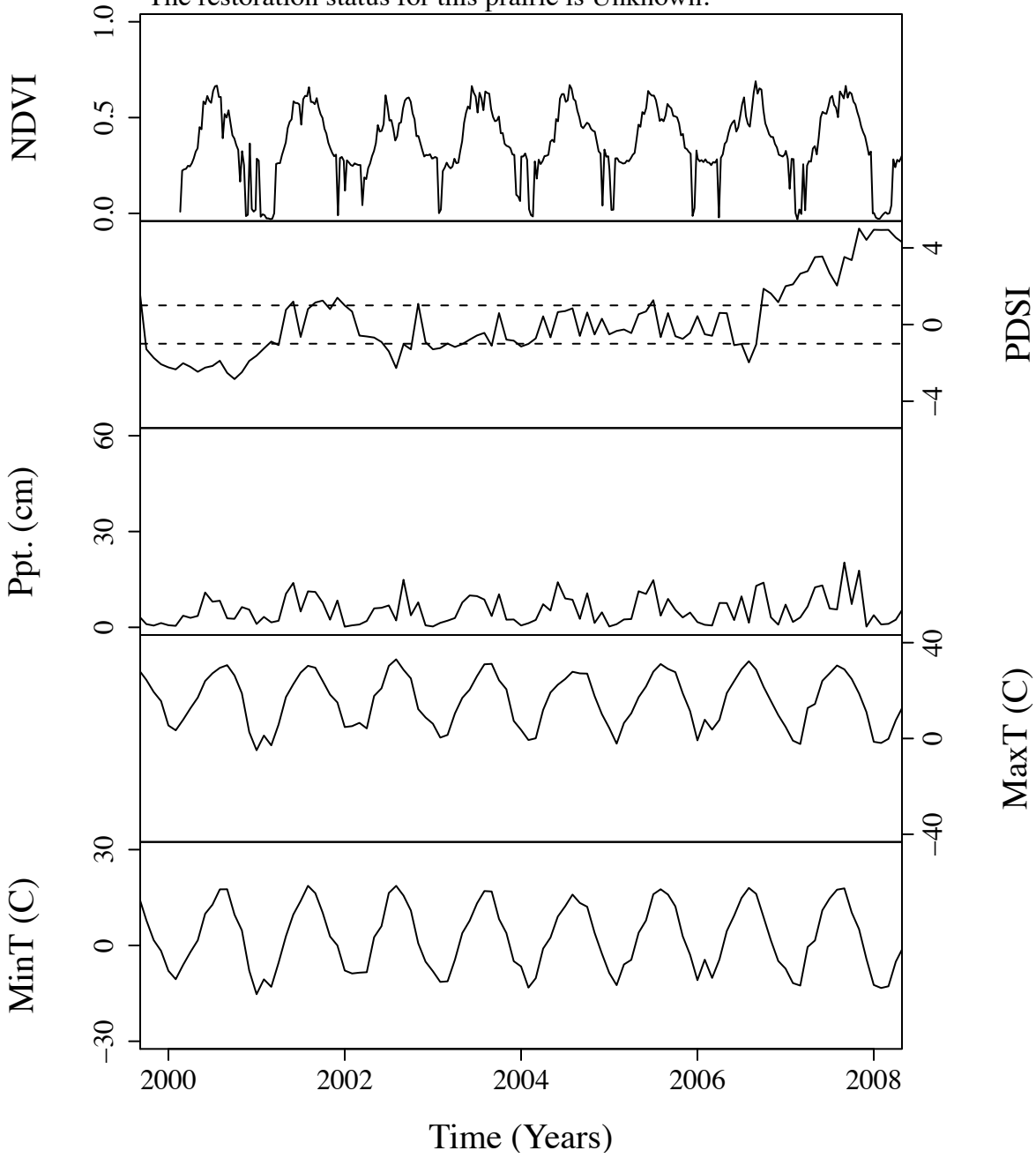

Figure B.66. Time series curves for nea434.
The community type for this prairie is Mixed.
The dominant photosynthetic pathway for this prairie is C4.
The restoration status for this prairie is Unknown.

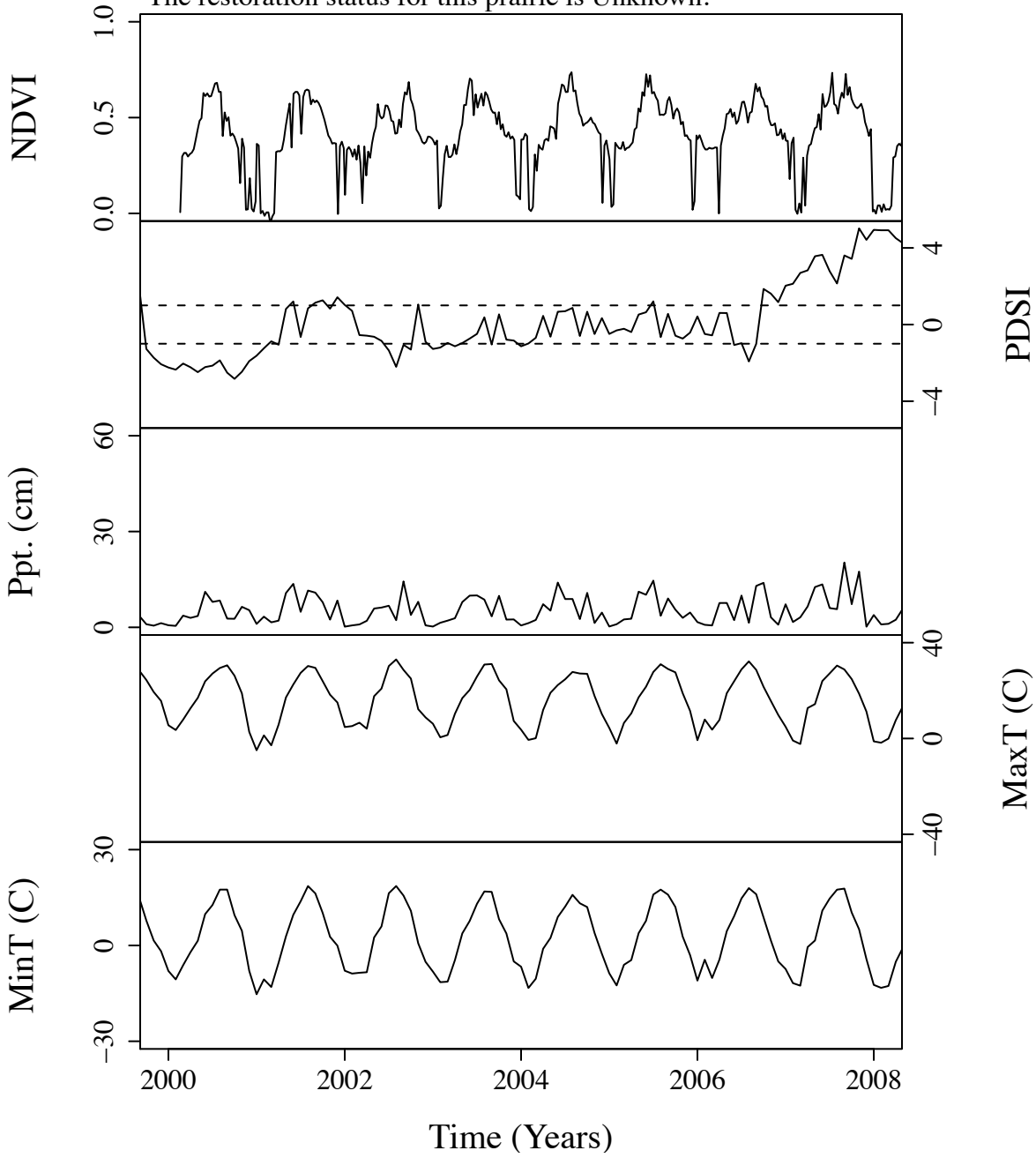

Figure B.67. Time series curves for nea435.
The community type for this prairie is Mixed.
The dominant photosynthetic pathway for this prairie is C4.
The restoration status for this prairie is Unknown.

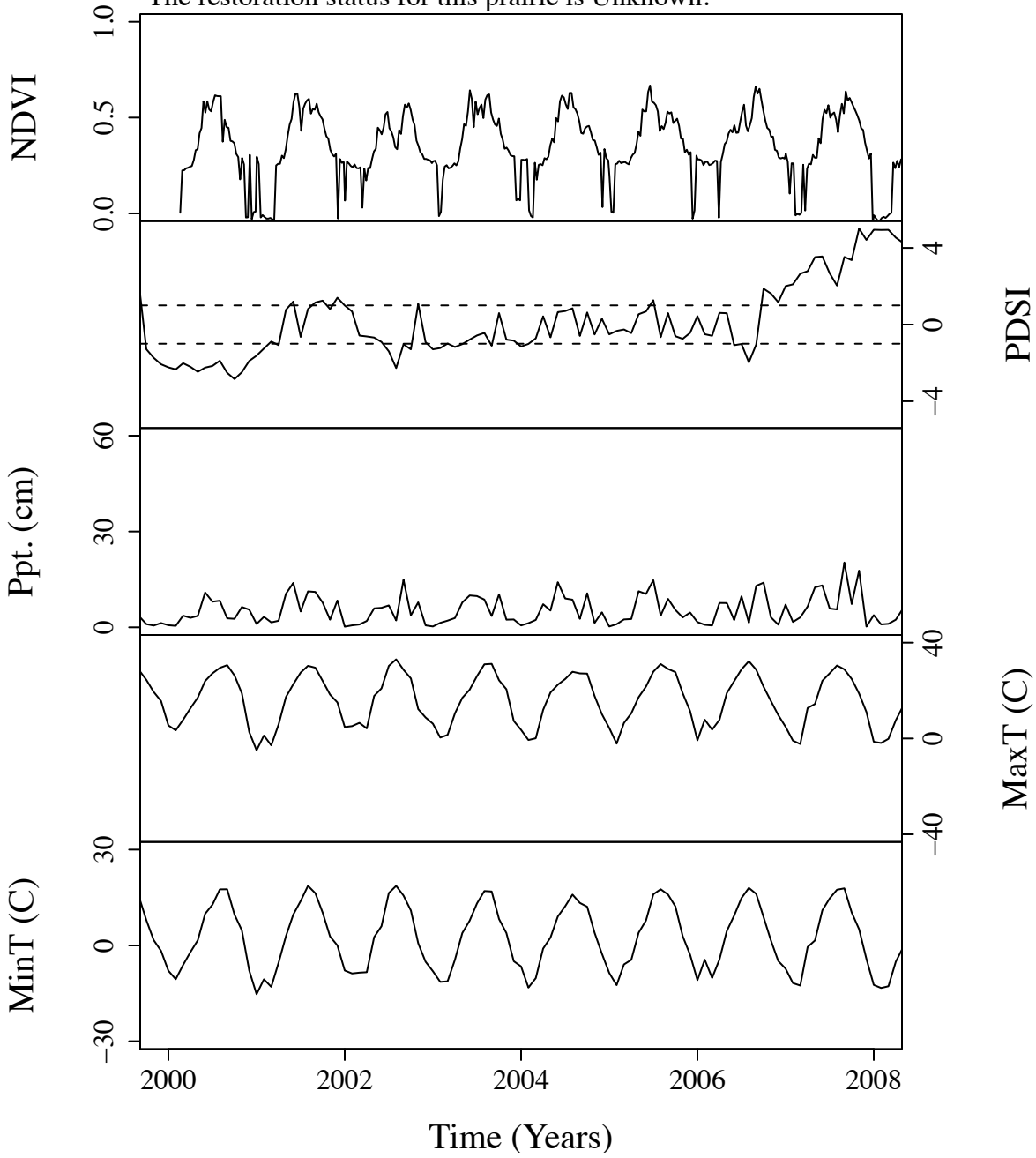

Figure B.68. Time series curves for nea436.
The community type for this prairie is Mixed.
The dominant photosynthetic pathway for this prairie is C4.
The restoration status for this prairie is Unknown.

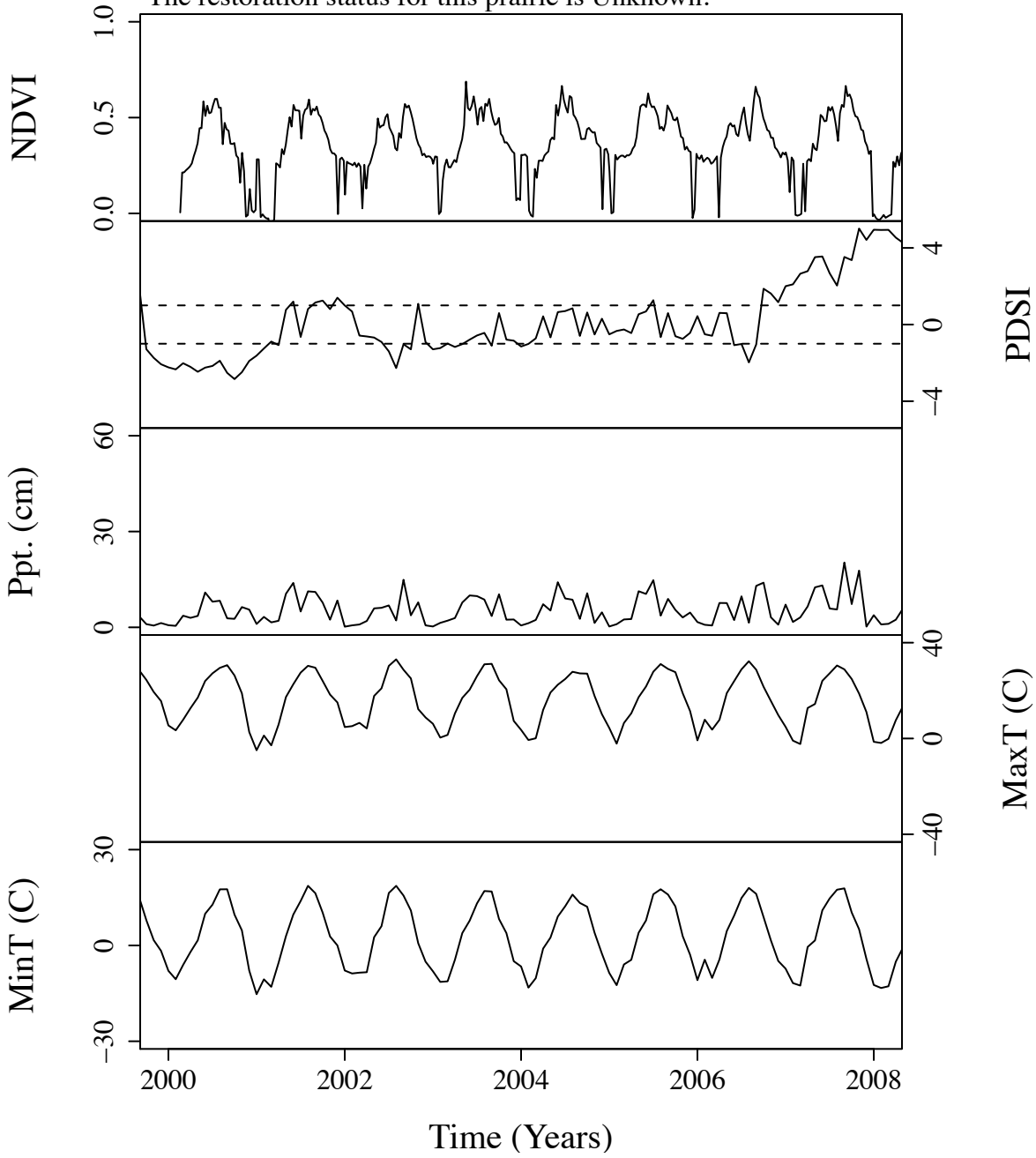

Figure B.69. Time series curves for nea462.
The community type for this prairie is Mixed.
The dominant photosynthetic pathway for this prairie is C4.
The restoration status for this prairie is Unknown.

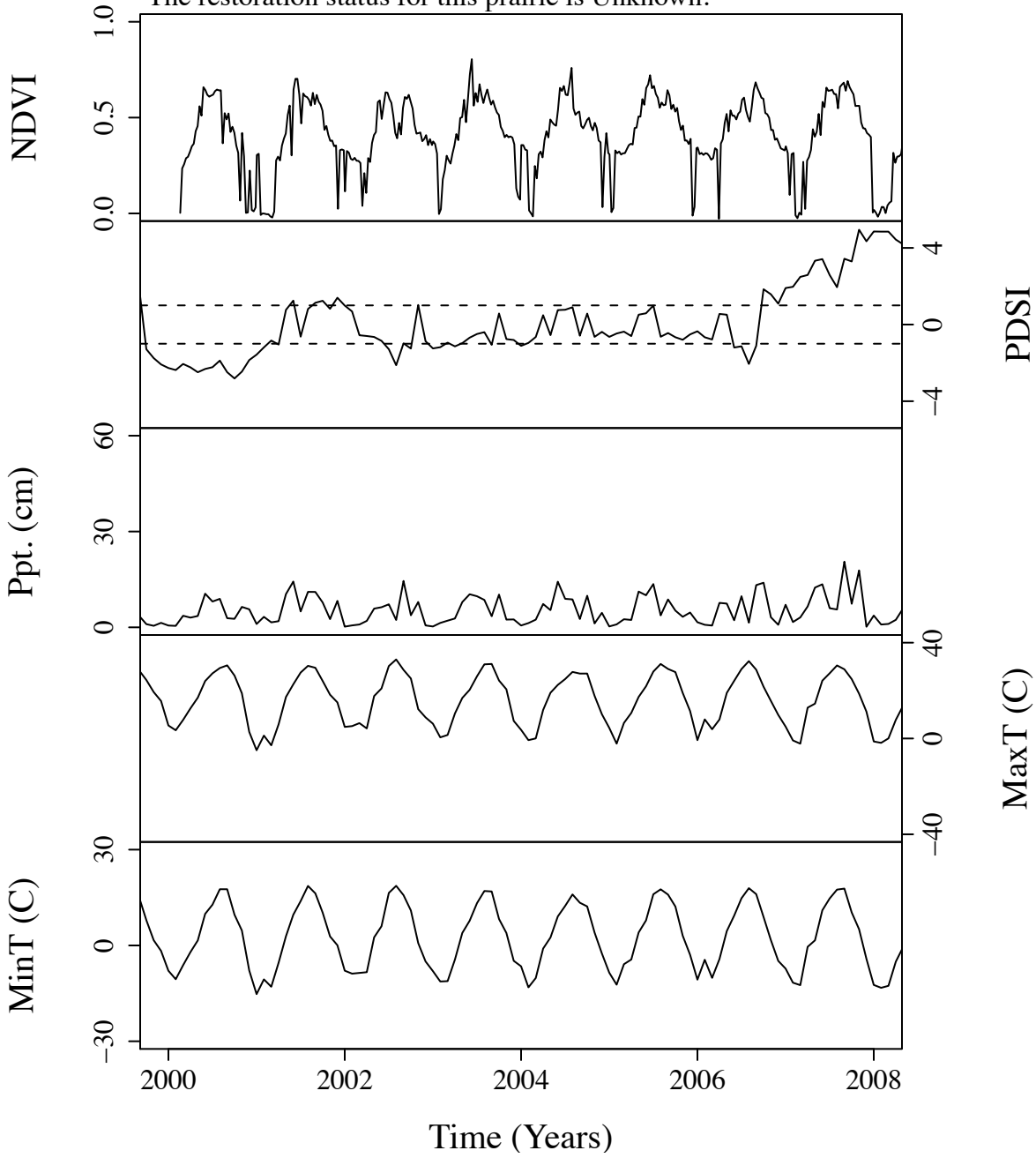

Figure B.70. Time series curves for nea470.
The community type for this prairie is Mixed.
The dominant photosynthetic pathway for this prairie is C4.
The restoration status for this prairie is Unknown.

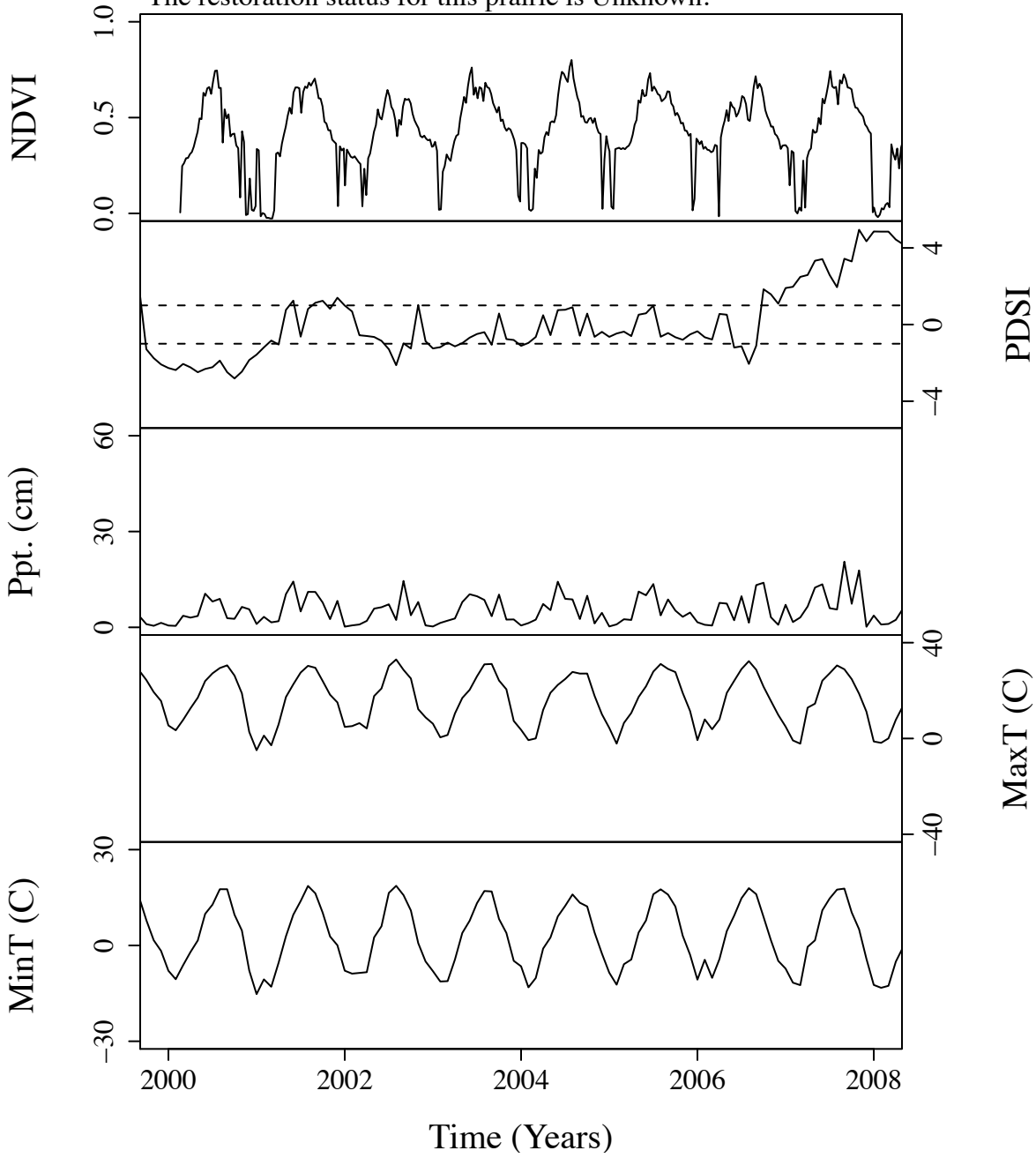

Figure B.71. Time series curves for nea471.
The community type for this prairie is Mixed.
The dominant photosynthetic pathway for this prairie is C4.
The restoration status for this prairie is Unknown.

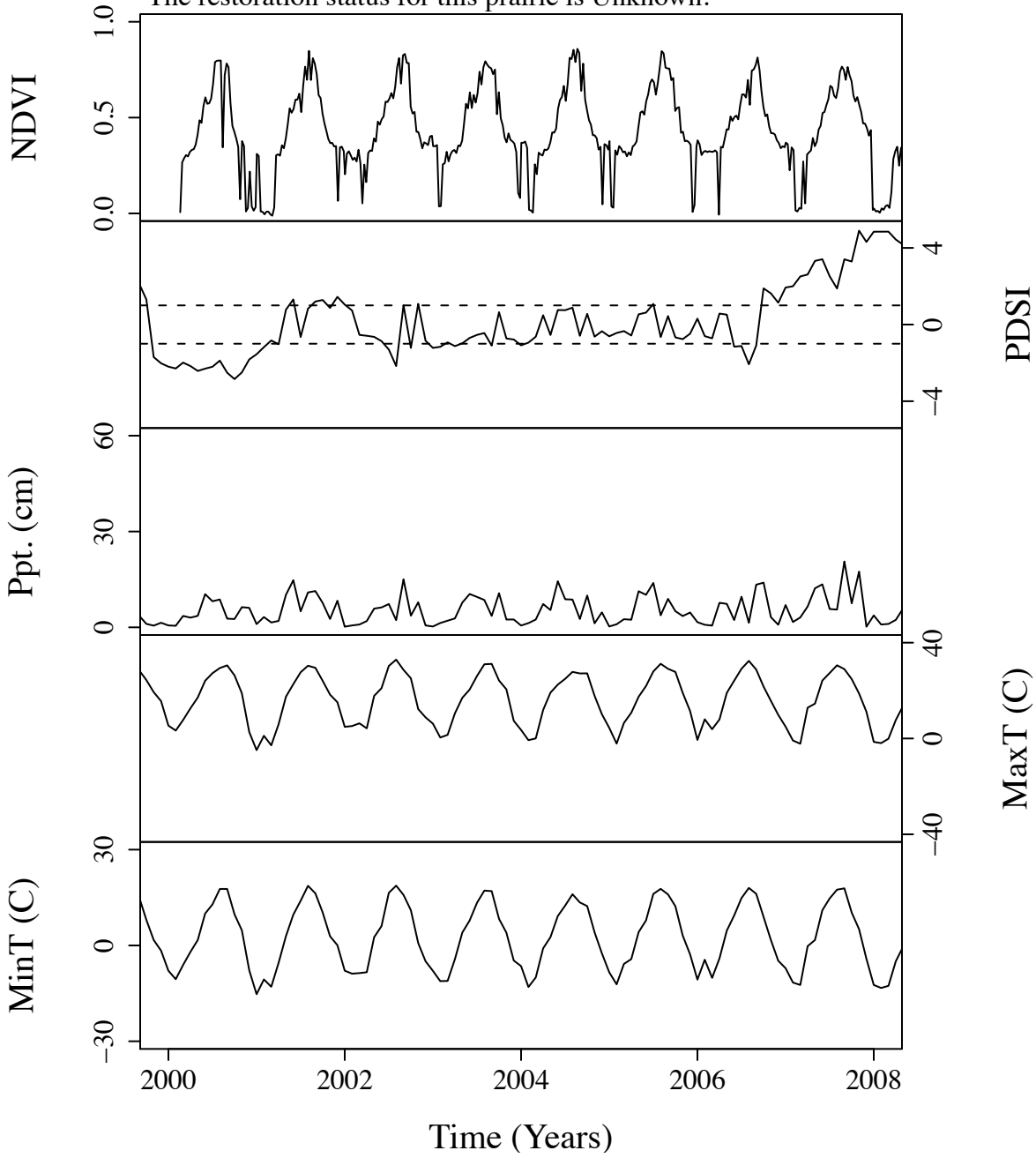

Figure B.72. Time series curves for nea479.
The community type for this prairie is Mixed.
The dominant photosynthetic pathway for this prairie is C4.
The restoration status for this prairie is Unknown.

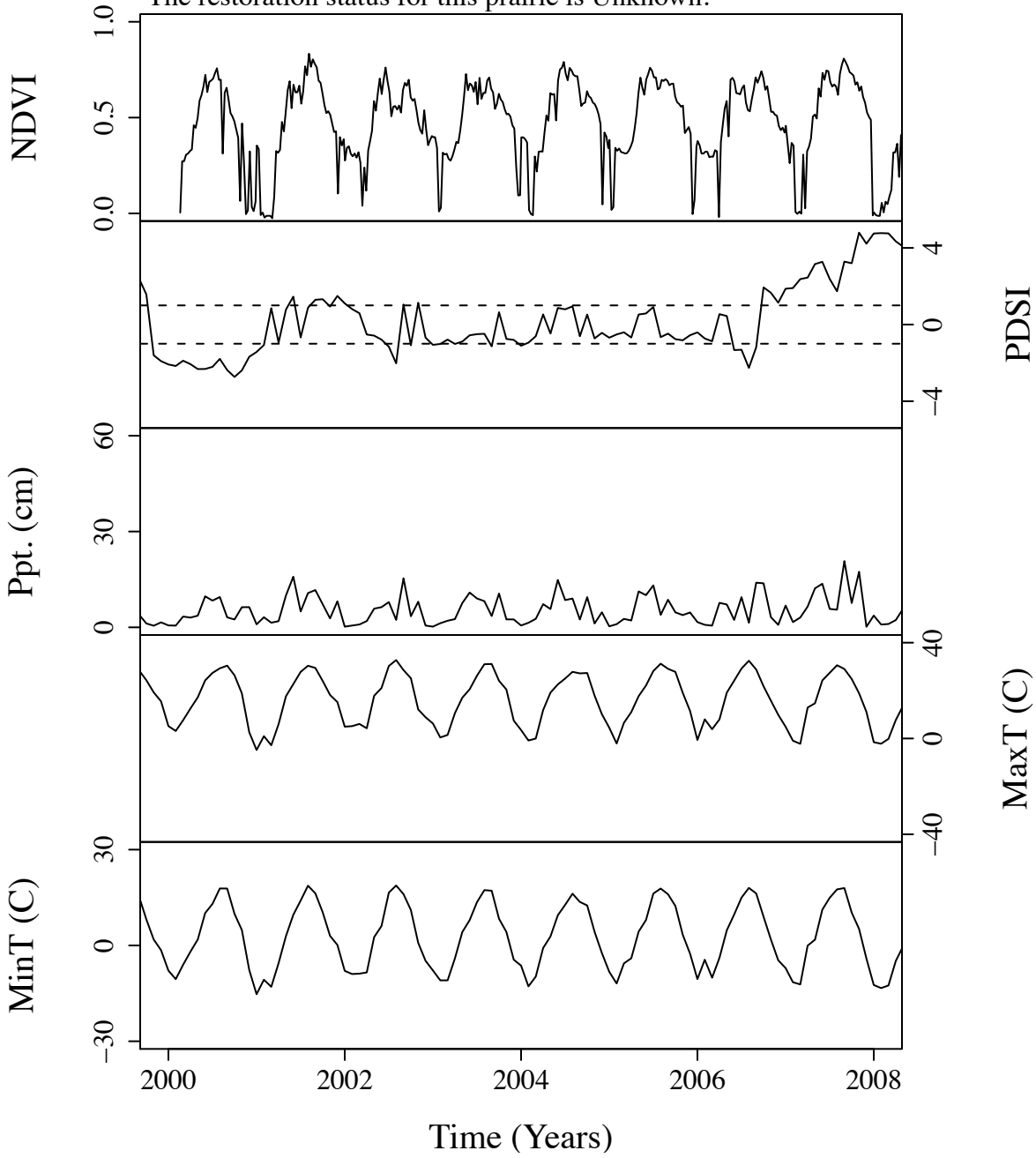

Figure B.73. Time series curves for nea482.
The community type for this prairie is Mixed.
The dominant photosynthetic pathway for this prairie is C4.
The restoration status for this prairie is Unknown.

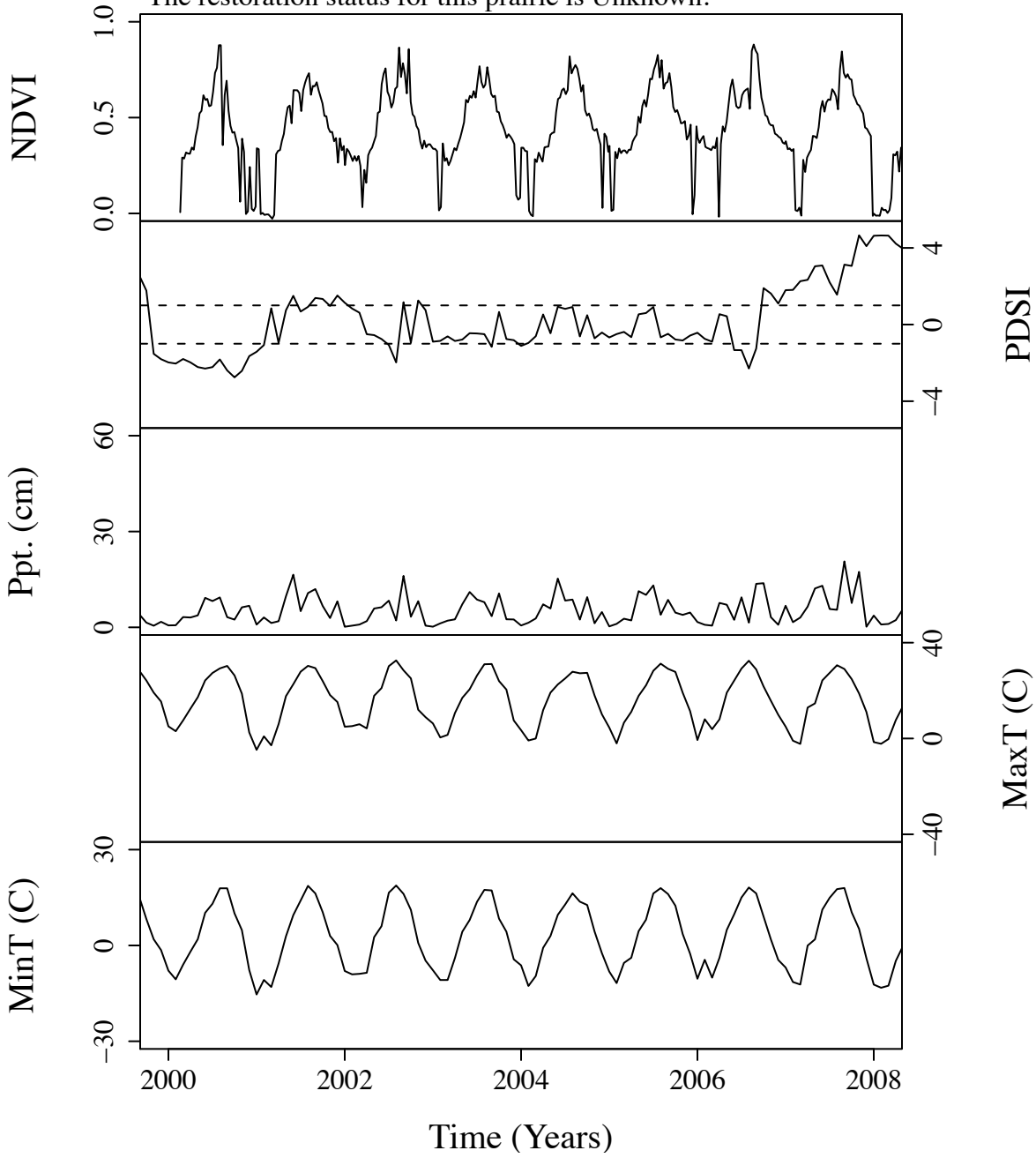

Figure B.74. Time series curves for nea491.
The community type for this prairie is Mixed.
The dominant photosynthetic pathway for this prairie is C4.
The restoration status for this prairie is Unknown.

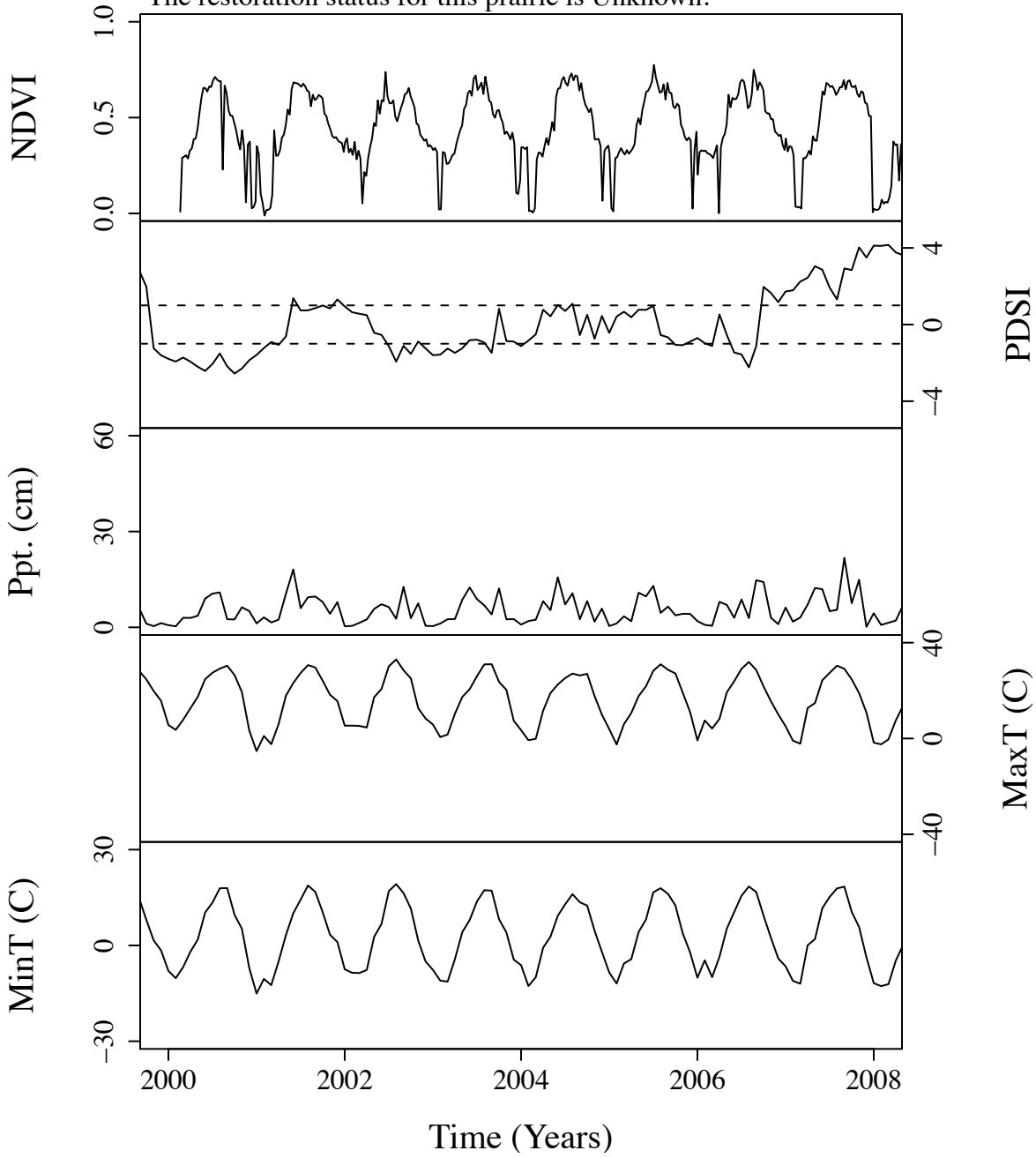

Figure B.75. Time series curves for nea510.
The community type for this prairie is Mixed.
The dominant photosynthetic pathway for this prairie is C4.
The restoration status for this prairie is Unknown.

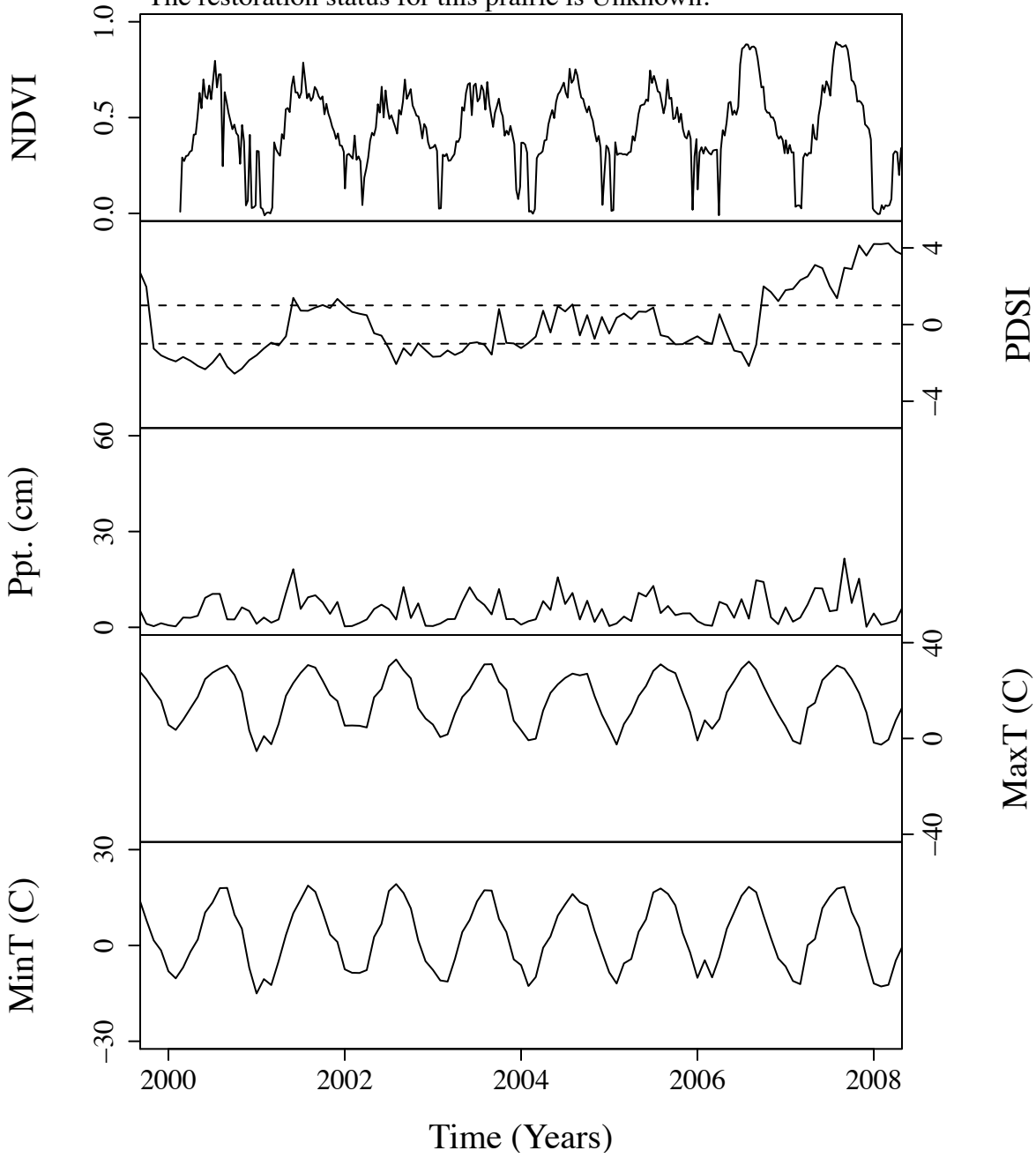

Figure B.76. Time series curves for nea511.
The community type for this prairie is Mixed.
The dominant photosynthetic pathway for this prairie is C4.
The restoration status for this prairie is Unknown.

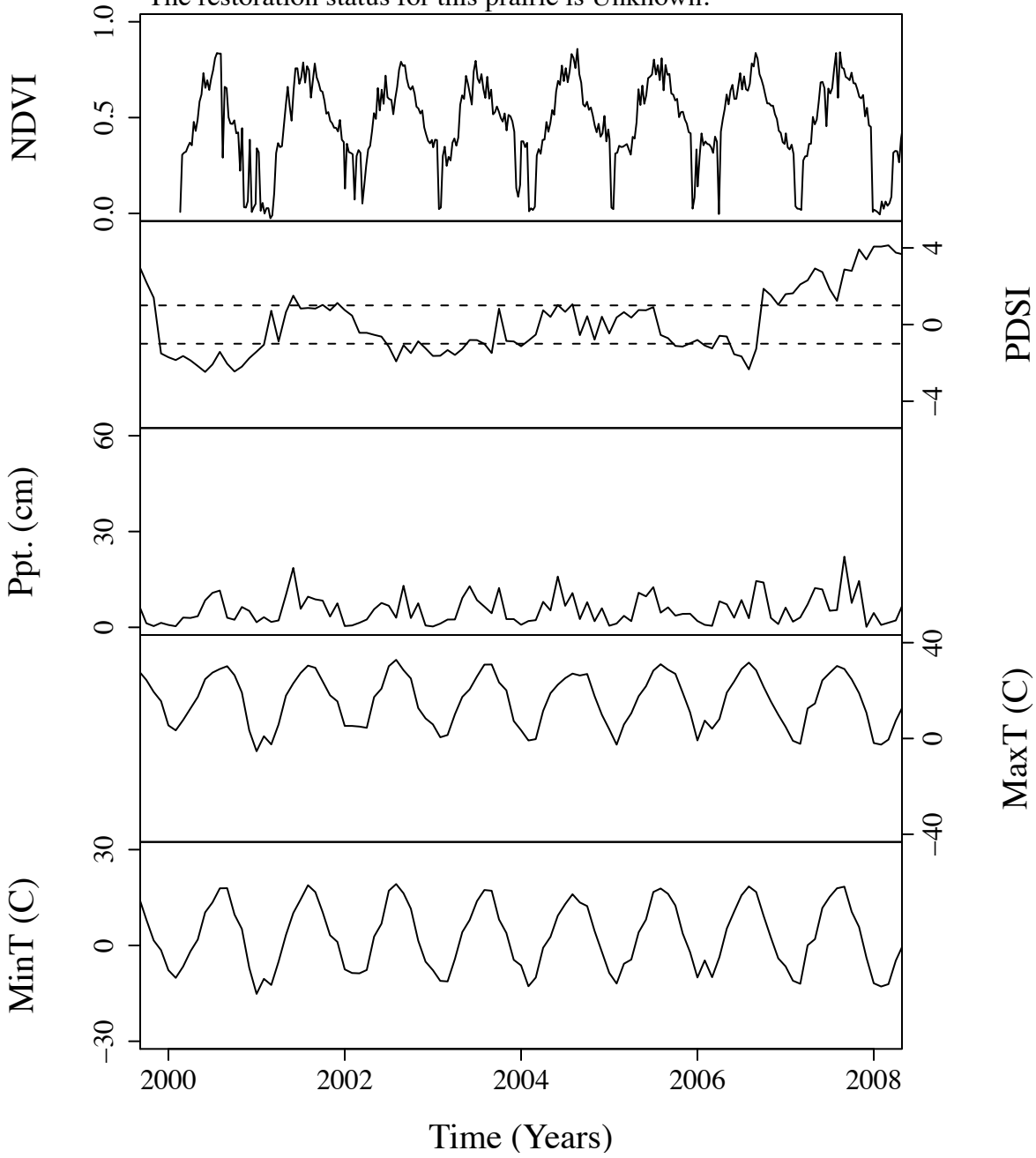

Figure B.77. Time series curves for nea530.
The community type for this prairie is Mixed.
The dominant photosynthetic pathway for this prairie is C4.
The restoration status for this prairie is Unknown.

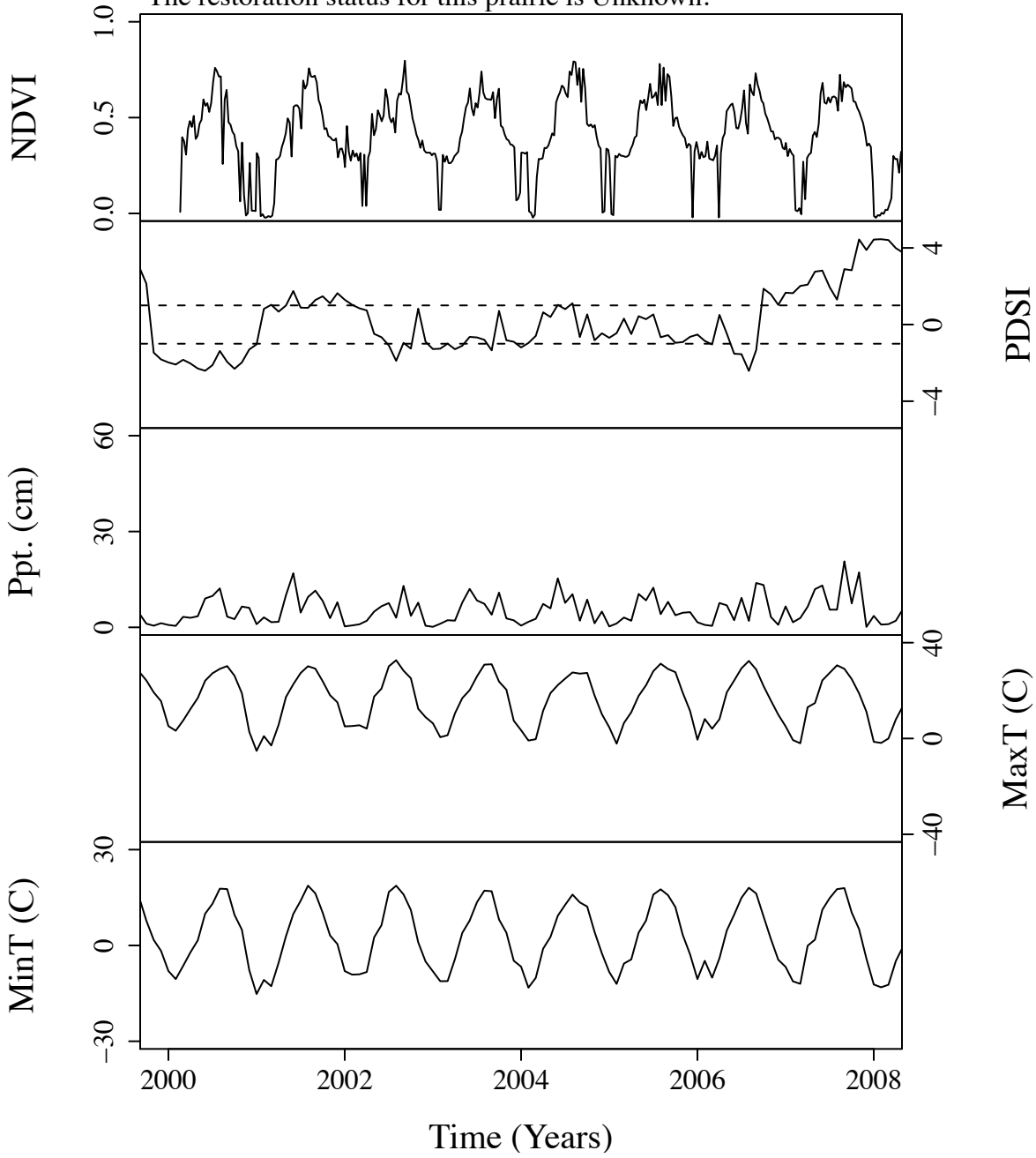

Figure B.78. Time series curves for nea541.
The community type for this prairie is Mixed.
The dominant photosynthetic pathway for this prairie is C4.
The restoration status for this prairie is Unknown.

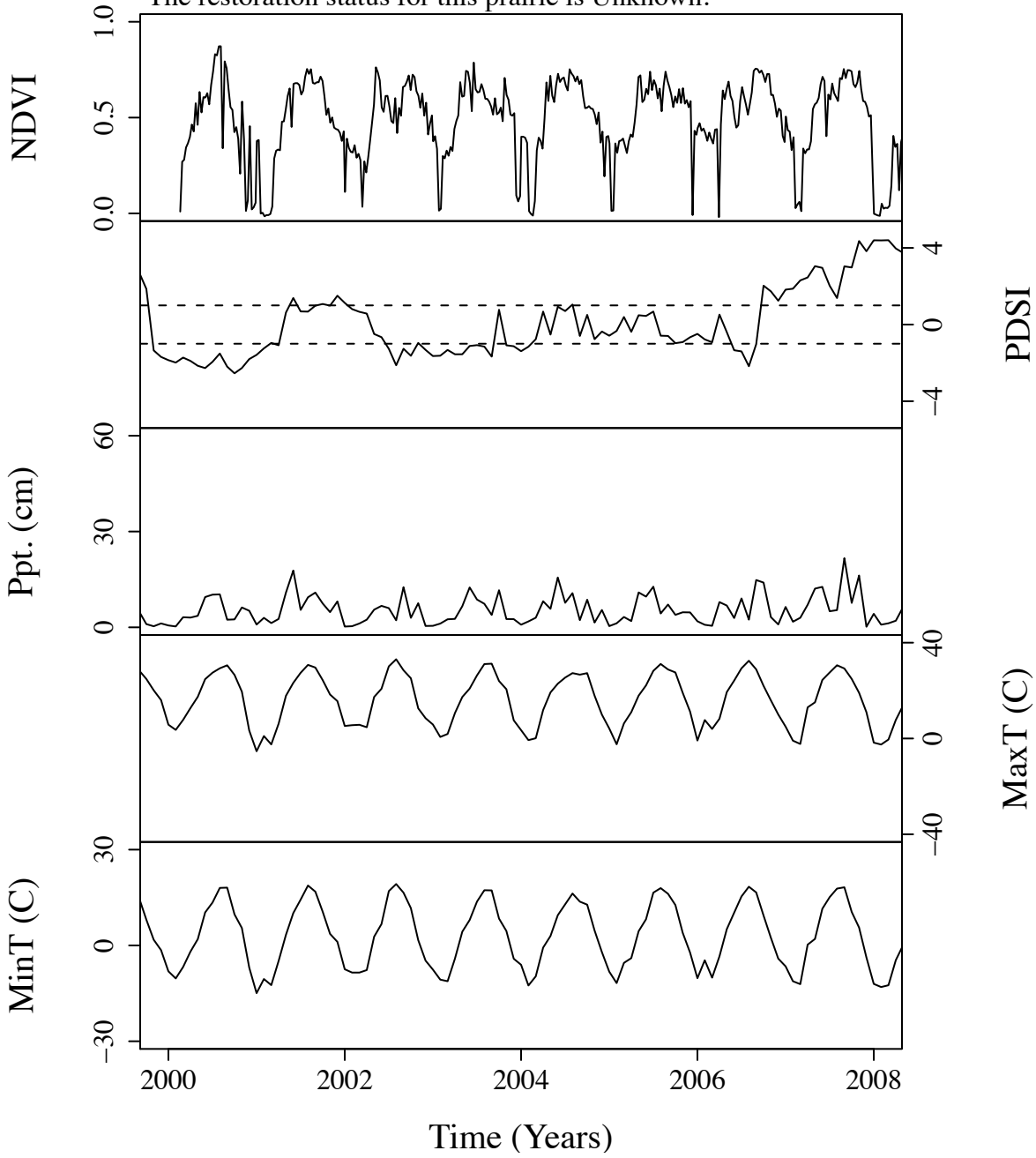

Figure B.79. Time series curves for nea542.
The community type for this prairie is Mixed.
The dominant photosynthetic pathway for this prairie is C4.
The restoration status for this prairie is Unknown.

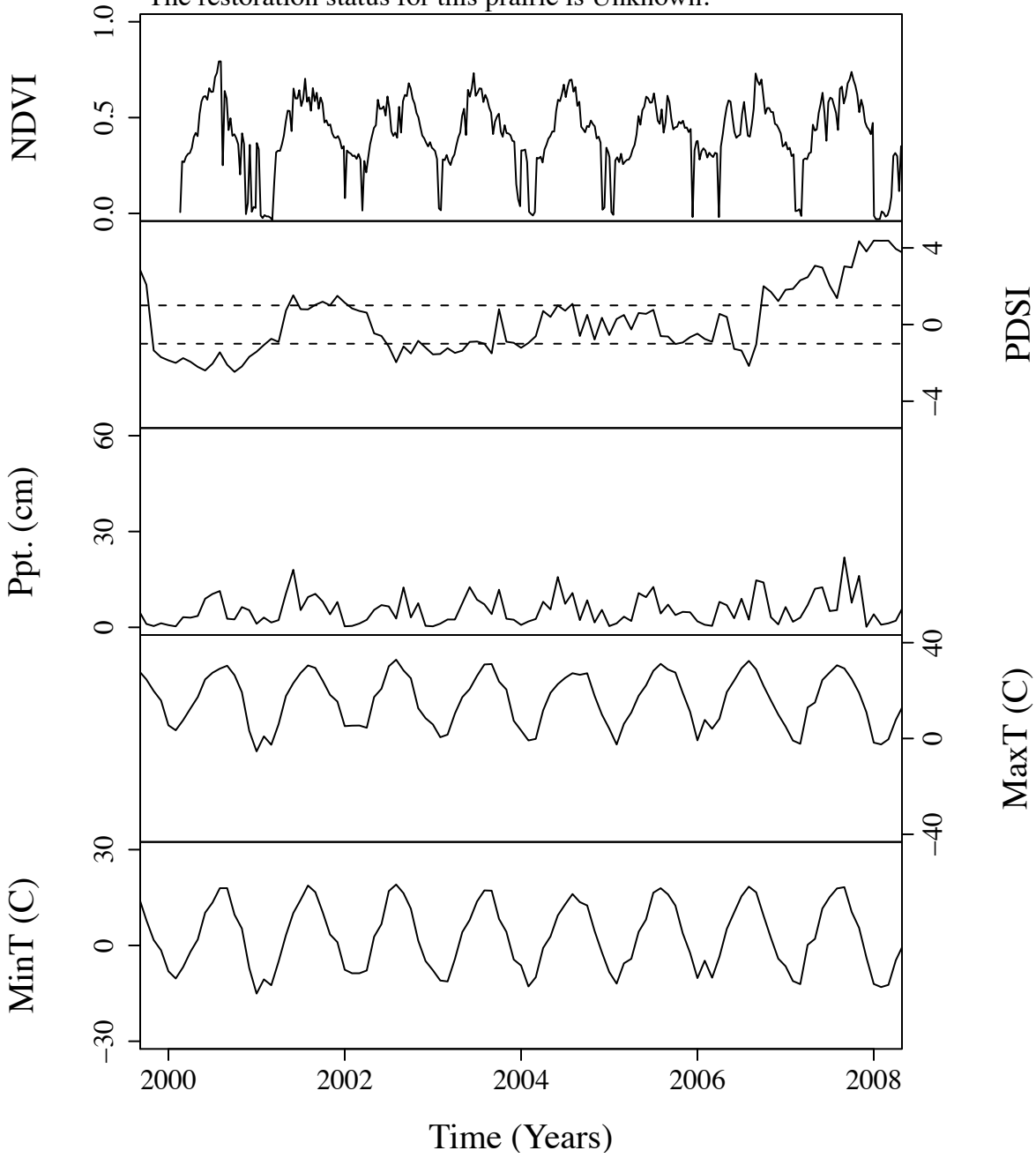

Figure B.80. Time series curves for nea543.
The community type for this prairie is Mixed.
The dominant photosynthetic pathway for this prairie is C4.
The restoration status for this prairie is Unknown.

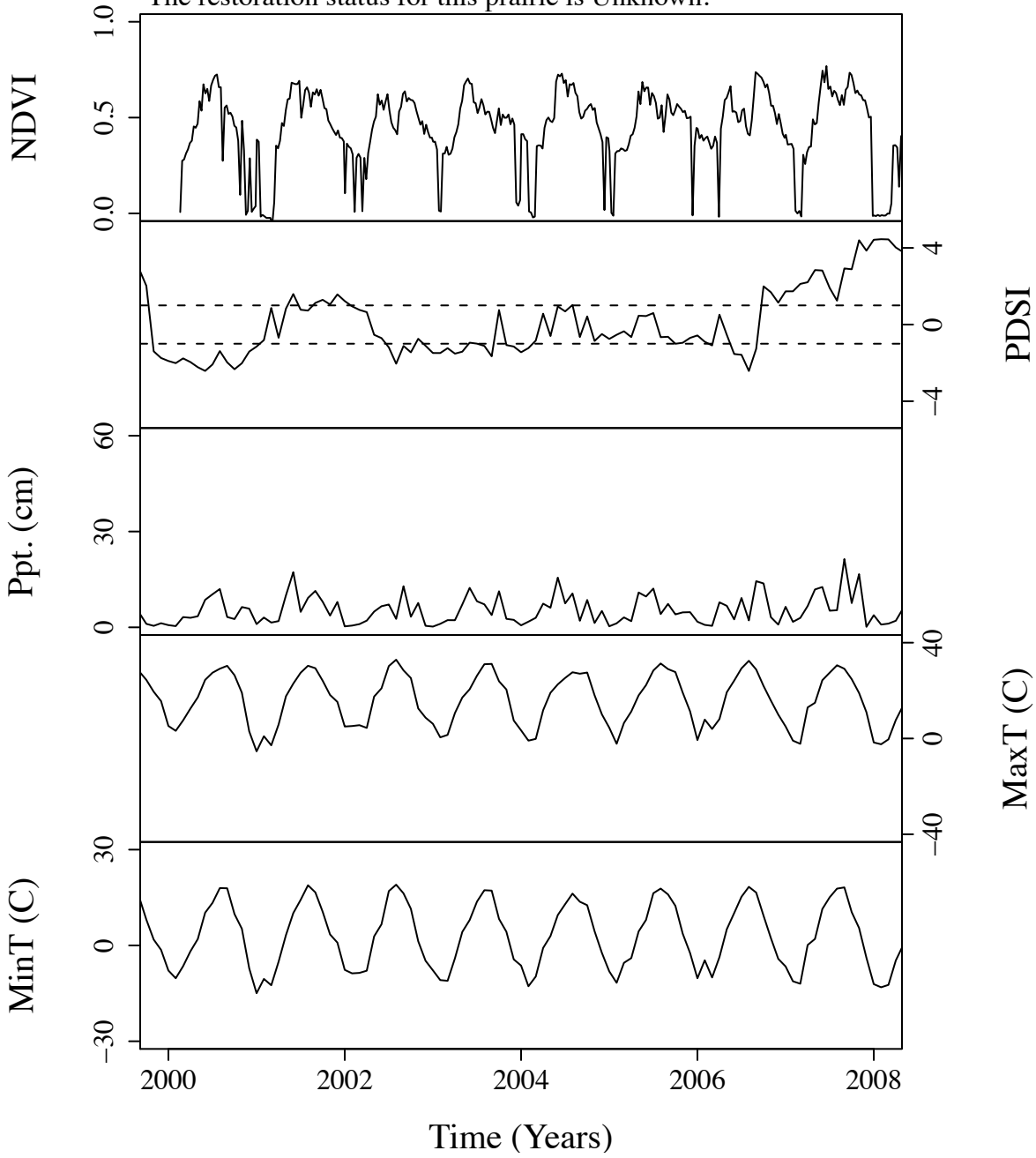

Figure B.81. Time series curves for nea598.
The community type for this prairie is Mixed.
The dominant photosynthetic pathway for this prairie is C4.
The restoration status for this prairie is Unknown.

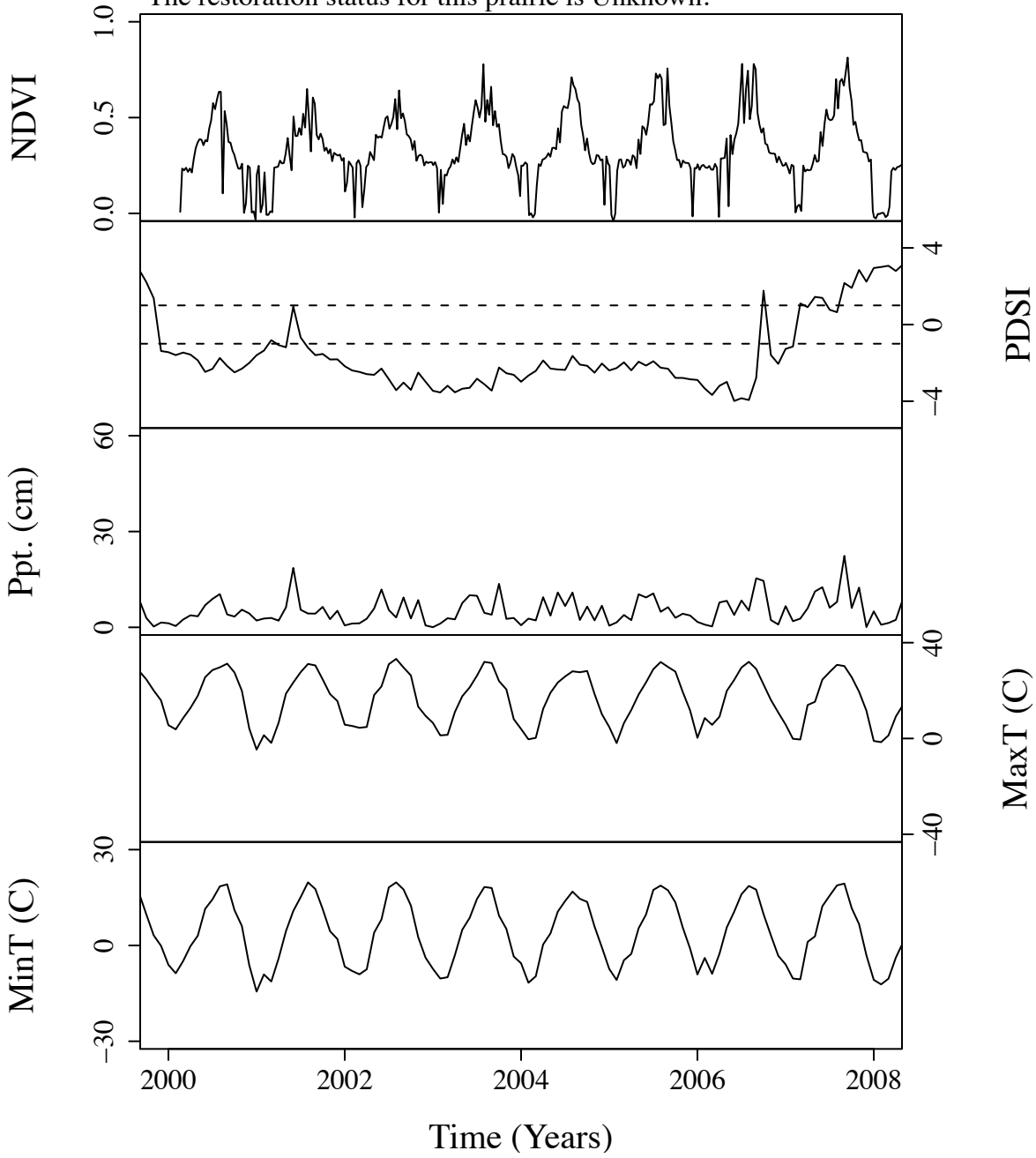

Figure B.82. Time series curves for nea636.
The community type for this prairie is Mixed.
The dominant photosynthetic pathway for this prairie is C4.
The restoration status for this prairie is Unknown.

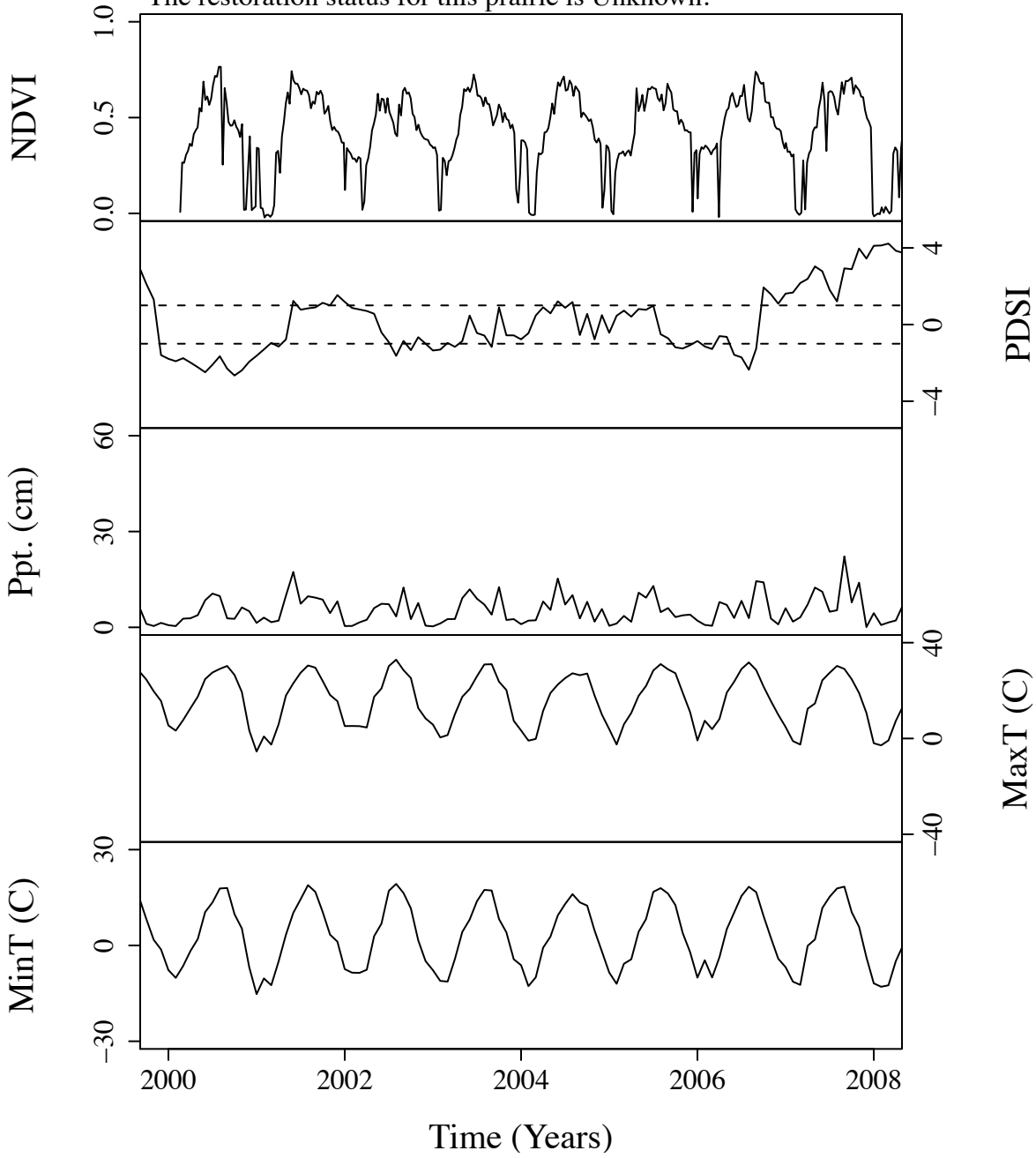

Figure B.83. Time series curves for nea640.
The community type for this prairie is Mixed.
The dominant photosynthetic pathway for this prairie is C4.
The restoration status for this prairie is Unknown.

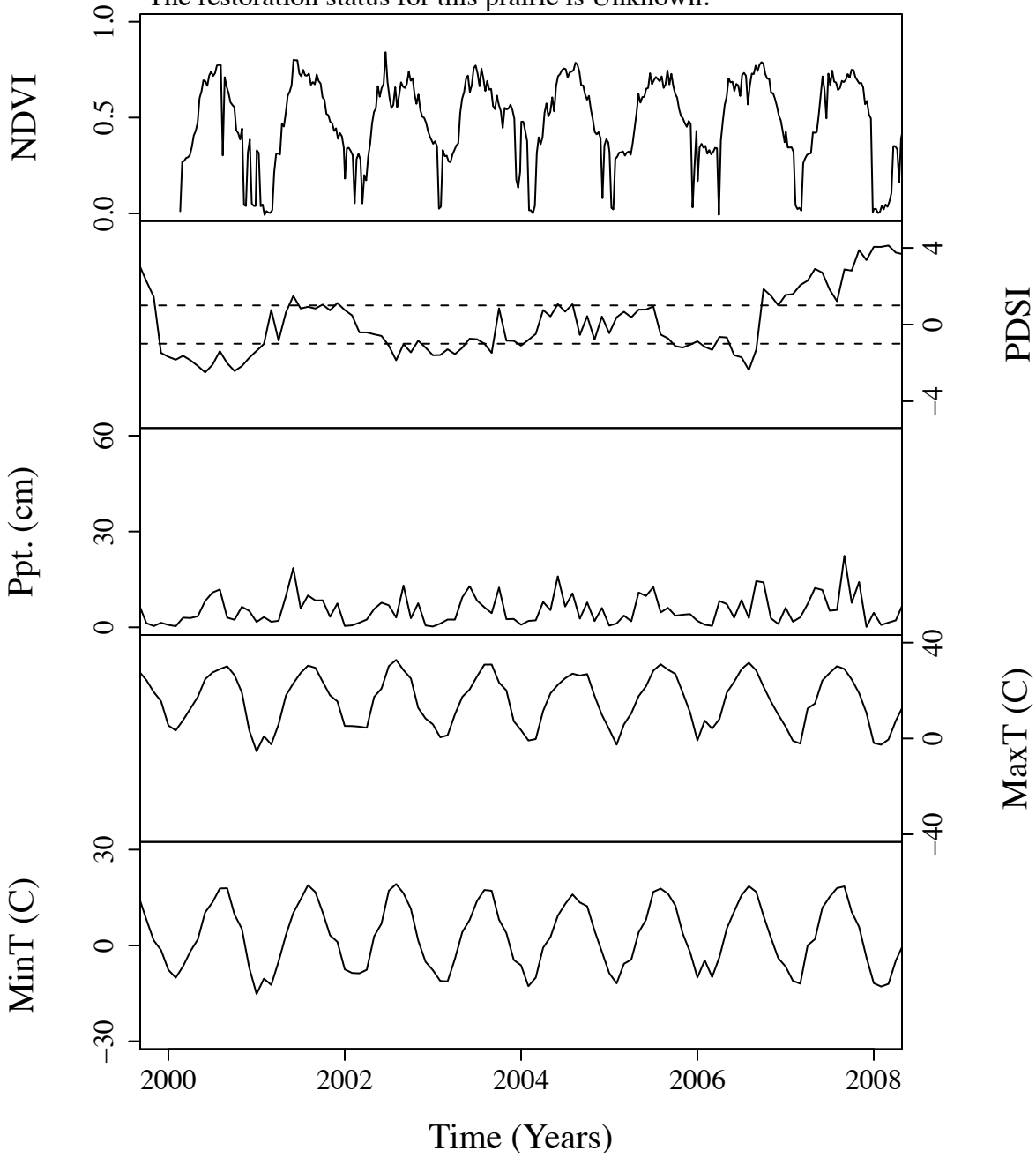

Figure B.84. Time series curves for nea641.
The community type for this prairie is Mixed.
The dominant photosynthetic pathway for this prairie is C4.
The restoration status for this prairie is Unknown.

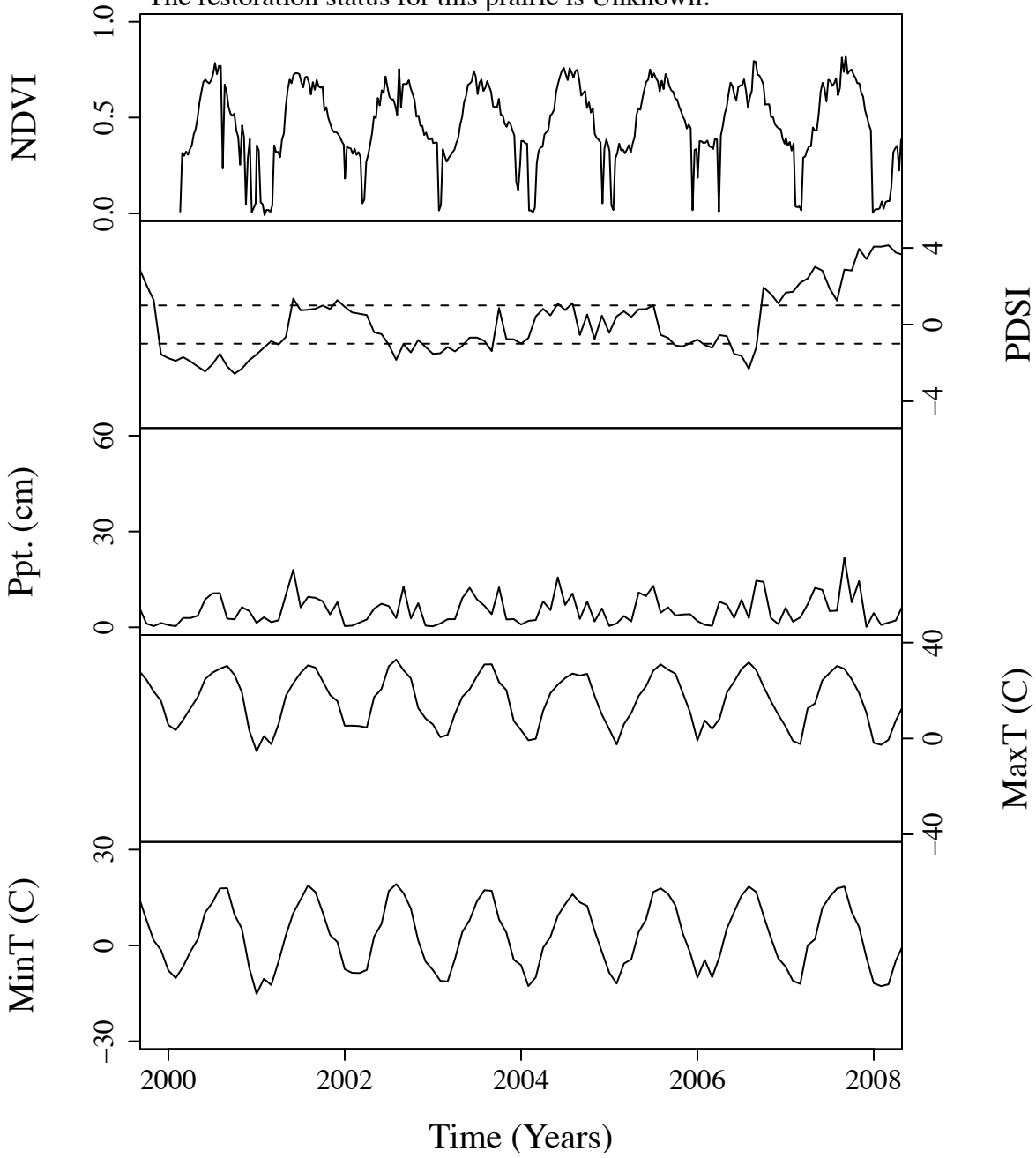

Figure B.85. Time series curves for nea642.
The community type for this prairie is Mixed.
The dominant photosynthetic pathway for this prairie is C4.
The restoration status for this prairie is Unknown.

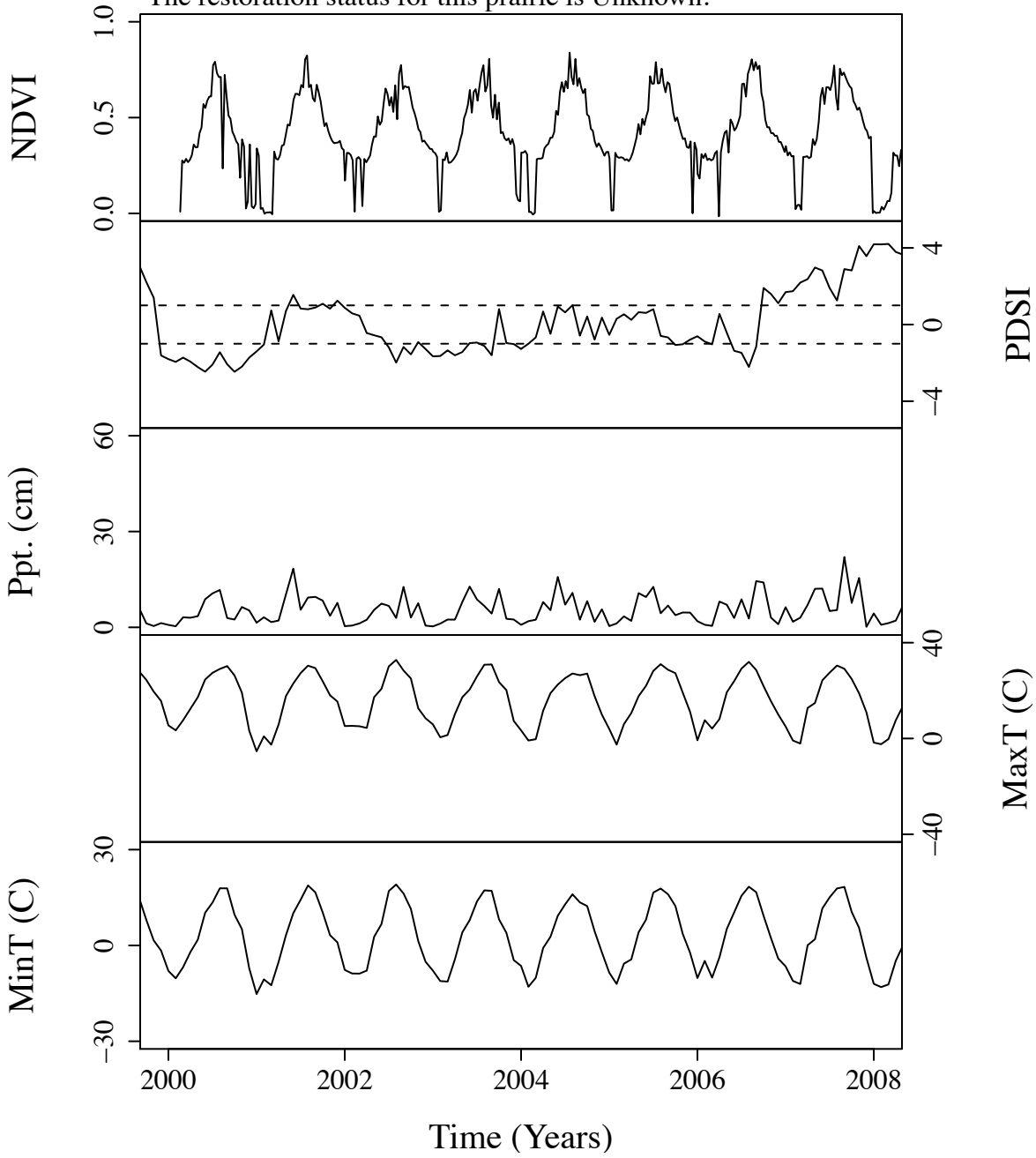

Figure B.86. Time series curves for nea655.
The community type for this prairie is Mixed.
The dominant photosynthetic pathway for this prairie is C4.
The restoration status for this prairie is Unknown.

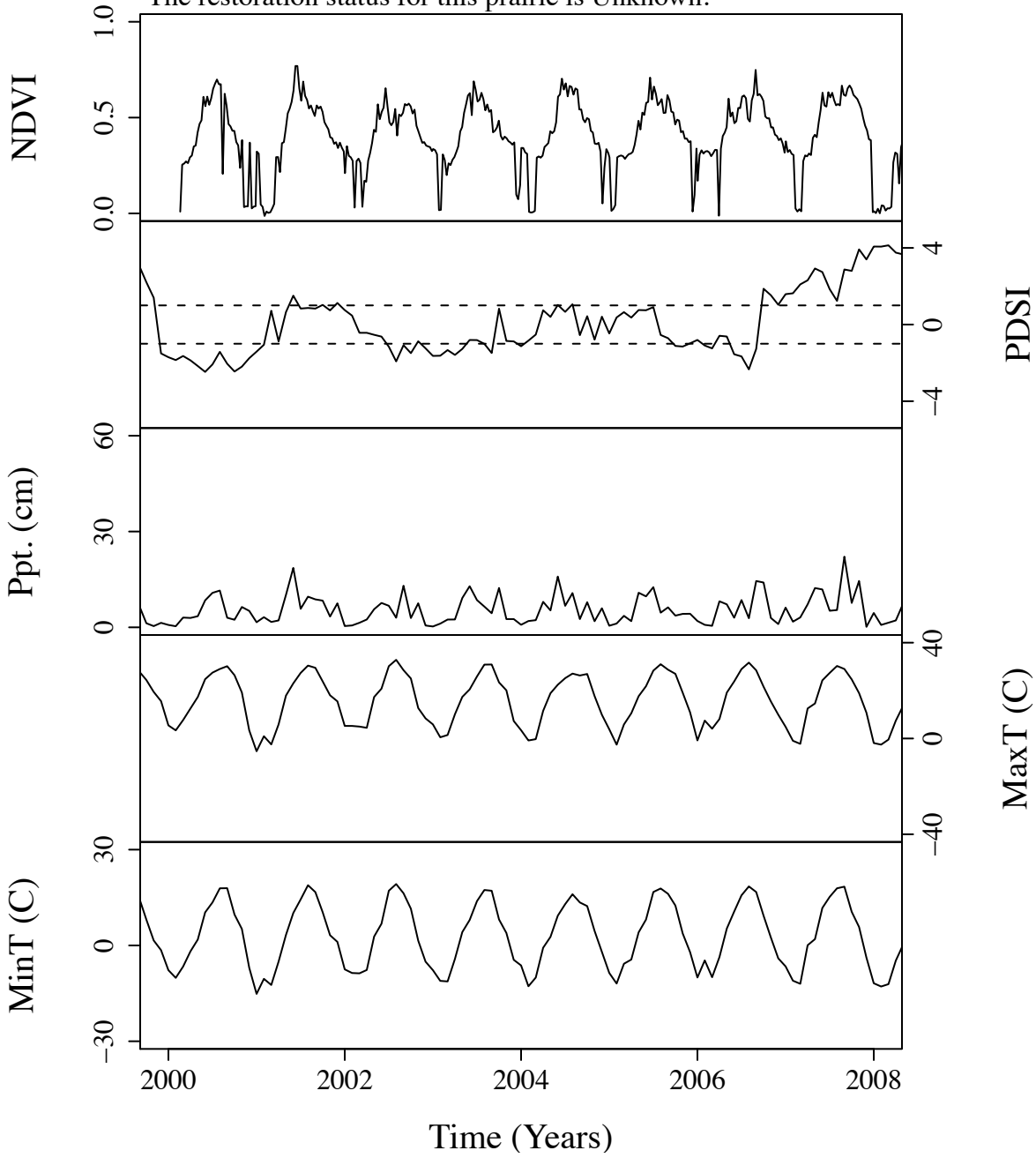

Figure B.87. Time series curves for nea689.
The community type for this prairie is Mixed.
The dominant photosynthetic pathway for this prairie is C4.
The restoration status for this prairie is Unknown.

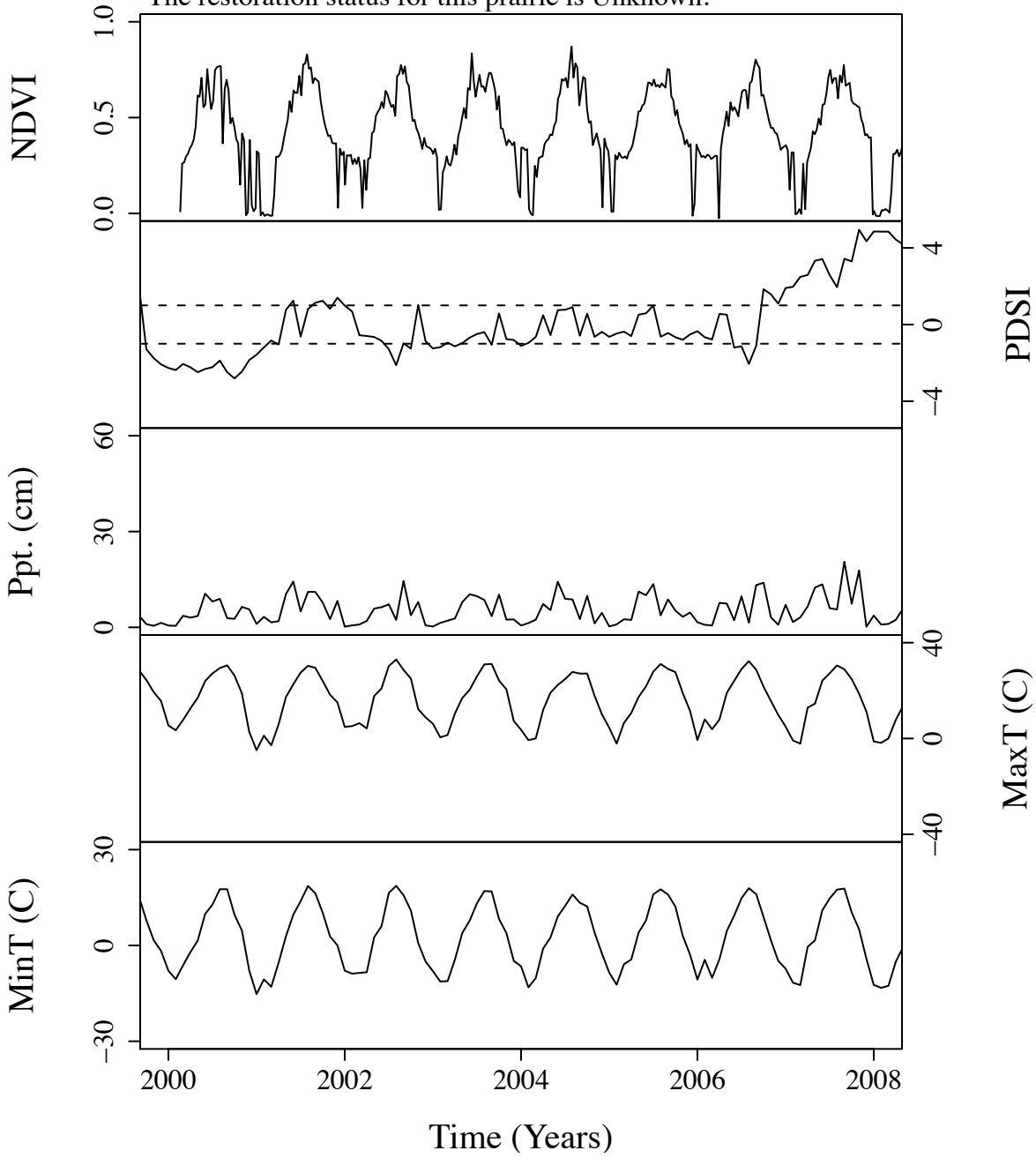

Figure B.88. Time series curves for nea690.
The community type for this prairie is Mixed.
The dominant photosynthetic pathway for this prairie is C4.
The restoration status for this prairie is Unknown.

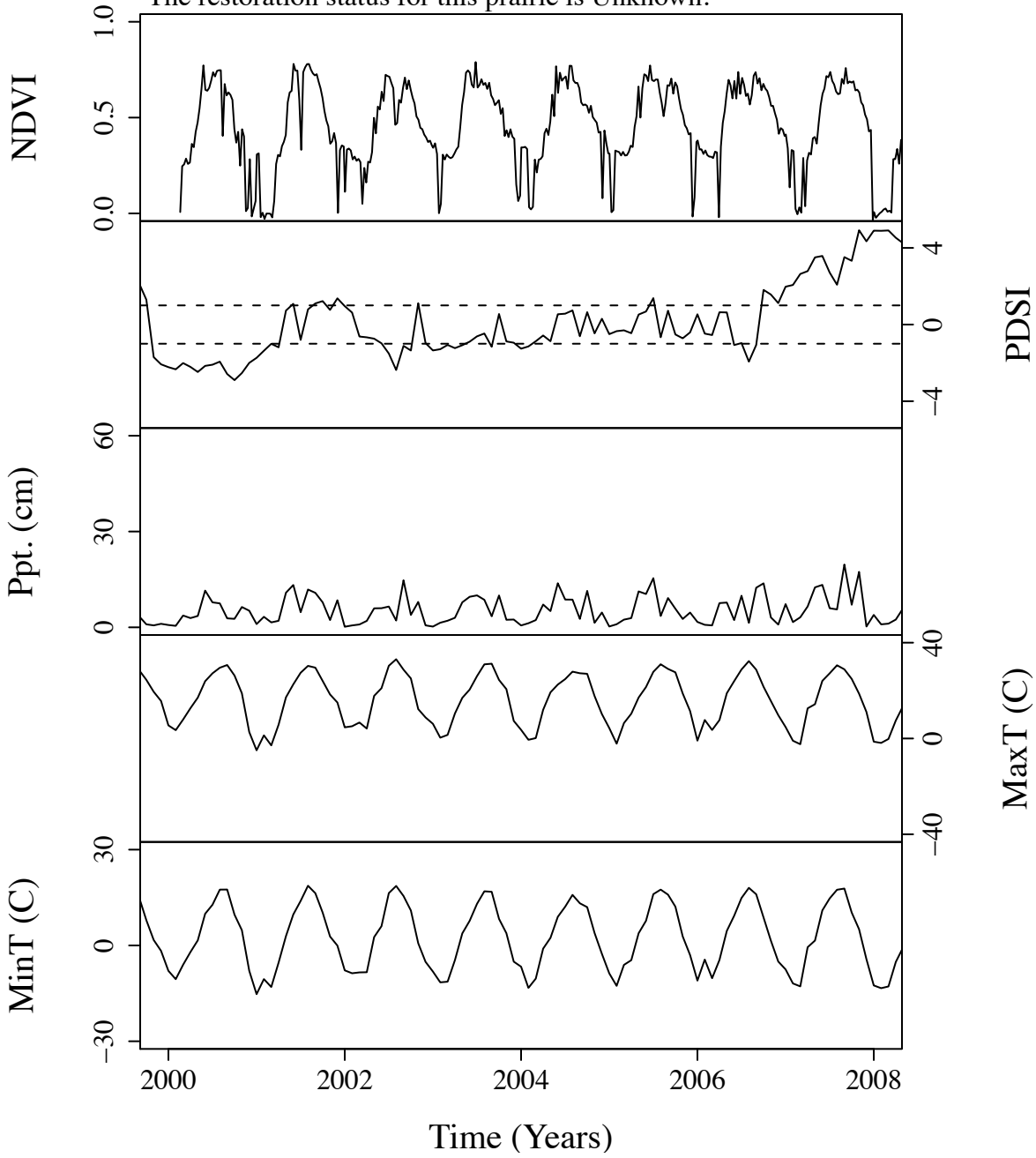

Figure B.89. Time series curves for nea692.
The community type for this prairie is Mixed.
The dominant photosynthetic pathway for this prairie is C4.
The restoration status for this prairie is Unknown.

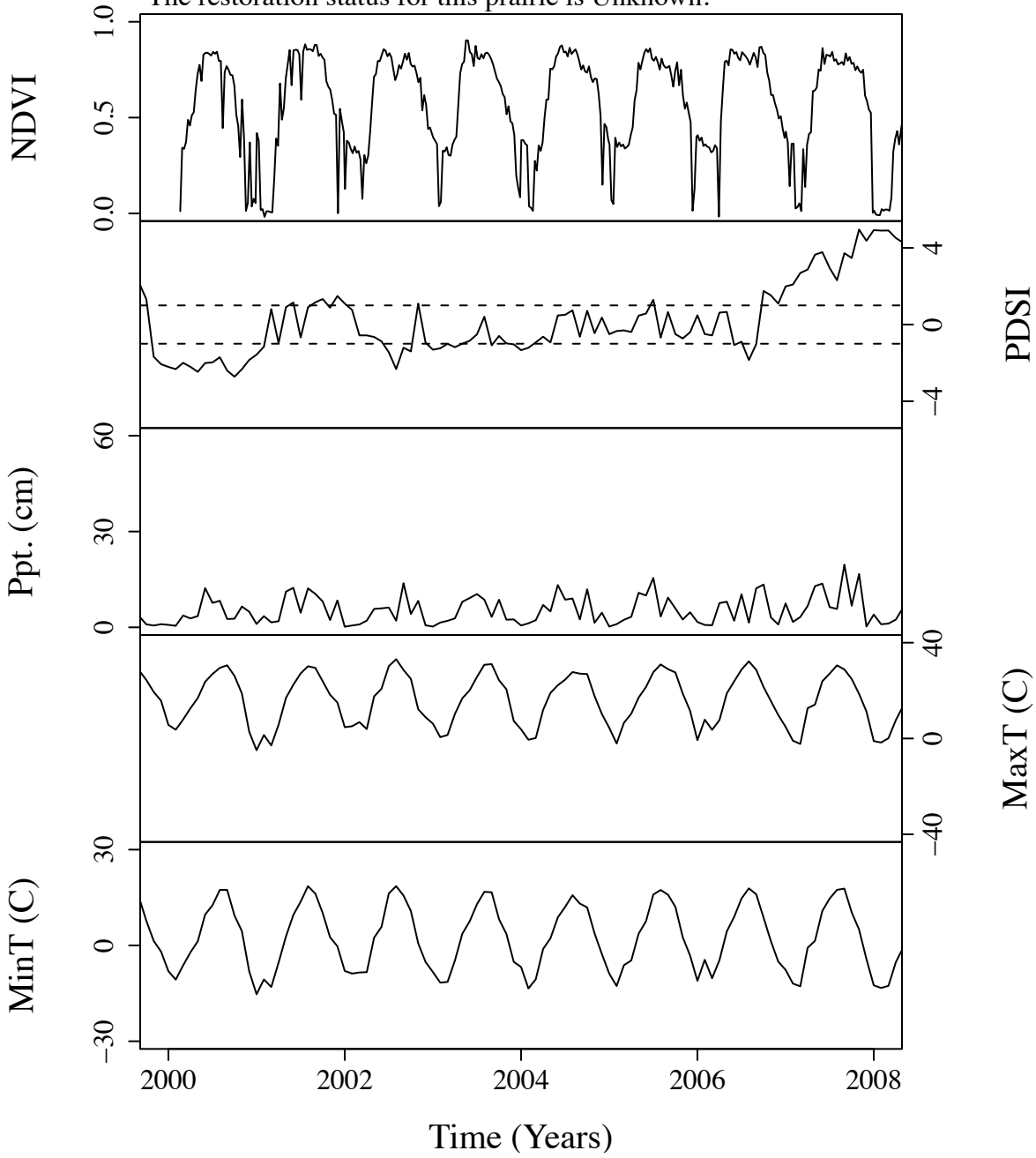

Figure B.90. Time series curves for nea694.
The community type for this prairie is Mixed.
The dominant photosynthetic pathway for this prairie is C4.
The restoration status for this prairie is Unknown.

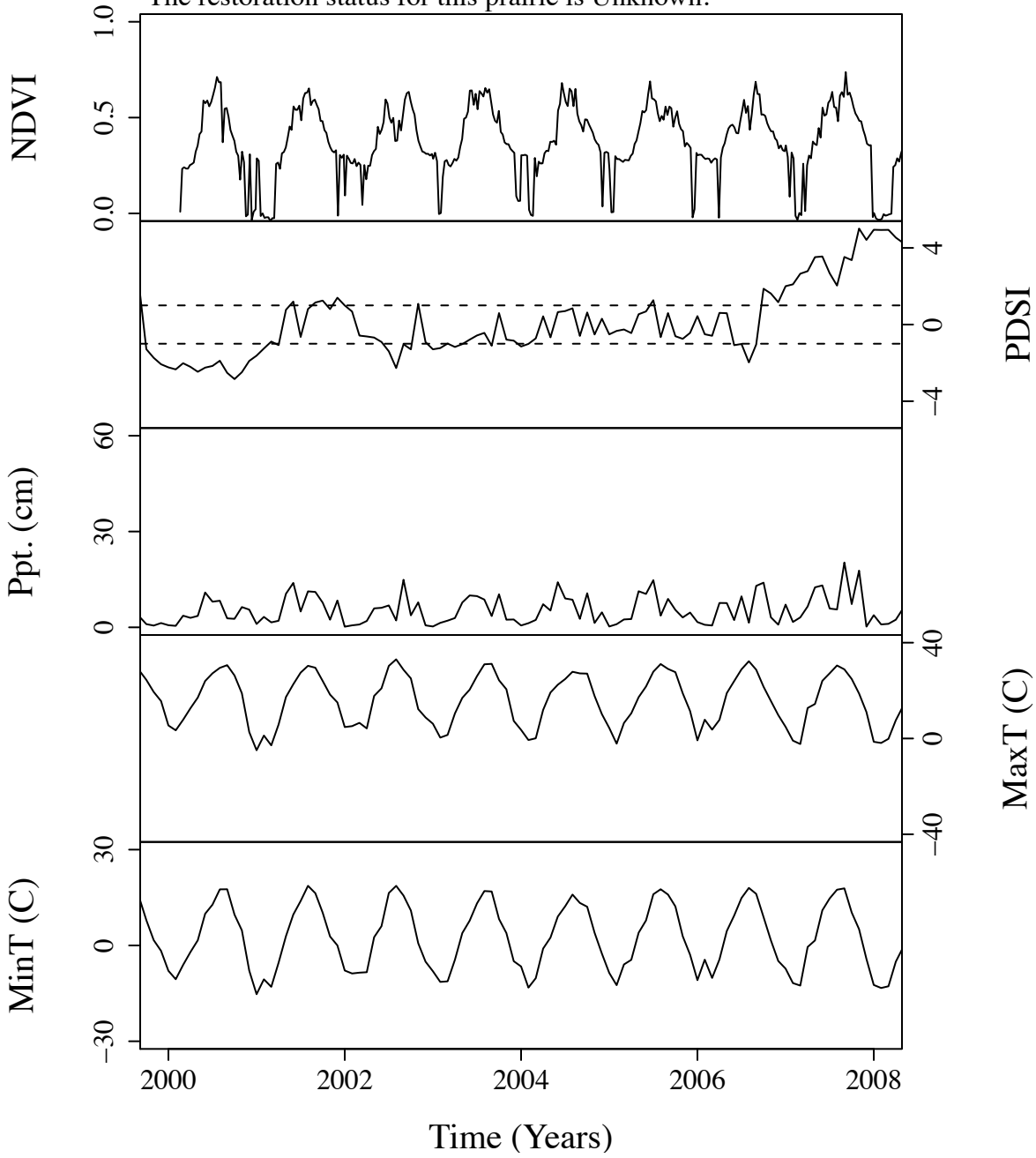

Figure B.91. Time series curves for nea695.
The community type for this prairie is Mixed.
The dominant photosynthetic pathway for this prairie is C4.
The restoration status for this prairie is Unknown.

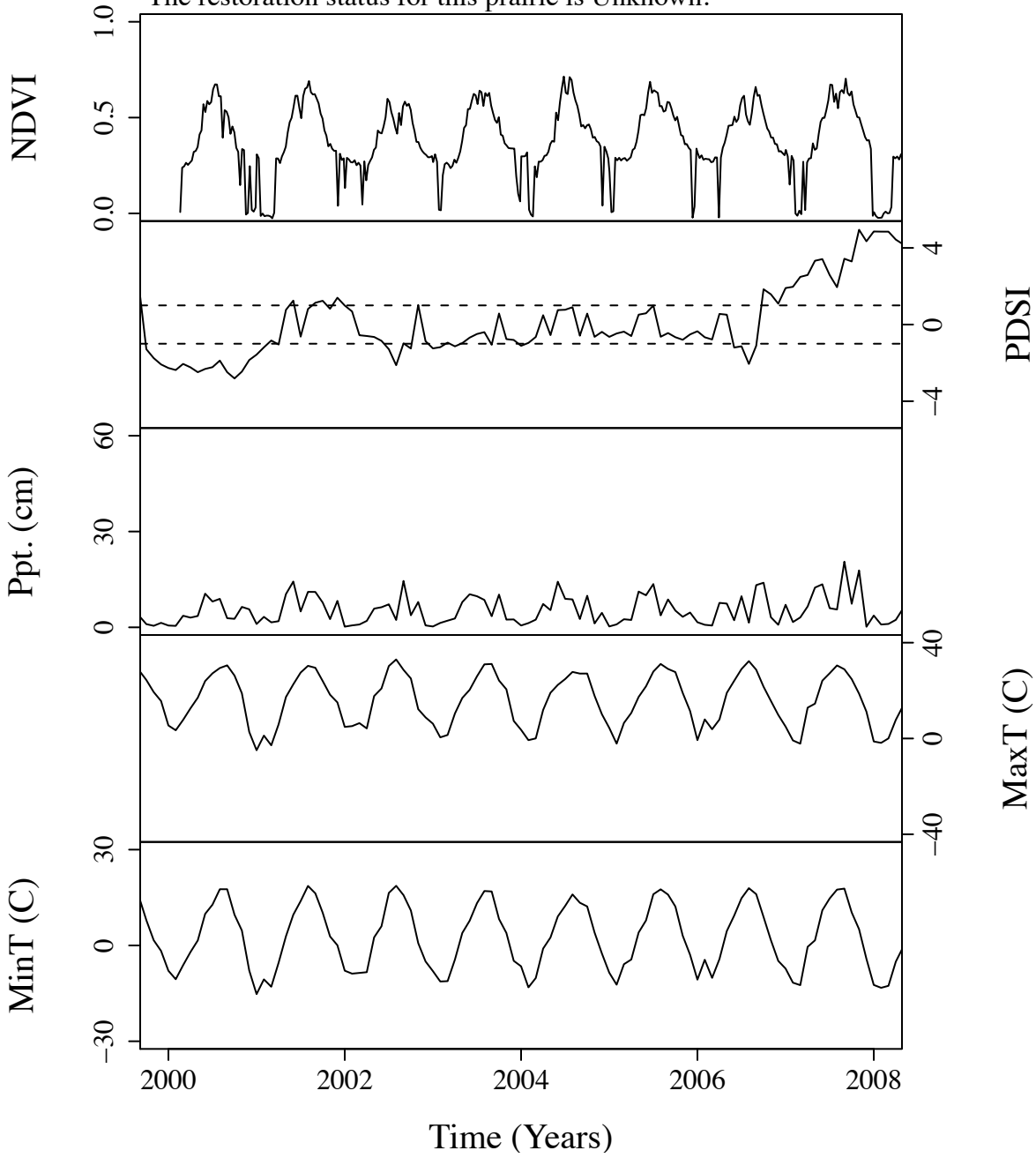

Figure B.92. Time series curves for nea696.
The community type for this prairie is Mixed.
The dominant photosynthetic pathway for this prairie is C4.
The restoration status for this prairie is Unknown.

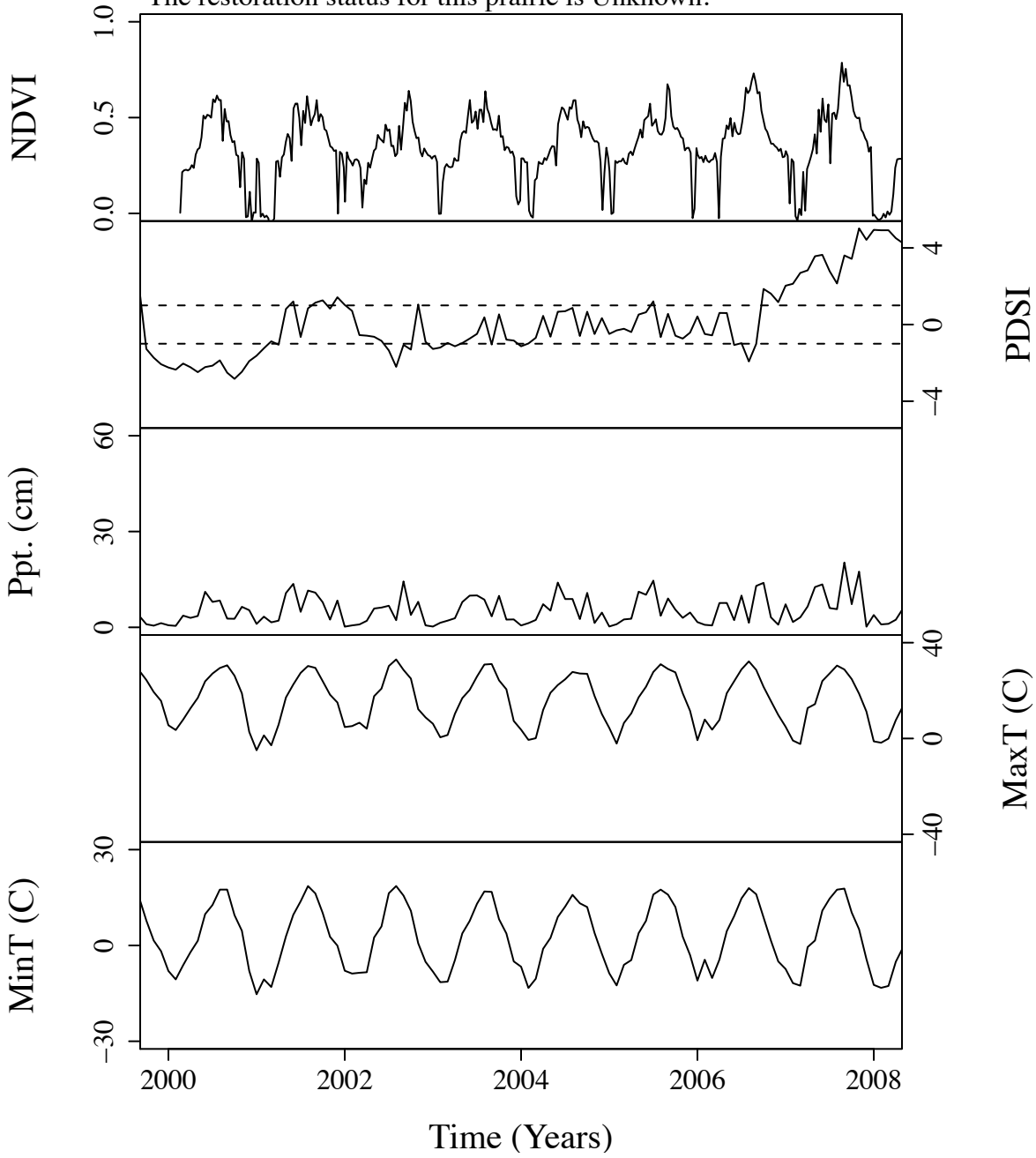

Figure B.93. Time series curves for nea701.
The community type for this prairie is Mixed.
The dominant photosynthetic pathway for this prairie is C4.
The restoration status for this prairie is Unknown.

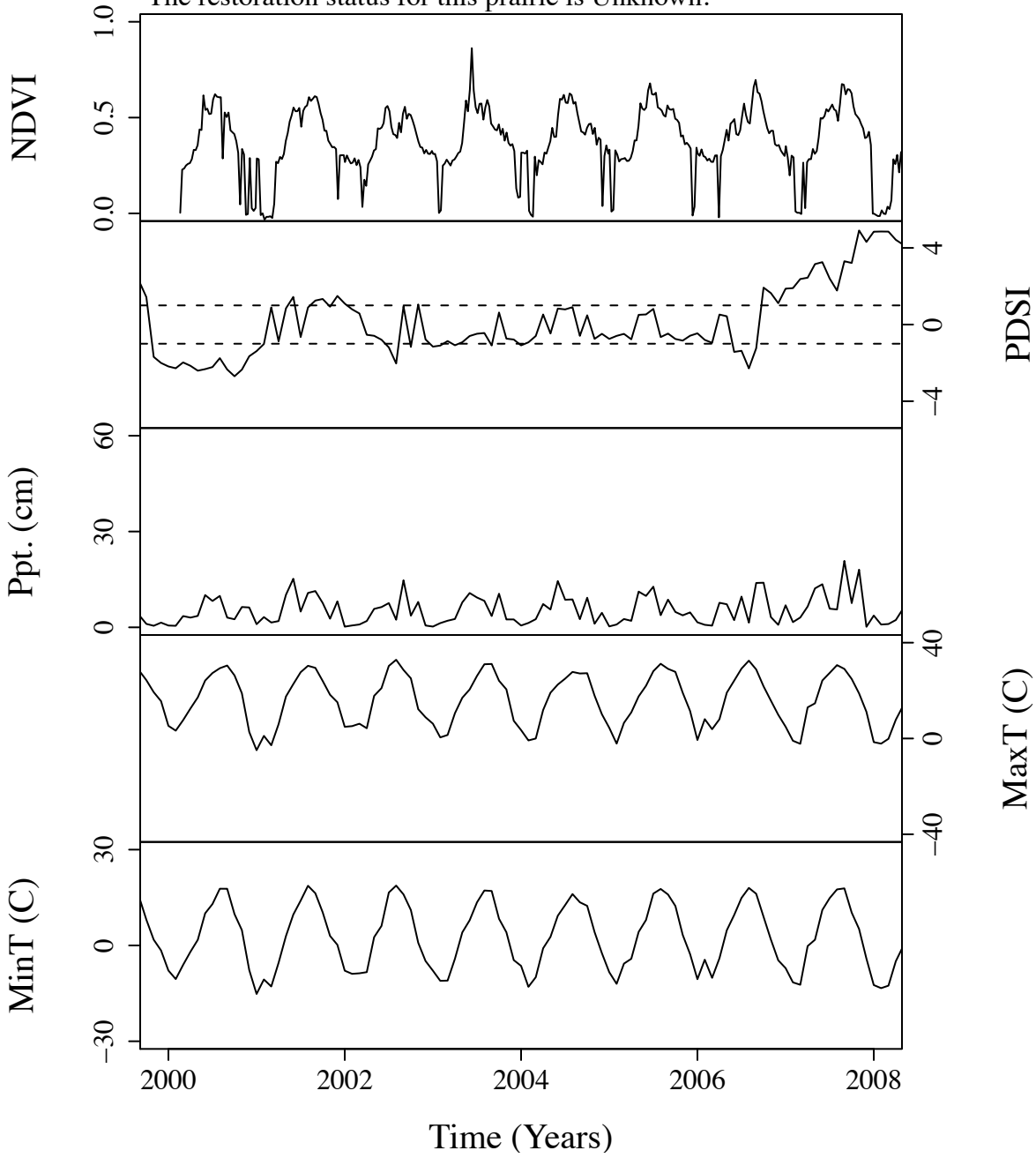

Figure B.94. Time series curves for nea703.
The community type for this prairie is Mixed.
The dominant photosynthetic pathway for this prairie is C4.
The restoration status for this prairie is Unknown.

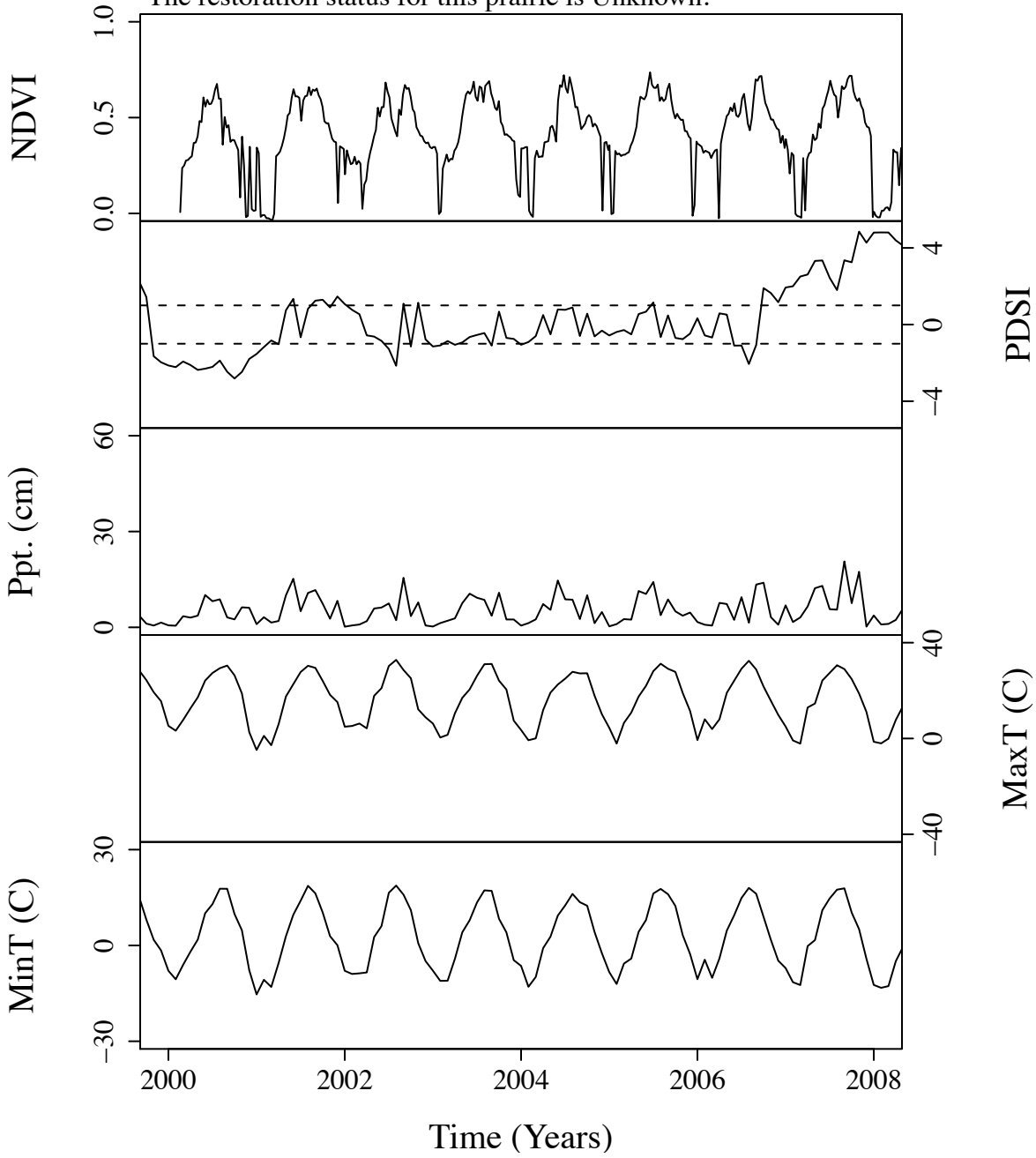

Figure B.95. Time series curves for nea705.
The community type for this prairie is Mixed.
The dominant photosynthetic pathway for this prairie is C4.
The restoration status for this prairie is Unknown.

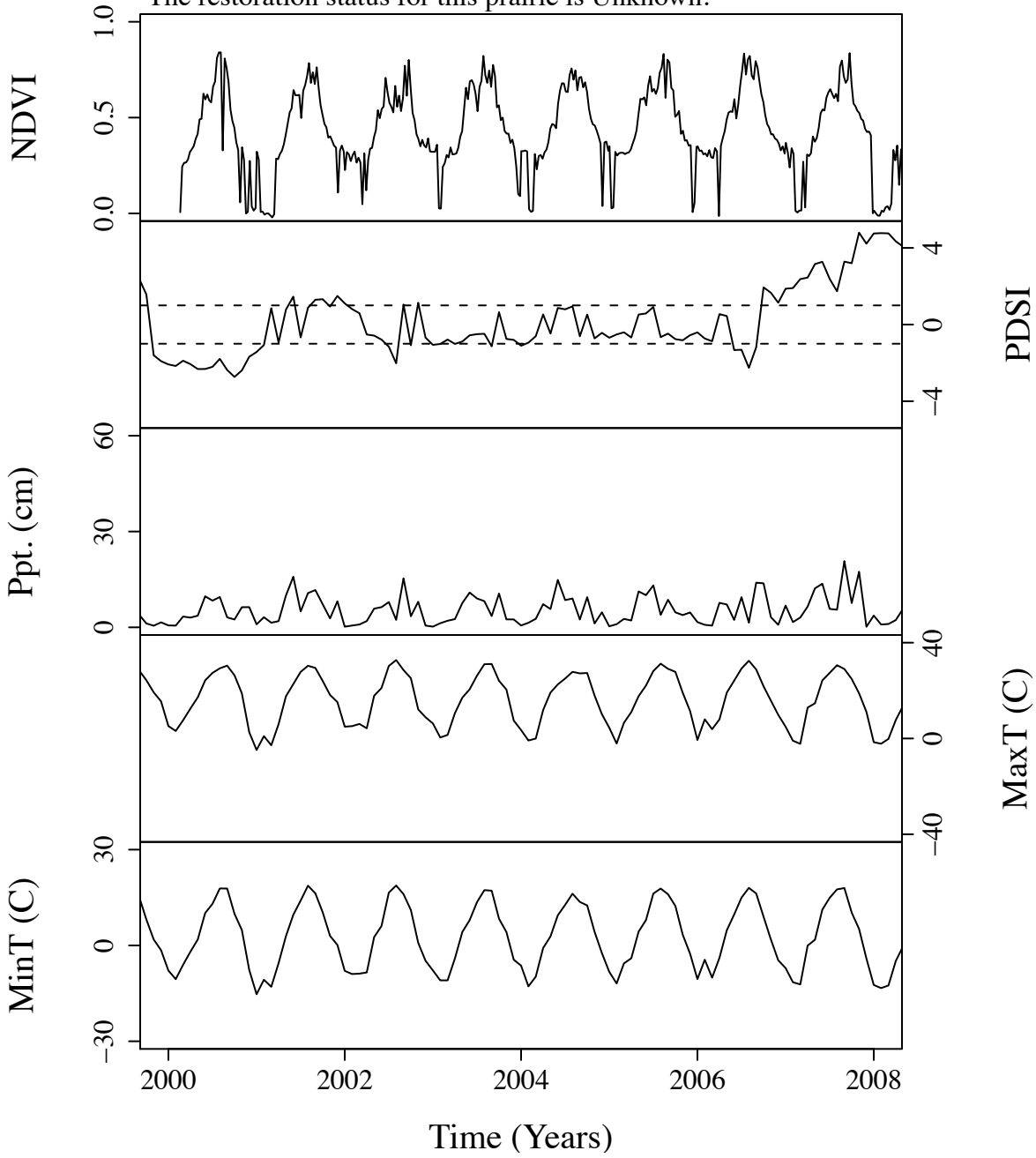

Figure B.96. Time series curves for nea710.
The community type for this prairie is Mixed.
The dominant photosynthetic pathway for this prairie is C4.
The restoration status for this prairie is Unknown.

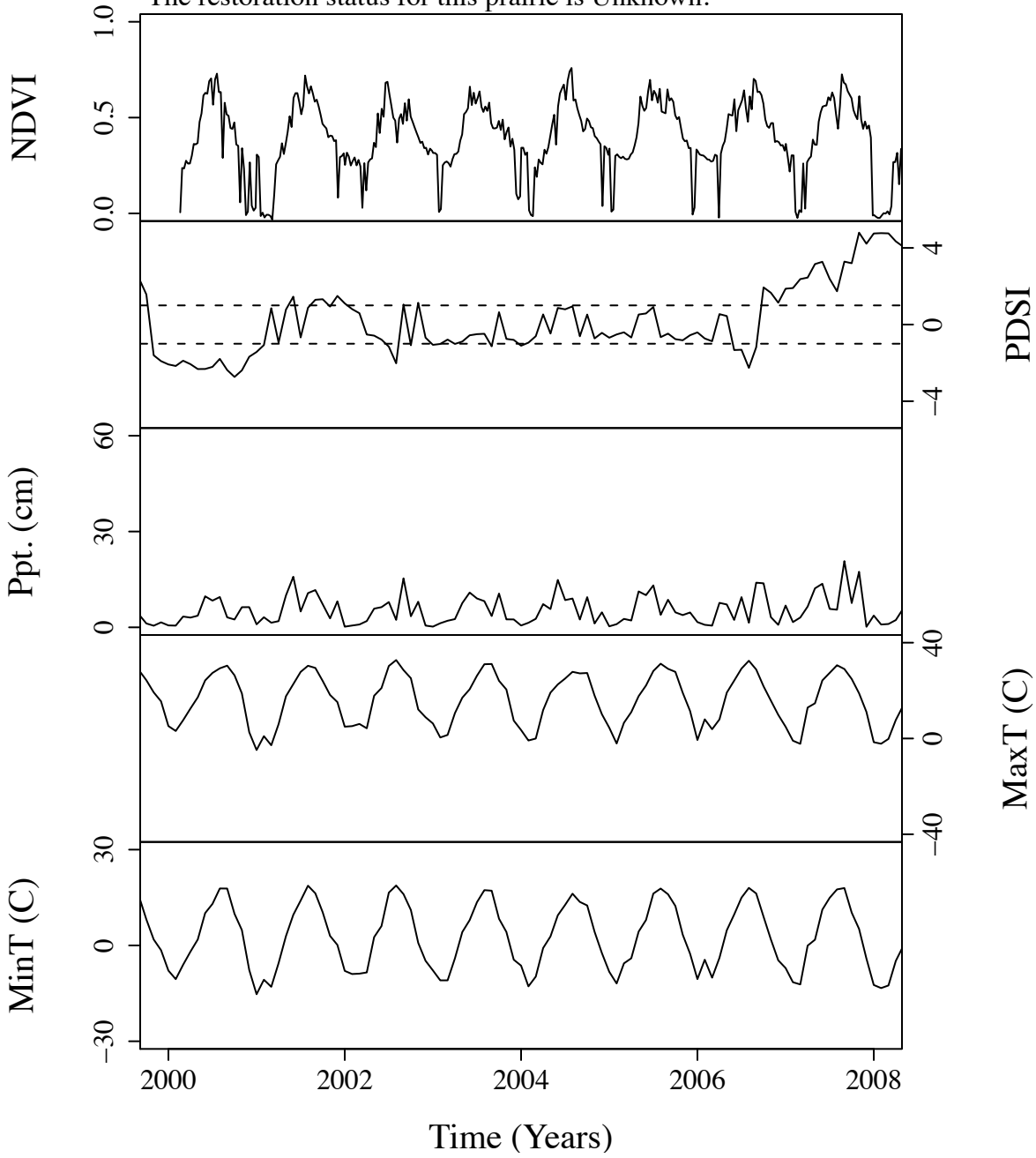

Figure B.97. Time series curves for ngn45.
The community type for this prairie is Mixed.
The dominant photosynthetic pathway for this prairie is C4.
The restoration status for this prairie is Unknown.

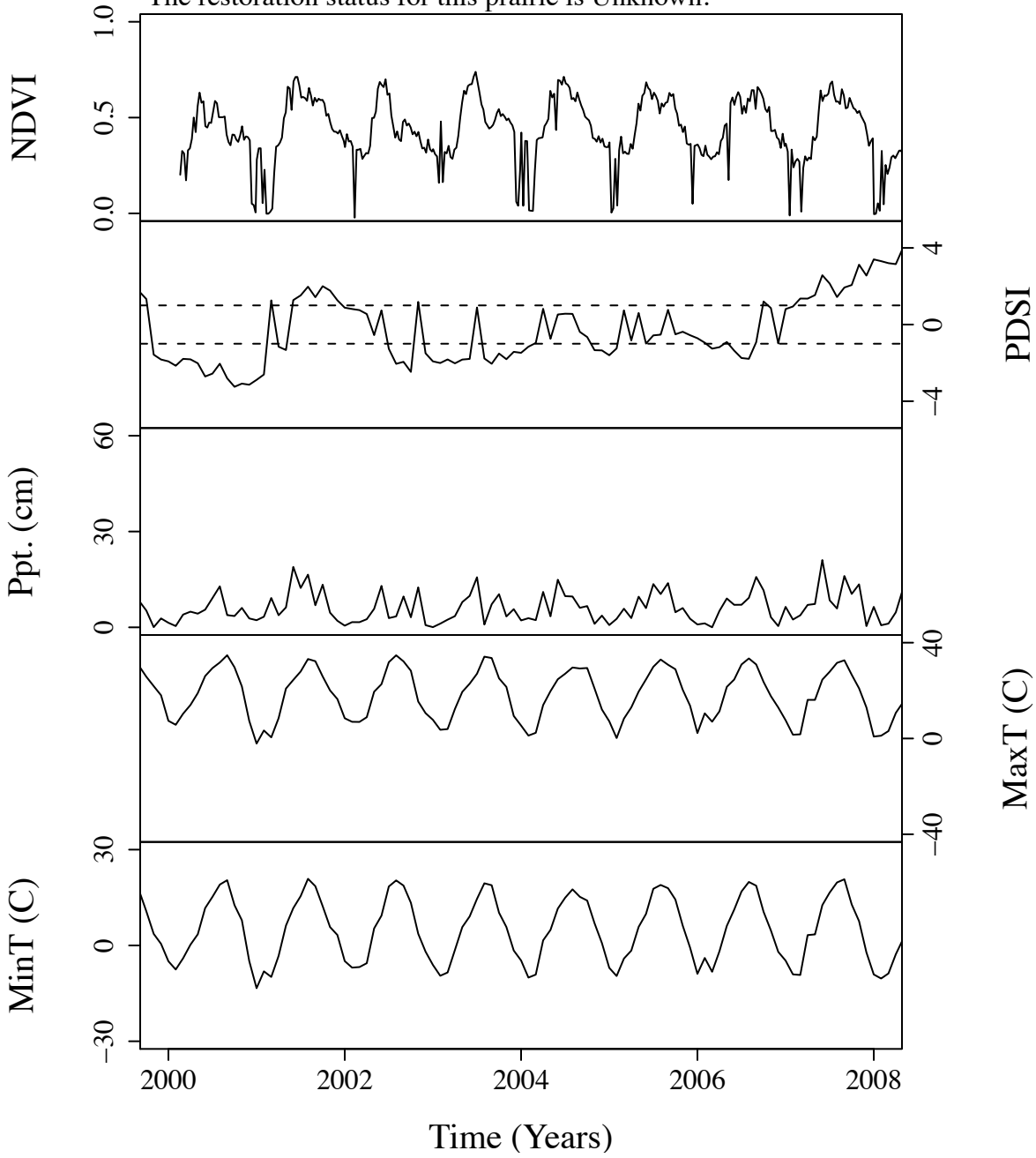

Figure B.98. Time series curves for ngn47.
The community type for this prairie is Mixed.
The dominant photosynthetic pathway for this prairie is C4.
The restoration status for this prairie is Unknown.

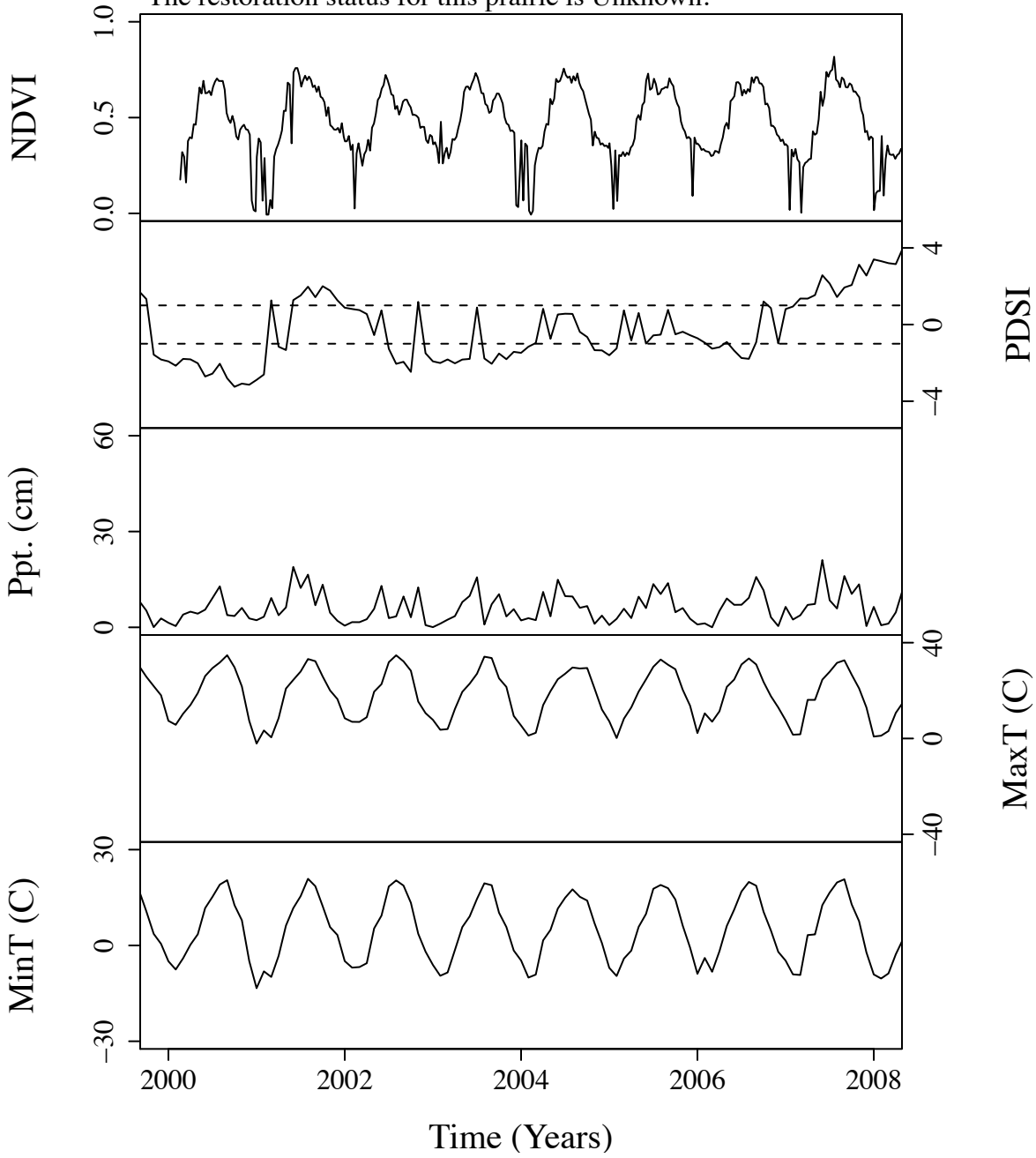

Figure B.99. Time series curves for ngn56.
The community type for this prairie is Mixed.
The dominant photosynthetic pathway for this prairie is C4.
The restoration status for this prairie is Unknown.

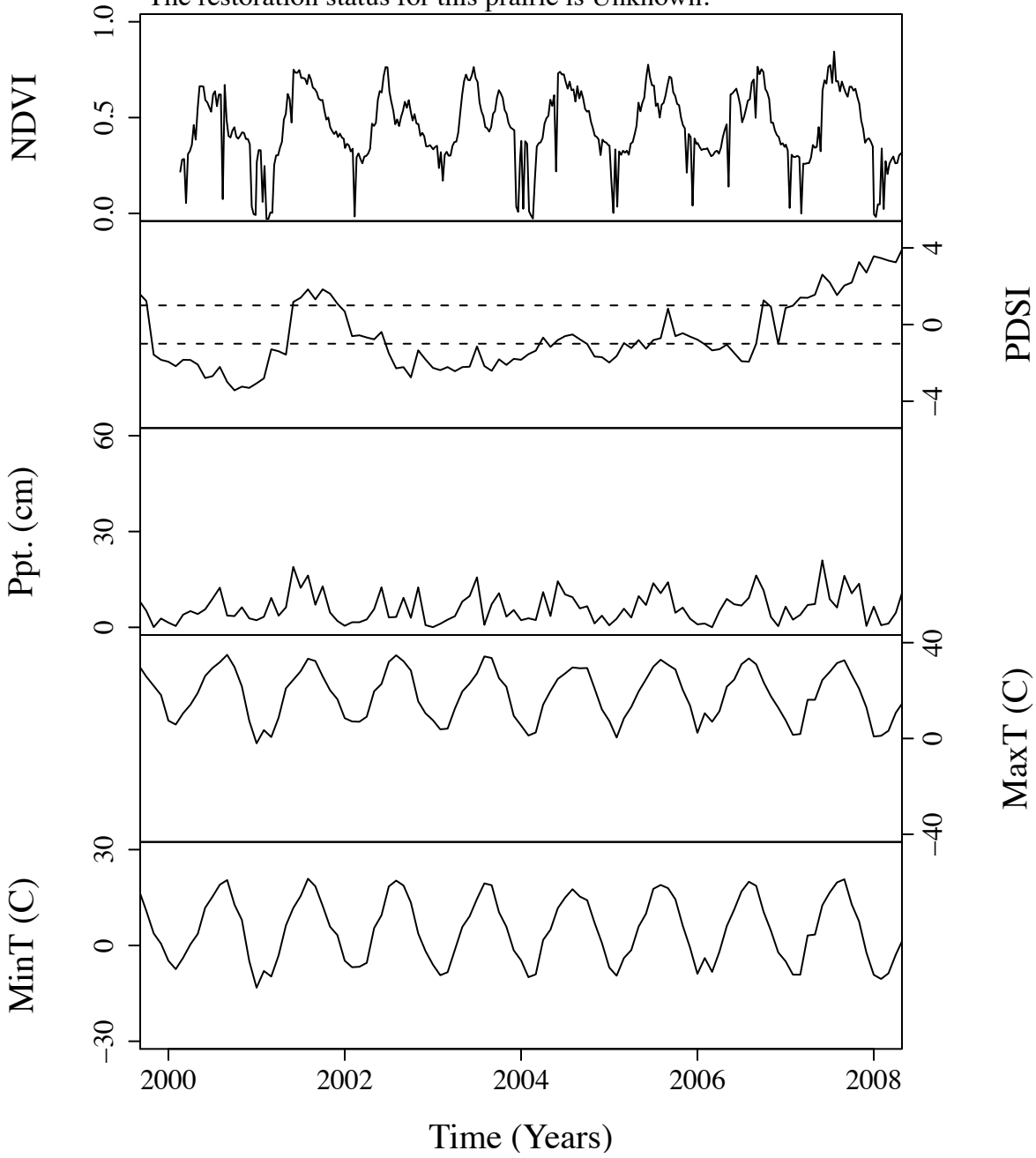

Figure B.100. Time series curves for ngn71.
The community type for this prairie is Mixed.
The dominant photosynthetic pathway for this prairie is C4.
The restoration status for this prairie is Unknown.

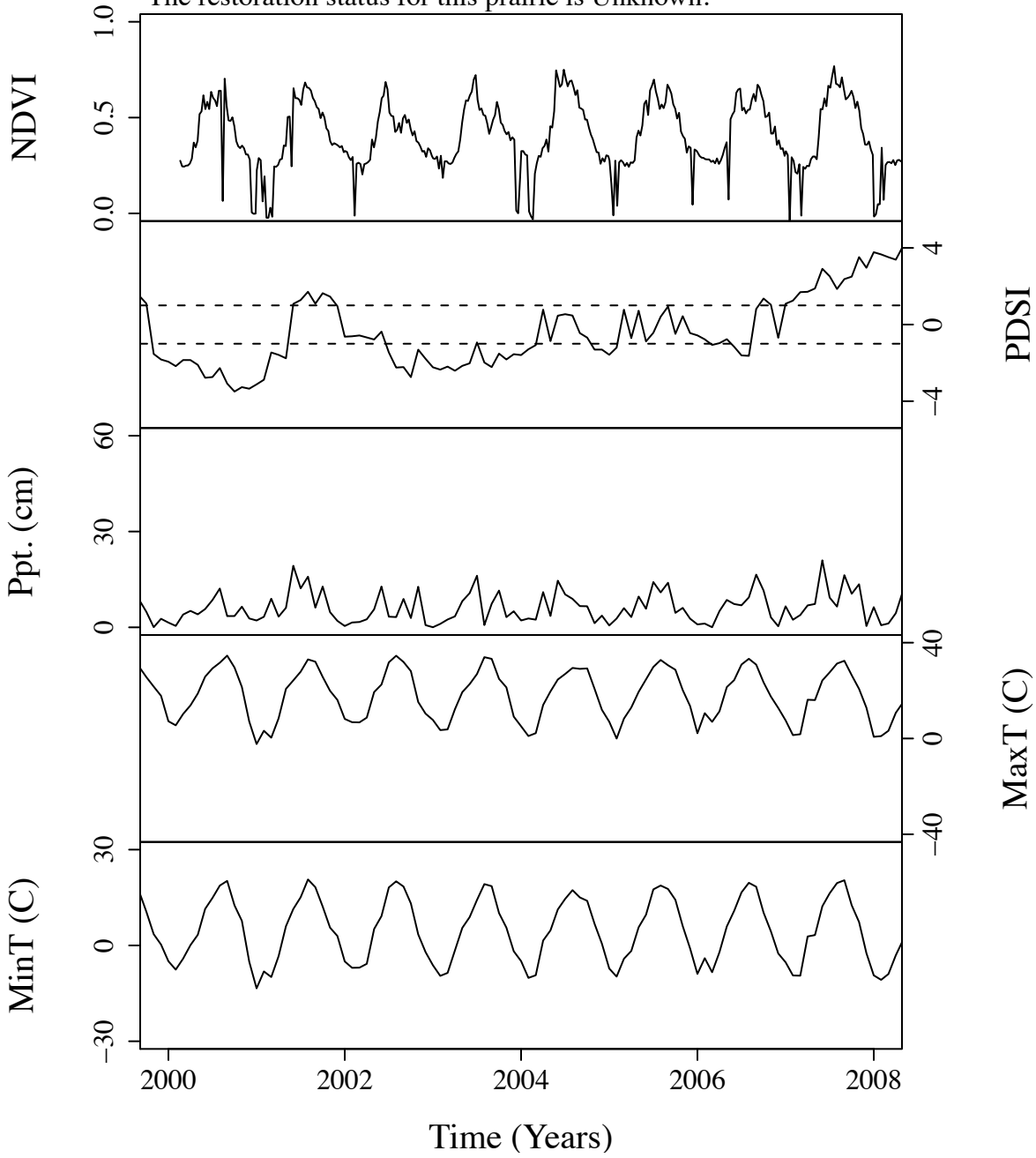

Figure B.101. Time series curves for ngn84.
The community type for this prairie is Mixed.
The dominant photosynthetic pathway for this prairie is C4.
The restoration status for this prairie is Unknown.

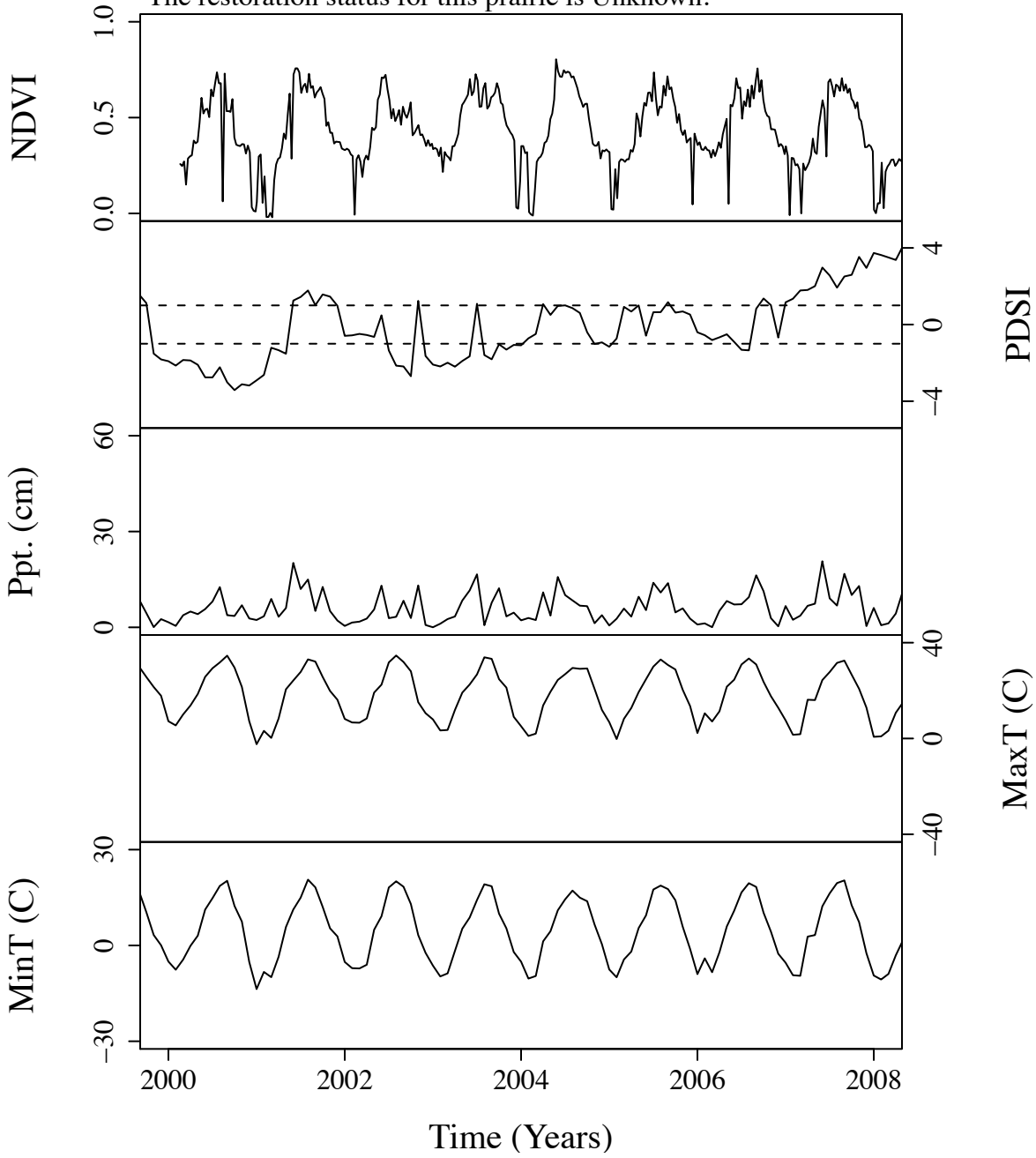

Figure B.102. Time series curves for ngn94.
The community type for this prairie is Mixed.
The dominant photosynthetic pathway for this prairie is C4.
The restoration status for this prairie is Unknown.

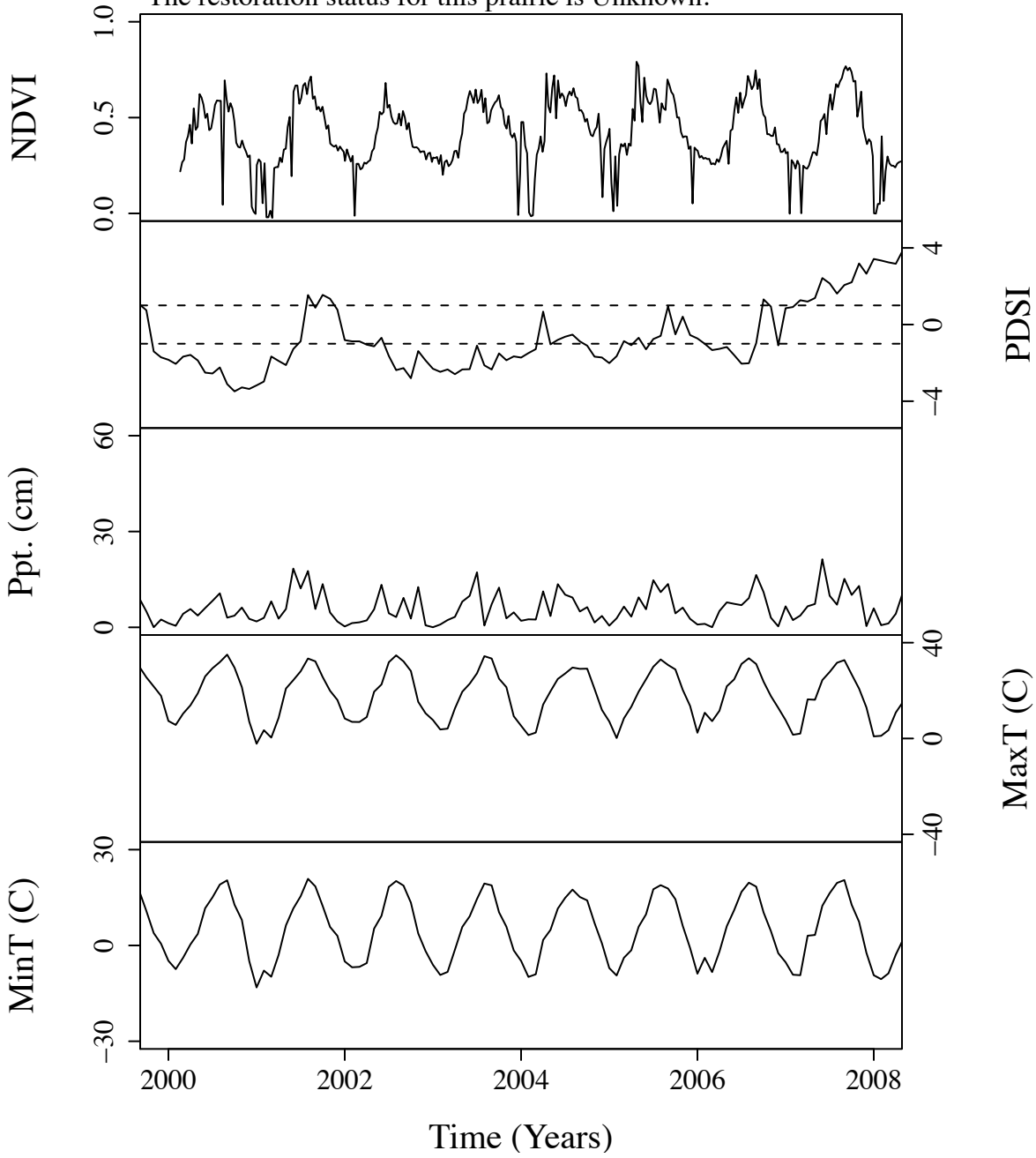

Figure B.103. Time series curves for ngn96.
The community type for this prairie is Mixed.
The dominant photosynthetic pathway for this prairie is C4.
The restoration status for this prairie is Unknown.

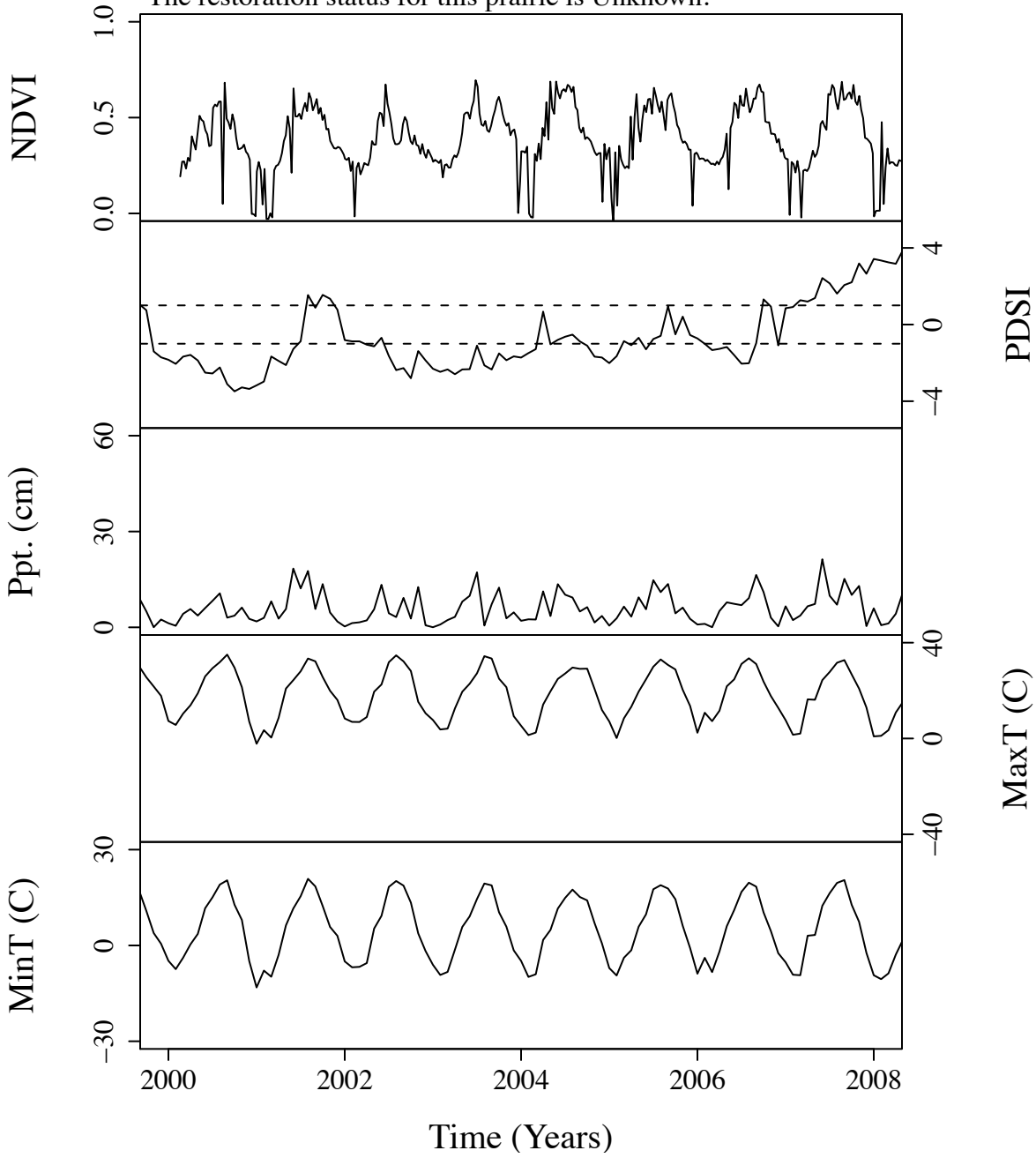

Figure B.104. Time series curves for ngn99.
The community type for this prairie is Mixed.
The dominant photosynthetic pathway for this prairie is C4.
The restoration status for this prairie is Unknown.

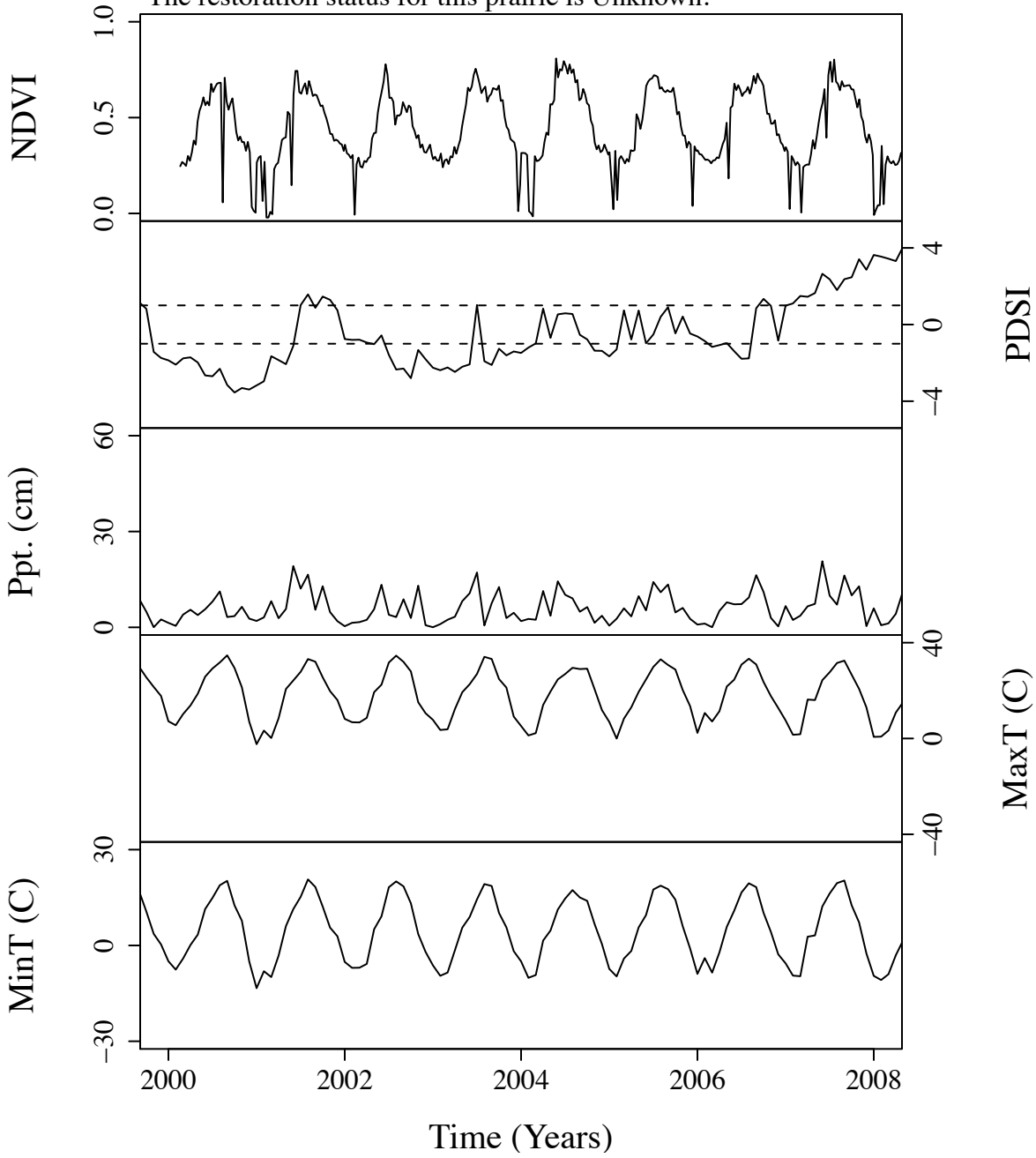

Figure B.105. Time series curves for nlo252.
The community type for this prairie is Mixed.
The dominant photosynthetic pathway for this prairie is C4.
The restoration status for this prairie is Unknown.

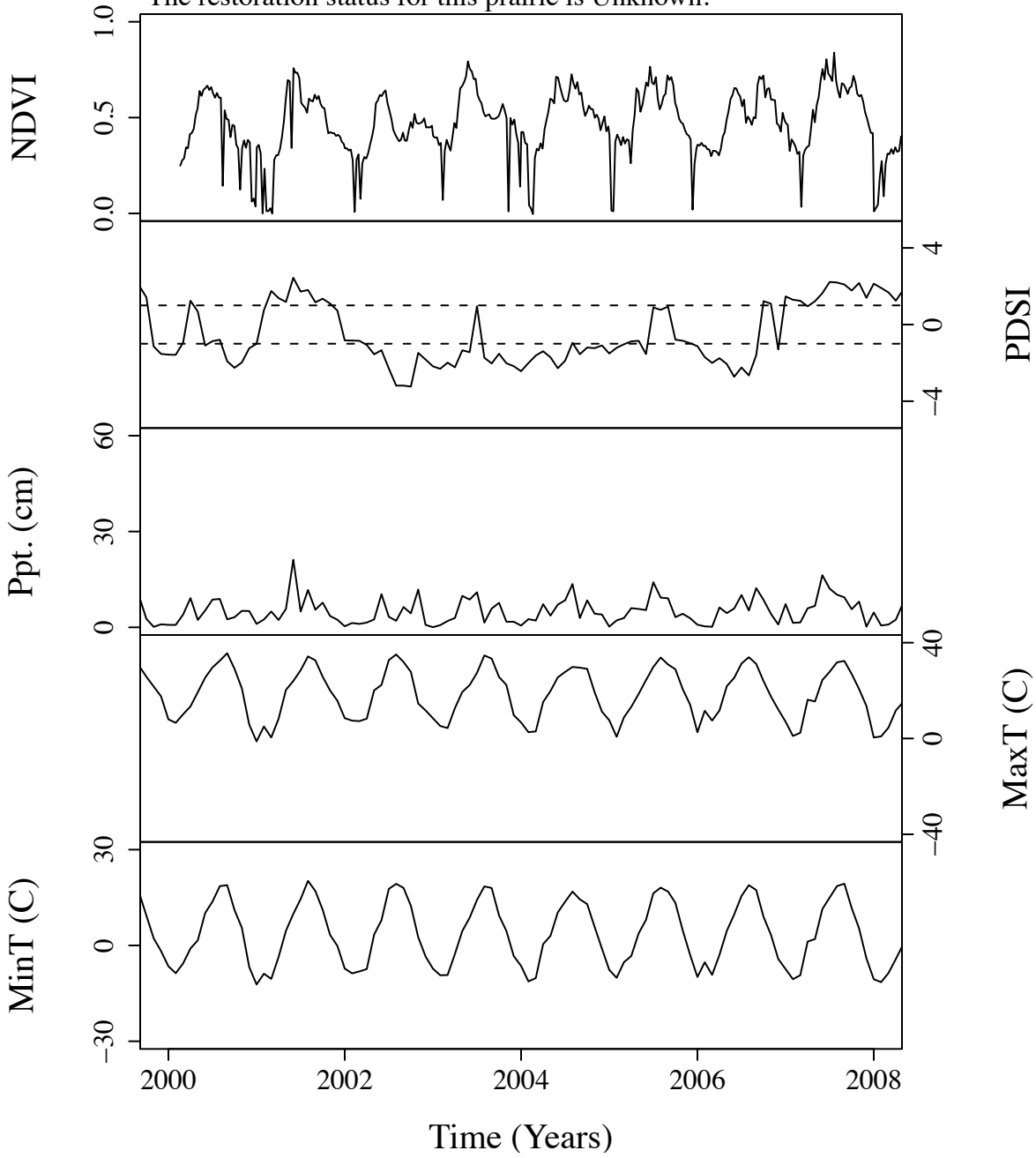

Figure B.106. Time series curves for nlo680.
The community type for this prairie is Short.
The dominant photosynthetic pathway for this prairie is C4.
The restoration status for this prairie is Unknown.

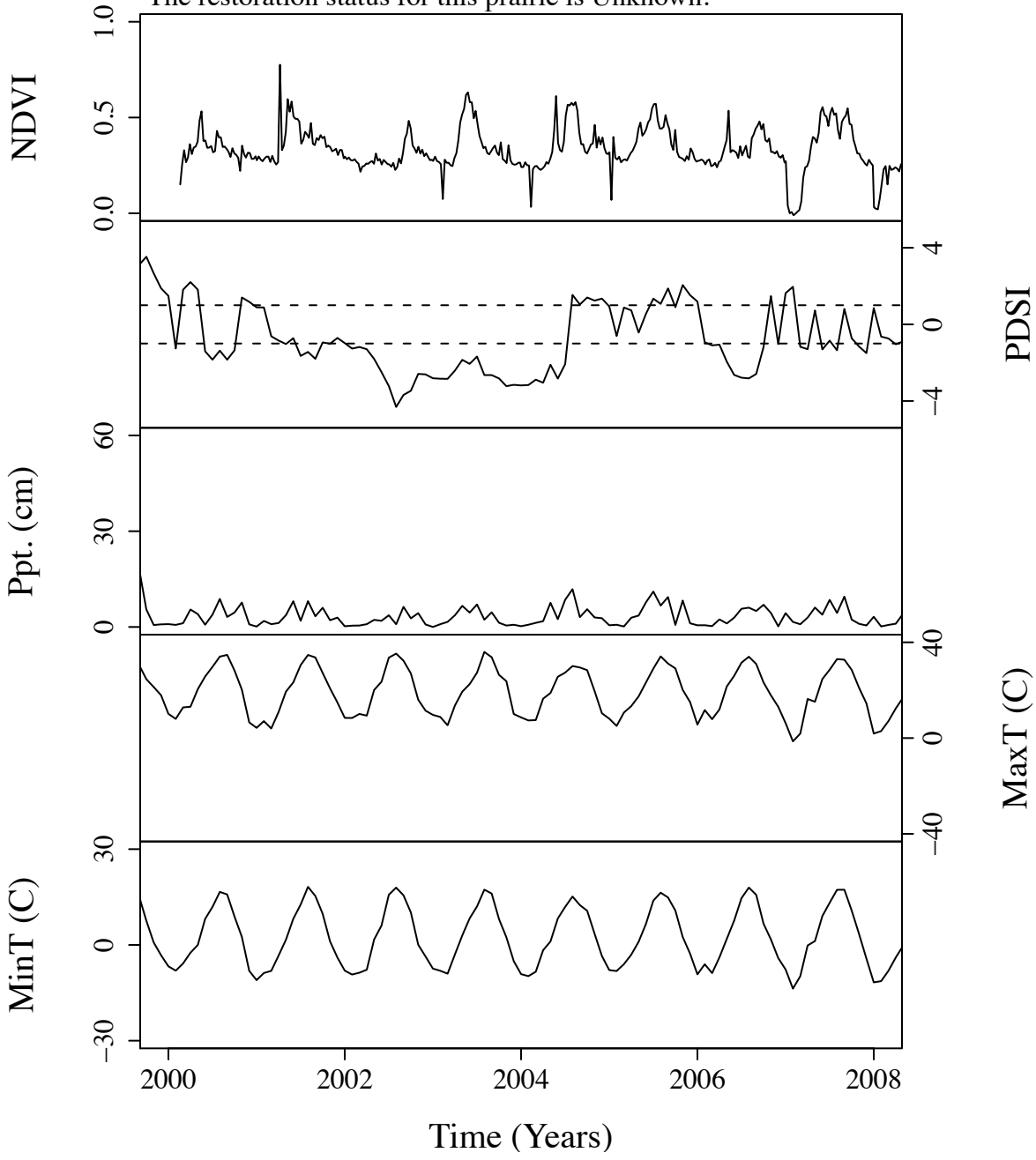

Figure B.107. Time series curves for nlo838.
The community type for this prairie is Mixed.
The dominant photosynthetic pathway for this prairie is C4.
The restoration status for this prairie is Unknown.

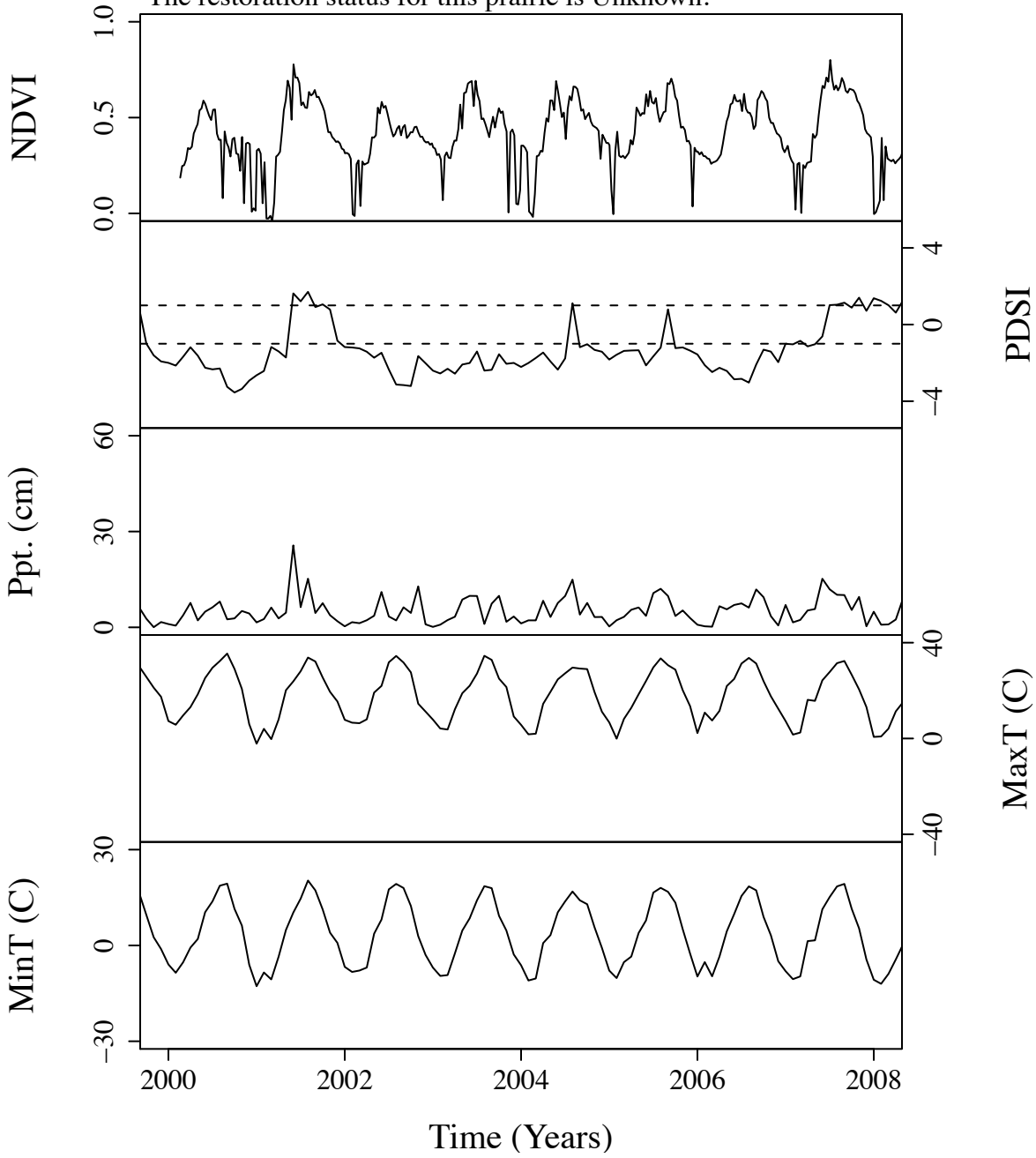

Figure B.108. Time series curves for nlo852.
The community type for this prairie is Mixed.
The dominant photosynthetic pathway for this prairie is C4.
The restoration status for this prairie is Unknown.

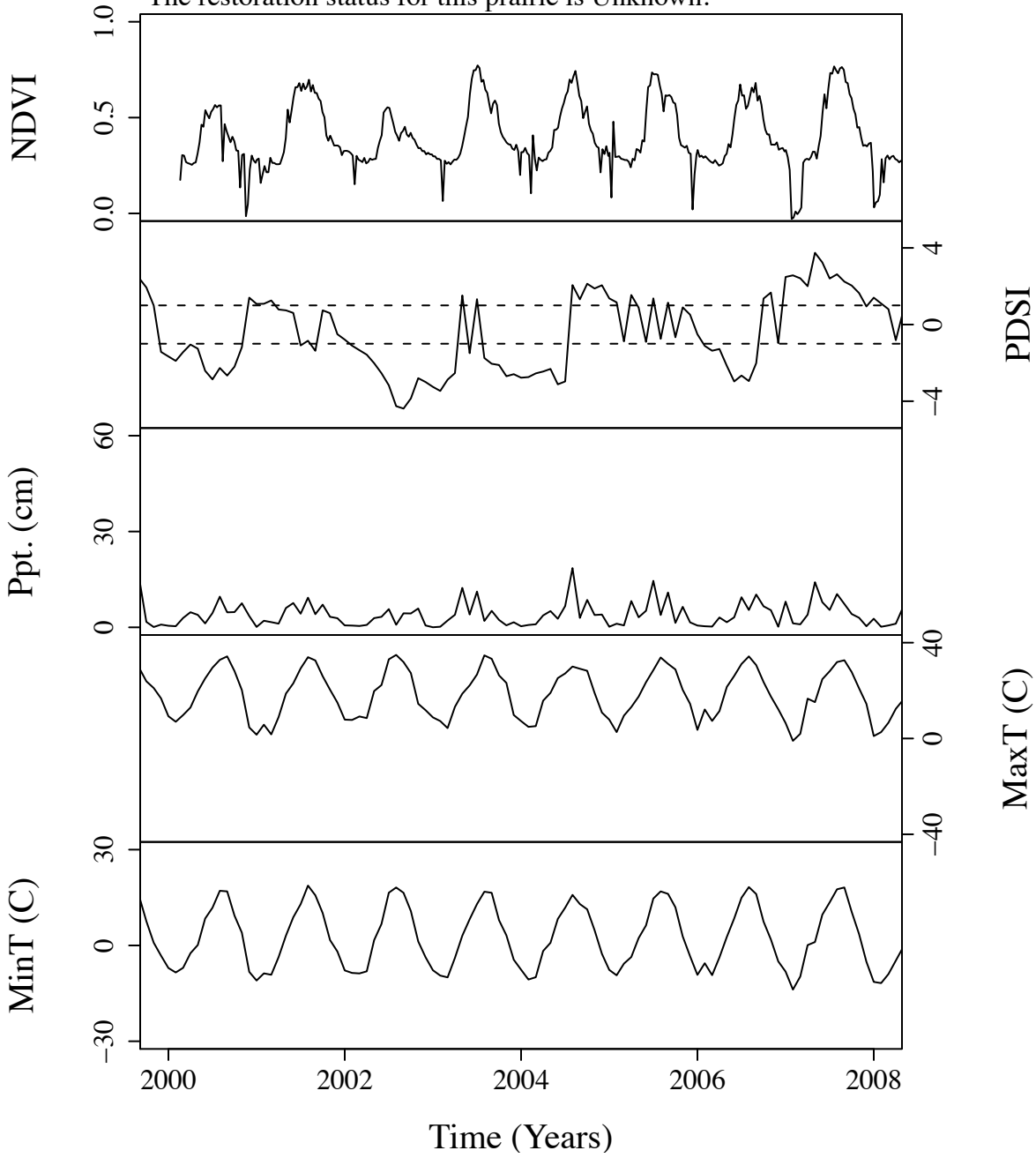

Figure B.109. Time series curves for nno1003.
The community type for this prairie is Mixed.
The dominant photosynthetic pathway for this prairie is C4.
The restoration status for this prairie is Unknown.

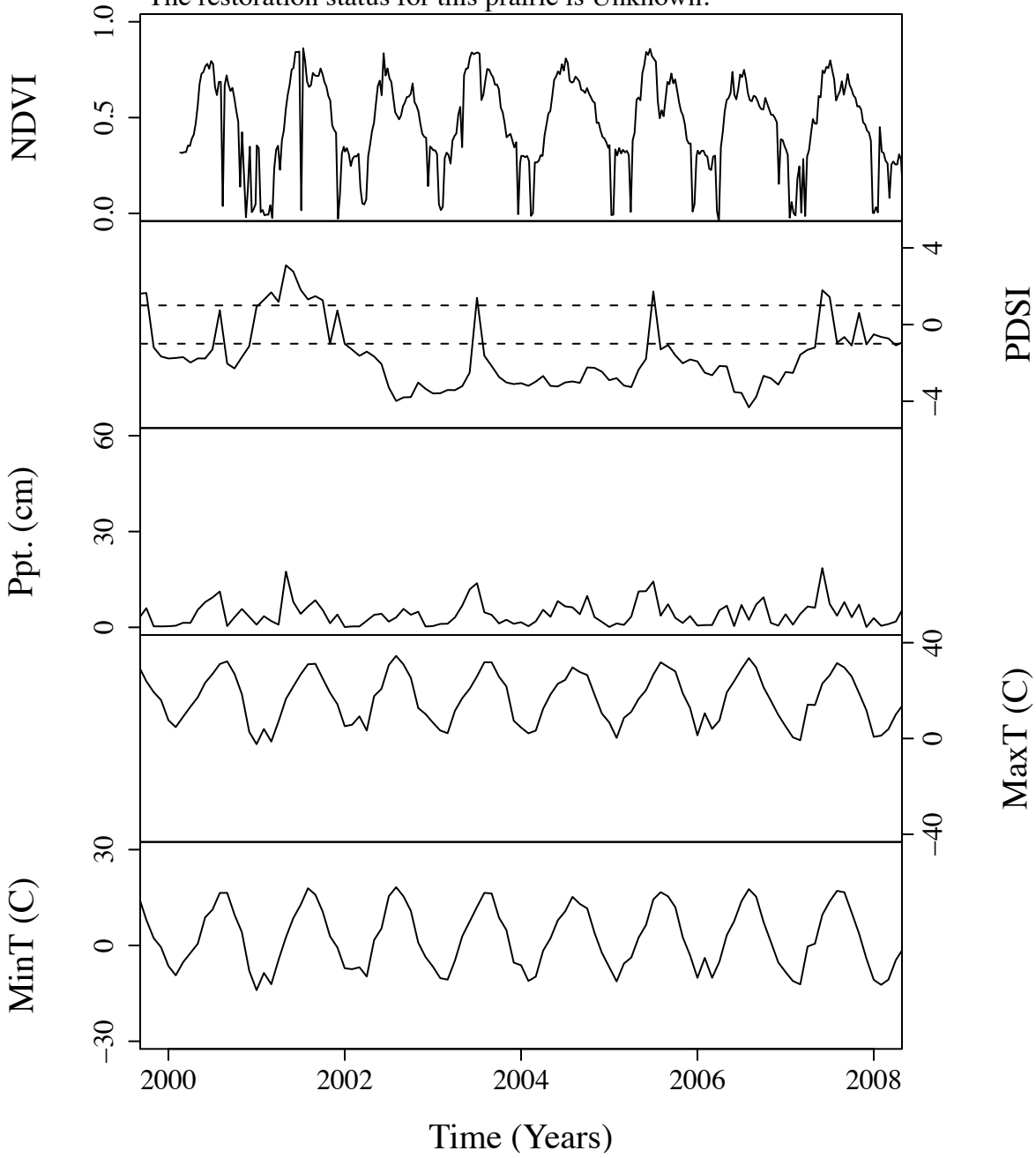

Figure B.110. Time series curves for nno143.
The community type for this prairie is Mixed.
The dominant photosynthetic pathway for this prairie is C4.
The restoration status for this prairie is Unknown.

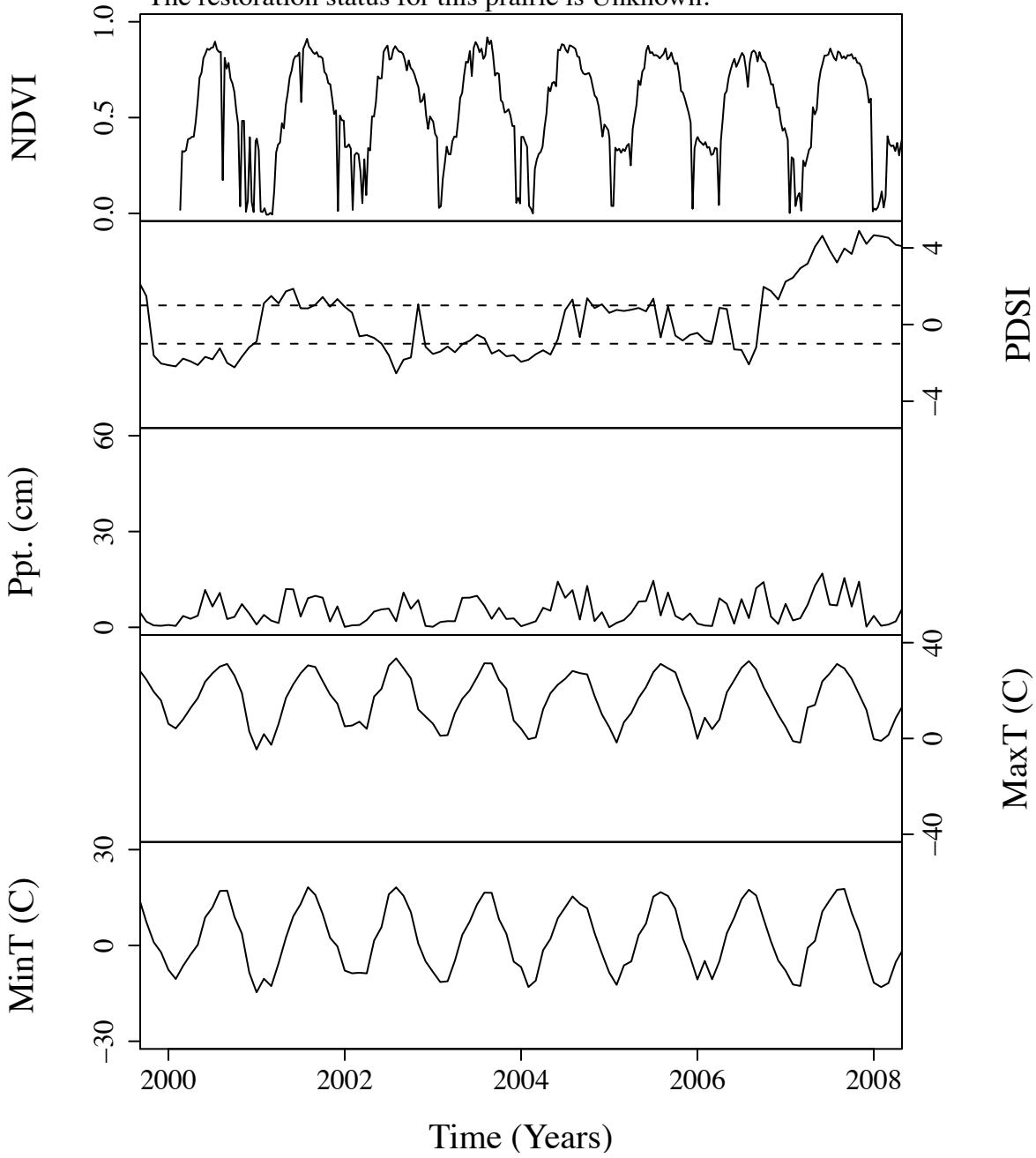

Figure B.111. Time series curves for nno3.
The community type for this prairie is Mixed.
The dominant photosynthetic pathway for this prairie is C4.
The restoration status for this prairie is Unknown.

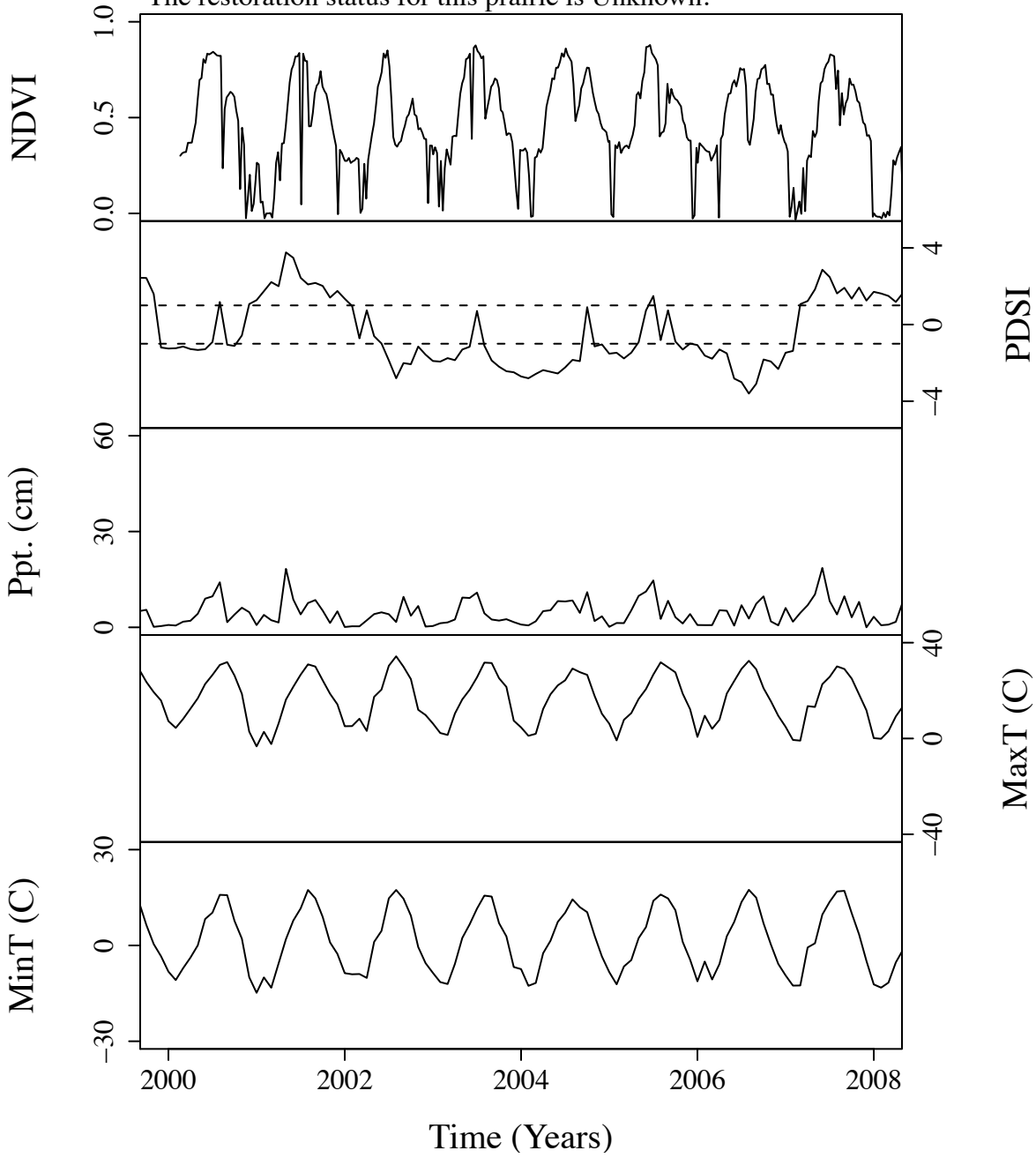

Figure B.112. Time series curves for nno311.
The community type for this prairie is Mixed.
The dominant photosynthetic pathway for this prairie is C4.
The restoration status for this prairie is Unknown.

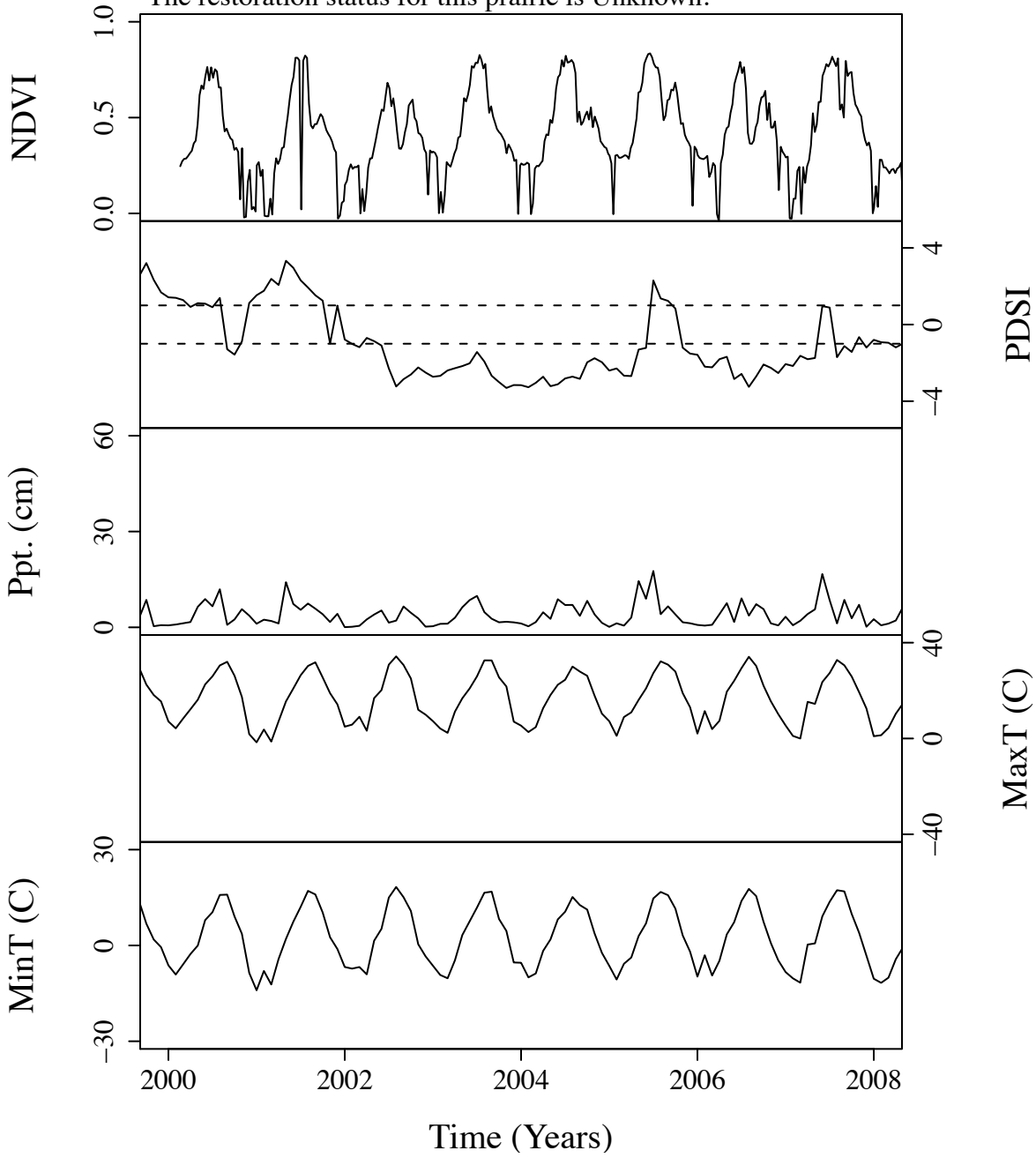

Figure B.113. Time series curves for nno596.
The community type for this prairie is Tall.
The dominant photosynthetic pathway for this prairie is C4.
The restoration status for this prairie is Unknown.

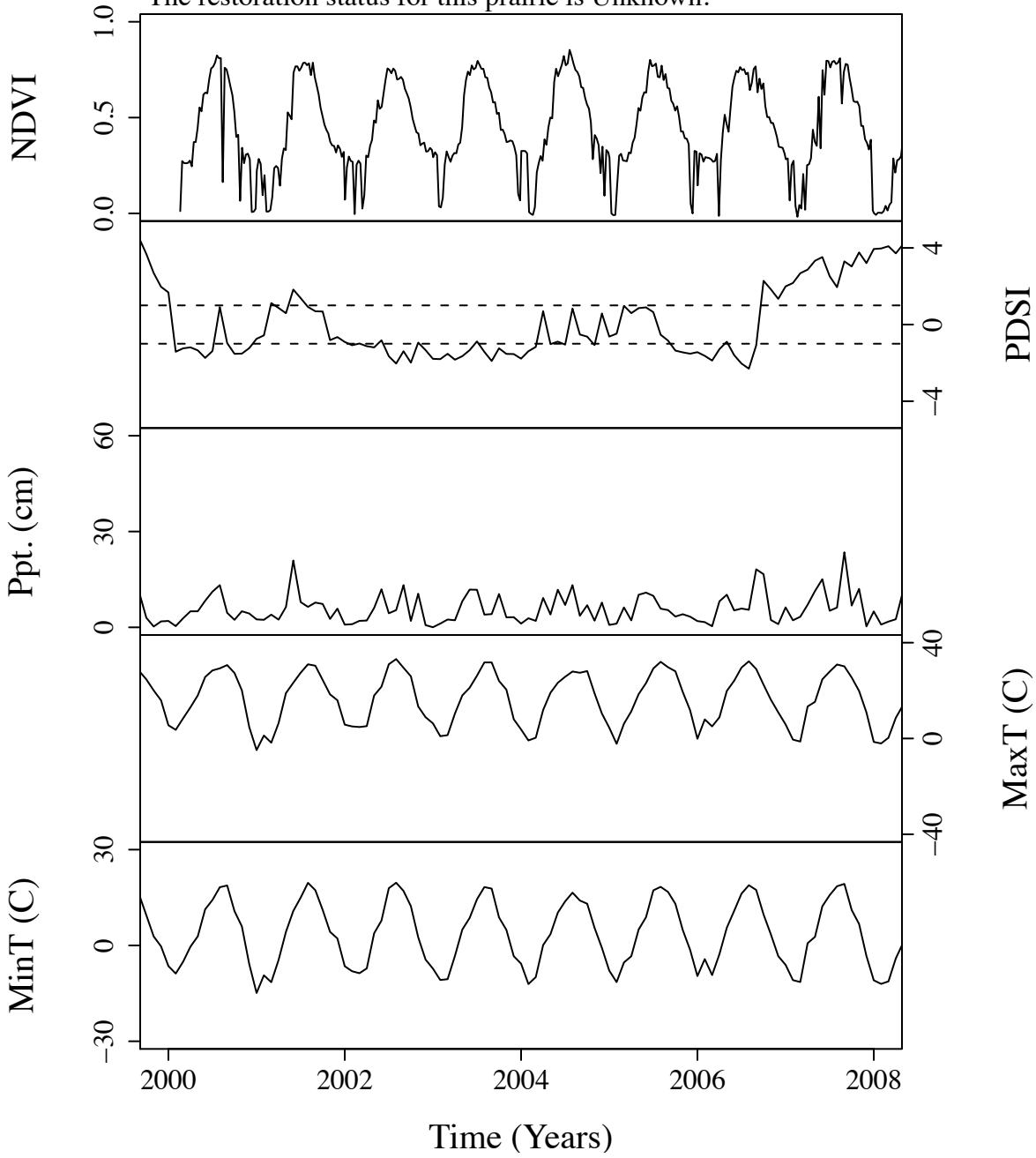

Figure B.114. Time series curves for nno64.
The community type for this prairie is Mixed.
The dominant photosynthetic pathway for this prairie is C4.
The restoration status for this prairie is Unknown.

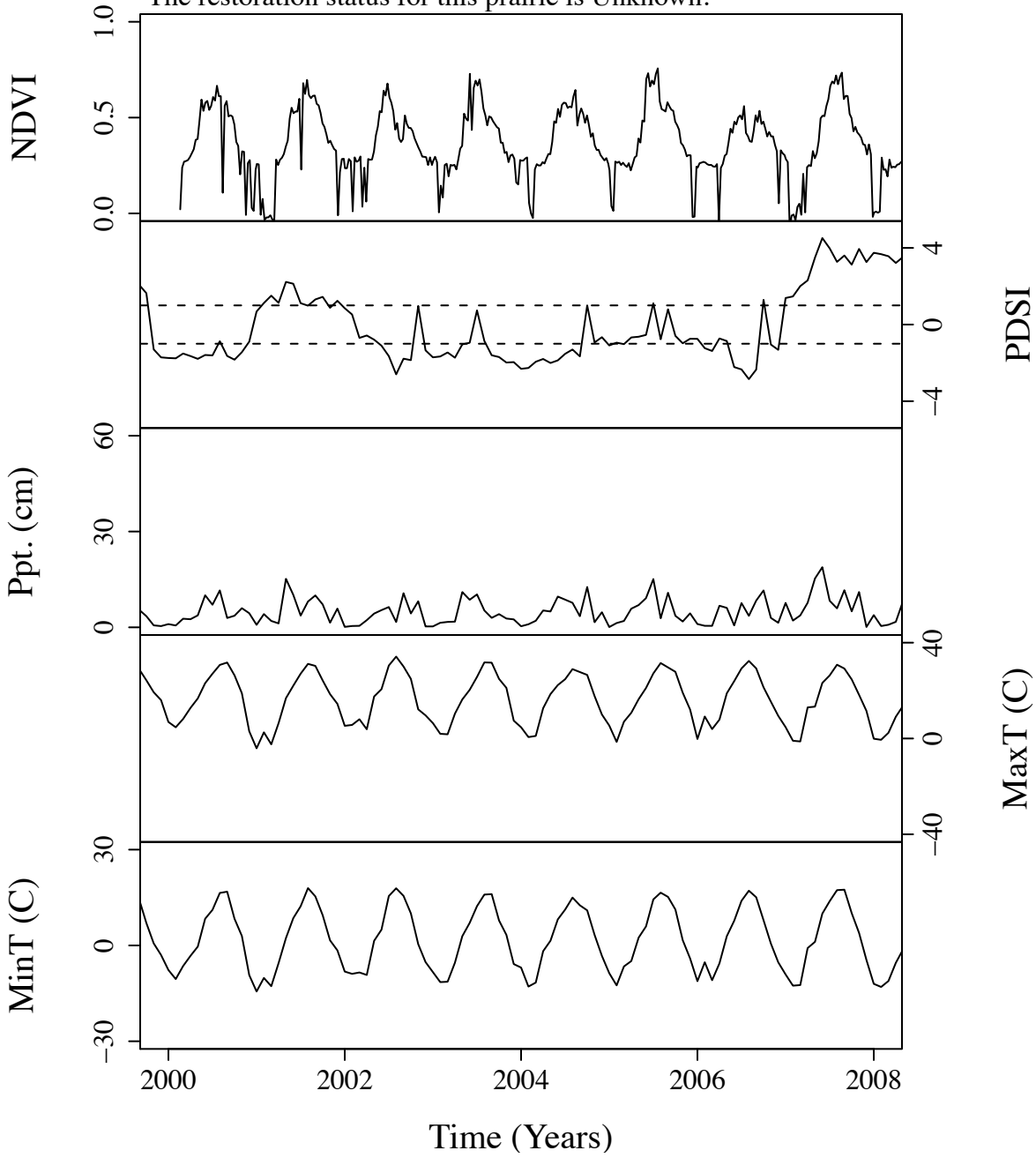

Figure B.115. Time series curves for nno732.
The community type for this prairie is Short.
The dominant photosynthetic pathway for this prairie is C4.
The restoration status for this prairie is Unknown.

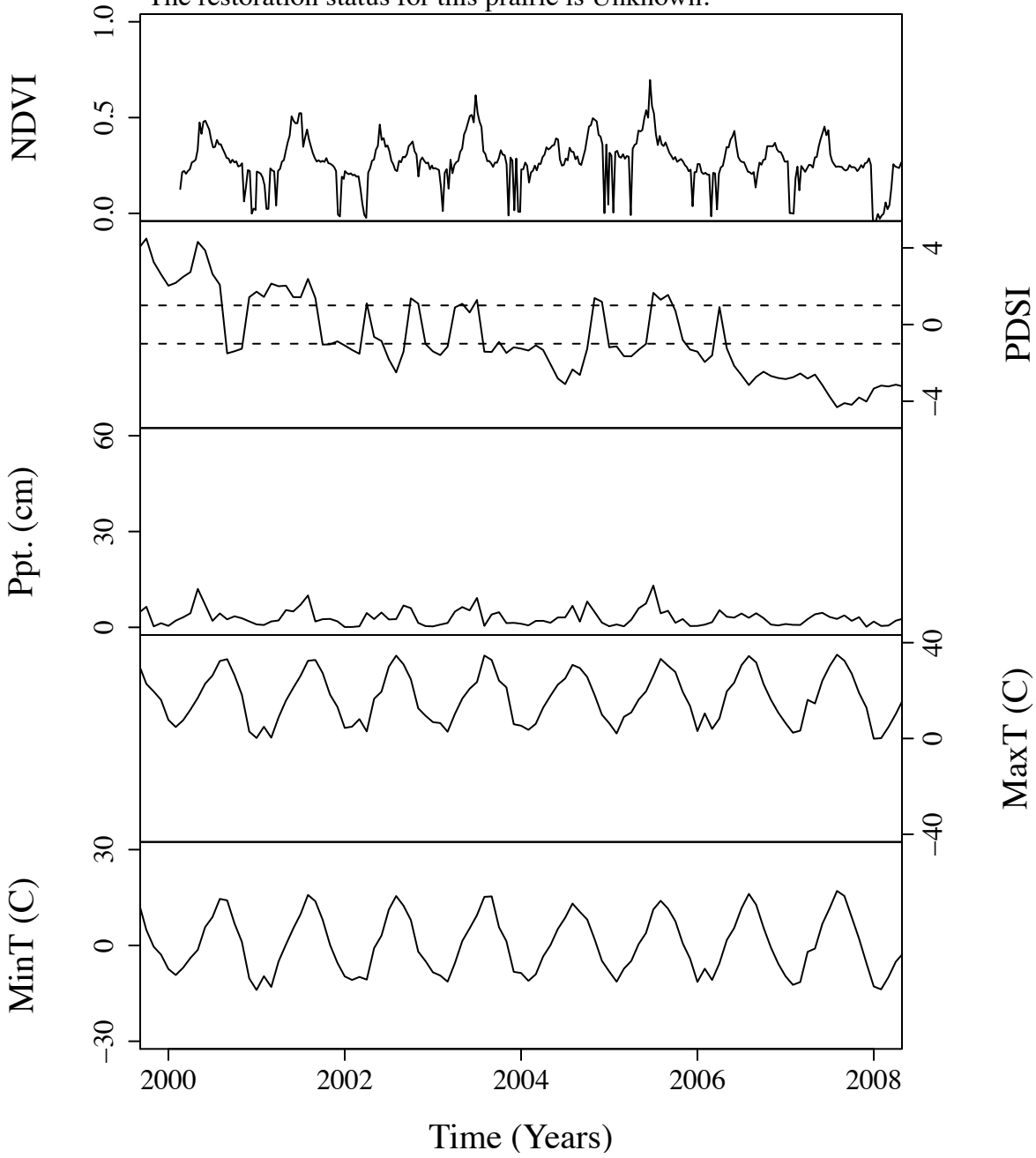

Figure B.116. Time series curves for nno740.
The community type for this prairie is Short.
The dominant photosynthetic pathway for this prairie is C4.
The restoration status for this prairie is Unknown.

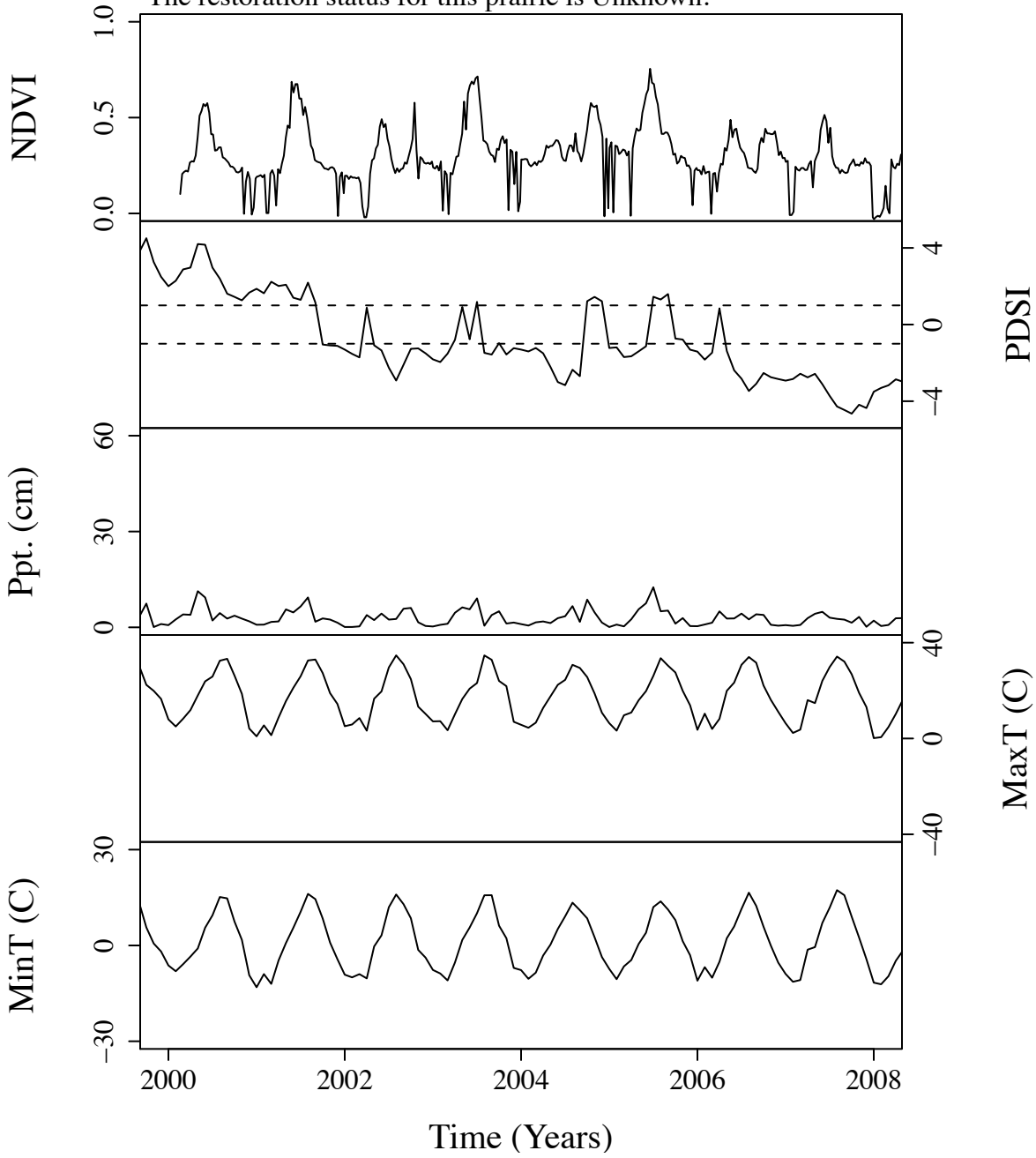

Figure B.117. Time series curves for nno741.
The community type for this prairie is Short.
The dominant photosynthetic pathway for this prairie is C4.
The restoration status for this prairie is Unknown.

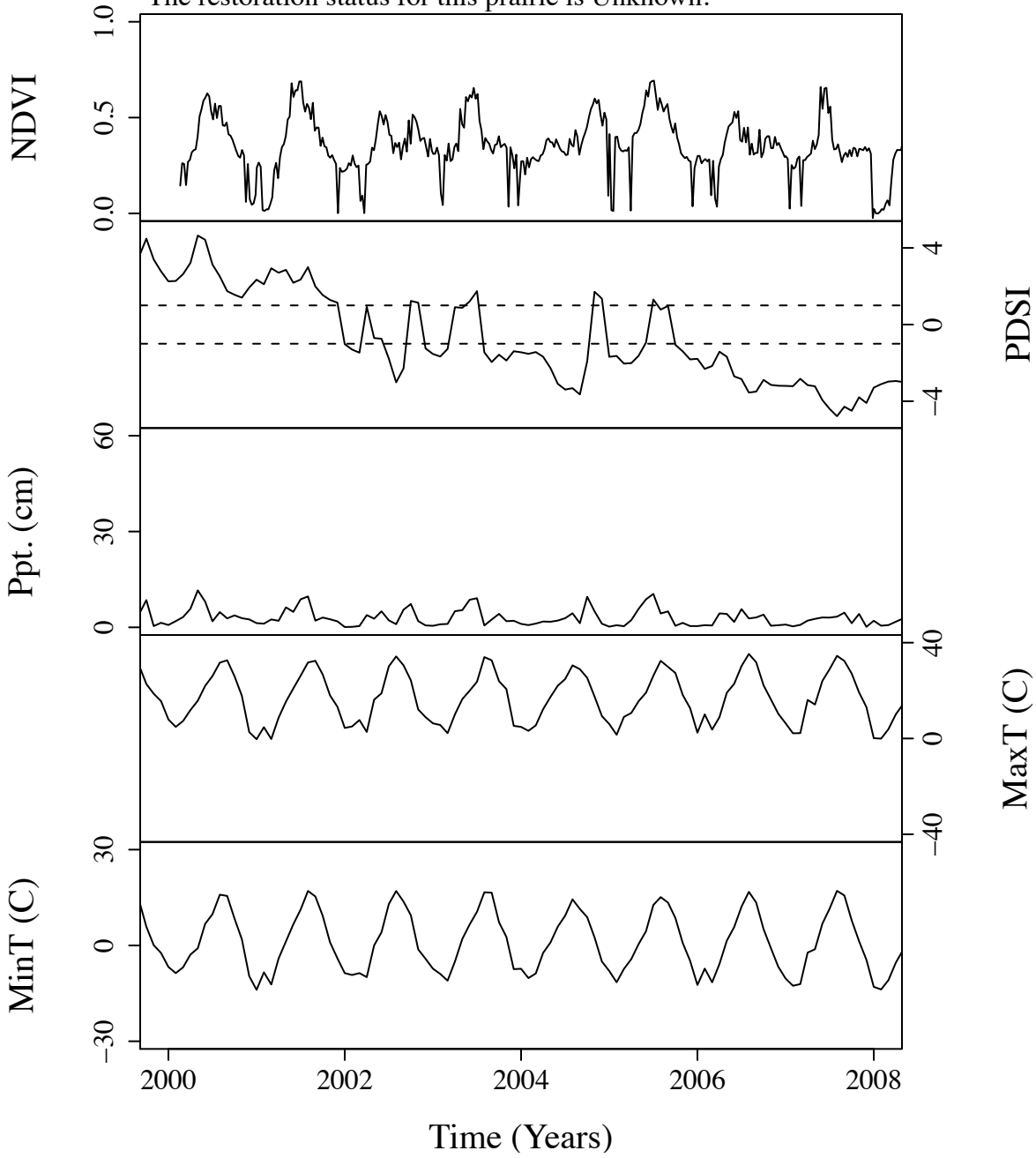

Figure B.118. Time series curves for nno83.
The community type for this prairie is Mixed.
The dominant photosynthetic pathway for this prairie is C4.
The restoration status for this prairie is Unknown.

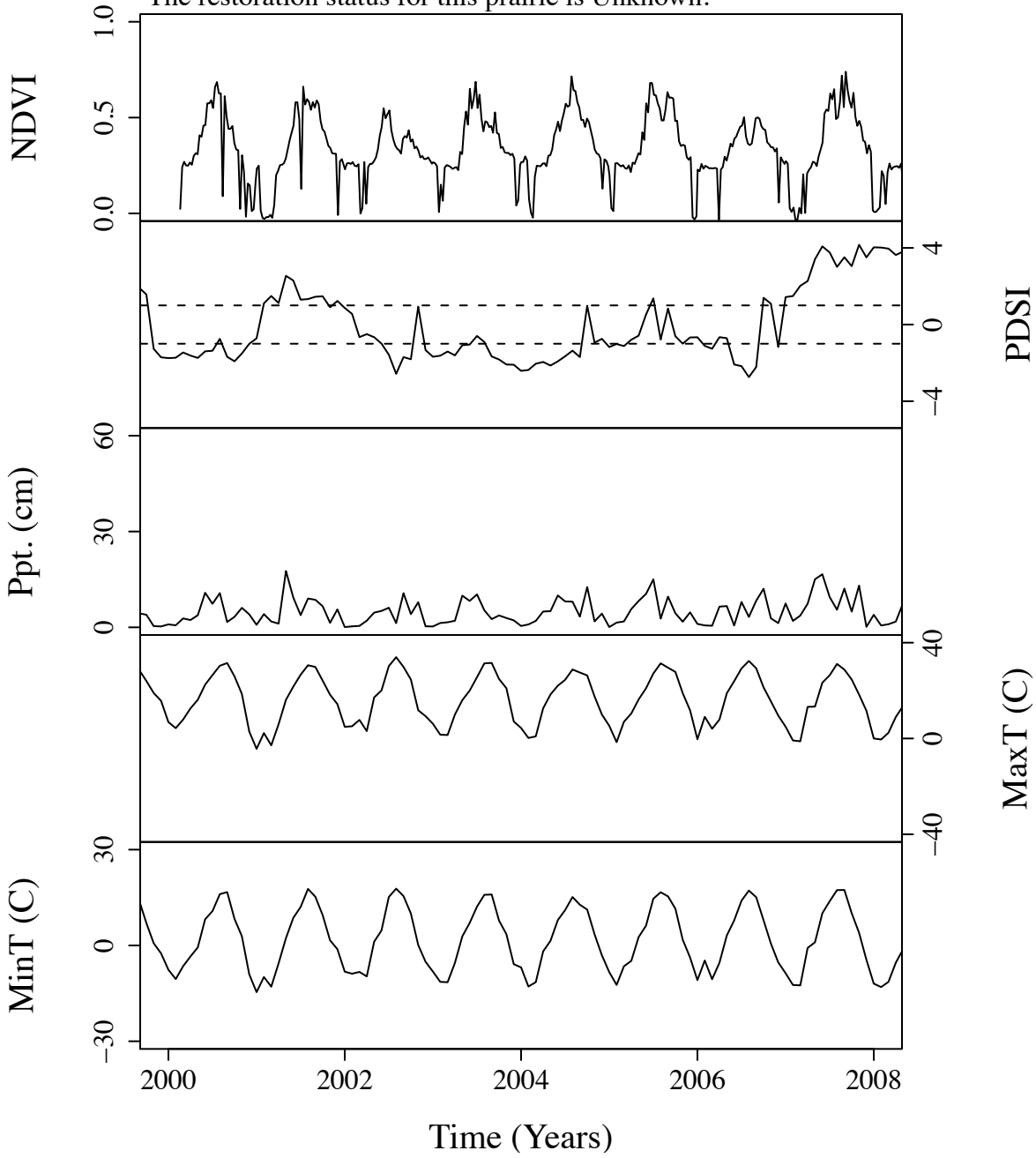

Figure B.119. Time series curves for nno846.
The community type for this prairie is Mixed.
The dominant photosynthetic pathway for this prairie is C4.
The restoration status for this prairie is Unknown.

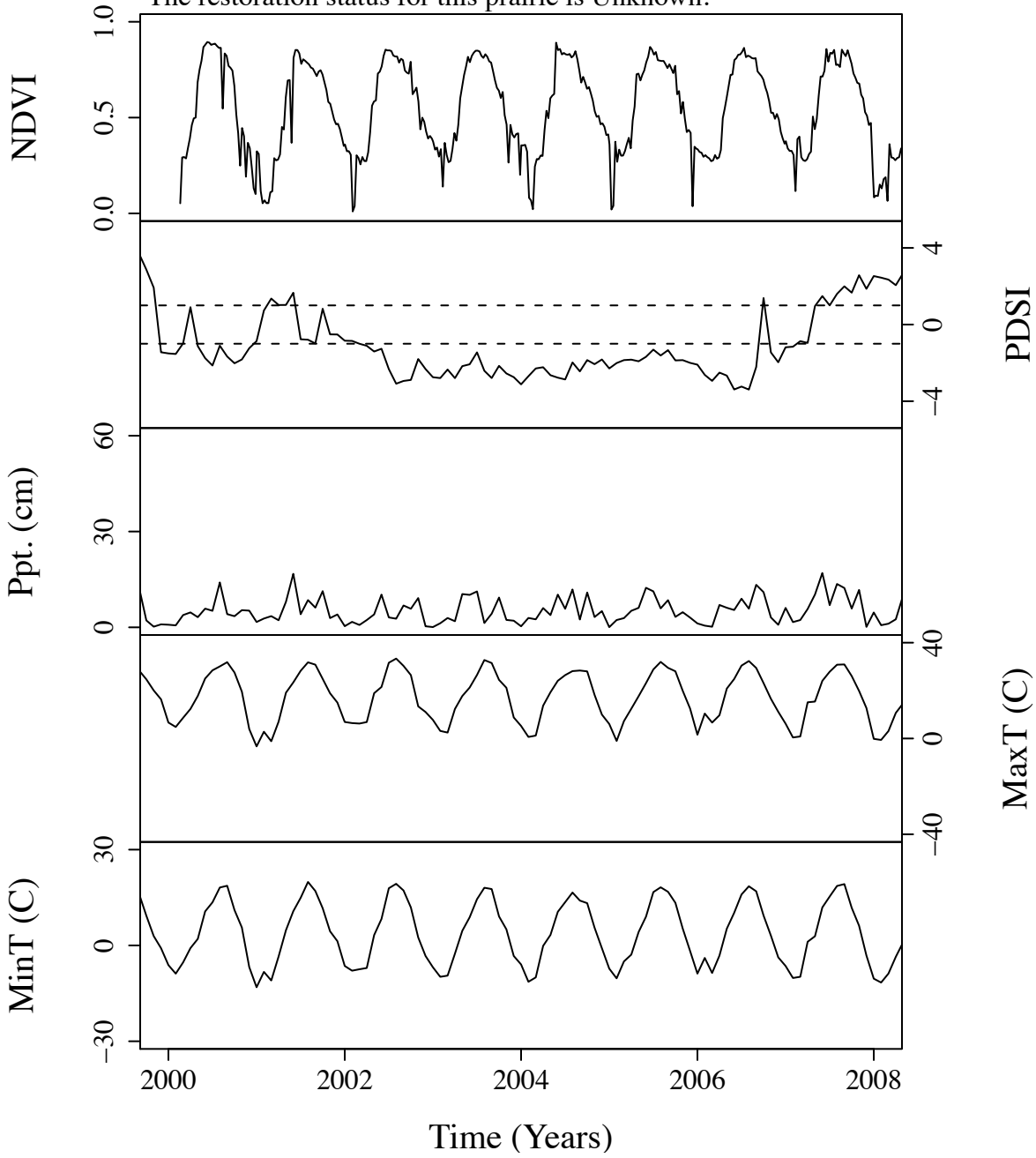

Figure B.120. Time series curves for nno866.
The community type for this prairie is Short.
The dominant photosynthetic pathway for this prairie is C4.
The restoration status for this prairie is Unknown.

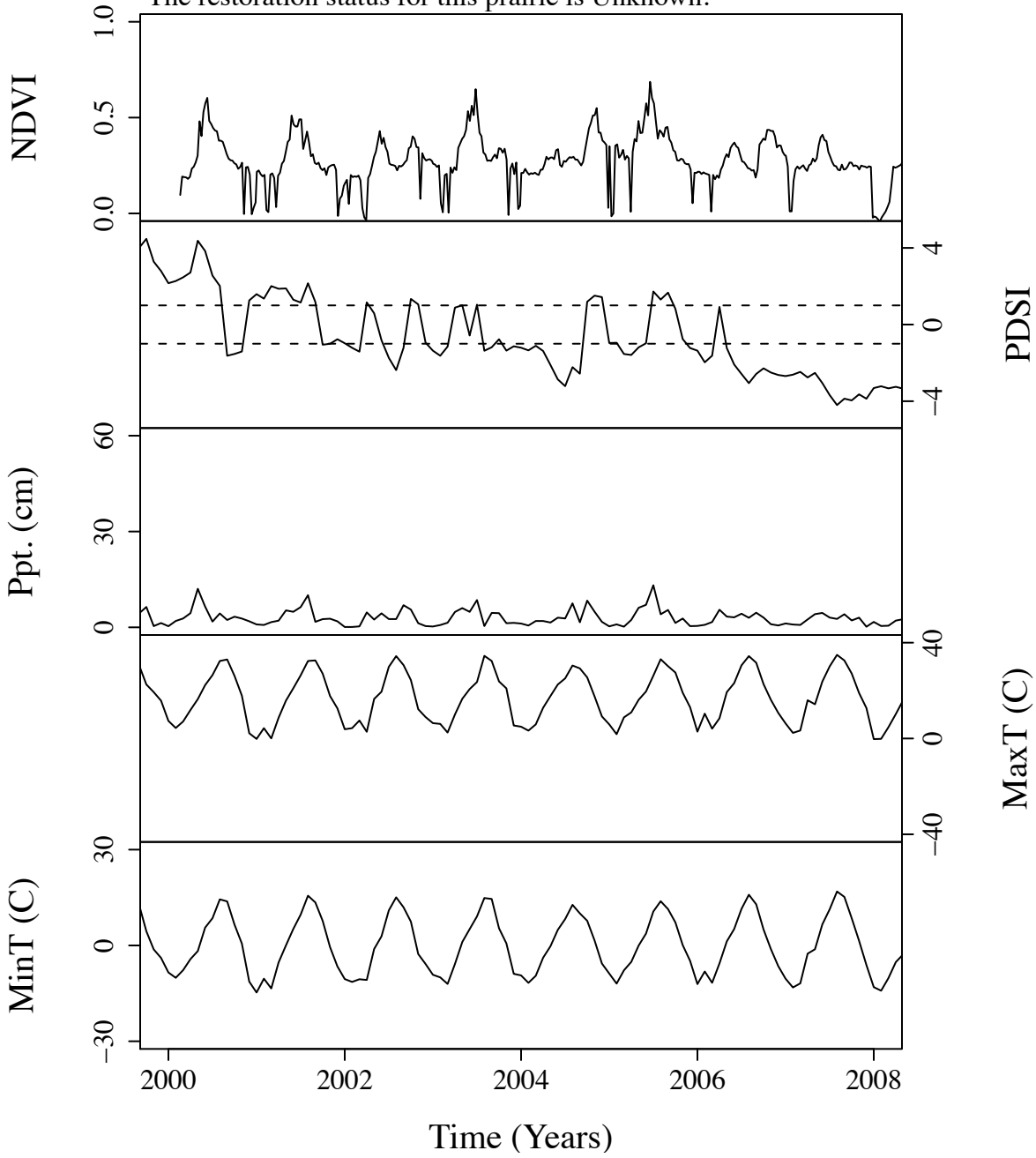

Figure B.121. Time series curves for nnor97.
The community type for this prairie is Short.
The dominant photosynthetic pathway for this prairie is C4.
The restoration status for this prairie is Unknown.

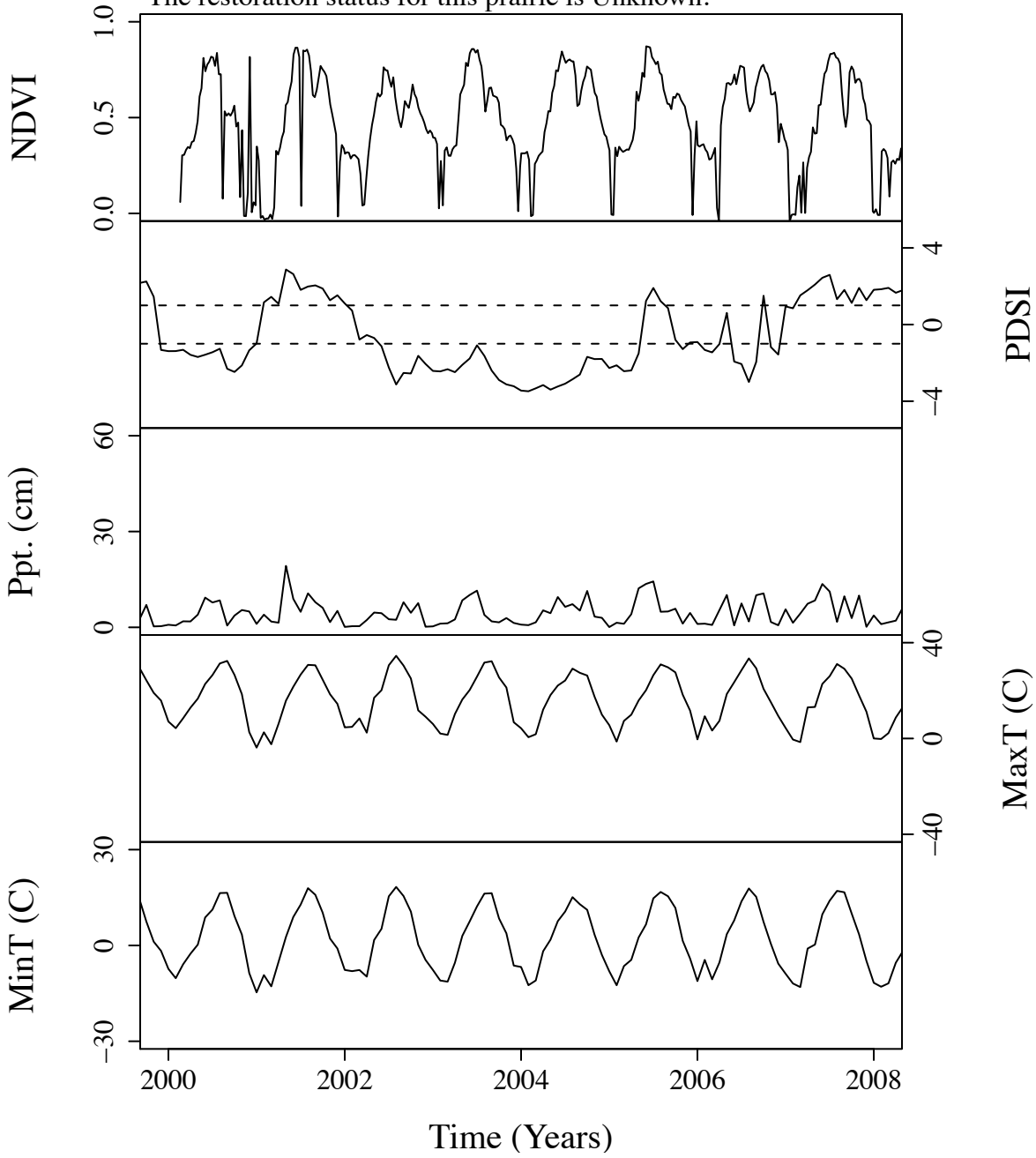

Figure B.122. Time series curves for nsa1007.
The community type for this prairie is Mixed.
The dominant photosynthetic pathway for this prairie is C4.
The restoration status for this prairie is Unknown.

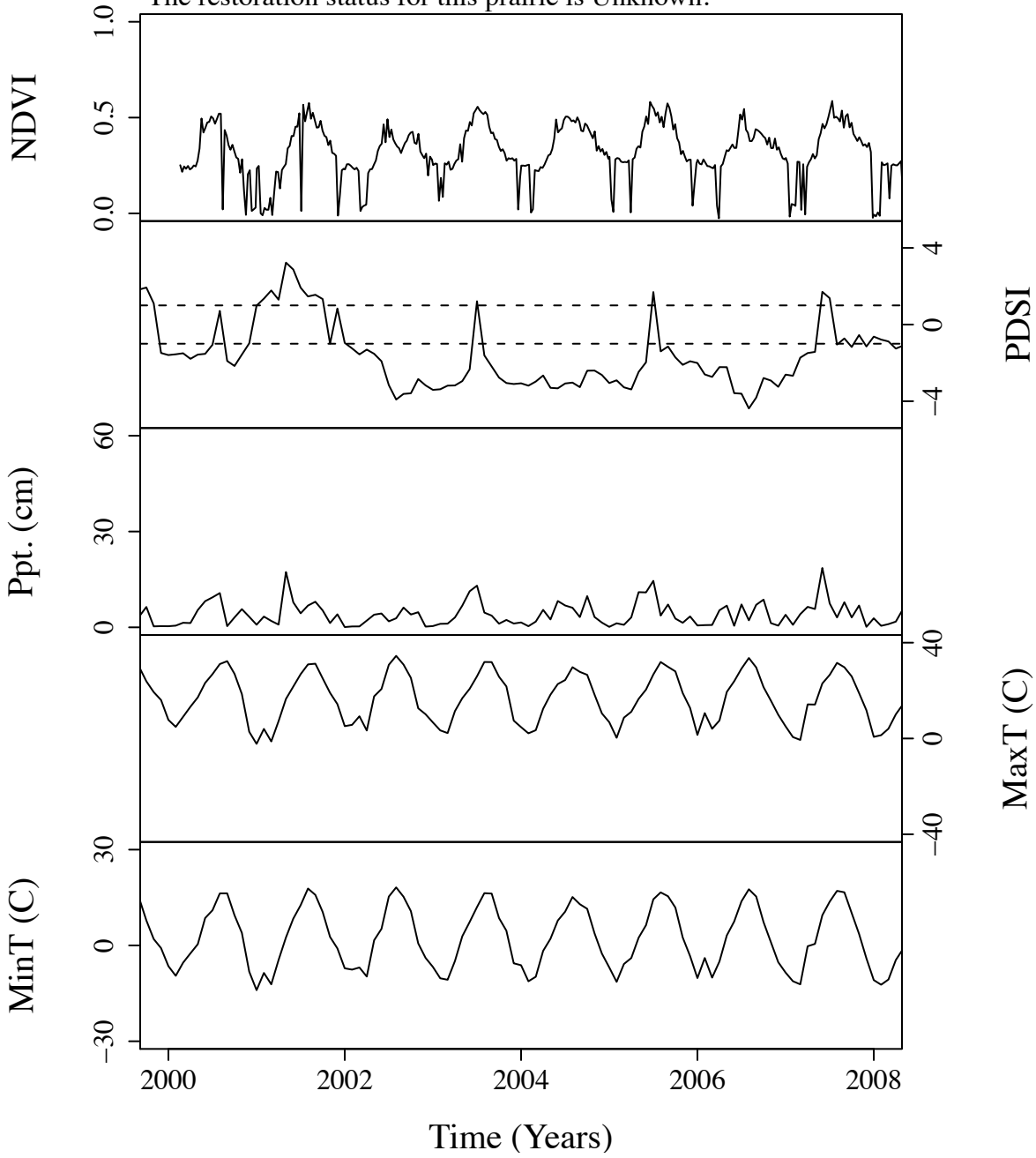

Figure B.123. Time series curves for nsa151.
The community type for this prairie is Mixed.
The dominant photosynthetic pathway for this prairie is C4.
The restoration status for this prairie is Unknown.

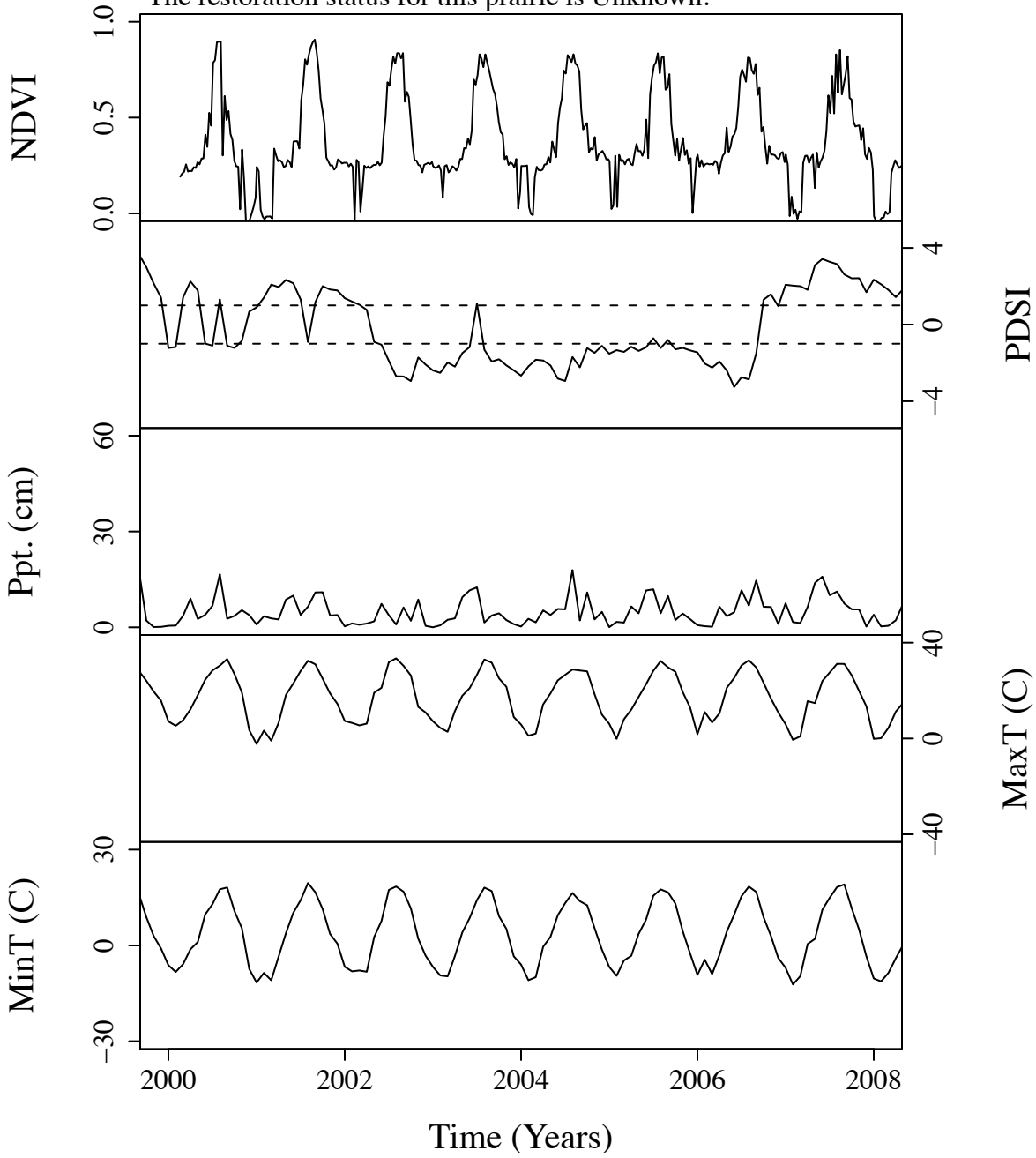

Figure B.124. Time series curves for nsa166.
The community type for this prairie is Short.
The dominant photosynthetic pathway for this prairie is C4.
The restoration status for this prairie is Unknown.

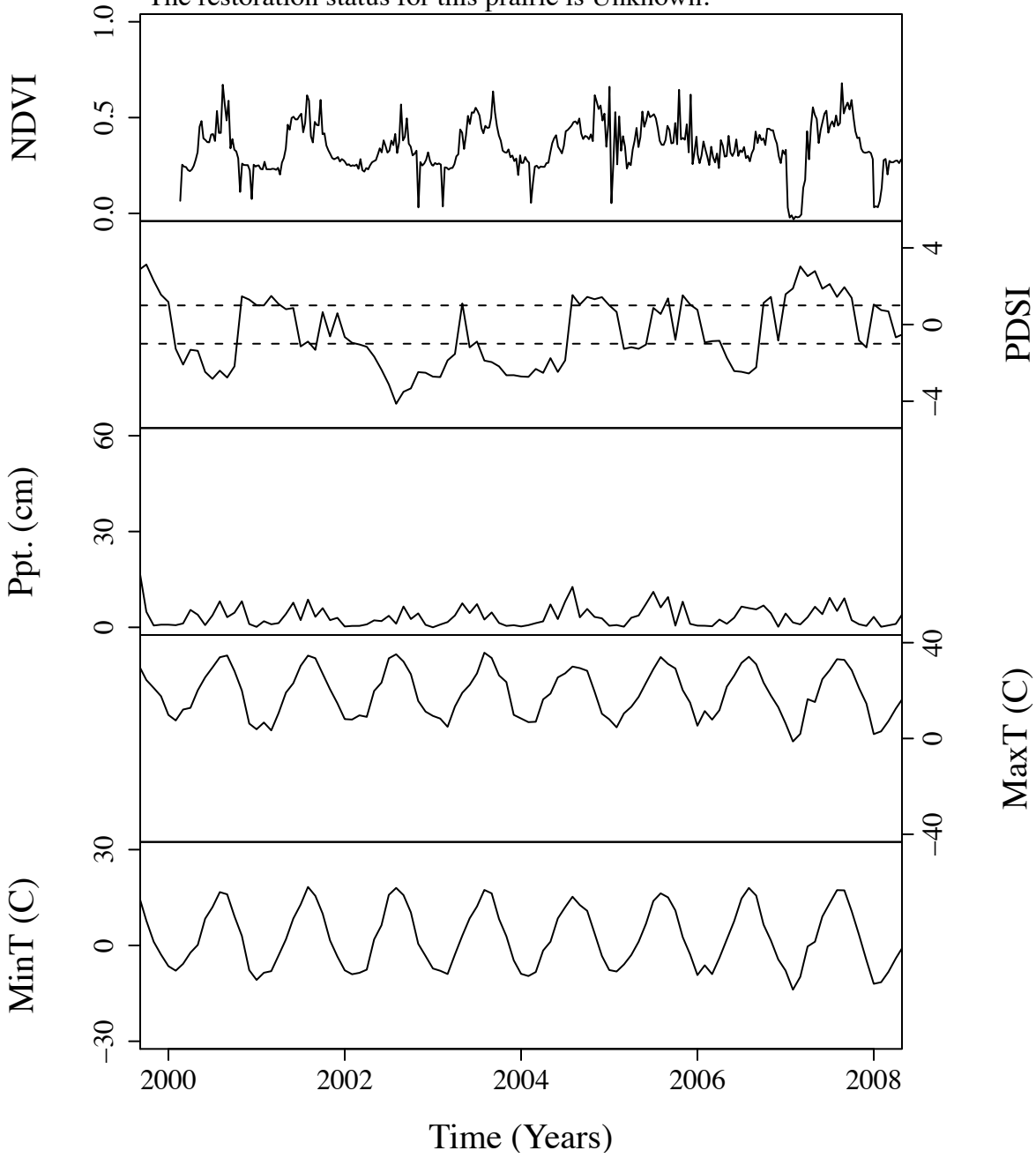

Figure B.125. Time series curves for nsa173.
The community type for this prairie is Short.
The dominant photosynthetic pathway for this prairie is C4.
The restoration status for this prairie is Unknown.

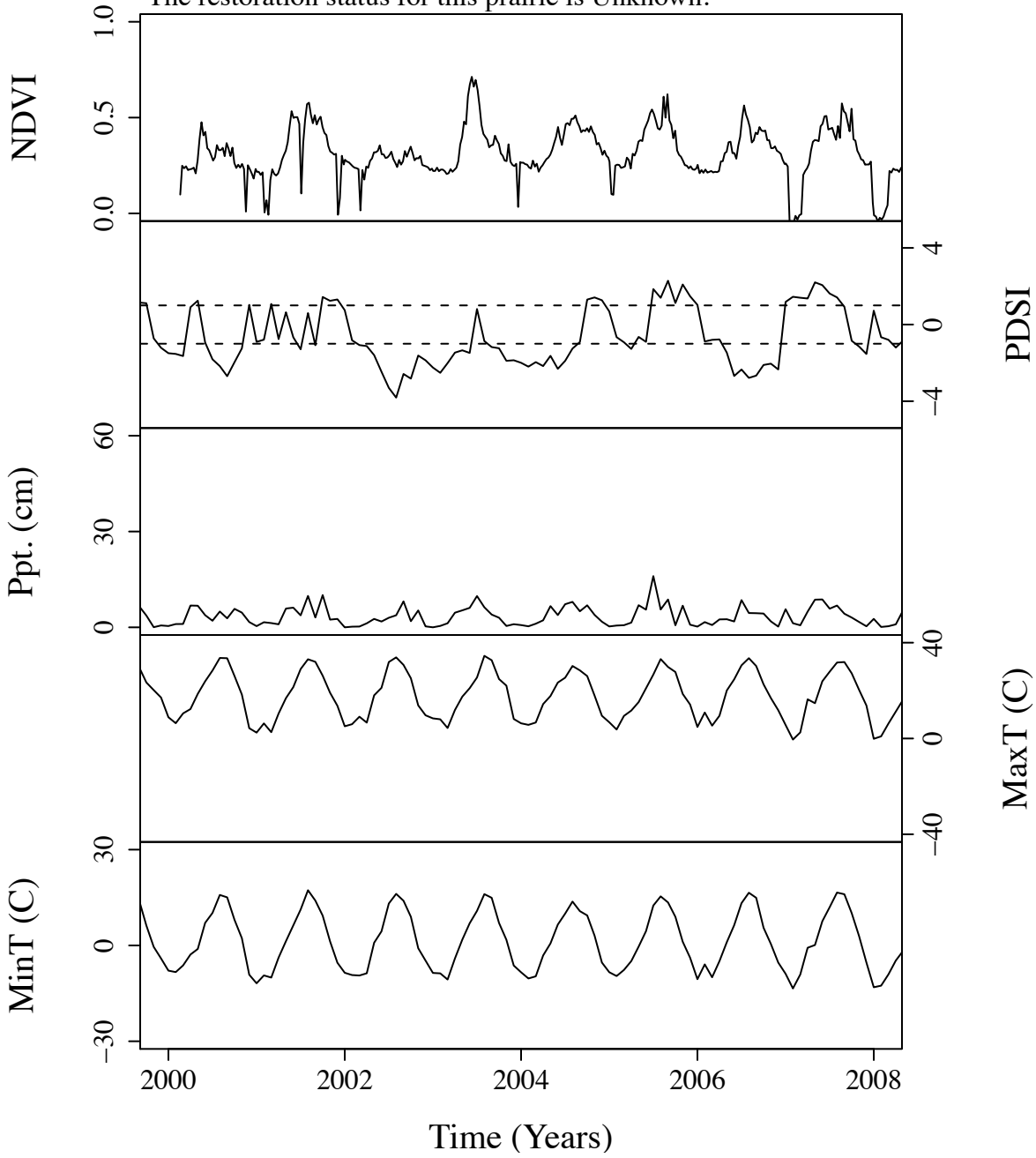

Figure B.126. Time series curves for nsa210.
The community type for this prairie is Mixed.
The dominant photosynthetic pathway for this prairie is C4.
The restoration status for this prairie is Unknown.

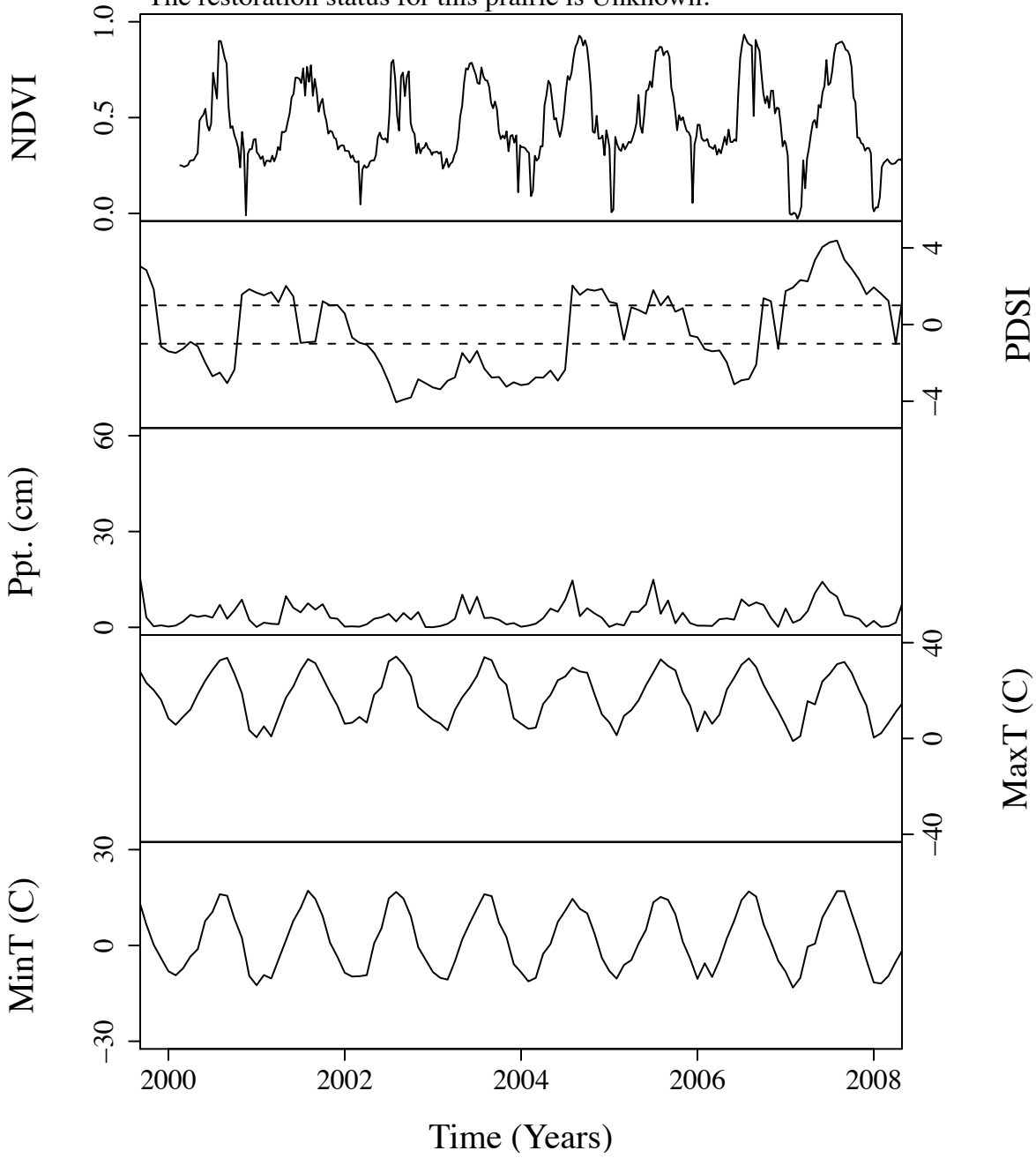

Figure B.127. Time series curves for nsa267.
The community type for this prairie is Short.
The dominant photosynthetic pathway for this prairie is C4.
The restoration status for this prairie is Unknown.

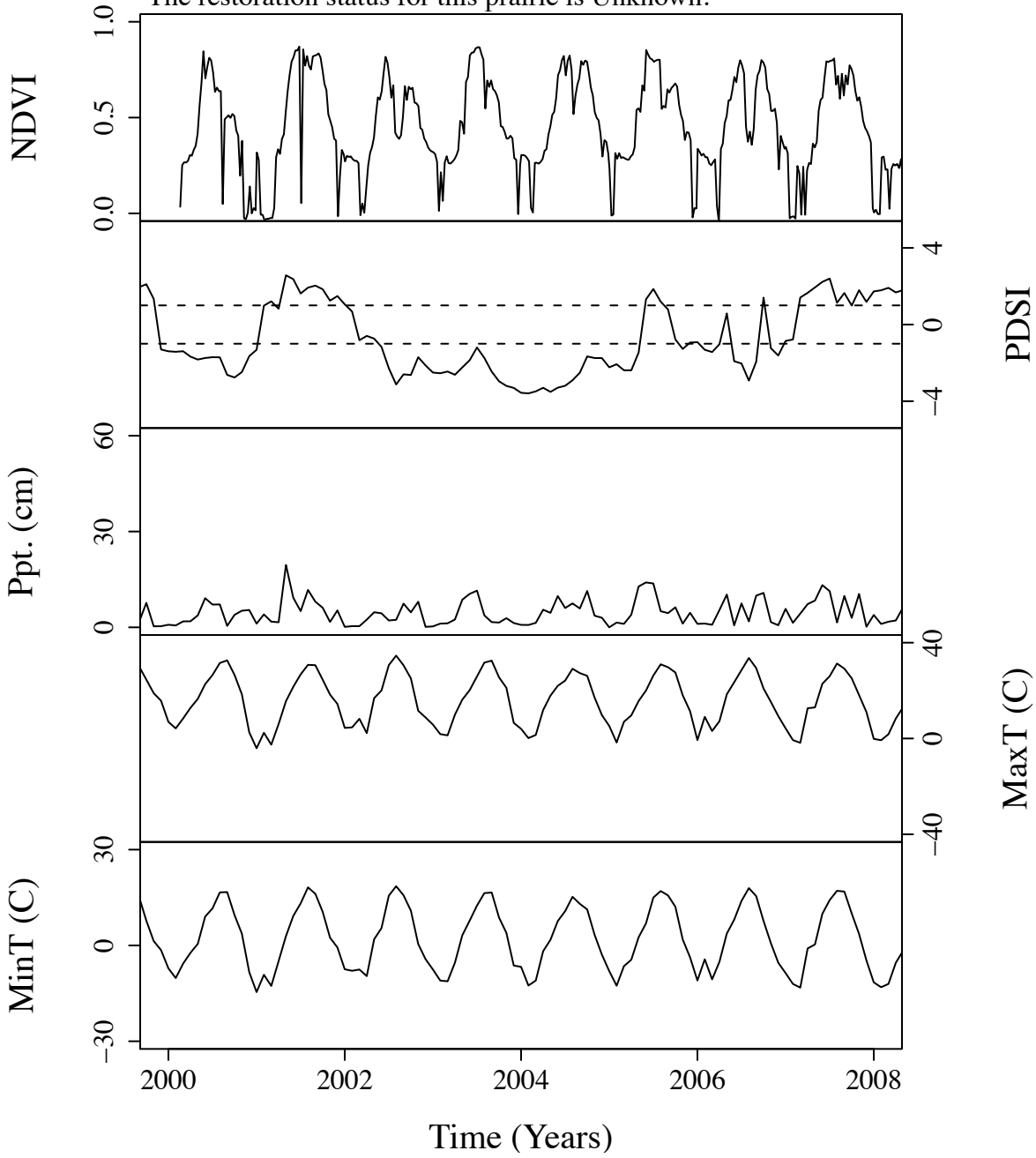

Figure B.128. Time series curves for nsa28.
The community type for this prairie is Short.
The dominant photosynthetic pathway for this prairie is C4.
The restoration status for this prairie is Unknown.

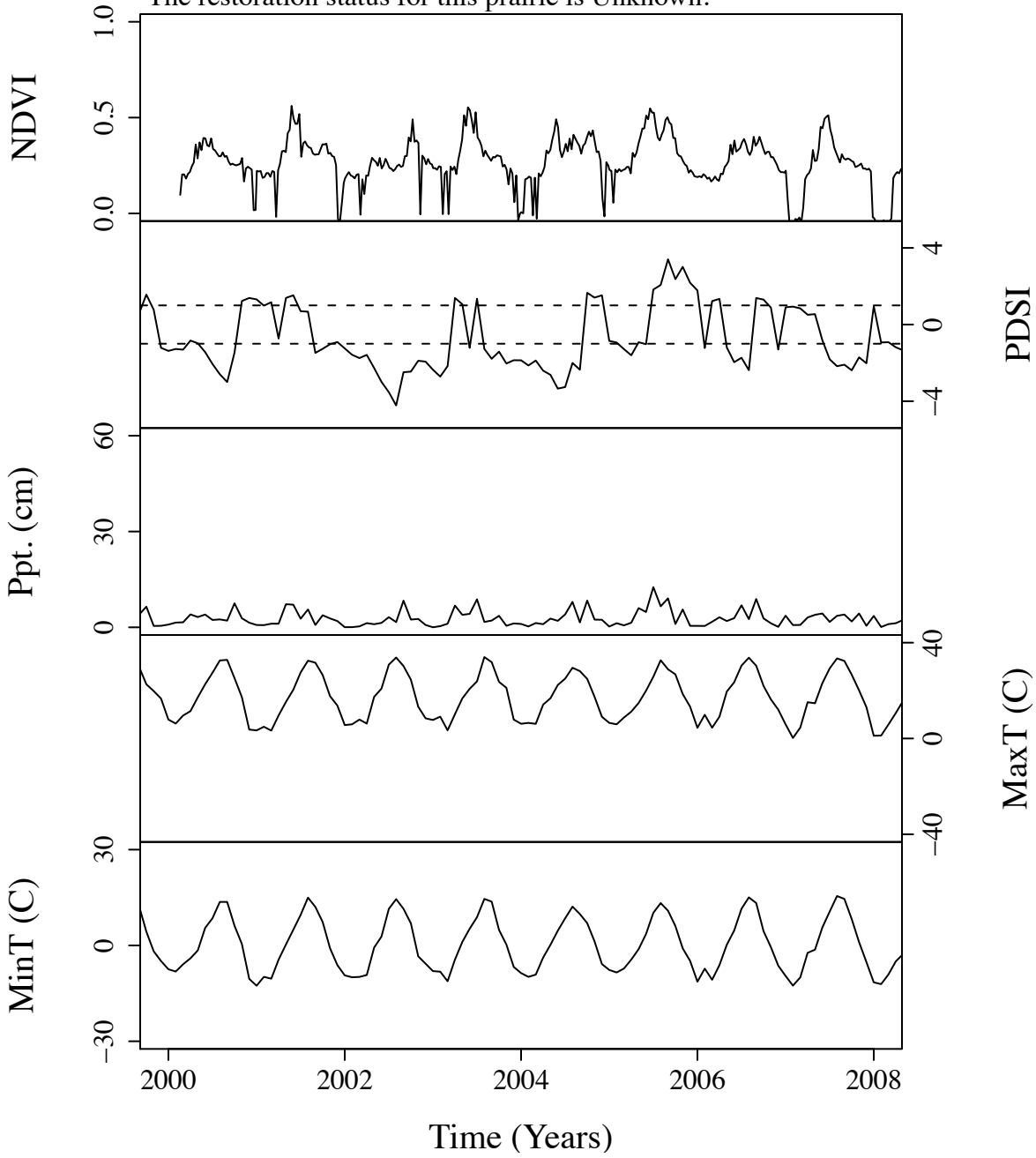

Figure B.129. Time series curves for nsa281.
The community type for this prairie is Short.
The dominant photosynthetic pathway for this prairie is C4.
The restoration status for this prairie is Unknown.

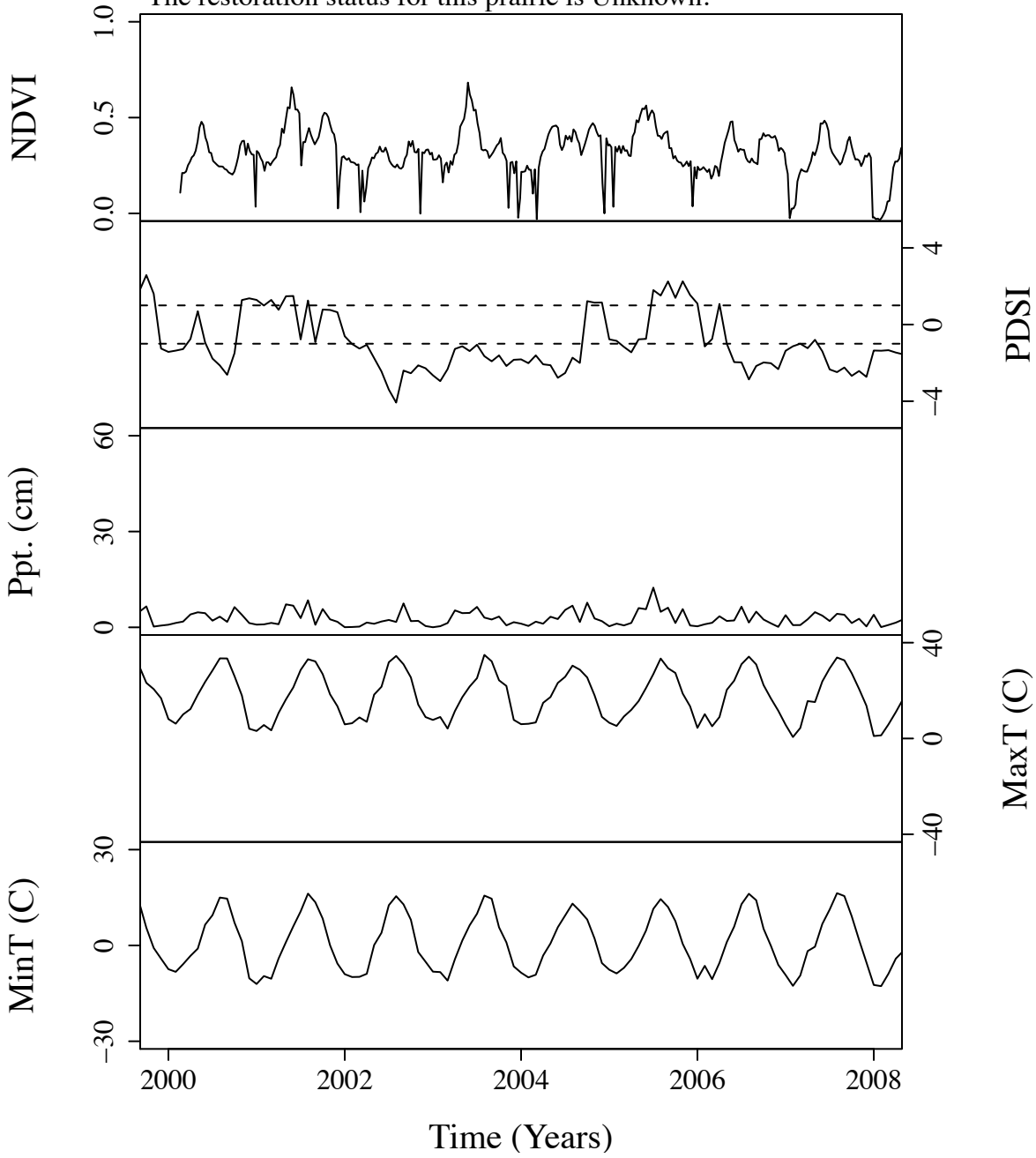

Figure B.130. Time series curves for nsa310.
The community type for this prairie is Mixed.
The dominant photosynthetic pathway for this prairie is C4.
The restoration status for this prairie is Unknown.

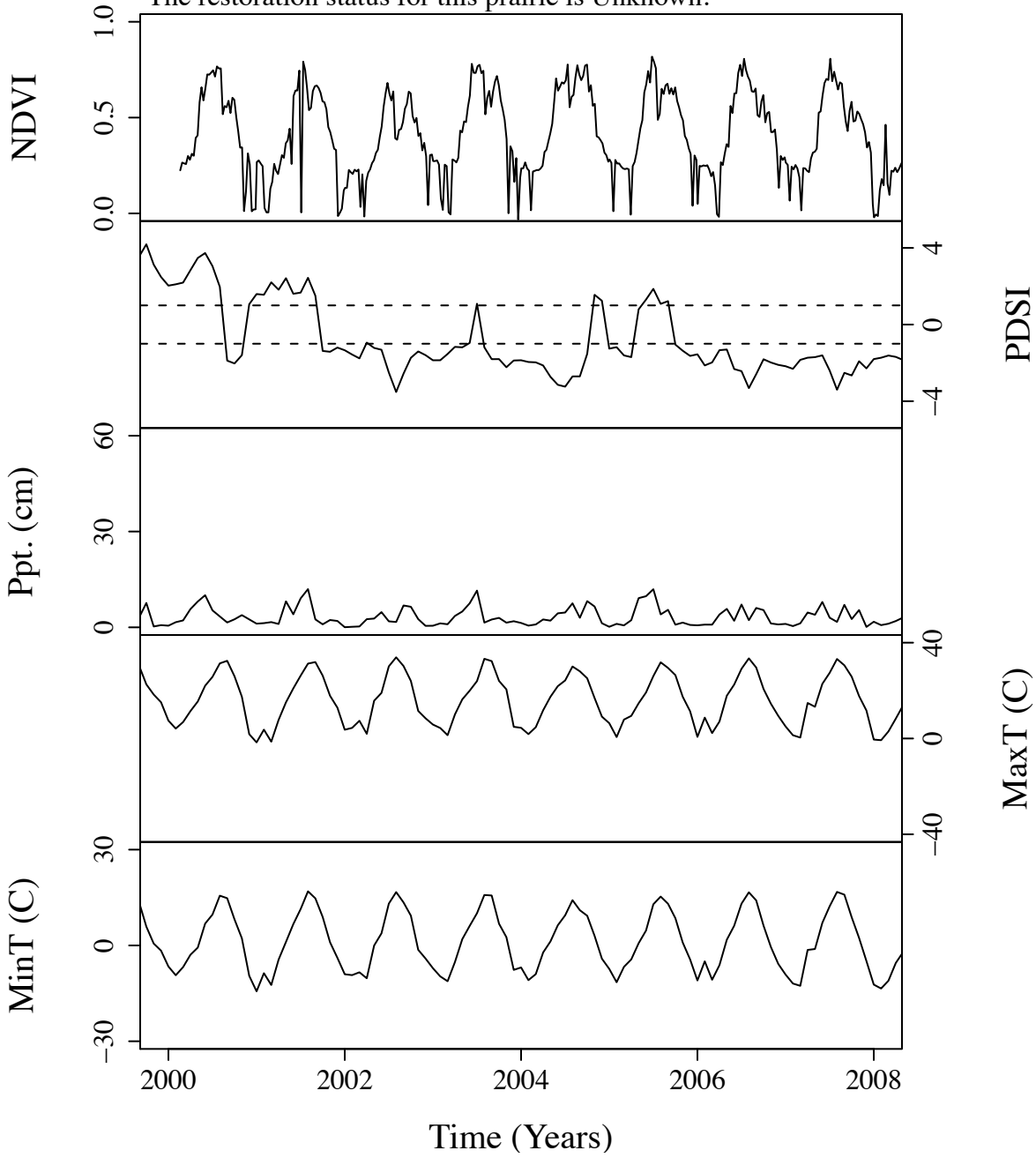

Figure B.131. Time series curves for nsa39.
The community type for this prairie is Short.
The dominant photosynthetic pathway for this prairie is C4.
The restoration status for this prairie is Unknown.

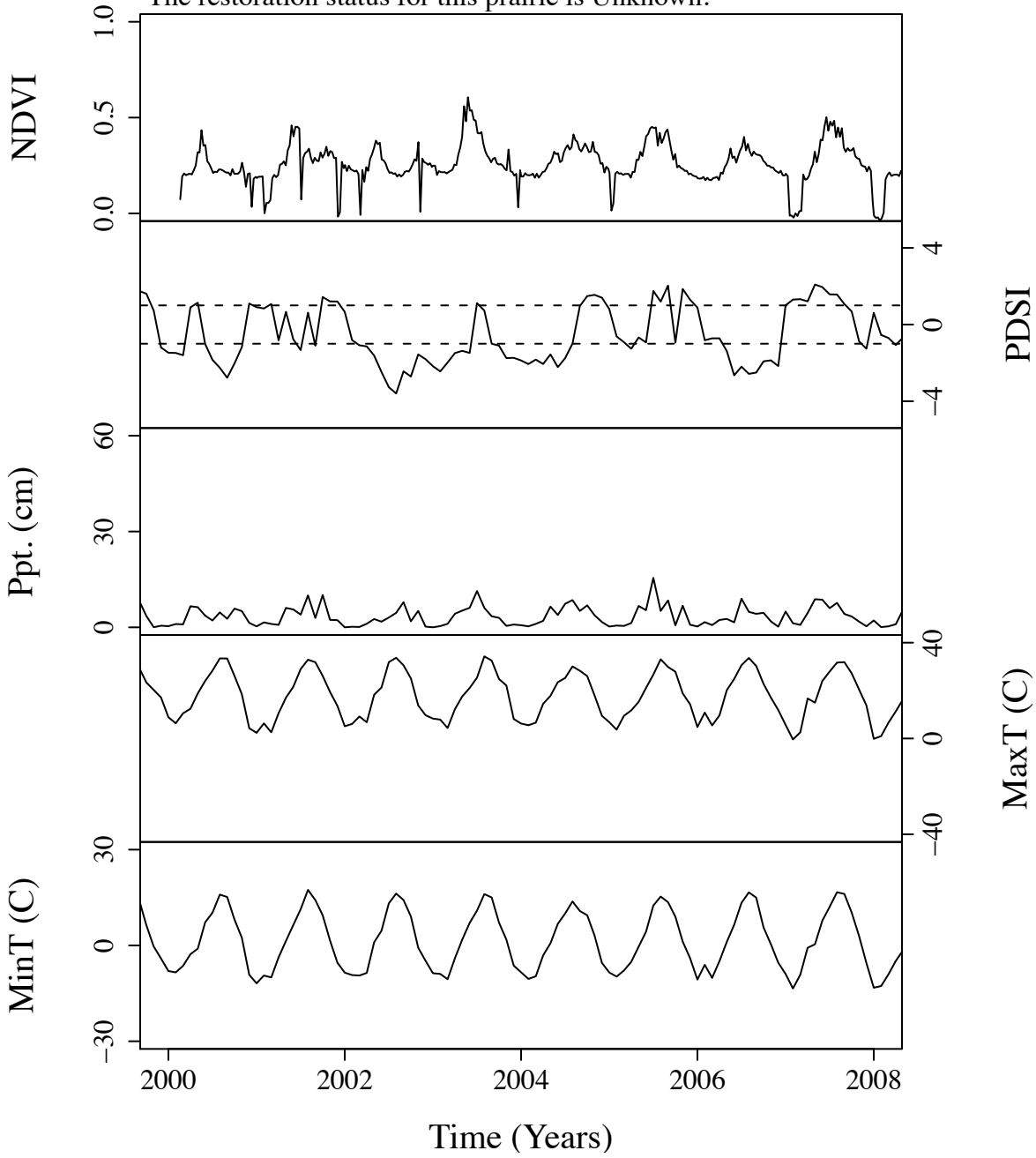

Figure B.132. Time series curves for nsa42.
The community type for this prairie is Short.
The dominant photosynthetic pathway for this prairie is C4.
The restoration status for this prairie is Unknown.

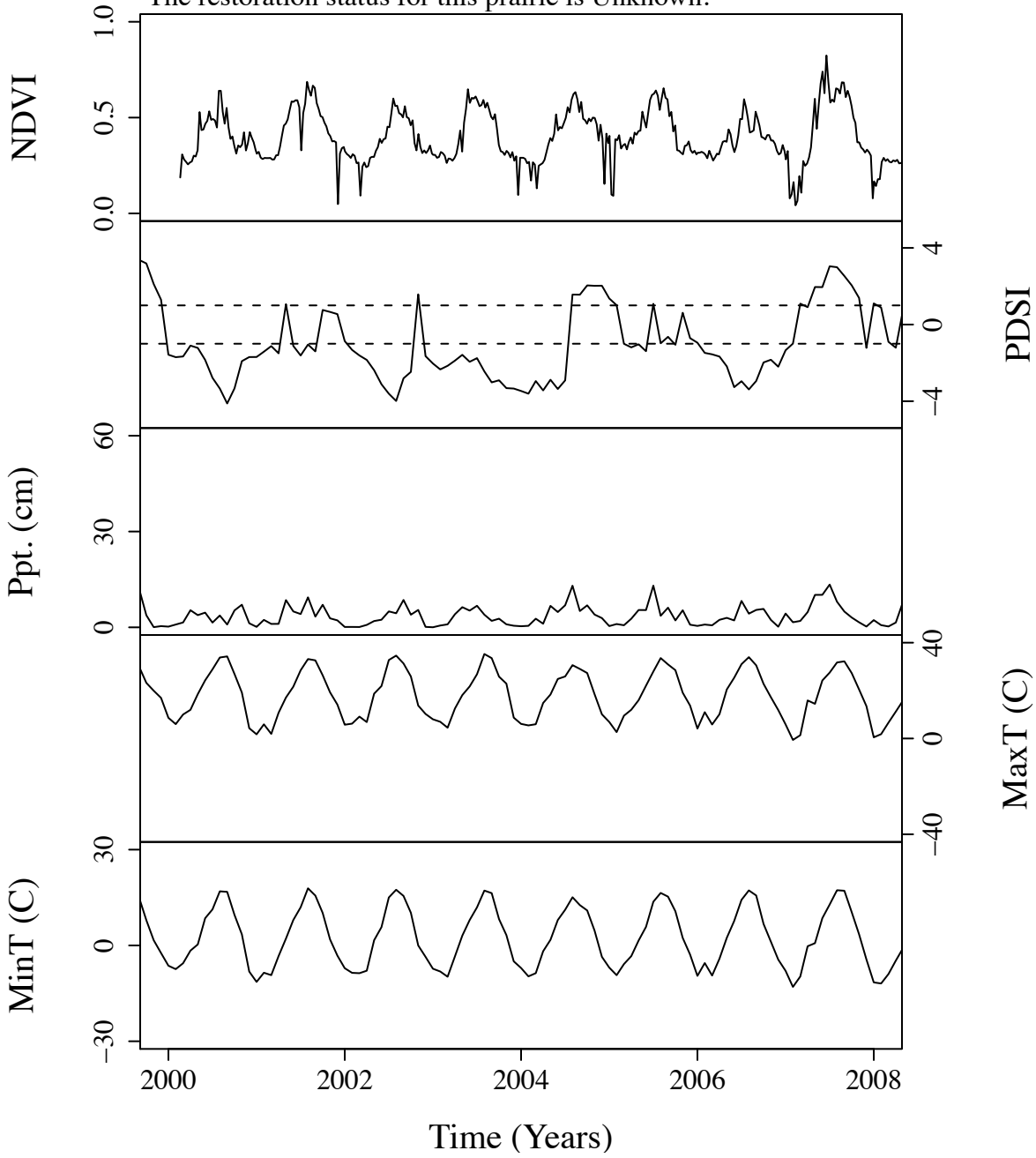

Figure B.133. Time series curves for nsa421.
The community type for this prairie is Mixed.
The dominant photosynthetic pathway for this prairie is C4.
The restoration status for this prairie is Unknown.

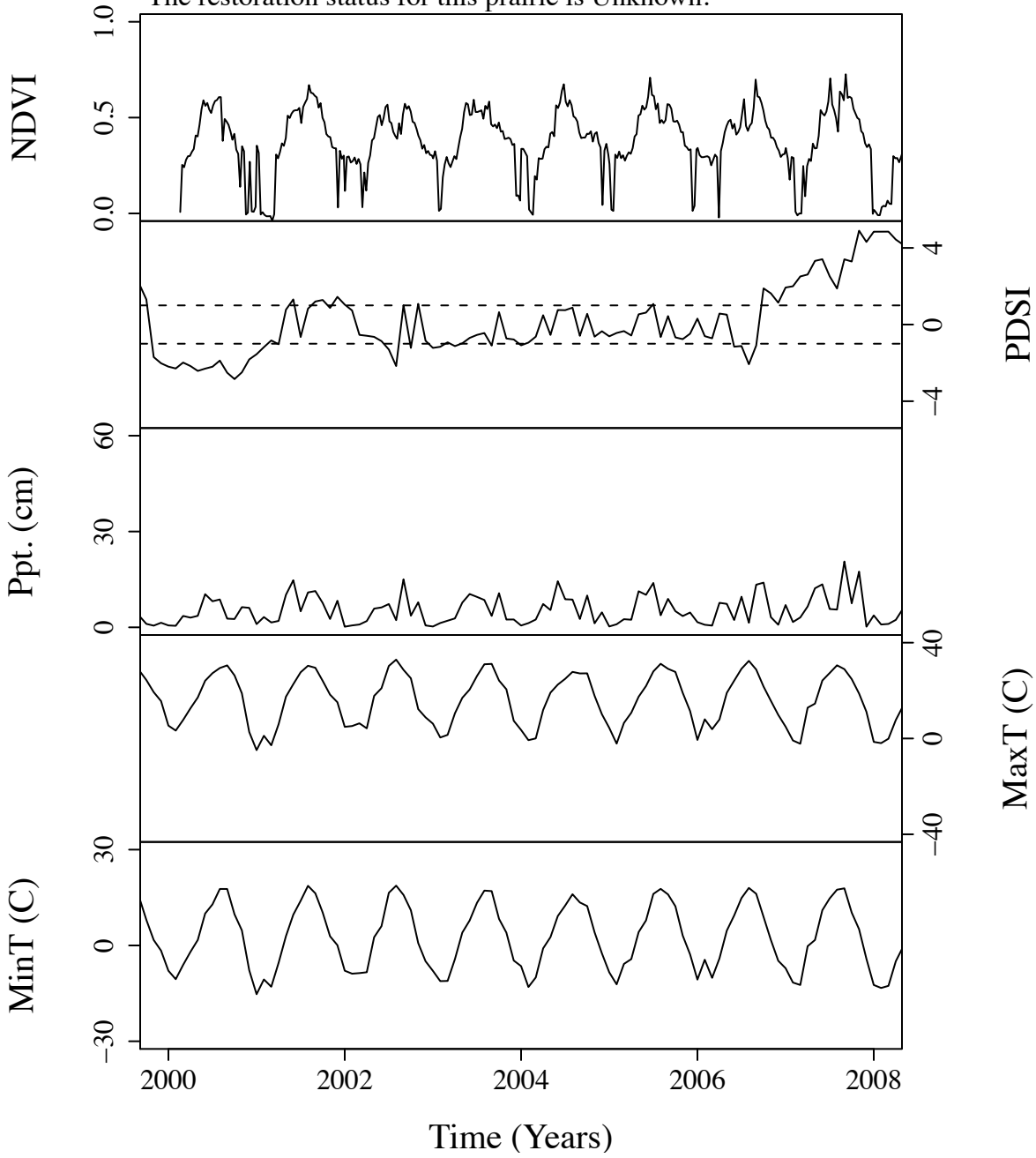

Figure B.134. Time series curves for nsa439.
The community type for this prairie is Short.
The dominant photosynthetic pathway for this prairie is C4.
The restoration status for this prairie is Unknown.

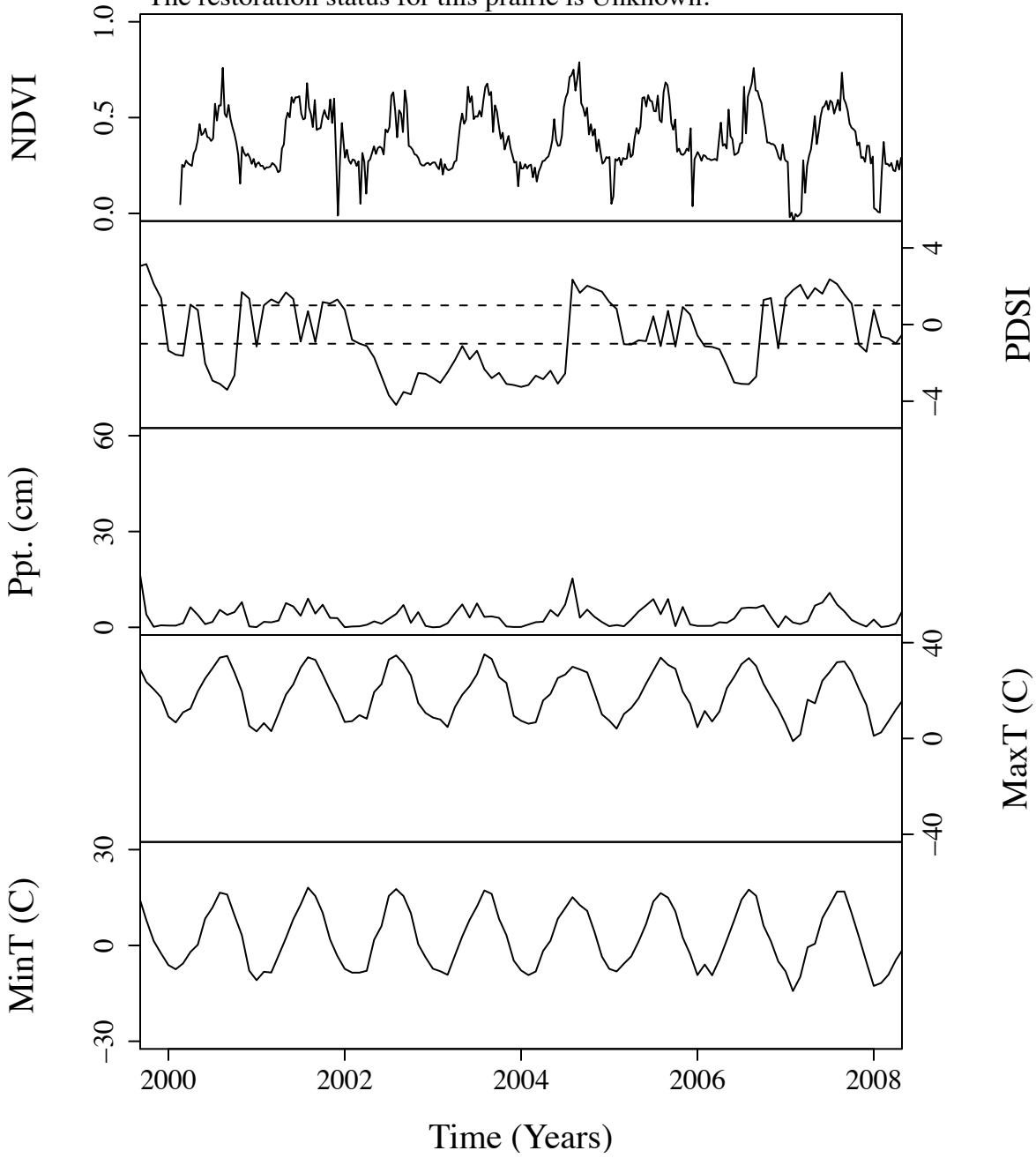

Figure B.135. Time series curves for nsa445.
The community type for this prairie is Short.
The dominant photosynthetic pathway for this prairie is C4.
The restoration status for this prairie is Unknown.

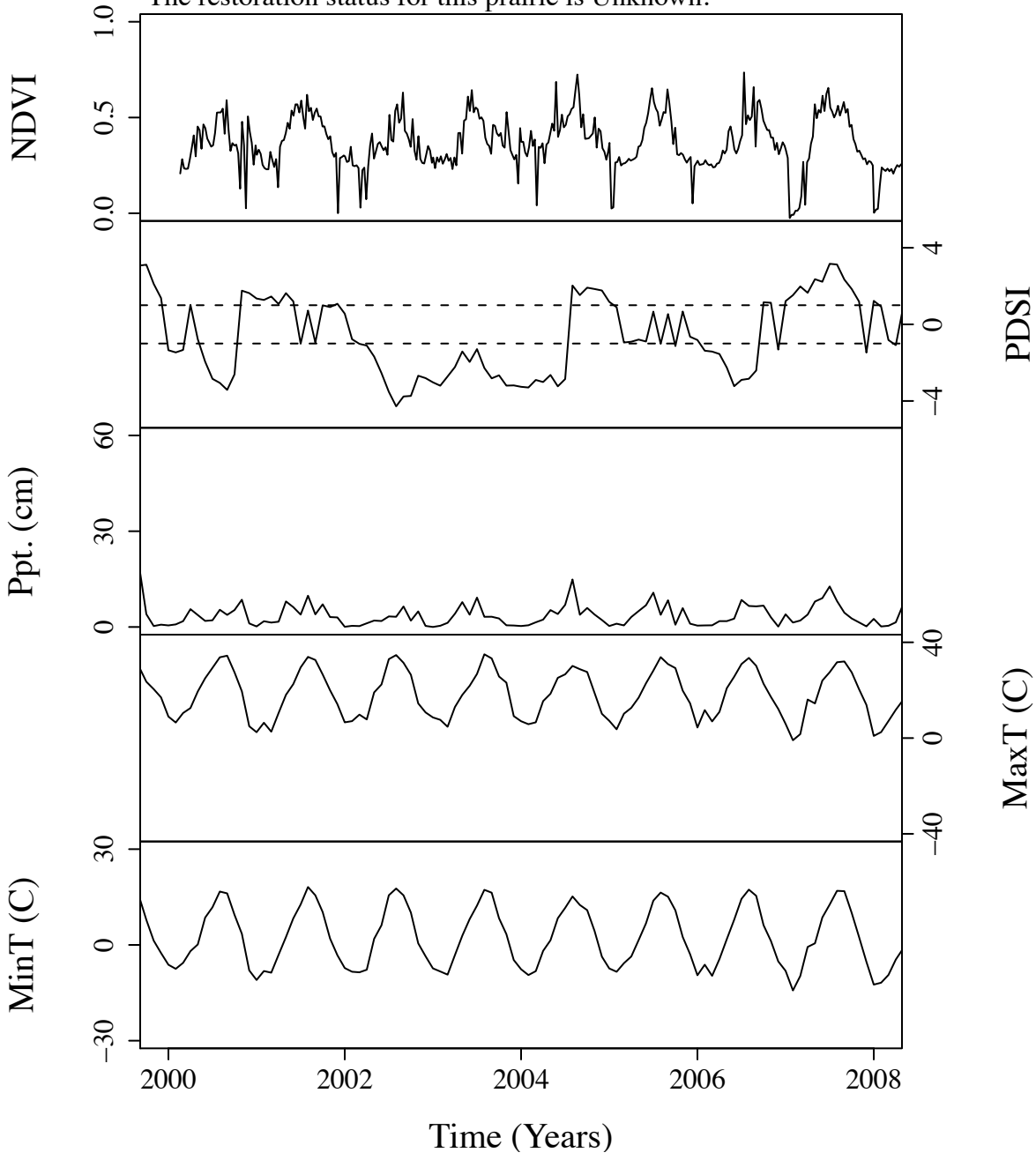

Figure B.136. Time series curves for nsa447.
The community type for this prairie is NoType.
The dominant photosynthetic pathway for this prairie is C4.
The restoration status for this prairie is Unknown.

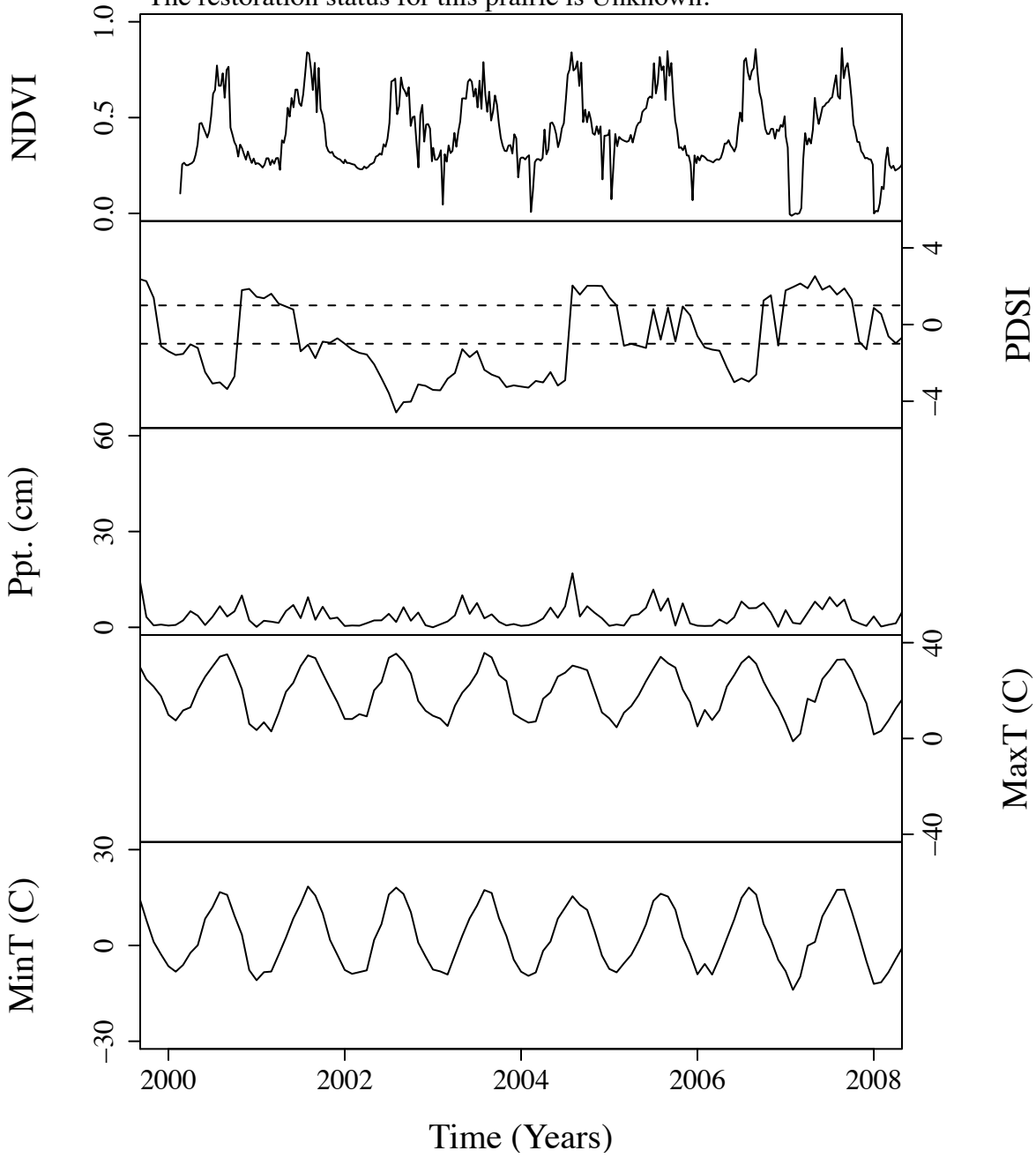

Figure B.137. Time series curves for nsa474.
The community type for this prairie is Short.
The dominant photosynthetic pathway for this prairie is C4.
The restoration status for this prairie is Unknown.

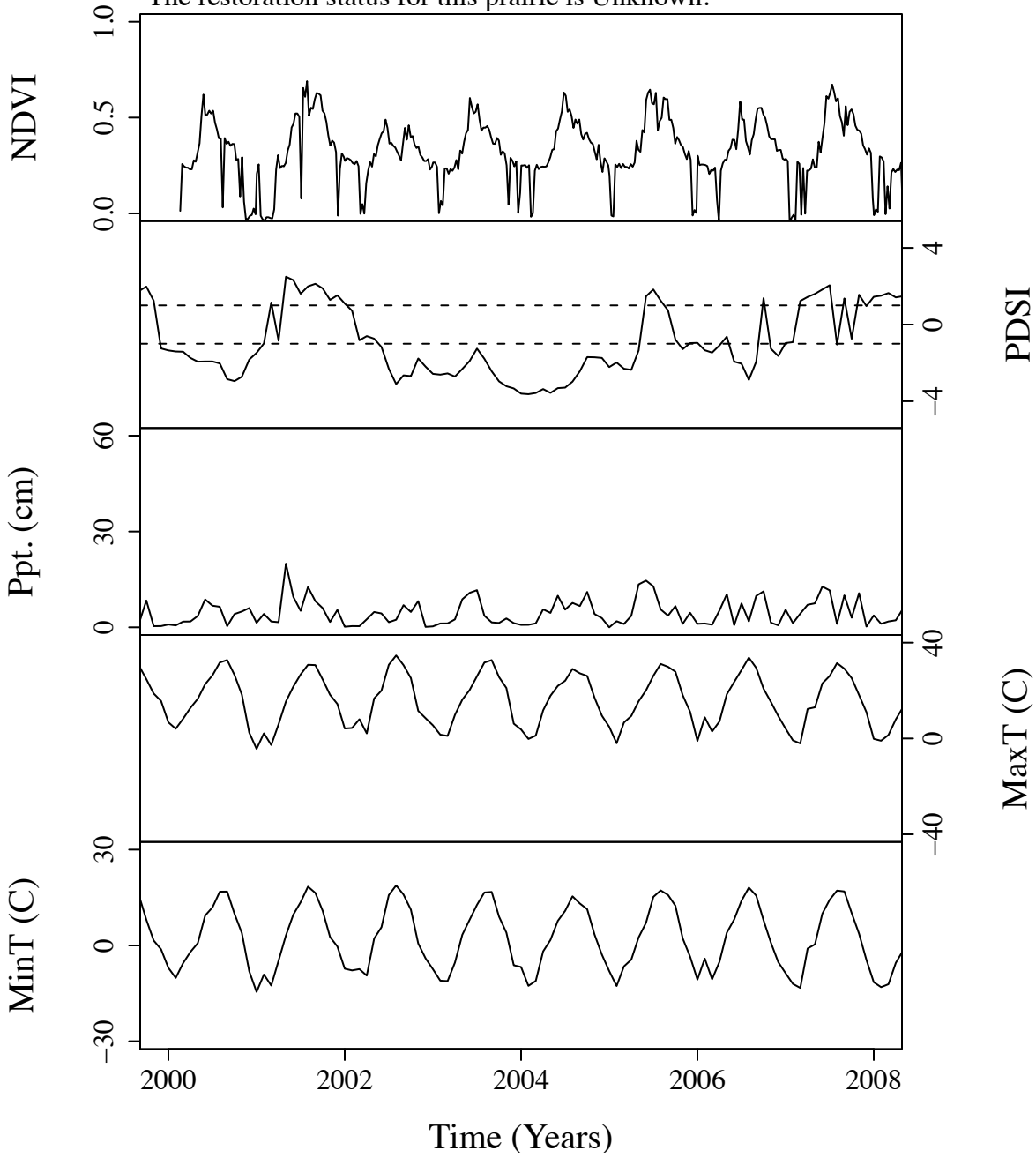

Figure B.138. Time series curves for nsa681.
The community type for this prairie is Mixed.
The dominant photosynthetic pathway for this prairie is C4.
The restoration status for this prairie is Unknown.

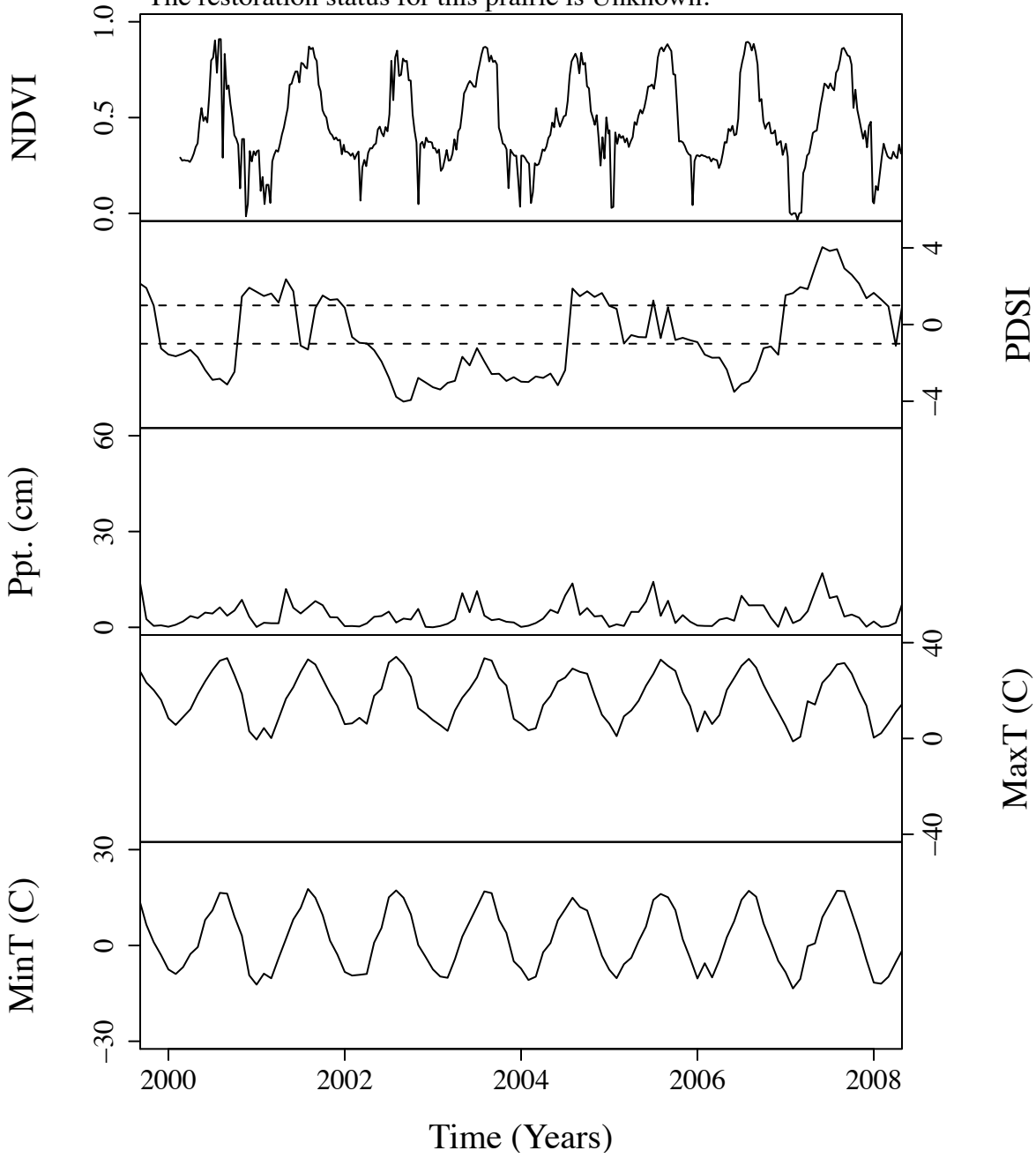

Figure B.139. Time series curves for nsa69.
The community type for this prairie is Mixed.
The dominant photosynthetic pathway for this prairie is C4.
The restoration status for this prairie is Unknown.

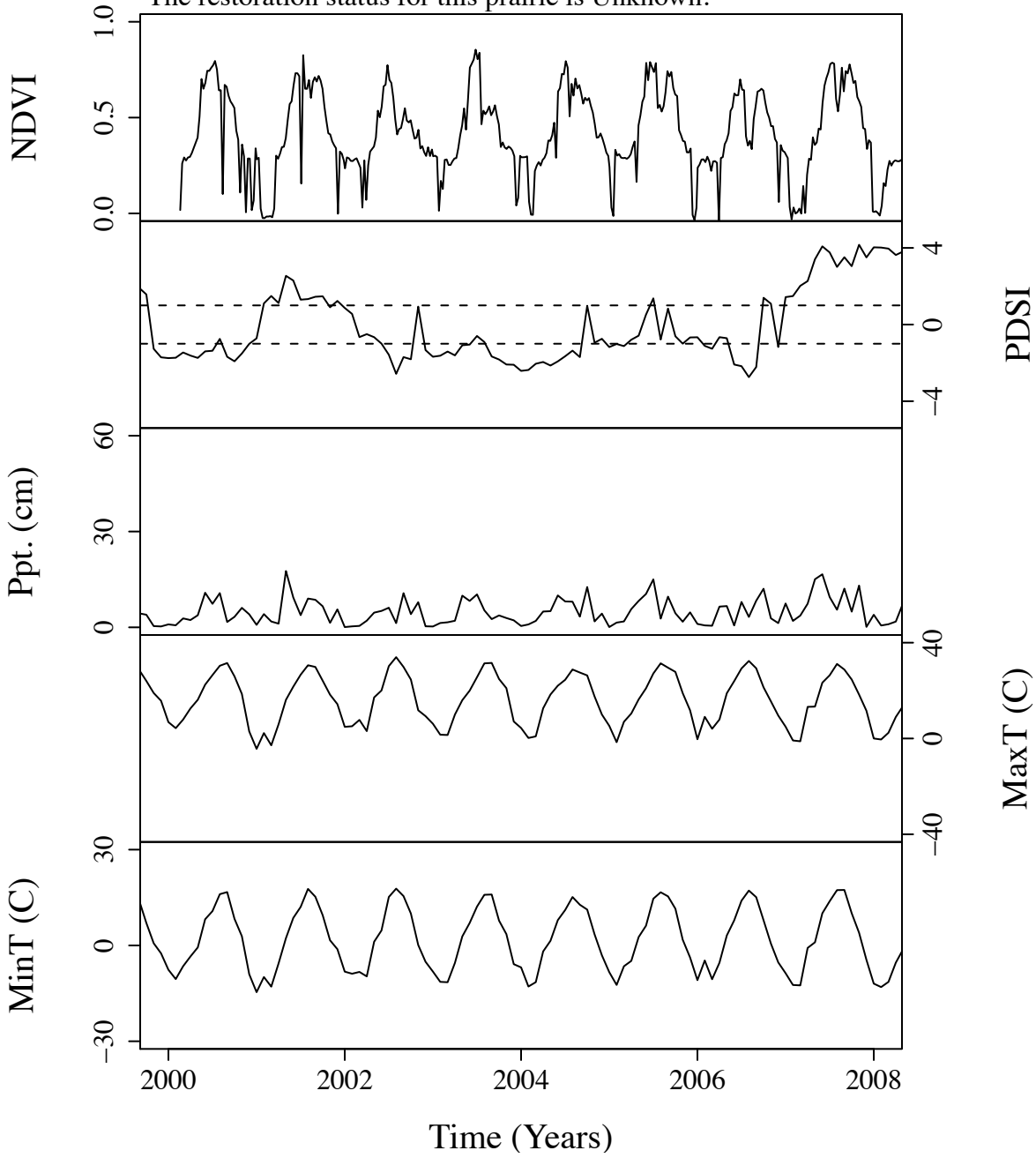

Figure B.140. Time series curves for nsa719.
The community type for this prairie is Mixed.
The dominant photosynthetic pathway for this prairie is C4.
The restoration status for this prairie is Unknown.

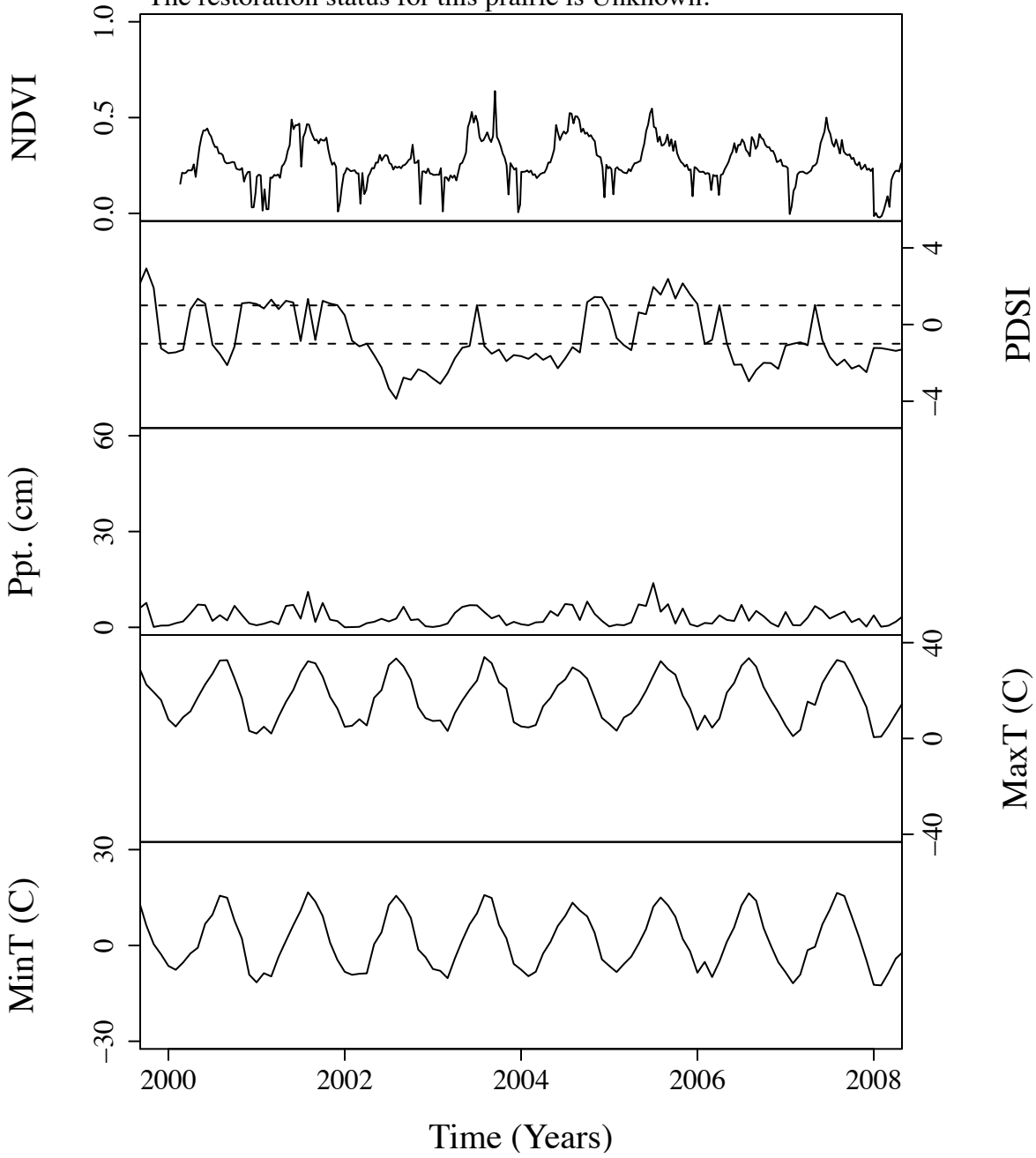

Figure B.141. Time series curves for nsa720.
The community type for this prairie is Short.
The dominant photosynthetic pathway for this prairie is C4.
The restoration status for this prairie is Unknown.

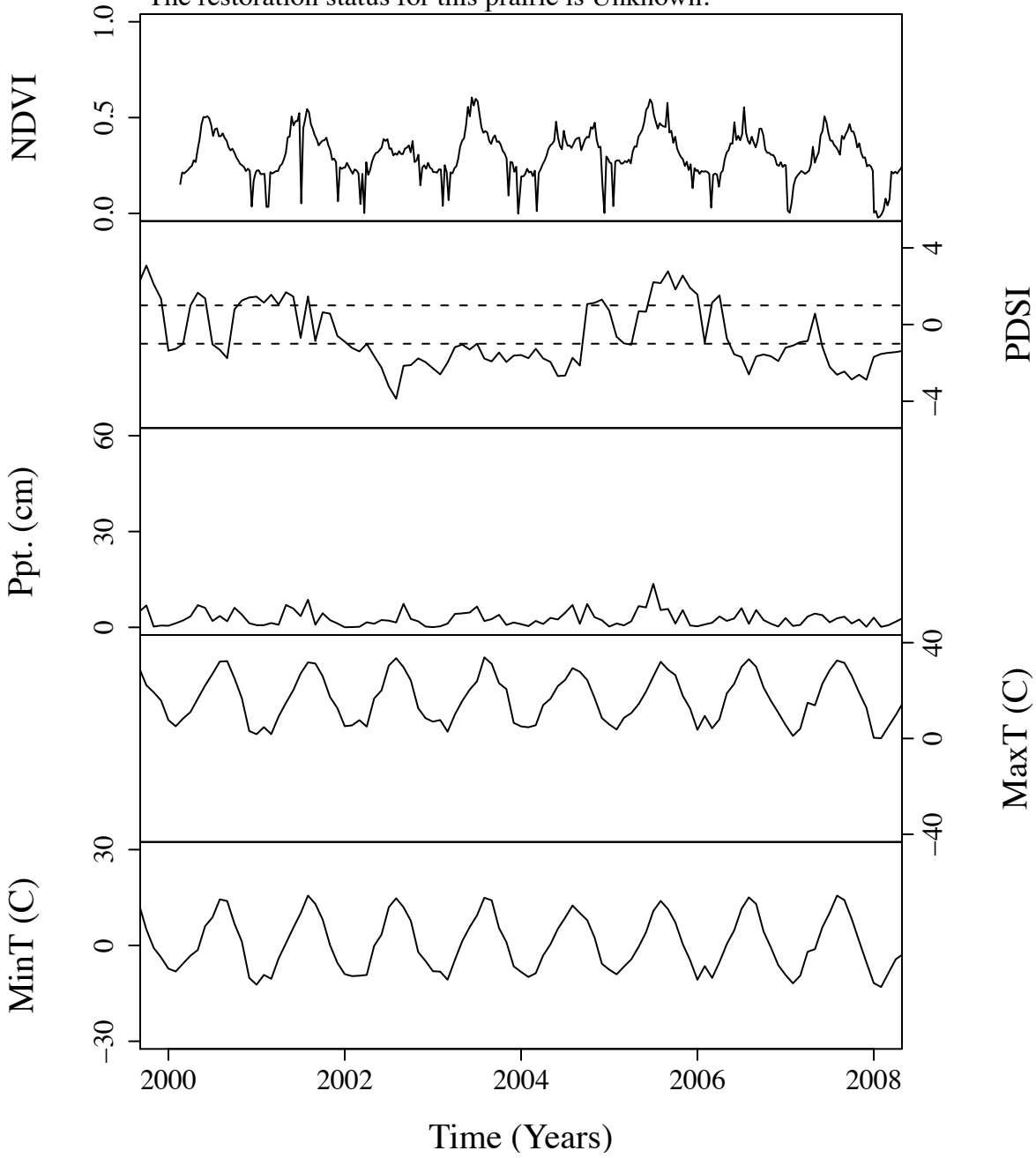

Figure B.142. Time series curves for nsa743.
The community type for this prairie is Short.
The dominant photosynthetic pathway for this prairie is C4.
The restoration status for this prairie is Unknown.

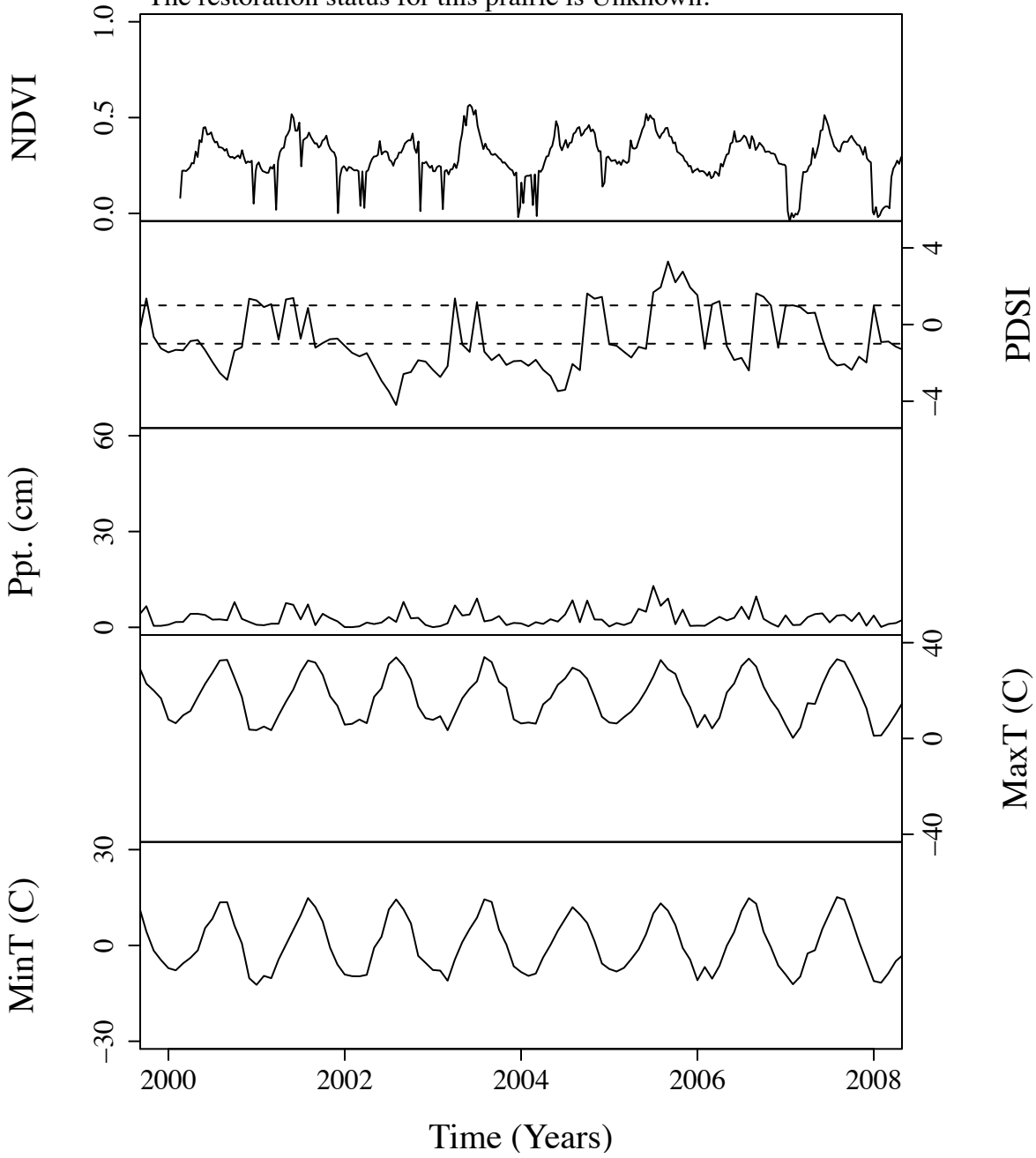

Figure B.143. Time series curves for nsa767.
The community type for this prairie is Short.
The dominant photosynthetic pathway for this prairie is C4.
The restoration status for this prairie is Unknown.

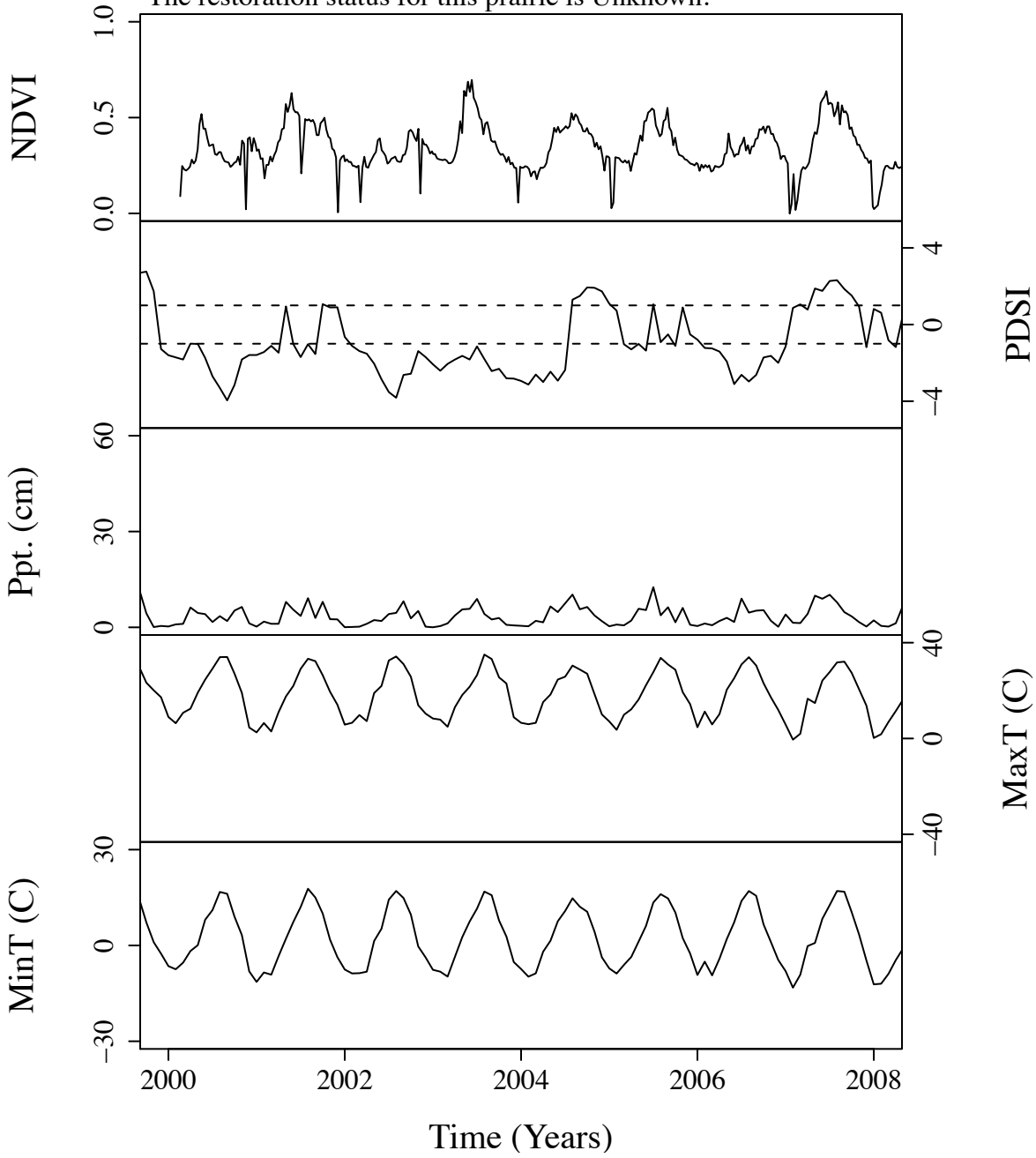

Figure B.144. Time series curves for nsa778.
The community type for this prairie is Short.
The dominant photosynthetic pathway for this prairie is C4.
The restoration status for this prairie is Unknown.

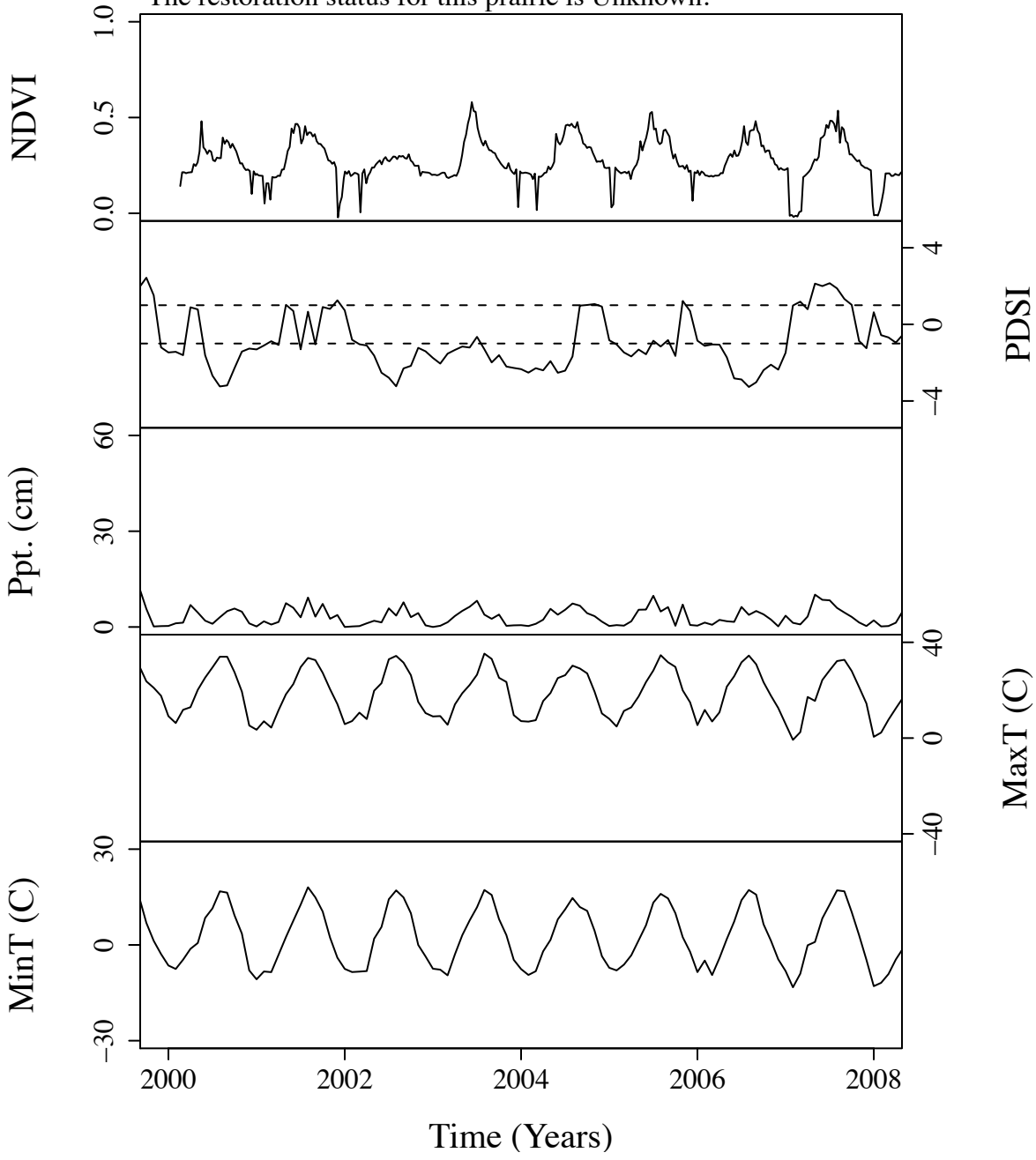

Figure B.145. Time series curves for nsa792.
The community type for this prairie is Mixed.
The dominant photosynthetic pathway for this prairie is C4.
The restoration status for this prairie is Unknown.

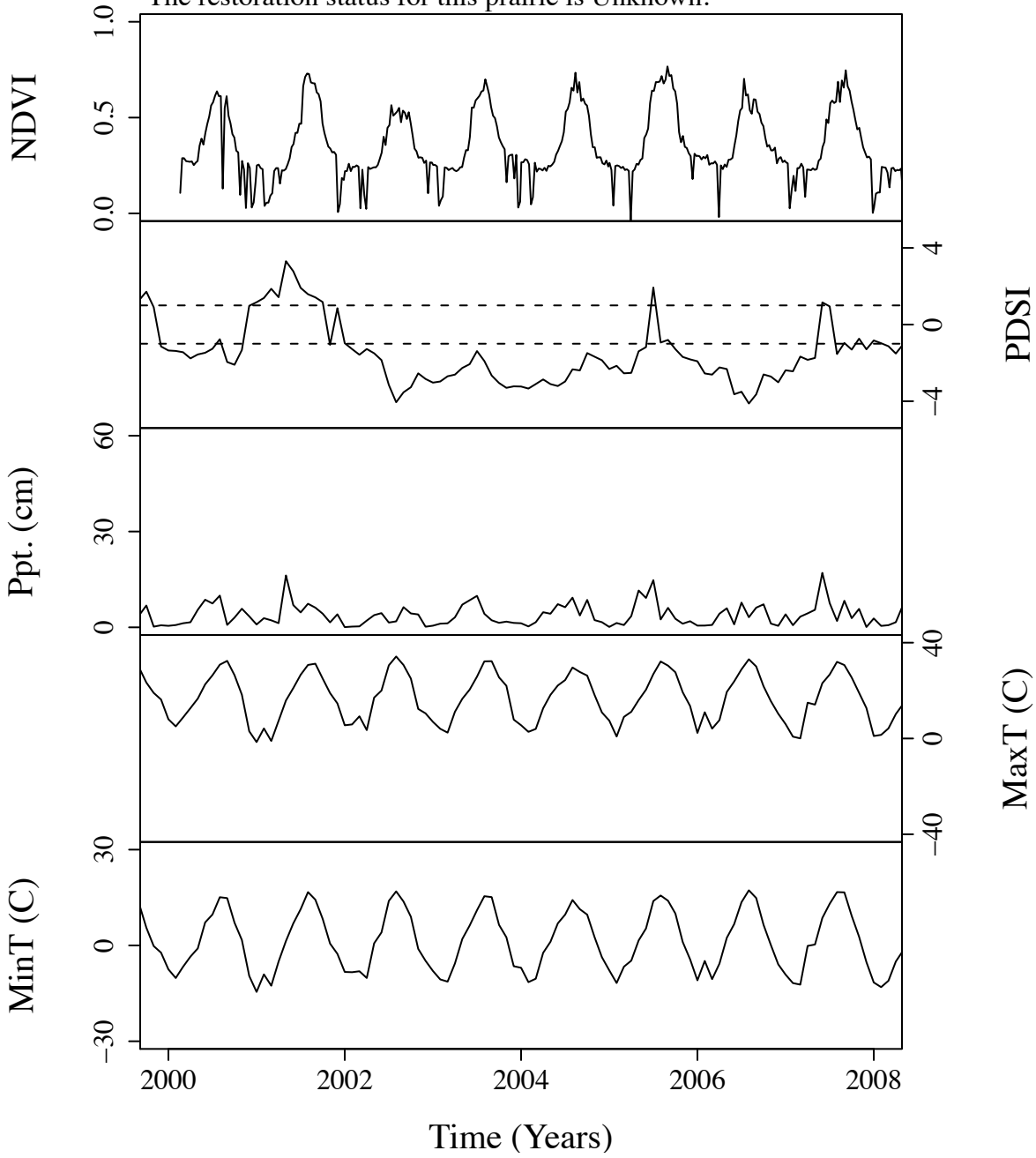

Figure B.146. Time series curves for nsa809.
The community type for this prairie is Short.
The dominant photosynthetic pathway for this prairie is C4.
The restoration status for this prairie is Unknown.

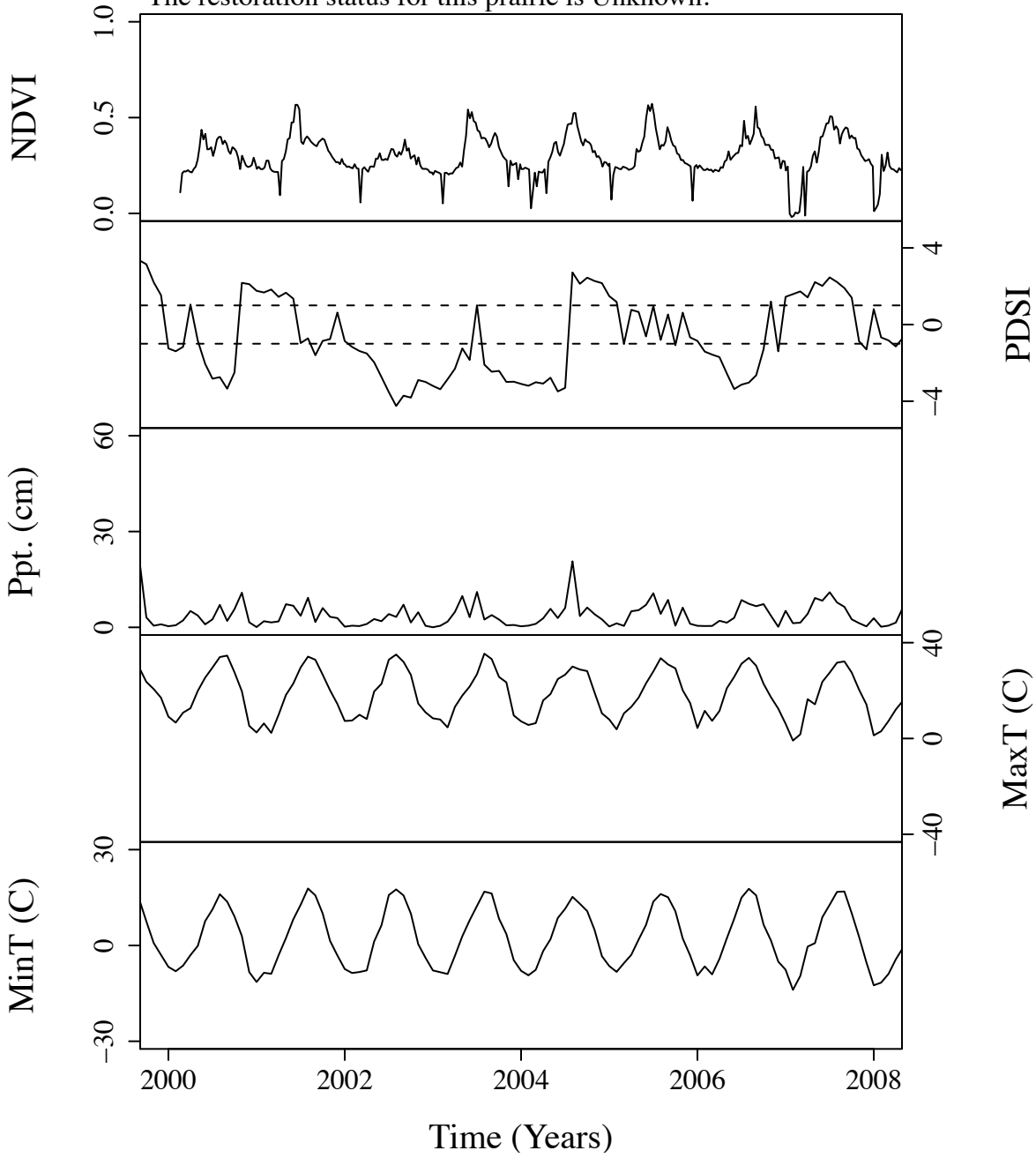

Figure B.147. Time series curves for nsa873.
The community type for this prairie is Mixed.
The dominant photosynthetic pathway for this prairie is C4.
The restoration status for this prairie is Unknown.

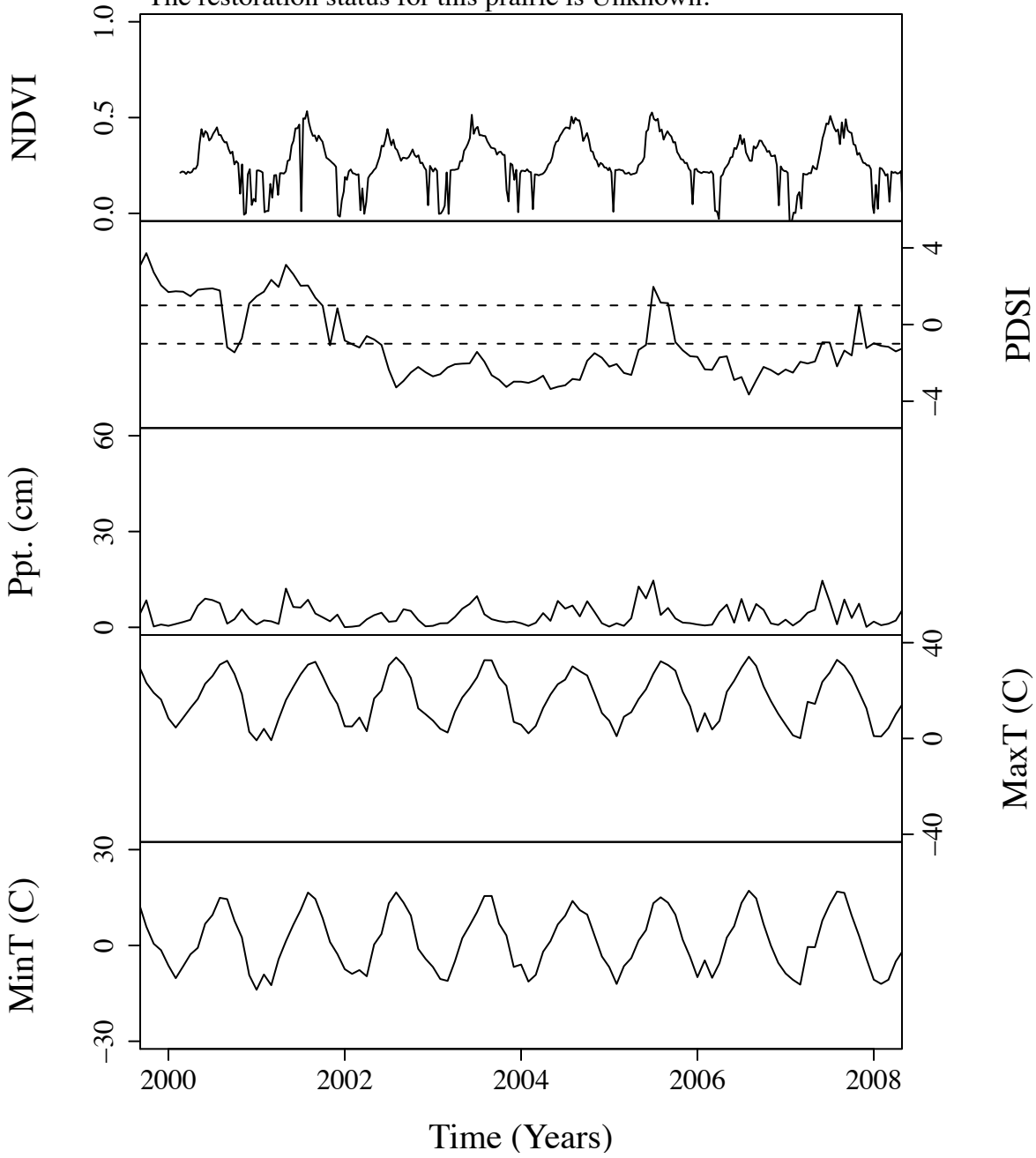

Figure B.148. Time series curves for nsa890.
The community type for this prairie is Mixed.
The dominant photosynthetic pathway for this prairie is C4.
The restoration status for this prairie is Unknown.

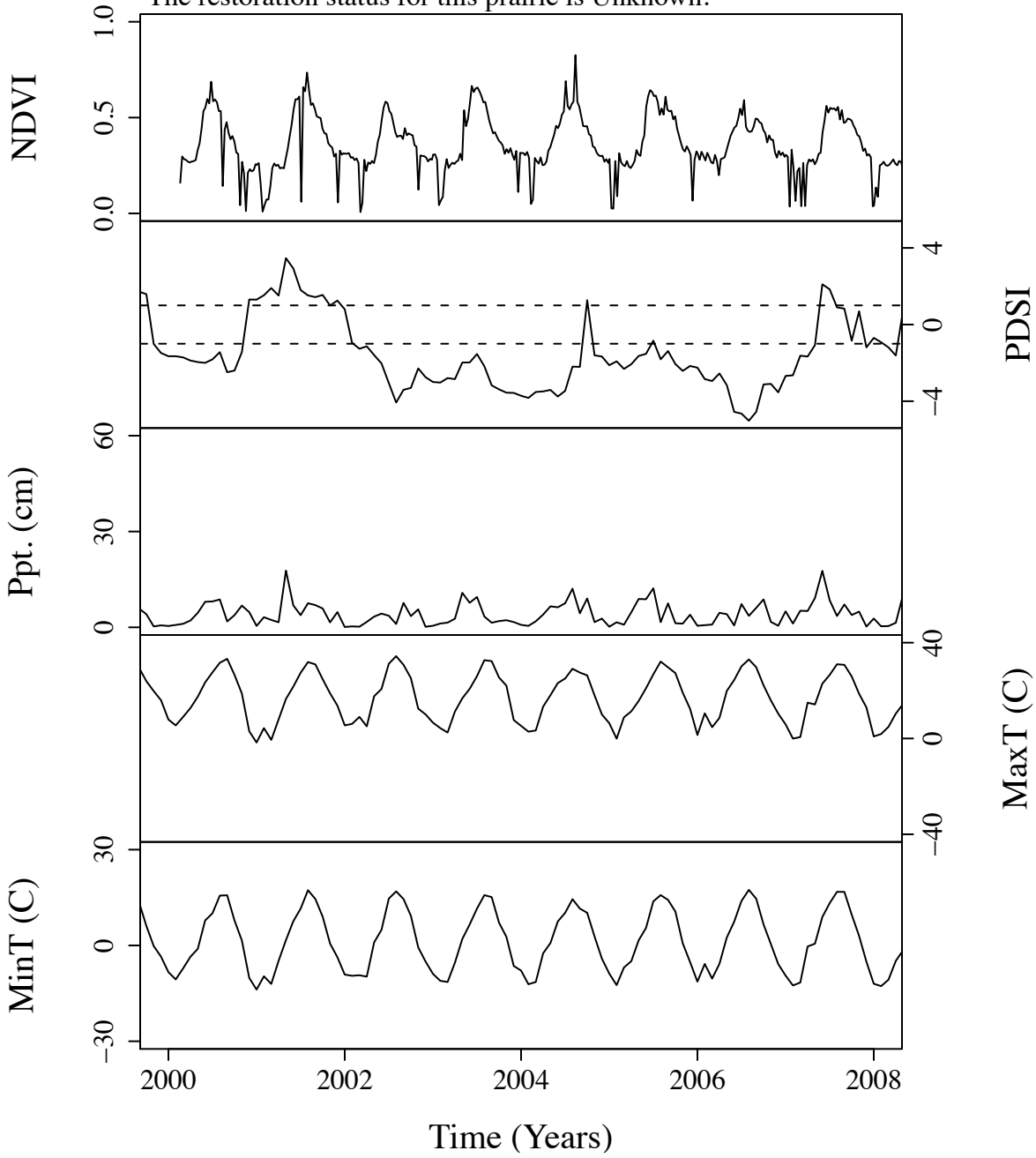

Figure B.149. Time series curves for nsa895.
The community type for this prairie is Mixed.
The dominant photosynthetic pathway for this prairie is C4.
The restoration status for this prairie is Unknown.

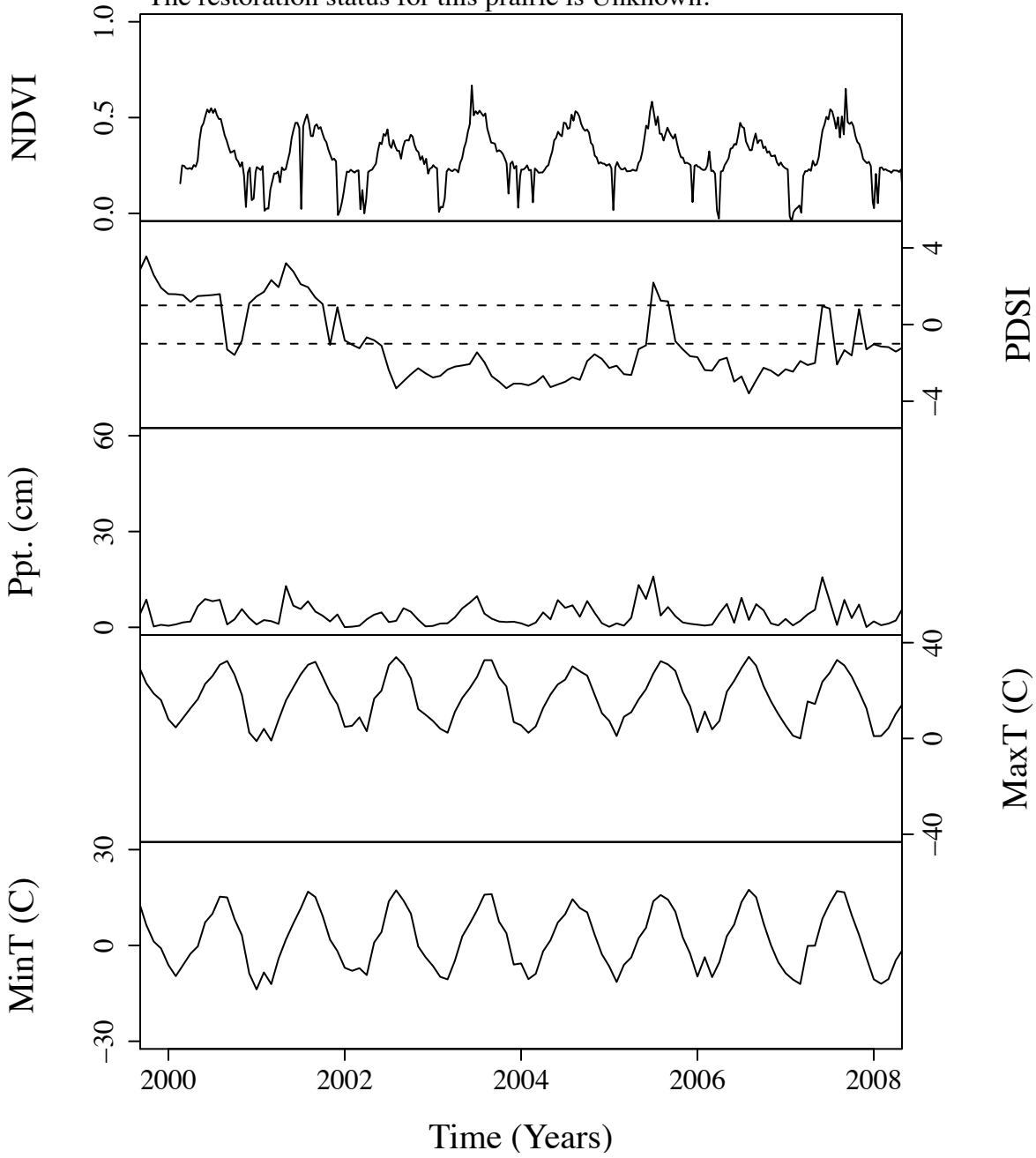

Figure B.150. Time series curves for nsa95.
The community type for this prairie is Mixed.
The dominant photosynthetic pathway for this prairie is C4.
The restoration status for this prairie is Unknown.

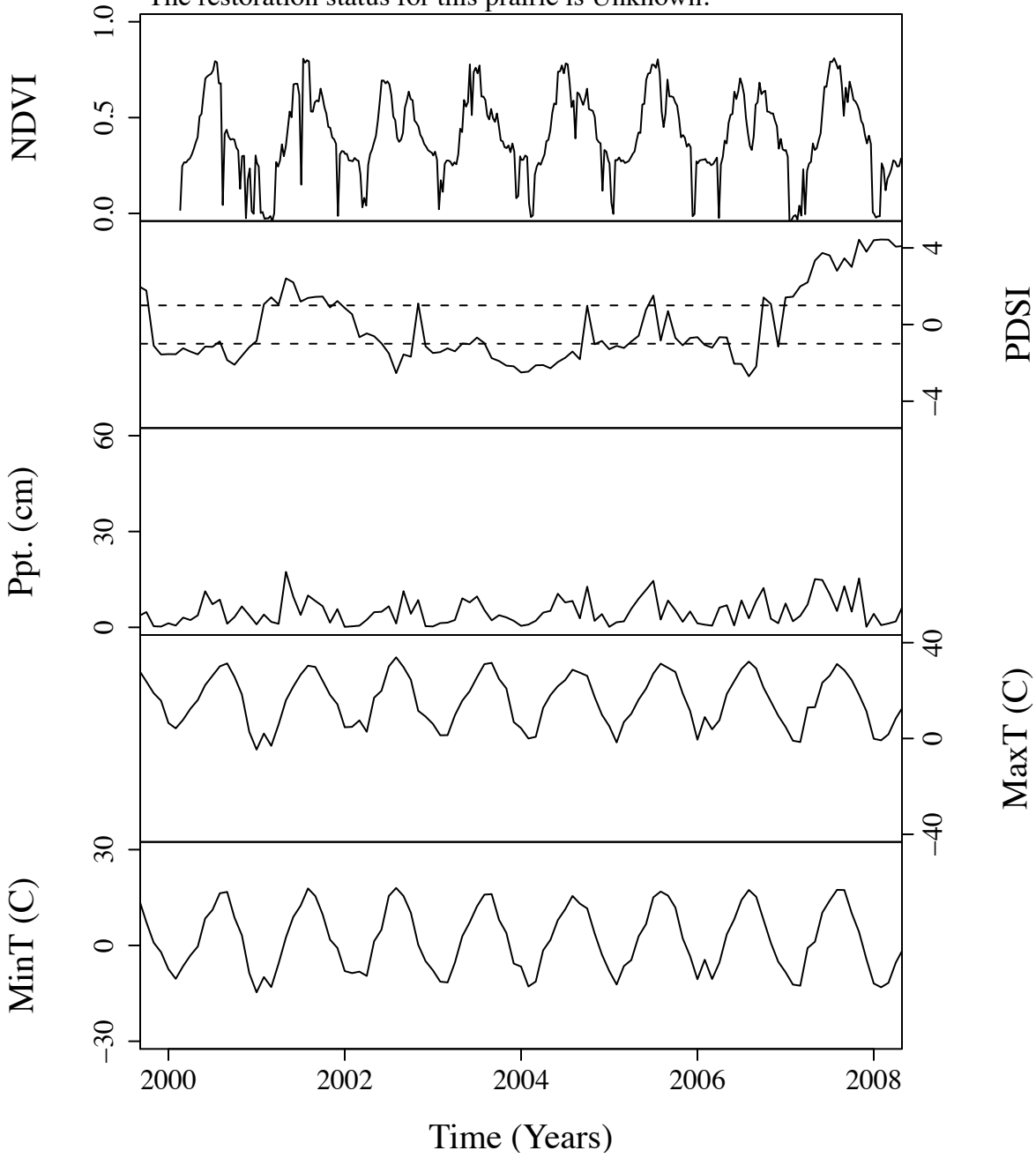

Figure B.151. Time series curves for nsan144.
The community type for this prairie is Mixed.
The dominant photosynthetic pathway for this prairie is C4.
The restoration status for this prairie is Unknown.

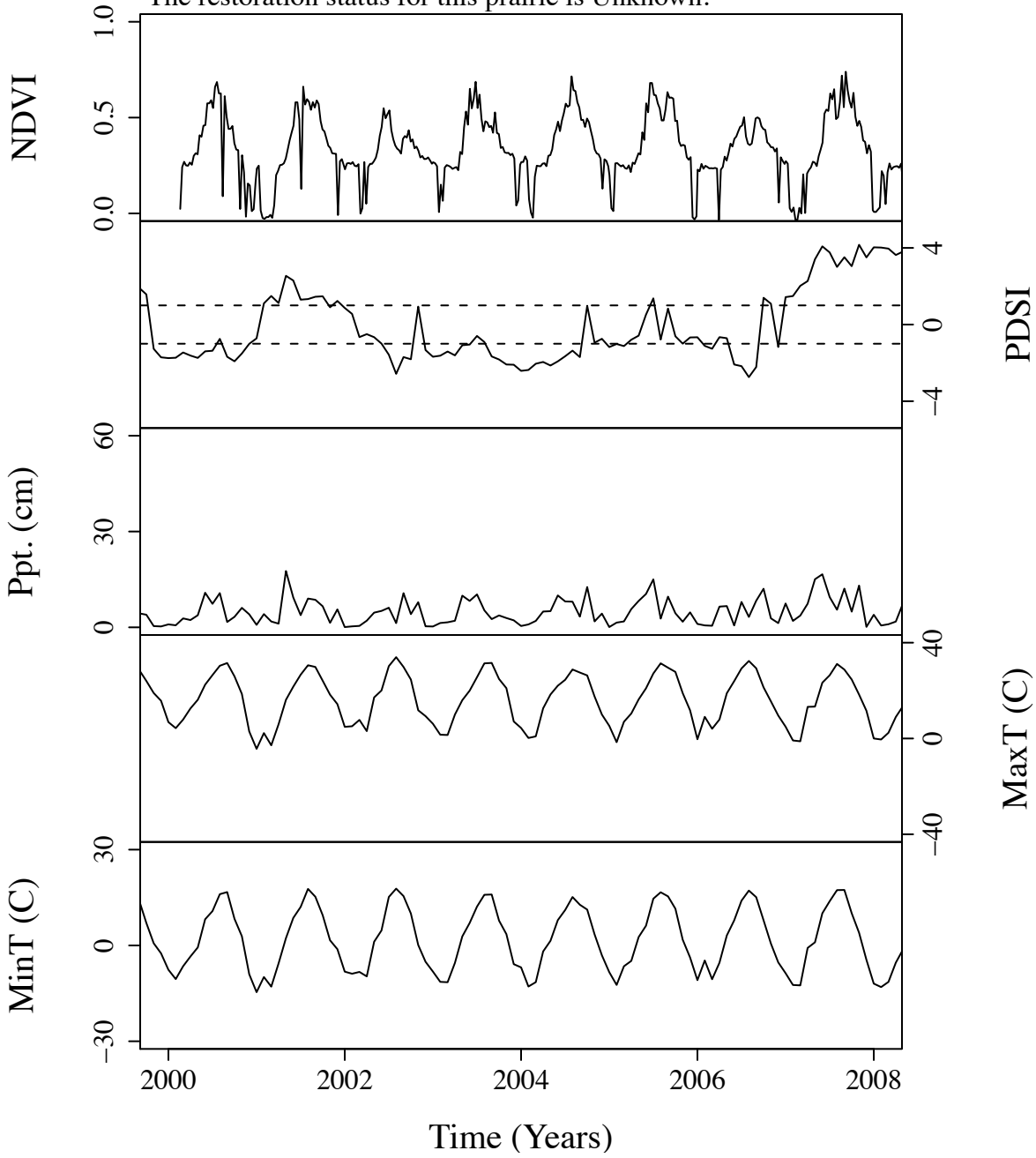

Figure B.152. Time series curves for nsh77.
The community type for this prairie is Short.
The dominant photosynthetic pathway for this prairie is C4.
The restoration status for this prairie is Unknown.

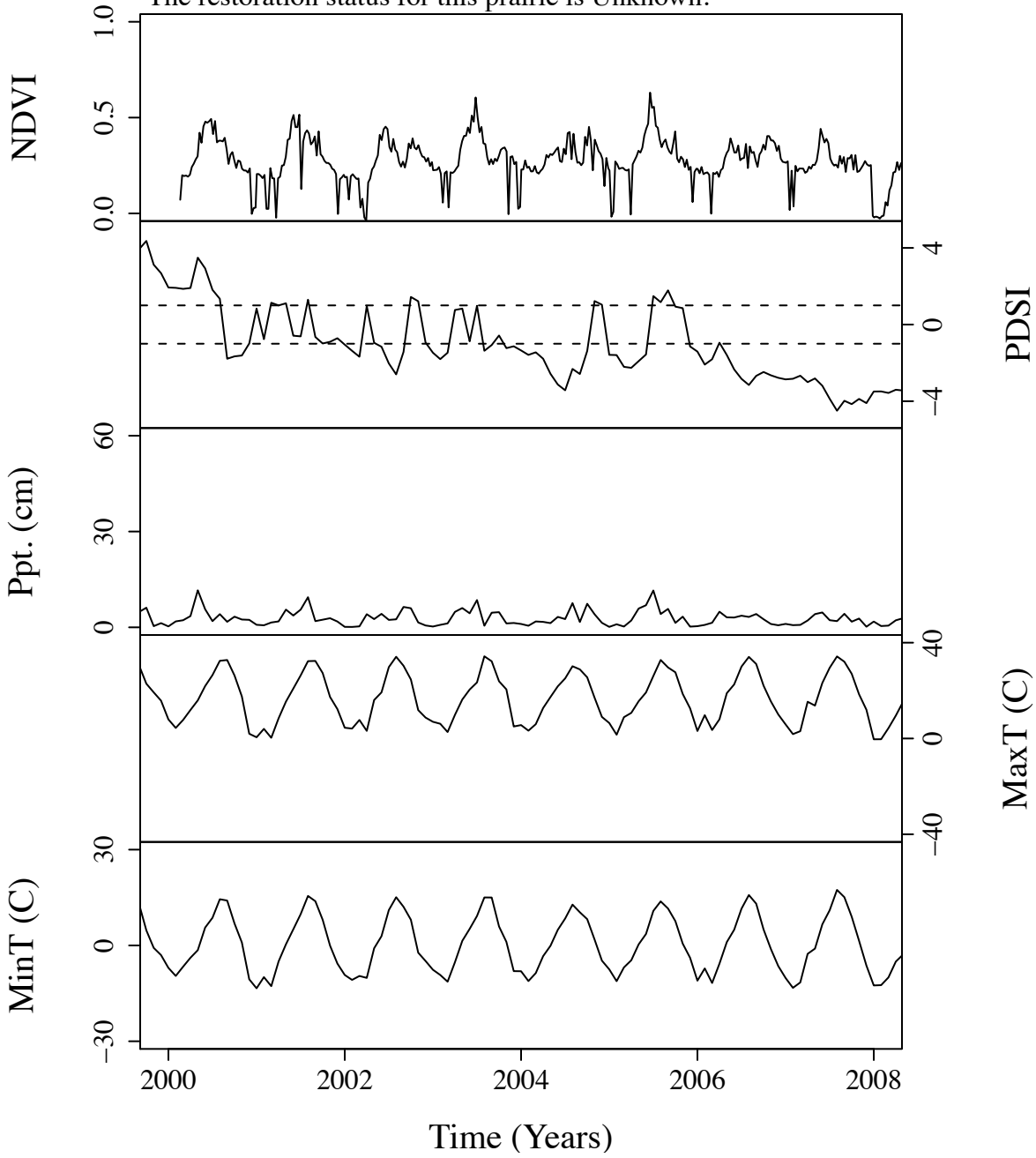

Figure B.153. Time series curves for nta362.
The community type for this prairie is Tall.
The dominant photosynthetic pathway for this prairie is C4.
The restoration status for this prairie is Unknown.

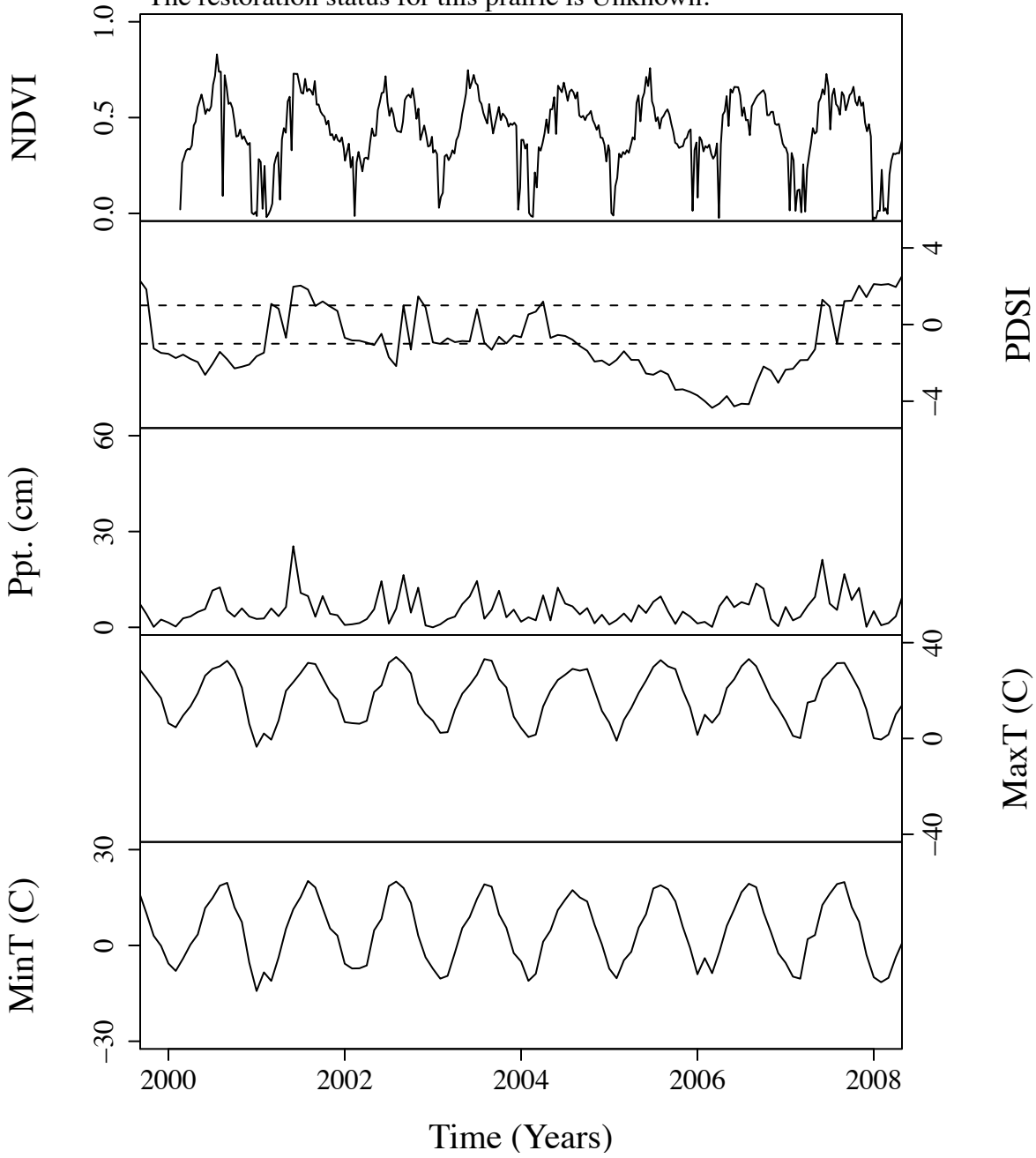

Figure B.154. Time series curves for nta377.
The community type for this prairie is Tall.
The dominant photosynthetic pathway for this prairie is C4.
The restoration status for this prairie is Unknown.

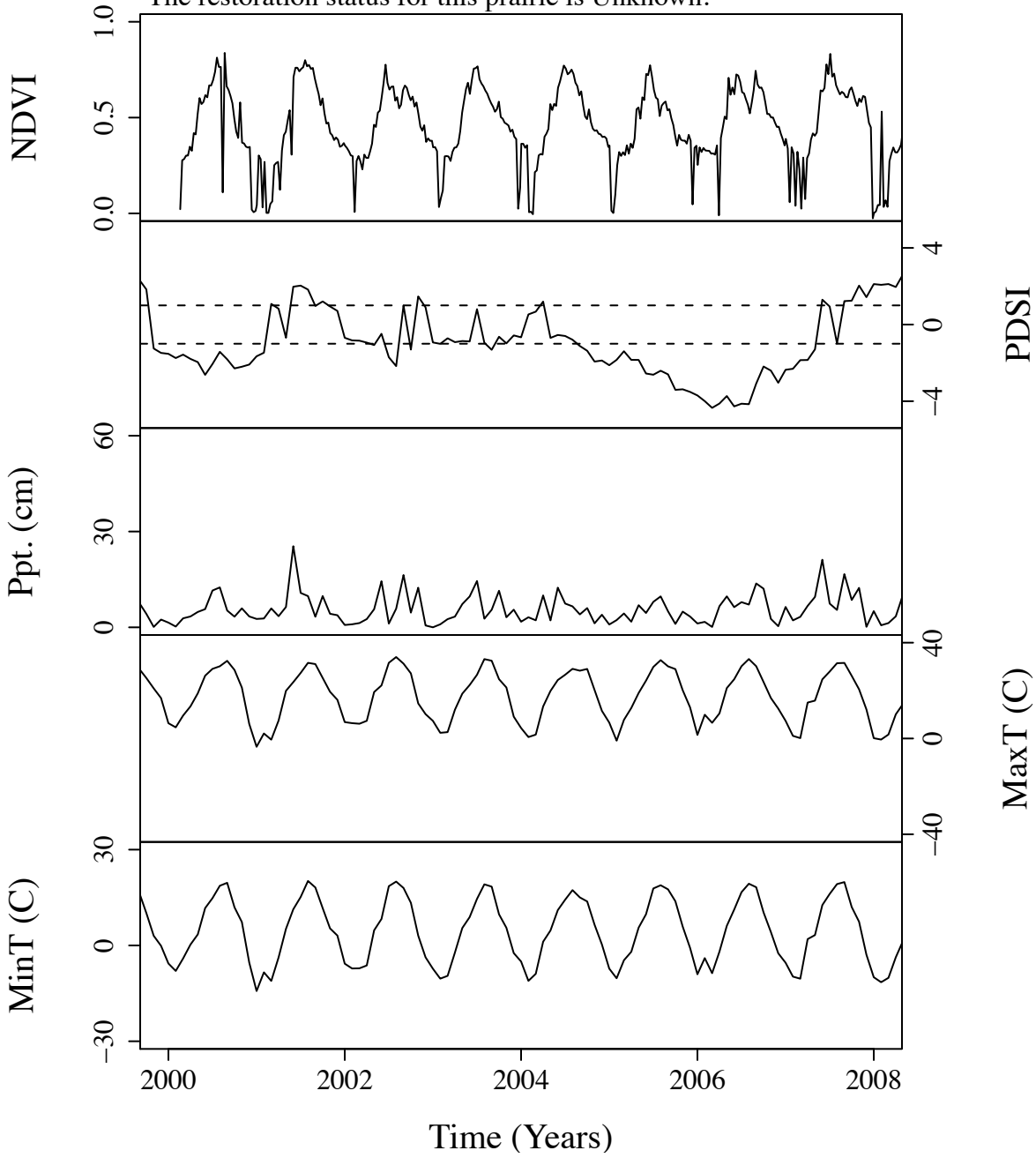

Figure B.155. Time series curves for nta383.
The community type for this prairie is Tall.
The dominant photosynthetic pathway for this prairie is C4.
The restoration status for this prairie is Unknown.

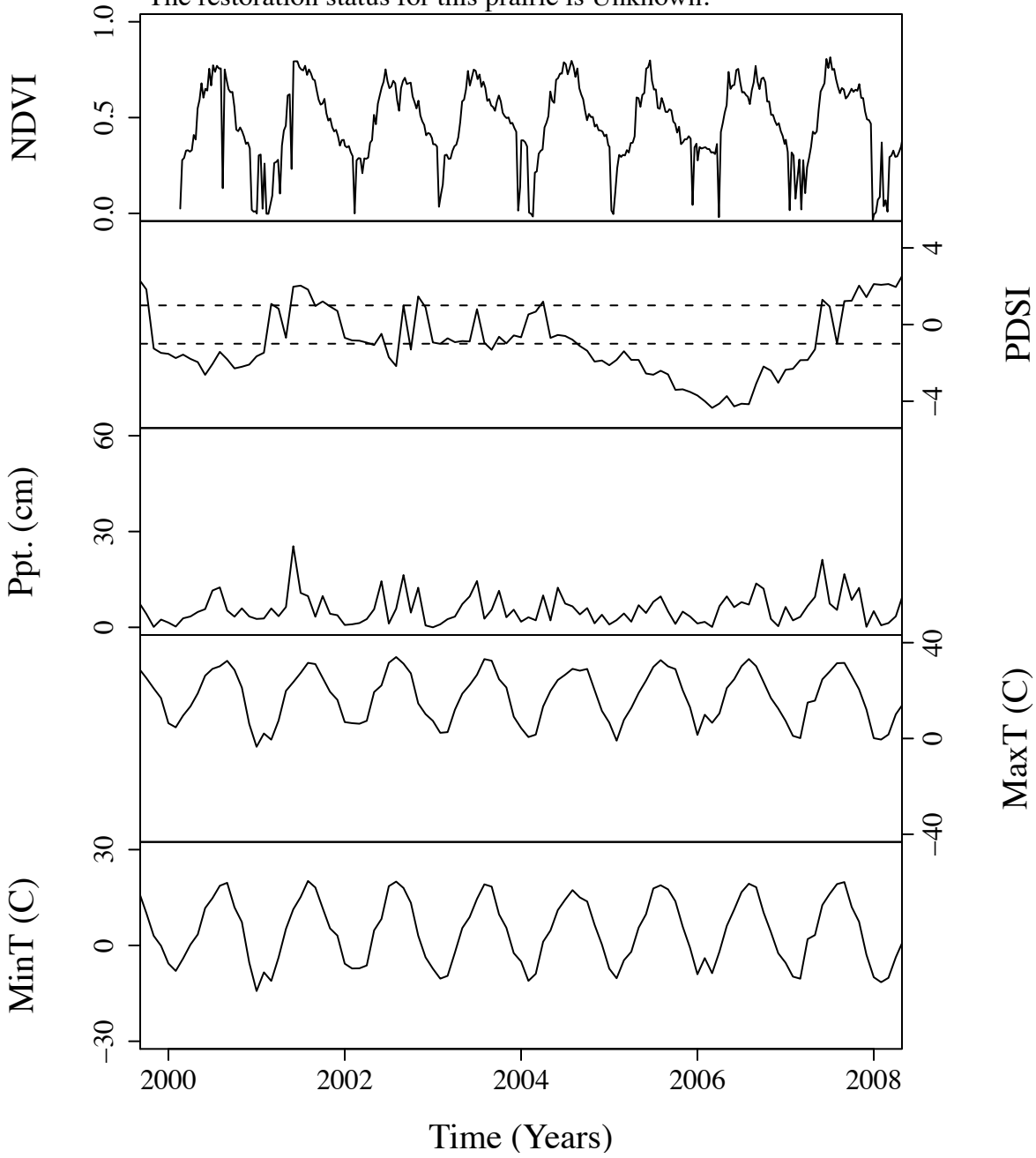

Figure B.156. Time series curves for nta406.
The community type for this prairie is Mixed.
The dominant photosynthetic pathway for this prairie is C4.
The restoration status for this prairie is Unknown.

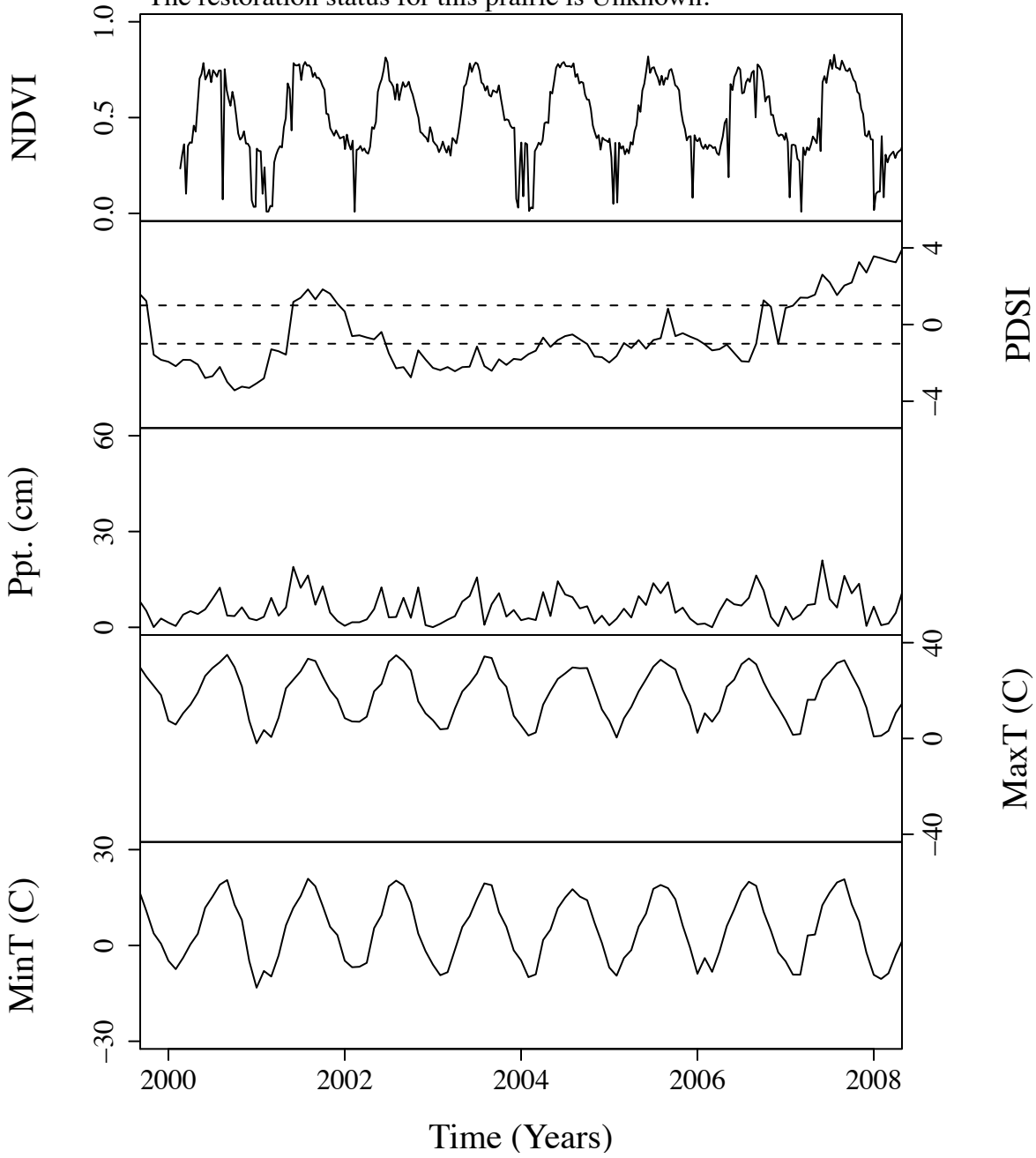

Figure B.157. Time series curves for nta408.
The community type for this prairie is Mixed.
The dominant photosynthetic pathway for this prairie is C4.
The restoration status for this prairie is Unknown.

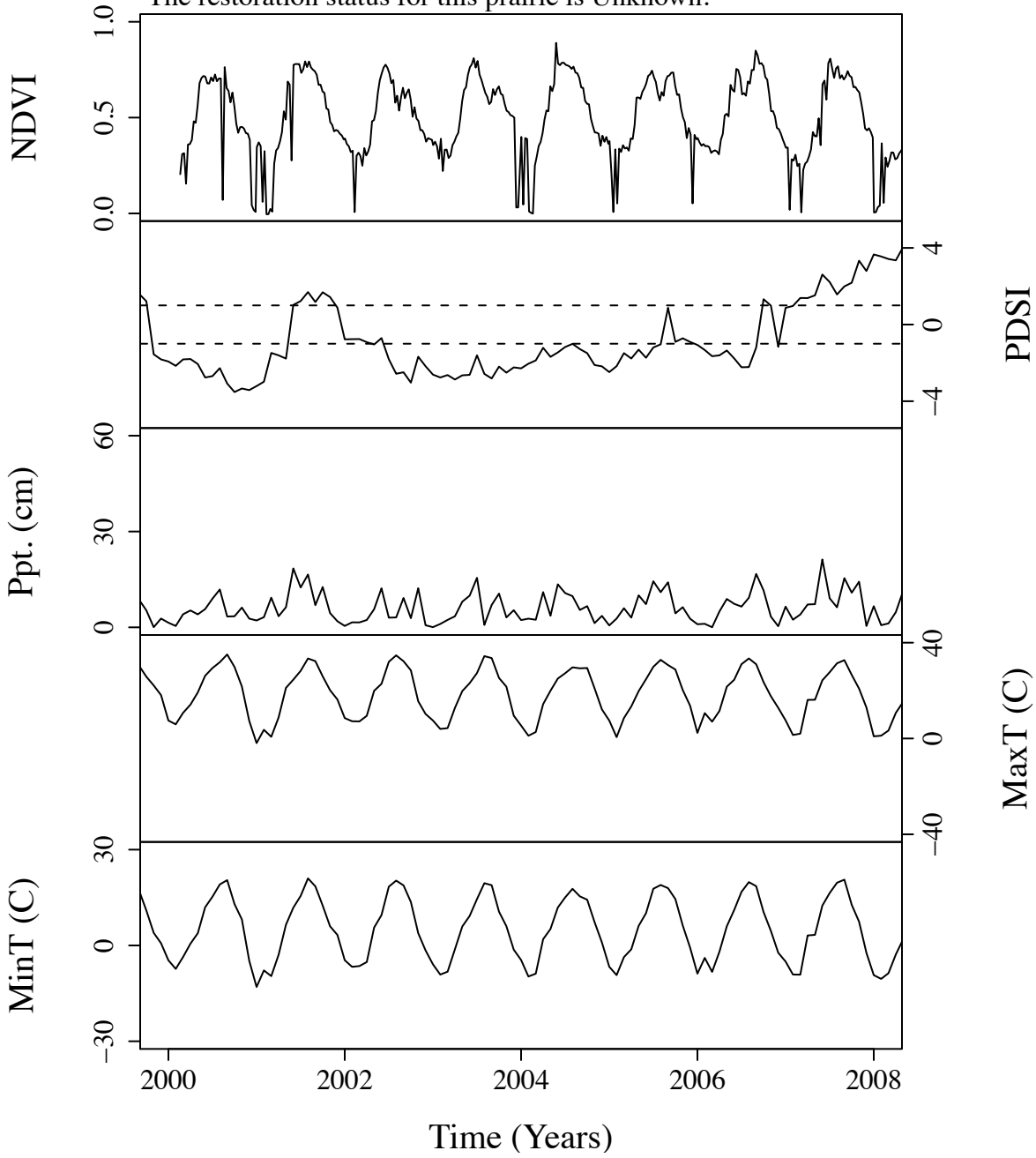

Figure B.158. Time series curves for nta409.
The community type for this prairie is Mixed.
The dominant photosynthetic pathway for this prairie is C4.
The restoration status for this prairie is Unknown.

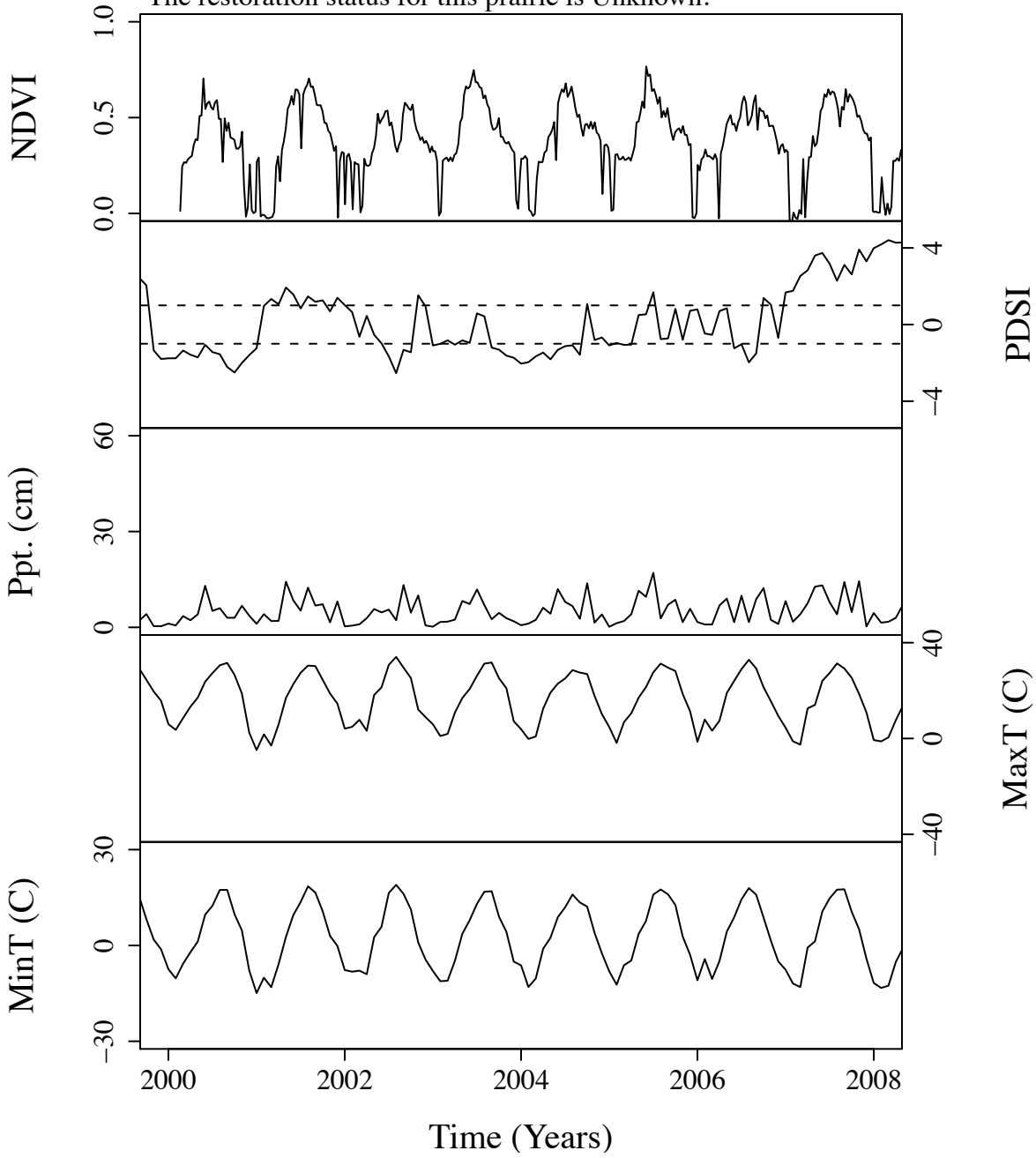

Figure B.159. Time series curves for nta413.
The community type for this prairie is Mixed.
The dominant photosynthetic pathway for this prairie is C4.
The restoration status for this prairie is Unknown.

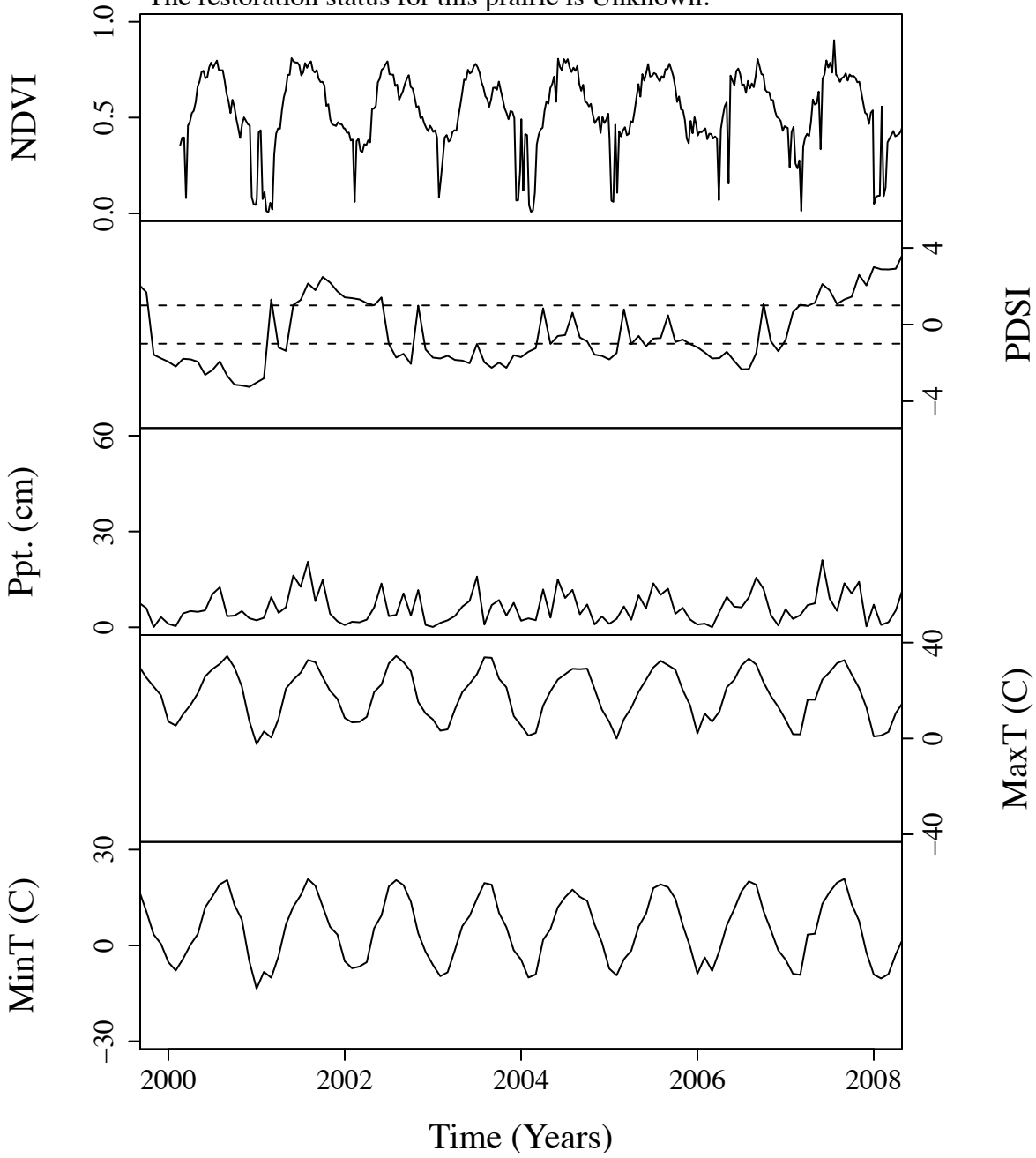

Figure B.160. Time series curves for nta501.
The community type for this prairie is Mixed.
The dominant photosynthetic pathway for this prairie is C4.
The restoration status for this prairie is Unknown.

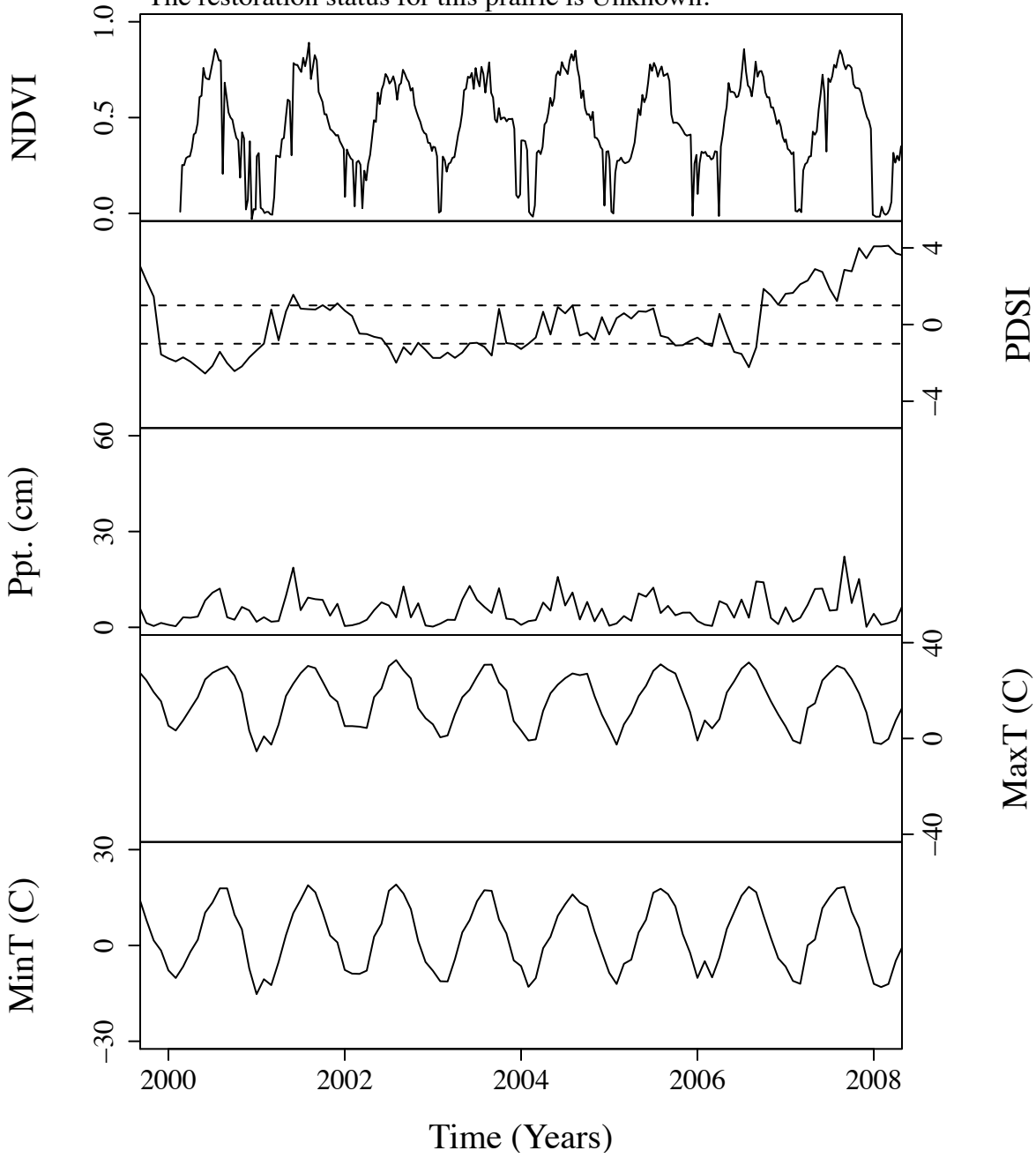

Figure B.161. Time series curves for nta573.
The community type for this prairie is Mixed.
The dominant photosynthetic pathway for this prairie is C4.
The restoration status for this prairie is Unknown.

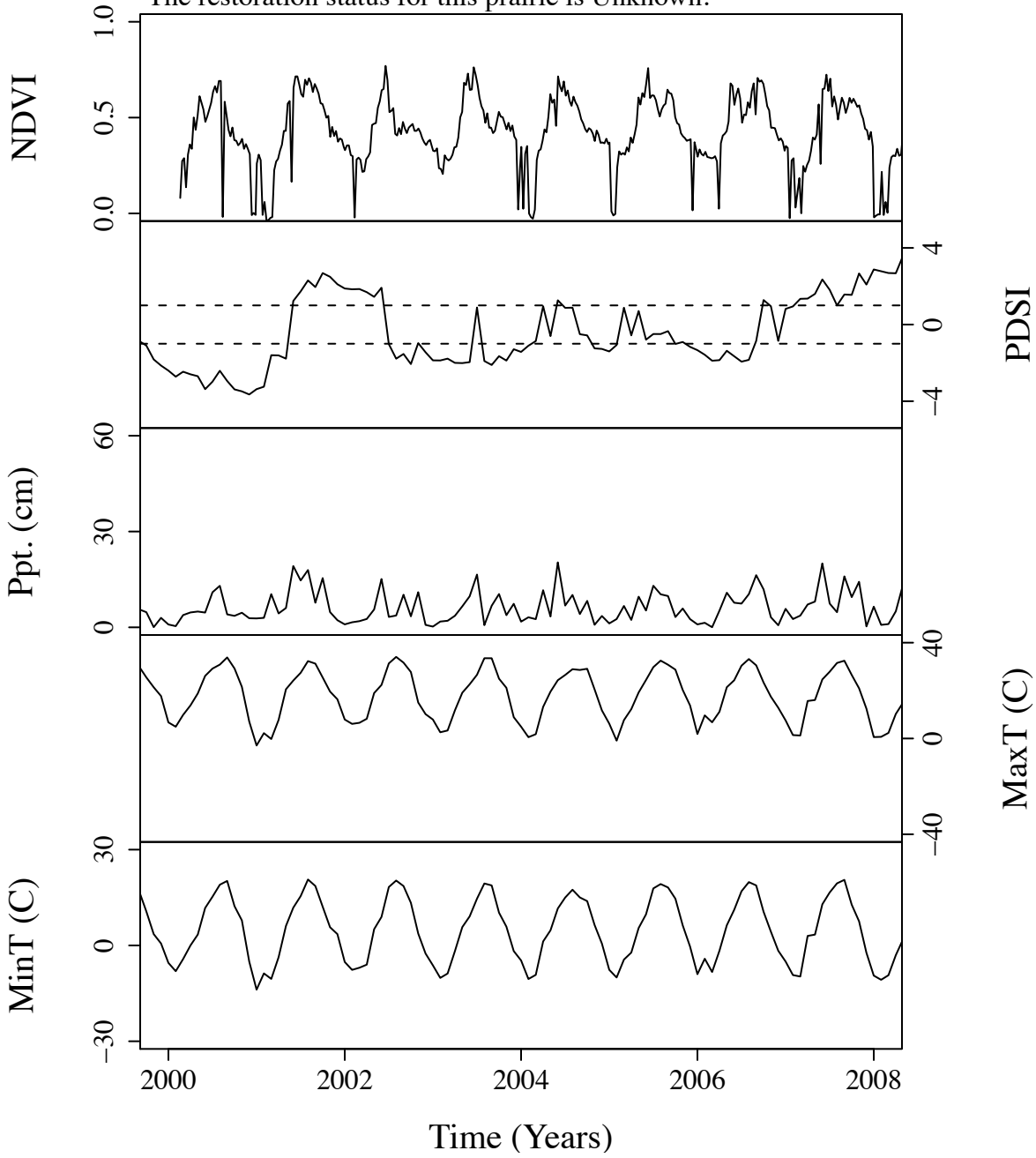

Figure B.162. Time series curves for nta621.
The community type for this prairie is Mixed.
The dominant photosynthetic pathway for this prairie is C4.
The restoration status for this prairie is Unknown.

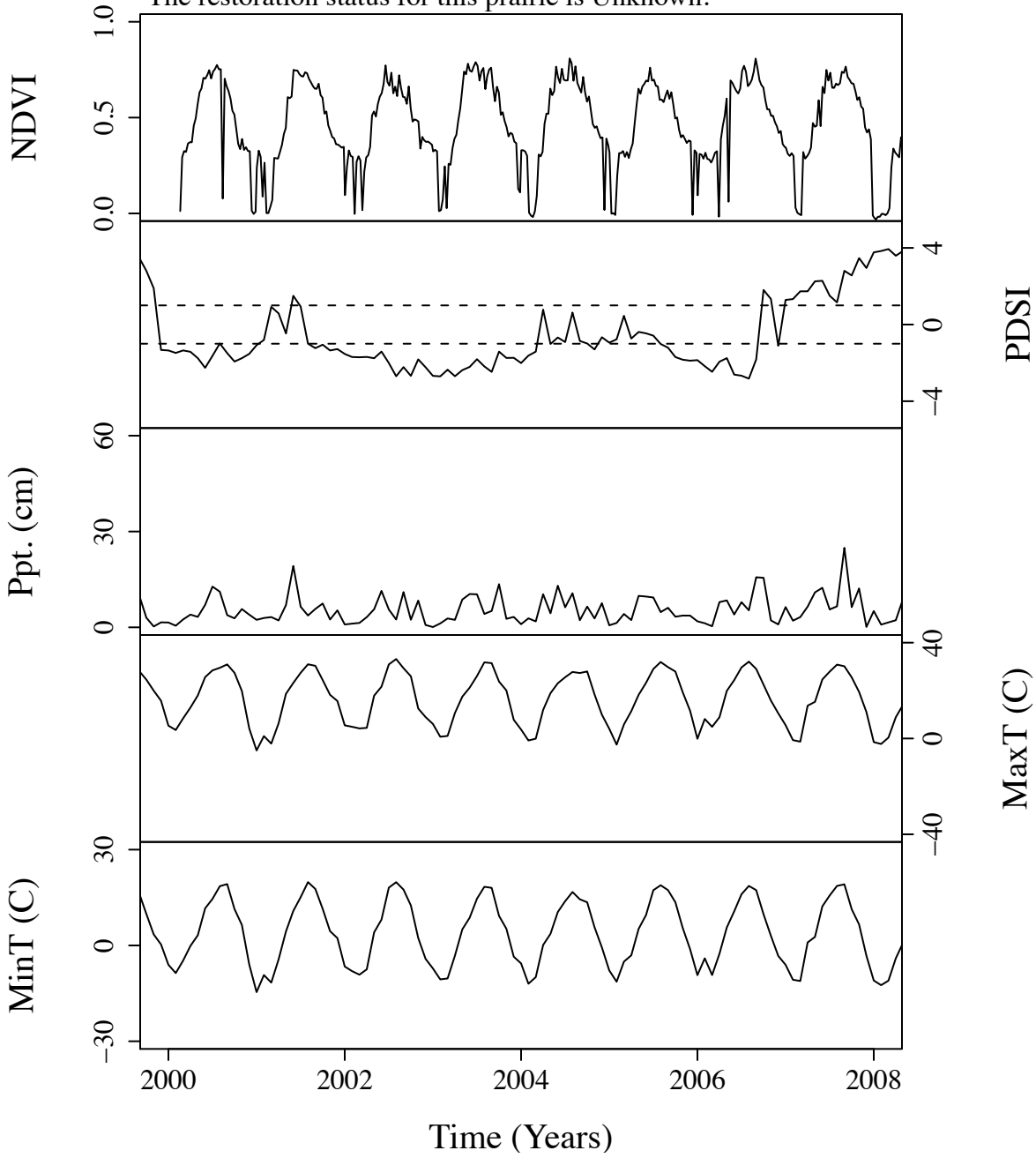

Figure B.163. Time series curves for nta783.
The community type for this prairie is Mixed.
The dominant photosynthetic pathway for this prairie is C4.
The restoration status for this prairie is Unknown.

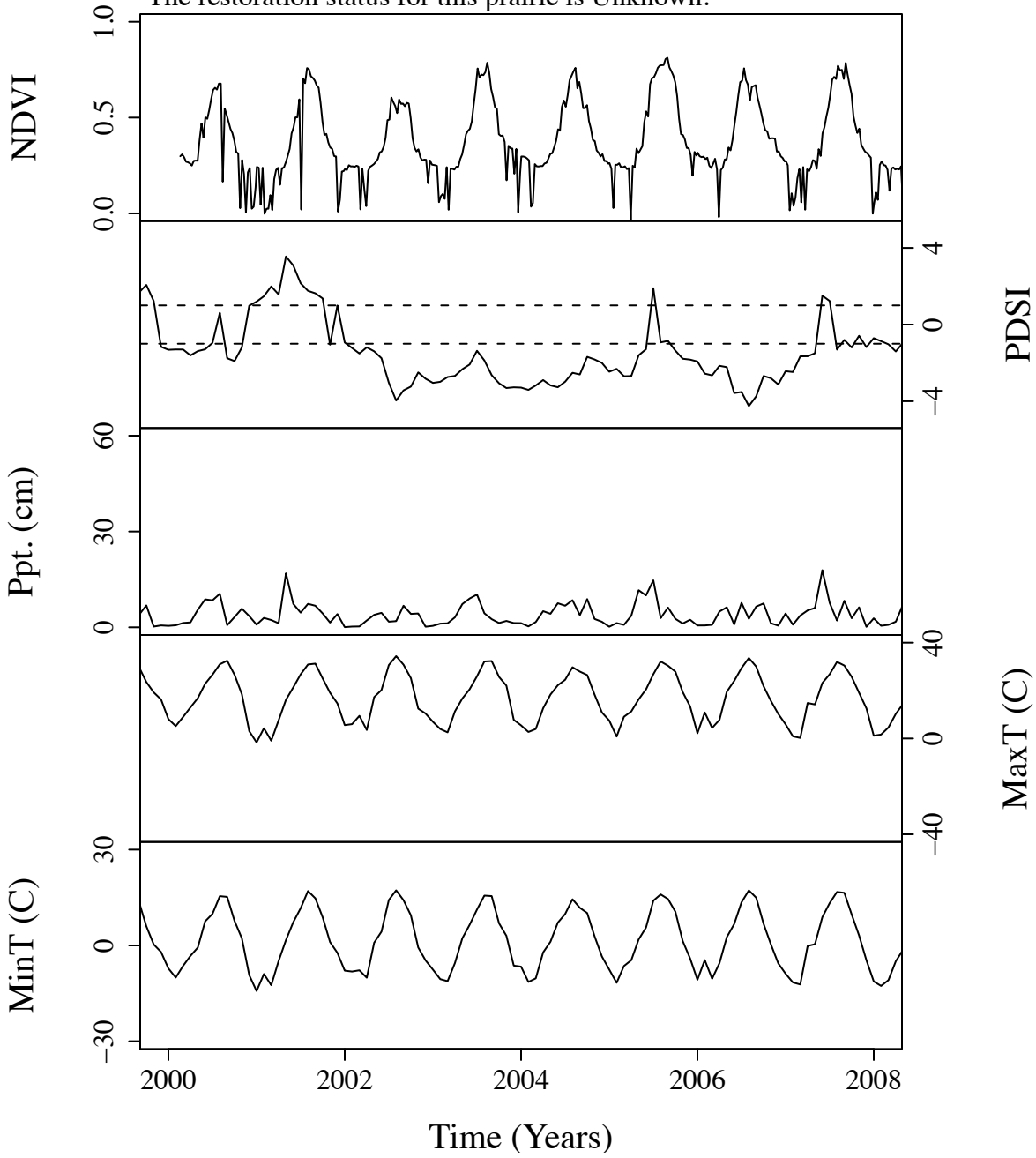

Figure B.164. Time series curves for nta791.
The community type for this prairie is Mixed.
The dominant photosynthetic pathway for this prairie is C4.
The restoration status for this prairie is Unknown.

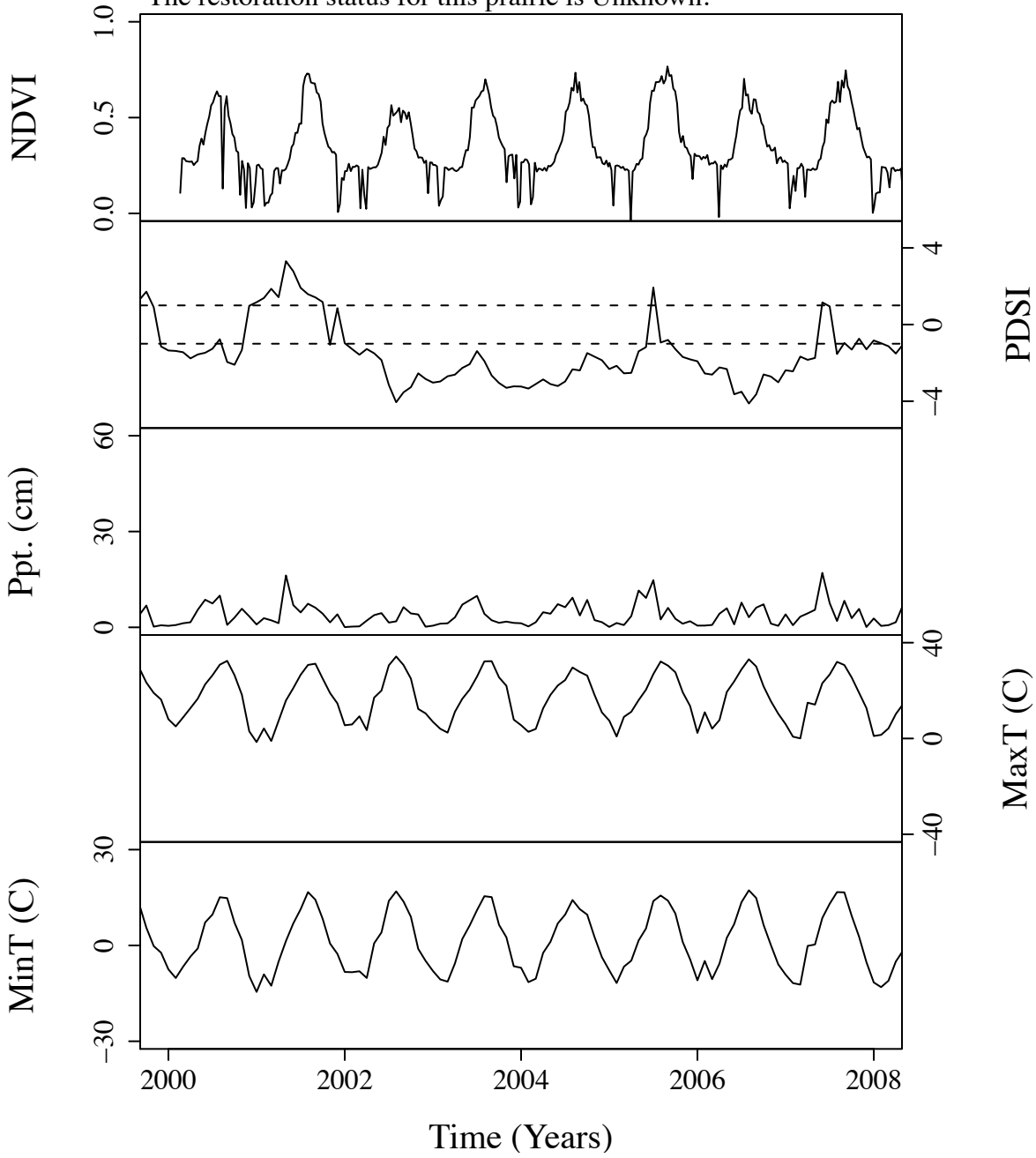

Figure B.165. Time series curves for nta835.
The community type for this prairie is Tall.
The dominant photosynthetic pathway for this prairie is C4.
The restoration status for this prairie is Unknown.

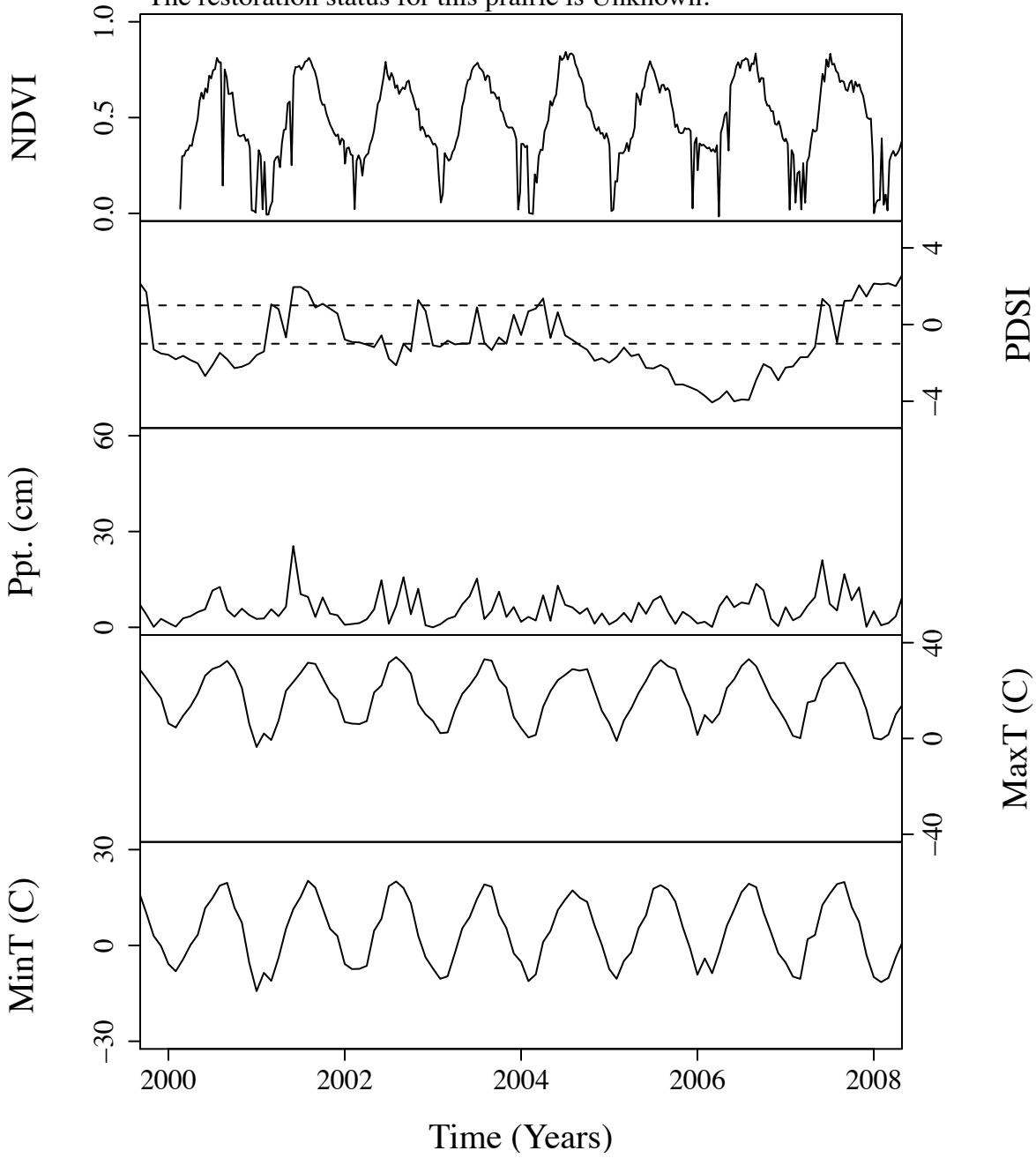

Figure B.166. Time series curves for nta906.
The community type for this prairie is Tall.
The dominant photosynthetic pathway for this prairie is C4.
The restoration status for this prairie is Unknown.

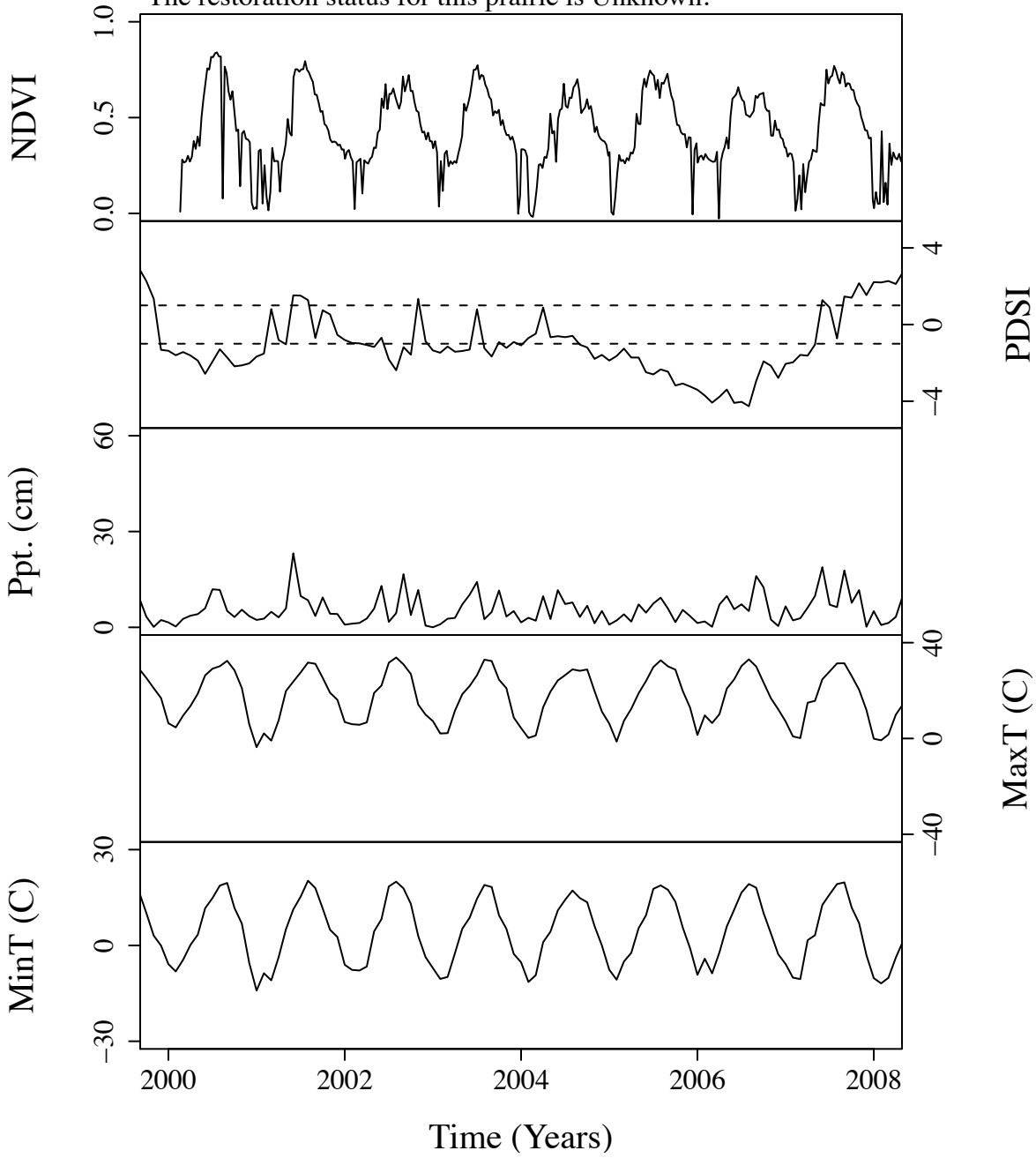

Figure B.167. Time series curves for nta934.
The community type for this prairie is Mixed.
The dominant photosynthetic pathway for this prairie is C4.
The restoration status for this prairie is Unknown.

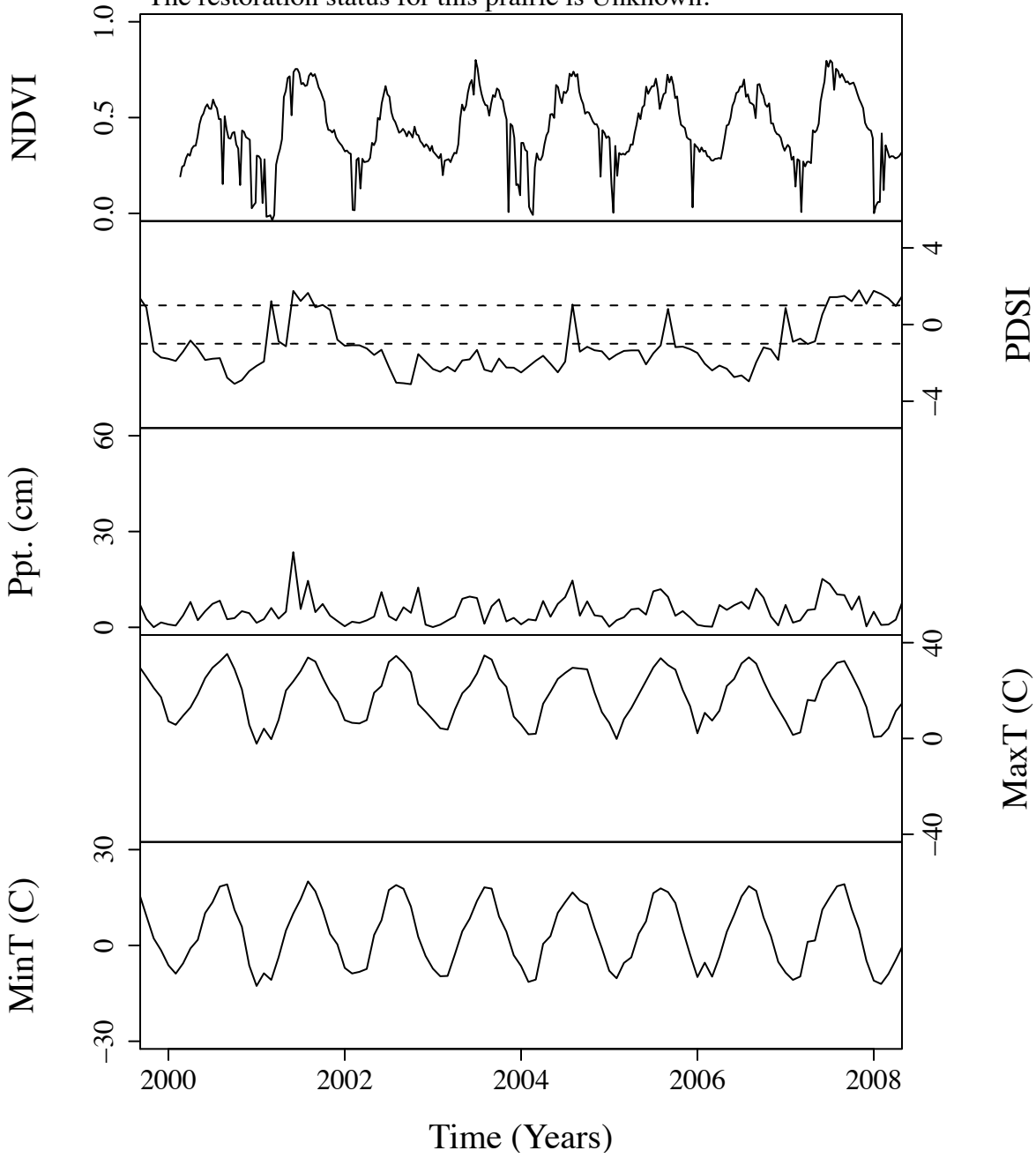

Figure B.168. Time series curves for nta941.
The community type for this prairie is Tall.
The dominant photosynthetic pathway for this prairie is C4.
The restoration status for this prairie is Unknown.

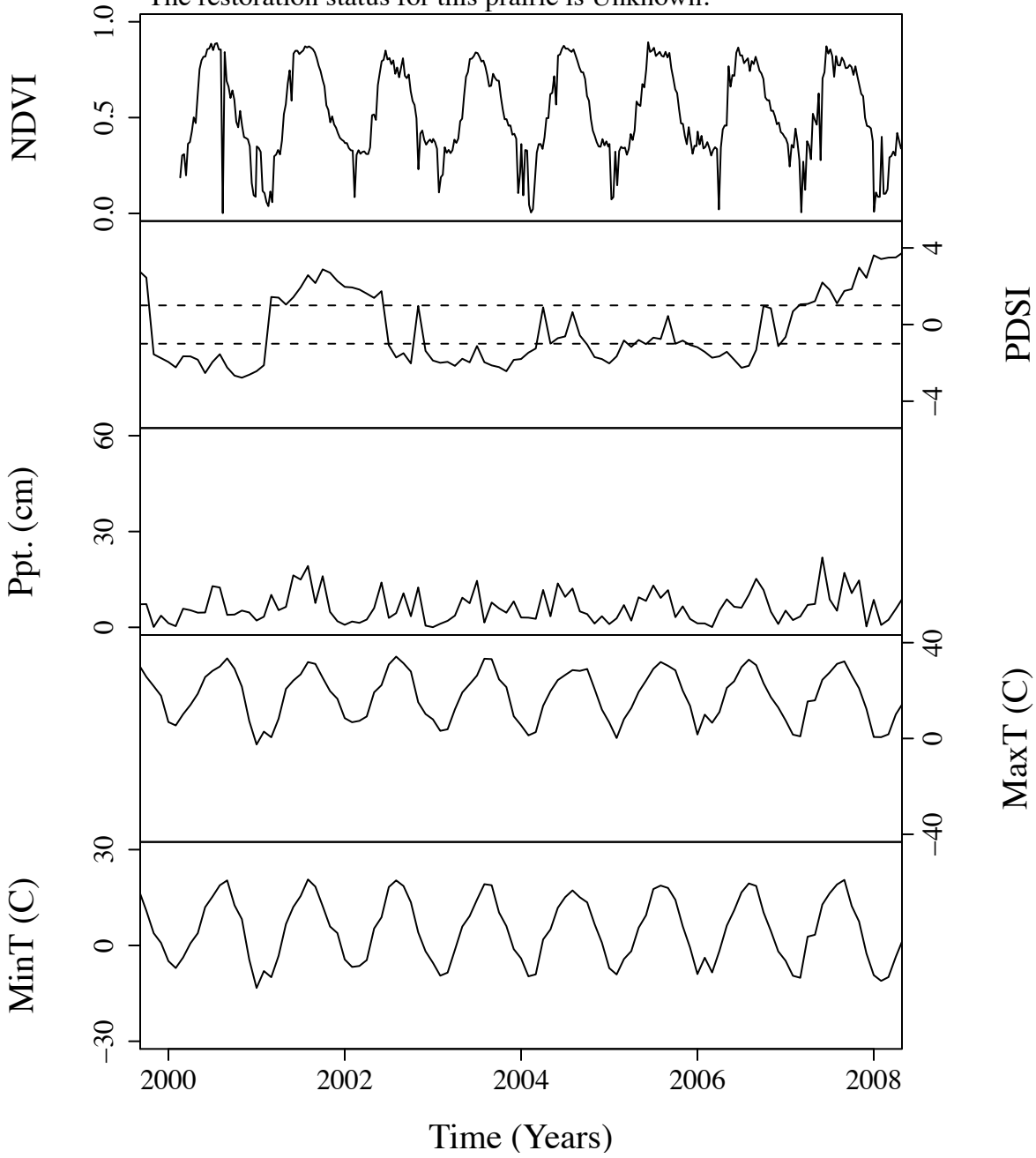

Figure B.169. Time series curves for nty186.
The community type for this prairie is Mixed.
The dominant photosynthetic pathway for this prairie is C4.
The restoration status for this prairie is Restored.

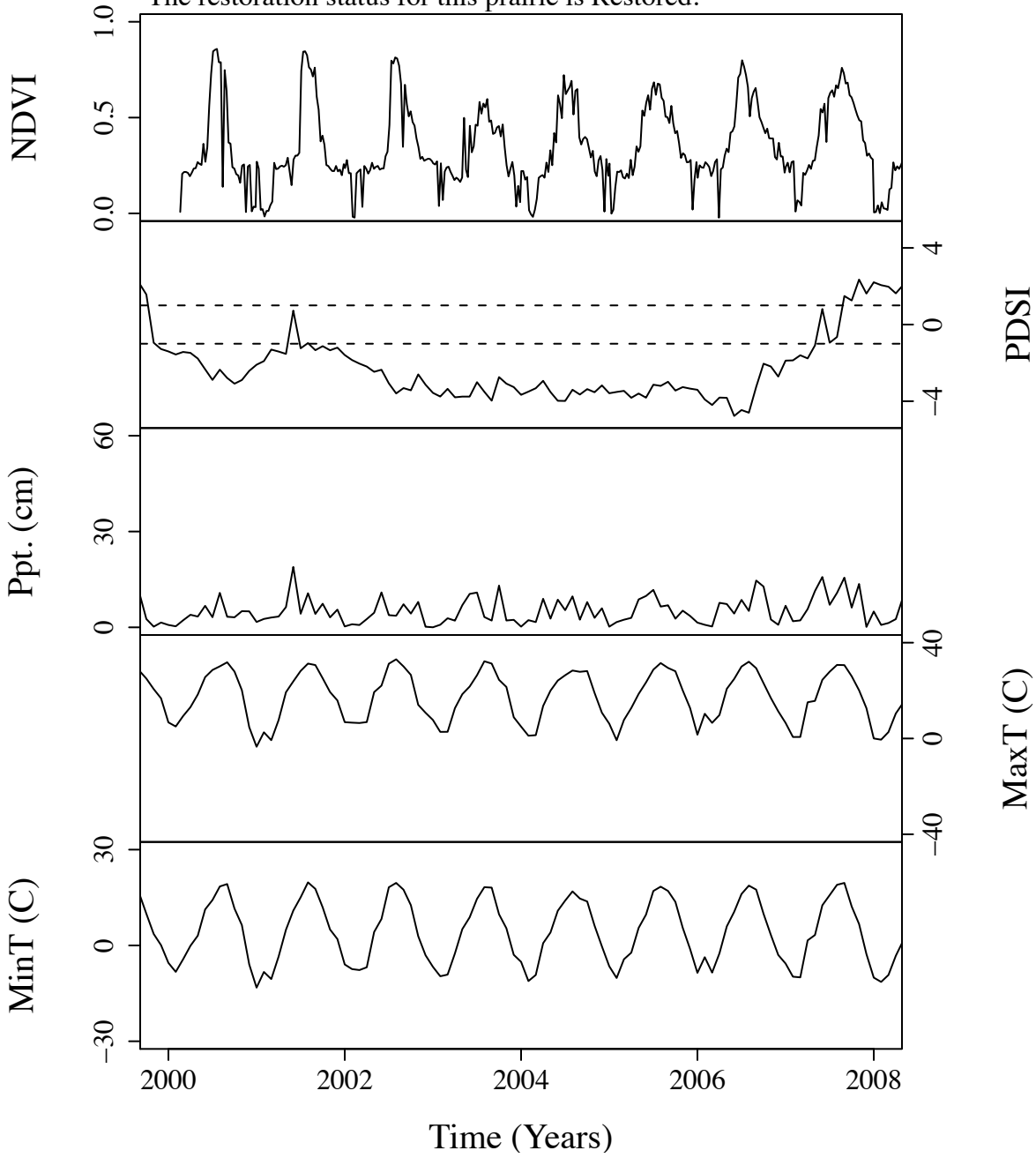

Figure B.170. Time series curves for nw30.
The community type for this prairie is Short.
The dominant photosynthetic pathway for this prairie is C4.
The restoration status for this prairie is Unknown.

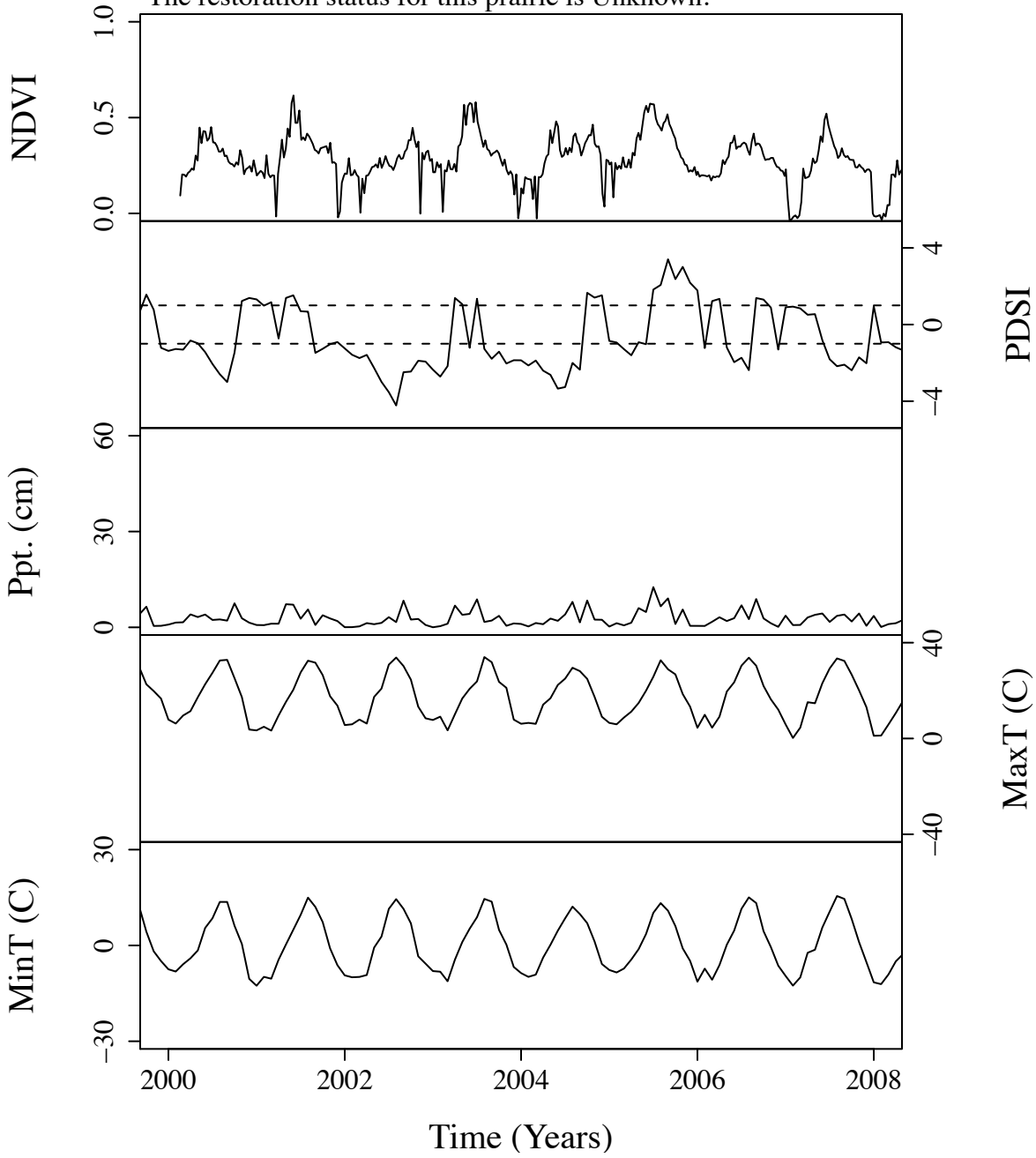

Figure B.171. Time series curves for nw40.
The community type for this prairie is Short.
The dominant photosynthetic pathway for this prairie is C4.
The restoration status for this prairie is Unknown.

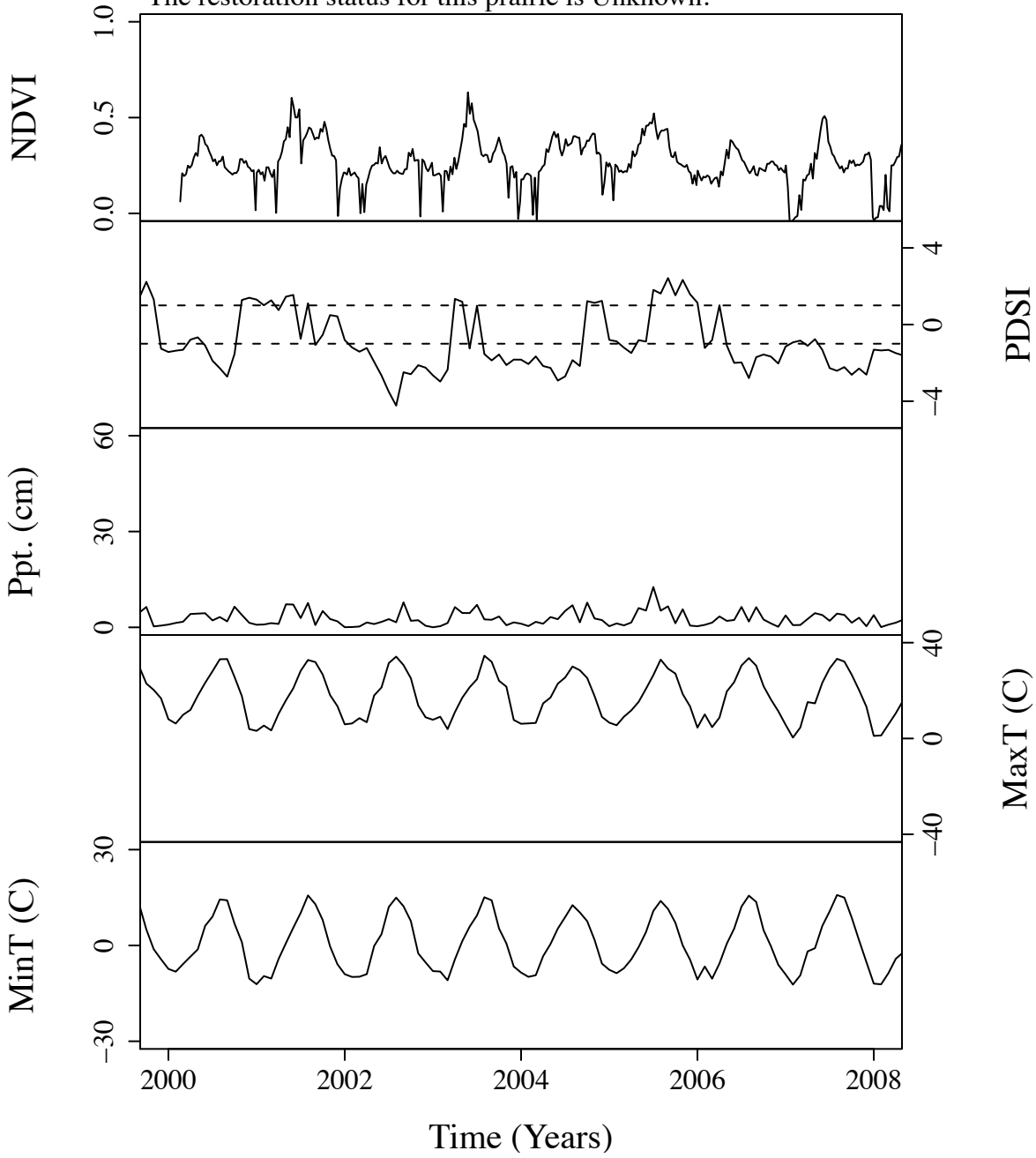

Figure B.172. Time series curves for nwe119.
The community type for this prairie is Mixed.
The dominant photosynthetic pathway for this prairie is C4.
The restoration status for this prairie is Unknown.

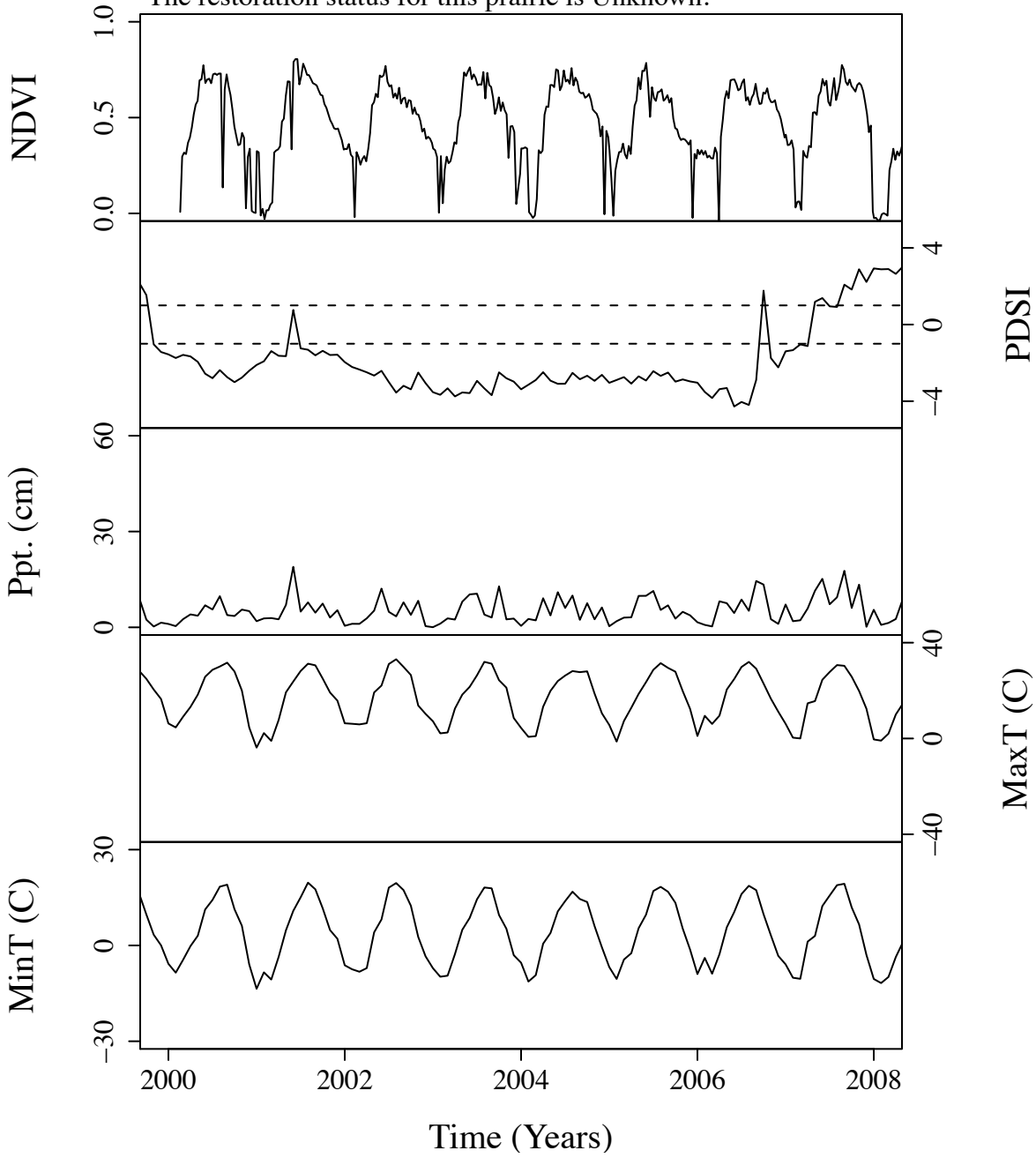

Figure B.173. Time series curves for nwe161.
The community type for this prairie is Short.
The dominant photosynthetic pathway for this prairie is C4.
The restoration status for this prairie is Unknown.

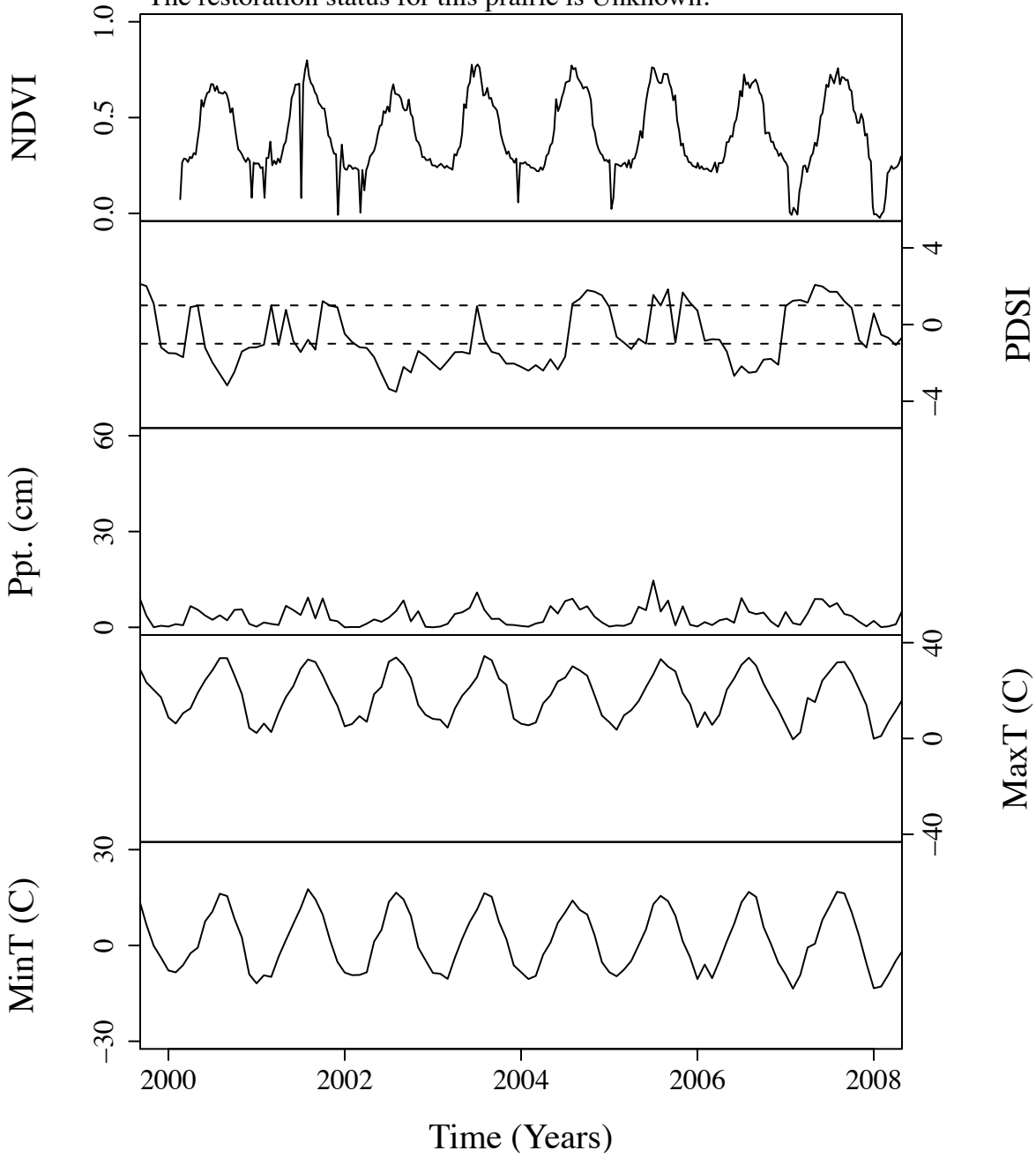

Figure B.174. Time series curves for nwe175.
The community type for this prairie is Mixed.
The dominant photosynthetic pathway for this prairie is C4.
The restoration status for this prairie is Unknown.

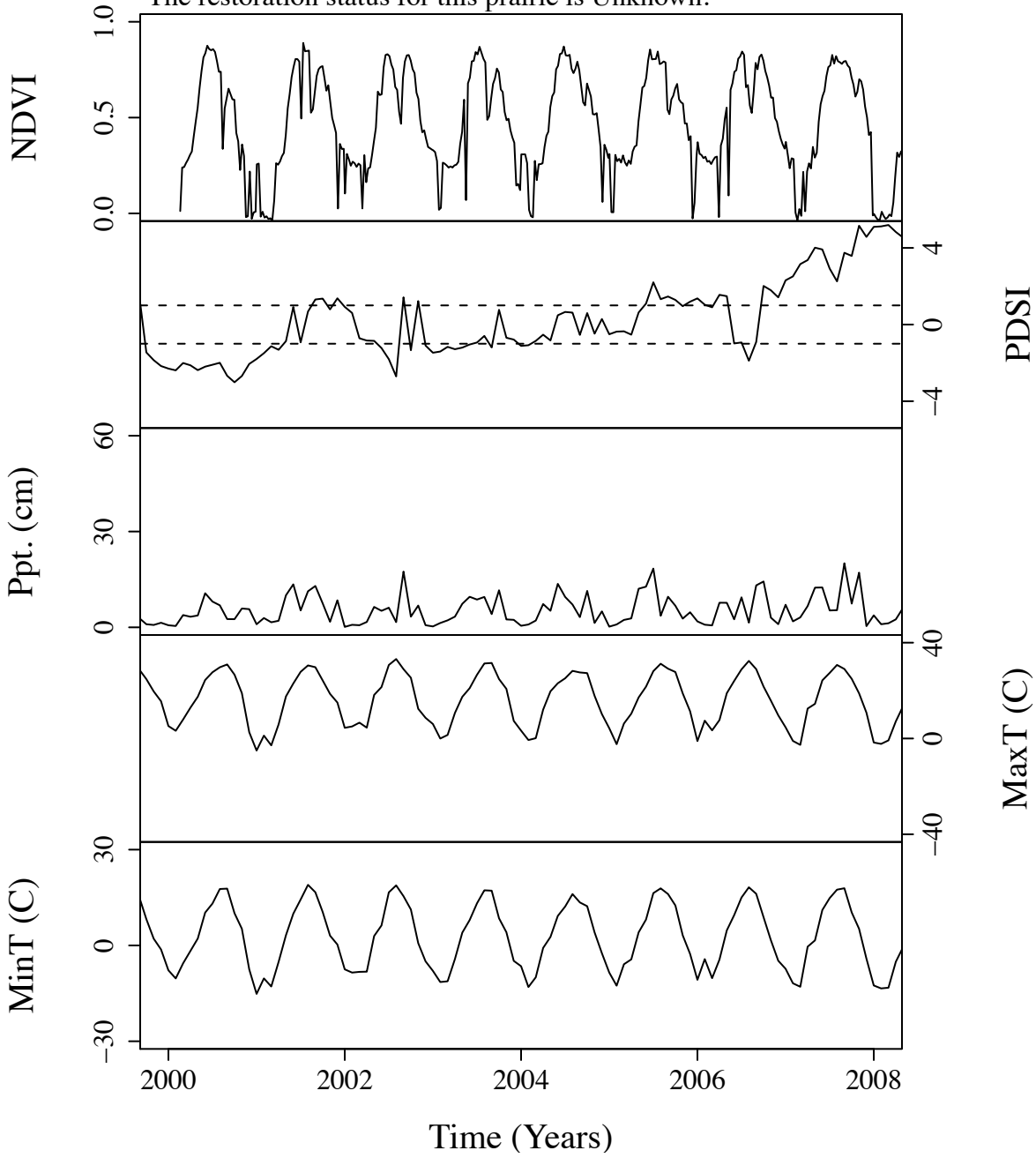

Figure B.175. Time series curves for nwe2.
The community type for this prairie is Short.
The dominant photosynthetic pathway for this prairie is C4.
The restoration status for this prairie is Unknown.

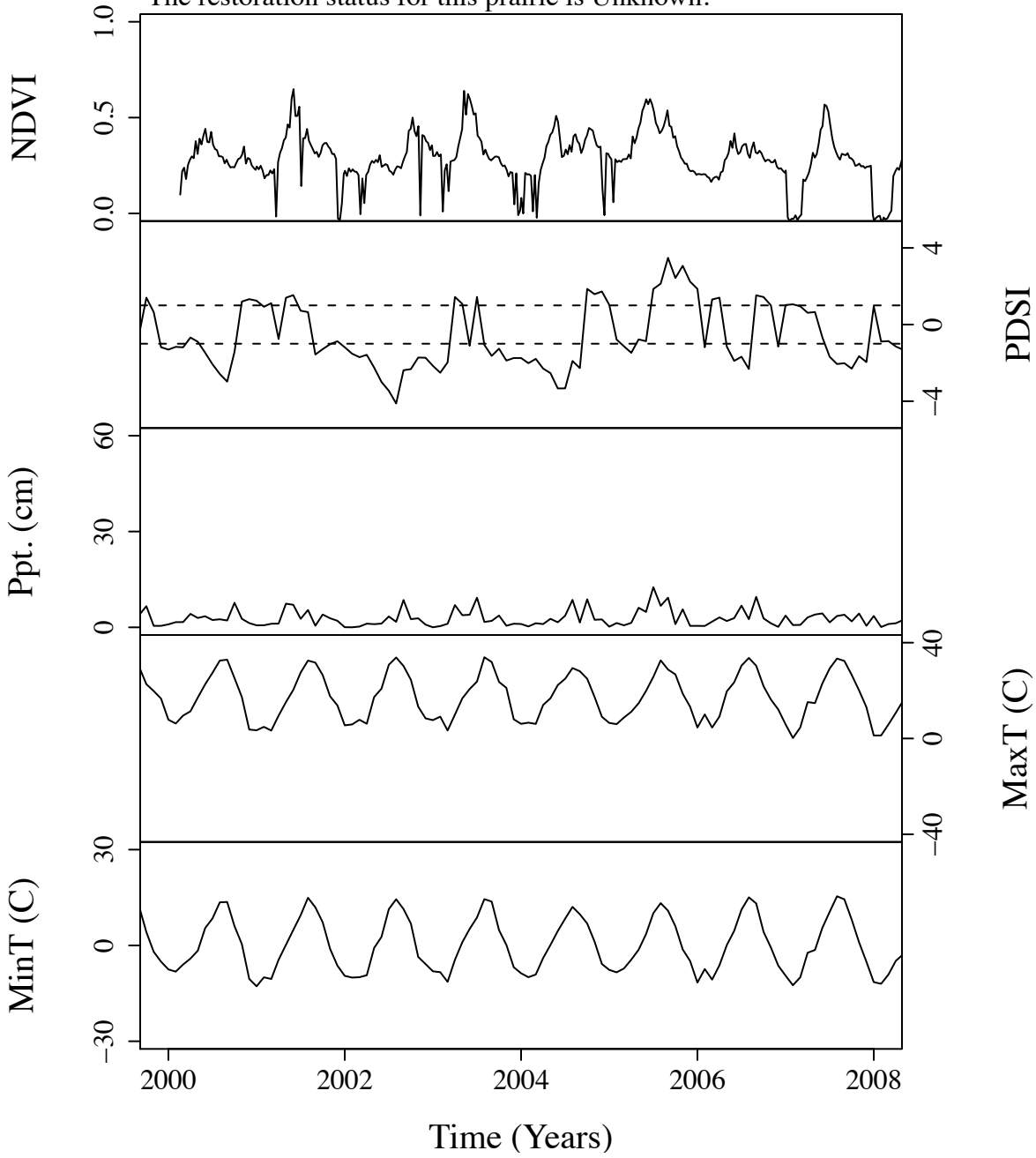

Figure B.176. Time series curves for nwe21.
The community type for this prairie is Short.
The dominant photosynthetic pathway for this prairie is C4.
The restoration status for this prairie is Unknown.

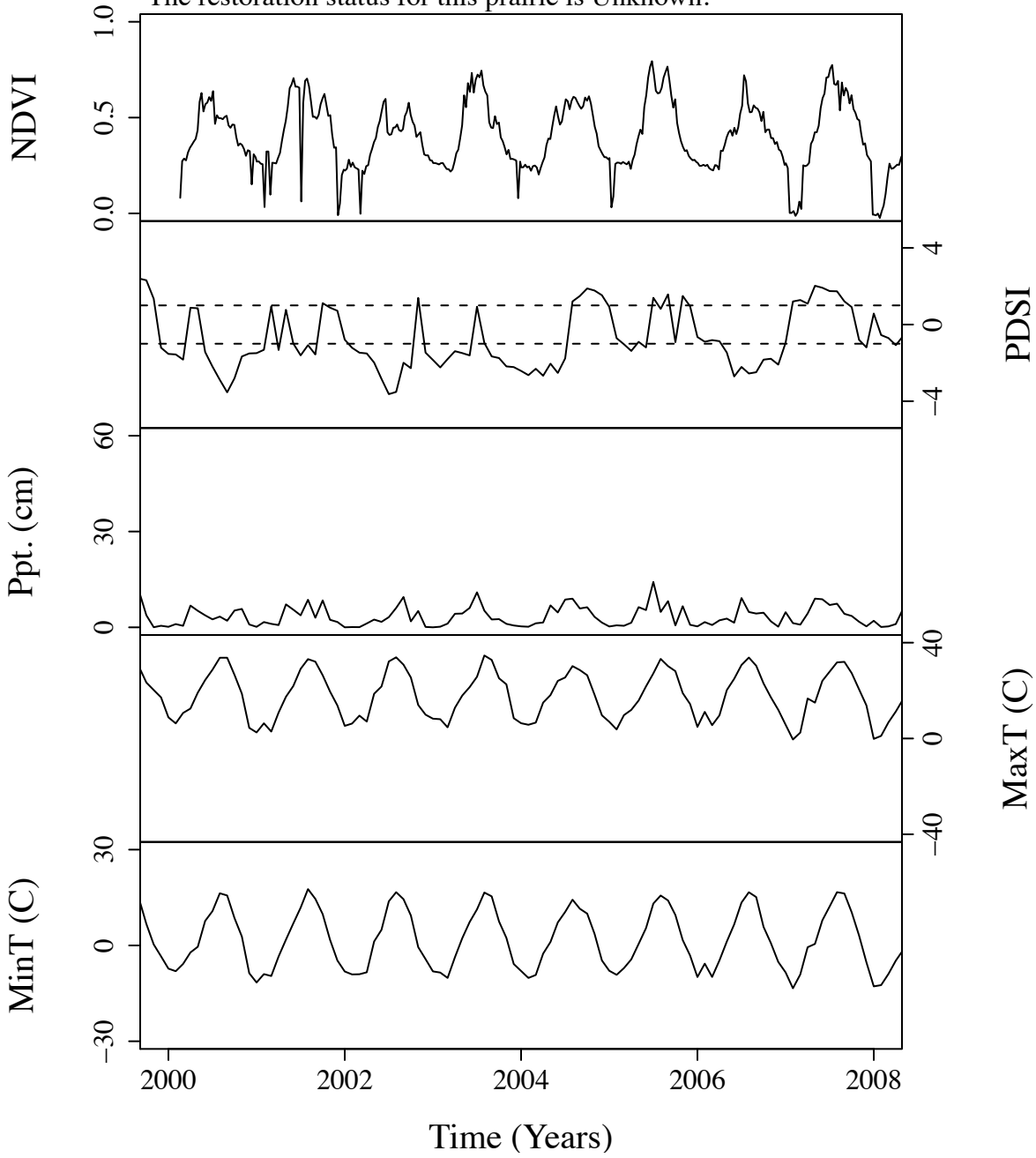

Figure B.177. Time series curves for nwe25.
The community type for this prairie is Short.
The dominant photosynthetic pathway for this prairie is C4.
The restoration status for this prairie is Unknown.

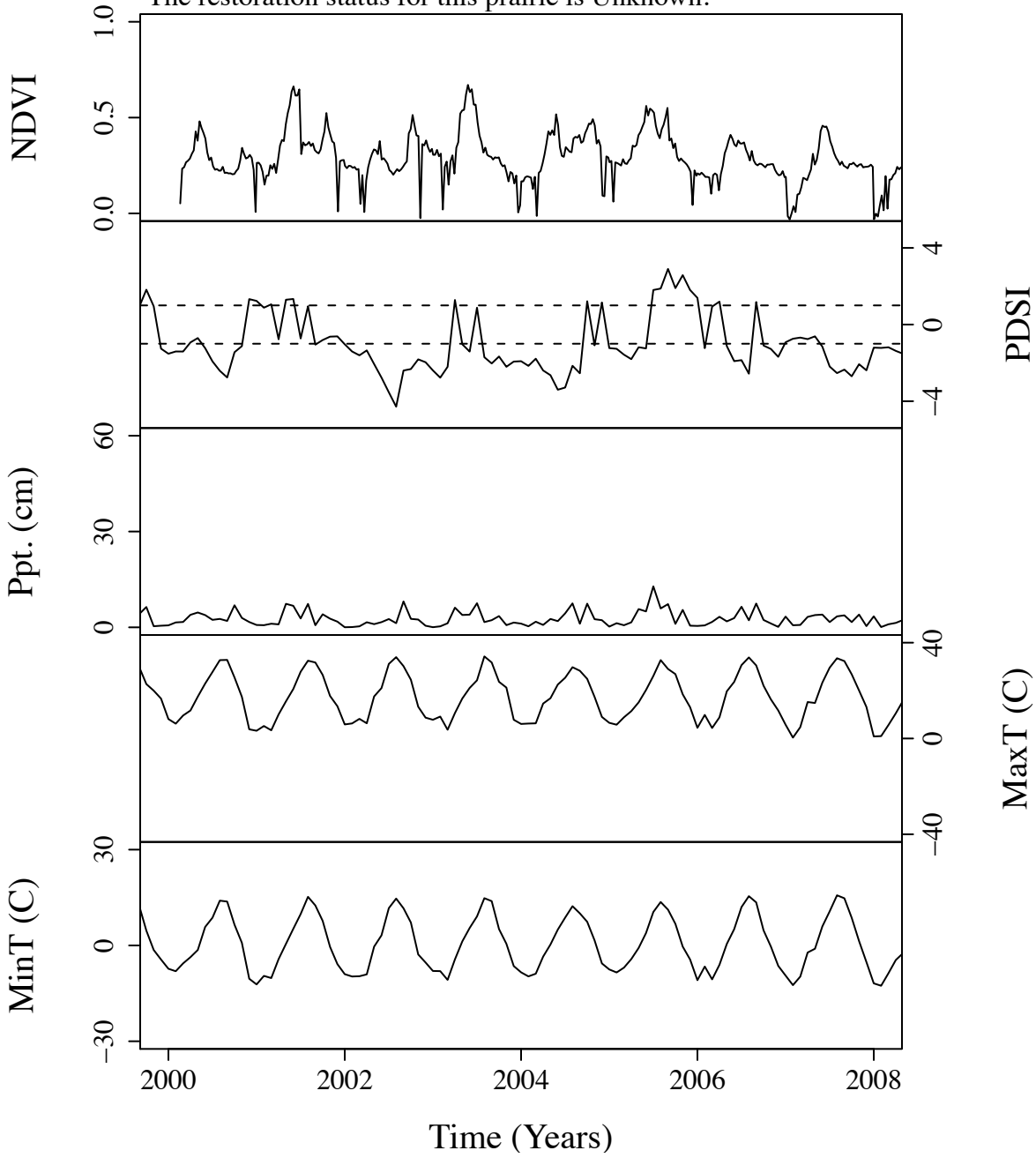

Figure B.178. Time series curves for nwe351.
The community type for this prairie is Tall.
The dominant photosynthetic pathway for this prairie is C4.
The restoration status for this prairie is Unknown.

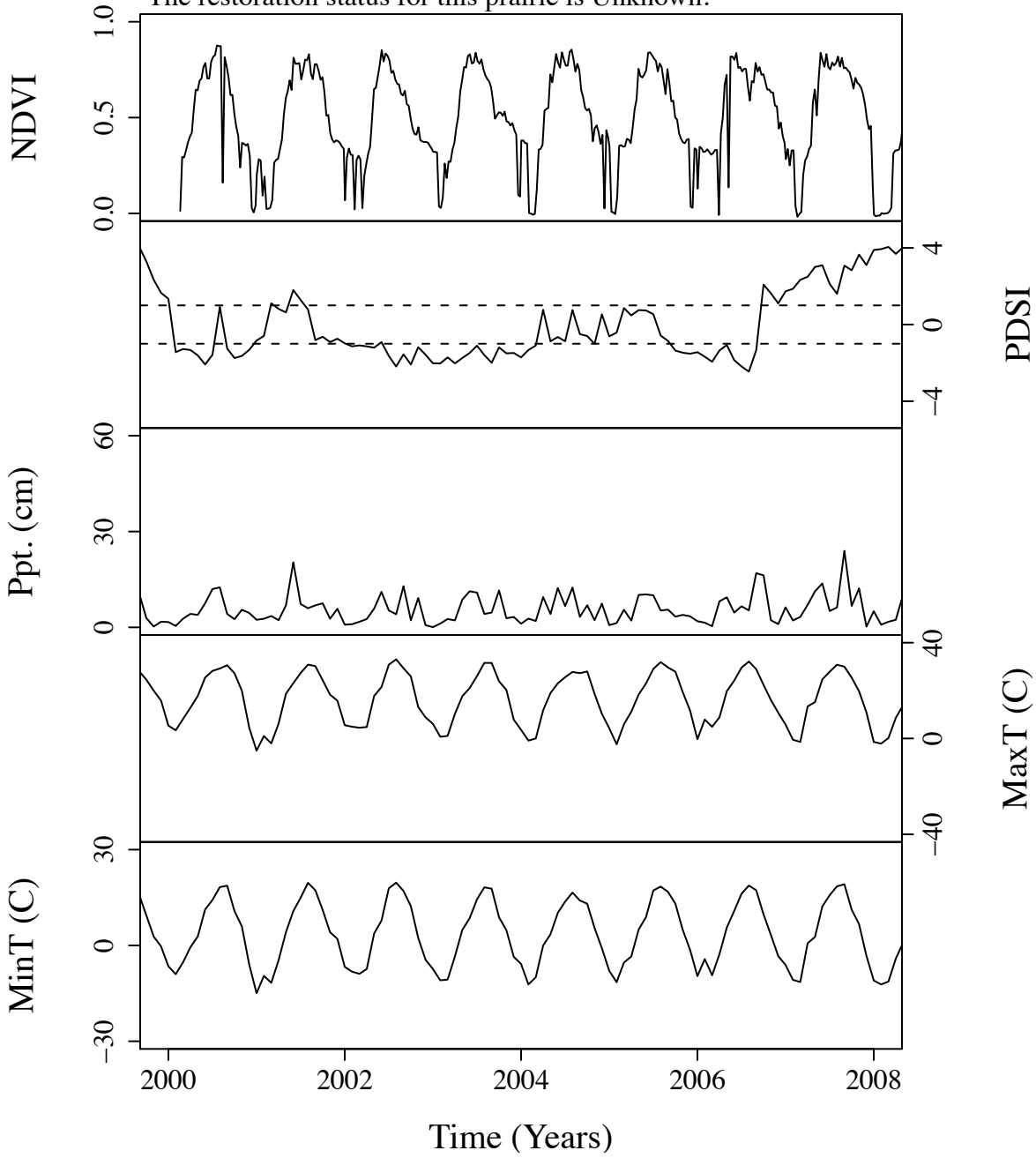

Figure B.179. Time series curves for nwe354.
The community type for this prairie is Tall.
The dominant photosynthetic pathway for this prairie is C4.
The restoration status for this prairie is Unknown.

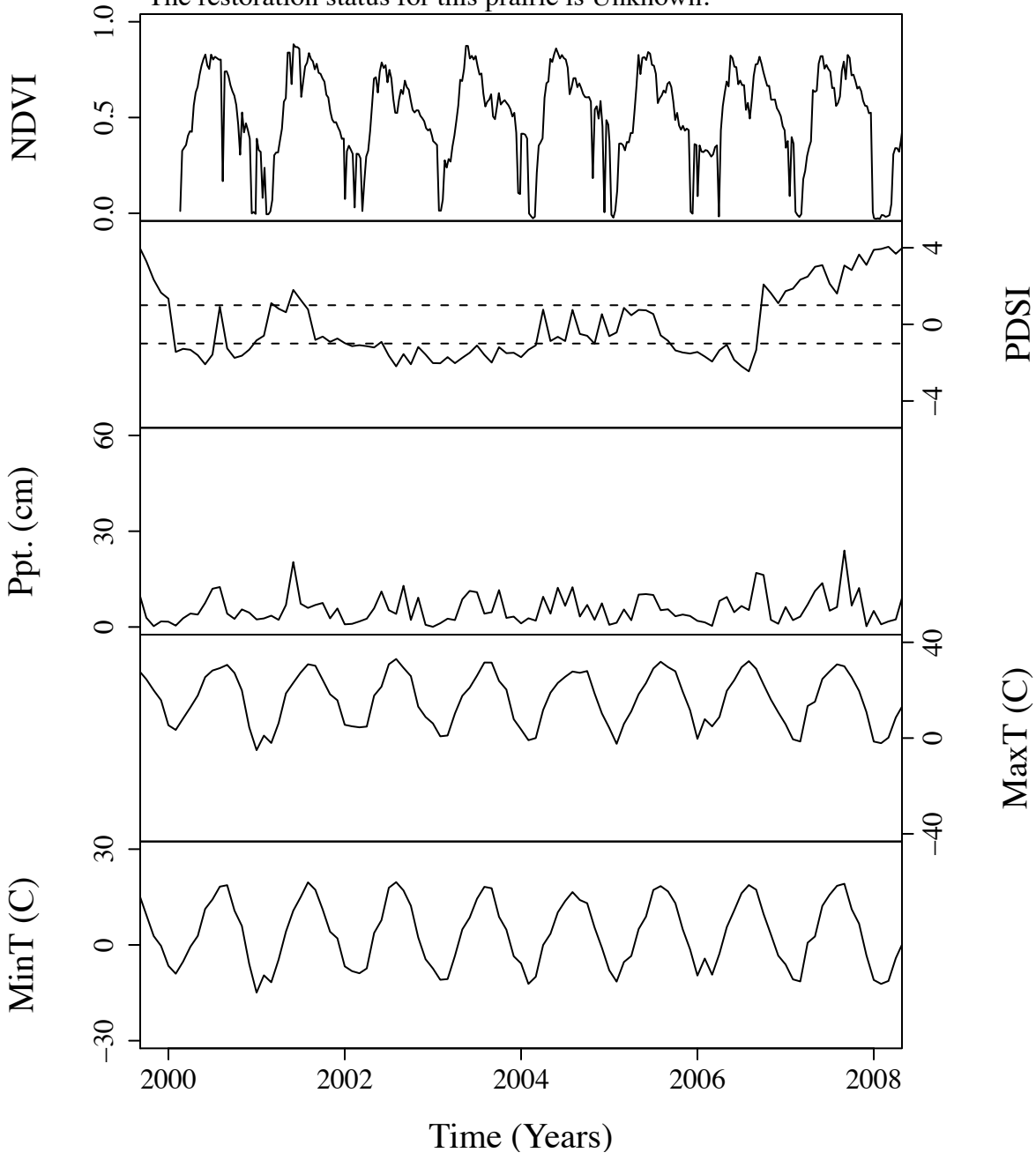

Figure B.180. Time series curves for nwe38.
The community type for this prairie is Short.
The dominant photosynthetic pathway for this prairie is C4.
The restoration status for this prairie is Unknown.

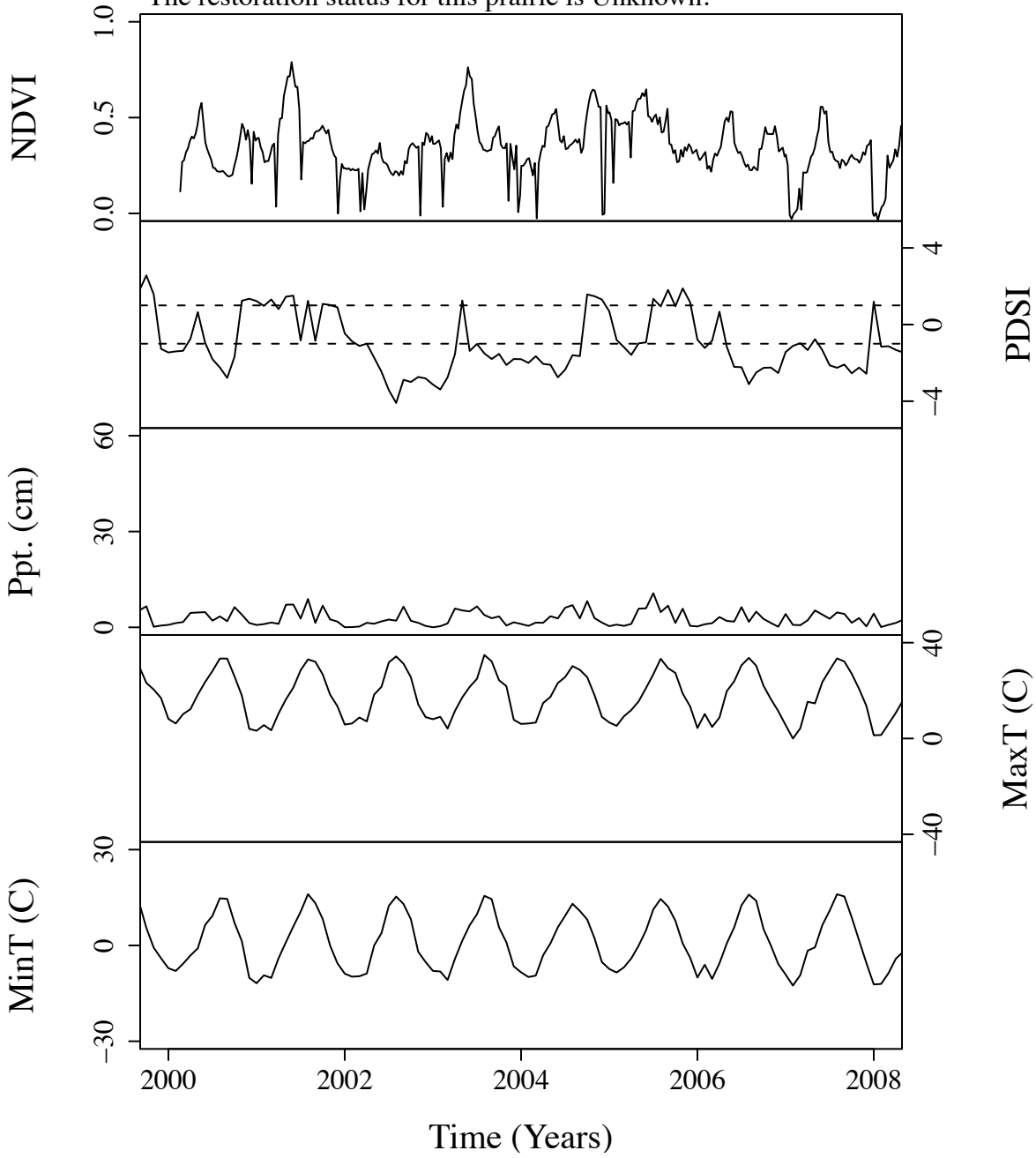

Figure B.181. Time series curves for nwe400.
The community type for this prairie is Tall.
The dominant photosynthetic pathway for this prairie is C4.
The restoration status for this prairie is Unknown.

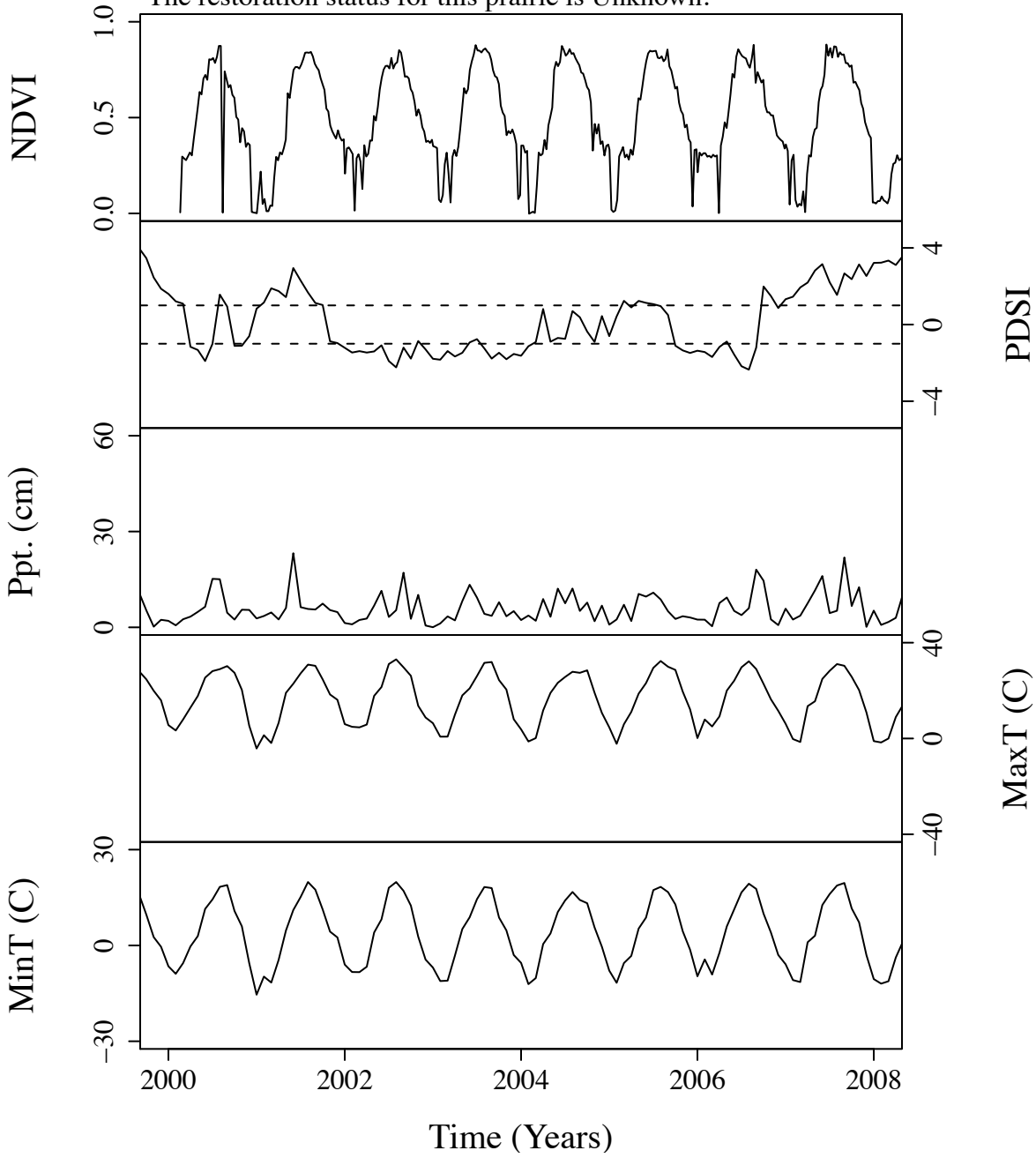

Figure B.182. Time series curves for nwe475.
The community type for this prairie is Mixed.
The dominant photosynthetic pathway for this prairie is C4.
The restoration status for this prairie is Unknown.

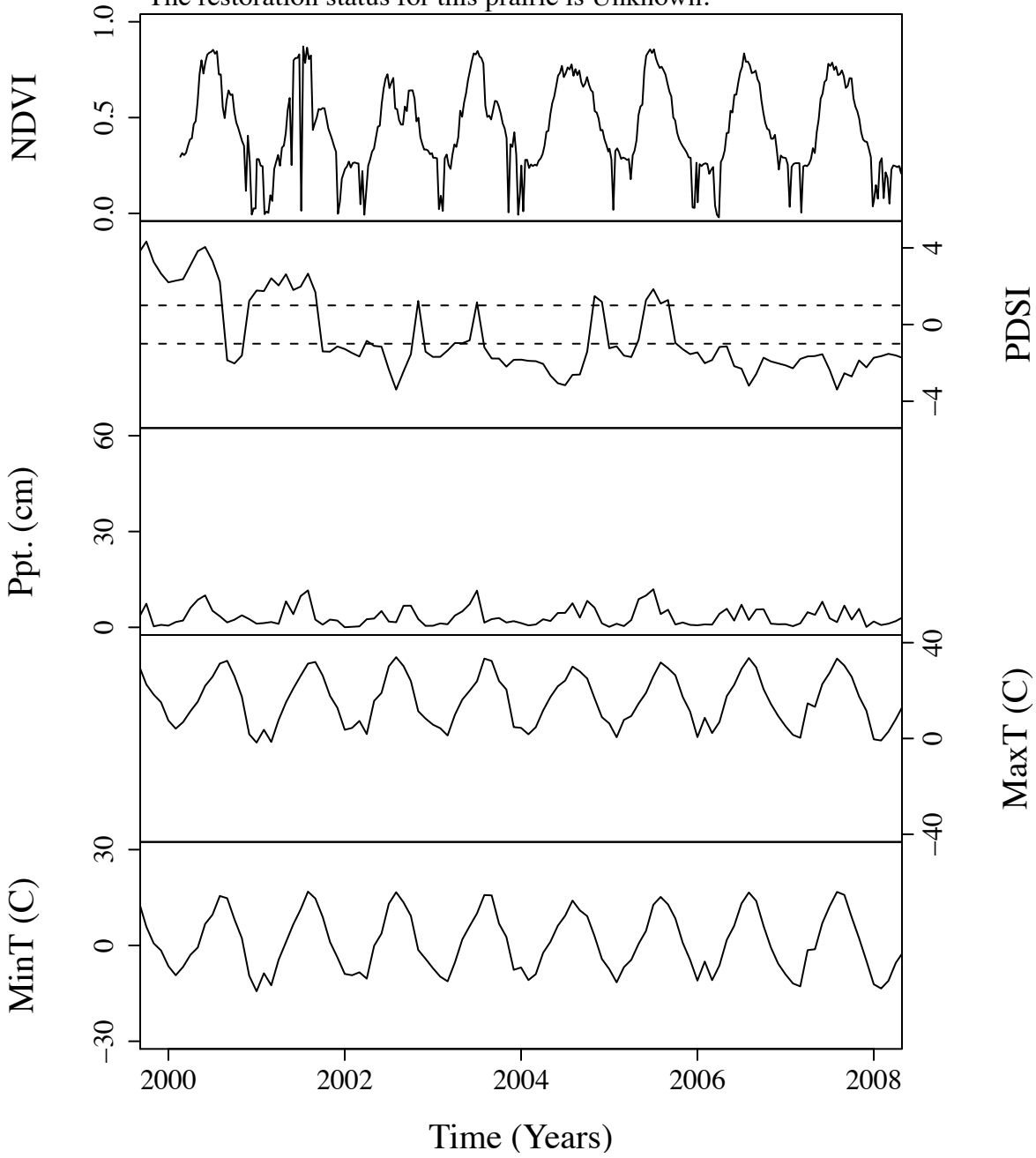

Figure B.183. Time series curves for nwe496.
The community type for this prairie is Short.
The dominant photosynthetic pathway for this prairie is C4.
The restoration status for this prairie is Unknown.

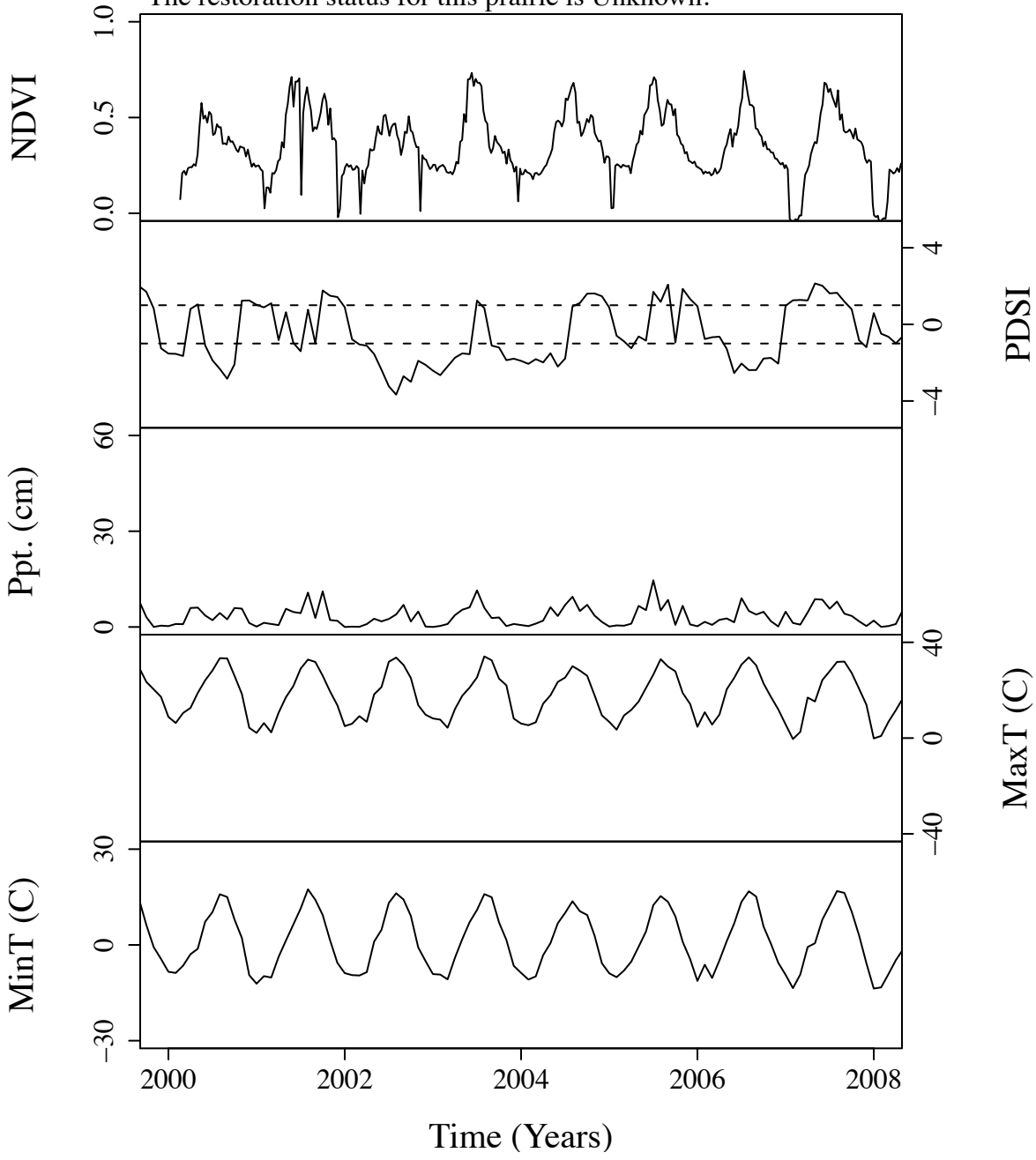

Figure B.184. Time series curves for nwe607.
The community type for this prairie is Tall.
The dominant photosynthetic pathway for this prairie is C4.
The restoration status for this prairie is Unknown.

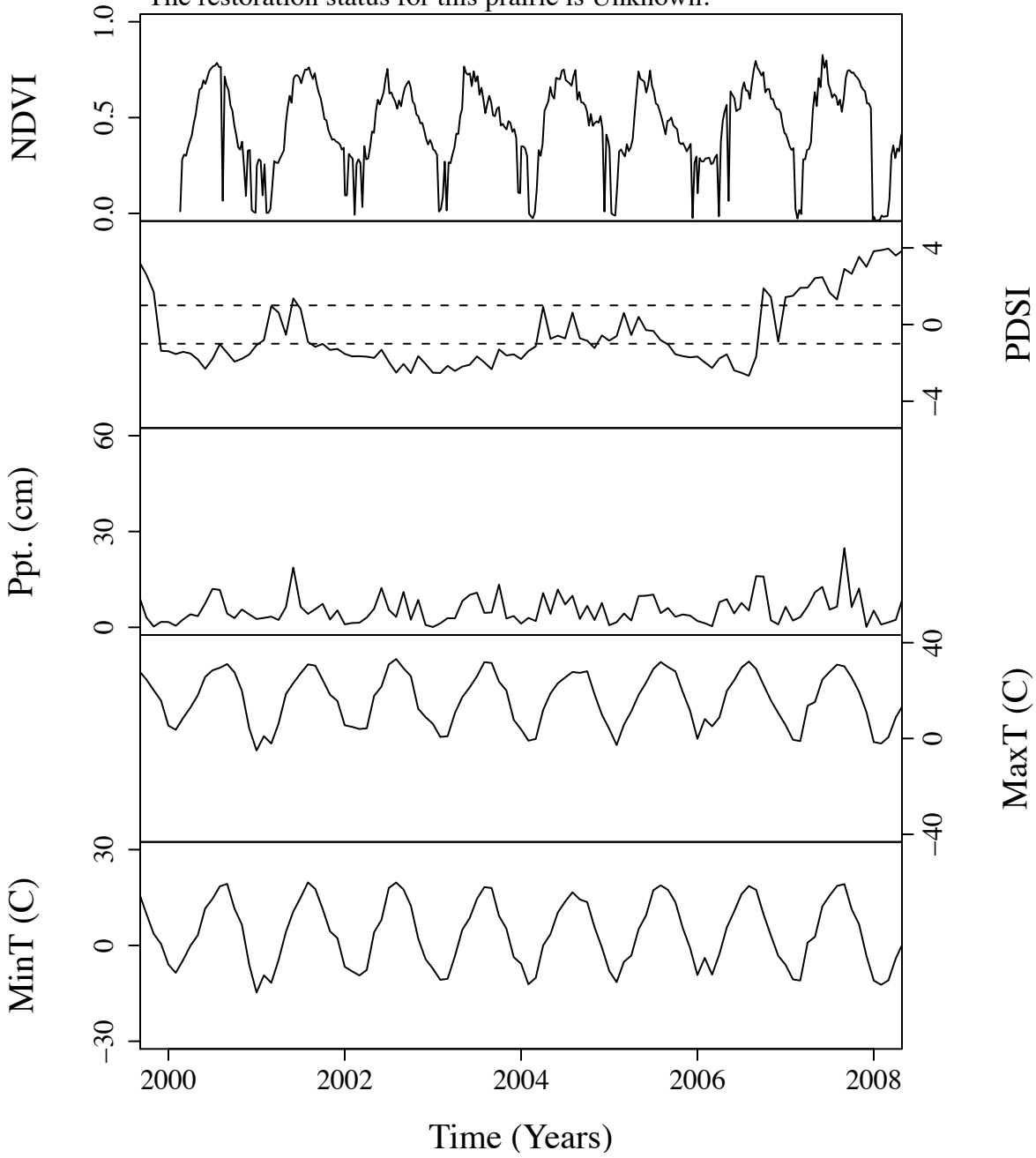

Figure B.185. Time series curves for nwe685.
The community type for this prairie is Mixed.
The dominant photosynthetic pathway for this prairie is C4.
The restoration status for this prairie is Unknown.

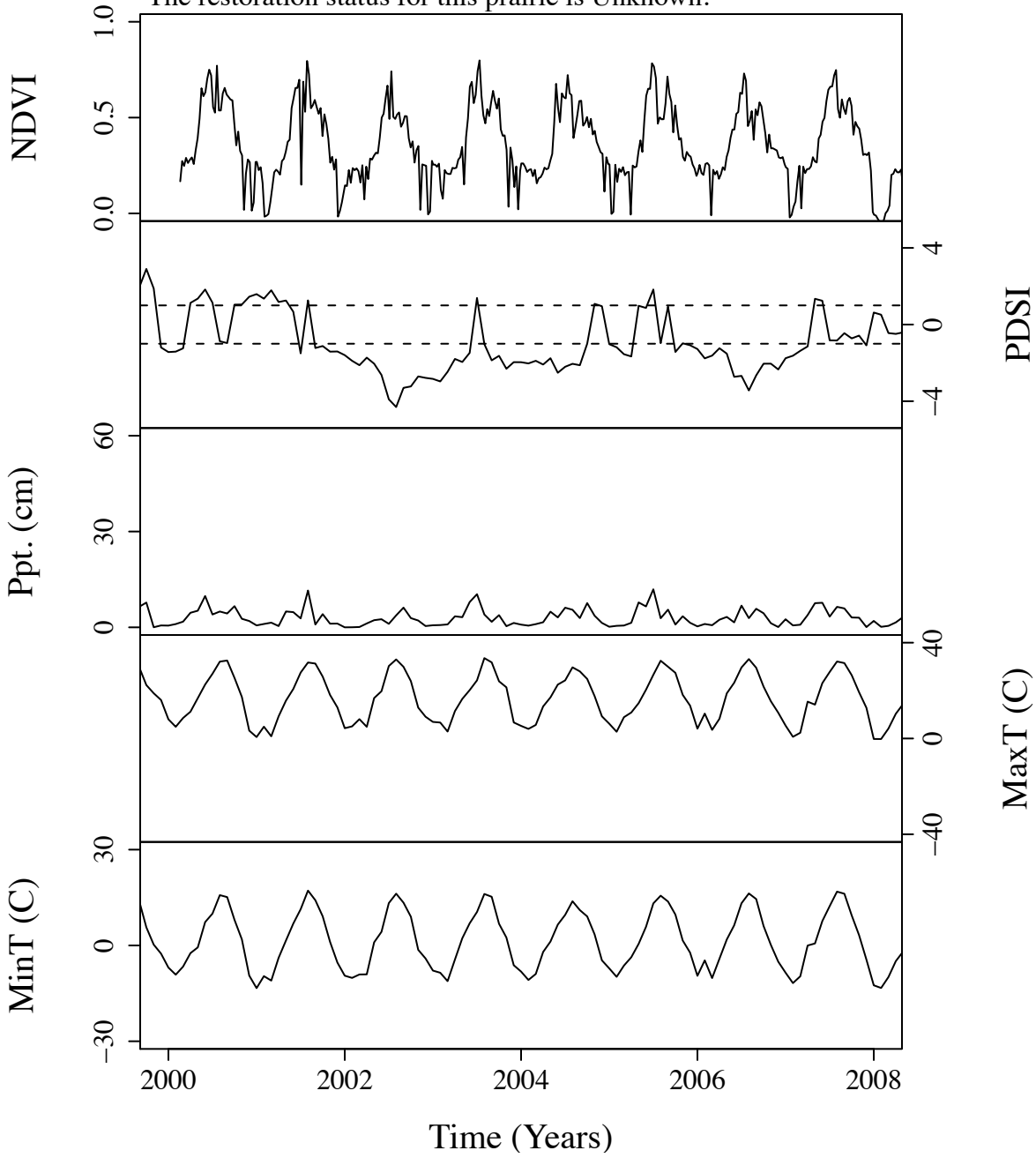

Figure B.186. Time series curves for nwe721.
The community type for this prairie is Short.
The dominant photosynthetic pathway for this prairie is C4.
The restoration status for this prairie is Unknown.

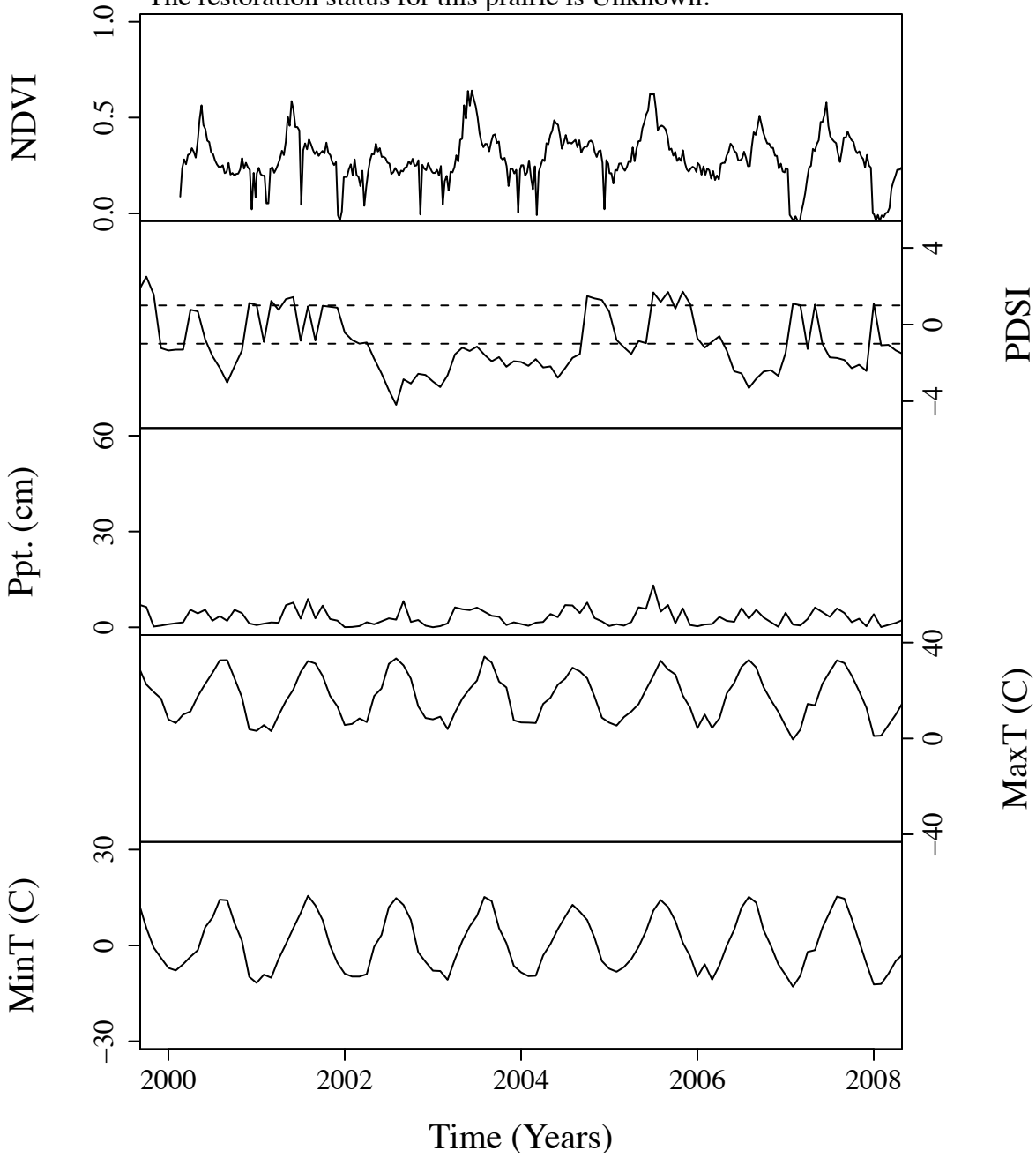

Figure B.187. Time series curves for nwe723.
The community type for this prairie is Short.
The dominant photosynthetic pathway for this prairie is C4.
The restoration status for this prairie is Unknown.

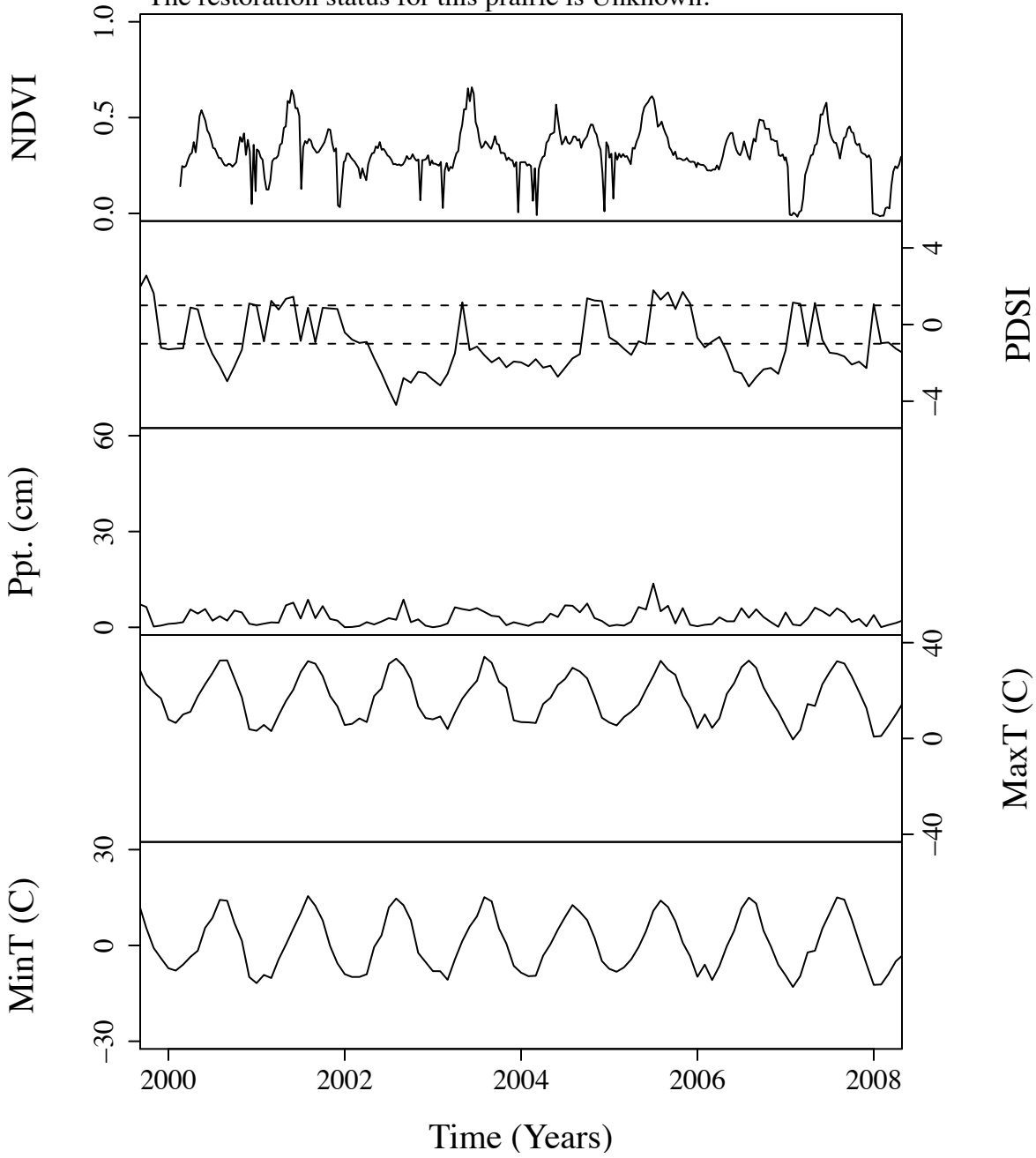

Figure B.188. Time series curves for nwe724.
The community type for this prairie is Short.
The dominant photosynthetic pathway for this prairie is C4.
The restoration status for this prairie is Unknown.

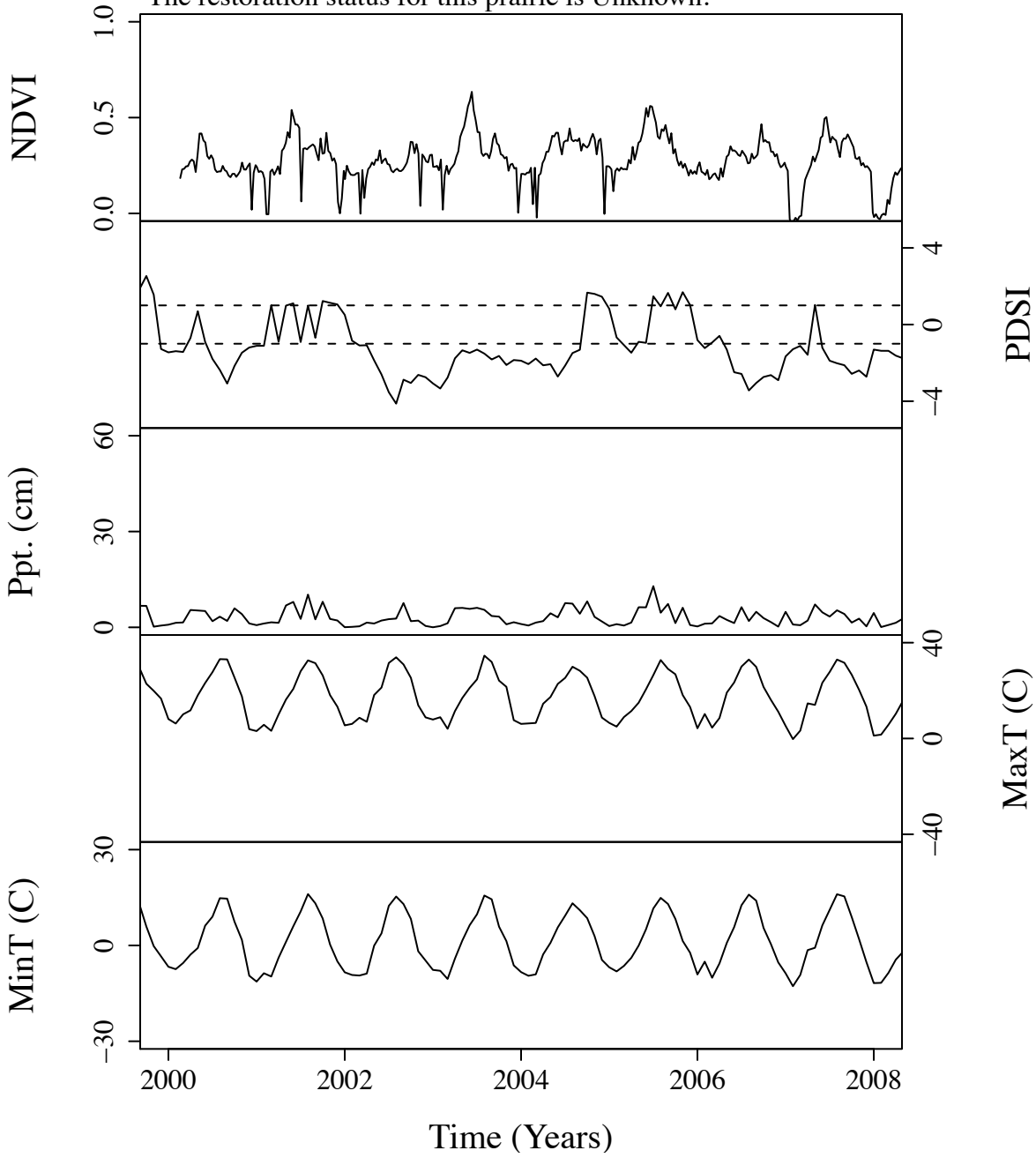

Figure B.189. Time series curves for nwe725.
The community type for this prairie is Short.
The dominant photosynthetic pathway for this prairie is C4.
The restoration status for this prairie is Unknown.

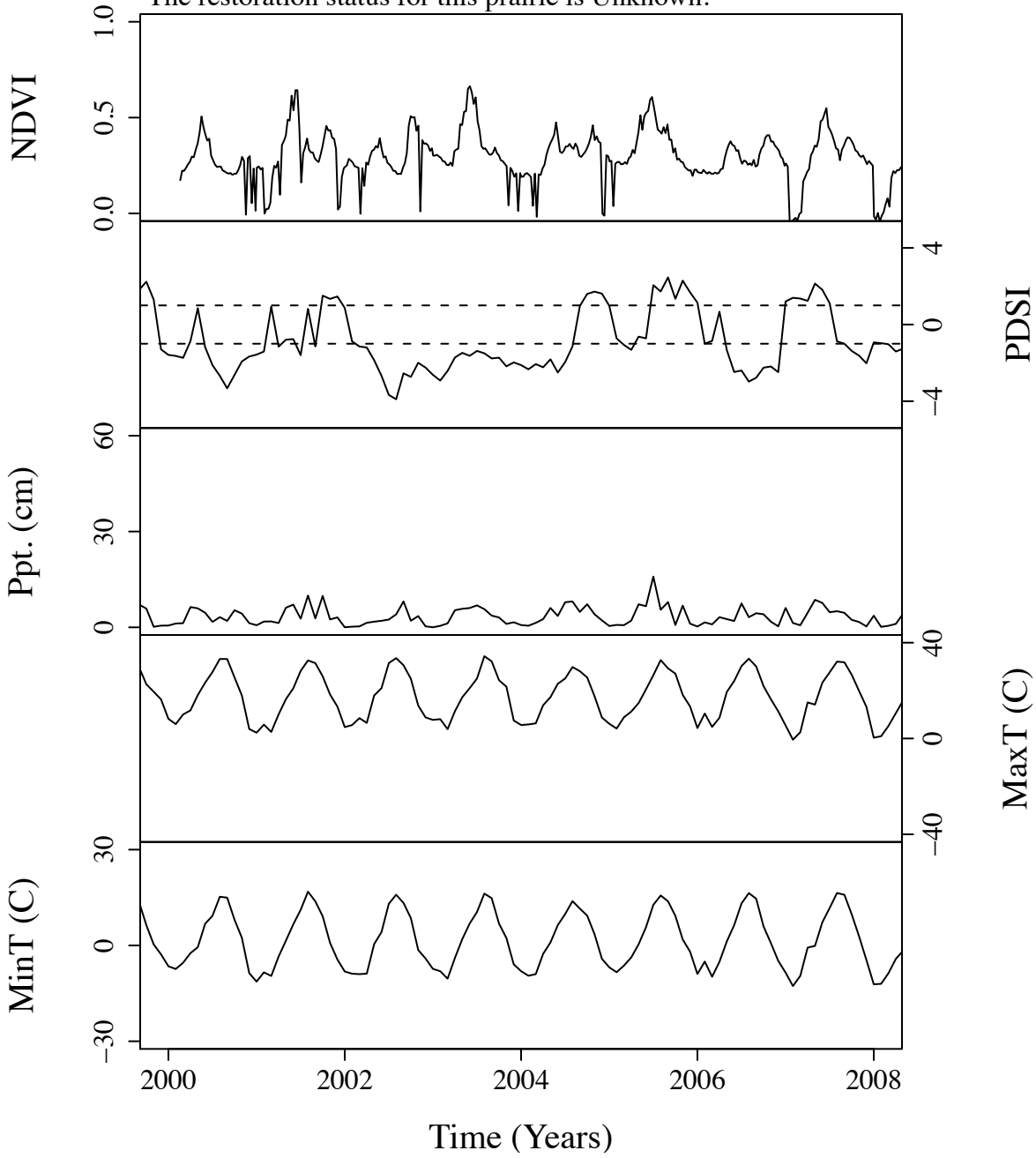

Figure B.190. Time series curves for nwe726.
The community type for this prairie is Short.
The dominant photosynthetic pathway for this prairie is C4.
The restoration status for this prairie is Unknown.

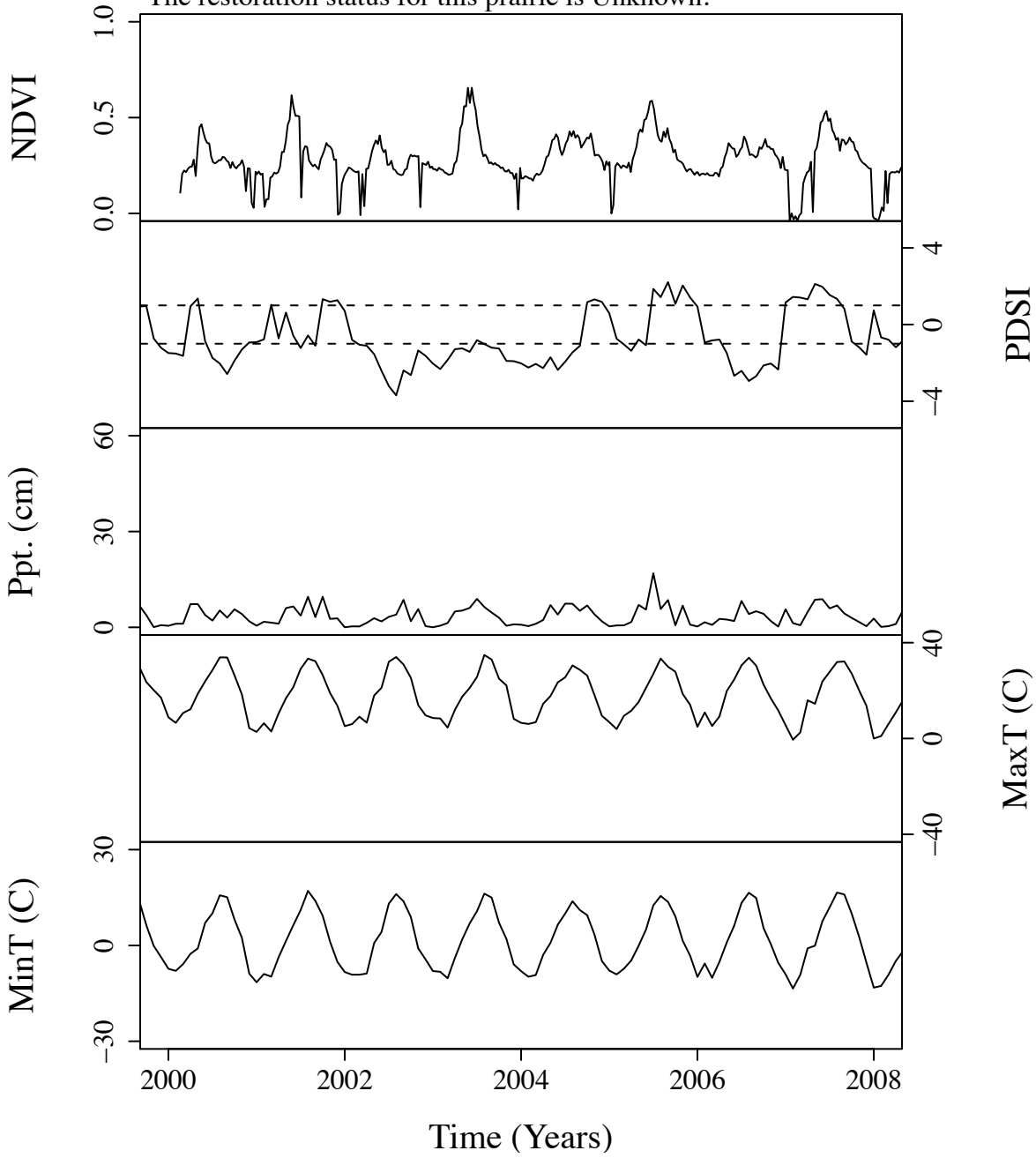

Figure B.191. Time series curves for nwe728.
The community type for this prairie is Short.
The dominant photosynthetic pathway for this prairie is C4.
The restoration status for this prairie is Unknown.

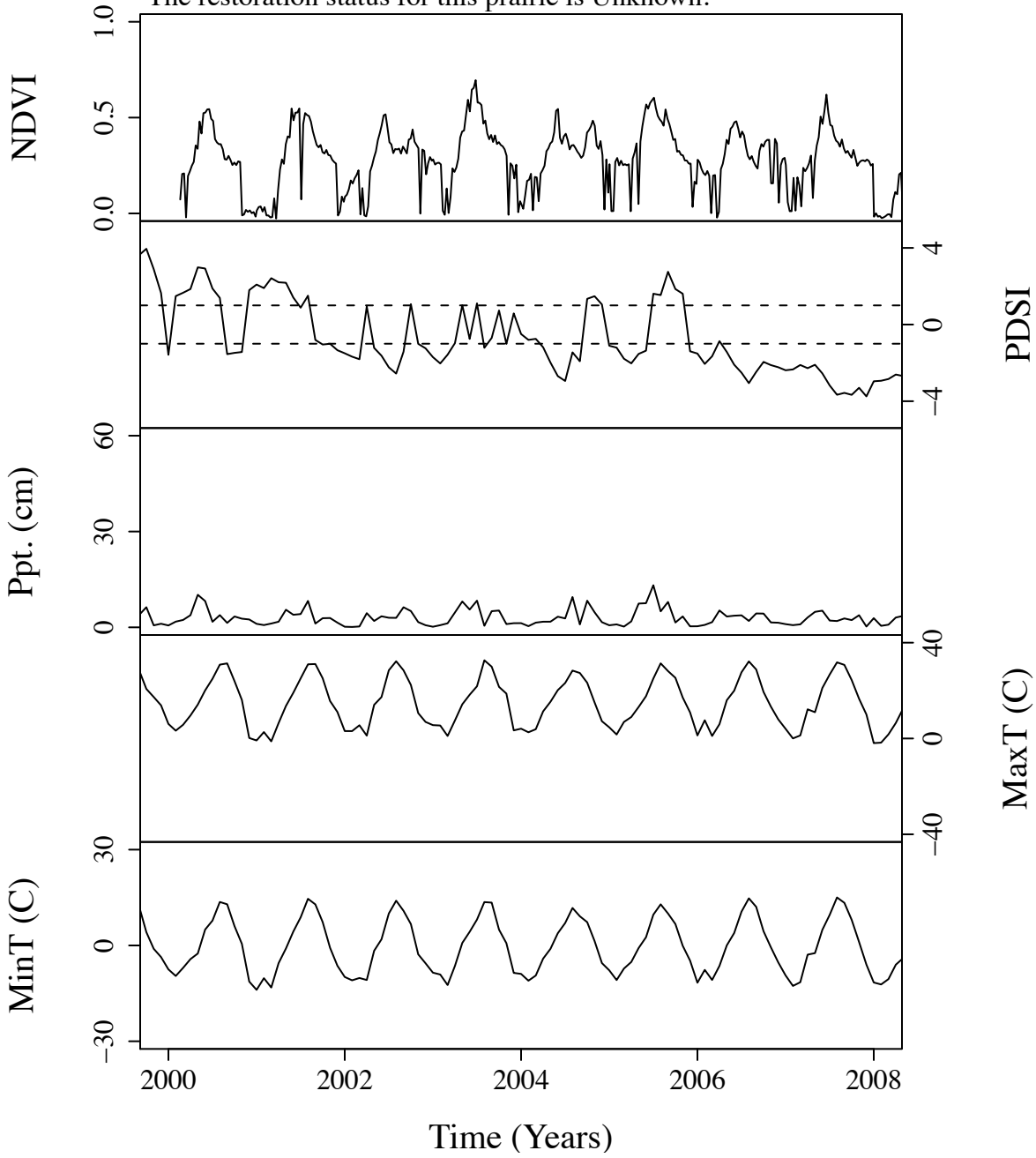

Figure B.192. Time series curves for nwe744.
The community type for this prairie is Short.
The dominant photosynthetic pathway for this prairie is C4.
The restoration status for this prairie is Unknown.

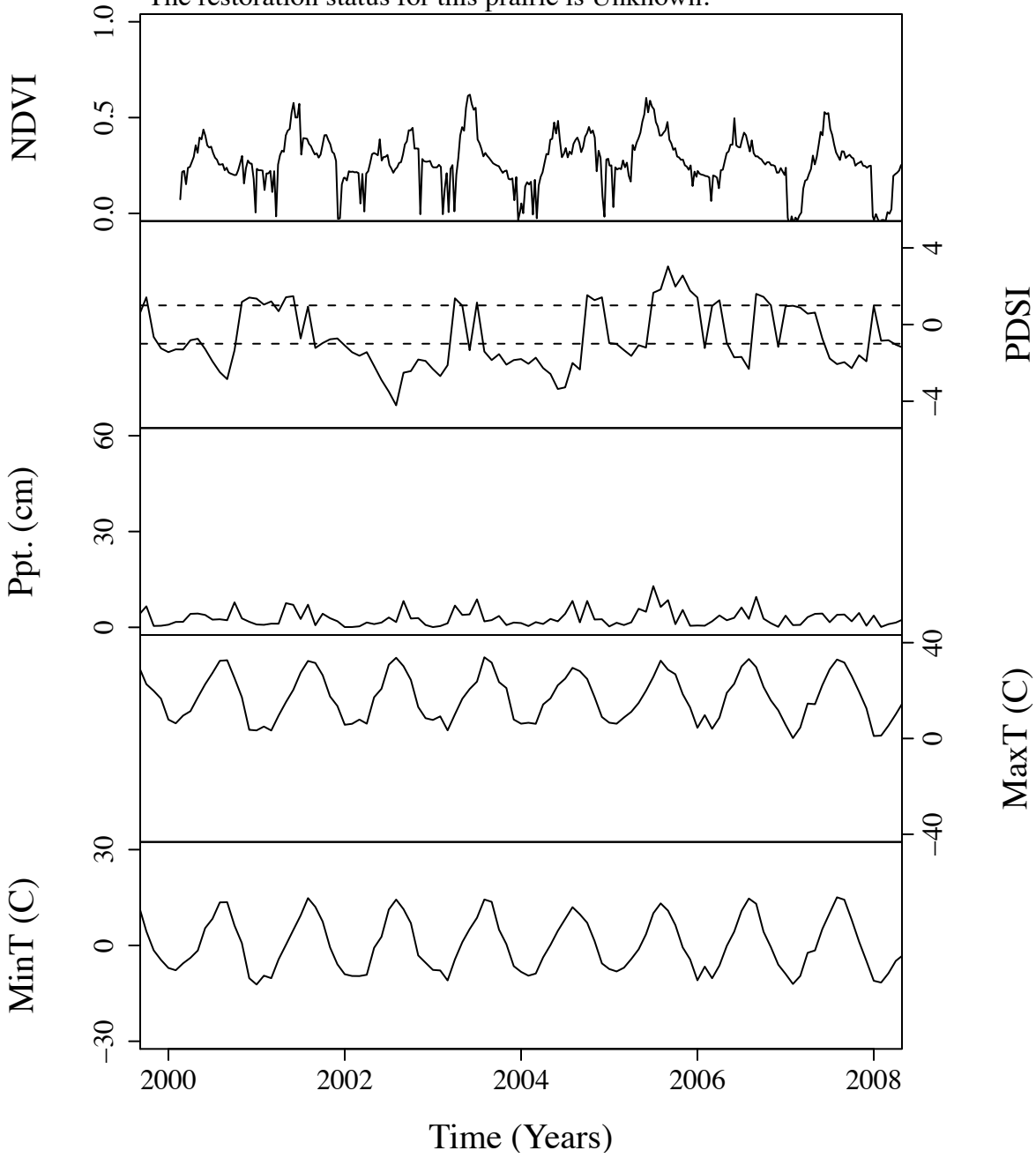

Figure B.193. Time series curves for nwe745.
The community type for this prairie is Short.
The dominant photosynthetic pathway for this prairie is C4.
The restoration status for this prairie is Unknown.

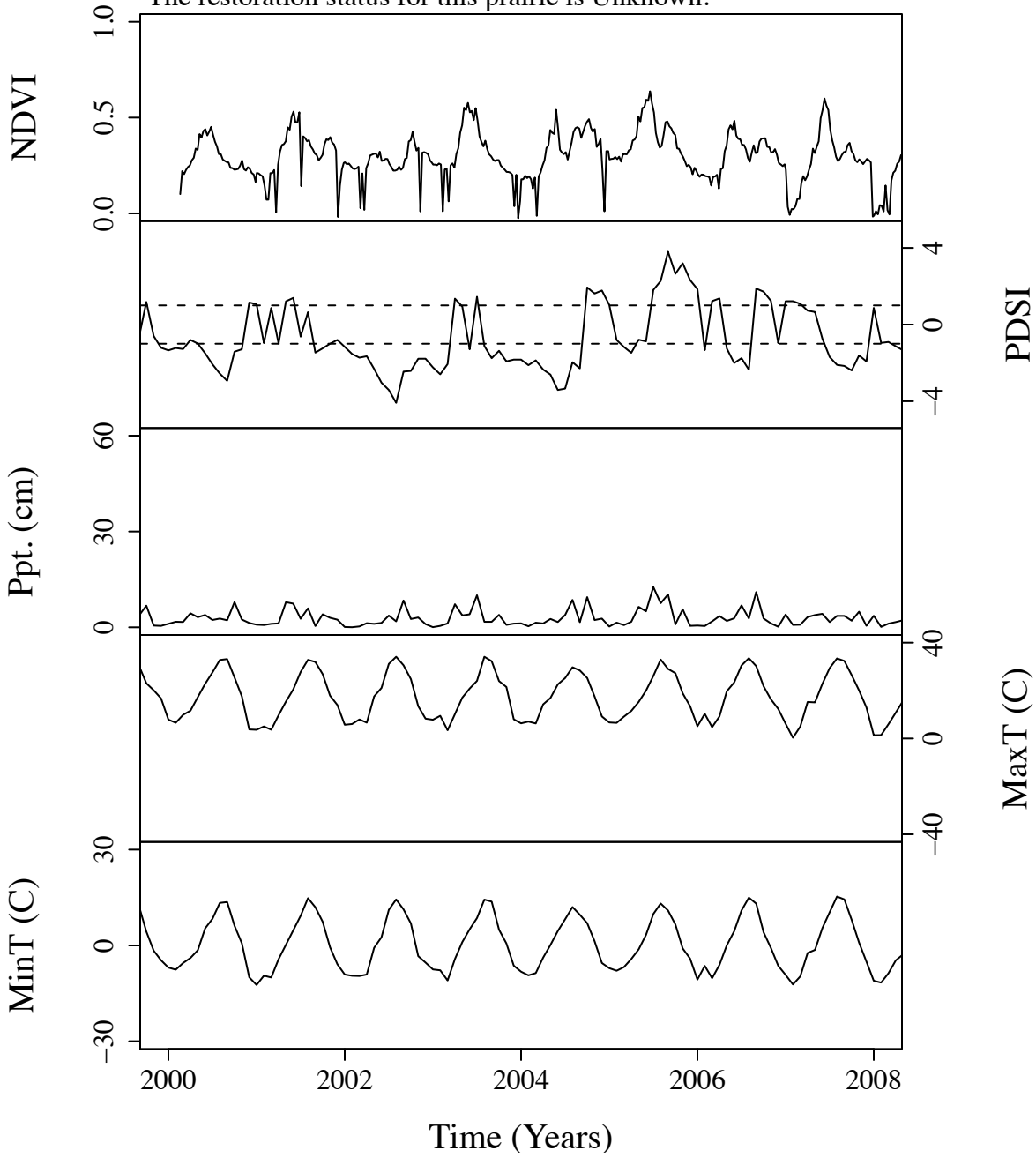

Figure B.194. Time series curves for nwe747.
The community type for this prairie is Short.
The dominant photosynthetic pathway for this prairie is C4.
The restoration status for this prairie is Unknown.

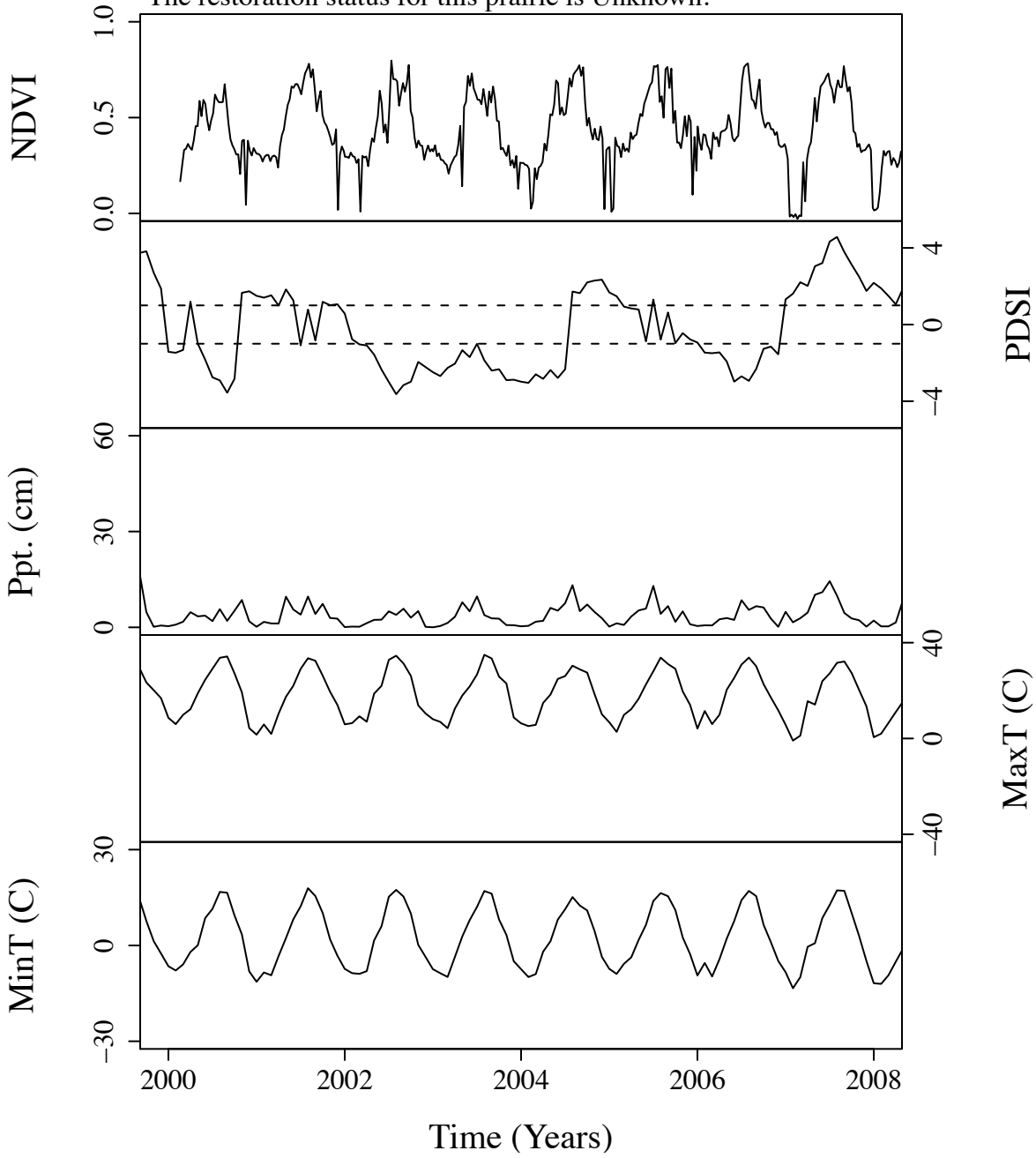

Figure B.195. Time series curves for nwe748.
The community type for this prairie is NoType.
The dominant photosynthetic pathway for this prairie is C4.
The restoration status for this prairie is Unknown.

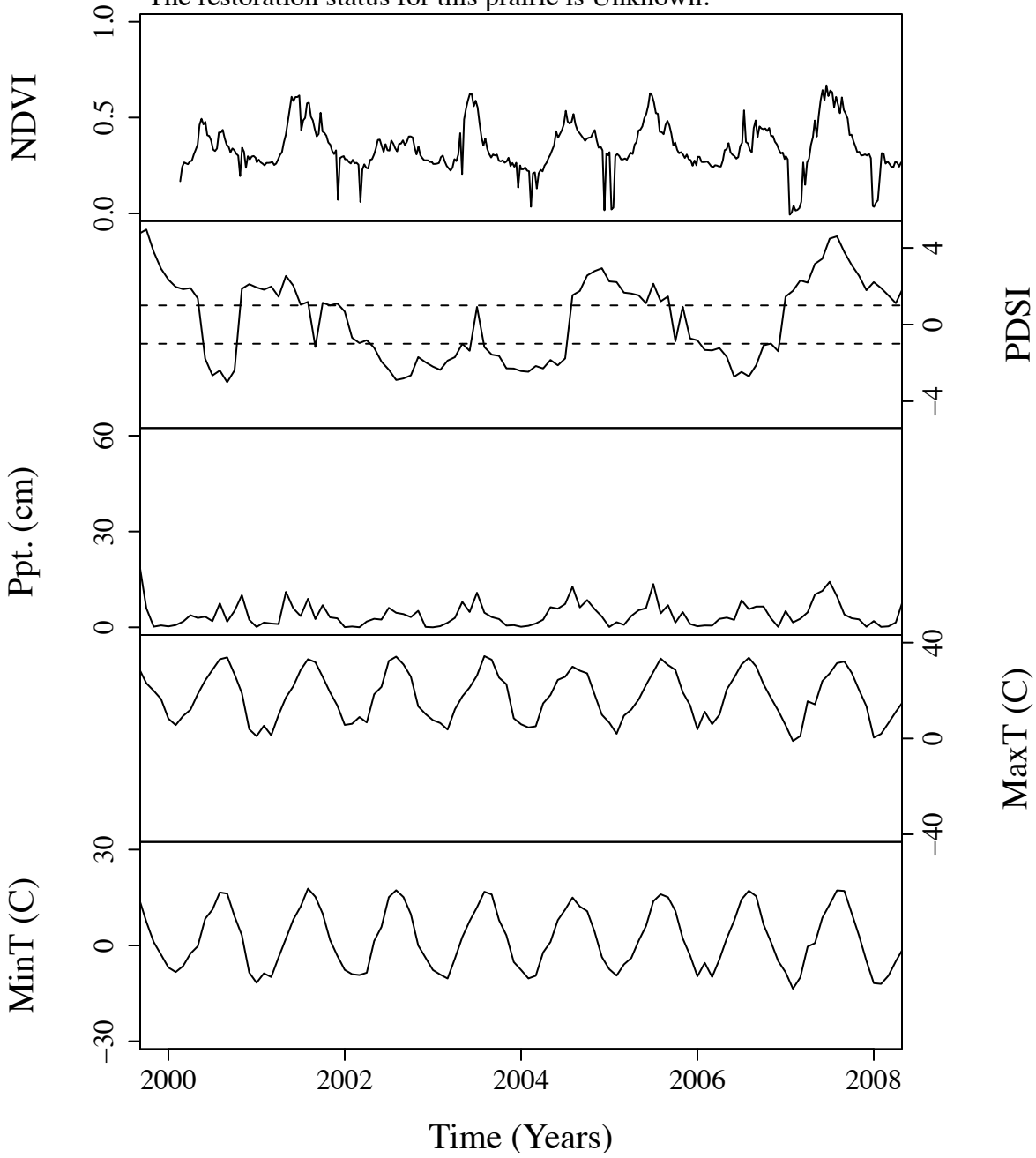

Figure B.196. Time series curves for nwe759.
The community type for this prairie is Short.
The dominant photosynthetic pathway for this prairie is C4.
The restoration status for this prairie is Unknown.

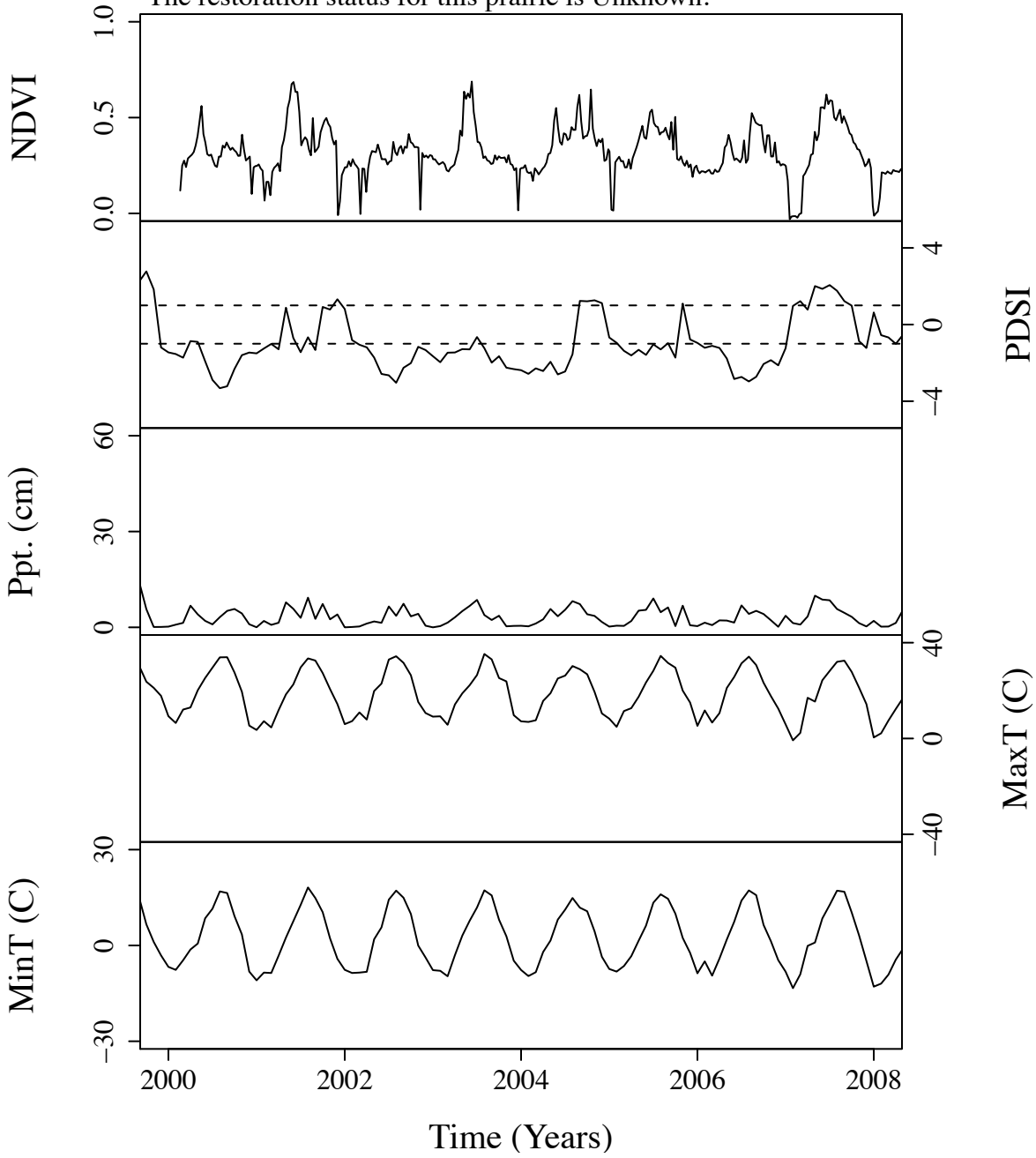

Figure B.197. Time series curves for nwe762.
The community type for this prairie is Short.
The dominant photosynthetic pathway for this prairie is C4.
The restoration status for this prairie is Unknown.

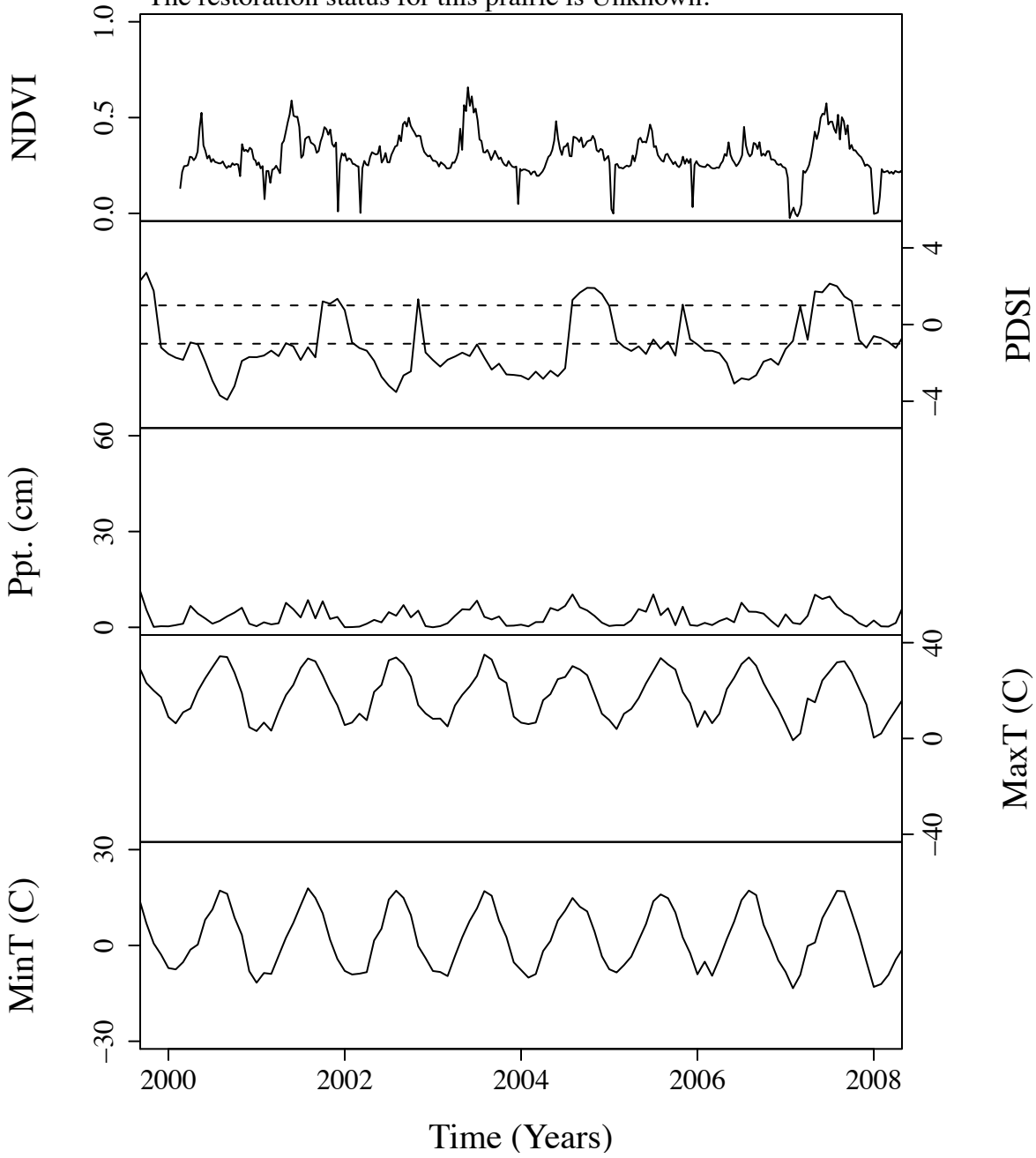

Figure B.198. Time series curves for nwe765.
The community type for this prairie is Short.
The dominant photosynthetic pathway for this prairie is C4.
The restoration status for this prairie is Unknown.

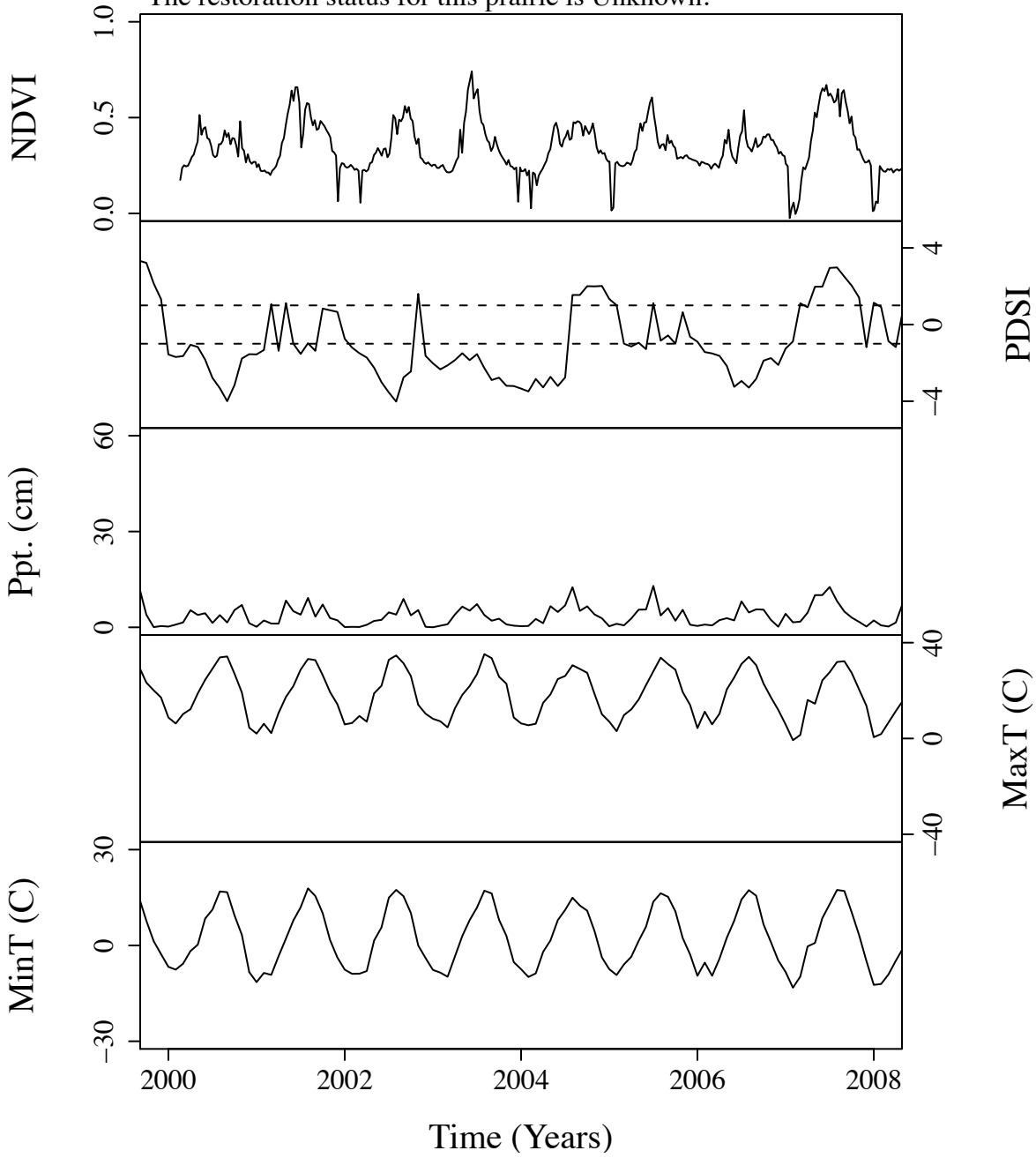

Figure B.199. Time series curves for nwe780.
The community type for this prairie is Mixed.
The dominant photosynthetic pathway for this prairie is C4.
The restoration status for this prairie is Unknown.

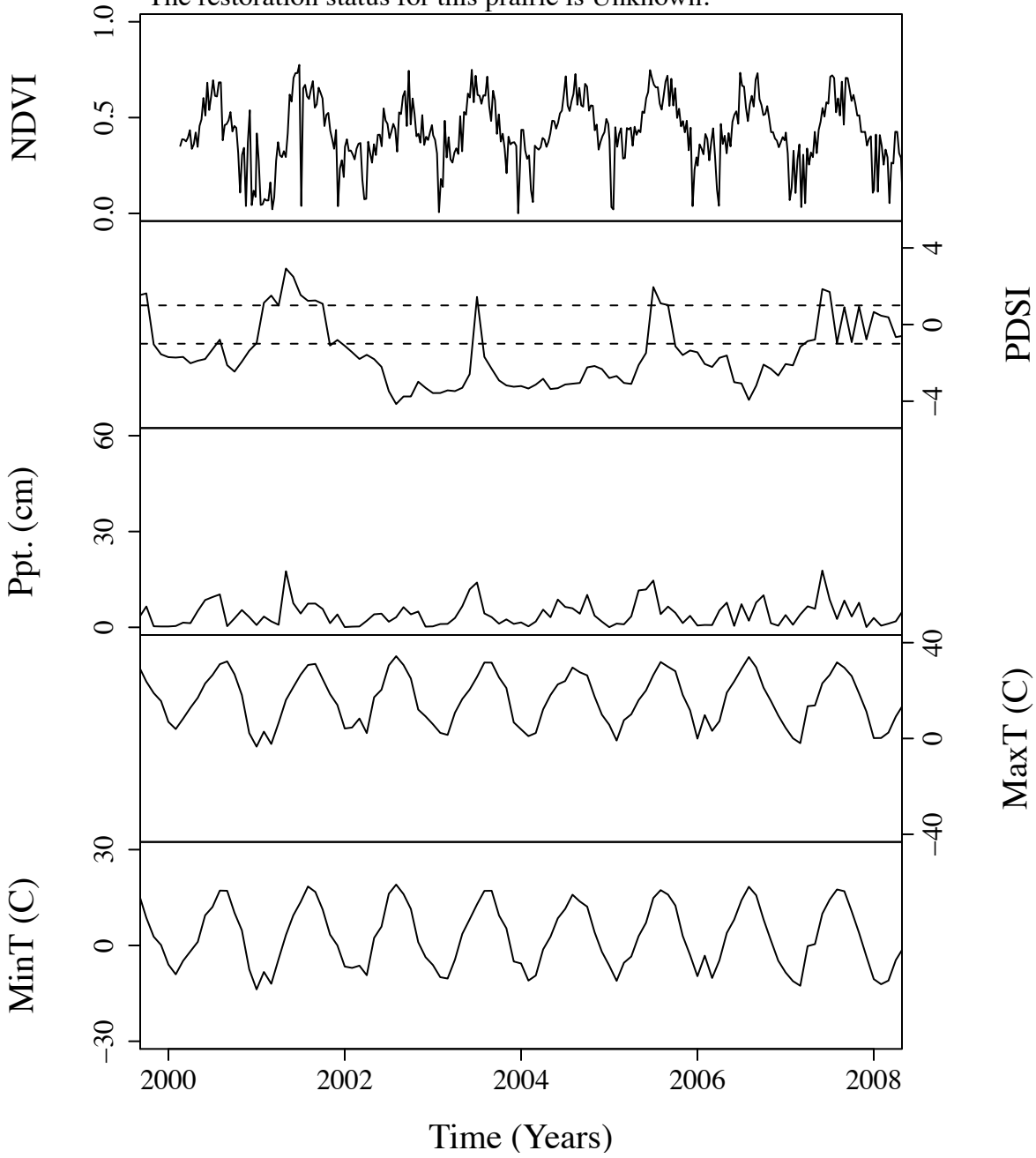

Figure B.200. Time series curves for nwe794.
The community type for this prairie is Short.
The dominant photosynthetic pathway for this prairie is C4.
The restoration status for this prairie is Unknown.

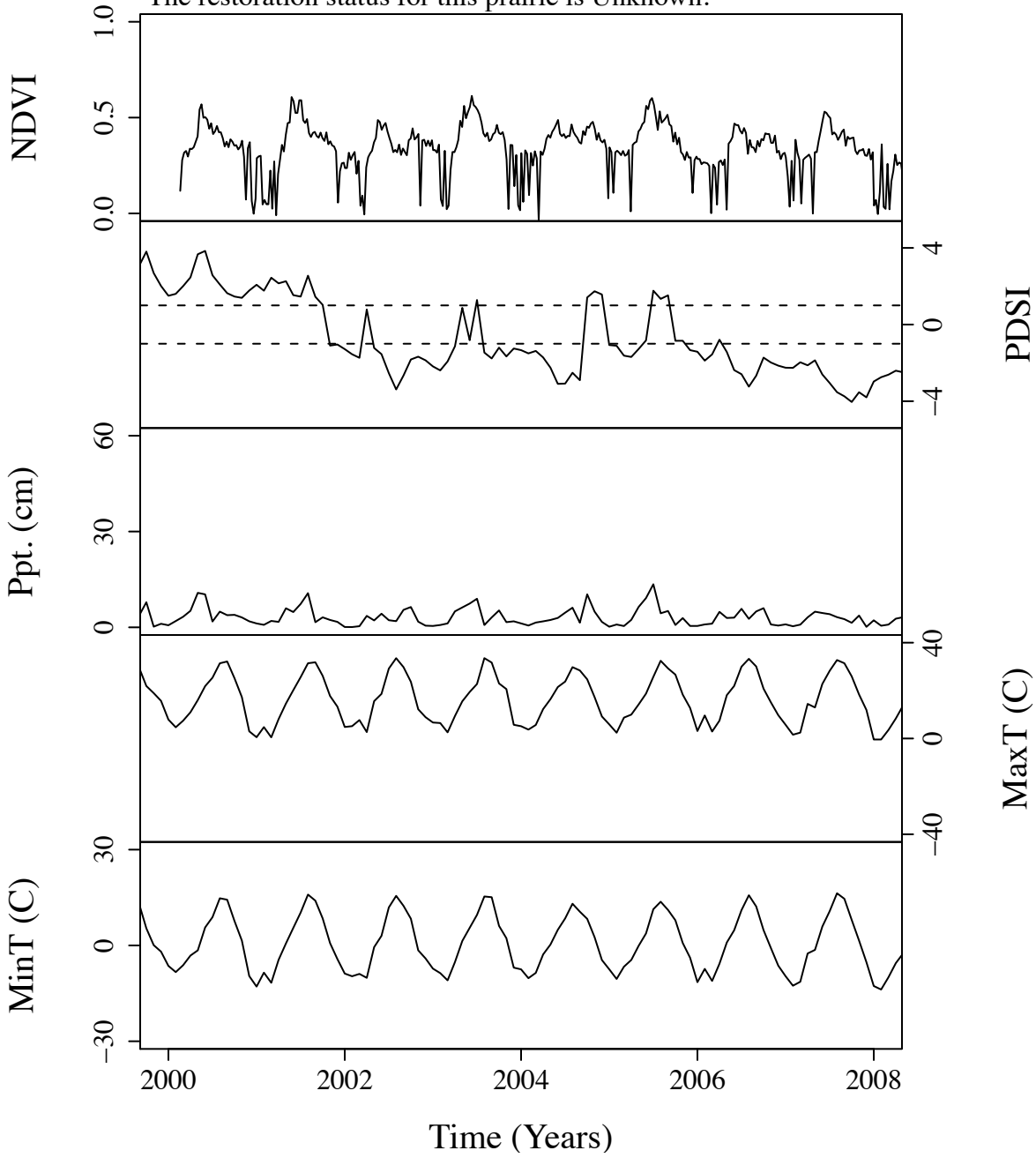

Figure B.201. Time series curves for nwe811.
The community type for this prairie is Mixed.
The dominant photosynthetic pathway for this prairie is C4.
The restoration status for this prairie is Unknown.

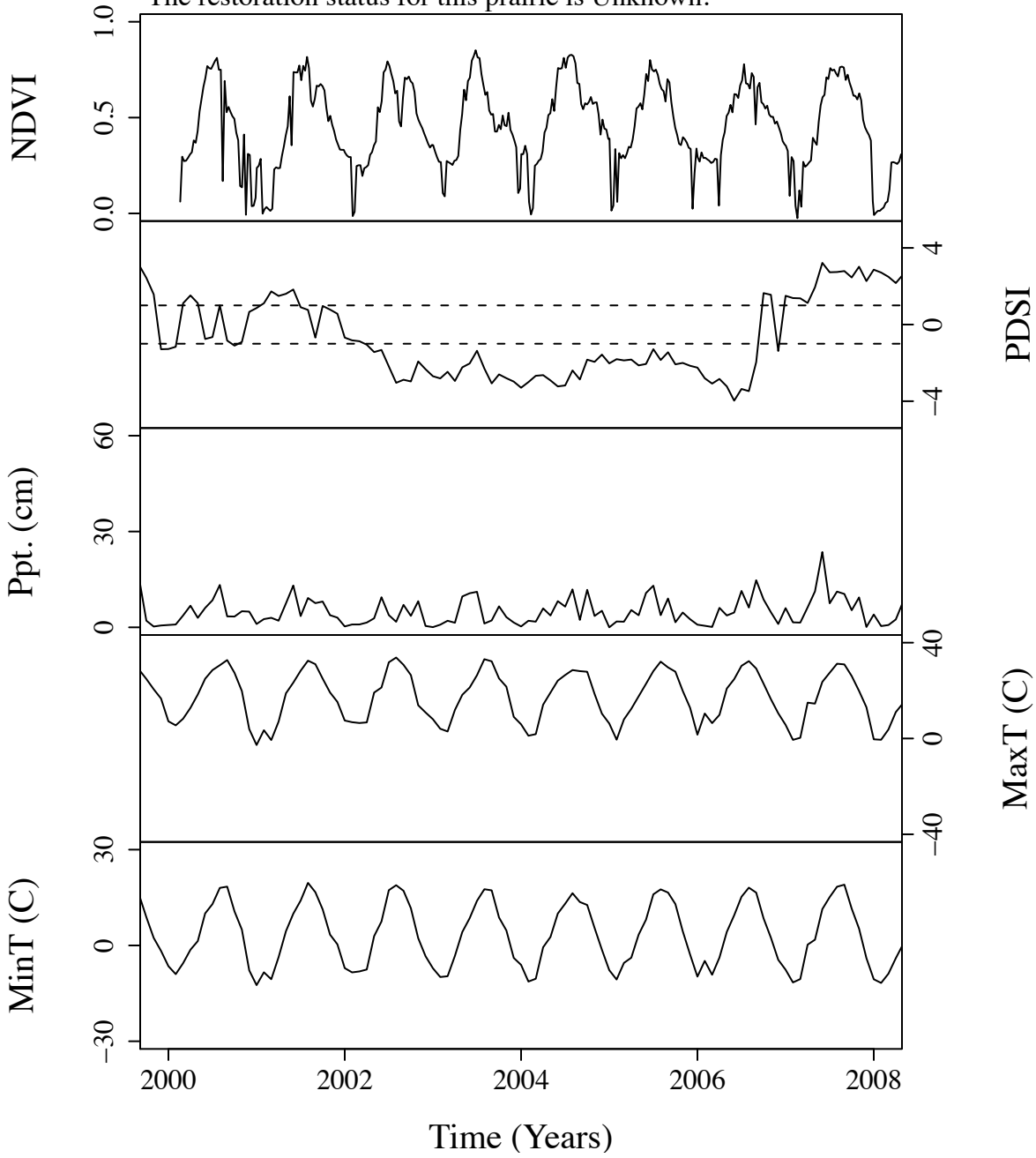

Figure B.202. Time series curves for nwe854.
The community type for this prairie is Short.
The dominant photosynthetic pathway for this prairie is C4.
The restoration status for this prairie is Unknown.

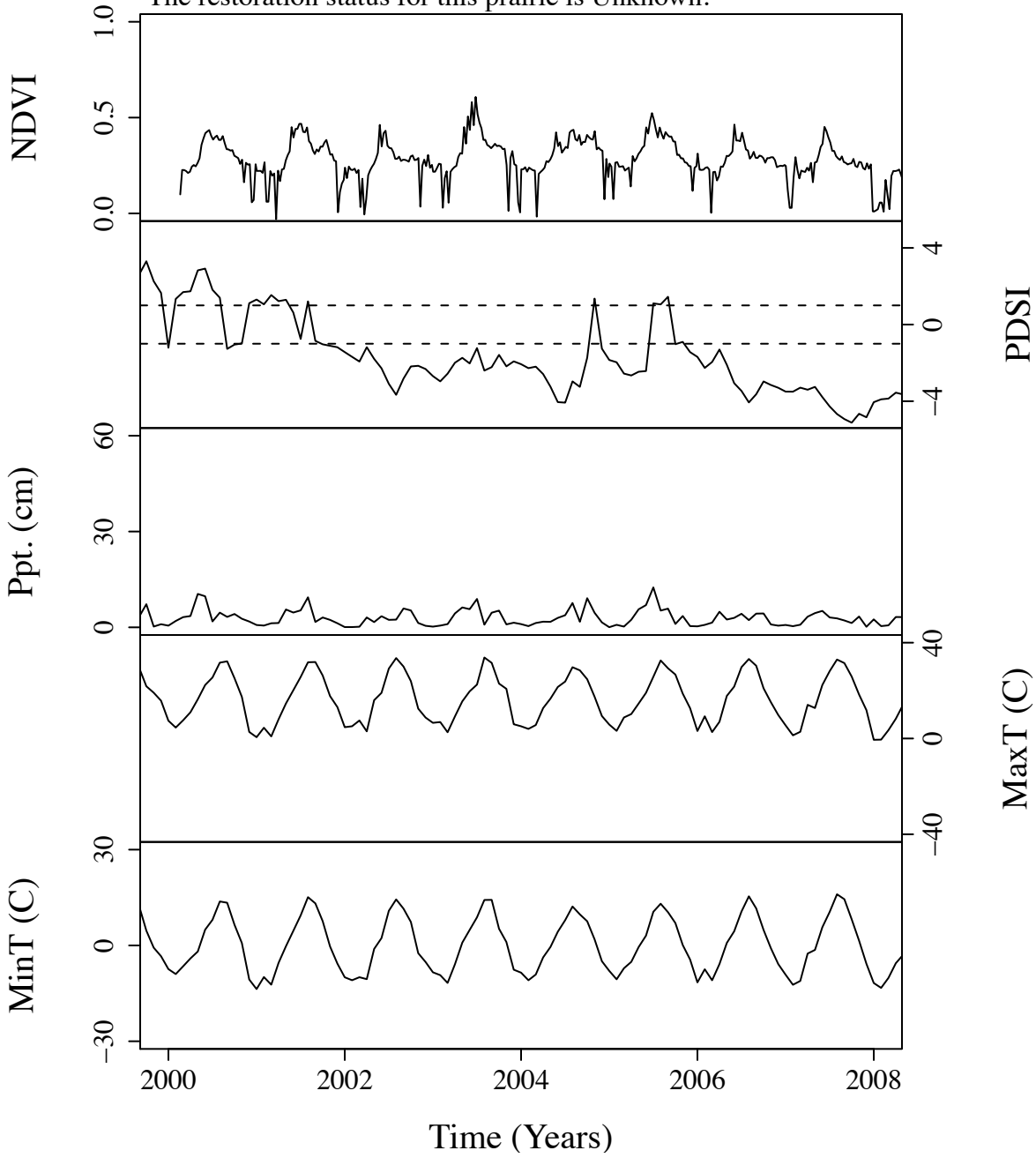

Figure B.203. Time series curves for nwe898.
The community type for this prairie is Mixed.
The dominant photosynthetic pathway for this prairie is C4.
The restoration status for this prairie is Unknown.

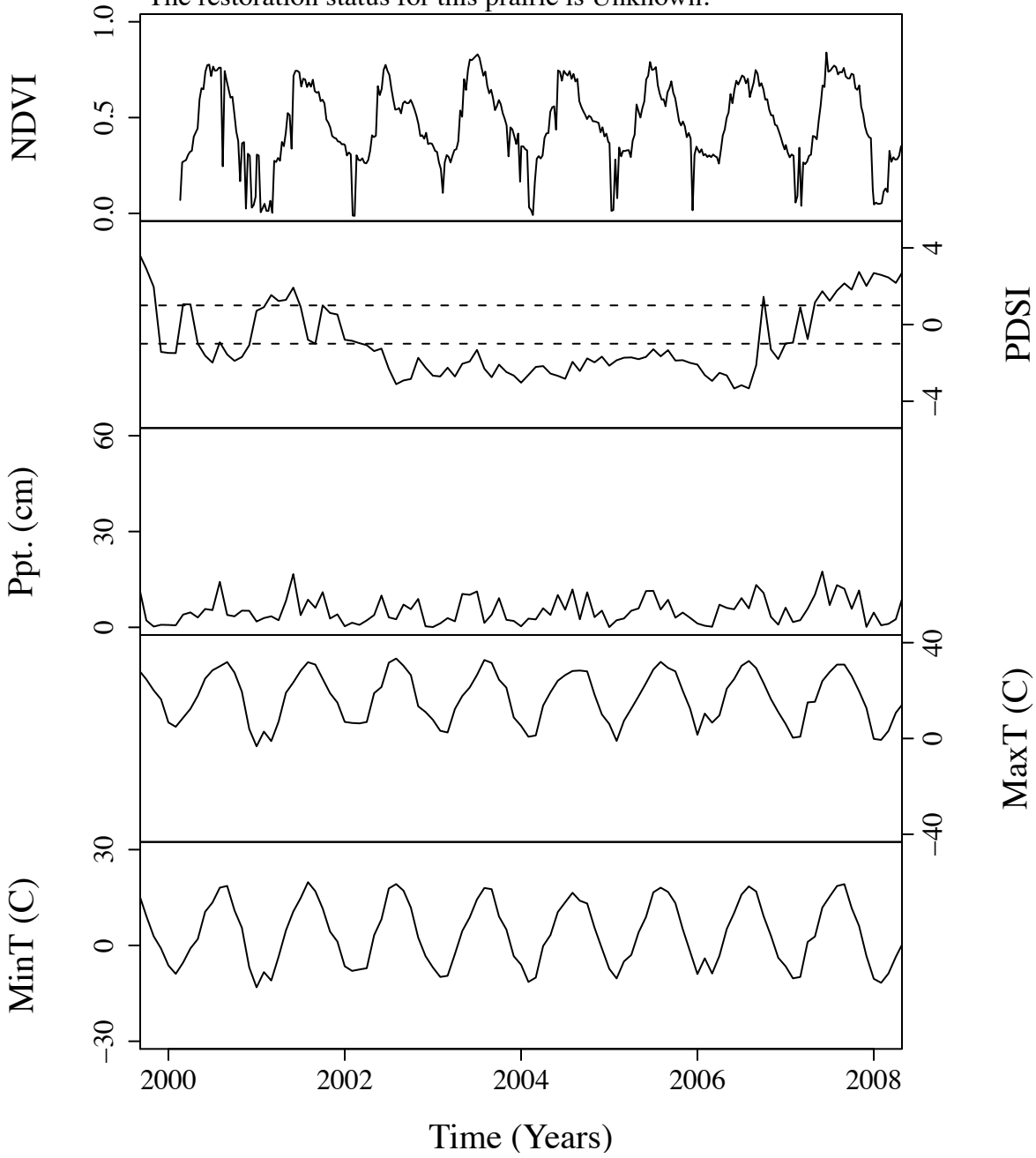

Figure B.204. Time series curves for nwe93.
The community type for this prairie is Short.
The dominant photosynthetic pathway for this prairie is C4.
The restoration status for this prairie is Unknown.

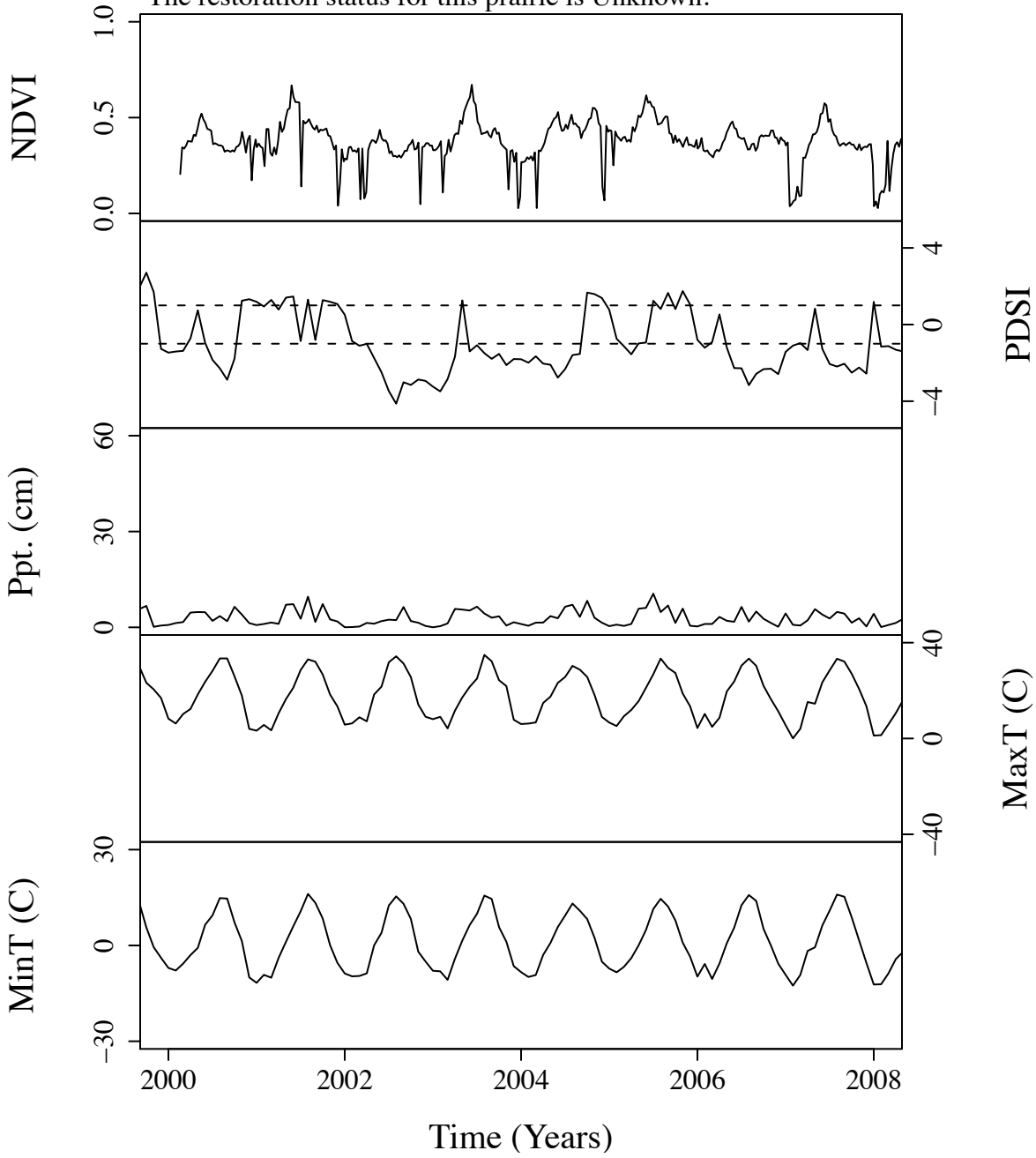

Figure B.205. Time series curves for nwe940.
The community type for this prairie is Short.
The dominant photosynthetic pathway for this prairie is C4.
The restoration status for this prairie is Unknown.

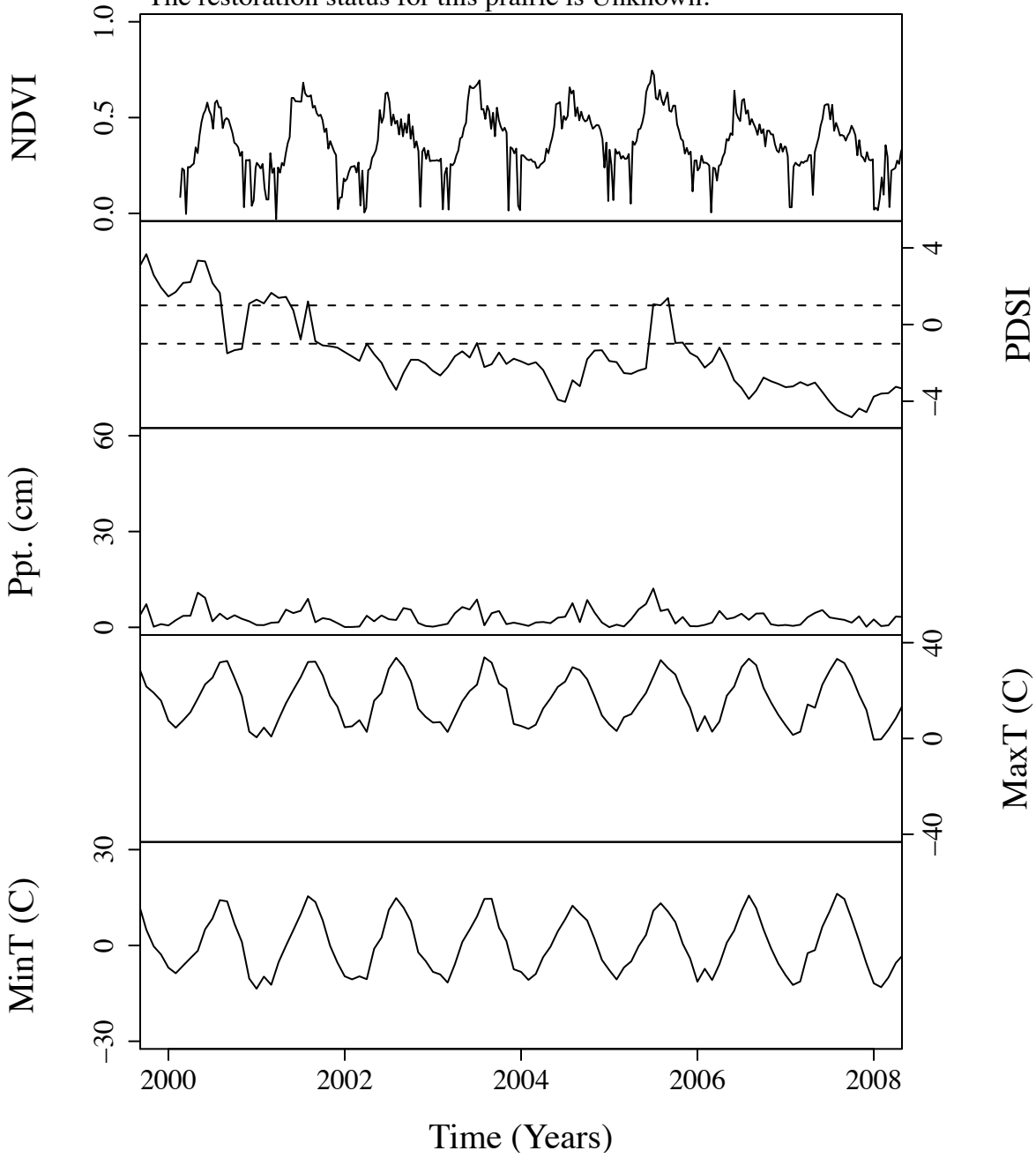

Figure B.206. Time series curves for nwe964.
The community type for this prairie is Mixed.
The dominant photosynthetic pathway for this prairie is C4.
The restoration status for this prairie is Unknown.

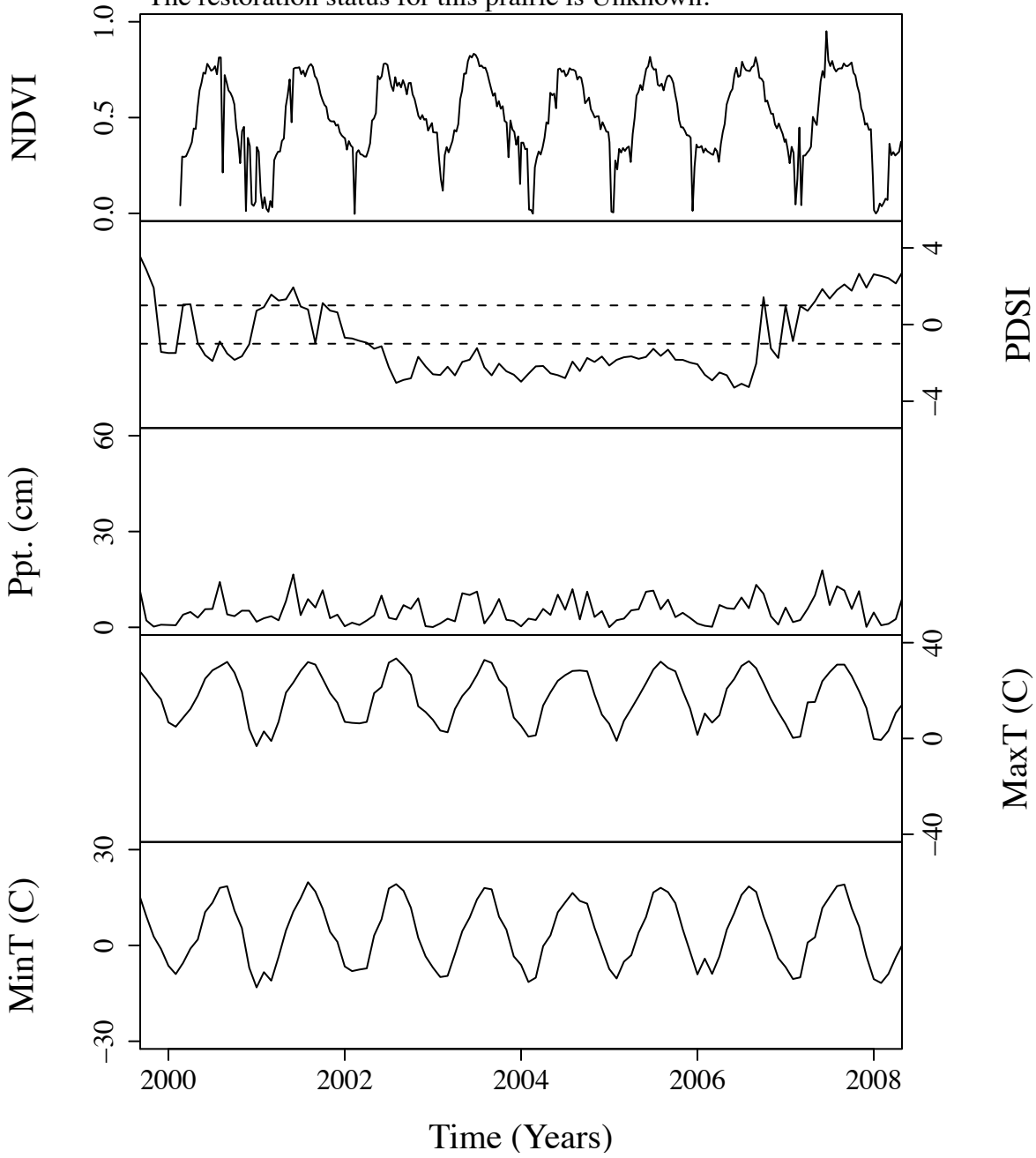

Figure B.207. Time series curves for s7.0.
The community type for this prairie is Tall.
The dominant photosynthetic pathway for this prairie is C4.
The restoration status for this prairie is Unknown.

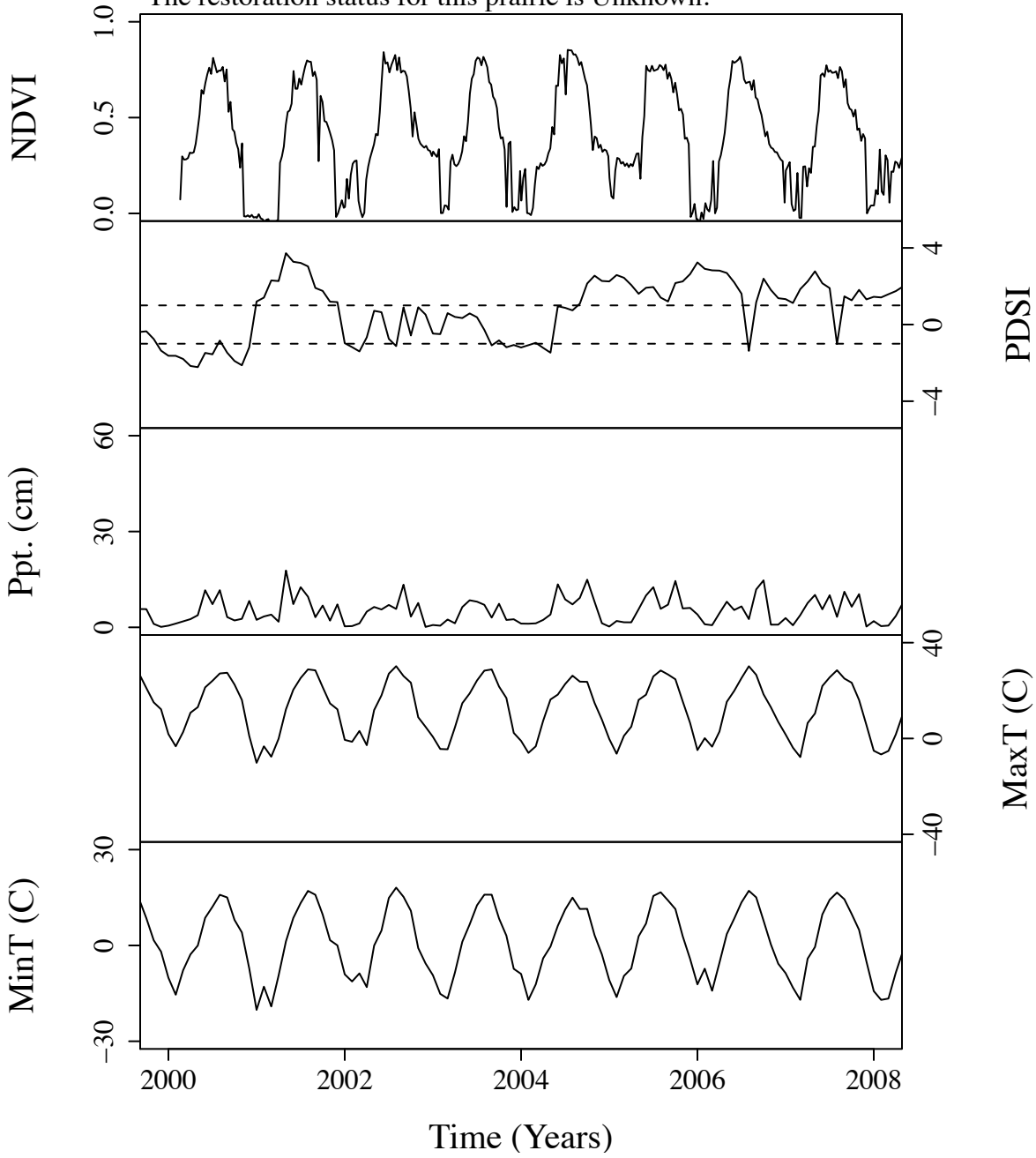

Figure B.208. Time series curves for sba2.
The community type for this prairie is Short.
The dominant photosynthetic pathway for this prairie is C4.
The restoration status for this prairie is Unknown.

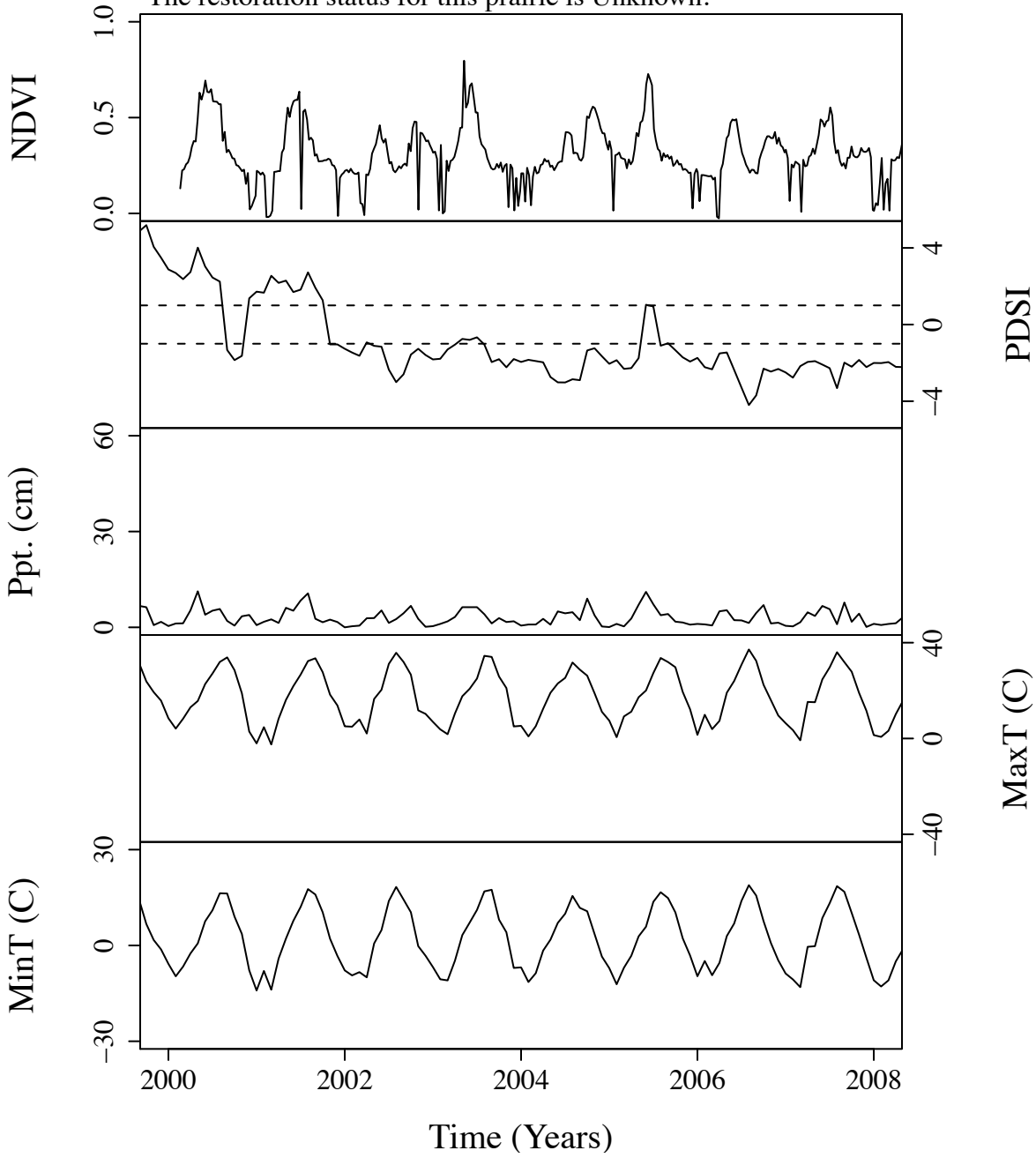

Figure B.209. Time series curves for sdo1.
The community type for this prairie is Short.
The dominant photosynthetic pathway for this prairie is C4.
The restoration status for this prairie is Unknown.

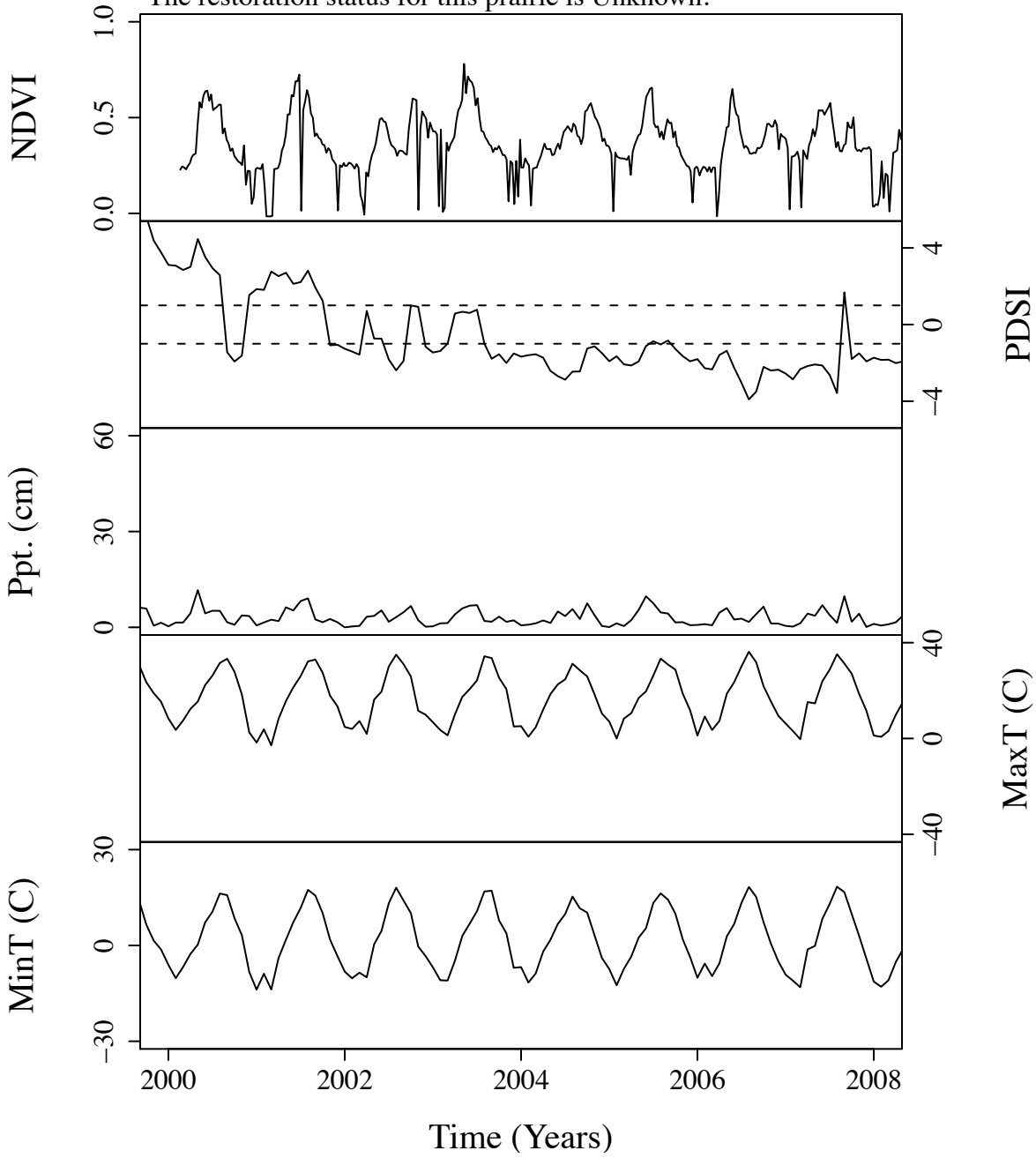

Figure B.210. Time series curves for sgo0.
The community type for this prairie is Short.
The dominant photosynthetic pathway for this prairie is C3.
The restoration status for this prairie is Unknown.

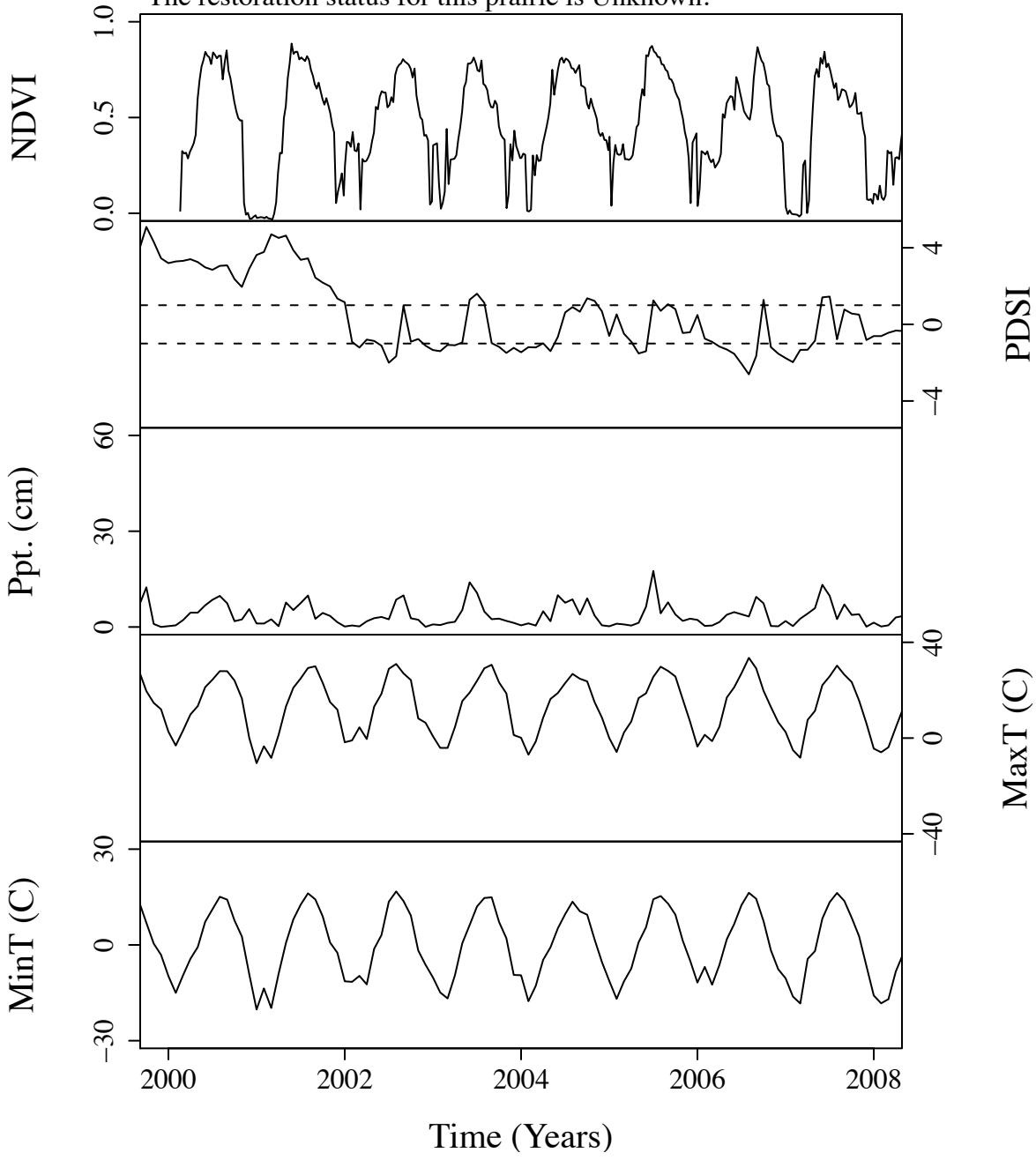

Figure B.211. Time series curves for sgo1.
The community type for this prairie is NoType.
The dominant photosynthetic pathway for this prairie is C3.
The restoration status for this prairie is Unknown.

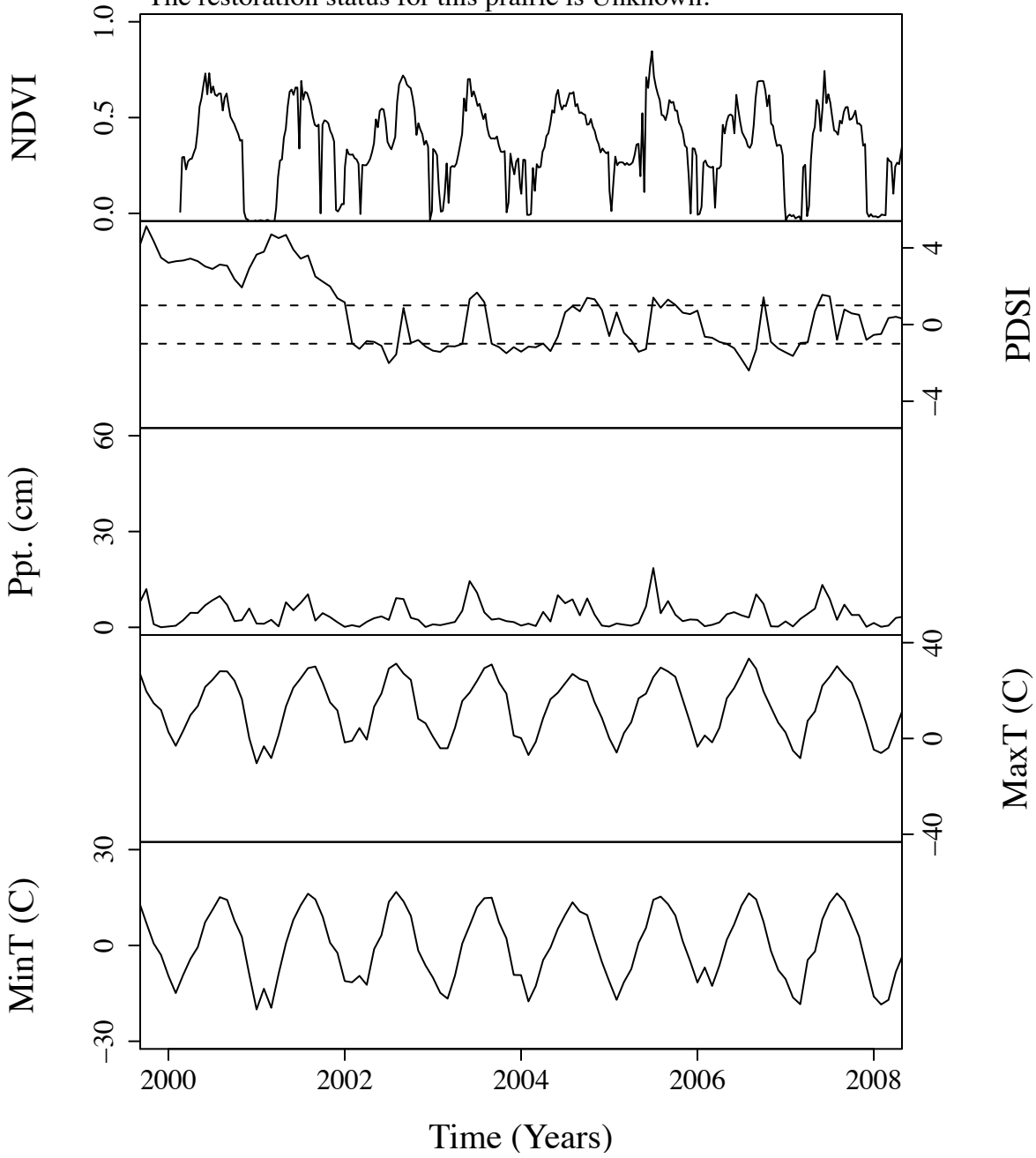

Figure B.212. Time series curves for sme16.
The community type for this prairie is Short.
The dominant photosynthetic pathway for this prairie is C3.
The restoration status for this prairie is Remnant.

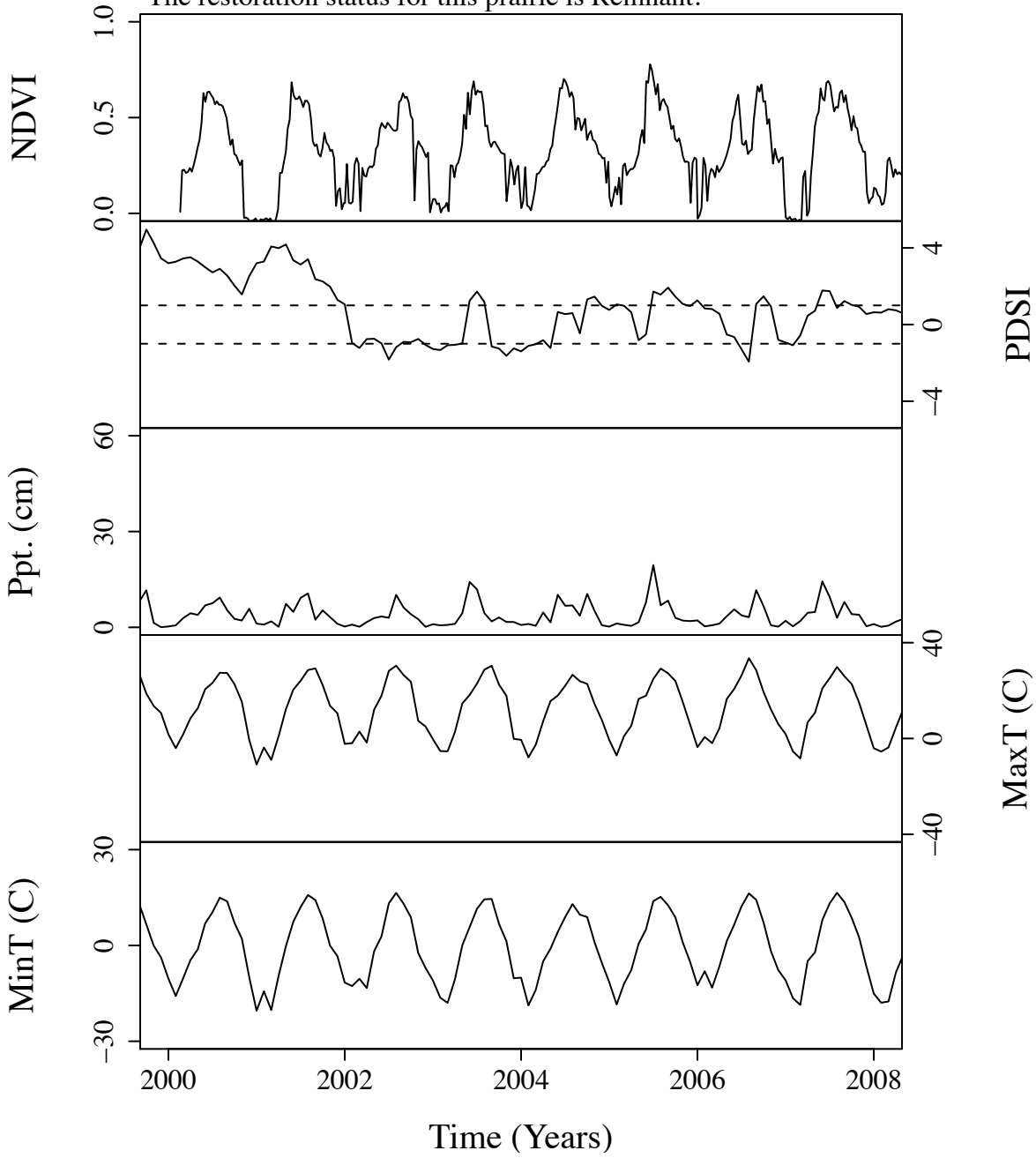

Figure B.213. Time series curves for sor0.
The community type for this prairie is Short.
The dominant photosynthetic pathway for this prairie is C3.
The restoration status for this prairie is Mixed.

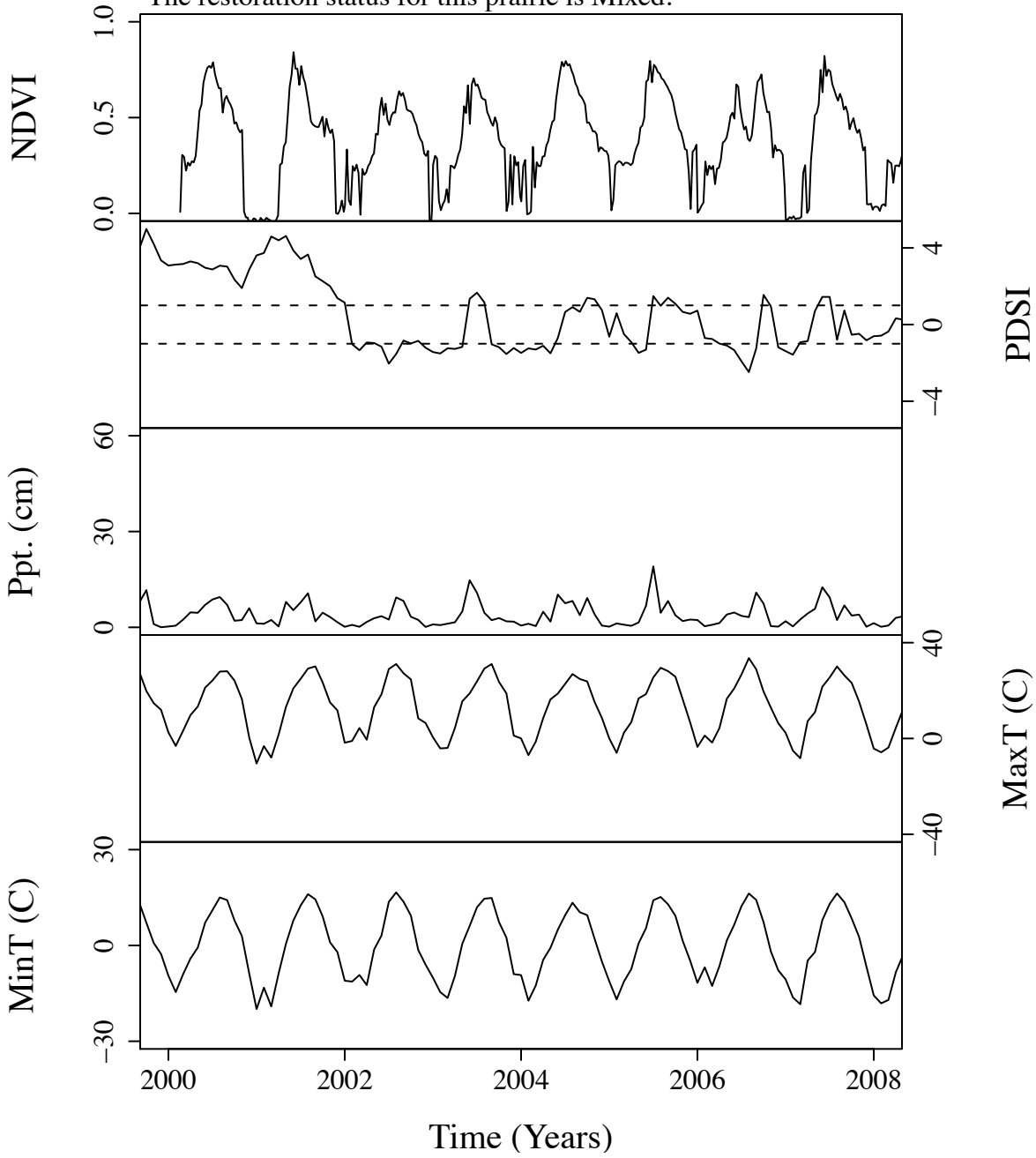

Figure B.214. Time series curves for sor1.
The community type for this prairie is Short.
The dominant photosynthetic pathway for this prairie is C3.
The restoration status for this prairie is Mixed.

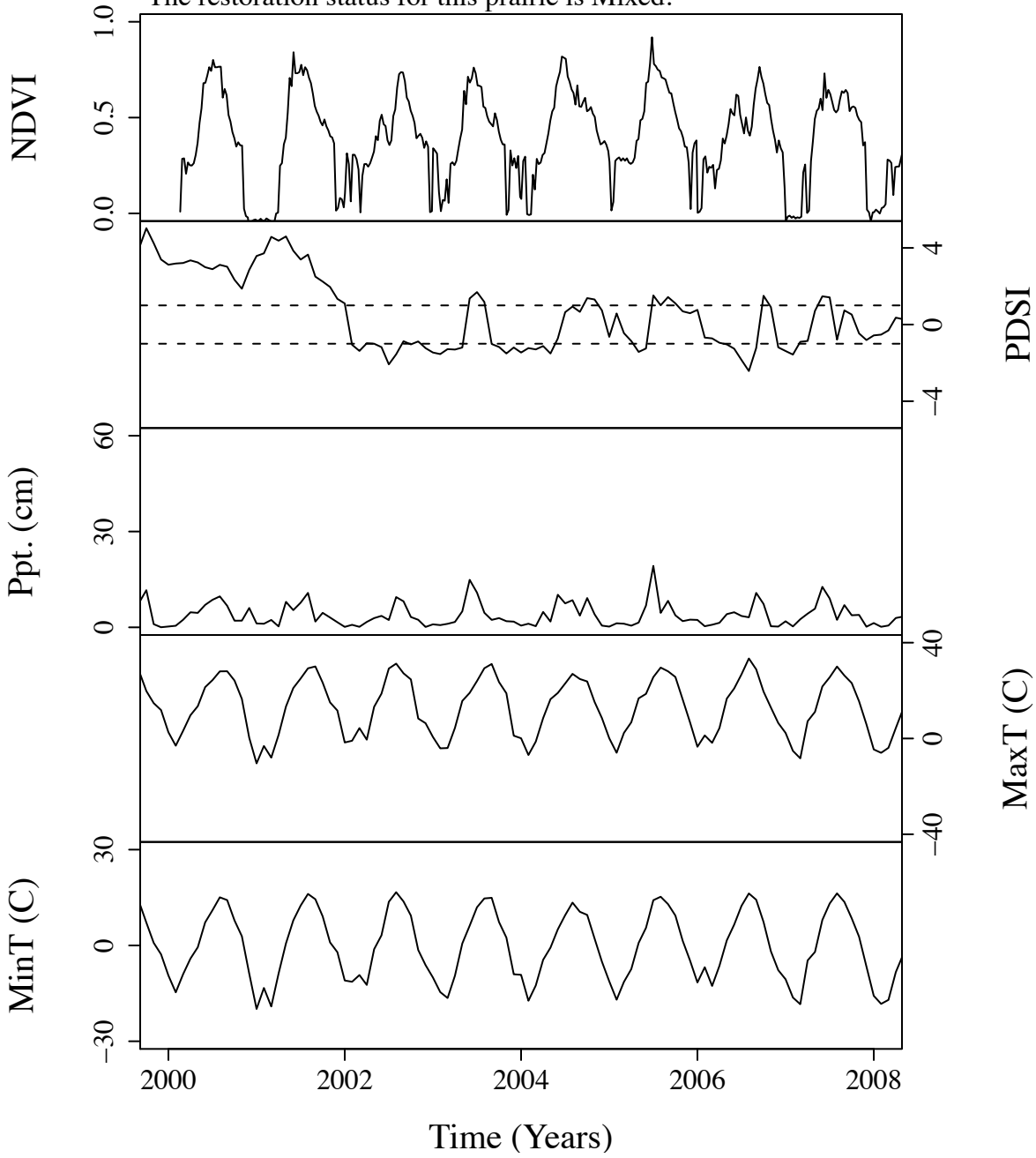

Figure B.215. Time series curves for sor10.
The community type for this prairie is Short.
The dominant photosynthetic pathway for this prairie is C3.
The restoration status for this prairie is Unknown.

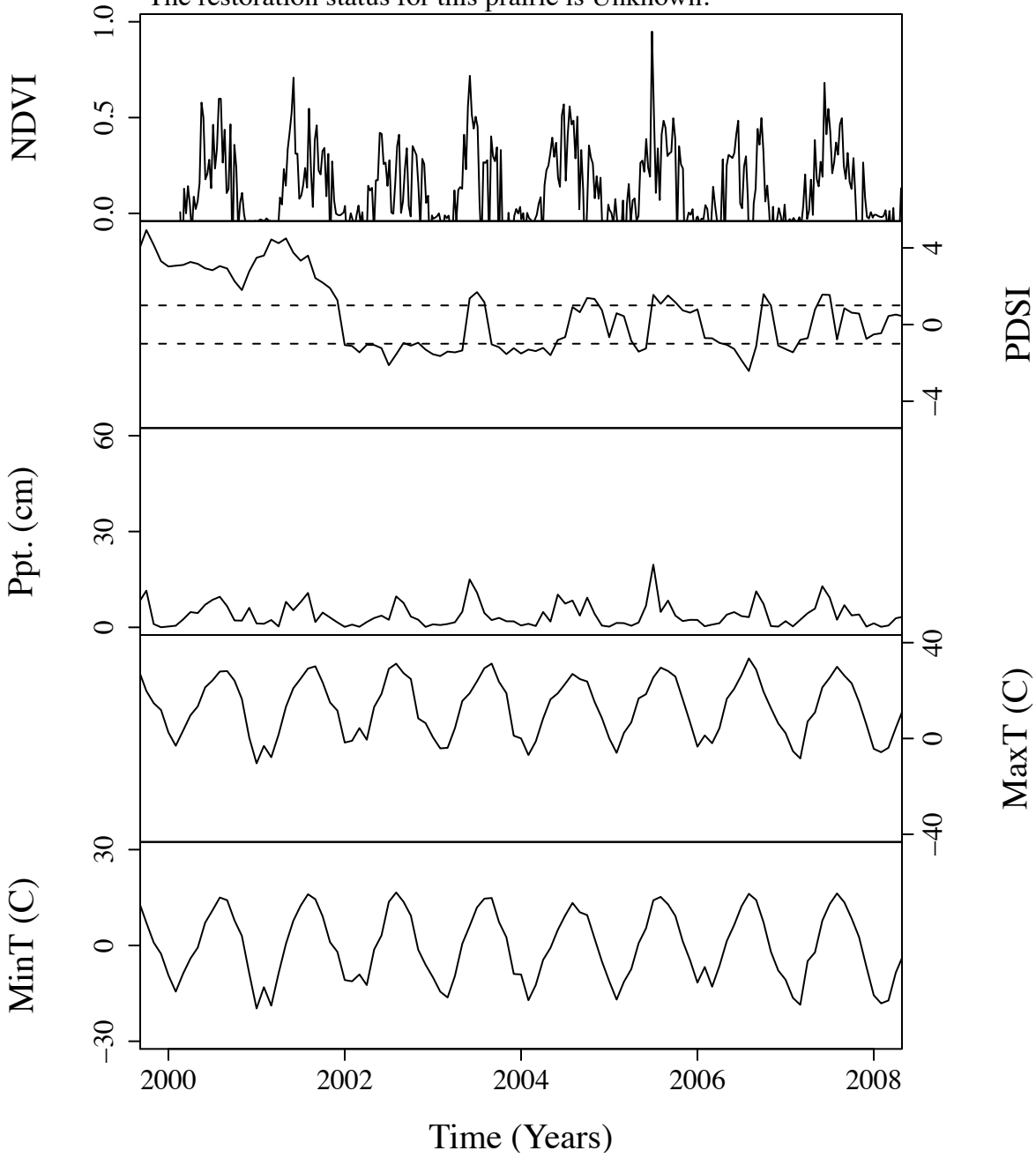

Figure B.216. Time series curves for sor11.
The community type for this prairie is Short.
The dominant photosynthetic pathway for this prairie is C3.
The restoration status for this prairie is Mixed.

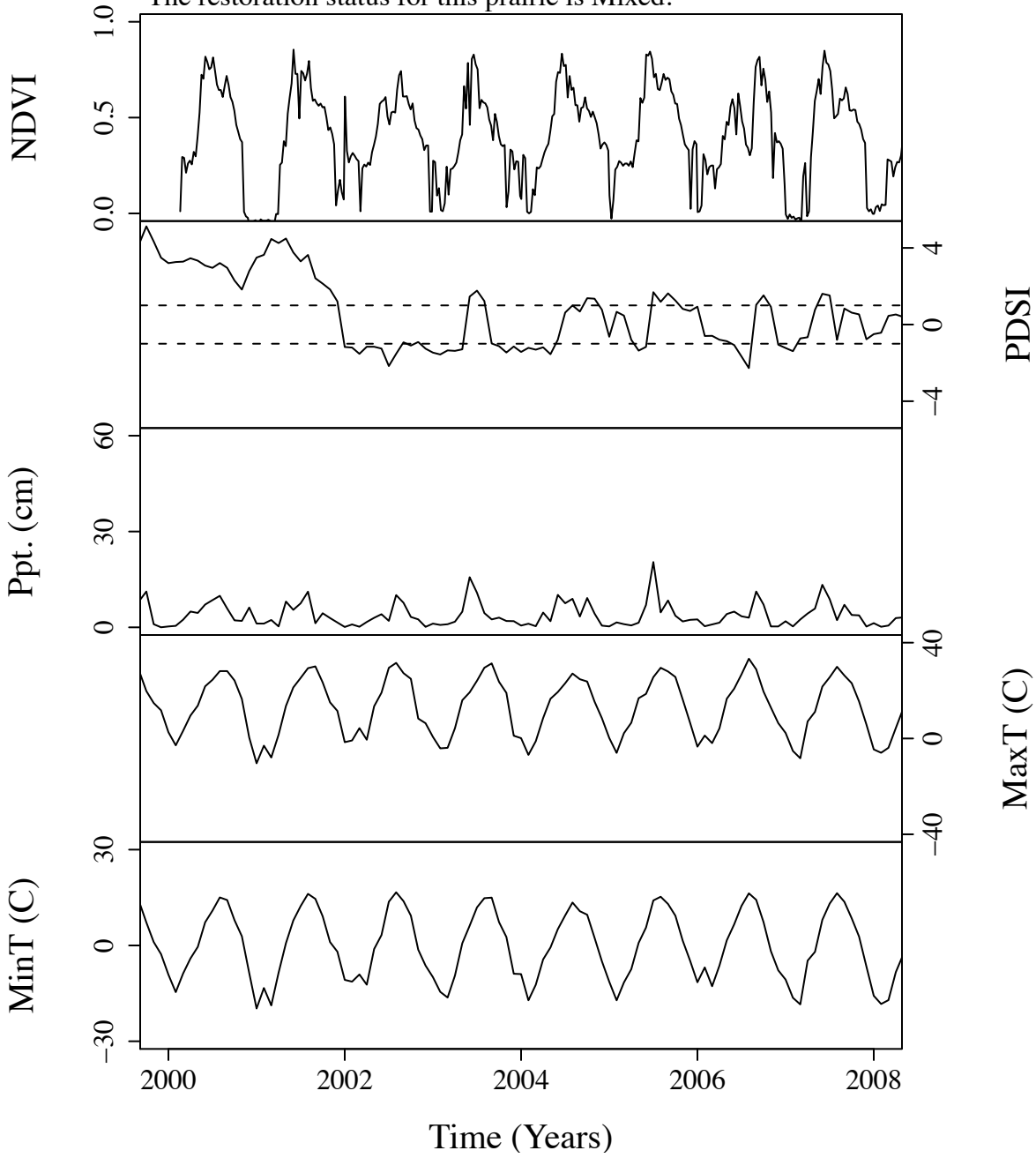

Figure B.217. Time series curves for sor15.
The community type for this prairie is Short.
The dominant photosynthetic pathway for this prairie is C3.
The restoration status for this prairie is Remnant.

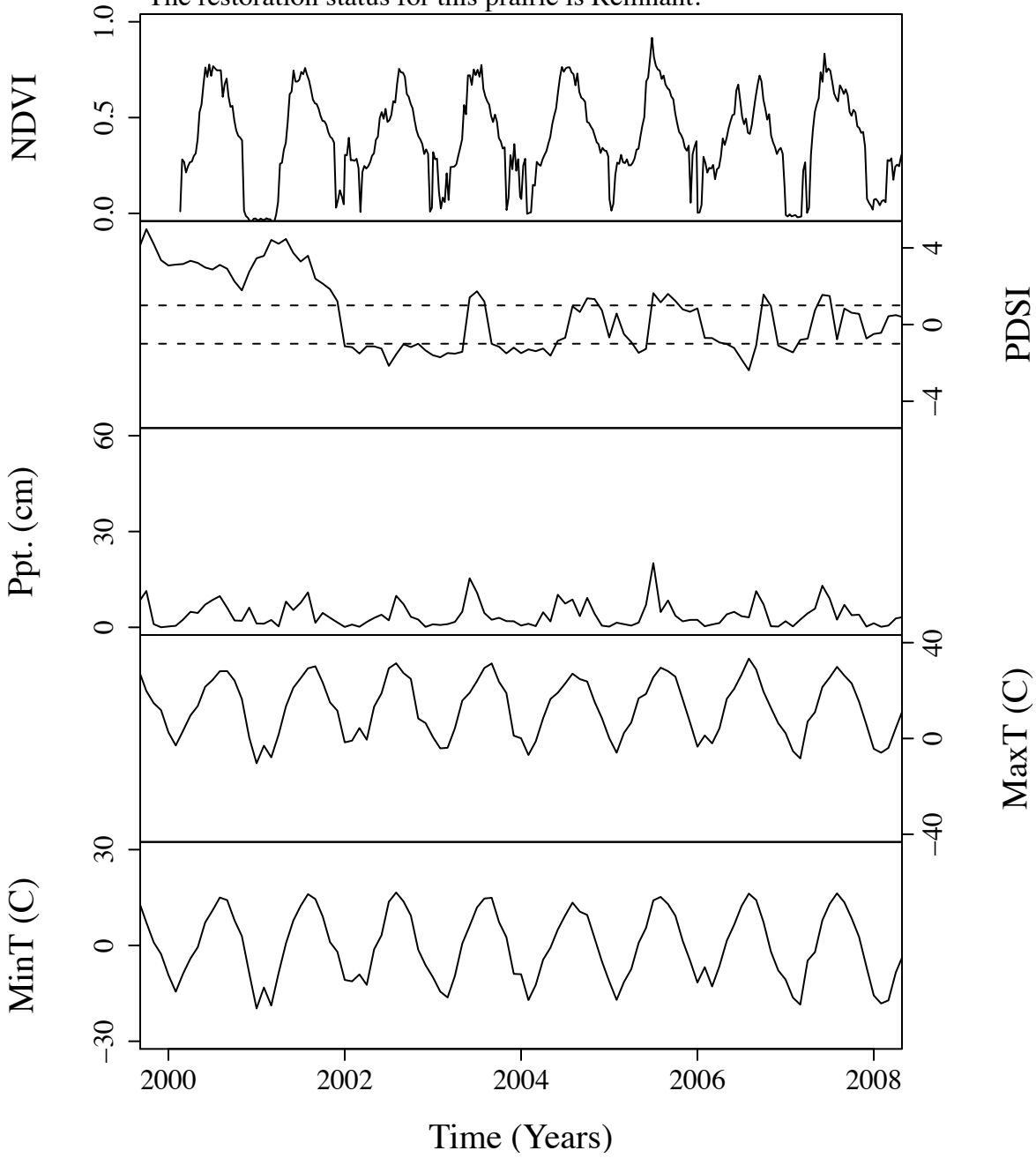

Figure B.218. Time series curves for sor19.
The community type for this prairie is Short.
The dominant photosynthetic pathway for this prairie is C3.
The restoration status for this prairie is Mixed.

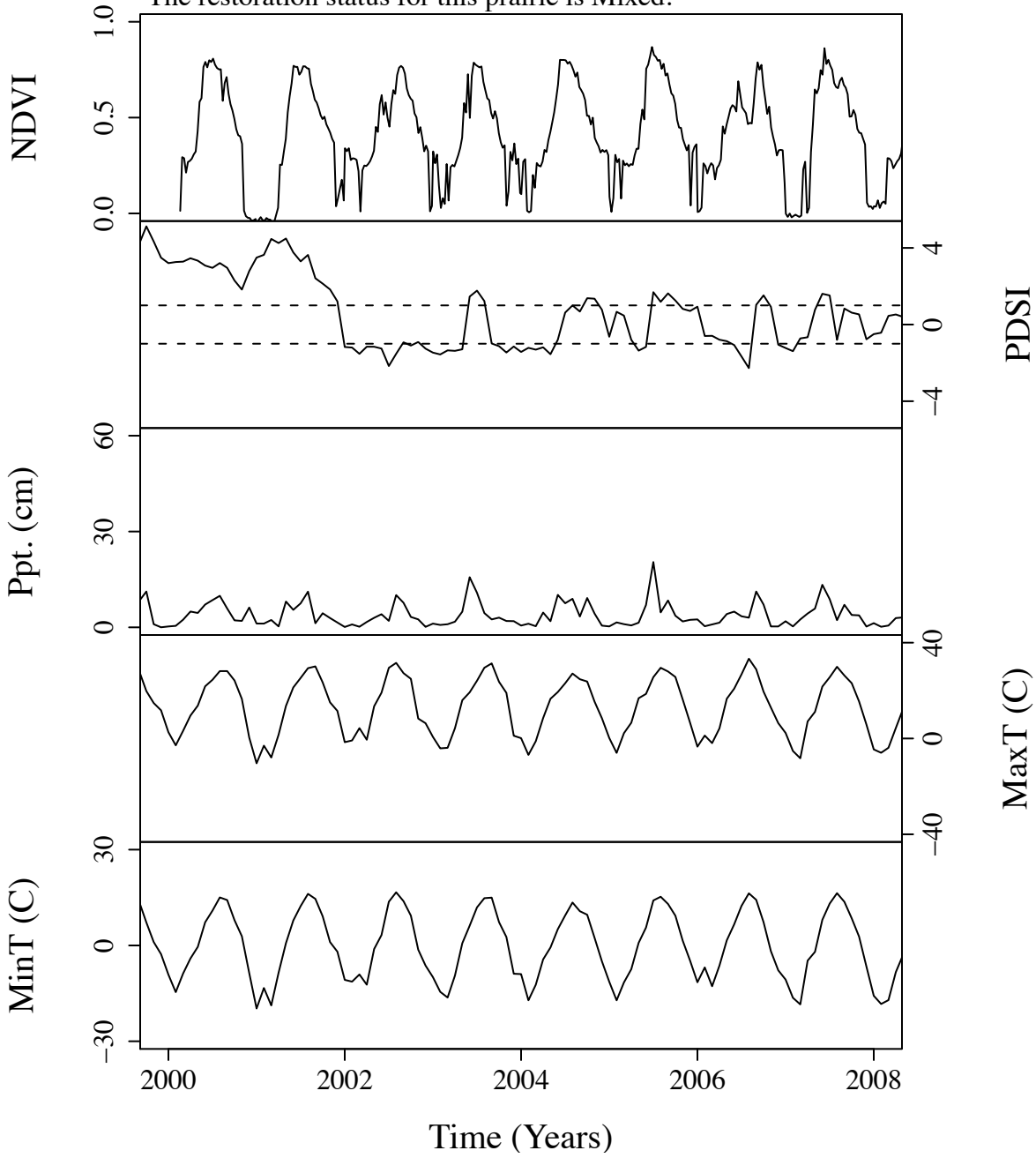

Figure B.219. Time series curves for sor21.
The community type for this prairie is Short.
The dominant photosynthetic pathway for this prairie is C3.
The restoration status for this prairie is Remnant.

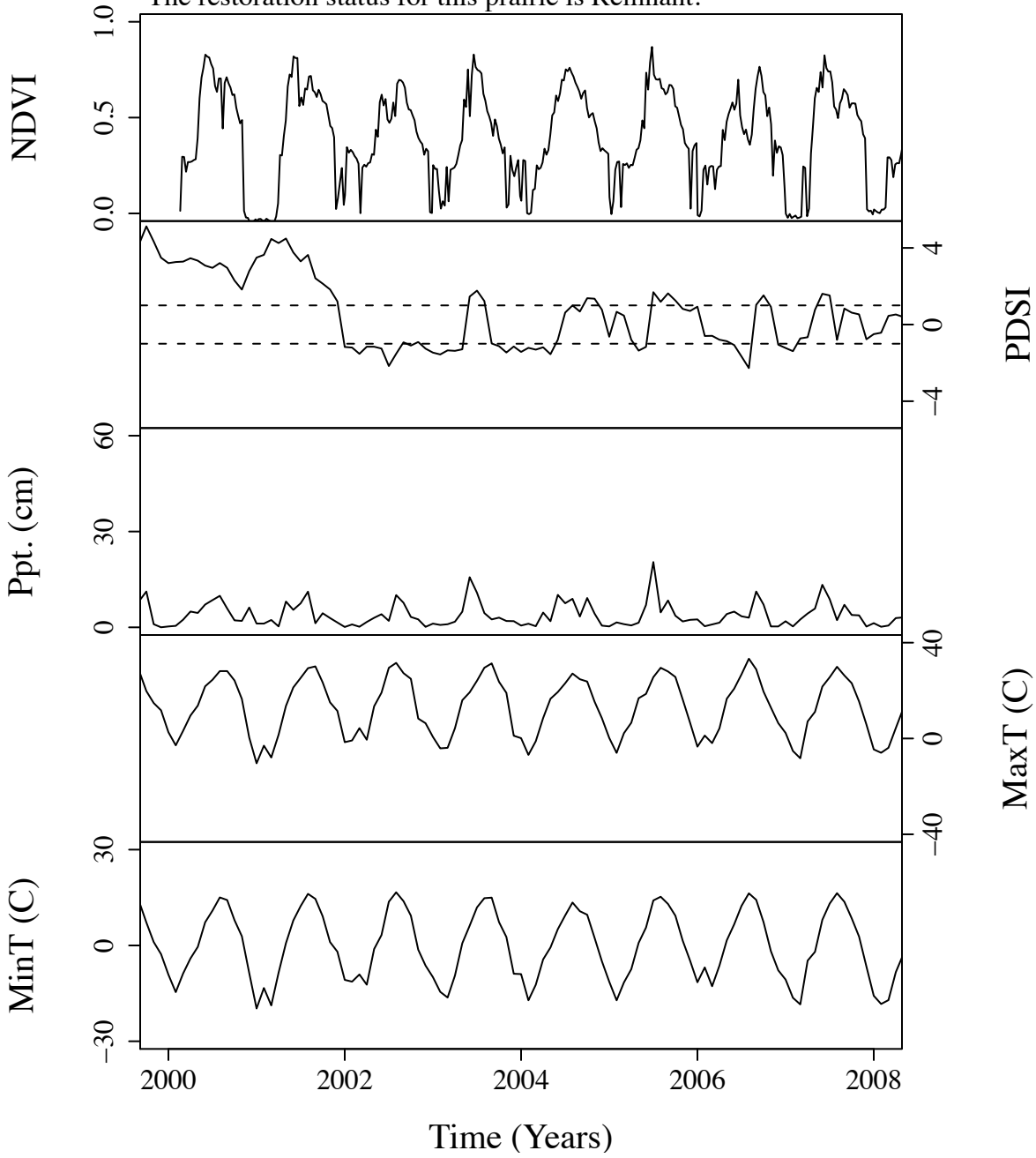

Figure B.220. Time series curves for sor4.
The community type for this prairie is Short.
The dominant photosynthetic pathway for this prairie is C3.
The restoration status for this prairie is Remnant.

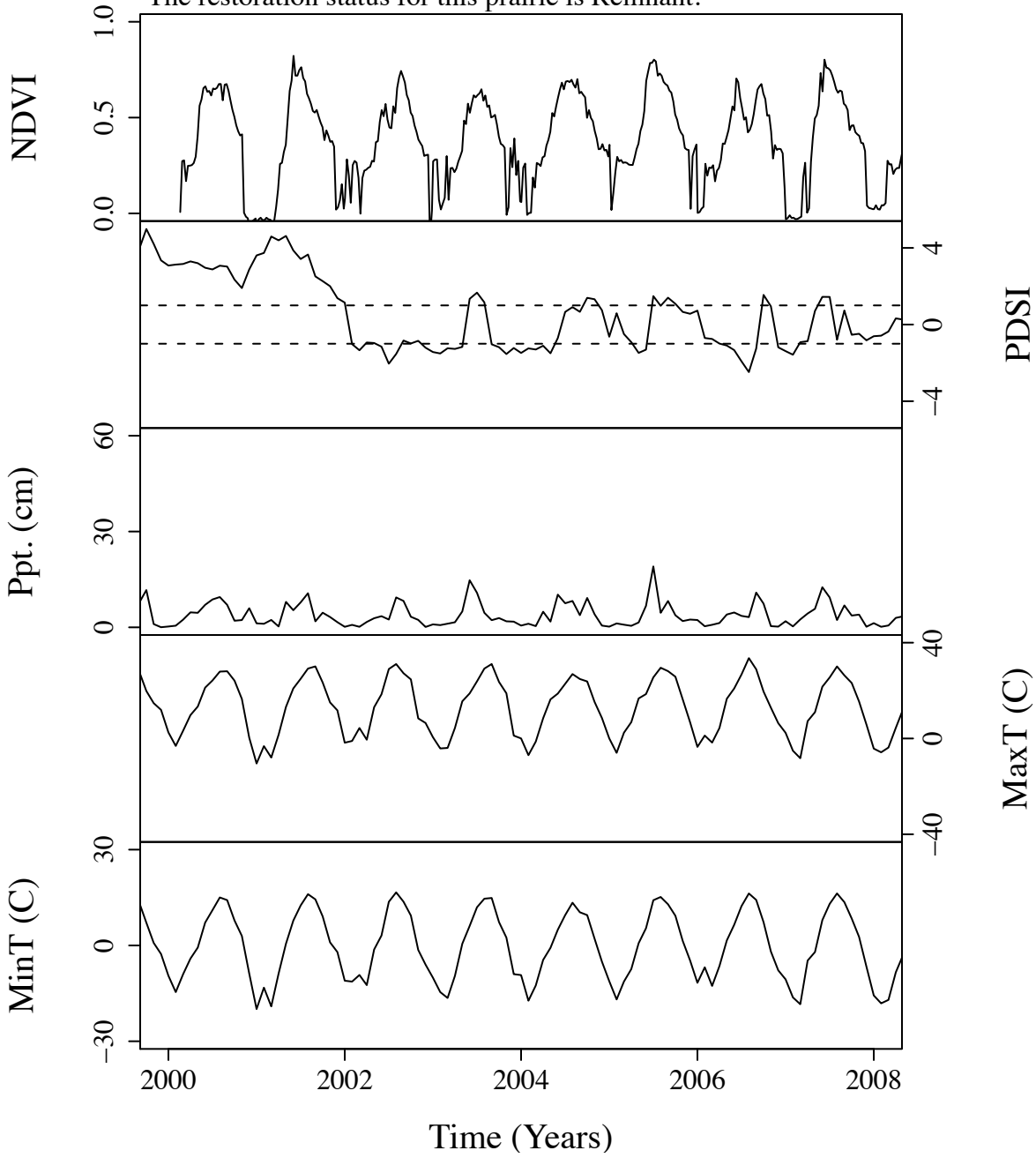

Figure B.221. Time series curves for sor6.
The community type for this prairie is Short.
The dominant photosynthetic pathway for this prairie is C3.
The restoration status for this prairie is Remnant.

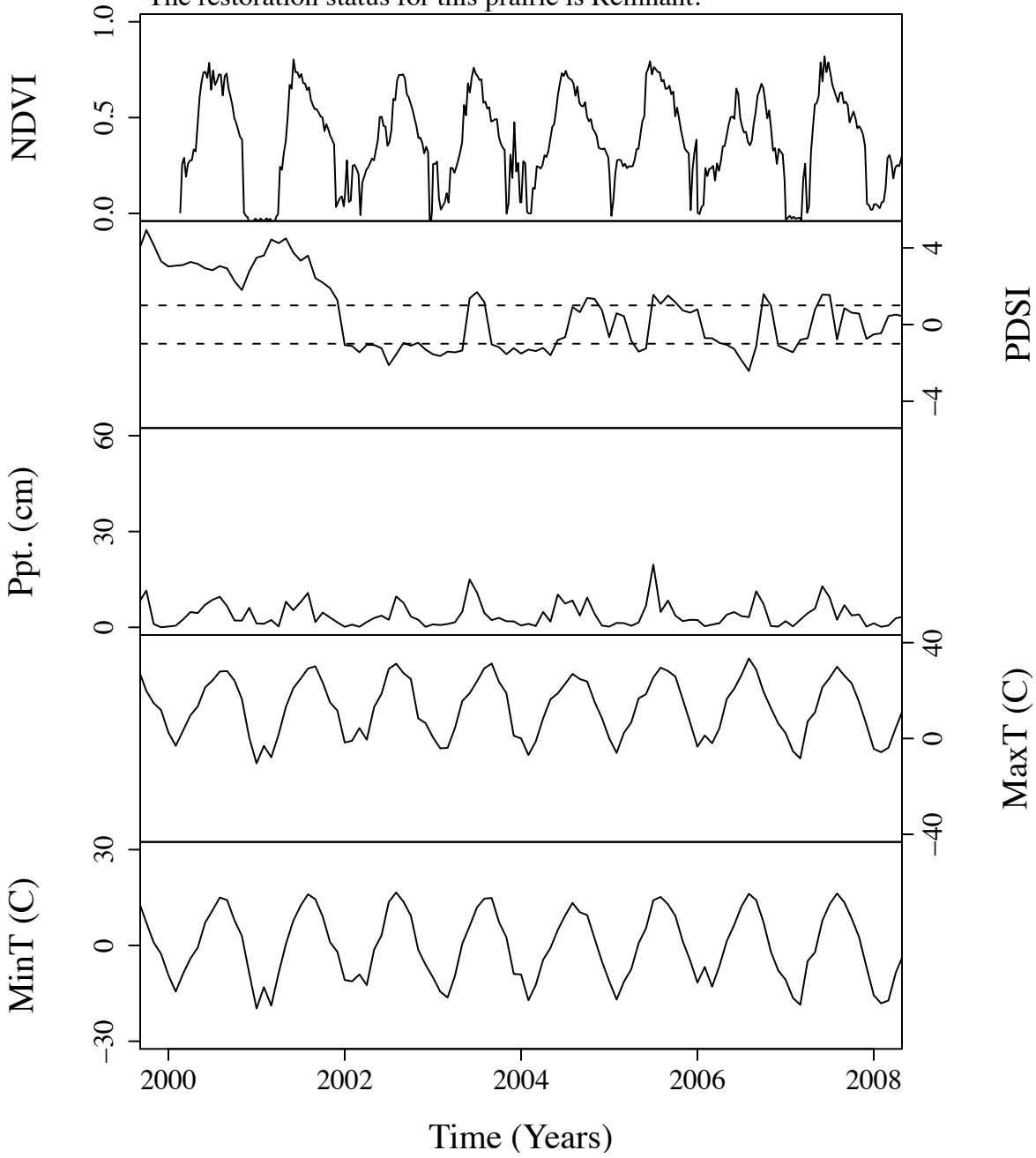

Figure B.222. Time series curves for sor7.
The community type for this prairie is Short.
The dominant photosynthetic pathway for this prairie is C3.
The restoration status for this prairie is Remnant.

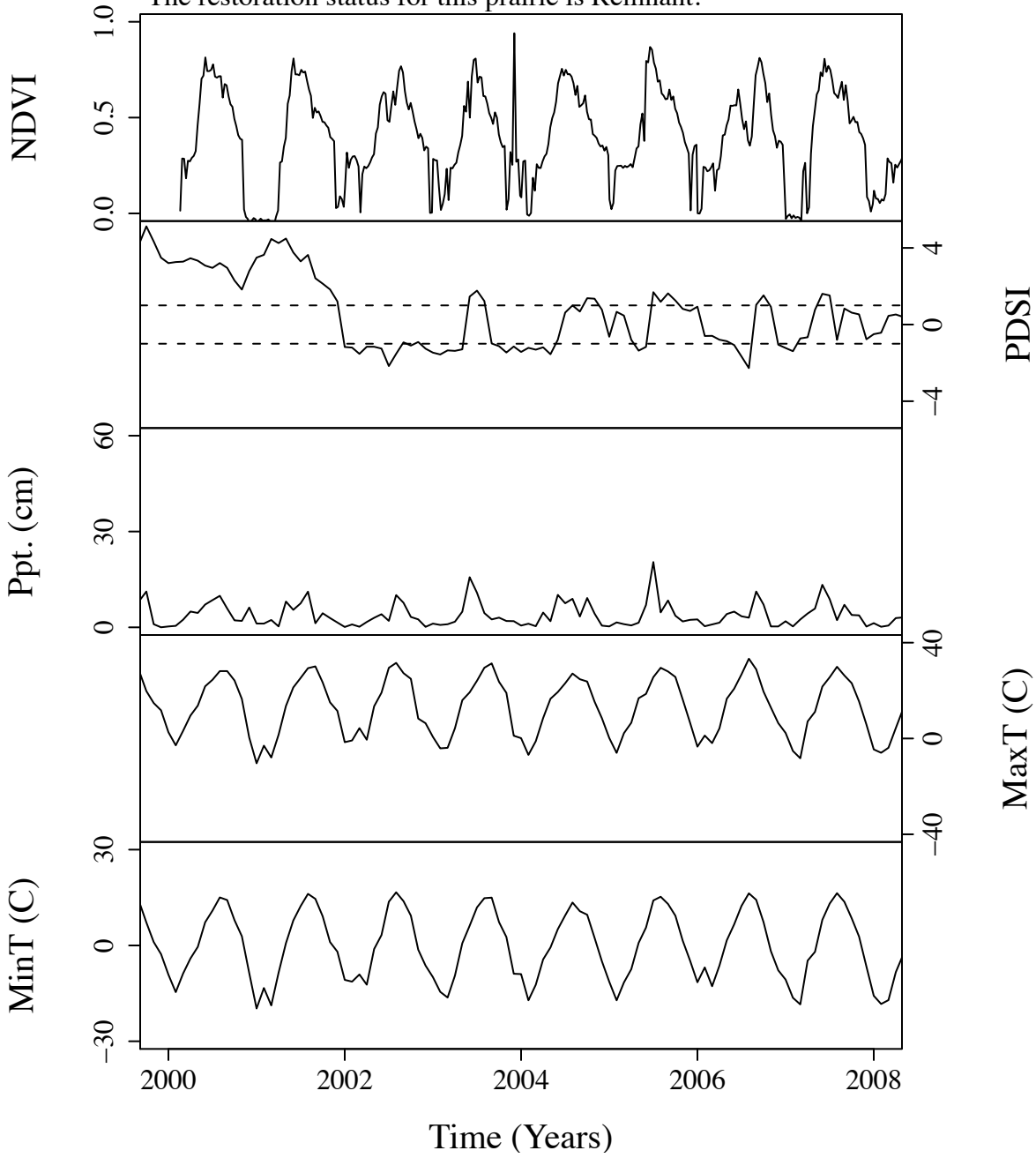

Figure B.223. Time series curves for sor8.
The community type for this prairie is Short.
The dominant photosynthetic pathway for this prairie is C3.
The restoration status for this prairie is Remnant.

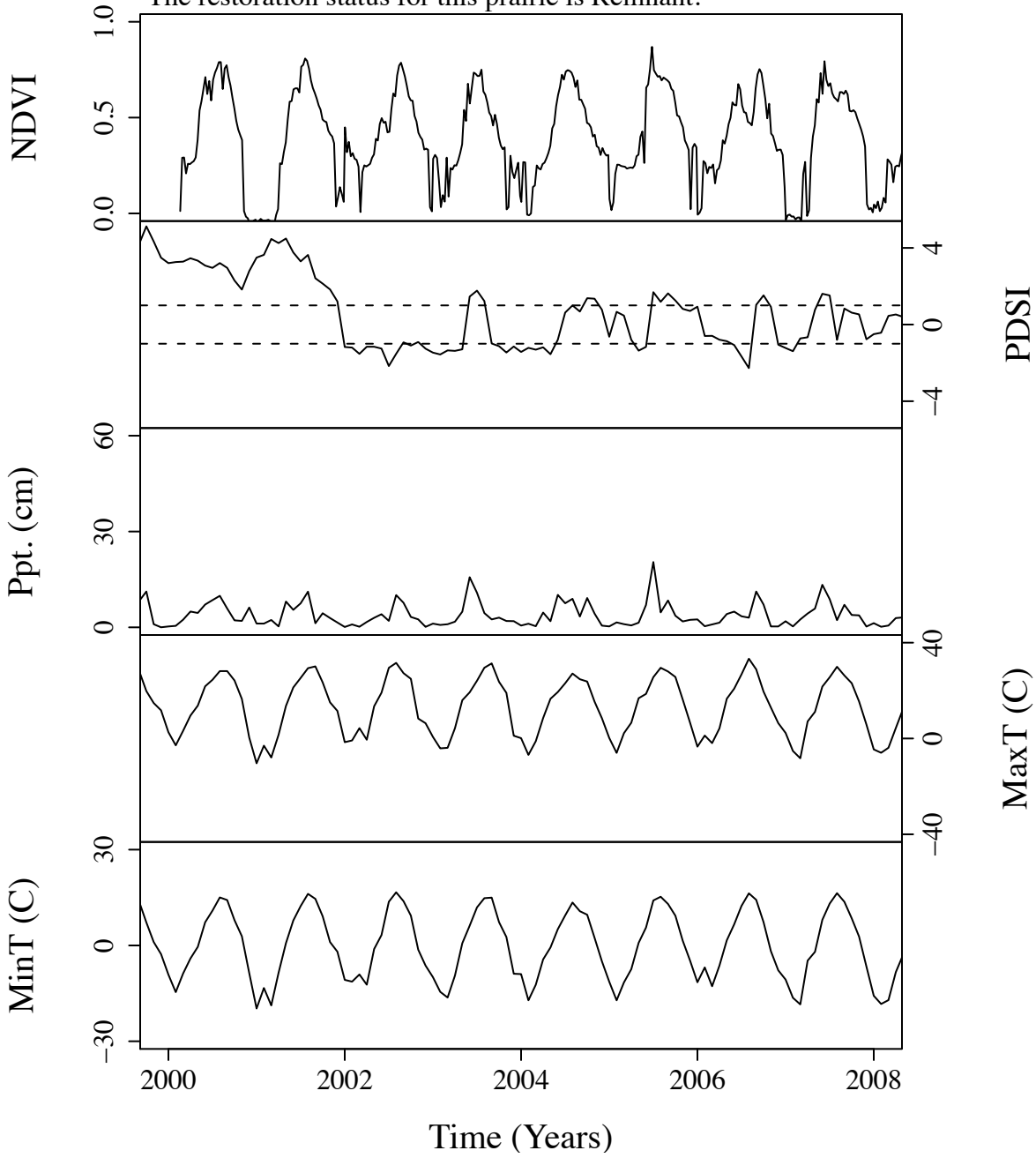

Figure B.224. Time series curves for sor9.
The community type for this prairie is Short.
The dominant photosynthetic pathway for this prairie is C3.
The restoration status for this prairie is Remnant.

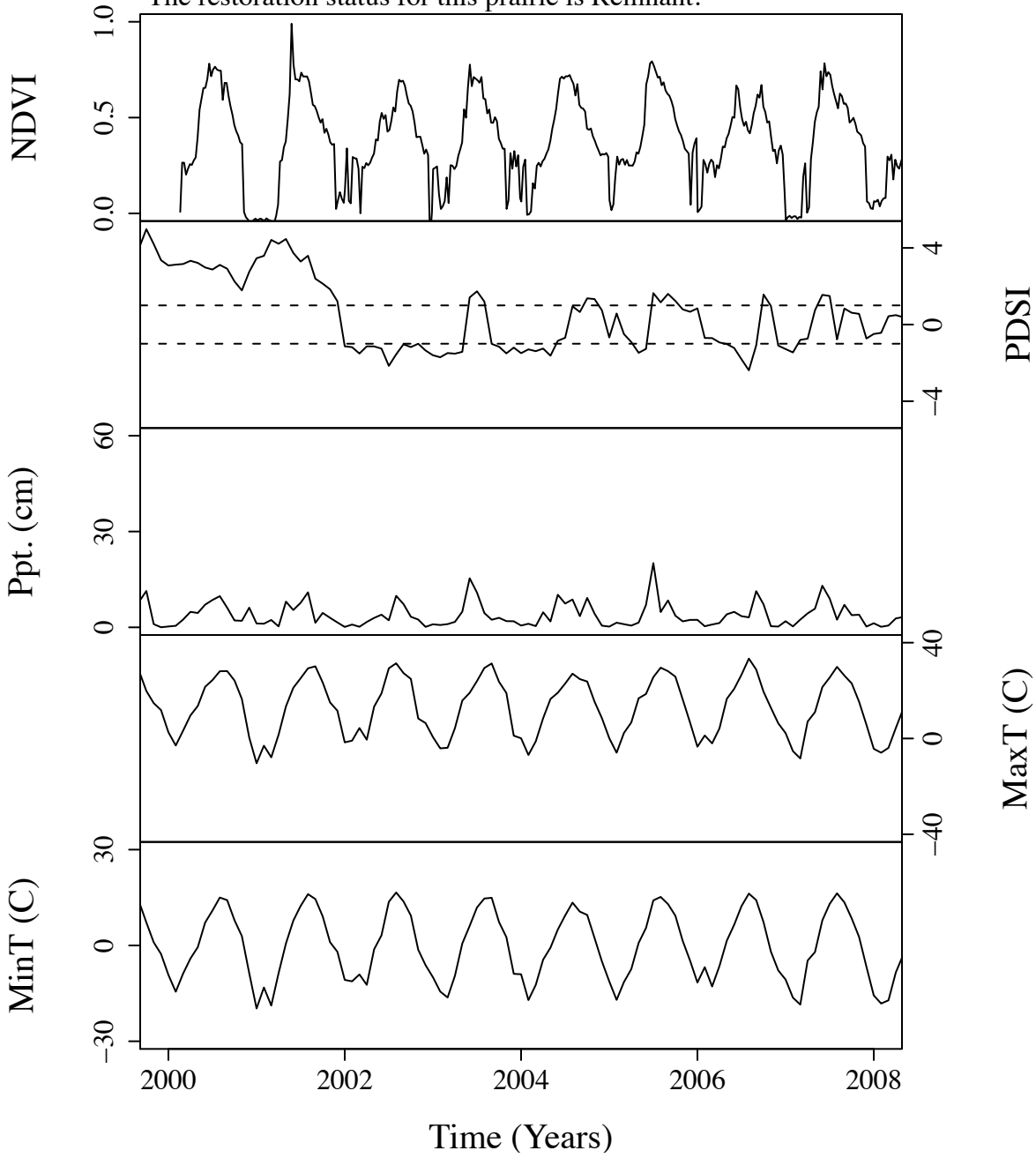

Figure B.225. Time series curves for ssi7.
The community type for this prairie is Tall.
The dominant photosynthetic pathway for this prairie is C4.
The restoration status for this prairie is Unknown.

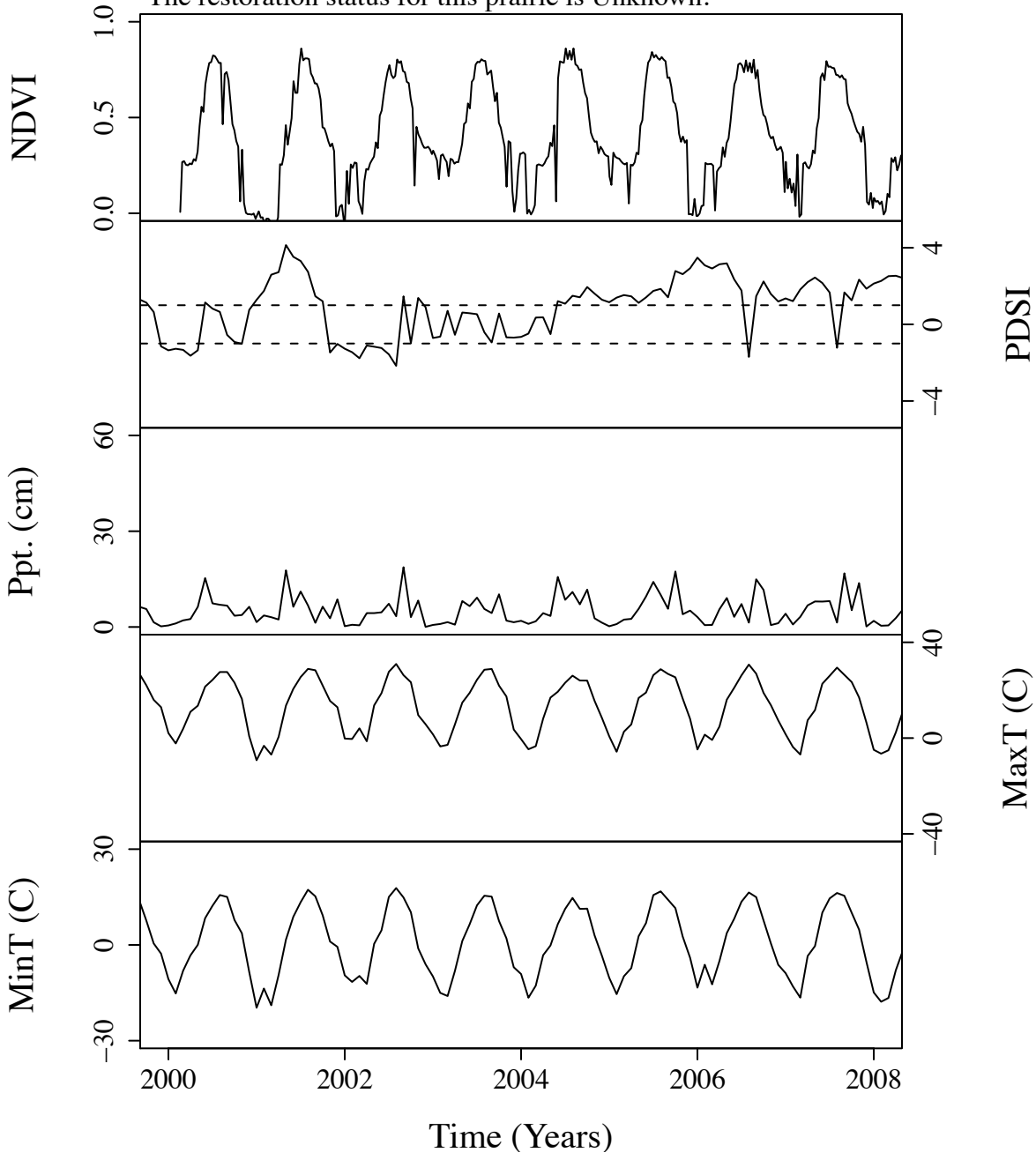

Figure B.226. Time series curves for wfc.
The community type for this prairie is NoType.
The dominant photosynthetic pathway for this prairie is C4.
The restoration status for this prairie is Unknown.